

Organic chemistry of singlet oxygen

Guest editor: Alexander Greer

Department of Chemistry and Graduate Center, The City University of New York (CUNY)—Brooklyn College, Brooklyn,
NY 11210, USA

Contents

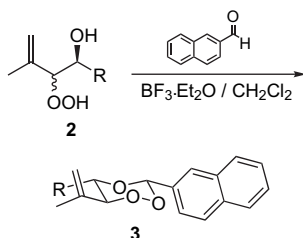
Announcement: Tetrahedron Symposia-in-Print
Preface

pp 10609–10611
p 10613

ARTICLES

Singlet oxygen addition to chiral allylic alcohols and subsequent peroxyacetalization with β -naphthaldehyde: synthesis of diastereomerically pure 3- β -naphthyl-substituted 1,2,4-trioxanes
Axel G. Griesbeck,* Tamer T. El-Idreesy and Johann Lex

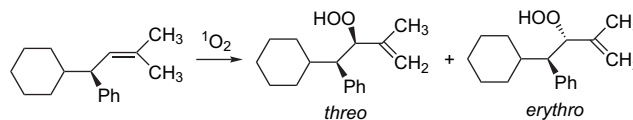
pp 10615–10622



Intrazeolite photooxygenation of chiral alkenes. Control of facial selectivity by confinement and cation- π interactions

pp 10623–10632

Manolis Stratakis,* Christos Raptis, Nikoleta Sofikiti, Constantinos Tsangarakis, Giannis Kosmas, Ioannis-Panagiotis Zaravinos, Dimitris Kalaitzakis, Dimitris Stavroulakis, Constantinos Baskakis and Aggeliki Stathoulopoulou



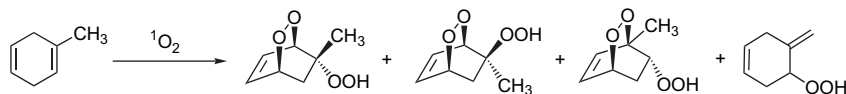
In solution: *threo/erythro* = 18/82

Within zeolite NaY: *threo/erythro* = 91/9

Regioselectivity in the ene-reaction of singlet oxygen with cyclic alkenes: photooxygenation of methyl-substituted 1,4-cyclohexadiene derivatives

pp 10633–10638

Sengül Dilem Yardımcı, Nihal Kaya and Metin Balci*

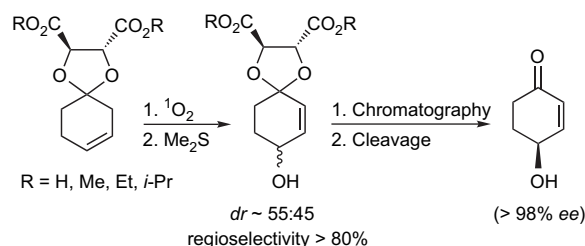


The photooxygenation of methyl-substituted cyclohexa-1,4-diene derivatives has been searched. The substituent effect is discussed.

Auxiliary controlled singlet-oxygen ene reactions of cyclohexenes

pp 10639–10646

Werner Fudickar, Katja Vorndran and Torsten Linker*

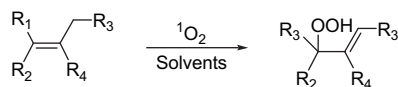

A comparative mechanistic analysis of the stereoselectivity trends observed in the oxidation of chiral oxazolidinone-functionalized encarbamates by singlet oxygen, ozone, and triazolidinone

J. Sivaguru, Thomas Poon, Catherine Hooper, Hideaki Saito, Marissa R. Solomon, Steffen Jockusch, Waldemar Adam, Yoshihisa Inoue and Nicholas J. Turro*

Reactive species	Stereo-differentiating structural factor	Stereoselectivity
	C ₄	Low
O ₃	C ₄ + alkene	Low to Moderate
¹ O ₂	C ₄ + alkene + C _{3'}	High

Stereoelectronic and solvent effects on the allylic oxyfunctionalization of alkenes with singlet oxygen

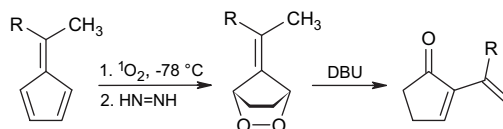
Mariza N. Alberti and Michael Orfanopoulos*



Unusual endoperoxide isomerizations: a convenient entry into 2-vinyl-2-cyclopentenones from saturated fulvene endoperoxides

pp 10676–10682

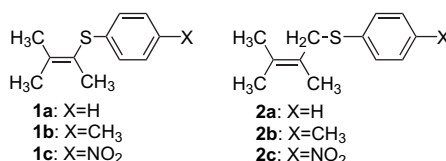
Ihsan Erden,* Nüket Öcal, Jianga Song, Cindy Gleason and Christian Gärtner



A comparison of hydrogen bonding solvent effects on the singlet oxygen reactions of allyl and vinyl sulfides, sulfoxides, and sulfones

pp 10683–10687

Kristina L. Stensaas,* Brent V. McCarty, Natacha M. Touchette and James B. Brock

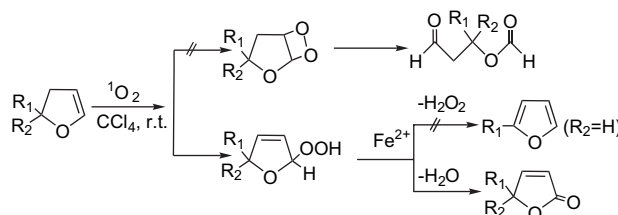


The singlet oxygen photooxidation of several allyl and vinyl sulfides, sulfoxides, and sulfones were conducted in deuterated solvents. The results indicate that only vinyl sulfides are susceptible to hydrogen bonding solvent effects.

Synthesis of α,β -unsaturated γ -lactones via photooxygenation of 2,3-dihydrofurans followed by ferrous ion-catalyzed *gem*-dehydration

pp 10688–10693

Yu-Zhe Chen, Li-Zhu Wu,* Ming-Li Peng, Dong Zhang, Li-Ping Zhang and Chen-Ho Tung*



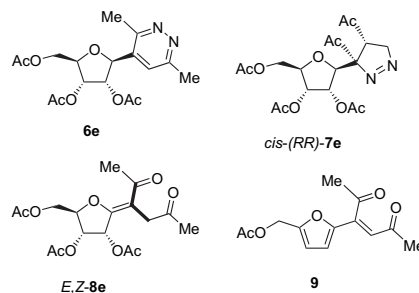
Photooxygenation of 2,3-dihydrofurans in CCl₄ at ambient temperature followed by ferrous ion-catalyzed *gem*-dehydration of the yielded allylic hydroperoxides afford the corresponding α,β -unsaturated γ -lactones in good to excellent yields.

Dye-sensitized photooxygenation of sugar-furans as synthetic strategy for novel C-nucleosides and functionalized *exo*-glycals

pp 10694–10699

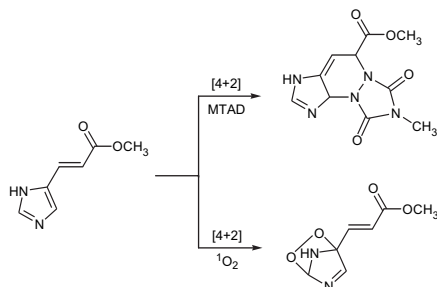
Flavio Cermola* and M. Rosaria Iesce

The methylene blue-sensitized photooxygenation of β -ribofuranosyl furan **1e** followed by in situ Et₂S treatment afforded the conformationally stable β -ribofuranoside **4e** almost quantitatively. The latter was converted to pyridazine C-nucleoside **6e** by cyclization with NH₂NH₂ and to pyrazoline **7e** through a 1,3-dipolar cycloaddition with diazomethane. Attempts to epoxidize the double bond failed both by dimethyldioxirane (DMDO), which left **4e** unchanged, and by NEt₃/*t*-BuOOH or NaOO-*t*-Bu which respectively afforded the new and unexpected *exo*-glycals *E,Z*-**8e** and the novel furan derivative **9**.



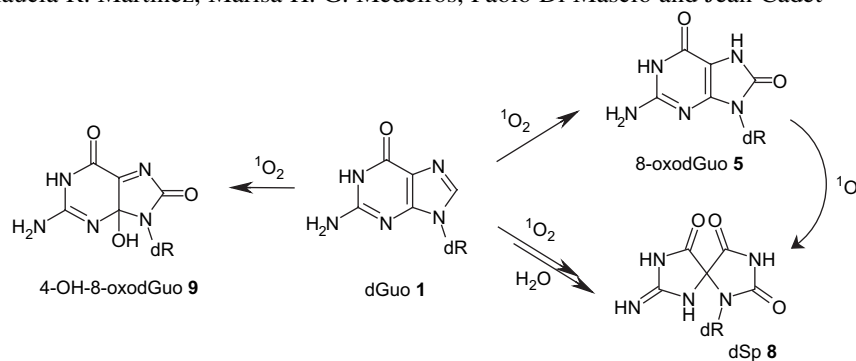
Reactions of urocanic acid (UCA) methyl esters with singlet oxygen and 4-methyl-1,2,4-triazoline-3,5-dione (MTAD) pp 10700–10708

Roberto Roa and Kevin E. O'Shea*


Singlet oxygen oxidation of 2'-deoxyguanosine. Formation and mechanistic insights

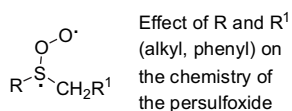
pp 10709–10715

Jean-Luc Ravanat, Glaucia R. Martinez, Marisa H. G. Medeiros, Paolo Di Mascio and Jean Cadet*


Reaction of singlet oxygen with some benzylic sulfides

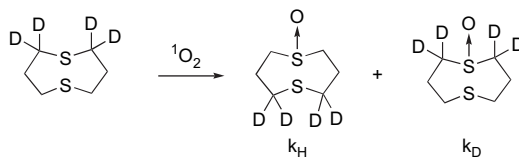
pp 10716–10723

Sergio M. Bonesi, Maurizio Fagnoni, Sandra Monti and Angelo Albini*


The hydroperoxysulfonium ylide. An aberration or a ubiquitous intermediate?

pp 10724–10728

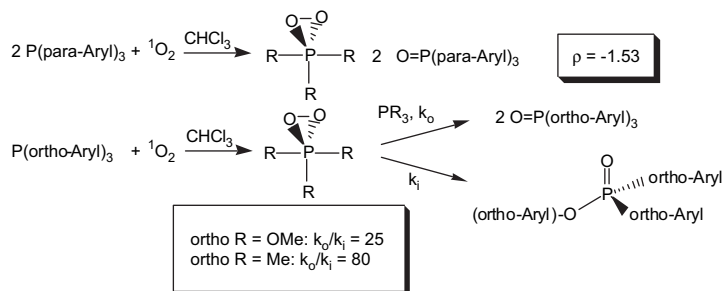
Edward L. Clennan* and Chen Liao



Chemistry of singlet oxygen with arylphosphines

pp 10729–10733

Dong Zhang, Bin Ye, David G. Ho, Ruomei Gao and Matthias Selke*

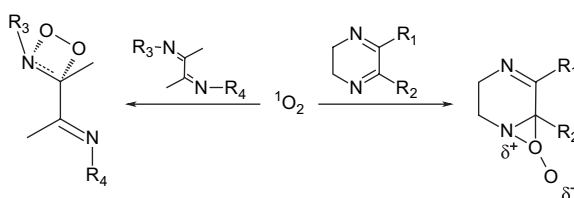


Steric and electronic effects on the reactivity of arylphosphines with singlet oxygen are reported.

Solvent effect on the sensitized photooxygenation of cyclic and acyclic α -diimines

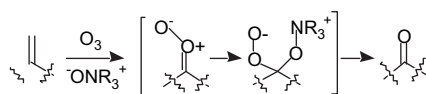
pp 10734–10746

Else Lemp,* Antonio L. Zanocco, German Günther and Nancy Pizarro

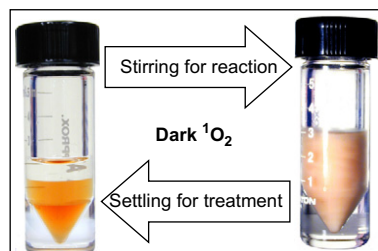
**'Reductive ozonolysis' via a new fragmentation of carbonyl oxides**

pp 10747–10752

Chris Schwartz, Joseph Raible, Kyle Mott and Patrick H. Dussault*

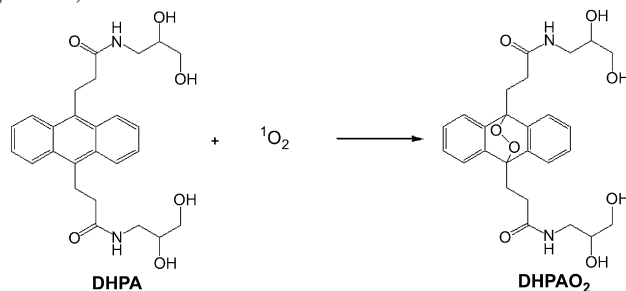
**Dark singlet oxygenation of organic substrates in single-phase and multiphase microemulsion systems** pp 10753–10761

Jean-Marie Aubry,* Waldemar Adam, Paul L. Alsters, Cédric Borde, Sébastien Queste, Jean Marko and Véronique Nardello

The chemical source of singlet oxygen $\text{H}_2\text{O}_2/\text{MoO}_4^{2-}$ can oxidize labile and hydrophobic substrates in microemulsion. The respective advantages and limitations of single-phase and multiphase microemulsion systems are shortly reviewed and discussed.

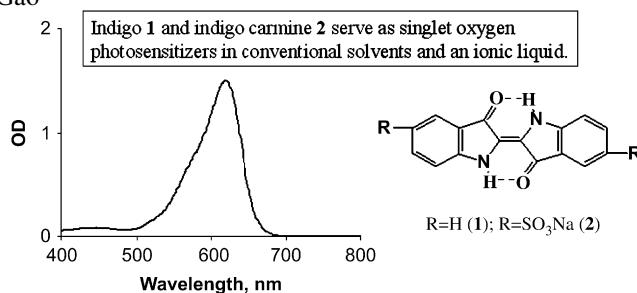
Synthesis of a hydrophilic and non-ionic anthracene derivative, the *N,N'*-di-(2,3-dihydroxypropyl)-9,10-pp 10762–10770 anthracenedipropanamide as a chemical trap for singlet molecular oxygen detection in biological systems

Glaucia R. Martinez, Flávia Garcia, Luiz H. Catalani, Jean Cadet, Mauricio C. B. Oliveira, Graziella E. Ronsein, Sayuri Miyamoto, Marisa H. G. Medeiros and Paolo Di Mascio*




Possible singlet oxygen generation from the photolysis of indigo dyes in methanol, DMSO, water, and ionic liquid, 1-butyl-3-methylimidazolium tetrafluoroborate pp 10771–10776

Naveen Gandra, Aaron T. Frank, Onica Le Gendre, Nahed Sawwan, David Aebisher, Joel F. Liebman, K. N. Houk, Alexander Greer* and Ruomei Gao*



*Corresponding author

 Supplementary data available via ScienceDirect

COVER

The cover figure shows the reaction of homochiral cyclohexene ketals with $^1\text{O}_2$, which gives hydroperoxides and after reduction the corresponding allylic alcohols with excellent regioselectivity. Mechanistic considerations were used to rationalize the regioselectivity. The work was conducted by Torsten Linker and co-workers.

© 2006 A. Greer. Published by Elsevier Ltd.



Full text of this journal is available, on-line from **ScienceDirect**. Visit www.sciencedirect.com for more information.

Abstracted/indexed in: AGRICOLA, Beilstein, BIOSIS Previews, CAB Abstracts, Chemical Abstracts. Current Contents: Life Sciences, Current Contents: Physical, Chemical and Earth Sciences, Current Contents Search, Derwent Drug File, Ei compendex, EMBASE/Excerpta Medica, Medline, PASCAL, Research Alert, Science Citation Index, SciSearch. Also covered in the abstract and citation database SCOPUS®. Full text available on ScienceDirect®



ELSEVIER

ISSN 0040-4020

Tetrahedron Symposia-in-Print

Series Editor

Professor H. H. Wasserman, Department of Chemistry, Yale University, P.O. Box 208107, New Haven, CT 06520-8107, U.S.A.

Tetrahedron Symposia-in-Print comprise collections of original research papers covering timely areas of organic chemistry.

Each symposium is organized by a Symposium Editor who will invite authors, active in the selected field, to submit original articles covering current research, complete with experimental sections. These papers will be rapidly reviewed and processed for publication by the Symposium Editor under the usual refereeing system.

Authors who have not already been invited, and who may have obtained recent significant results in the area of the announced symposium, may also submit contributions for Editorial consideration and possible inclusion. Before submitting such papers authors should send an abstract to the Symposium Editor for preliminary evaluation. Firm deadlines for receipt of papers will allow sufficient time for completion and presentation of ongoing work without loss of the freshness and timeliness of the research results.

Symposia-in-Print—already published

1. Recent trends in organic photochemistry, Albert Padwa, Ed. *Tetrahedron* **1981**, *37*, 3227–3420.
2. New general synthetic methods, E. J. Corey, Ed. *Tetrahedron* **1981**, *37*, 3871–4119.
3. Recent developments in polycyclopentanoid chemistry, Leo A. Paquette, Ed. *Tetrahedron* **1981**, *37*, 4357–4559.
4. Biradicals, Josef Michl, Ed. *Tetrahedron* **1982**, *38*, 733–867.
5. Electron-transfer initiated reactions, Gary B. Schuster, Ed. *Tetrahedron* **1982**, *38*, 1025–1122.
6. The organic chemistry of animal defense mechanisms, Jerrold Meinwald, Ed. *Tetrahedron* **1982**, *38*, 1853–1970.
7. Recent developments in the use of silicon in organic synthesis, Hans Reich, Ed. *Tetrahedron* **1983**, *39*, 839–1009.
8. Linear tetrapyrroles, Ray Bonnett, Ed. *Tetrahedron* **1983**, *39*, 1837–1954.
9. Heteroatom-directed metallations in heterocyclic synthesis, George R. Newkome, Ed. *Tetrahedron* **1983**, *39*, 1955–2091.
10. Recent aspects of the chemistry of β -lactams, J. E. Baldwin, Ed. *Tetrahedron* **1983**, *39*, 2445–2608.
11. New spectroscopic techniques for studying metabolic processes, A. I. Scott, Ed. *Tetrahedron* **1983**, *39*, 3441–3626.
12. New developments in indole alkaloids, Martin E. Kuehne, Ed. *Tetrahedron* **1983**, *39*, 3627–3780.
13. Recent aspects of the chemistry of nucleosides, nucleotides and nucleic acids, Colin B. Reese, Ed. *Tetrahedron* **1984**, *40*, 1–164.
14. Bioorganic studies on receptor sites, Koji Nakanishi, Ed. *Tetrahedron* **1984**, *40*, 455–592.
15. Synthesis of chiral non-racemic compounds, A. I. Meyers, Ed. *Tetrahedron* **1984**, *40*, 1213–1418.
16. Control of acyclic stereochemistry, Teruaki Mukaiyama, Ed. *Tetrahedron* **1984**, *40*, 2197–2344.
17. Recent aspects of anthracycline chemistry, T. Ross Kelly, Ed. *Tetrahedron* **1984**, *40*, 4537–4794.
18. The organic chemistry of marine products, Paul J. Scheuer, Ed. *Tetrahedron* **1985**, *41*, 979–1108.
19. Recent aspects of carbene chemistry, Matthew Platz, Ed. *Tetrahedron* **1985**, *41*, 1423–1612.
20. Recent aspects of singlet oxygen chemistry of photooxidation, Isao Saito and Teruo Matsuura, Eds. *Tetrahedron* **1985**, *41*, 2037–2236.
21. Synthetic applications of dipolar cycloaddition reactions, Wolfgang Oppolzer, Ed. *Tetrahedron* **1985**, *41*, 3447–3568.
22. Selectivity and synthetic applications of radical reactions, Bernd Giese, Ed. *Tetrahedron* **1985**, *41*, 3887–4302.
23. Recent aspects of organoselenium chemistry, Dennis Liotta, Ed. *Tetrahedron* **1985**, *41*, 4727–4890.
24. Application of newer organometallic reagents to the total synthesis of natural products, Martin Semmelhack, Ed. *Tetrahedron* **1985**, *41*, 5741–5900.
25. Formal transfers of hydride from carbon–hydrogen bonds, James D. Wuest, Ed. *Tetrahedron* **1986**, *42*, 941–1208.
26. Synthesis of non-natural products: challenge and reward, Philip E. Eaton, Ed. *Tetrahedron* **1986**, *42*, 1549–1916.
27. New synthetic methods—II, F. E. Ziegler, Ed. *Tetrahedron* **1986**, *42*, 2777–3028.
28. Structure and reactivity of organic radical ions, Heinz D. Roth, Ed. *Tetrahedron* **1986**, *42*, 6097–6350.
29. Organic chemistry in anisotropic media, V. Ramamurthy, J. R. Scheffer and N. J. Turro, Eds. *Tetrahedron* **1987**, *43*, 1197–1746.
30. Current topics in sesquiterpene synthesis, John W. Huffman, Ed. *Tetrahedron* **1987**, *43*, 5467–5722.
31. Peptide chemistry: design and synthesis of peptides, conformational analysis and biological functions, Victor J. Hruby and Robert Schwyzler, Eds. *Tetrahedron* **1988**, *44*, 661–1006.
32. Organosilicon chemistry in organic synthesis, Ian Fleming, Ed. *Tetrahedron* **1988**, *44*, 3761–4292.
33. α -Amino acid synthesis, Martin J. O'Donnell, Ed. *Tetrahedron* **1988**, *44*, 5253–5614.
34. Physical-organic/theoretical chemistry: the Dewar interface, Nathan L. Bauld, Ed. *Tetrahedron* **1988**, *44*, 7335–7626.
35. Recent developments in organocopper chemistry, Bruce H. Lipshutz, Ed. *Tetrahedron* **1989**, *45*, 349–578.
36. Organotin compounds in organic synthesis, Yoshinori Yamamoto, Ed. *Tetrahedron* **1989**, *45*, 909–1230.

37. Mycotoxins, Pieter S. Steyn, Ed. *Tetrahedron* **1989**, *45*, 2237–2464.
38. Strain-assisted syntheses, Léon Ghosez, Ed. *Tetrahedron* **1989**, *45*, 2875–3232.
39. Covalently linked donor-acceptor species for mimicry of photosynthetic electron and energy transfer, Devens Gust and Thomas A. Moore, Eds. *Tetrahedron* **1989**, *45*, 4669–4912.
40. Aspects of modern carbohydrate chemistry, S. Hanessian, Ed. *Tetrahedron* **1990**, *46*, 1–290.
41. Nitroalkanes and nitroalkenes in synthesis, Anthony G. M. Barrett, Ed. *Tetrahedron* **1990**, *46*, 7313–7598.
42. Synthetic applications of anodic oxidations, John S. Swenton and Gary W. Morrow, Eds. *Tetrahedron* **1991**, *47*, 531–906.
43. Recent advances in bioorganic chemistry, Dale L. Boger, Ed. *Tetrahedron* **1991**, *47*, 2351–2682.
44. Natural product structure determination, R. B. Bates, Ed. *Tetrahedron* **1991**, *47*, 3511–3664.
45. Frontiers in natural products biosynthesis. Enzymological and molecular genetic advances, D. E. Cane, Ed. *Tetrahedron* **1991**, *47*, 5919–6078.
46. New synthetic methods—III, S. E. Denmark, Ed. *Tetrahedron* **1992**, *48*, 1959–2222.
47. Organotitanium reagents in organic chemistry, M. T. Reetz, Ed. *Tetrahedron* **1992**, *48*, 5557–5754.
48. Total and semi-synthetic approaches to taxol, J. D. Winkler, Ed. *Tetrahedron* **1992**, *48*, 6953–7056.
49. Synthesis of optically active compounds—prospects for the 21st century, Kenji Koga and Takayuki Shioiri, Eds. *Tetrahedron* **1993**, *49*, 1711–1924.
50. Peptide secondary structure mimetics, Michael Kahn, Ed. *Tetrahedron* **1993**, *49*, 3433–3689.
51. Transition metal organometallics in organic synthesis, Anthony J. Pearson, Ed. *Tetrahedron* **1993**, *49*, 5415–5682.
52. Palladium in organic synthesis, Jan-E. Bäckvall, Ed. *Tetrahedron* **1994**, *50*, 285–572.
53. Recent progress in the chemistry of enediyne antibiotics, Terrence W. Doyle and John F. Kadow, Eds. *Tetrahedron* **1994**, *50*, 1311–1538.
54. Catalytic asymmetric addition reactions, Stephen F. Martin, Ed. *Tetrahedron* **1994**, *50*, 4235–4574.
55. Mechanistic aspects of polar organometallic chemistry, Manfred Schlosser, Ed. *Tetrahedron* **1994**, *50*, 5845–6128.
56. Molecular recognition, Andrew D. Hamilton, Ed. *Tetrahedron* **1995**, *51*, 343–648.
57. Recent advances in the chemistry of zirconocene and related compounds, Ei-ichi Negishi, Ed. *Tetrahedron* **1995**, *51*, 4255–4570.
58. Fluoroorganic chemistry: synthetic challenges and biomedical rewards, Giuseppe Resnati and Vadim A. Soloshonok, Eds. *Tetrahedron* **1996**, *52*, 1–330.
59. Novel applications of heterocycles in synthesis, A. R. Katritzky, Ed. *Tetrahedron* **1996**, *52*, 3057–3374.
60. Fullerene chemistry, Amos B. Smith III, Ed. *Tetrahedron* **1996**, *52*, 4925–5262.
61. New synthetic methods—IV. Organometallics in organic chemistry, István E. Markó, Ed. *Tetrahedron* **1996**, *52*, 7201–7598.
62. Cascade reactions, Ron Grigg, Ed. *Tetrahedron* **1996**, *52*, 11385–11664.
63. Applications of solid-supported organic synthesis in combinatorial chemistry, James A. Bristol, Ed. *Tetrahedron* **1997**, *53*, 6573–6706.
64. Recent applications of synthetic organic chemistry, Stephen F. Martin, Ed. *Tetrahedron* **1997**, *53*, 8689–9006.
65. Chemical biology, Gregory L. Verdine and Julian Simon, Eds. *Tetrahedron* **1997**, *53*, 11937–12066.
66. Recent aspects of S, Se, and Te chemistry, Richard S. Glass and Renji Okazaki, Eds. *Tetrahedron* **1997**, *53*, 12067–12318.
67. Modern organic chemistry of polymerization, H. K. Hall Jr., Ed. *Tetrahedron* **1997**, *53*, 15157–15616.
68. New synthetic methods—V, John L. Wood, Ed. *Tetrahedron* **1997**, *53*, 16213–16606.
69. New developments in organonickel chemistry, Bruce H. Lipshutz and Tien-Yau Luh, Eds. *Tetrahedron* **1998**, *54*, 1021–1316.
70. Solution phase combinatorial chemistry, David L. Coffen, Ed. *Tetrahedron* **1998**, *54*, 3955–4150.
71. Heterocycles in asymmetric synthesis, Alexandre Alexakis, Ed. *Tetrahedron* **1998**, *54*, 10239–10554.
72. Recent advances of phase-transfer catalysis, Takayuki Shioiri, Ed. *Tetrahedron* **1999**, *55*, 6261–6402.
73. Olefin metathesis in organic synthesis, Marc L. Snapper and Amir H. Hoveyda, Eds. *Tetrahedron* **1999**, *55*, 8141–8262.
74. Stereoselective carbon–carbon bond forming reactions, Harry H. Wasserman, Stephen F. Martin and Yoshinori Yamamoto, Eds. *Tetrahedron* **1999**, *55*, 8589–9006.
75. Applications of combinatorial chemistry, Miles G. Siegel and Stephen W. Kaldor, Eds. *Tetrahedron* **1999**, *55*, 11609–11710.
76. Advances in carbon–phosphorus heterocyclic chemistry, François Mathey, Ed. *Tetrahedron* **2000**, *56*, 1–164.
77. Transition metal organometallics in organic synthesis, Kenneth M. Nicholas, Ed. *Tetrahedron* **2000**, *56*, 2103–2338.
78. Organocopper chemistry II, Norbert Krause, Ed. *Tetrahedron* **2000**, *56*, 2727–2904.
79. Carbene complexes in organic chemistry, James W. Herndon, Ed. *Tetrahedron* **2000**, *56*, 4847–5044.
80. Recent aspects of the chemistry of β -lactams—II, Marvin J. Miller, Ed. *Tetrahedron* **2000**, *56*, 5553–5742.
81. Molecular assembly and reactivity of organic crystals and related structures, Miguel A. Garcia-Garibay, Vaidhyathan Ramamurthy and John R. Scheffer, Eds. *Tetrahedron* **2000**, *56*, 6595–7050.
82. Protein engineering, Richard Chamberlin, Ed. *Tetrahedron* **2000**, *56*, 9401–9526.
83. Recent advances in peptidomimetics, Jeffrey Aubé, Ed. *Tetrahedron* **2000**, *56*, 9725–9842.
84. New synthetic methods—VI, George A. Kraus, Ed. *Tetrahedron* **2000**, *56*, 10101–10282.
85. Oxidative activation of aromatic rings: an efficient strategy for arene functionalization, Stéphane Quideau and Ken S. Feldman, Eds. *Tetrahedron* **2001**, *57*, 265–424.
86. Lewis acid control of asymmetric synthesis, Keiji Maruoka, Ed. *Tetrahedron* **2001**, *57*, 805–914.
87. Novel aromatic compounds, Lawrence T. Scott and Jay S. Siegel, Eds. *Tetrahedron* **2001**, *57*, 3507–3808.
88. Asymmetric synthesis of novel sterically constrained amino acids, Victor J. Hruby and Vadim A. Soloshonok, Eds. *Tetrahedron* **2001**, *57*, 6329–6650.
89. Recognition-mediated self-assembly of organic systems, Vincent M. Rotello, Ed. *Tetrahedron* **2002**, *58*, 621–844.
90. Synthesis of marine natural products containing polycyclic ethers, Masahiro Hirama and Jon D. Rainier, Eds. *Tetrahedron* **2002**, *58*, 1779–2040.

91. Fluorous chemistry, John A. Gladysz and Dennis P. Curran, Eds. *Tetrahedron* **2002**, 58, 3823–4132.
92. Recent developments in chiral lithium amide base chemistry, Peter O'Brien, Ed. *Tetrahedron* **2002**, 58, 4567–4734.
93. Beyond natural product synthesis (Tetrahedron Prize for Creativity in Organic Chemistry 2001 – Yoshito Kishi), Harry H. Wasserman and Stephen F. Martin, Eds. *Tetrahedron* **2002**, 58, 6223–6602.
94. Strained heterocycles as intermediates in organic synthesis, Amy R. Howell, Ed. *Tetrahedron* **2002**, 58, 6979–7194.
95. Molecular design of Lewis and Brønsted acid catalysts—the key to environmentally benign reagents (Tetrahedron Chair 2002), Hisashi Yamamoto, Ed. *Tetrahedron* **2002**, 58, 8153–8364.
96. Recent developments in dendrimer chemistry, David K. Smith, Ed. *Tetrahedron* **2003**, 59, 3787–4024.
97. Art, science and technology in total synthesis (Tetrahedron Prize for Creativity in Organic Chemistry 2002 – K. C. Nicolaou), Stephen F. Martin and Harry H. Wasserman, Eds. *Tetrahedron* **2003**, 59, 6667–7070.
98. New synthetic methods—VII, Brian M. Stoltz, Ed. *Tetrahedron* **2003**, 59, 8843–9030.
99. Oxiranyl and aziridinyl anions as reactive intermediates in synthetic organic chemistry, S. Florio, Ed. *Tetrahedron* **2003**, 59, 9683–9864.
100. Recent advances in rare earth chemistry, Shū Kobayashi, Ed. *Tetrahedron* **2003**, 59, 10339–10598.
101. Biocatalysts in synthetic organic chemistry, S. M. Roberts, Ed. *Tetrahedron* **2004**, 60, 483–806.
102. Recent advances in the chemistry of zirconocenes, Keisuke Suzuki and Peter Wipf, Eds. *Tetrahedron* **2004**, 60, 1257–1424.
103. Atropisomerism, Jonathan Clayden, Ed. *Tetrahedron* **2004**, 60, 4325–4558.
104. Chemistry of biologically and physiologically intriguing phenomena, Daisuke Uemura, Ed. *Tetrahedron* **2004**, 60, 6959–7098.
105. Olefin metathesis: a powerful and versatile instrument for organic synthesis (Tetrahedron prize for creativity in organic chemistry 2003 – R. H. Grubbs), Stephen F. Martin and Harry H. Wasserman, Eds. *Tetrahedron* **2004**, 60, 7099–7438.
106. From synthetic methodology to biomimetic target assembly (Tetrahedron prize for creativity in organic chemistry 2003 – D. Seebach), Léon A. Ghosez, Ed. *Tetrahedron* **2004**, 60, 7439–7794.
107. Solid and solution phase combinatorial chemistry, Rolf Breinbauer and Herbert Waldmann, Eds. *Tetrahedron* **2004**, 60, 8579–8738.
108. Catalytic tools enabling total synthesis (Tetrahedron Chair 2004), Alois Fürstner, Ed. *Tetrahedron* **2004**, 60, 9529–9784.
109. Synthesis and applications of non-racemic cyanohydrins and α -amino nitriles, Michael North, Ed. *Tetrahedron* **2004**, 60, 10371–10568.
110. Synthetic receptors as sensors, Eric V. Anslyn, Ed. *Tetrahedron* **2004**, 60, 11041–11316.
111. Functionalised organolithium compounds, Carmen Nájera and Miguel Yus, Eds. *Tetrahedron* **2005**, 61, 3125–3450.
112. Applications of catalysis in academia and industry, Michael J. Krische, Ed. *Tetrahedron* **2005**, 61, 6155–6472.
113. Development and application of highly active and selective palladium catalysts, Ian J. S. Fairlamb, Ed. *Tetrahedron* **2005**, 61, 9647–9918.
114. Multicomponent reactions, Ilan Marek, Ed. *Tetrahedron* **2005**, 61, 11299–11520.
115. Polymer-supported reagents and catalysts: increasingly important tools for organic synthesis, Patrick Toy and Min Shi, Eds. *Tetrahedron* **2005**, 61, 12013–12192.
116. Organocatalysis in organic synthesis, Pavel Kočovský and Anderi V. Malkov, Eds. *Tetrahedron* **2006**, 62, 243–502.
117. Supramolecular chemistry of fullerenes, Nazario Martín and Jean-François Nierengarten, Eds. *Tetrahedron* **2006**, 62, 1905–2132.
118. Chemistry of electron-deficient ynamines and ynamides, Richard P. Hsung, Ed. *Tetrahedron* **2006**, 62, 3771–3938.
119. Microwave assisted organic synthesis, Nicholas E. Leadbeater, Ed. *Tetrahedron* **2006**, 62, 4623–4732.
120. Nature-inspired approaches to chemical synthesis, Erik J. Sorensen and Emmanuel A. Theodorakis, Eds. *Tetrahedron* **2006**, 62, 5159–5354.
121. The chemistry of radical ions, Paul E. Floreancig, Ed. *Tetrahedron* **2006**, 62, 6447–6594.
122. Recent advances in oxidation chemistry, Dan Yang, Ed. *Tetrahedron* **2006**, 62, 6595–6718.
123. Stereoselective and catalyzed halogenation reactions, Thomas Lectka, Ed. *Tetrahedron* **2006**, 62, 7141–7204.
124. Recent advances in organonickel chemistry, Timothy F. Jamison, Ed. *Tetrahedron* **2006**, 62, 7493–7610.
125. New applications of metal catalysis in natural product synthesis, Kay M. Brummond, Ed. *Tetrahedron* **2006**, 62, 10467–10602.
126. Organic chemistry of singlet oxygen, Alexander Greer, Ed. *Tetrahedron* **2006**, 62, 10603–10776.



ELSEVIER

Preface

Organic chemistry of singlet oxygen

This special issue on singlet oxygen chemistry consists of 20 papers, from laboratories around the world—in China, Italy, France, Turkey, United States, Brazil, Germany, Chile, and Greece. Some of the papers explore singlet oxygen's unique ability to oxidize molecules. Other papers describe methods in the generation of $^1\text{O}_2$. The formation and subsequent reactions of $^1\text{O}_2$ are reported in a variety of media, such as common organic solvents, aqueous media, zeolites, and an ionic liquid.

The focus on $^1\text{O}_2$ chemistry in ene, [2+2], and [2+4] reactions with unsaturated molecules plays a leading role in this symposium. The contributors include Iesce, Erden, Griesbeck, Balci, Linker, Stratakis, Orfanopoulos, Turro, Tung, and Stensaas. The research is largely driven by an attempt to find selective reactions. The study of mechanisms of $^1\text{O}_2$ reactions also fuels the research.

Cadet and O'Shea have probed $^1\text{O}_2$ chemistry to learn about reactions with biologically important (unsaturated) molecules, such as deoxyguanosine and methyl urocanate. There, the $^1\text{O}_2$ reactions yield unstable endoperoxides, which readily rearrange to stable products.

Singlet oxygen reactions with heteroatom-containing molecules are also under intense study. Albin and Clennan describe the latest of what has been learned about reactions of $^1\text{O}_2$ with sulfides. The reaction of $^1\text{O}_2$ with phosphines and diimines are described by Selke and Lemp, respectively, to get a handle on the reactions and how they may be of interest from a synthetic point of view.

As a reactive species, $^1\text{O}_2$ has a short lifetime in solution. The effectiveness in how $^1\text{O}_2$ oxidizes compounds depends

on the relative chemical and physical reaction pathways. Lemp, Selke, and Albin provide insight on these relative contributions. Turro discusses a provocative idea for vibrational deactivation of $^1\text{O}_2$ by which regioselective oxidation is achieved.

The symposium papers also include data on the chemical generation of $^1\text{O}_2$. In an ozone reaction, Dussault presents data in support of generating $^1\text{O}_2$ via a new reaction. In another study, Aubry discusses the chemical generation of $^1\text{O}_2$ in microemulsions by the reaction of sodium molybdate with H_2O_2 . Di Mascio describes the thermal decomposition of a water-soluble anthracene endoperoxide.

The symposium highlights information on the chemistry of singlet oxygen. There are many challenges that remain for the application of $^1\text{O}_2$ in organic chemistry. Research will continue toward an ever better understanding of mechanisms. During the period of collection of manuscripts, I sensed an enthusiasm felt by the researchers in many ways. This makes the area inviting to exploit and rich with new research opportunities. I thank Harry H. Wasserman for the invitation to serve as guest editor.

Alexander Greer
*Department of Chemistry and Graduate Center,
The City University of New York (CUNY)—Brooklyn College,
Brooklyn, NY 11210,
USA*

E-mail address: agreer@brooklyn.cuny.edu

Available online 25 September 2006



ELSEVIER

Available online at www.sciencedirect.com

Tetrahedron 62 (2006) 10615–10622

Tetrahedron

Singlet oxygen addition to chiral allylic alcohols and subsequent peroxyacetalization with β -naphthaldehyde: synthesis of diastereomerically pure 3- β -naphthyl-substituted 1,2,4-trioxanes

Axel G. Griesbeck,* Tamer T. El-Idreesy and Johann Lex

Institute of Organic Chemistry, University of Cologne, Greinstr. 4, D-50939 Köln/Cologne, Germany

Received 15 February 2006; revised 18 May 2006; accepted 18 May 2006

Available online 7 September 2006

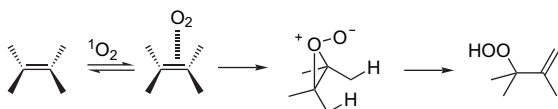
Abstract—The synthesis of a series of eight β -naphthyl-substituted 1,2,4-trioxanes **3a–h** by a sequence of singlet oxygen ene reaction of allylic alcohols **1a–h** and Lewis acid catalyzed peroxyacetalization of the allylic hydroperoxides **2a–h** with β -naphthaldehyde is reported. The ene reactions were performed by solid-state photooxygenation in dye-crosslinked polystyrene beads and resulted in mixtures of diastereoisomeric hydroperoxides **2**. Boron trifluoride catalyzed peroxyacetalization resulted in the formation of **3**, as well as the 1,2,4-trioxanes **4** and **5**, which were formed via acid catalyzed β -hydroperoxy alcohol cleavage.

© 2006 Elsevier Ltd. All rights reserved.

1. Introduction

1.1. Singlet oxygen chemistry

In 1948, Schenck was the first to describe the singlet oxygen ene reaction¹ (therefore often termed Schenck reaction).² In the course of this reaction, $^1\text{O}_2$ attacks one center of a CC double bond with abstraction of an allylic hydrogen atom or an allylic silyl group (from a silyl enoether in case of the *silyl-ene reaction*) with simultaneous allylic shift of the double bond. As a result of this reaction, allylic hydroperoxides or *O*-silylated α -hydroperoxy carbonyl compounds are formed (Scheme 1). Since the first report, the $^1\text{O}_2$ ene reaction has attracted major interest not only in the mechanistic photochemistry but also in modern organic synthesis. Several mechanisms have been postulated for this reaction with concerted or 'concerted two-stage' mechanisms,³ as well as 1,4-biradicals,⁴ 1,4-zwitterions,⁵ perepoxide, dioxetane⁶ or exciplex intermediates.



Scheme 1. Singlet oxygen ene reaction.

The results of Stephenson's elegant inter- and intramolecular isotope effect experiment⁷ with isotopically labeled tetramethylethylenes provided evidence for the perepoxide intermediate. Also, the small negative activation enthalpies and highly negative activation entropies observed for the singlet oxygen ene reaction from kinetic measurements have shown that the reaction of $^1\text{O}_2$ with electron-rich olefins proceed 10^3 times slower than the diffusion rate, which accounts for the presence of non-productive encounters between $^1\text{O}_2$ and the alkene favoring the participation of a reversibly formed exciplex as intermediate.⁸ As a result, a three-step mechanism involving exciplex and perepoxide can be assumed for the ene reaction.

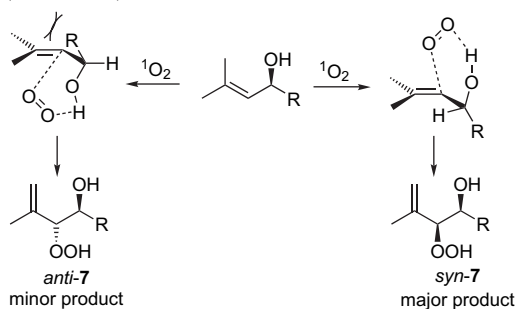
The *regiochemistry* of the ene reaction with substrates with multiple sites for allylic hydrogen transfer was extensively studied and several general effects can predict the regioselective introduction of the hydroperoxy group: (a) the *cis-effect*⁹ (*syn-effect*): in the reaction of $^1\text{O}_2$ with trisubstituted alkenes¹⁰ or enol ethers,¹¹ the allylic hydrogen atoms on the more substituted side of the double bond are more reactive for H-abstraction by $^1\text{O}_2$; (b) the *gem-effect*¹² that leads to highly selective abstraction of an allylic hydrogen atom from a substituent in α position of an α,β -unsaturated carbonyl compound; (c) the large-group effect¹³ that leads to selective (moderate) abstraction of an allylic hydrogen from the substituent geminal to a large group.

Several factors that control the π -facial selectivity of singlet oxygen ene reaction are known and can be summarized as follows: (a) steric factors: in view of the small size of the

Keywords: Ene reaction; Singlet oxygen; 1,2,4-Trioxanes; Peroxyacetalization; Catalysis.

* Corresponding author. E-mail: griesbeck@uni-koeln.de

reactive molecule singlet oxygen, steric interactions are expected to be less important in directing the facial approach. However, in rigid (cyclic and polycyclic) substrates where changes in conformation that minimize steric factors are restricted, this effect is more pronounced and steric shielding of one face of the double bond may bias $^1\text{O}_2$ attack to occur predominantly on the other face of the π -system;¹⁴ (b) conformational effects: for an efficient hydrogen abstraction to occur, the reactive allylic hydrogen atoms must adopt a conformation, which places them perpendicular to the alkene plane.¹⁵ This factor is often highly effective in rigid compounds in which allylic hydrogen atoms can be conformationally fixed in an optimal transfer geometry on one face of the double bond; (c) electronic effects and hydrogen bonding: the simplest tetrasubstituted alkene, 2,3-dimethyl-2-butene with a highly nucleophilic double bond reacts more than 30 times faster than the corresponding trisubstituted alkene, 2-methyl-2-butene, and the latter reacts about 15 times faster than the disubstituted alkene *Z*-2-butene. Adam and Brünker elegantly used hydrogen bonding interactions between the substrate and the incoming singlet oxygen for control of the diastereoselectivity in the photooxygenation of allylic alcohols and other substrates.¹⁶ The coordination of singlet oxygen to the hydroxy group in the more stable conformer (not destabilized by 1,3-allylic strain) directs the approach of the electrophilic $^1\text{O}_2$ to one face of the double bond (Scheme 2).



Scheme 2. Mechanism of the singlet oxygen ene reaction with chiral allylic alcohols.

We have recently demonstrated that the use of polymer support as reaction media with non-covalently adsorbed or covalently linked porphyrin dyes are convenient processes for the solvent-free photooxygenation of unsaturated organic substrates.¹⁷ Especially the use of chiral allylic alcohols is informative in that the diastereoselectivity is a tool for analyzing the reaction environment and supramolecular effects.¹⁸ We have used this concept for the synthesis of β -hydroperoxy alcohols, which we have applied as substrates for the synthesis of a series of 1,2,4-trioxanes in the context of a study on antimalarial peroxides.

1.2. Artemisinin and antimalarial peroxides

One of the major drawbacks of artemisinin is its poor solubility in both water and oil.¹⁹ To overcome this problem artemisinin is reduced to dihydroartemisinin, which leads to the preparation of a series of semisynthetic first-generation artemisinin analogues, including artemether, arteether, and artesunate, which are used broadly in many areas of the world where malaria is endemic (Fig. 1).²⁰ Venugopalan et al. synthesized various ethers and thioethers of dihydroartemisinin

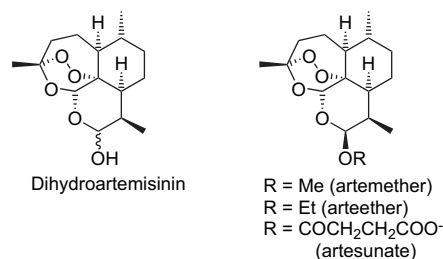


Figure 1. Artemisinin-derivatives with improved pharmacological properties.

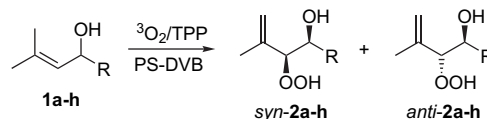
by treatment with alkyl, aryl, alkynyl, and heteroalkyl alcohols or thiols in the presence of boron trifluoride. The products were tested in vivo and some show antimalarial activity comparable to arteether.²¹

The moderate bioavailability and rapid clearance (short pharmacological half-life) observed with these artemisinin-derived drugs are the major disadvantages. This often results from the poor chemical and metabolic stability of the additional acetal functional group present in such derivatives. To overcome this problem, many C-10-carba analogues and C-10-aryl analogues of dihydroartemisinin that are metabolically more robust were synthesized. Of relevance are the C-10-alkyl and the C-10-aryl or heteroaromatic derivatives prepared by Haynes,²² Posner,²³ O'Neill,²⁴ Jung,²⁵ and Ziffer.²⁶ The development of the artemisinin combination therapy concept was recently achieved by the synthesis of effective drugs that simultaneously contain the 1,2,4-trioxane moiety covalently bound with another active antimalarial pharmacophore, such as aminoquinolines²⁷ or aliphatic diamines.²⁸ The high activity of these molecules, termed trioxaquinones, is rationalized by the combination of a peroxidic entity that is a fast and potential alkylating agent, in the same molecule with the aminoquinoline unit, which is characterized by easy penetration of the infected erythrocytes.²⁹

The goal of the present work is to show that aromatic side groups can be easily incorporated into 1,2,4-trioxanes that are produced by a sequence of $^1\text{O}_2$ ene reaction with chiral allylic alcohols and subsequent peroxyacetalization. As a model compound for aromatic and heteroaromatic carbonyl compounds, β -naphthaldehyde was applied.

2. Results and discussion

The photooxygenation of a series of allylic alcohols **1a–h** using PS–DVB polymer matrix doped with adsorbed porphyrin sensitizers resulted in the formation of a *syn* (or *threo*) and *anti* (or *erythro*) diastereomeric mixture of the *vic*-hydroperoxy alcohols in good yields (Scheme 3). The β -hydroperoxy alcohols are stable at rt and can be kept in the refrigerator for weeks without decomposition.



Scheme 3. Solvent-free photooxygenation of the allylic alcohols **1a–h** using TPP embedded in PS–DVB matrix.

The diastereoselectivity of the ene reaction using the commercial PS–DVB that were modified with adsorbed porphyrin sensitizer (Table 1) showed similar values to that obtained with the polymer-bound sensitizer systems, TSP–S–DVB or PP–S–DVB (TSP=tetrastyrilporphyrin; PP=protoporphyrin IX),³⁰ but lower than for solution phase (e.g., tetrachloromethane), accounting for an intermolecular hydrogen bonding between the concentrated substrate molecules in both polymer systems. Comparison of the chemical yields and the diastereoselectivities in the solvent-free photooxygenation reaction of the allylic alcohols **1a–h** is shown in Table 1.

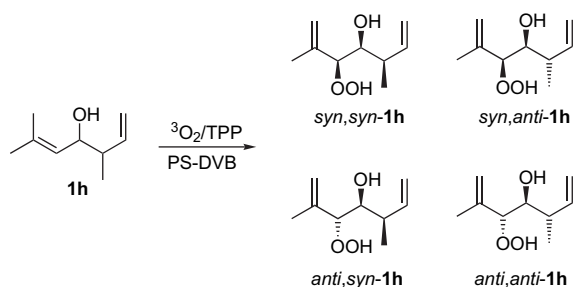
Table 1. Photooxygenation of the allylic alcohols **1a–h** using solvent-free approach with PS–DVB copolymer

Compound	R	d.r. ^a <i>syn:anti</i>	Yield (%)
2a	Et	77:23	72
2b	<i>n</i> -Pr	79:21	78
2c	<i>n</i> -Bu	79:21	78
2d	<i>i</i> -Bu	80:20	77
2e	<i>c</i> -Pr	62:38	80
2f	<i>c</i> -Hex	88:12	65
2g	CH ₂ CH=CH ₂	75:25	69
2h	CH(Me)CH=CH ₂	^b	63

^a The diastereoselectivity was determined from the integration of the characteristic signals in the NMR of the crude reaction mixture.

^b Four diastereomers were obtained in a ratio of 39:39:11:11.

The photooxygenation of the allylic alcohol **1h** (possessing two stereogenic centers, applied as a 1:1 diastereoisomeric mixture) afforded four diastereomers of the β-hydroxy allylic hydroperoxides, two correspond to the major products with reaction-induced *syn* configuration (assigned as *syn,syn-2h* and *syn,anti-2h*) and two to the minor compounds with reaction-induced *anti* configuration (assigned as *anti,syn-2h* and *anti,anti-2h*). The photooxygenation of **1h** is depicted in Scheme 4. The diastereomeric ratio of the individual pairs of major and minor isomers is about 1:1. The major diastereomers constitute about 85% of the product mixture (determined from ¹³C NMR).



Scheme 4. Solvent-free photooxygenation of the allylic alcohol **1h**.

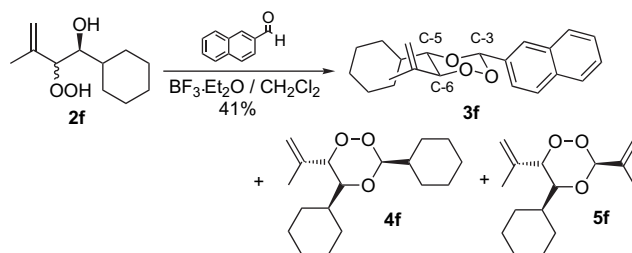
The peroxyacetalization reaction of 2-naphthaldehyde with the β-hydroperoxy alcohols proceeded under standard reaction conditions³¹ with boron trifluoride as Lewis acid catalyst and resulted in the 1,2,4-trioxanes **3a–h** in moderate yields (Table 2). The carbonyl component was applied in slight excess and thus, appreciable amounts of the BF₃-catalyzed cleavage and cross-peroxyacetalization products were isolated in each case. This is shown for the reaction of the cyclohexyl-substituted β-hydroperoxy alcohol **2f** (Scheme 5)

Table 2. Peroxyacetalization of the allylic hydroperoxides **2a–h** with β-naphthaldehyde

Compound	R	Yield ^a (%)
3a	Et	24
3b	<i>n</i> -Pr	40
3c	<i>n</i> -Bu	43
3d	<i>i</i> -Bu	21
3e	<i>c</i> -Pr	31
3f	<i>c</i> -Hex	41
3g	CH ₂ CH=CH ₂	14
3h	CH(Me)CH=CH ₂	15

^a Yields after purification of the crude materials.

with β-naphthaldehyde. The hydroperoxy alcohol **2f** is reacted with 1.1 equiv of the aldehyde in CH₂Cl₂ in the presence of a catalytic amount of BF₃ to form the 1,2,4-trioxane **3f** in 41% yield in addition to the cross-peroxyacetalization products **4f** and **5f** in 22 and 16% yields, respectively. In most cases, these side-products were not isolated and characterized solely from the NMR spectra (not reported in Section 4). It is, however, possible to obtain these compounds (also 1,2,4-trioxane structures) in good yields by BF₃-catalyzed oxidative cleavage and cross-peroxyacetalization of the hydroperoxides in the absence of an additional carbonyl component. The assignment of the structure of **3f** is based on ¹H as well as ¹³C NMR spectra, IR, elemental, and HRMS analyses. The IR spectrum shows the characteristic C–O stretching at 1112, 1074 cm⁻¹ and O–O at 906, 822 cm⁻¹. The ¹H NMR shows the characteristic singlet at 6.38 ppm corresponding to the peroxyacetal proton (H-3) and the doublet at 4.87 ppm related to the peroxy proton (H-6) due to coupling with H-5 (³J_{HH}=9.5 Hz) indicating *trans* configuration. Surprisingly, H-5 appears also as doublet (and not doublet of doublet as expected); this can be ascribed to a dihedral angle of roughly 90° between this proton and the CH proton of the cyclohexyl group. The 2-naphthyl group is located also in equatorial position as confirmed by X-ray for the two analogous examples **3a** and **3b** (Fig. 2 and Table 3). In no case were the products from the minor diastereoisomeric allylic hydroperoxides (*anti* isomers) isolated from the crude reaction mixtures (where they appear with about 5–10% relative yields).



Scheme 5. Lewis acid catalyzed peroxyacetalization of the β-hydroperoxy alcohol **2f** with β-naphthaldehyde.

3. Conclusion

In summary, the singlet oxygen ene reaction with chiral allylic alcohols **1** in polystyrene matrices proceeds with excellent yields and gives the allylic hydroperoxides **2** with good (*syn*) diastereoselectivities. Subsequent Lewis acid catalyzed peroxyacetalization with β-naphthaldehyde results

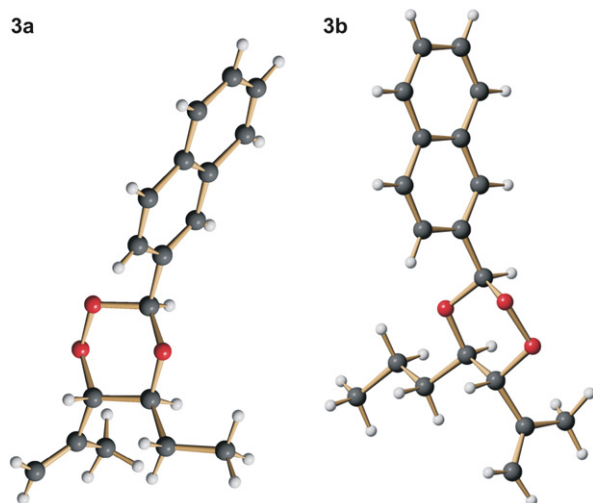


Figure 2. Structure of 1,2,4-trioxanes **3a** and **3b** in the crystal.

Table 3. Crystal structure analyses data for 1,2,4-trioxanes **3a** and **3b**

Crystal data	3a	3b
Empirical formula	C ₁₈ H ₂₀ O ₃	C ₁₉ H ₂₂ O ₃
Formula weight	284.34	298.37
Temperature [K]	100(2)	100(2)
Crystal system	Monoclinic	Monoclinic
Space group	<i>P</i> 2 ₁ / <i>c</i>	<i>C</i> 2/ <i>c</i>
<i>a</i> [Å]	13.614(2)	34.338(1)
<i>b</i> [Å]	5.6245(5)	5.362(1)
<i>c</i> [Å]	19.903(3)	20.740(1)
α [°]	90	90
β [°]	97.456(4)	121.32(1)
γ [°]	90	90
Volume [Å ³]	1511.1(4)	3262.2(6)
<i>Z</i>	4	8
<i>d</i> _{calcd} [g cm ⁻³]	1.250	1.215
Crystal size [mm]	0.1×0.1×0.3	0.35×0.25×0.25
No. refl. collected	6492	10220
No. unique refl.	3146	3554
No. obsd refl.	1251	2305
<i>R</i> 1	0.0663	0.0427
<i>wR</i> 2	0.1452	0.0900
Largest diff. peak/hole [e/Å ⁻³]	0.428/−0.215	0.232/−0.166

in the formation of diastereomerically pure (all-equatorial) 3-naphthyl-1,2,4-trioxanes **3** in moderate yields besides the cross-peroxyacetalization products **4** and **5**.

4. Experimental

4.1. General procedures (GP)

4.1.1. GP 1. Solvent-free type-II photooxygenation reaction in polymer matrices.

4.1.1.1. Using commercial PS-DVB copolymer. The polymer beads (ca. 2–3 g, Fluka, polystyrene copolymer with 1% divinylbenzene) were introduced into a Petri dish (19 cm diameter) and were pretreated with CH₂Cl₂ (20 mL) and the excess solvent evaporated by a vacuum line. The substrate (ca. 10 mmol) and the non-polar sensitizer (tetraphenylporphyrin, TPP, or tetratolylporphyrin, TTP, ca. 3–6 mg) in ethyl acetate (20 mL) were subsequently added and the excess solvent evaporated by leaving

the Petri dish in a well ventilated hood. The Petri dish is covered with a glass plate and the sandy solid is irradiated with halogen lamp or sodium street lamp. The polymer beads were subsequently washed with ethanol (3×30 mL) and filtered (the beads can be used again for at least six cycles without pre-swelling). The solvent was evaporated under reduced pressure (CAUTION: water bath temperature should not exceed 30 °C.) and the composition of the product was determined by ¹H as well as ¹³C NMR and the crude products applied directly for peroxyacetalization.

4.1.1.2. Using synthetic TSP-S-DVB or PP-S-DVB copolymers.³⁰ The dye-cross-linked polymer beads (TSP-S-DVB or PP-S-DVB, ca. 0.60 g) in a Petri dish (14 cm in diameter) were swollen by CH₂Cl₂ (20 mL), then the substrate (ca. 5 mmol) in ethyl acetate (20 mL) was added. Subsequent treatment as in Section 4.1.1.1 affords the product.

4.1.2. GP 2. General procedure for the peroxyacetalization reaction and 1,2,4-trioxanes synthesis. To a stirred solution of β -hydroxy hydroperoxides and the carbonyl reagent in dry CH₂Cl₂ (100 mL) was added at rt a catalytic amount of boron trifluoride etherate (ca. 0.2 mL) and the mixture was further stirred for about 12 h (overnight) at the same temperature. Volatile carbonyl compounds were used in 5–10-fold molar excess, less volatile carbonyl compounds were used in 1.2–1.5-fold molar excess. The reaction mixture was then partitioned between CH₂Cl₂ and saturated NaHCO₃ solution and the phases were separated. The aqueous phase was extracted with CH₂Cl₂ (3×30 mL) and the combined organic phases were washed with brine, water, and dried over Na₂SO₄. Solvent evaporation (CAUTION: water bath temperature should not exceed 30 °C.) followed by chromatographic purification afforded the 1,2,4-trioxane as pure product.

4.1.2.1. 4-Hydroperoxy-5-methylhex-5-en-3-ol (2a). Photooxygenation of 5-methylhex-4-en-3-ol (**1a**) (1.0 g, 8.77 mmol) for 48 h according to GP 1 afforded a diastereomeric mixture (d.r. *syn:anti*, 77:23) of β -hydroxy allylic hydroperoxides **2a** (0.92 g, 6.30 mmol, 72%) as colorless oil.

syn-2a: ¹H NMR: δ 0.92 (t, 3H, *J*=7.5 Hz, CH₃CH₂), 1.23–1.58 (m, 2H, CH₂CH₃), 1.68 (m, 3H, CH₃C=), 3.55 (ddd, 1H, *J*=5.9, 5.9, 8.5 Hz, CH–OH), 4.15 (d, 1H, *J*=8.5 Hz, CH–OOH), 5.01 (m, 2H, CH₂=C). ¹³C NMR: δ 9.6 (q, CH₃CH₂), 17.8 (q, CH₃C=), 25.5 (t, CH₂CH₃), 71.8 (d, CH–OH), 93.4 (d, CH–OOH), 116.5 (t, CH₂=C), 141.4 (s, C=CH₂).

anti-2a: ¹H NMR additional significant signals: δ 0.93 (t, 3H, *J*=7.4 Hz, CH₃CH₂), 1.76 (s, 3H, CH₃C=), 3.69 (m, 1H, CH–OH), 4.30 (d, 1H, *J*=4.7 Hz, CH–OOH), 5.04 (m, 2H, CH₂=C). ¹³C NMR: δ 10.3 (q, CH₃CH₂), 19.3 (q, CH₃C=), 25.0 (t, CH₂CH₃), 72.2 (d, CH–OH), 91.4 (d, CH–OOH), 115.3 (t, CH₂=C), 141.2 (s, C=CH₂).

4.1.2.2. 3-Hydroperoxy-2-methylhept-1-en-4-ol (2b). Photooxygenation of 2-methylhept-2-en-4-ol (**1b**) (1.0 g, 7.81 mmol) for 48 h according to GP 1 afforded a diastereomeric mixture (d.r. *syn:anti*, 79:21) of β -hydroxy allylic hydroperoxides **2b** (0.98 g, 6.13 mmol, 78%) as colorless oil.

syn-2b: ^1H NMR: δ 0.87 (t, 3H, $J=7.1$ Hz, CH_3CH_2), 1.20–1.58 (m, 4H, CH_2CH_2), 1.68 (m, 3H, $\text{CH}_3\text{C}=\text{C}$), 3.63 (m, 1H, CH-OH), 4.13 (d, 1H, $J=8.5$ Hz, CH-OOH), 5.01 (m, 2H, $\text{CH}_2=\text{C}$). ^{13}C NMR: δ 13.8 (q, CH_3CH_2), 17.8 (t, CH_2CH_3), 18.3 (q, $\text{CH}_3\text{C}=\text{C}$), 34.6 (t, CH_2CH_2), 70.3 (d, CH-OH), 93.8 (d, CH-OOH), 116.6 (t, $\text{CH}_2=\text{C}$), 141.4 (s, $\text{C}=\text{CH}_2$).

anti-2b: ^1H NMR additional significant signals: δ 0.87 (t, 3H, $J=7.1$ Hz, CH_3CH_2), 1.76 (m, 3H, $\text{CH}_3\text{C}=\text{C}$), 3.78 (m, 1H, CH-OH), 4.29 (d, 1H, $J=4.4$ Hz, CH-OOH). ^{13}C NMR: $\delta=13.9$ (q, CH_3CH_2), 19.0 (t, CH_2CH_3), 19.4 (q, $\text{CH}_3\text{C}=\text{C}$), 34.0 (t, CH_2CH_2), 70.5 (d, CH-OH), 91.6 (d, CH-OOH), 115.2 (t, $\text{CH}_2=\text{C}$), 141.2 (s, $\text{C}=\text{CH}_2$).

4.1.2.3. 3-Hydroperoxy-2-methyloct-1-en-4-ol (2c).

Photooxygenation of 2-methyloct-2-en-4-ol (**1c**) (1.19 g, 8.38 mmol) for 60 h according to GP 1 afforded a diastereomeric mixture (d.r. *syn:anti*, 79:21) of β -hydroxy allylic hydroperoxides **2c** (1.14 g, 6.55 mmol, 78%) as faint yellow oil.

syn-2c: ^1H NMR: δ 0.85 (t, 3H, $J=7.1$ Hz, CH_3CH_2), 1.21–1.57 (m, 6H, $\text{CH}_2\text{CH}_2\text{CH}_2$), 1.70 (s, 3H, $\text{CH}_3\text{C}=\text{C}$), 3.64 (m, 1H, CH-OH), 4.15 (d, 1H, $J=8.4$ Hz, CH-OOH), 5.03 (m, 2H, $\text{CH}_2=\text{C}$). ^{13}C NMR: δ 13.9 (q, CH_3CH_2), 17.9 (q, $\text{CH}_3\text{C}=\text{C}$), 22.5 (t, CH_2CH_3), 27.3 (t, CH_2CH_2), 32.2 (t, CH_2CH_2), 70.6 (d, CH-OH), 93.7 (d, CH-OOH), 116.6 (t, $\text{CH}_2=\text{C}$), 141.3 (s, $\text{C}=\text{CH}_2$).

anti-2c: ^1H NMR additional significant signals: δ 1.77 (s, 3H, $\text{CH}_3\text{C}=\text{C}$), 3.75 (m, 1H, CH-OH), 4.30 (d, 1H, $J=4.7$ Hz, CH-OOH). ^{13}C NMR: δ 13.9 (q, CH_3CH_2), 19.3 (q, $\text{CH}_3\text{C}=\text{C}$), 22.5 (t, CH_2CH_3), 28.0 (t, CH_2CH_2), 32.2 (t, CH_2CH_2), 70.7 (d, CH-OH), 91.7 (d, CH-OOH), 116.6 (t, $\text{CH}_2=\text{C}$), 141.2 (s, $\text{C}=\text{CH}_2$).

4.1.2.4. 3-Hydroperoxy-2,6-dimethylhept-1-en-4-ol (2d). Photooxygenation of 2,6-dimethylhept-2-en-4-ol (**1d**) (1.25 g, 8.80 mmol) for 60 h according to GP 1 afforded a diastereomeric mixture (d.r. *syn:anti*, 80:20) of β -hydroxy allylic hydroperoxides **2d** (1.18 g, 6.78 mmol, 77%) as colorless oil.

syn-2d: ^1H NMR: δ 0.83 (d, 3H, $J=6.5$ Hz, CH_3CH), 0.87 (d, 3H, $J=6.8$ Hz, CH_3CH), 1.03 (m, 1H, CH_2CH), 1.32 (m, 1H, CH_2CH), 1.68 (s, 3H, $\text{CH}_3\text{C}=\text{C}$), 1.81 (m, 1H, CHCH_2), 3.68 (m, 1H, CH-OH), 4.09 (d, 1H, $J=8.4$ Hz, CH-OOH), 5.0 (m, 2H, $\text{CH}_2=\text{C}$). ^{13}C NMR: δ 17.9 (q, CH_3CH), 21.1 (q, $\text{CH}_3\text{C}=\text{C}$), 23.8 (d, CHCH_2), 24.0 (q, CH_3CH), 41.6 (t, CH_2CH), 68.7 (d, CH-OH), 94.2 (d, CH-OOH), 116.6 (t, $\text{CH}_2=\text{C}$), 141.4 (s, $\text{C}=\text{CH}_2$).

anti-2d: ^1H NMR additional significant signals: δ 0.84 (d, 3H, $J=6.7$ Hz, CH_3CH), 1.76 (s, 3H, $\text{CH}_3\text{C}=\text{C}$), 3.83 (m, 1H, CH-OH), 4.26 (d, 1H, $J=4.5$ Hz, CH-OOH), 5.05 (m, 2H, $\text{CH}_2=\text{C}$). ^{13}C NMR: δ 19.4 (q, CH_3CH), 21.4 (q, $\text{CH}_3\text{C}=\text{C}$), 23.6 (d, CHCH_2), 24.7 (q, CH_3CH), 41.1 (t, CH_2CH), 68.9 (d, CH-OH), 92.0 (d, CH-OOH), 115.2 (t, $\text{CH}_2=\text{C}$), 141.3 (s, $\text{C}=\text{CH}_2$).

4.1.2.5. 1-Cyclopropyl-2-hydroperoxy-3-methylbut-3-en-1-ol (2e). Photooxygenation of 1-cyclopropyl-3-

methylbut-2-en-1-ol (**1e**) (1.0 g, 7.94 mmol) for 60 h according to GP 1 afforded a diastereomeric mixture (d.r. *syn:anti*, 62:38) of β -hydroxy allylic hydroperoxides **2e** (1.0 g, 6.33 mmol, 80%) as colorless oil.

syn-2e: ^1H NMR: δ 0.20–0.52 (m, 4H, CH_2CH_2), 0.78–0.99 (m, 1H, CH), 1.75 (m, 3H, $\text{CH}_3\text{C}=\text{C}$), 3.07 (dd, 1H, $J=7.9$, 7.9 Hz, CH-OH), 4.29 (d, 1H, $J=9.3$ Hz, CH-OOH), 5.05 (m, 2H, $\text{CH}_2=\text{C}$). ^{13}C NMR: δ 1.8 (t, CH_2CH_2), 3.2 (t, CH_2CH_2), 14.0 (d, CH), 18.9 (q, $\text{CH}_3\text{C}=\text{C}$), 75.0 (d, CH-OH), 93.3 (d, CH-OOH), 115.5 (t, $\text{CH}_2=\text{C}$), 141.6 (s, $\text{C}=\text{CH}_2$).

anti-2e: ^1H NMR additional significant signals: δ 1.82 (m, 3H, $\text{CH}_3\text{C}=\text{C}$), 3.14 (dd, 1H, $J=4.3$, 8.8 Hz, CH-OH), 4.41 (d, 1H, $J=4.3$ Hz, CH-OOH). ^{13}C NMR: δ 2.6 (t, CH_2CH_2), 2.9 (t, CH_2CH_2), 13.3 (d, CH), 19.6 (q, $\text{CH}_3\text{C}=\text{C}$), 75.6 (d, CH-OH), 91.2 (d, CH-OOH), 115.4 (t, $\text{CH}_2=\text{C}$), 141.3 (s, $\text{C}=\text{CH}_2$).

4.1.2.6. 1-Cyclohexyl-2-hydroperoxy-3-methylbut-3-en-1-ol (2f). Photooxygenation of 1-cyclohexyl-3-methylbut-2-en-1-ol (**1f**) (1.30 g, 7.74 mmol) for 60 h according to GP 1 afforded a diastereomeric mixture (d.r. *syn:anti*, 88:12) of β -hydroxy allylic hydroperoxides **2f** (1.0 g, 5.0 mmol, 65%) as faint yellow oil.

syn-2f: ^1H NMR: δ 0.83–1.90 (m, 11H, CH and CH_2), 1.64 (s, 3H, $\text{CH}_3\text{C}=\text{C}$), 3.43 (m, 1H, CH-OH), 4.24 (d, 1H, $J=8.5$ Hz, CH-OOH), 4.97 (s, 2H, $\text{CH}_2=\text{C}$). ^{13}C NMR: δ 17.7 (q, $\text{CH}_3\text{C}=\text{C}$), 25.3 (t, CH_2), 25.9 (t, CH_2), 26.1 (t, CH_2), 26.4 (t, CH_2), 30.3, 30.5 (t, CH_2), 39.1 (d, CH), 74.3 (d, CH-OH), 91.0 (d, CH-OOH), 115.9 (t, $\text{CH}_2=\text{C}$), 141.6 (s, $\text{C}=\text{CH}_2$).

anti-2f: ^1H NMR additional significant signals: δ 4.29 (d, 1H, $J=6.0$ Hz, CH-OOH). ^{13}C NMR additional significant signals: δ 39.3 (d, CH), 89.2 (d, CH-OOH), 112.9 (t, $\text{CH}_2=\text{C}$).

4.1.2.7. 3-Hydroperoxy-2-methylhepta-1,6-dien-4-ol (2g). Photooxygenation of 6-methylhepta-1,5-dien-4-ol (**1g**) (1.16 g, 9.21 mmol) for 60 h according to GP 1 afforded a diastereomeric mixture (d.r. *syn:anti*, 75:25) of β -hydroxy allylic hydroperoxides **2g** (1.0 g, 6.33 mmol, 69%) as faint yellow oil.

syn-2g: ^1H NMR: δ 1.70 (m, 3H, $\text{CH}_3\text{C}=\text{C}$), 2.02–2.37 (m, 2H, CH_2), 3.71 (ddd, 1H, $J=3.7$, 8.3, 8.3 Hz, CH-OH), 4.17 (d, 1H, $J=8.4$ Hz, CH-OOH), 5.05 (m, 4H, $\text{CH}_2=\text{C}$ and $\text{CH}_2=\text{CH}$), 5.79 (m, 1H, $\text{CH}=\text{CH}_2$). ^{13}C NMR: δ 17.9 (q, $\text{CH}_3\text{C}=\text{C}$), 37.1 (t, CH_2), 70.0 (d, CH-OH), 92.8 (d, CH-OOH), 116.8 (t, $\text{CH}_2=\text{CH}$), 118.1 (t, $\text{CH}_2=\text{C}$), 133.8 (d, $\text{CH}=\text{CH}_2$), 141.1 (s, $\text{C}=\text{CH}_2$).

anti-2g: ^1H NMR additional significant signals: δ 1.76 (m, 3H, $\text{CH}_3\text{C}=\text{C}$), 3.82 (m, 1H, CH-OH), 4.31 (d, 1H, $J=4.9$ Hz, CH-OOH). ^{13}C NMR: δ 19.1 (q, $\text{CH}_3\text{C}=\text{C}$), 36.6 (t, CH_2), 69.9 (d, CH-OH), 91.0 (d, CH-OOH), 115.6 (t, $\text{CH}_2=\text{CH}$), 117.9 (t, $\text{CH}_2=\text{C}$), 134.5 (d, $\text{CH}=\text{CH}_2$), 141.0 (s, $\text{C}=\text{CH}_2$).

4.1.2.8. 3-Hydroperoxy-2,5-dimethylhepta-1,6-dien-4-ol (2h). Photooxygenation of 3,6-dimethylhepta-1,5-dien-4-ol

(**1h**) (1.20 g, 8.57 mmol) for 60 h according to GP 1 afforded an oil composed of the inseparable diastereomeric mixture (0.92 g, 5.35 mmol, 63%) composed of *syn,syn-2h*, *syn,anti-2h* (d.r. 1:1) as major product and a diastereomeric mixture of *anti,syn-2h* and *anti,anti-2h* (d.r. 1:1) as minor products (major/minor: 78:22 ratio).

syn,syn-2h: $^1\text{H NMR}$: δ 0.90 (d, 3H, $J=6.9$ Hz, CH_3CH), 1.63 (s, 3H, $\text{CH}_3\text{C}=\text{C}$), 2.17 (m, 1H, CHCH_3), 3.50 (m, 1H, CH-OH), 4.12 (d, 1H, $J=8.8$ Hz, CH-OOH), 4.94 (m, 4H, $\text{CH}_2=\text{C}$ and $\text{CH}_2=\text{CH}$), 5.74 (m, 1H, $\text{CH}=\text{CH}_2$). $^{13}\text{C NMR}$: δ 12.1 (q, CH_3CH), 17.8 (q, $\text{CH}_3\text{C}=\text{C}$), 38.7 (d, CHCH_3), 73.1 (d, CH-OH), 90.8 (d, CH-OOH), 114.3 (t, $\text{CH}_2=\text{CH}$), 116.2 (t, $\text{CH}_2=\text{C}$), 141.1 (s, $\text{C}=\text{CH}_2$), 141.2 (d, $\text{CH}=\text{CH}_2$).

syn,anti-2h: $^1\text{H NMR}$ additional significant signals: δ 0.99 (d, 3H, $J=5.4$ Hz, CH_3CH), 3.52 (m, 1H, CH-OH), 4.22 (d, 1H, $J=8.0$ Hz, CH-OOH). $^{13}\text{C NMR}$: δ 17.6 (q, $\text{CH}_3\text{C}=\text{C}$), 39.0 (d, CHCH_3), 73.4 (d, CH-OH), 91.3 (d, CH-OOH), 116.2 (t, $\text{CH}_2=\text{CH}$), 116.8 (t, $\text{CH}_2=\text{C}$), 137.8 (d, $\text{CH}=\text{CH}_2$), 140.6 (s, $\text{C}=\text{CH}_2$).

anti,syn-2h: $^{13}\text{C NMR}$ significant signals: δ 72.5 (d, CH-OH), 89.2 (d, CH-OOH).

anti,anti-2h: $^{13}\text{C NMR}$ significant signals: δ 72.5 (d, CH-OH), 89.5 (d, CH-OOH).

4.1.2.9. (3RS,5RS,6RS)-5-Ethyl-3-(naphthalen-2-yl)-6-(prop-1-en-2-yl)-1,2,4-trioxane (3a). Following GP 2, a solution of 4-hydroperoxy-5-methylhex-5-en-3-ol (**2a**) (1.22 g, 8.36 mmol) and β -naphthaldehyde (1.30 g, 8.33 mmol) in CH_2Cl_2 was treated with a catalytic amount of $\text{BF}_3 \cdot \text{Et}_2\text{O}$ (0.2 mL). Usual work-up and further purification of the crude product by preparative thick-layer chromatography (SiO_2 , EA/*n*-hex, 1:10, $R_f=0.71$) affords the 1,2,4-trioxane (0.57 g, 2.0 mmol, 24%) as viscous oil, which crystallizes into white solid on standing, mp 73–75 °C. $^1\text{H NMR}$: δ 1.14 (dd, 3H, $J=7.4, 7.4$ Hz, CH_3CH_2), 1.70 (m, 2H, CH_2CH_3), 1.86 (m, 3H, $\text{CH}_3\text{C}=\text{C}$), 3.96 (ddd, 1H, $J=3.8, 7.9, 9.3$ Hz, OCH), 4.67 (d, 1H, $J=9.3$ Hz, OOCH), 5.18 (m, 1H, $\text{CH}_2=\text{C}$), 5.23 (s, 1H, $\text{CH}_2=\text{C}$), 6.43 (s, 1H, OCHOO), 7.48–8.07 (m, 7H, H_{arom}); $^{13}\text{C NMR}$: δ 9.4 (q, CH_3CH_2), 19.9 (q, $\text{CH}_3\text{C}=\text{C}$), 23.6 (t, CH_2CH_3), 78.5 (d, OCH), 87.4 (d, OOCH), 104.0 (d, OCHOO), 118.4 (t, $\text{CH}_2=\text{C}$), 124.0 (d, CH_{arom}), 126.1 (d, CH_{arom}), 126.6 (d, CH_{arom}), 126.8 (d, CH_{arom}), 127.6 (d, CH_{arom}), 128.0 (d, CH_{arom}), 128.3 (d, CH_{arom}), 131.9 (s, C_{qarom}), 132.8 (s, C_{qarom}), 133.9 (s, C_{qarom}), 138.7 (s, $\text{C}=\text{CH}_2$); IR: (CsI) ν (cm^{-1})=3064, 2980, 2925, 2898, 1664, 1605, 1071, 908, 824; MS: (EI, 70 eV) m/z (%)=284 (M^+ , 4), 156 ($\text{C}_{11}\text{H}_8\text{O}^+$, 100), 155 ($\text{C}_{11}\text{H}_7\text{O}^+$, 95), 128 ($\text{C}_{10}\text{H}_8^+$, 22), 127 ($\text{C}_{10}\text{H}_7^+$, 73), 96 (C_7H_7^+ , 47), 81 (C_6H_6^+ , 17); HRMS: (EI, 70 eV, $\text{C}_{18}\text{H}_{20}\text{O}_3$) calcd: $M=284.141$ g/mol, found: $M=284.141 \pm 0.005$ g/mol; CH-analysis: ($\text{C}_{18}\text{H}_{20}\text{O}_3$, $M=284.35$ g/mol) calcd: C, 76.03; H, 7.09, found: C, 75.53; H, 7.11.

4.1.2.10. (3RS,5RS,6RS)-3-(Naphthalen-2-yl)-6-(prop-1-en-2-yl)-5-propyl-1,2,4-trioxane (3b). Following GP 2, a solution of 3-hydroperoxy-2-methylhept-1-en-4-ol (**2b**) (1.20 g, 7.50 mmol) and β -naphthaldehyde (1.18 g, 7.56 mmol) in CH_2Cl_2 was treated with a catalytic amount

of $\text{BF}_3 \cdot \text{Et}_2\text{O}$ (0.2 mL). Usual work-up and further purification of the crude product by preparative thick-layer chromatography (SiO_2 , EA/*n*-hex, 1:10, $R_f=0.66$) afforded the pure 1,2,4-trioxane (0.89 g, 2.99 mmol, 40%) as colorless oil, which crystallizes on standing, mp 78–80 °C. $^1\text{H NMR}$: δ 1.02 (t, 3H, $J=7.1$ Hz, CH_3CH_2), 1.47–1.79 (m, 4H, CH_2CH_2), 1.86 (m, 3H, $\text{CH}_3\text{C}=\text{C}$), 4.04 (ddd, 1H, $J=3.1, 8.1, 9.3$ Hz, OCH), 4.67 (d, 1H, $J=9.3$ Hz, OOCH), 5.19 (m, 1H, $\text{CH}_2=\text{C}$), 5.24 (s, 1H, $\text{CH}_2=\text{C}$), 6.43 (s, 1H, OCHOO), 7.47–8.07 (m, 7H, H_{arom}); $^{13}\text{C NMR}$: δ 13.9 (q, CH_3CH_2), 18.1 (t, CH_2CH_3), 19.7 (q, $\text{CH}_3\text{C}=\text{C}$), 32.5 (t, CH_2CH_2), 77.1 (d, OCH), 87.7 (d, OOCH), 104.0 (d, OCHOO), 118.5 (t, $\text{CH}_2=\text{C}$), 124.0 (d, CH_{arom}), 126.1 (d, CH_{arom}), 126.6 (d, CH_{arom}), 126.7 (d, CH_{arom}), 127.6 (d, CH_{arom}), 128.0 (d, CH_{arom}), 128.3 (d, CH_{arom}), 131.9 (s, C_{qarom}), 132.8 (s, C_{qarom}), 133.9 (s, C_{qarom}), 138.7 (s, $\text{C}=\text{CH}_2$); IR: (CsI) ν (cm^{-1})=2957, 2934, 1664, 1605, 1576, 1362, 1340, 1092, 1075, 907; MS: (EI, 70 eV) m/z (%)=298 (M^+ , 3), 226 ($\text{M}^+-\text{C}_4\text{H}_8\text{O}$, 2), 156 ($\text{C}_{11}\text{H}_8\text{O}^+$, 92), 155 ($\text{C}_{11}\text{H}_7\text{O}^+$, 100), 128 ($\text{C}_{10}\text{H}_8^+$, 22), 127 ($\text{C}_{10}\text{H}_7^+$, 77), 110 (C_8H_7^+ , 27), 95 (C_7H_7^+ , 8); HRMS: (EI, 70 eV, $\text{C}_{19}\text{H}_{22}\text{O}_3$) calcd: $M=298.157$ g/mol, found: $M=298.157 \pm 0.005$ g/mol; CH-analysis: ($\text{C}_{19}\text{H}_{22}\text{O}_3$, $M=298.39$) calcd: C, 76.48; H, 7.43, found: C, 76.25; H, 7.27.

4.1.2.11. (3RS,5RS,6RS)-5-Butyl-3-(naphthalen-2-yl)-6-(prop-1-en-2-yl)-1,2,4-trioxane (3c). Following GP 2, a solution of 3-hydroperoxy-2-methyloct-1-en-4-ol (**2c**) (1.24 g, 7.13 mmol) and β -naphthaldehyde (1.11 g, 7.12 mmol) in CH_2Cl_2 was treated with a catalytic amount of $\text{BF}_3 \cdot \text{Et}_2\text{O}$ (0.2 mL). Usual work-up and further purification of the crude product by preparative thick-layer chromatography (SiO_2 , EA/*n*-hex, 1:10, $R_f=0.85$) afforded the pure 1,2,4-trioxane (0.96 g, 3.08 mmol, 43%) as viscous oil, which crystallizes on standing, mp 51–53 °C. $^1\text{H NMR}$: δ 0.96 (t, 3H, $J=7.2$ Hz, CH_3CH_2), 1.25–1.70 (m, 6H, CH_2), 1.85 (s, 3H, $\text{CH}_3\text{C}=\text{C}$), 4.01 (m, 1H, OCH), 4.64 (d, 1H, $J=9.3$ Hz, OOCH), 5.18 (m, 1H, $\text{CH}_2=\text{C}$), 5.22 (s, 1H, $\text{CH}_2=\text{C}$), 6.41 (s, 1H, OCHOO), 7.49–8.05 (m, 7H, H_{arom}); $^{13}\text{C NMR}$: δ 13.9 (q, CH_3CH_2), 19.7 (q, $\text{CH}_3\text{C}=\text{C}$), 22.6 (t, CH_2CH_3), 27.0 (t, CH_2CH_2), 30.1 (t, CH_2CH_2), 77.4 (d, OCH), 87.7 (d, OOCH), 104.1 (d, OCHOO), 118.5 (t, $\text{CH}_2=\text{C}$), 124.1 (d, CH_{arom}), 126.1 (d, CH_{arom}), 126.6 (d, CH_{arom}), 126.8 (d, CH_{arom}), 127.6 (d, CH_{arom}), 128.1 (d, CH_{arom}), 128.4 (d, CH_{arom}), 132.0 (s, C_{qarom}), 132.8 (s, C_{qarom}), 133.9 (s, C_{qarom}), 138.8 (s, $\text{C}=\text{CH}_2$); MS: (EI, 70 eV) m/z (%)=312 (M^+ , 1), 226 ($\text{M}^+-\text{C}_5\text{H}_{10}\text{O}$, less than 1), 156 ($\text{C}_{11}\text{H}_8\text{O}^+$, 100), 155 ($\text{C}_{11}\text{H}_7\text{O}^+$, 93), 127 ($\text{C}_{10}\text{H}_7^+$, 72), 124 (C_9H_7^+ , 38); HRMS: (EI, 70 eV, $\text{C}_{20}\text{H}_{24}\text{O}_3$) calcd: $M=312.173$ g/mol, found: $M=312.173 \pm 0.005$ g/mol; CH-analysis: ($\text{C}_{20}\text{H}_{24}\text{O}_3$, $M=312.40$) calcd: C, 76.61; H, 7.78.

4.1.2.12. (3RS,5RS,6RS)-5-Isobutyl-3-(naphthalen-2-yl)-6-(prop-1-en-2-yl)-1,2,4-trioxane (3d). Following GP 2, a solution of 3-hydroperoxy-2,6-dimethylhept-1-en-4-ol (**2d**) (1.21 g, 6.95 mmol) and β -naphthaldehyde (1.09 g, 6.99 mmol) in CH_2Cl_2 was treated with a catalytic amount of $\text{BF}_3 \cdot \text{Et}_2\text{O}$ (0.2 mL). Usual work-up and further purification of the crude product by preparative thick-layer chromatography (SiO_2 , EA/*n*-hex, 1:10, $R_f=0.71$) affords the 1,2,4-trioxane (0.46 g, 1.47 mmol, 21%) as an oil, which crystallizes on standing to white solid, mp 60–62 °C.

^1H NMR: δ 1.01 (d, 3H, $J=6.6$ Hz, CH_3CH), 1.04 (d, 3H, $J=6.8$ Hz, CH_3CH), 1.33 (m, 1H, CH_2CH), 1.70 (m, 1H, CH_2CH), 1.87 (s, 3H, $\text{CH}_3\text{C}=\text{C}$), 2.08 (m, 1H, CHCH_2), 4.12 (ddd, 1H, $J=2.3, 9.1, 10.3$ Hz, OCH), 4.65 (d, 1H, $J=9.1$ Hz, OUCH), 5.19 (m, 1H, $\text{CH}_2=\text{C}$), 5.24 (m, 1H, $\text{CH}_2=\text{C}$), 6.45 (s, 1H, OCHOO), 7.49–8.07 (m, 5H, H_{arom}); ^{13}C NMR: δ 19.6 (q, $\text{CH}_3\text{C}=\text{C}$), 21.5 (q, CH_3CH), 23.6 (d, CHCH_2), 23.7 (q, CH_3CH), 39.2 (t, CH_2CH), 75.6 (d, OCH), 88.0 (d, OUCH), 104.0 (d, OCHOO), 118.7 (t, $\text{CH}_2=\text{C}$), 124.0 (d, CH_{arom}), 126.1 (d, CH_{arom}), 126.6 (d, CH_{arom}), 126.7 (d, CH_{arom}), 127.6 (d, CH_{arom}), 128.0 (d, CH_{arom}), 128.3 (d, CH_{arom}), 131.9 (s, C_{qarom}), 132.8 (s, C_{qarom}), 133.9 (s, C_{qarom}), 138.6 (s, $\text{C}=\text{CH}_2$); IR: (CsI) ν (cm^{-1})=3095, 2956, 2934, 1605, 1347, 1098, 1080, 997, 863, 817; MS: (EI, 70 eV) m/z (%)=312 (M^+ , 3), 226 ($\text{M}^+-\text{C}_5\text{H}_{10}\text{O}$, 2), 156 ($\text{C}_{11}\text{H}_8\text{O}^+$, 100), 155 ($\text{C}_{11}\text{H}_7\text{O}^+$, 97), 128 ($\text{C}_{10}\text{H}_8^+$, 30), 127 ($\text{C}_{10}\text{H}_7^+$, 70), 124 ($\text{C}_9\text{H}_{16}^+$, 27), 109 ($\text{C}_8\text{H}_{13}^+$, 17); HRMS: (EI, 70 eV, $\text{C}_{20}\text{H}_{24}\text{O}_3$) calcd: $M=312.173$ g/mol, found: $M=312.173\pm 0.005$ g/mol; CH-analysis: ($\text{C}_{20}\text{H}_{24}\text{O}_3$, $M=312.40$ g/mol) calcd: C, 76.89; H, 7.74, found: C, 76.61; H, 7.63.

4.1.2.13. (3RS,5RS,6RS)-5-Cyclopropyl-3-(naphthalen-2-yl)-6-(prop-1-en-2-yl)-1,2,4-trioxane (3e). Following GP 2, a solution of 1-cyclopropyl-2-hydroperoxy-3-methylbut-3-en-1-ol (**2e**) (1.25 g, 7.91 mmol) and β -naphthaldehyde (1.23 g, 7.88 mmol) in CH_2Cl_2 was treated with a catalytic amount of $\text{BF}_3\cdot\text{Et}_2\text{O}$ (0.2 mL). Usual work-up and further purification of the crude product by preparative thick-layer chromatography (SiO_2 , EA/*n*-hex, 1:10, $R_f=0.67$) affords the pure 1,2,4-trioxane as yellow oil, which crystallizes upon standing (0.72 g, 2.43 mmol, 31%). ^1H NMR: δ 0.39–0.64 (m, 4H, CH_2CH_2), 0.98 (m, 1H, $\text{CH}(\text{CH}_2)_2$), 1.87 (m, 3H, $\text{CH}_3\text{C}=\text{C}$), 3.44 (dd, 1H, $J=7.4, 9.1$ Hz, OCH), 4.68 (d, 1H, $J=9.12$ Hz, OUCH), 5.14 (m, 2H, $\text{CH}_2=\text{C}$), 6.31 (s, 1H, OCHOO), 7.46–7.98 (m, 7H, H_{arom}); ^{13}C NMR: δ 2.0 (t, CH_2), 2.8 (t, CH_2), 11.6 (d, $\text{CH}(\text{CH}_2)_2$), 20.7 (q, $\text{CH}_3\text{C}=\text{C}$), 81.0 (d, OCH), 87.8 (d, OUCH), 104.0 (d, OCHOO), 117.5 (t, $\text{CH}_2=\text{C}$), 124.2 (d, CH_{arom}), 126.2 (d, CH_{arom}), 126.7 (d, CH_{arom}), 127.0 (d, CH_{arom}), 127.7 (d, CH_{arom}), 128.2 (d, CH_{arom}), 128.5 (d, CH_{arom}), 131.8 (s, C_{qarom}), 132.9 (s, C_{qarom}), 134.1 (s, C_{qarom}), 139.9 (s, $\text{C}=\text{CH}_2$); IR: (Film) ν (cm^{-1})=3088, 3011, 2968, 2934, 1647, 1603, 1126, 1071, 904, 859, 814; HRMS: (EI, 70 eV, $\text{C}_{19}\text{H}_{20}\text{O}_3$) calcd: $M=296.141$ g/mol, found: $M=296.141\pm 0.005$ g/mol; CH-analysis: ($\text{C}_{19}\text{H}_{20}\text{O}_3$, $M=296.36$) calcd: C, 77.00; H, 6.80, found: C, 76.47; H, 6.83.

4.1.2.14. (3RS,5RS,6RS)-5-Cyclohexyl-3-(naphthalen-2-yl)-6-(prop-1-en-2-yl)-1,2,4-trioxane (3f). Following GP 2, a solution of 1-cyclohexyl-2-hydroperoxy-3-methylbut-3-en-1-ol (**2f**) (1.20 g, 6.0 mmol) and β -naphthaldehyde (0.94 g, 6.03 mmol) in CH_2Cl_2 was treated with a catalytic amount of $\text{BF}_3\cdot\text{Et}_2\text{O}$ (0.2 mL). Usual work-up and further purification of the crude product by preparative thick-layer chromatography (SiO_2 , EA/*n*-hex, 1:10, $R_f=0.65$) afforded the pure 1,2,4-trioxanes (0.83 mg, 2.46 mmol, 41%) as white solid, mp 88–90 °C. Additionally, the cross-peroxyacetalization products **4f** and **5**, were isolated in 22 and 16% yields, respectively (by NMR from the crude reaction mixture). ^1H NMR: δ 1.06–1.94 (m, 11H, CH and CH_2), 1.85 (s, 3H, $\text{CH}_3\text{C}=\text{C}$), 3.87 (d, 1H, $J=9.5$ Hz, OCH), 4.87 (d, 1H,

$J=9.5$ Hz, OUCH), 5.18 (m, 2H, $\text{CH}_2=\text{C}$), 6.38 (s, 1H, OCHOO), 7.47–8.02 (m, 7H, H_{arom}); ^{13}C NMR: δ 19.7 (q, $\text{CH}_3\text{C}=\text{C}$), 26.2 (t, CH_2), 26.2 (t, CH_2), 26.3 (t, CH_2), 26.5 (t, CH_2), 30.1 (t, CH_2), 38.4 (d, CH), 81.4 (d, OCH), 85.2 (d, OUCH), 104.1 (d, OCHOO), 118.5 (t, $\text{CH}_2=\text{C}$), 124.1 (d, CH_{arom}), 126.1 (d, CH_{arom}), 126.6 (d, CH_{arom}), 126.9 (d, CH_{arom}), 127.6 (d, CH_{arom}), 128.0 (d, CH_{arom}), 128.4 (d, CH_{arom}), 132.1 (s, C_{qarom}), 132.8 (s, C_{qarom}), 133.9 (s, C_{qarom}), 138.9 (s, $\text{C}=\text{CH}_2$); IR: (CsI) ν (cm^{-1})=2933, 2856, 1653, 1647, 1605, 1560, 1112, 1074, 1004, 906, 822; MS: (EI, 70 eV) m/z (%)=338 (M^+ , 1), 226 ($\text{M}^+-\text{C}_5\text{H}_{10}\text{O}$, 2), 156 ($\text{C}_{11}\text{H}_8\text{O}^+$, 95), 155 ($\text{C}_{11}\text{H}_7\text{O}^+$, 96), 128 ($\text{C}_{10}\text{H}_8^+$, 27), 127 ($\text{C}_{10}\text{H}_7^+$, 100), 83 ($\text{C}_6\text{H}_{11}^+$, 17); HRMS: (EI, 70 eV, $\text{C}_{22}\text{H}_{26}\text{O}_3$) calcd: $M=338.188$ g/mol, found: $M=338.188\pm 0.005$ g/mol; CH-analysis: ($\text{C}_{22}\text{H}_{26}\text{O}_3$, $M=338.44$) calcd: C, 78.07; H, 7.74, found: C, 77.49; H, 7.90.

4.1.2.15. (3RS,5RS,6RS)-3,5-Dicyclohexyl-6-(prop-1-en-2-yl)-1,2,4-trioxane (4f). ^1H NMR: δ 0.92–2.12 (m, 22H, CH and CH_2), 1.71 (s, 3H, $\text{CH}_3\text{C}=\text{C}$), 3.48 (d, 1H, $J=9.6$ Hz, OCH), 4.54 (d, 1H, $J=9.5$ Hz, OUCH), 4.95 (d, 1H, $J=5.6$ Hz, OCHOO), 5.05 (m, 2H, $\text{CH}_2=\text{C}$). ^{13}C NMR: δ 19.7 (q, $\text{CH}_3\text{C}=\text{C}$), 25.7 (t, CH_2), 25.7 (t, CH_2), 25.8 (t, CH_2), 26.0 (t, CH_2), 26.2 (t, CH_2), 26.3 (t, CH_2), 26.5 (t, CH_2), 27.1 (t, CH_2), 27.3 (t, CH_2), 30.1 (t, CH_2), 38.3 (d, CH), 40.6 (d, CH), 80.6 (d, OCH), 85.2 (d, OUCH), 107.1 (d, OCHOO), 118.1 (t, $\text{CH}_2=\text{C}$), 139.1 (s, $\text{C}=\text{CH}_2$).

4.1.2.16. (3RS,5RS,6RS)-5-Allyl-3-(naphthalen-2-yl)-6-(prop-1-en-2-yl)-1,2,4-trioxane (3g). Following GP 2, a solution of 3-hydroperoxy-2-methylhepta-1,6-dien-4-ol (**2g**) (0.39 g, 2.47 mmol) and β -naphthaldehyde (388 mg, 2.49 mmol) in CH_2Cl_2 was treated with a catalytic amount of $\text{BF}_3\cdot\text{Et}_2\text{O}$ (0.2 mL). Usual work-up and further purification of the crude product by preparative thick-layer chromatography (SiO_2 , EA/*n*-hex, 1:10, $R_f=0.69$) afforded the pure 1,2,4-trioxanes (30 mg, 0.10 mmol, 4%) as viscous colorless oil, which crystallizes on standing, mp 55–57 °C. ^1H NMR: δ 1.82 (m, 3H, $\text{CH}_3\text{C}=\text{C}$), 2.47 (m, 2H, CH_2), 4.06 (ddd, 1H, $J=3.9, 7.2, 9.2$ Hz, OCH), 4.64 (d, 1H, $J=9.2$ Hz, OUCH), 5.15 (m, 4H, $\text{CH}_2=\text{CH}$ and $\text{CH}_2=\text{C}$), 6.0 (m, 1H, $\text{CH}=\text{CH}_2$), 6.37 (s, 1H, OCHOO), 7.45–8.0 (m, 7H, H_{arom}); ^{13}C NMR: δ 19.7 (q, $\text{CH}_3\text{C}=\text{C}$), 35.1 (t, CH_2), 76.8 (d, OCH), 87.1 (d, OUCH), 104.1 (d, OCHOO), 117.7 (t, $\text{CH}_2=\text{CH}$), 119.0 (t, $\text{CH}_2=\text{C}$), 124.1 (d, CH_{arom}), 126.2 (d, CH_{arom}), 126.7 (d, CH_{arom}), 126.9 (d, CH_{arom}), 127.7 (d, CH_{arom}), 128.2 (d, CH_{arom}), 128.5 (d, CH_{arom}), 131.8 (s, C_{qarom}), 132.9 (s, C_{qarom}), 133.4 (d, $\text{CH}=\text{CH}_2$), 134.0 (s, C_{qarom}), 138.5 (s, $\text{C}=\text{CH}_2$); MS: (EI, 70 eV) m/z (%)=296 (M^+ , 7), 156 ($\text{C}_{11}\text{H}_8\text{O}^+$, 100), 155 ($\text{C}_{11}\text{H}_7\text{O}^+$, 86), 127 ($\text{C}_{10}\text{H}_7^+$, 62); HRMS: (EI, 70 eV, $\text{C}_{19}\text{H}_{20}\text{O}_3$) calcd: $M=296.141$ g/mol, found: $M=296.141\pm 0.005$ g/mol; CH-analysis: ($\text{C}_{19}\text{H}_{20}\text{O}_3$, $M=296.36$) calcd: C, 77.00; H, 6.80, found: C, 76.85; H, 6.71.

4.1.2.17. (3RS,5RS,6RS)-5-((RS)-But-3-en-2-yl)-3-(naphthalen-2-yl)-6-(prop-1-en-2-yl)-1,2,4-trioxane and (3RS,5RS,6RS)-5-((SR)-but-3-en-2-yl)-3-(naphthalen-2-yl)-6-(prop-1-en-2-yl)-1,2,4-trioxane (3h). Following GP 2, a solution of 3-hydroperoxy-2,5-dimethylhepta-1,6-dien-4-ol (**2h**) (1.16 g, 6.74 mmol) and 2-naphthaldehyde (1.07 g, 6.86 mmol) in CH_2Cl_2 was treated with a catalytic amount of $\text{BF}_3\cdot\text{Et}_2\text{O}$ (0.2 mL). Usual work-up and further

purification of the crude product (1.62 g, 5.23 mmol, 77.5%) by preparative thick-layer chromatography (SiO₂, EA/*n*-hex, 1:10, *R_f*=0.69) afforded a diastereomeric mixture of the pure 1,2,4-trioxanes **3h** in a ratio 1:1 (0.31 g, 1.0 mmol, 15%) as white solid. ¹H NMR first diastereomer: δ 1.30 (d, 3H, *J*=7.0 Hz, CH₃CH), 1.88 (t, 3H, *J*=1.5 Hz, CH₃C=), 2.55 (m, 1H, CHCH₃), 4.02 (dd, 1H, *J*=1.9, 9.5 Hz, OCH), 4.83 (d, 1H, *J*=9.5 Hz, OOCH), 5.20 (m, 4H, CH₂=CH and CH₂=), 6.15 (m, 1H, CH=CH₂), 6.40 (s, 1H, OCHOO), 7.50–8.10 (m, 7H, H_{arom}); ¹³C NMR first diastereomer: δ 13.5 (q, CH₃CH), 19.5 (q, CH₃C=), 38.1 (d, CHCH₃), 79.9 (d, OCH), 85.4 (d, OOCH), 103.9 (d, OCHOO), 114.3 (t, CH₂=CH), 118.9 (t, CH₂=C), 124.0 (d, CH_{arom}), 126.1 (d, CH_{arom}), 126.6 (d, CH_{arom}), 126.8 (d, CH_{arom}), 126.9 (d, CH_{arom}), 127.6 (d, CH_{arom}), 128.0 (d, CH_{arom}), 131.9 (s, C_qarom), 132.7 (s, C_qarom), 133.9 (s, C_qarom), 138.5 (d, CH=CH₂), 138.6 (s, C=CH₂); ¹H NMR additional signals of the other diastereomer: δ 4.12 (dd, 1H, *J*=2.51, 9.6 Hz, OCH), 4.89 (d, 1H, *J*=9.6 Hz, OOCH), 6.41 (s, 1H, OCHOO); ¹³C NMR other diastereomer: δ 18.2 (q, CH₃CH), 19.5 (q, CH₃C=), 38.8 (d, CHCH₃), 80.0 (d, OCH), 85.6 (d, OOCH), 104.0 (d, OCHOO), 116.1 (t, CH₂=CH), 118.9 (t, CH₂=C), 124.0 (d, CH_{arom}), 126.1 (d, CH_{arom}), 126.6 (d, CH_{arom}), 126.8 (d, CH_{arom}), 126.9 (d, CH_{arom}), 127.6 (d, CH_{arom}), 128.3 (d, CH_{arom}), 131.9 (s, C_qarom), 132.7 (s, C_qarom), 133.9 (s, C_qarom), 138.4 (s, C=CH₂), 140.8 (d, CH=CH₂); IR: (CsI) ν (cm⁻¹)=3078, 2978, 2923, 1653, 1647, 1605, 1127, 1076, 999, 987, 904, 866, 818; MS: (EI, 70 eV) *m/z* (%)=310 (M⁺, 2), 226 (M⁺-C₅H₈O, 1), 156 (C₁₁H₈O⁺, 100), 155 (C₁₁H₇O⁺, 89), 128 (C₁₀H₈⁺, 20), 127 (C₁₀H₇⁺, 68), 107 (C₈H₁₁⁺, 20); HRMS: (EI, 70 eV, C₂₀H₂₂O₃) calcd: M=310.157 g/mol, found: M=310.157±0.005 g/mol; CH-analysis: (C₂₀H₂₂O₃, M=310.39) calcd: C, 77.39; H, 7.14, found: C, 77.28; H, 7.02.

Acknowledgements

This research was supported by the Deutsche Forschungsgemeinschaft. T.T.E. thanks the Egyptian government and the Kurt-Alder foundation (University of Cologne) for a Ph.D. grant.

References and notes

- Schenck, G. O. *Naturwissenschaften* **1948**, *35*, 28–29.
- Recent reviews: Clennan, E. L. *Tetrahedron* **2005**, *61*, 6665–6691; Clennan, E. L. *Tetrahedron* **2000**, *56*, 9151–9179.
- Singleton, D. A.; Hang, C.; Szymanski, M. J.; Meyer, M. P.; Leach, A. G.; Kuwata, K. T.; Chen, J. S.; Greer, A.; Foote, C. S.; Houk, K. N. *J. Am. Chem. Soc.* **2003**, *125*, 1319–1328.
- Maranzana, A.; Canepa, C.; Ghigo, G.; Tonachini, G. *Eur. J. Org. Chem.* **2005**, 3643–3649.
- Jefford, C. W.; Kohmoto, S.; Boukouvalas, J.; Burger, U. *J. Am. Chem. Soc.* **1983**, *105*, 6498–6500.
- Gollnick, K.; Kuhn, H. J. *Singlet Oxygen*; Wasserman, H. H., Murray, R. W., Eds.; Academic: New York, NY, 1979; pp 287–427.
- Orfanopoulos, M.; Stephenson, L. M. *J. Am. Chem. Soc.* **1980**, *102*, 1417–1418.
- Hurst, J. R.; Wilson, S. L.; Schuster, G. B. *Tetrahedron* **1985**, *41*, 2191–2197.
- Adam, W.; Prein, M. *Angew. Chem., Int. Ed.* **1996**, *35*, 477–494.
- (a) Orfanopoulos, M.; Gardina, M. B.; Stephenson, L. M. *J. Am. Chem. Soc.* **1979**, *101*, 275–276; (b) Rautenstrauch, V.; Thommen, W.; Schulte-Elte, K. H. *Helv. Chim. Acta* **1986**, *69*, 1638–1643.
- (a) Rousseau, G.; Le Perchec, P.; Conia, J. M. *Tetrahedron Lett.* **1977**, *18*, 2517–2520; (b) Jefford, C. W. *Tetrahedron Lett.* **1979**, *20*, 985–988.
- (a) Adam, W.; Griesbeck, A. G. *Synthesis* **1986**, 1050–1052; (b) Orfanopoulos, M.; Foote, C. S. *Tetrahedron Lett.* **1985**, *26*, 5991–5994.
- (a) Clennan, E. L.; Chen, X. *J. Am. Chem. Soc.* **1989**, *111*, 5787–5792; (b) Orfanopoulos, M.; Stratakis, M.; Elemis, Y. *J. Am. Chem. Soc.* **1990**, *112*, 6417–6419.
- (a) Jefford, C. W.; Laffer, M. H.; Boschung, A. F. *J. Am. Chem. Soc.* **1972**, *94*, 8904–8905; (b) Jefford, C. W.; Boschung, A. F. *Helv. Chim. Acta* **1974**, *57*, 2242–2257.
- Kropf, H.; Reichwaldt, R. *J. Chem. Res.* **1987**, 412–413.
- Adam, W.; Brünker, H.-G. *J. Am. Chem. Soc.* **1995**, *117*, 3976–3982.
- Griesbeck, A. G.; Bartoschek, A. *Chem. Commun.* **2002**, 1594–1595.
- Griesbeck, A. G.; Bartoschek, A.; Brodwolf, A.; Miara, C. *Photochem. Photobiol.* **2006**, *82*, in press.
- China Cooperative Research Group on Qinghaosu and its Derivatives as Antimalarials. *J. Tradit. Chin. Med.* **1982**, *2*, 9–16.
- Meshnick, S. R.; Taylor, T. E.; Kamchonwongpaisan, S. *Microbiol. Rev.* **1996**, *60*, 301–315.
- Venugopalan, B.; Karnik, P. J.; Bapat, C. P.; Chatterjee, D. K.; Iyer, N.; Lepcha, D. *Eur. J. Med. Chem.* **1995**, *30*, 697–706.
- Haynes, R. K.; Chan, H.-W.; Cheung, M.-K.; Chung, S. T.; Lam, W.-L.; Tsang, H.-W.; Voerste, A.; Williams, I. D. *Eur. J. Org. Chem.* **2003**, 2098–2114.
- (a) Posner, G. H.; Paik, I. H.; Sur, S.; McRiner, A. J.; Borstnik, K. *J. Med. Chem.* **2003**, *46*, 1060–1065; (b) Borstnik, K.; Paik, I. H.; Posner, G. H. *Int. J. Parasitol.* **2002**, *32*, 1661–1667.
- O'Neill, P. M.; Searle, N. L.; Kan, K. W.; Storr, R. C.; Maggs, J. L. *J. Med. Chem.* **1999**, *42*, 5487–5493.
- Jung, M.; Bae, J. *Heterocycles* **2000**, *45*, 1055–1058.
- Pu, Y. M.; Ziffer, H. *J. Med. Chem.* **1995**, *38*, 613–616.
- (a) Robert, A.; Dechy-Cabaret, O.; Cazelles, J.; Meunier, B. *Acc. Chem. Res.* **2002**, *35*, 167–174; (b) Dechy-Cabaret, O.; Benoitvical, F.; Robert, A.; Meunier, B. *ChemBioChem* **2000**, *1*, 281–283.
- Hindley, S.; Ward, S. A.; Storr, R. C.; Searle, N. L.; Bray, P. G.; Park, B. K.; Davies, J.; O'Neill, P. M. *J. Med. Chem.* **2002**, *45*, 1052–1063.
- Meunier, B. *J. Porphyrins Phthalocyanines* **2002**, *6*, 271–273.
- Griesbeck, A. G.; El-Idreesy, T. T. *Photochem. Photobiol. Sci.* **2005**, *5*, 205–209.
- Griesbeck, A. G.; El-Idreesy, T. T.; Fiege, M.; Brun, R. *Org. Lett.* **2002**, *4*, 4193–4195.



Intrazeolite photooxygenation of chiral alkenes. Control of facial selectivity by confinement and cation– π interactions

Manolis Stratakis,^{*} Christos Raptis, Nikoletta Sofikiti, Constantinos Tsangarakis, Giannis Kosmas, Ioannis-Panagiotis Zaravinos, Dimitris Kalaitzakis, Dimitris Stavroulakis, Constantinos Baskakis and Aggeliki Stathouloupoulou

Department of Chemistry, University of Crete, Voutes, 71003 Iraklion, Greece

Received 27 April 2006; revised 5 July 2006; accepted 5 July 2006

Available online 7 September 2006

Abstract—Depending on the nature of the substituents on the stereogenic carbon atom, the ene reaction of singlet oxygen with several chiral alkenes by confinement within thionin-supported zeolite NaY, may exhibit significant changes on facial selectivity by comparison to their photooxygenation reaction in solution. It is proposed that, apart from the conformational consequences as a result of the alkene confinement within the zeolite cavities, a synergism between Na^+ – π interactions and singlet oxygen– Na^+ interactions plays a significant role in the transition states of ene hydroperoxidation. Within NaY, the diastereoselectivity may significantly depend on the site selectivity, as probed through specific deuterium labelling of trisubstituted alkenes bearing a *gem*-dimethyl group. In certain cases, a remote stereogenic centre relative to the reacting double bond may induce enhanced diastereoselection and regioselectivity.

© 2006 Elsevier Ltd. All rights reserved.

1. Introduction

Mechanistic studies and synthetic applications of singlet oxygen ($^1\text{O}_2$) reactions with organic compounds, have attracted the interest of organic chemists for the past 50 years.¹ The singlet oxygen reactions are typically performed in a homogeneous environment in which the dissolved photosensitizing dye is vulnerable to decomposition. In recent years, however, immobilizing the dyes on solid supports has attracted considerable attention, as it contributes to the green character of the oxidation process, while their stability is considerably enhanced, as well.² Apart from the practical advantages of using solid materials as singlet oxygen generators, a large number of studies have been focused, on studying the product selectivity of the $^1\text{O}_2$ reactions by confining the reacting substrates within supramolecular assemblies as microreactors.³ Typical examples are zeolites with small pores,⁴ Nafion membranes⁵ and surfactant vesicles.⁶ One of the most practical and efficient systems, which has been studied extensively for the past 10 years is thionin or methylene blue-supported zeolite NaY.⁷ In pioneering work, Li and Ramamurthy⁸ confined through partial ion exchange dyes, that are organic cations, in the interior of the zeolite

NaY supercages, and generated a novel photosensitizing system capable of producing very efficiently $^1\text{O}_2$ upon visible light irradiation. Pace and Clennan⁹ improved the efficiency of methylene blue-supported NaY as a photosensitizing system, by replacing the solvent hexane with perfluorohexane. The fluorophobicity of the alkenes in perfluorohexane allows their facile migration into the zeolite cavities. Thus, the zeolite medium may be used for preparative scale photooxygenation reactions, without significant changes in product selectivity or loss of the reaction mass balance. In the same study, the upper limit of the $^1\text{O}_2$ lifetime within NaY was extrapolated to be around 7.5 μs . More recently, Ramamurthy and co-workers¹⁰ measured directly the $^1\text{O}_2$ lifetime within NaY, and found to depend on the alumina content of the zeolite lattice and the intrazeolite water content.

From the early studies, it was clearly evident that a new trend existed for the intrazeolite photooxygenation of trisubstituted alkenes. The reaction is regioselective with predominant or even exclusive formation of the secondary allylic hydroperoxides.^{8,11} Moreover, in contrast to the reaction in solution, enhanced reactivity of the less hindered allylic hydrogens was found through specific labelling in the photooxygenation of several *gem*-dimethyl trisubstituted alkenes within NaY.¹² Several models have been postulated to explain the intrazeolite regioselectivity trends,^{1,7c} however, none of them is widely acceptable and each specific model is rather considered as a working hypothesis. Yet, the

Keywords: Singlet oxygen; Hydroperoxides; Zeolites; Regioselectivity; Diastereoselection; Cation– π interactions.

^{*} Corresponding author. Tel.: +30 2810 545087; fax: +30 2810 545001; e-mail: stratakis@chemistry.uoc.gr

majority of them consider a favourable electrostatic interaction between the intrazeolite alkali metal cations and $^1\text{O}_2$ in the transition state of the ene hydroperoxidation reaction. Apart from the changes in the regioselectivity for the case of trisubstituted alkenes, it was reported that isobutenylarenes afford within NaY primarily the ene products relative to the Diels–Alder cycloadducts, in a highly chemoselective manner.¹³ This selectivity was attributed to the higher destabilization of an open zwitterion (leading to the [4+2] products) relative to a peroxide intermediate (leading to the ene products) as a consequence of the strong Na^+ –arene interactions. Generally, cation– π interactions seem to play a major role in intrazeolite reactions¹⁴ and will be postulated as one of the main driving forces to explain the changes of the diastereoselection trends in the photooxygenation of the chiral alkenes presented throughout this paper.

The study of the diastereoselection in the electrophilic addition of $^1\text{O}_2$ to the π face of chiral alkenes is of primary interest in organic synthesis.¹⁵ The confined environment of zeolite and cation– π interactions as well, might be expected to affect significantly the facial selectivity in the intrazeolite photooxygenation of chiral alkenes. One general aspect would be that blocking the less sterically hindered face of a double bond through cation binding within the zeolite, would leave the other face accessible to $^1\text{O}_2$ attack. For example, Na^+ – π interactions have been postulated to alter the π facial photoreduction of some enone steroids confined within NaY,¹⁶ relative to their reaction in a homogeneous environment. In addition, diastereoselection might be expected even in cases where a stereogenic centre resides at a remote position with respect to the reacting double bond. As a result of ‘substrate-coiling’ within the zeolite cavities, a remote chiral centre may be brought proximal to the reacting double bond and thus affect the facial selectivity. Ramamurthy and co-workers¹⁷ have elegantly shown this aspect in the photochemical disrotatory electrocyclic reaction of a chiral tropolone ether. Having in mind these possible contributing parameters to the π facial selectivity of the intrazeolite reactions, we focused our interest on the photooxygenation of chiral alkenes bearing a stereogenic centre at the α - or at more remote positions with respect to the reacting double bond. In addition, specific labelling of the less hindered methyl group for the majority of the *gem*-dimethyl trisubstituted alkenes studied herein was accomplished, to examine the interplay of site selectivity on diastereoselection, as abstraction of an allylic hydrogen atom from the two geminal methyls occurs through the participation of two non-equilibrating diastereomeric peroxide type-intermediates,^{12c} which may induce a different degree of diastereoselection.

2. Results and discussion

2.1. Synthesis of chiral alkenes

The chiral alkenes (**1–7**) whose photooxygenation was studied are presented in Chart 1. The synthesis of **1–7** was accomplished by Wittig coupling of isopropylidene-triphenylphosphorane with the corresponding aldehydes. The necessary aldehydes for the synthesis of substrates **1** and **4** are commercially available, while the rest were prepared according to trivial procedures described in Section 4.

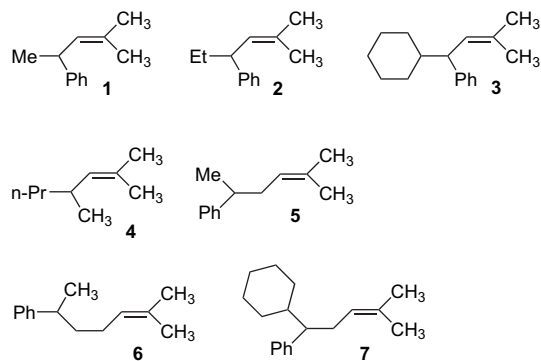


Chart 1. Structures of the chiral alkenes **1–7** whose intrazeolite photooxygenation was examined.

2.2. Diastereoselectivity in the photooxygenation of chiral alkenes bearing a stereogenic centre at the α -position with respect to the double bond (**1–4**)

Among the chiral alkenes presented in Chart 1, the first four (**1–4**) possess a stereogenic centre at the α -position with respect to the reacting double bond. The distribution of the ene products for the photooxygenation of **1–4** in solution (dichloromethane, methylene blue as sensitizer, 0°C) is presented in Table 1. The *erythro* secondary allylic hydroperoxides were primarily formed relative to the *threo* isomers, while the labile tertiary allylic hydroperoxides were formed in up to 14% relative yield, depending on the nature of the substituents R_1 and R_2 . Analysis by NOE clearly revealed that they have the *Z* configuration on the newly formed trisubstituted double bond. It is surprising,¹⁸ from the first point of view, that alkene **3** in which the two substituents on the stereogenic carbon atom (phenyl and cyclohexyl) have more or less similar steric demands, affording the highest diastereomeric ratio among **1–4**. It is obvious, therefore, that for the phenyl-substituted alkenes **1–3**, steric effects cannot explain the stereochemical outcome. The possible reasons will be analyzed below.

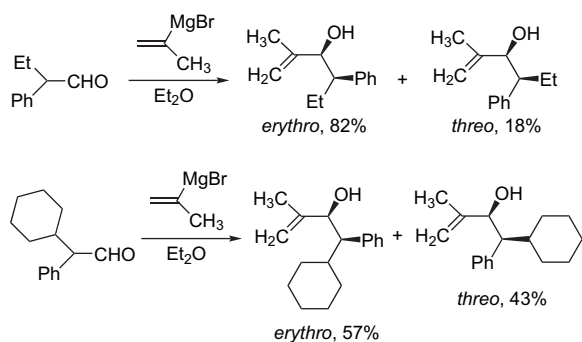
Apart from the photooxygenation of **1** for which the relative configuration of the allylic hydroperoxides is known,²⁰ the

Table 1. Photooxygenation of chiral alkenes **1–4** in solution

Alkene	Tertiary (%) ^a	<i>erythro</i> (%) ^a	<i>threo</i> (%) ^a
$\text{R}_1=\text{Me}$, $\text{R}_2=\text{Ph}$ (1)	6	72	22
$\text{R}_1=\text{Et}$, $\text{R}_2=\text{Ph}$ (2)	10	70	20
$\text{R}_1=\text{Cyclohexyl}$, $\text{R}_2=\text{Ph}$ (3)	14	71	15
$\text{R}_1=\text{Me}$, $\text{R}_2=n\text{-Pr}$ (4)	—	62	38

^a Relative percentages.

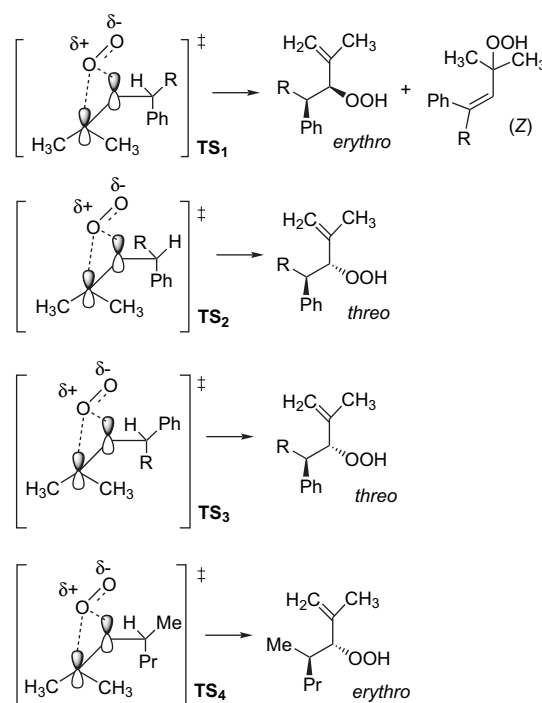
ene products for the case of **2** and **3** were reduced in situ with PPh_3 and the resulting allylic alcohols were compared to the diastereomeric alcohols produced from the reaction of 2-propenylmagnesium bromide with α -ethyl or cyclohexyl-phenylacetaldehyde (Scheme 1). It is well known²¹ that the addition of organolithium or Grignard reagents to α -alkyl substituted phenylacetaldehydes is *erythro* diastereoselective. In our case, reaction of 2-propenylmagnesium bromide with 2-phenylbutyraldehyde afforded the allylic alcohols in a ratio *erythro*/*threo*=4.6/1, while α -cyclohexylphenylacetaldehyde gave a product ratio of *erythro*/*threo*=1.4/1. The predominant formation of the *erythro* allylic hydroperoxide in the photooxygenation of **4**, was reasonably ascribed from the photooxygenation results of similar chiral trisubstituted alkenes²⁰ bearing alkyl substituents on the stereogenic centre.



Scheme 1. Addition of 2-propenylmagnesium bromide to α -substituted phenylacetaldehydes.

The selective formation of the *erythro* stereoisomer in the photooxygenation of **1–3** in solution can be explained considering preferential facial approach of $^1\text{O}_2$ to the double bond as shown in transition state **TS**₁ of Scheme 2. The phenyl group is placed to the opposite face of the double bond with respect to the attacking singlet oxygen, due to the unfavourable oxygen–arene electronic repulsions. In addition, for **TS**₁, the 1,3-allylic strain between the tertiary allylic hydrogen atom and the more hindered allylic methyl group is minimized. Abstraction of the suitably oriented tertiary allylic hydrogen atom leads to the formation of the minor (*Z*)-tertiary allylic hydroperoxides. Transition states **TS**₂ and **TS**₃, which lead to the *threo* diastereomers are expected to be less stable compared to **TS**₁, due to the substantial 1,3-allylic strain between the R group and the proximal allylic methyl for the case of **TS**₂, or to unfavourable oxygen–arene electronic repulsions for the case of **TS**₃. By increasing the bulkiness of the alkyl group (R) from methyl to cyclohexyl, enhanced *erythro* diastereoselection is found as reasonably expected (**TS**₁ vs **TS**₂). For alkene **4**, the moderate *erythro* selectivity arises through the more favourable transition state **TS**₄ in which the steric effects (methyl vs *n*-propyl) and the minimum 1,3-allylic strain as well, dictate the facial selectivity.

Photooxygenation of **1–4**²² by confinement within thionin-supported zeolite NaY is highly regioselective, since only the secondary allylic hydroperoxides were obtained, however, with an inverse diastereoselection trend, which is more profound and even remarkable in the case of the cyclohexyl-substituted alkene **3** (Table 2). The *threo* diastereomers were



Scheme 2. Possible transition states for the photooxygenation of alkenes **1–4** in solution.

predominantly formed, and the ratio *threo*/*erythro* increases with increasing the bulkiness of the R group (for alkenes **1–3**).

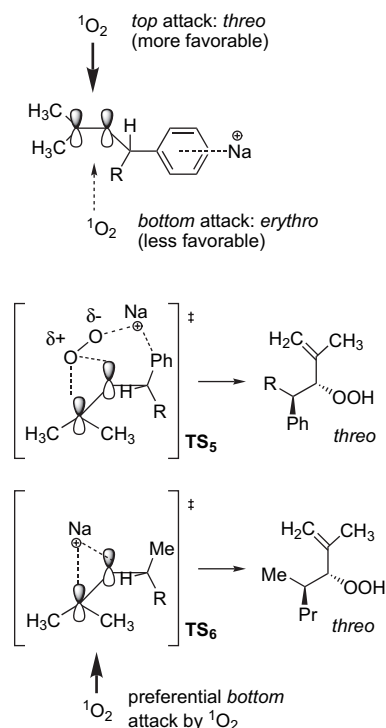
The predominant formation of the *threo* secondary allylic hydroperoxides by zeolite confinement can be rationalized as follows. Taking into account the strong electrostatic interaction²³ of the phenyl ring to the Na^+ within the NaY supercages, the alkene most likely adopts the conformation shown in Scheme 3. Preferential attack of $^1\text{O}_2$ from the less hindered *top* face gives the major *threo* secondary allylic hydroperoxides, while attack from the less accessible *bottom* face gives the minor *erythro* diastereomers. As the bulkiness of the R group increases, the energy difference between the *threo* and *erythro* forming transition states increases as well, in favour of the *threo* isomer. The participation of the *threo*-forming transition state **TS**₅ (Scheme 3), in which apart from the cation–arene interaction, a favourable $^1\text{O}_2$ – Na^+ interaction operates cannot be excluded. In the case of alkene **4**, we postulate that preferential interaction of the Na^+ with the less hindered face of the double bond allows the *threo*-forming transition state **TS**₆ (Scheme 3) to predominate

Table 2. Photooxygenation of chiral alkenes **1–4** within zeolite NaY

Alkene	<i>erythro</i> (%) ^a	<i>threo</i> (%) ^a
$\text{R}_1=\text{Me}, \text{R}_2=\text{Ph}$ (1)	46	54
$\text{R}_1=\text{Et}, \text{R}_2=\text{Ph}$ (2)	23	77
$\text{R}_1=\text{Cyclohexyl}, \text{R}_2=\text{Ph}$ (3)	9	91
$\text{R}_1=\text{Me}, \text{R}_2=n\text{-Pr}$ (4)	47	53

^a Relative percentage.

slightly. Furthermore, for alkene **4**, the change of the diastereoselection trend on going from the reaction in solution to the confined zeolite environment, is not as impressive as in the case of **1–3**. We postulate that since the electrostatic interaction between **4** and an Na^+ is not expected to be as strong²⁴ as with the phenyl-substituted alkenes **1–3**, reaction of $^1\text{O}_2$ with non- Na^+ bound alkene **4** conformers within NaY^{25} may also occur.

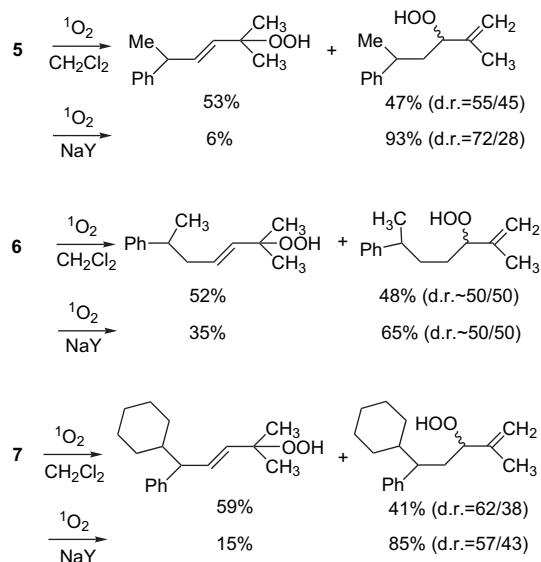


Scheme 3. Possible *threo*-forming transition states for the photooxygenation of **1–4** within NaY .

2.3. Diastereoselectivity in the photooxygenation of chiral alkenes bearing a stereogenic centre at a remote position with respect to the double bond (**5–7**)

As we discussed earlier, due to the adsorption of the reactant alkenes in the confined environment, increased diastereoselectivity might be expected in cases where a chiral centre resides at a remote position with respect to the reacting double bond, as a consequence of ‘substrate-coiling’ in the limited space of zeolite cavities. To examine this interesting aspect we performed the photooxygenation of alkenes **5**,²⁶ **6**, and **7**, which possess a stereogenic centre at the β - or γ -position with respect to the double bond. Reaction of **5** with $^1\text{O}_2$ in solution gave the expected ene product distribution (secondary vs tertiary allylic hydroperoxides=47/53), while for the secondary hydroperoxides a low diastereomeric ratio was found ($\sim 10\%$ dr, not specified). By NaY confinement, however, the reaction is 94% regioselective in favour of the secondary hydroperoxides (**Scheme 4**), and the diastereomeric ratio enhances significantly (dr=72/28). We postulate that, upon interaction of the alkene with the Na^+ within the cages, the substrate folds, and the chirality is ‘transferred’ close to the reaction centre (double bond). Consequently, the facial selectivity of $^1\text{O}_2$ to the double bond is significantly affected. For a further examination of this enhanced diastereoselection, we prepared alkene **7**,²⁷

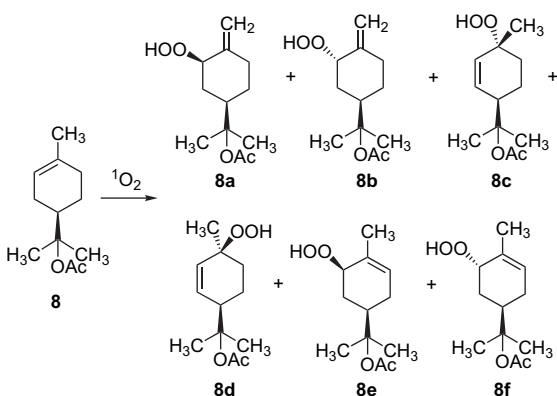
in which the more bulky cyclohexyl group has replaced the methyl group on the stereogenic centre of **5**. Photooxygenation of **7** in solution gave a mixture of tertiary and secondary allylic hydroperoxides in a ratio 59/41, and a relatively enhanced diastereomeric ratio for the case of the secondary allylic hydroperoxides (dr=62/38, not specified). While the reaction by zeolite confinement is 85% regioselective in favour of the formation of the secondary allylic hydroperoxides, the diastereoselection was not enhanced, as in the case of **5**, but essentially slightly decreased to 57/43 (**Scheme 4**). We assume that the bulkiness of the cyclohexyl ring may force **7** at NaY to adopt a conformation in which the stereogenic centre may not become proximal to the reacting double bond, and thus, affect substantially the facial selectivity. We next studied the photooxygenation of the chiral alkene **6** (**Scheme 4**), which bears the same substituents on the stereogenic centre as alkene **5**, however, situated at the more remote γ -position with respect to the double bond. In solution, the expected regioselectivity trend was found, while the diastereomeric ratio for the secondary allylic hydroperoxides was negligible (by GC and ^1H NMR). Photooxygenation of **6** within NaY gave predominantly the secondary allylic hydroperoxides (65% relative ratio), yet, the diastereoselection, as for the reaction in solution, was negligible. We would like to point out the significant difference in the regioselectivity on going from **5** to **7** within NaY . The relative ratio of the tertiary allylic hydroperoxide in the case of **5** is remarkably low (6%) and increases to 35% for **7**. Similar regioselectivity changes had been reported by our group^{12c} on studying the regioselectivity in the photooxygenation of structurally analogous phenyl-substituted alkenes and had been explained in terms of different substrate conformations within NaY which allow methylene allylic hydrogen abstraction to occur with different energetic consequences. From the above results we conclude that it is difficult to predict an enhancement of facial selectivity for the case of alkenes bearing remote stereogenic centres, since the relative bulkiness of the substituents in the interior of the zeolite cage, may or may not provide suitable proximity of the pre-existing chirality to the reacting double bond.



Scheme 4. Photooxygenation of chiral alkenes **5–7** in solution and within zeolite NaY .

A dramatic change in regioselectivity and diastereoselection was found in the photooxygenation of α -terpinyl acetate (**8**), by zeolite confinement relative to reaction in solution (Table 3), and exemplifies the role of the zeolite confinement as a powerful medium to control product selectivity, even if a stereogenic centre resides at a remote position with respect to the reacting double bond. In contrast to the photooxygenation of **8** in solution, which gives the expected ene product distribution based on the already published results of similar cycloalkenes such as limonene,²⁹ the intrazeolite photooxygenation of **8**³⁰ gave mainly one regioisomeric adduct (**8d**) in >90% dr. It is worthy to emphasize here, the predominant formation of a tertiary allylic hydroperoxide (**8d**), which is unique for an intrazeolite reaction, since trisubstituted alkenes afford within NaY primarily it is the secondary allylic hydroperoxides.

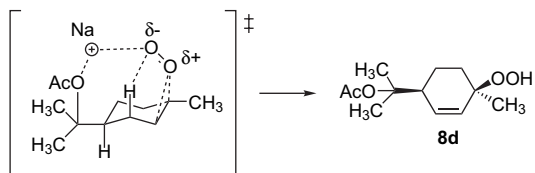
Table 3. Photooxygenation of α -terpinyl acetate (**8**) in solution and within NaY



	8a (%) ^a	8b (%) ^a	8c (%) ^a	8d (%) ^a	8e/8f (%) ^a
In solution	27	17	7	40	9
Within NaY	5	4	2	87	2

^a Relative percentage.

The enhanced regioselectivity/diastereoselectivity within NaY can be explained considering a synergism of $^1\text{O}_2$ -Na⁺ and Na⁺-acetate interactions. Essentially, an Na⁺ bound to the -OAc functionality directs singlet oxygen to abstract a pseudoaxially oriented allylic hydrogen atom at the more substituted side of the alkene (Scheme 5).

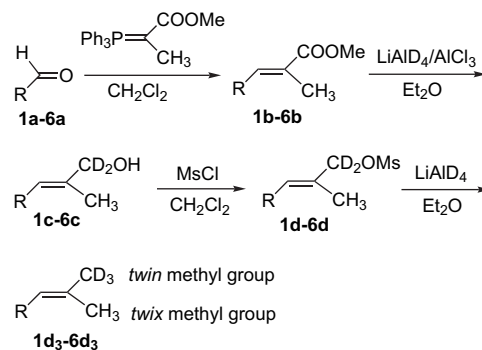


Scheme 5. Transition state for the selective formation of the hydroperoxide **8d** in the intrazeolite photooxygenation of α -terpinyl acetate.

2.4. Interplay of regioselectivity and diastereoselectivity in the photooxygenation of the chiral alkenes 1–6, through specific methyl group labelling

To determine the ratio of the *threolerythro* stereoisomers induced by abstraction of an allylic hydrogen atom either from the more (*twix* CH₃)³¹ or from the less (*twin* CH₃)³¹

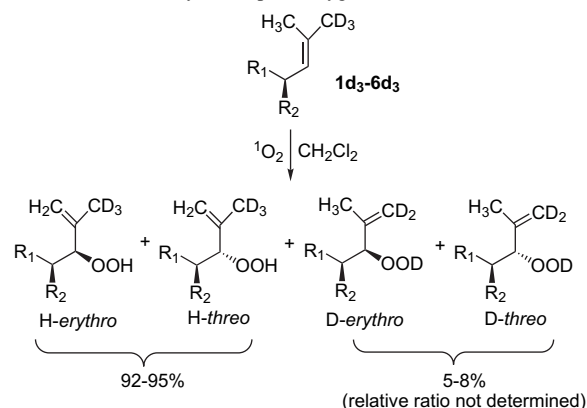
substituted side of the double bond, we prepared stereoselectively the deuterium labelled at the *twin* position chiral alkenes **1d₃–6d₃**. The synthesis was accomplished in >95% purity for the (*E*)-isomer as shown in Scheme 6, applying an already well known methodology.^{12c}



Scheme 6. Synthesis of the chiral labelled alkenes **1d₃–6d₃**.

Photooxygenation of **1d₃–6d₃** in solution (Table 4) afforded the mixture of tertiary and secondary allylic hydroperoxides, as shown in Table 1 and in Scheme 4 for their perprotio analogues. For clarity purposes, since photooxygenation of **1d₃–6d₃** in solution is around 92–95% regioselective for allylic hydrogen atom abstraction from the more substituted side of the alkene (*cis* effect selectivity),³² we will analyze below the diastereoselectivity arising only from the reaction of the *twix* methyl group. We define *H-threo* or *H-erythro* as the diastereomeric secondary allylic hydroperoxides resulting from allylic hydrogen atom abstraction from the *twix* methyl group (CH₃), and *D-threo* and *D-erythro* as the hydroperoxides resulting from allylic deuterium atom abstraction from the labelled *twin* methyl group (CD₃). The ratio of secondary *H-threo*/*H-erythro* allylic hydroperoxides was assessed by integration of the terminal olefinic hydrogen atoms in the region of 5 ppm.

Table 4. Stereochemistry in the photooxygenation of **1d₃–6d₃** in solution



Alkene	<i>H-erythro</i> / <i>H-threo</i> (%)
R ₁ =Me, R ₂ =Ph (1d₃)	77/23
R ₁ =Et, R ₂ =Ph (2d₃)	78/22
R ₁ =Cyclohexyl, R ₂ =Ph (3d₃)	83/17
R ₁ =Me, R ₂ = <i>n</i> -Pr (4d₃)	62/38
5d₃	55/45 ^a
6d₃	~50/50 ^a

^a The relative configuration of the major and minor *erythro* or *threo* diastereomers in the photooxygenation of **5d₃** and **6d₃** was not assessed.

The intrazeolite photooxygenation of **1d₃–6d₃** afforded the mixture of tertiary and secondary allylic hydroperoxides, with the latest being predominant or only products. For discussion purposes we will emphasize only to the stereochemical analysis of the secondary allylic hydroperoxides (Table 5). Enhanced *twin* selectivity was found, in accordance with the previously reported studies on other labelled trisubstituted alkenes,^{7c} and therefore, analysis of the diastereoselectivity obtained from allylic hydrogen abstraction either from the labelled *twin* (CD₃) or from the *twix* methyl group became possible.

Table 5. Stereochemistry in the photooxygenation of **1d₃–6d₃** within NaY

Alkene	<i>twin</i> / <i>twix</i> (%)	H- <i>erythro</i> / H- <i>threo</i> (%)	H- <i>erythro</i> / H- <i>threo</i> (%)
R ₁ =Me, R ₂ =Ph (1d₃)	62/38	52/48	44/56
R ₁ =Et, R ₂ =Ph (2d₃)	60/40	23/77	22/78
R ₁ =Cyclohexyl, R ₂ =Ph (3d₃)	55/45	11/89	08/92
R ₁ =Me, R ₂ = <i>n</i> -Pr (4d₃)	52/48	44/56	50/50
5d₃	30/70	77/23 ^a	58/42 ^a
6d₃	47/54	~50/50 ^a	~50/50 ^a

^a The relative configuration of the major and minor *erythro* or *threo* diastereomers in the photooxygenation of **5d₃** and **6d₃** was not assessed.

The ratio of secondary H-*threo*/H-*erythro* allylic hydroperoxides was assessed by integration of the terminal olefinic hydrogen atoms in the region of 5 ppm. On the other hand, the ratio D-*threo*/D-*erythro*, formed by abstraction of an allylic deuterium atom from the *twin* methyl group (CD₃), was assessed either by integration of the diastereotopic allylic methyls, or extrapolated, taking into account the total ratio of *threo/erythro* hydroperoxides and the ratio H-*threo*/H-*erythro*, as well. The typical ¹H NMR spectra, based on which the H-*threo*/H-*erythro* and D-*threo*/D-*erythro* ratios were calculated, for the photooxygenation of **3d₃** in solution and within NaY are shown in Figure 1.

The intrazeolite results present in Table 5 indicate that for alkenes **1d₃–4d₃** the diastereoselection arisen from abstraction of an allylic H or D atom (from the *twix* or the *twin* methyl group, respectively), is more or less very similar. The only significant change was found in the intrazeolite photooxygenation of **5d₃**, where the diastereoselectivity depends significantly on the orientation of singlet oxygen to form the peroxide intermediates, either towards the more or towards the less substituted side of the double bond. Thus, abstraction of a D atom from the *twin* methyl group proceeds with moderate diastereoselection (18% dr), while H atom abstraction from the *twix* methyl group proceeds with significantly higher facial selectivity (54% dr). The significant dependence of diastereoselectivity on site selectivity, most probably indicates that upon folding of the alkene within NaY cages, the stereogenic centre is more proximal to the more substituted side of the double bond, and therefore, control of the facial approach in the case of the *twix*-oriented peroxide intermediate is more profound.

3. Conclusions

As a conclusion, we have shown that the confined environment of zeolite NaY may in certain cases remarkably alter

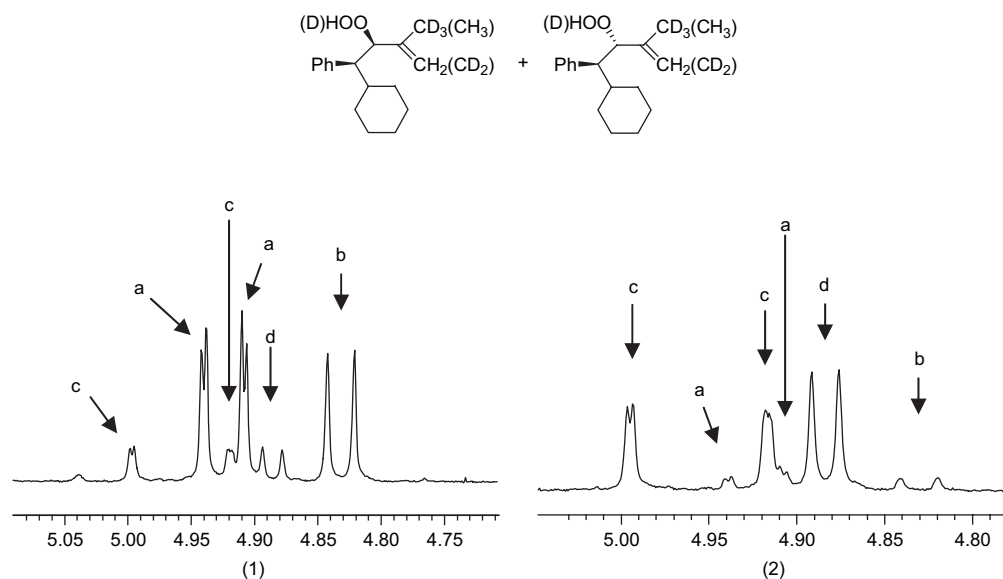


Figure 1. Part of the crude ¹H NMR spectrum in the region 4.7–5.1 ppm for the photooxygenation of **3d₃** in solution (1) and within NaY (2). Abbreviations: (a) terminal olefinic hydrogen (H-*erythro*); (b) allylic hydrogen on the carbon bearing the –OOH(D) functionality (H-*erythro*+D-*erythro*); (c) terminal olefinic hydrogen (H-*threo*); (d) allylic hydrogen on the carbon bearing the –OOH(D) functionality (H-*threo*+D-*threo*).

the facial selectivity in the photooxygenation of some chiral alkenes compared to their reaction in solution. It is postulated that within zeolite, a synergism between cation- π and singlet oxygen-cation interactions as well, are the main driving forces for the facial selectivity changes. In certain cases, enhanced regioselectivity and diastereoselection can be induced by a remote stereogenic centre relative to the reacting double bond, as a consequence of substrate confinement within the limited space of a cavity. We believe that the current results may provide a basis for the development of models with predictive capability in order to tune the behaviour of $^1\text{O}_2$ reactions by zeolite confinement.

4. Experimental

4.1. General

Nuclear magnetic resonance spectra were obtained on a 300 and 500 MHz instruments. Isomeric purities were determined by ^1H NMR and by GC analysis on a 60 m HP-5 capillary column. All spectra reported herein were taken in CDCl_3 . Since, in addition to the synthesis of **1–6**, the stereoselectively labelled at the *twin* position analogous substrates **1d₃–6d₃** were prepared, we will describe below the synthesis of the labelled alkenes only. The only chiral alkene, which was not prepared in its labelled form was (1-cyclohexyl-4-methylpent-3-enyl)benzene (**7**) and the details of its synthesis are presented separately below.

4.2. Synthesis of (1-cyclohexyl-4-methylpent-3-enyl)-benzene (**7**)

4.2.1. Methyl 3-cyclohexyl-3-hydroxy-3-phenylpropanoate. In a flame-dried flask were added 2-bromoacetate (55 mmol), cyclohexylphenyl ketone (30 mmol), 2 g of activated Zn, and as a solvent was used a mixture of 100 mL dry benzene and 50 mL of dry ether. The slurry was refluxed for 1 day and then it was poured into 100 mL 2 N H_2SO_4 . After extraction, the organic layer was dried and the solvent was removed under vacuum to produce methyl 3-cyclohexyl-3-hydroxy-3-phenylpropanoate in 75% yield as a white solid. The starting material cyclohexylphenyl ketone, was obtained in two steps by phenylmagnesium bromide addition to cyclohexanecarboxaldehyde, followed by oxidation of the resulting alcohol with Jones' reagent (70% yield over two steps). ^1H NMR of the hydroxyl ester: 7.19–7.35 (m, 5H), 4.30 (br s, 1H), 3.49 (s, 3H), 3.02 (d, 1H, $J=16$ Hz), 2.84 (d, 1H, $J=16$ Hz), 0.96–1.75 (m, 11H).

4.2.2. 1-Cyclohexyl-1-phenylpropane-1,3-diol. The methyl 3-cyclohexyl-3-hydroxy-3-phenylpropanoate was reduced into 95% yield by reacting for 8 h at ambient temperature and under inert atmosphere, with 1 mol equiv of LiAlH_4 in dry ether. ^1H NMR: 7.21–7.36 (m, 5H), 3.70 (m, 2H), 3.47 (t, 2H, $J=7.5$ Hz), 0.86–1.97 (m, 11H).

4.2.3. 3-Cyclohexyl-3-phenylpropan-1-ol. In a flame-dried flask were placed 0.99 g of 1-cyclohexyl-1-phenylpropane-1,3-diol (4 mmol) and 15 mL dry dichloromethane. At 0 °C were added by syringe 10 mmol (1.5 mL) of BF_3 etherated and then 0.73 mL of triethylsilane.²⁸ After 24 h the reduction of the benzylic hydroxyl was complete by TLC.

The reaction mixture was washed with saturated solution of NaHCO_3 , the organic layer was dried and the solvent was evaporated to yield after column chromatography (hexane/ethyl acetate=6/1) 0.62 g of 3-cyclohexyl-3-phenylpropan-1-ol (70%). ^1H NMR: 7.11–7.29 (m, 5H), 3.45 (m, 1H), 3.36 (m, 1H), 3.36 (m, 1H), 0.75–2.10 (m, 13H).

4.2.4. 3-Cyclohexyl-3-phenylpropanal. The alcohol was oxidized to the corresponding aldehyde (3-cyclohexyl-3-phenylpropanal) in 75% isolated yield by PCC oxidation of 3-cyclohexyl-3-phenylpropan-1-ol in dry dichloromethane. ^1H NMR: 9.70 (s, 1H), 7.13–7.29 (m, 5H), 2.97 (t, 1H, $J=6.0$ Hz), 2.78 (m, 2H), 0.82–1.81 (m, 11H).

4.2.5. (1-Cyclohexyl-4-methylpent-3-enyl)benzene (7**).** The aldehyde reacted with the ylide obtained from the reaction of triphenylphosphoniumisopropyl iodide with *n*-BuLi in dry THF, to obtain after column chromatography (hexane as eluent) the desired alkene **7** in 59% isolated yield. ^1H NMR: 7.09–7.27 (m, 5H), 4.94 (t, 1H, $J=7.0$ Hz), 2.52 (m, 2H), 2.34 (m, 1H), 2.24 (m, 1H), 1.59 (s, 3H), 1.53 (s, 3H), 0.77–1.91 (m, 10H). ^{13}C NMR: 144.5, 131.7, 128.7, 127.7, 125.6, 123.2, 52.4, 42.5, 31.5, 31.1, 30.7, 26.7, 25.7, 17.7.

4.3. Synthesis of the labelled chiral alkenes **1d₃–6d₃**

4.3.1. Chiral aldehydes **1a–6a.** The aldehydes **1a** and **4a** are commercially available. The rest were prepared as follows. Aldehyde **2a**: it was prepared in 71% isolated yield by oxidation of 2-phenyl-1-butanol with PCC in dichloromethane. ^1H NMR: 9.69 (br s, 1H), 7.20–7.47 (m, 5H), 3.43 (t, 1H, $J=7.0$ Hz), 2.13 (m, 1H), 1.78 (m, 1H), 0.92 (t, 3H, $J=7.5$ Hz). Aldehyde **3a**: it was prepared in two steps from reduction of α -cyclohexylphenylacetic acid with LiAlH_4 , followed by PCC oxidation of the resulting alcohol (60% yield, over two steps). ^1H NMR: 9.71 (d, 1H, $J=3.5$ Hz), 7.18–7.38 (m, 5H), 3.25 (dd, 1H, $J_1=9.5$ Hz, $J_2=3.5$ Hz), 2.12 (m, 1H), 0.80–1.86 (m, 10H). Aldehyde **6a**: it was prepared in two steps as follows: 3-phenyl-1-butanol was transformed to corresponding bromide in 96% yield by reacting with the $\text{PPh}_3\text{-Br}_2$ complex. ^1H NMR of the bromide: 7.19–7.35 (m, 5H), 3.32 (m, 1H), 3.18 (m, 1H), 2.96 (m, 1H), 2.11 (q, 2H, $J=7.5$ Hz), 1.29 (d, 3H, $J=7.0$ Hz). The bromide was transformed to the organomagnesium reagent in the presence of 1.4 mol equiv of Mg turnings, and then the Grignard reagent reacted with *N*-formylpiperidine³³ at 0 °C for 30 min. Acidic work up (3 N HCl) and extraction of the crude reaction mixture afforded the crude aldehyde **6a**, which was purified by flash column chromatography using hexane as eluent (56% isolated yield). ^1H NMR: 9.69 (t, 1H, $J=1.5$ Hz), 7.16–7.33 (m, 5H), 2.72 (m, 2H), 2.32 (m, 2H), 1.90 (m, 2H), 1.29 (d, 3H, $J=7.0$ Hz).

4.3.2. α,β -Unsaturated esters **1b–6b.** In a one-necked flask were placed 60 mL of dry CH_2Cl_2 , and 40 mmol of the stabilized ylide methyl(triphenylphosphoranylidene)propionate and 25 mmol of the aldehydes **1a–6a**. The solution was refluxed until consumption of the aldehyde (normally 2–6 h is necessary). For the case of the bulkiest aldehyde **6c**, the reaction time was 2 days. Most of the solvent was removed by evaporation and then 50 mL of hexane were added. The

solid residue was washed with hexane (4×50 mL), the solvent was evaporated and the oily residue was chromatographed or distilled at reduced pressure (for volatile derivative **4b**). The α,β -unsaturated esters were isolated in 50–75% yield and in >95% purity for the (*E*)-isomer. ^1H NMR data: compound **1b**: 7.22–7.35 (m, 5H), 6.87 (d, 1H, $J=11.0$ Hz), 3.77 (m, 1H), 3.72 (s, 3H), 1.91 (s, 3H), 1.39 (d, 3H, $J=7.0$ Hz). Compound **2b**: 7.19–7.35 (m, 5H), 6.88 (d, 1H, $J=10.0$ Hz), 3.73 (s, 3H), 3.50 (m, 1H), 1.90 (s, 3H), 1.78 (m, 2H), 0.88 (t, 3H, $J=7.5$ Hz). Compound **3b**: 7.16–7.31 (m, 5H), 6.97 (dd, 1H, $J_1=10.5$ Hz, $J_2=1.5$ Hz), 3.72 (s, 3H), 3.28 (t, 1H, $J=10.0$ Hz), 1.86 (d, 3H, $J=1.5$ Hz), 0.80–1.85 (m, 11H). Compound **4b**: 6.51 (d, 1H, $J=8.0$ Hz), 3.72 (s, 3H), 2.50 (m, 1H), 1.83 (s, 3H), 1.25 (m, 4H), 0.97 (d, 3H, $J=7.0$ Hz), 0.87 (t, 3H, $J=7.0$ Hz). Compound **5b**: 7.19–7.32 (m, 5H), 6.73 (t, 1H, $J=6.5$ Hz), 3.71 (s, 3H), 2.87 (m, 1H), 2.44 (m, 2H), 1.77 (s, 3H), 1.28 (d, 3H, $J=6.5$ Hz). Compound **6b**: 7.19–7.34 (m, 5H), 6.76 (t, 1H, $J=7.0$ Hz), 3.75 (s, 3H), 2.74 (m, 1H), 2.08 (m, 2H), 1.76 (m, 2H), 1.75 (s, 3H), 1.29 (d, 3H, $J=7.0$ Hz).

4.3.3. Allylic alcohols- d_2 , 1c–6c. In a flame-dried two-necked flask were placed 12 mmol of LiAlD_4 and 15 mL of dry ether. The flask was cooled to 0 °C and subsequently 4 mmol of anhydrous AlCl_3 were added in portions. The resulting slurry was stirred for an additional 20 min, followed by the dropwise addition of the α,β -unsaturated ester **1b–6b** (15 mmol). The reaction mixture was stirred for 1–2 h and then treated with 1 mL of water. After extraction with diethyl ether, the deuterated allylic alcohols **1c–6c** were isolated in 85–95% yield. ^1H NMR: compound **1c**: 7.18–7.34 (m, 5H), 5.58 (d, 1H, $J=9.5$ Hz), 3.73 (m, 1H), 1.75 (s, 3H), 1.58 (br s, 1H), 1.29 (t, 3H, $J=7.0$ Hz). Compound **2c**: 7.17–7.36 (m, 5H), 5.57 (dd, 1H, $J_1=9.5$ Hz, $J_2=1.0$ Hz), 3.41 (m, 1H), 1.73 (d, 3H, $J=1.0$ Hz), 1.62–1.78 (m, 2H), 1.49 (br s, 1H), 0.87 (t, 3H, $J=7.0$ Hz). Compound **3c**: 7.15–7.30 (m, 5H), 5.63 (d, 1H, $J=9.5$ Hz), 3.19 (t, 1H, $J=9.5$ Hz), 1.87 (m, 1H), 1.69 (s, 3H), 0.78–1.74 (m, 10H). Compound **4c**: 5.11 (d, 1H, $J=8.0$ Hz), 2.37 (m, 1H), 1.66 (s, 3H), 1.54 (br s, 1H), 1.17–1.30 (m, 4H), 0.92 (d, 3H, $J=7.0$ Hz), 0.87 (t, 3H, $J=7.0$ Hz). Compound **5c**: 7.18–7.32 (m, 5H), 5.37 (t, 1H, $J=7.5$ Hz), 2.73 (m, 1H), 2.31 (m, 2H), 1.60 (s, 3H), 1.56 (br s, 1H), 1.25 (d, 3H, $J=7.0$ Hz). Compound **6c**: 7.20–7.33 (m, 5H), 5.39 (t, 1H, $J=7.0$ Hz), 2.73 (m, 1H), 1.97 (m, 2H), 1.68 (m, 2H), 1.60 (s, 3H), 1.28 (d, 3H, $J=7.0$ Hz), 1.29 (br s, 1H).

4.3.4. Mesylates of the allylic alcohols- d_2 , 1d–6d. The allylic alcohols- d_2 , **1c–6c** (10 mmol) were placed into a flask charged with 30 mmol of dry triethylamine and 30 mL of dry dichloromethane. Subsequently, 11 mmol of methanesulfonyl chloride were added dropwise at 0 °C. After 25 min the reaction was complete (by TLC). The solids were removed by filtration and the organic layer was washed with 5% HCl (until pH was acidic), then with saturated solution of NaHCO_3 , and finally with 50 mL of brine. The allylic mesylates do not persist and were used immediately in the next step without purification.

4.3.5. Chiral alkenes- d_3 , 1d₃–6d₃. To a flame-dried flask charged with 20 mL of dry ether were suspended 4 mmol of LiAlD_4 . The crude mesylates **1d–6d** (10 mmol) were

added dropwise at 0 °C. The reaction mixture was stirred overnight. After treatment with 2 mL of water and extraction with ether, the resulting crude alkenes **1d₃–6d₃** were purified by flash silica gel chromatography using hexane as eluent. The geometric purity of the (*E*)-alkenes was >95% and was estimated by comparison with the spectra of their corresponding perprotio alkenes. ^1H NMR of **1d₃**: 7.17–7.33 (m, 5H), 5.29 (dq, 1H, $J_1=9.5$ Hz, $J_2=1.0$ Hz), 3.67 (m, 1H), 1.69 (d, 3H, $J=1.0$ Hz), 1.30 (t, 3H, $J=7.5$ Hz); ^{13}C NMR of **1d₃**: 147.3, 130.4, 130.2, 128.3, 126.9, 125.7, 38.1, 25.1 (septet, $J_{\text{C-D}}=19$ Hz), 22.4, 17.9; MS, $m/z=163$ (100%, $m/z=148$). ^1H NMR of **2d₃**: 7.14–7.32 (m, 5H), 5.28 (dq, 1H, $J_1=9.5$ Hz, $J_2=1.0$ Hz), 3.36 (m, 1H), 1.57–1.76 (m, 2H), 1.67 (d, 3H, $J=1.0$ Hz), 0.86 (t, 3H, $J=7.5$ Hz); ^{13}C NMR of **2d₃**: 146.2, 131.2, 128.9, 128.3, 127.3, 125.7, 46.1, 30.1, 25.0 (septet, $J_{\text{C-D}}=19$ Hz), 18.0, 12.2; MS, $m/z=177$ (100%, $m/z=148$); HRMS calcd for $\text{C}_{13}\text{H}_{15}\text{D}_3$: 177.1597, found: 177.1597. ^1H NMR of **3d₃**: 7.15–7.29 (m, 5H), 5.35 (dq, 1H, $J_1=10.0$ Hz, $J_2=1.0$ Hz), 3.14 (t, 1H, $J=10.0$ Hz), 0.77–1.89 (m, 11H), 1.63 (d, 3H, $J=1.0$ Hz); ^{13}C NMR of **3d₃**: 145.3, 131.3, 128.2, 127.9, 125.5, 51.16, 43.6, 31.5, 31.1, 26.6, 26.5, 26.4, 25.1 (septet, $J_{\text{C-D}}=19$ Hz), 18.1; HRMS calcd for $\text{C}_{17}\text{H}_{21}\text{D}_3$: 231.2066, found: 231.2064. ^1H NMR of **4d₃**: 4.90 (d, 1H, $J=9.0$ Hz), 2.34 (m, 1H), 1.62 (s, 3H), 1.17–1.30 (m, 4H), 0.92 (d, 3H, $J=7.0$ Hz), 0.89 (t, 3H, $J=7.0$ Hz). ^{13}C NMR of **4d₃**: 131.6, 129.3, 40.1, 32.1, 24.8 (septet, $J_{\text{C-D}}=19$ Hz), 21.2, 20.5, 17.8, 14.2. ^1H NMR of **5d₃**: 7.19–7.32 (m, 5H), 5.10 (t, 1H, $J=6.5$ Hz), 2.72 (m, 1H), 2.25 (m, 2H), 1.56 (s, 3H), 1.24 (d, 3H, $J=7.0$ Hz). ^1H NMR of **6d₃**: 7.19–7.33 (m, 5H), 5.12 (t, 1H, $J=7.0$ Hz), 2.73 (m, 1H), 1.91 (m, 2H), 1.59–1.68 (m, 2H), 1.55 (s, 3H), 1.27 (d, 3H, $J=7.0$ Hz).

4.4. Photooxygenation of chiral alkenes 1–7 and their labelled analogues

The photooxygenation of the alkenes in solution was accomplished by dissolving 10 mg of each alkene in a solution of 10^{-4} M methylene blue in dichloromethane (5 mL). The solution was bubbled with oxygen gas and then irradiated with a 300 W Xenon lamp until the alkene was consumed (by TLC). The intrazeolite reactions were carried as follows. In a test tube were added 1 g of freshly dried thionin-supported zeolite NaY and 5 mL of dry hexane, which contained 10 μL of pyridine. After 5 min, a hexane solution (5 mL) containing each alkenes- d_3 or their perprotio analogues (10 mg) was added. The tube was immediately photolyzed at 0 °C under a constant slow stream of oxygen gas for 1–2 min, followed by immediate addition of 10 mL of moistened tetrahydrofuran. The slurry was stirred for 3 h and then the solid was removed by filtration. The solvent was removed by rotary evaporation and the ^1H NMR spectrum was taken directly on the crude reaction mixture. The spectroscopic data for the ene allylic hydroperoxides obtained from the photooxygenation of **1** have been reported (see Ref. 19). Photooxygenation of **2** (or **2d₃**): tertiary hydroperoxide {7.10–7.35 (m, 5H), 5.56 (s, 1H), 2.31 (q, 2H, $J=7.5$ Hz), 1.16 (s, 6H), 0.98 (t, 3H, $J=7.5$ Hz)}; *erythro* secondary hydroperoxide {7.83 (br s, 1H), 7.10–7.35 (m, 5H), 4.89 (br s, 1H), 4.87 (br s, 1H), 4.51 (d, 1H, $J=9.5$ Hz), 2.60 (m, 1H), 2.12 (m, 1H), 1.57 (s, 3H), 1.62 (m, 1H), 0.73 (t, 3H, $J=7.0$ Hz)}; *threo* secondary

hydroperoxide {7.65 (br s, 1H), 7.10–7.35 (m, 5H), 5.11 (br s, 1H), 5.06 (br s, 1H), 4.51 (d, 1H, $J=9.5$ Hz), 2.58 (m, 1H), 1.78 (s, 3H), 1.64 (m, 1H), 1.52 (m, 1H), 0.71 (t, 3H, $J=7.0$ Hz)}. Photooxygenation of **3** (or **3d₃**): tertiary hydroperoxide {7.05–7.30 (m, 5H), 5.55 (s, 1H), 2.09 (br t, 1H, $J=11.0$ Hz), 1.12 (s, 6H), 0.80–1.85 (m, 10H)}; *erythro* secondary hydroperoxide {7.75 (br s, 1H), 7.05–7.30 (m, 5H), 4.94 (br s, 1H), 4.91 (br s, 1H), 4.83 (d, 1H, $J=10.5$ Hz), 2.70 (dd, 1H, $J_1=10.5$ Hz, $J_2=4.5$ Hz), 1.61 (s, 3H), 0.80–1.85 (m, 10H)}; *threo* secondary hydroperoxide {7.60 (br s, 1H), 7.05–7.30 (m, 5H), 4.99 (br s, 1H), 4.92 (br s, 1H), 4.88 (d, 1H, $J=7.5$ Hz), 2.55 (t, 1H, $J=7.0$ Hz), 1.68 (s, 3H), 0.80–1.85 (m, 10H)}. Photooxygenation of **4** (or **4d₃**): *erythro* secondary hydroperoxide (as alcohol obtained after reduction with PPh₃, characteristic absorptions) {4.97 (br s, 1H), 4.90 (br s, 1H), 3.88 (d, 1H, $J=6.5$ Hz), 1.72 (s, 3H)}; *threo* secondary hydroperoxide (as alcohol obtained after reduction with PPh₃, characteristic absorptions) {4.93 (br s, 1H), 4.88 (br s, 1H), 3.79 (d, 1H, $J=6.5$ Hz), 1.73 (s, 3H)}. Photooxygenation of **5** (or **5d₃**): tertiary hydroperoxide (as alcohol obtained after reduction with PPh₃, characteristic absorptions) {5.85 (dd, 1H, $J_1=16.0$ Hz, $J_2=7.0$ Hz), 5.61 (d, 1H, $J=16.0$ Hz), 3.45 (m, 1H), 1.46 (s, 6H), 1.41 (d, 3H, $J=7.5$ Hz)}; main diastereomeric secondary hydroperoxide (as alcohol obtained after reduction with PPh₃, characteristic absorptions) {4.90 (d, 1H, $J=1.5$ Hz), 4.80 (d, 1H, $J=1.5$ Hz), 3.84 (dd, 1H, $J_1=8.5$ Hz, $J_2=4.5$ Hz), 2.99 (m, 1H), 1.78–1.90 (m, 2H), 1.70 (s, 3H), 1.29 (d, 3H, $J=7.0$ Hz)}; minor diastereomeric secondary hydroperoxide (as alcohol obtained after reduction with PPh₃, characteristic absorptions) {4.88 (d, 1H, $J=1.5$ Hz), 4.86 (d, 1H, $J=1.5$ Hz), 4.04 (t, 1H, $J=8.5$ Hz), 2.85 (m, 1H), 1.78–1.90 (m, 2H), 1.76 (s, 3H), 1.29 (d, 3H, $J=7.0$ Hz)}. Photooxygenation of **6** (or **6d₃**): tertiary hydroperoxide (characteristic absorptions) {5.62 (dt, 1H, $J_1=16$ Hz, $J_2=7.5$ Hz), 5.41 (d, 1H, $J=16.0$ Hz), 2.85 (m, 1H), 2.37 (m, 2H), 1.27 (s, 6H)}; secondary hydroperoxides (characteristic absorptions) {5.03 (br s, 1H), 5.00 (br s, 1H), 4.31 (t, 1H, $J=7.5$ Hz) corresponding to the one diastereomer, 4.30 (t, 1H, $J=7.5$ Hz) corresponding to the other diastereomer, 2.72 (m, 2H), 1.70 (s, 3H) corresponding to the one diastereomer, 1.66 (s, 3H) corresponding to the other diastereomer}. Photooxygenation of **7**: tertiary hydroperoxide (characteristic absorptions) {5.87 (dd, 1H, $J_1=16$ Hz, $J_2=7.5$ Hz), 5.53 (d, 1H, $J=16.0$ Hz), 2.94 (t, 1H, $J=9.0$ Hz), 1.34 (s, 3H), 1.31 (s, 3H)}; major secondary hydroperoxide (characteristic absorptions) {7.65 (s, 1H, –OOH), 4.90 (br s, 1H), 4.85 (br s, 1H), 3.98 (m, 1H), 2.60 (m, 1H), 1.62 (s, 3H)}; minor secondary hydroperoxide (characteristic absorptions) {7.56 (s, 1H, –OOH), 5.05 (br s, 1H), 4.79 (br s, 1H), 4.00 (m, 1H), 2.21 (m, 1H), 1.73 (s, 3H)}.

Acknowledgements

This work was supported by the community initiative INTERREG IIB, MEDOCC programme (Aquatex project). This European programme supports projects aimed at transnational co-operation in the field of territorial development of Mediterranean countries. The authors are indebted to Professors Michael Orfanopoulos and Georgios Vassilikogiannakis for fruitful discussions and productive collaboration in the field of singlet oxygen chemistry for the past 15–20 years.

References and notes

- (a) Wasserman, H. H.; Murray, R. W. *Singlet Oxygen*; Academic: New York, NY, 1979; (b) For a recent review article, see: Clennan, E. L.; Pace, A. *Tetrahedron* **2005**, *61*, 6665–6691.
- Wahlen, J.; de Vos, D. E.; Jacobs, P. A.; Alsters, P. L. *Adv. Synth. Catal.* **2004**, *346*, 152–164.
- Tung, C.-H.; Wu, L.-Z.; Zhang, L.-P.; Chen, B. *Acc. Chem. Res.* **2003**, *36*, 39–47.
- (a) Tung, C.-H.; Wang, H.; Ying, Y.-M. *J. Am. Chem. Soc.* **1998**, *120*, 5179–5186; (b) Chen, Y.-Z.; Wu, L.-Z.; Zhang, L.-P.; Tung, C.-H. *J. Org. Chem.* **2005**, *70*, 4676–4681.
- Tung, C.-H.; Guan, J.-Q. *J. Am. Chem. Soc.* **1998**, *120*, 11874–11879.
- Tung, C.-H.; Wu, L. Z.; Zhang, L. P.; Li, H. R.; Yi, X. Y.; Ming, K. S.; Yuan, Z. Y.; Guan, J. Q.; Wang, H. W.; Ying, Y. M.; Xu, X. H. *Pure Appl. Chem.* **2000**, *72*, 2289–2298.
- (a) Ramamurthy, V.; Lakshminarasimhan, P.; Grey, C. P.; Johnston, L. J. *Chem. Commun.* **1998**, 2411–2424; (b) Sen, S. E.; Smith, S. M.; Sullivan, K. A. *Tetrahedron* **1999**, *55*, 12657–12698; (c) Stratakis, M. *Curr. Org. Synth.* **2005**, *2*, 281–299.
- Li, X.; Ramamurthy, V. *J. Am. Chem. Soc.* **1996**, *118*, 10666–10667.
- Pace, A.; Clennan, E. L. *J. Am. Chem. Soc.* **2002**, *124*, 11236–11237.
- Jockusch, S.; Sivaguru, J.; Turro, N. J.; Ramamurthy, V. *Photochem. Photobiol. Sci.* **2005**, *4*, 403–405.
- Robbins, R. J.; Ramamurthy, V. *Chem. Commun.* **1997**, 1071–1072.
- (a) Stratakis, M.; Froudakis, G. *Org. Lett.* **2000**, *2*, 1369–1372; (b) Clennan, E. L.; Sram, J. P. *Tetrahedron* **2000**, *56*, 6945–6950; (c) Stratakis, M.; Nencka, R.; Rabalakos, C.; Adam, W.; Krebs, O. *J. Org. Chem.* **2002**, *67*, 8758–8763.
- Stratakis, M.; Rabalakos, C.; Mpourmpakis, G.; Froudakis, G. E. *J. Org. Chem.* **2003**, *68*, 2839–2843.
- Ramamurthy, V.; Shailaja, J.; Kaanumalle, L. S.; Sunoj, R. B.; Chandrasekhar, J. *Chem. Commun.* **2003**, 1987–1999.
- Prein, M.; Adam, W. *Angew. Chem., Int. Ed.* **1996**, *35*, 477–494.
- Rao, V. J.; Uppili, S. R.; Corbin, D. R.; Schwarz, S.; Lustig, S. R.; Ramamurthy, V. *J. Am. Chem. Soc.* **1998**, *120*, 2480–2481.
- Joy, A.; Uppili, S.; Netherthon, M. R.; Scheffer, J. R.; Ramamurthy, V. *J. Am. Chem. Soc.* **2000**, *122*, 728–729.
- The relevant to the **1–4** chiral alkene, for which R₁=methyl and R₂=*tert*-butyl(2,4,5,5-tetramethyl-2-hexene) affords a ratio *erythro*/*threo* secondary allylic hydroperoxides=71/29 (see Ref. 19). This diastereomeric ratio is lower compared to the *erythro*/*threo* ratio obtained from the photooxygenation of **3**.
- Adam, W.; Nestler, B. *Liebigs Ann. Chem.* **1990**, 1051–1053.
- Adam, W.; Brunker, H.-G.; Kumar, A. S.; Peters, E.-M.; Peters, K.; Schneider, U.; von Schnering, H. G. *J. Am. Chem. Soc.* **1996**, *118*, 1899–1905.
- Karabatsos, G. J. *J. Am. Chem. Soc.* **1967**, *89*, 1367–1371 and references cited therein.
- A preliminary account for the intrazeolite photooxygenation of the phenyl-substituted alkenes **1–3** has been published: Stratakis, M.; Kalaitzakis, D.; Stavroulakis, D.; Kosmas, G.; Tsangarakis, C. *Org. Lett.* **2003**, *5*, 3471–3474.
- Feller, D. *Chem. Phys. Lett.* **2000**, *322*, 543–548.

24. The interaction of an isolated double bond to the Na⁺ is at least 10 kcal/mol less exothermic compared to the Na⁺–benzene interaction. Ma, J. C.; Dougherty, D. A. *Chem. Rev.* **1997**, *97*, 1303–1324.
25. Clennan, E. L.; Sram, J. P.; Pace, A.; Vincer, K.; White, S. *J. Org. Chem.* **2002**, *67*, 3975–3978.
26. Stratakis, M.; Kosmas, G. *Tetrahedron Lett.* **2001**, *42*, 6007–6009.
27. Alkene **7** was prepared as follows. Reformatsky coupling of 2-bromoacetate with phenyl cyclohexyl ketone in the presence of activated Zn, afforded methyl 3-cyclohexyl-3-hydroxy-3-phenylpropanoate, which was reduced to 1-cyclohexyl-1-phenylpropane-1,3-diol by LiAlH₄. Selective reduction²⁸ of the tertiary benzylic hydroxyl with Et₃SiH/BF₃ yielded 3-cyclohexyl-3-phenylpropan-1-ol, which was oxidized with PCC to form 3-cyclohexyl-3-phenylpropanal. Finally, Wittig coupling of the aldehyde with isopropylidene-triphenylphosphorane afforded **7**.
28. Orfanopoulos, M.; Smonou, I. *Synth. Commun.* **1988**, *18*, 833–839.
29. Gollnick, K.; Schade, G. *Tetrahedron Lett.* **1973**, *11*, 857–860.
30. Stratakis, M.; Sofikiti, N.; Baskakis, C.; Raptis, C. *Tetrahedron Lett.* **2004**, *45*, 5433–5436.
31. For the definition of the terminology *twin* and *twix*, see: Adam, W.; Bottke, N.; Krebs, O. *J. Am. Chem. Soc.* **2000**, *122*, 6791–6792.
32. Stratakis, M.; Orfanopoulos, M. *Tetrahedron* **2000**, *56*, 1595–1615.
33. Olah, G. A.; Arvanaghi, M. *Angew. Chem., Int. Ed. Engl.* **1981**, *20*, 878–879.

Regioselectivity in the ene-reaction of singlet oxygen with cyclic alkenes: photooxygenation of methyl-substituted 1,4-cyclohexadiene derivatives

Şengül Dilem Yardımcı, Nihal Kaya and Metin Balci*

Middle East Technical University, Department of Chemistry, 06531 Ankara, Turkey

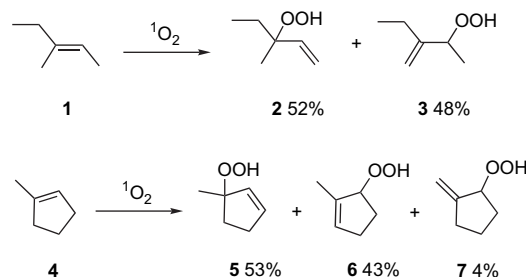
Received 10 July 2006; accepted 14 July 2006

Available online 18 September 2006

Abstract—The photooxygenation of the 1-methyl-, 2,3-dimethyl-, and 1,4-dimethylcyclohexa-1,4-dienes, which are readily available through Birch reduction, yielded the corresponding ene-products. The formed endocyclic dienes were trapped by the addition of singlet oxygen to give the corresponding bicyclic endoperoxy hydroperoxides. In the case of 1-methylcyclohexa-1,4-diene and 1,4-dimethylcyclohexa-1,4-diene, the cis-effect determined the product distribution. Photooxygenation of 2,3-dimethylcyclohexa-1,4-dienes gave mainly exocyclic olefin, which was attributed to the lowered rotational barrier of the methyl group and increased reactivity of the methyl groups. © 2006 Elsevier Ltd. All rights reserved.

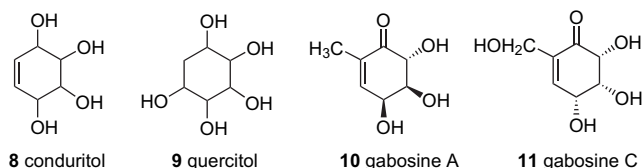
1. Introduction

Singlet oxygen is an important and reactive specie in oxidation reactions and has received remarkable attention by chemists.¹ It exhibits a diverse reactivity with organic unsaturated molecules, giving in particular [4+2] and [2+2] cycloaddition reactions.² Wherever an allylic hydrogen is available, an additional reaction channel forming a hydroperoxide is available: this is called the ene-reaction.³ The ene-reaction was originally discovered by Schenck in 1953.⁴ The ene-reaction has attracted major interest due to its controversial reaction mechanism and fascinating regiochemistry and stereochemistry. Various reaction mechanisms have been proposed, which vary from the concerted⁵ to non-concerted and include diradical,⁶ open-chain zwitterionic,⁷ and perepoxide⁸ intermediates. Perepoxide or exciplex intermediates have been proposed in some cases and a transition state in others.^{3c,9} The reaction of trisubstituted olefins with singlet oxygen gave products derived from the most substituted side of the olefin. For example, the photooxygenation of (*E*)-3-methylpent-2-ene (**1**) formed ene-products **2** and **3** (Scheme 1). These products are derived from the hydrogen abstraction from the side of the olefin with two substituents. This selectivity is referred to as the cis-effect.¹⁰ For the singlet oxygen reaction of cyclic alkenes; it was proposed that the geometry of the allylic hydrogen in the ground state determines the regioselectivity (Scheme 1).



Scheme 1.

The reaction of singlet oxygen with 1-methyl-cyclopent-1-ene (**4**) produced ene-products **5** and **6** where the proton abstraction took place from the allylic protons located in the five-membered ring.¹¹ The exocyclic olefin **7** was only formed in 4% yield. It has been proposed that the stabilizing effect by the interaction of singlet oxygen with two allylic hydrogens on the same side of the molecule during the formation of the perepoxide plays an important role in determining the regioselectivity.¹²



Keywords: Singlet oxygen; Endoperoxide; Hydroperoxide; Photooxygenation; Ene-reaction; Hydrocarbons.

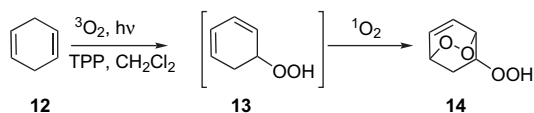
* Corresponding author. Tel.: +90 312 210 5140; fax: +90 312 210 3200; e-mail: mbalci@metu.edu.tr

As an extension of our work that is directed toward to the synthesis of highly hydroxylated cyclohexene derivatives

such as conduritols **8**, quercitols **9**,¹³ and gabosines **10/11**¹⁴ we were interested in the singlet oxygen ene-reaction of the methyl substituted 1,4-cyclohexadiene derivatives. Herein we report our results.

2. Results and discussions

Recently, we reported that the tetraphenylporphyrin-sensitized photooxygenation of 1,4-cyclohexadiene (**12**) resulted in the formation of the bicyclic endoperoxide **14**.¹⁵ The singlet oxygen first undergoes an ene-reaction to give **13**. The conjugated diene system in **13** is then easily trapped by a second mole of singlet oxygen to give isomeric **14**. Similar reactions have been observed by the reaction of singlet oxygen with isotetraline (Scheme 2).¹⁶



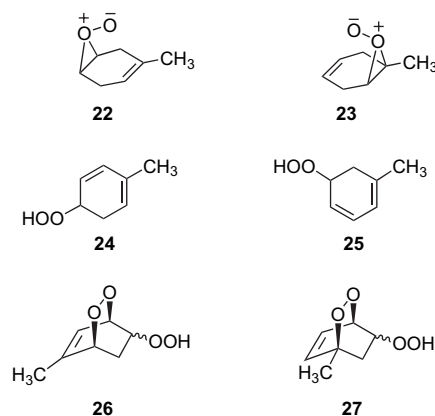
Scheme 2.

As the first reaction, 1-methylcyclohexa-1,4-diene (**15**)¹⁷ was reacted with singlet oxygen. Tetraphenylporphyrin-sensitized photooxygenation of **15** in methylene chloride at room temperature produced three bicyclic endoperoxides **16–18** and a monocyclic hydroperoxide **19** in a ratio of 3:1:2.5:2. The isolated endoperoxides are quite stable at room temperature for many days.

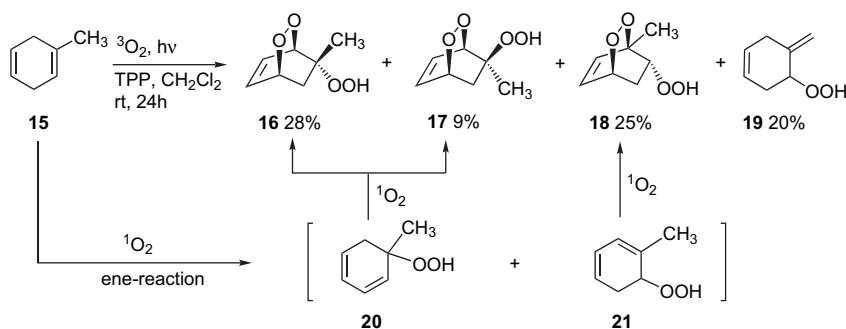
The structures of **16** and **17** were assigned by ¹H and ¹³C NMR spectra. The most conspicuous features in the ¹H NMR spectra of the endoperoxide **16** and **17** are the presence of double bond protons and two bridgehead protons along with one AB-system that corresponds to methylenic protons. This clearly indicates that the methyl group is attached to the carbon-atom bearing the hydroperoxide. The presence of two olefinic protons and one bridgehead proton in the ¹H NMR spectrum of **18** showed that the methyl group is attached to the bridgehead carbon atom. The structure of **19** was established based on the presence of four olefinic protons (two of them are methylenic) and two methylene groups with large geminal couplings ($J_{5a,5c}=21.0$ Hz, $J_{2a,2c}=20.1$ Hz) that indicate the location of these methylene groups between the double bonds.¹⁸ For the mechanism of the formation of these interesting endoperoxides containing

hydroperoxide groups, we assume that the 1,4-cyclohexadiene unit in **15** first undergoes an ene-reaction with the double bond activated methylene and methyl groups. The addition of singlet oxygen to diene units in **20** and **21** results in the formation of the isolated products **16–18**. The proposed intermediates **20** and **21** were not detected. Probably, the rate of the cycloaddition of singlet oxygen to the diene unit in **20** and **21** is most likely much faster than the rate of the ene-reaction with **15** (Scheme 3).

Because of the unsymmetrical arrangement of the double bonds in **15**, singlet oxygen can attack two double bonds. If the singlet oxygen would attack the sterically less crowded double bond, the perepoxide **22** would be formed, which would then rearrange to the hydroperoxides **24** and **25**. Trapping of the diene units in **24** and **25** would end up with the formation of the bicyclic endoperoxides **26** and **27**. However, careful analysis of the different fractions did not reveal the formation of any trace of the endoperoxides **26** and **27**. The structures of the isolated products clearly show that singlet oxygen exclusively attacks the higher substituted double bond in **15**.¹⁹



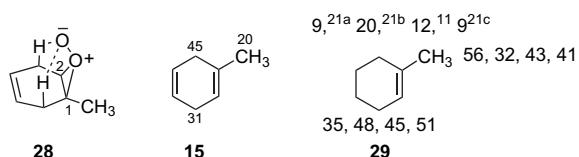
The site selection of singlet oxygen for the higher substituted double bond in **15** can be rationalized in terms of the electrophilic character of this species. The product distribution shows that the ratio of the products (**16**, **17**, and **18**), which were derived from the cis-effect to the product from the *anti*-side is 76:24, and in turn indicates that the more-substituted side of the double bond is more reactive. The formation of the perepoxide on the more-substituted side is



Scheme 3.

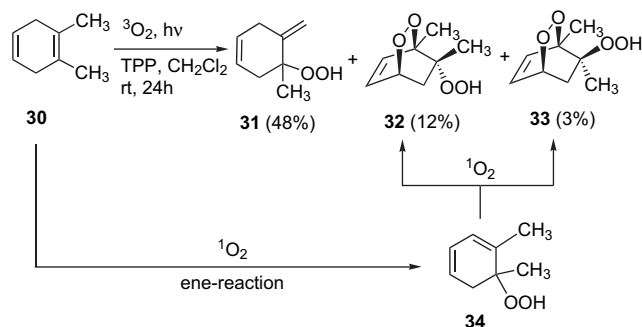
avored. Thus, the stabilizing interaction of oxygen with two allylic hydrogens on the same side of the double bond determines the mode of singlet oxygen attack to the double bond. Once the singlet oxygen has selected the favored face of the double bond by hydrogen bonding, it still has the choice for hydrogen abstraction between the two sides of two different allylic hydrogens.

Geminal selectivity was also observed in this case. The product distribution ratio was 45:31. The factors affecting the geminal regioselectivity have been studied by several groups.^{3b,3c,20} A methyl group can interact with the peroxide ring system (1,3-repulsion between the oxygen atom and methyl group) and lengthen the $^+O-C_1$ bond. As a consequence of this interaction the hydrogen abstraction from the end of the double bond bearing the methyl group will take place as shown in **28**.



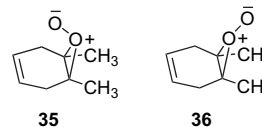
It is worth comparing the results of the photooxygenation of **15** with that of 1-methylcyclohexene (**29**). 1-Methylcyclohexene reacts with singlet oxygen and furnishes a mixture of three hydroperoxides, whereas the major product is the *exo*-cyclic alkene.²¹ Methylcyclohexene exhibits anti 'cis-effect' selectivity. The stabilizing interaction between the pendant oxygen and two allylic hydrogens is probably not the dominating interaction in **29**. This can be attributed to the unfavorable conformation of the molecule. Probably the conformation of 1,4-cyclohexadiene in **15** allows the orthogonal orientation of the allylic hydrogen to the double bond plane much better than in **29**.

Next, the 1,2-dimethylcyclohexa-1,4-diene (**30**)²² was submitted to the photooxygenation reaction under the same reaction conditions as described above. After the separation of the reaction mixture on silica gel, three peroxides **31**, **32**, and **33** were separated. The structures were determined by NMR spectral data. The major product was identified as the exocyclic ene-product **31**. The minor products **32** and **33** were formed by the ene-reaction of singlet oxygen with **30** followed by the [2+4] cycloaddition reaction of singlet oxygen with the primarily formed diene **34** (Scheme 4).



Scheme 4.

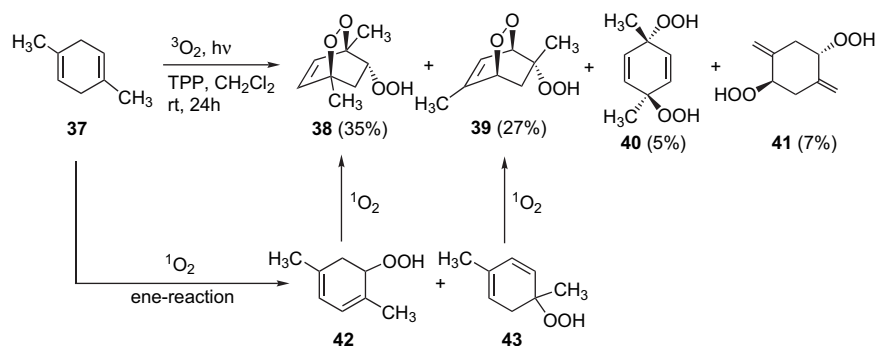
The structures of the products show that singlet oxygen exclusively attacks the more-substituted double bond. Any product derived from the attack of the less-substituted double bond was not detected. Singlet oxygen reacts with the tetrasubstituted double bond in **30** and forms two diastereomeric peroxides **35** and **36** as illustrated below.



Because of the symmetrical environment in **35** as well as in **36**, the pendant oxygen can abstract the allylic hydrogen from one of the neighboring allyl hydrogens and form the corresponding products **32** and **33**. The product distribution shows that the diastereoisomer **36** was formed as the major intermediate. Houk et al.^{12a} suggested that the barrier to rotate the allylic hydrogen to the perpendicular geometry desired for hydrogen abstraction determines the mode of singlet oxygen attack. Thus, the greater reactivity of the methyl groups of this molecule may arise from the relative ease of rotating one C–H bond on one of these methyls to the perpendicular conformation in the transition state. The presence of a second methyl group at the C-2 position in **30** most likely decreases the rotational barrier of the methyl group and increases their reactivity.

As the last compound, we searched the photooxygenation of 1,4-dimethylcyclohexa-1,4-diene (**37**).^{17a} We isolated four products **38–41**. Two of them were bicyclic endoperoxides **38** and **39**, which were formed by an ene-reaction followed by the [2+4] cycloaddition reaction of singlet oxygen. The diene **43** also undergoes an ene-reaction besides the cycloaddition reaction to form **40**. Singlet oxygen attacks the trisubstituted double bond in **43** and forms a *syn*-peroxide, which is responsible for the formation of **40**. The hydroperoxide **41** is derived from the formation of an *exo*-peroxide formed by the reaction of singlet oxygen with one of the double bonds in **37**. Based on the product distribution it can be easily rationalized that the major products are derived from the *endo*-peroxide (10:1). The reaction of singlet oxygen with dienes **30** and **37** clearly demonstrates that the position of the second methyl group in 1,4-cyclohexadiene unit has a dramatic effect on product distribution. In the case of **30** the products derived from the *exo*-peroxide were major (1:4); however, in the case of **37**, the major products are derived from the *endo*-peroxide (10:1). The product distribution is completely reversed. On the other hand, the product distribution of **37** resembles the product distribution from **15** as expected (Scheme 5).

In conclusion, the photooxygenation of three different methyl substituted cyclohexa-1,4-dienes shows complete side-selectivity. The more-substituted double bond is preferentially attacked. The cis-effect is mainly observed. In the case of 2,3-dimethylcyclohexa-1,4-diene **37** the major products are derived from the *exo*-peroxide. It has attributed to the lower rotational barrier of the methyl groups that in turn increases their reactivity. Further work with different substituents are currently under progress.



Scheme 5.

3. Experimental

3.1. General

Melting points are uncorrected. Infrared spectra were obtained from a solution in 0.1-mm cells or KBr pellets on a regular instrument. The ^1H and ^{13}C NMR spectra were recorded on 400 (100) MHz spectrometers. Apparent splitting is given in all cases. Column chromatography was performed on silica gel (60-mesh, Merck). TLC was carried out on Merck 0.2-mm silica gel 60 F₂₅₄ analytical aluminum plates. All of the substances reported in this paper are in their racemic form.

3.2. Photooxygenation of 1-methylcyclohexa-1,4-diene (15)

To a stirred solution of 1-methylcyclohexa-1,4-diene (15) (5.0 g, 53.14 mmol) in 500 mL of CH_2Cl_2 was added 85 mg of tetraphenylporphyrin (TPP). The resulting mixture was irradiated with a projection lamp (500 W) while oxygen was passed through solution, in which the mixture was stirred for 24 h at room temperature. The ^1H NMR spectrum of the mixture showed that the conversion was approximately 80% and the products 16, 17, 18, and 19 were formed in a ratio of 3:1:2.5:2, respectively (6.5 g). Evaporation of the solvent (30 °C, 20 mmHg) and chromatography of the residue on a silica gel column (200 g) eluting with hexane/ether (3:2) gave as the first fraction hydroperoxide 19, the second fraction a mixture of the endoperoxide 16 and 18, and as the third fraction 17, 16, and 18 were separated by crystallization from hexane/ether mixture. Pure samples were obtained by repeated column chromatography.

3.2.1. (1R(S),4S(R),5R(S))-5-Methyl-2,3-dioxabicyclo-[2.2.2]oct-7-en-5-yl hydroperoxide (16). Colorless solid, mp 108–109 °C from ether/hexane (28%); ^1H NMR (400 MHz, CDCl_3) δ 7.52 (br s, 1H, –OOH), 6.68 (quasi t, 2H, H₇ and H₈), 4.70 (m, 2H, H₁ and H₄), 2.10 (dd, A-part of AB-system, $^2J_{gem}=14.1$ Hz, $^3J_{1,6endo}=3.7$ Hz, 1H, H_{6endo}), 1.70 (s, 3H, –CH₃), 1.42 (dd, B-part of AB-system, $^2J_{gem}=14.1$ Hz, $^3J_{1,6exo}=1.9$ Hz, 1H, H_{6exo}). ^{13}C NMR (100 MHz, CDCl_3) δ 131.8, 130.7, 78.6, 75.7, 71.0, 36.5, 21.8. IR (KBr, cm^{-1}) 3339, 2979, 2935, 1368, 1105, 925, 707. Anal. Calcd for $\text{C}_7\text{H}_{10}\text{O}_4$: C, 53.16; H, 6.37. Found: C, 53.01; H, 6.51.

3.2.2. (1R(S),4S(R),5S(R))-5-Methyl-2,3-dioxabicyclo-[2.2.2]oct-7-en-5-yl hydroperoxide (17). Colorless liquid,

purity 95% (9%). ^1H NMR (400 MHz, CDCl_3) δ 8.17 (br s, 1H, –OOH), 6.60 (m, 2H, H₇ and H₈), 4.75 (m, 1H, H₄), 4.64 (m, 1H, H₁), 2.1 (dd, A-part of AB-system, $^2J_{gem}=14.2$ Hz, $^3J_{1,6endo}=4.1$ Hz, 1H, H_{6endo}), 1.45 (dd, B-part of AB-system, $^2J_{gem}=14.1$ Hz, $^3J_{1,6exo}=1.8$ Hz, 1H, H_{6exo}), 1.25 (s, 3H, CH₃). ^{13}C NMR (100 MHz, CDCl_3) δ 133.0, 130.9, 80.2, 74.9, 70.9, 35.2, 23.3. IR (KBr, cm^{-1}) 3402, 2976, 2930, 1369, 1103, 974, 762. Anal. Calcd for $\text{C}_7\text{H}_{10}\text{O}_4$: C, 53.16; H, 6.37. Found: C, 52.90; H, 6.49.

3.2.3. (1R(S),4S(R),5R(S))-4-Methyl-2,3-dioxabicyclo-[2.2.2]oct-7-en-5-yl hydroperoxide (18). Viscous liquid (25%). ^1H NMR (400 MHz, CDCl_3) δ 8.1 (br s, 1H), 6.66 (dd, A-part of AB-system, $J_{7,8}=8.3$ Hz, $J_{7,6}=6.1$ Hz, 1H, H₇), 6.21 (br d, B-part of AB-system, $J_{7,8}=8.3$ Hz, 1H, H₈), 4.65 (m, 1H, H₁), 4.32 (dd, $J_{5,6endo}=8.1$ Hz, $J_{5,6exo}=2.3$ Hz, 1H₅), 2.55 (ddd, A-part of AB-system, $^2J_{gem}=14.8$ Hz, $J_{5,6endo}=8.1$ Hz, $J_{1,6endo}=3.7$ Hz, 1H, H_{6endo}), 1.50 (s, 3H, –CH₃), 1.41 (dt, B-part of AB-system, $^2J_{gem}=14.8$ Hz, $J_{5,6exo}=J_{1,6exo}=2.2$ Hz, 1H, H_{6exo}). ^{13}C NMR (100 MHz, CDCl_3) δ 133.6, 133.1, 80.9, 76.0, 70.9, 31.6, 19.8. IR (KBr, cm^{-1}) 3403, 2979, 2940, 1432, 1381, 1105. Anal. Calcd for $\text{C}_7\text{H}_{10}\text{O}_4$: C, 53.16; H, 6.37. Found: C, 53.45; H, 6.56.

3.2.4. (1R(S))-6-Methylenecyclohex-3-en-1-yl hydroperoxide (19). Colorless liquid (20%), purity 95%. ^1H NMR (400 MHz, CDCl_3) δ 7.98 (s, 1H, –OOH), 5.62 (d, AB-system, $J_{3,4}=9.7$ Hz, 1H, H₃ or H₄), 5.54 (br d, B-part of AB-system, $J=9.9$ Hz, 1H, H₃ or H₄), 5.04 (s, 1H, C=CH₂), 5.0 (s, 1H, C=CH₂), 4.60 (t, $J_{1,2a}=J_{1,2}=4.6$ Hz, 1H, H₁), 2.96–2.75 (br, AB-system, $J_{5a,5e}=21.0$ Hz, 2H, H₅), 2.5–2.42 (m, AB-system, $J_{2a,2}=20.1$ Hz, 1H, H₂). ^{13}C NMR (100 MHz, CDCl_3) δ 142.6, 128.5, 126.6, 111.3, 83.3, 30.8, 21.6. IR (KBr, cm^{-1}) 3340, 2936, 1598, 1452, 1400, 1178, 1076.

3.3. Photooxygenation of 1,2-dimethylcyclohexa-1,4-diene (30)

To a stirred solution of 1,2-dimethylcyclohexa-1,4-diene (5.0 g, 46.25 mmol) in 500 mL of CH_2Cl_2 was added 75 mg of tetraphenylporphyrin (TPP). The resulting mixture was irradiated with a projection lamp (500 W) while oxygen was passed through solution, in which the mixture was stirred for 24 h at room temperature. The ^1H NMR spectrum of the mixture showed that the conversion was about 60% and the products 31 and 32/33 were formed in a ratio of 4:1 (4.06 g). Evaporation of the solvent (30 °C, 20 mmHg) and

chromatography of the residue on a silica gel column (200 g) eluting with hexane/ether (3:2) gave as the first fraction hydroperoxide **31**, and as the second fraction endoperoxide **32** and as the third fraction **33**. Pure samples were obtained by repeated column chromatography.

3.3.1. (1R(S),1-Methyl-6-methylenecyclohex-3-en-1-yl hydroperoxide (31). Viscous liquid (48%). ¹H NMR (400 MHz, CDCl₃) δ 7.75 (s, 1H, –OOH), 5.69 (br d, A-part of AB-system, *J*=9.8 Hz, 1H, C₃ or C₄), 5.45 (br d, B-part of AB-system, *J*=9.8 Hz, 1H, C₃ or C₄), 5.06 (s, 1H, –C=CH₂), 5.03 (s, 1H, –C=CH₂), 3.08 (br d, A-part of AB-system, *J*=18.4 Hz, 1H, H₅), 2.81 (br d, B-part of AB-system, *J*=18.4 Hz, 1H, H₅), 2.44 (br d, A-part of AB-system, *J*=21.3 Hz, 1H, H₂), 2.23 (br d, B-part of AB-system, *J*=21.3 Hz, 1H, H₂), 1.49 (s, 3H, –CH₃). ¹³C NMR (100 MHz, CDCl₃) δ 145.9, 126.0, 123.2, 110.1, 82.9, 37.4, 33.1, 21.5. IR (KBr, cm⁻¹) 3400, 3089, 3030, 2979, 2934, 1423, 1370, 912, 744. Anal. Calcd for C₈H₁₂O₂: C, 68.54; H, 8.63. Found: C, 68.01; H, 8.44.

3.3.2. (1R(S),4S(R),5R(S))-4,5-Dimethyl-2,3-dioxabicyclo-[2.2.2]oct-7-en-5-yl hydroperoxide (32). Viscous liquid (9%). ¹H NMR (400 MHz, CDCl₃) δ 7.5 (s, 1H, –OOH), 6.59 (dd, A-part of AB-system, *J*_{7,8}=8.3 Hz, *J*_{1,7}=6.1 Hz, 1H, H₇), 6.25 (dd, B-part of AB-system, *J*_{7,8}=8.31 Hz, *J*_{1,8}=1.4 Hz, 1H, H₈), 4.59 (m, 1H, H₁), 2.08 (dd, A-part of AB-system, *J*_{6,6'}=14.1 Hz, *J*_{1,6}=3.6 Hz, 1H, H₆), 1.74 (dd, B-part of AB-system, *J*_{6,6'}=14.1 Hz, *J*_{1,6}=2.1 Hz, 1H, H_{6'}), 1.52 (s, 3H, –CH₃), 1.37 (s, 3H, –CH₃). ¹³C NMR (100 MHz, CDCl₃) δ 134.8, 131.8, 81.7, 78.3, 71.4, 37.8, 18.9, 16.6. IR (KBr, cm⁻¹) 3421, 2988, 1452, 1380, 1124, 1082, 1059, 835, 748. Anal. Calcd for C₈H₁₂O₄: C, 55.81; H, 7.02. Found: C, 55.35; H, 7.01.

3.3.3. (1R(S),4S(R),5S(R))-4,5-Dimethyl-2,3-dioxabicyclo-[2.2.2]oct-7-en-5-yl hydroperoxide (33). Viscous liquid (3%). ¹H NMR (400 MHz, CDCl₃) δ 9.13 (s, 1H, –OOH), 6.70 (dd, A-part of AB-system, *J*_{7,8}=8.2 Hz, *J*_{1,7}=5.8 Hz, 1H, H₇), 6.25 (br d, B-part of AB-system, *J*_{7,8}=8.2 Hz, 1H, H₈), 4.76 (m, 1H, H₁), 2.97 (br d, A-part of AB-system, *J*_{6,6'}=14.2 Hz, 1H, H₆), 1.50 (d, B-part of AB-system, *J*_{6,6'}=14.2 Hz, 1H, H_{6'}), 1.45 (s, 3H, –CH₃), 1.19 (s, 3H, –CH₃). ¹³C NMR (100 MHz, CDCl₃) δ 135.1, 133.3, 82.9, 81.1, 71.9, 33.1, 24.1, 15.0. IR (KBr, cm⁻¹) 3392, 2984, 2940, 1371, 913, 745. Anal. Calcd for C₈H₁₂O₄: C, 55.81; H, 7.02. Found: C, 55.51; H, 7.23.

3.4. Photooxygenation of 1,4-dimethylcyclohexa-1,4-diene (37)

To a stirred solution of 1,4-dimethylcyclohexa-1,4-diene **37** (5.0 g, 46.25 mmol) in 500 mL of CH₂Cl₂ was added 75 mg of tetraphenylporphyrin (TPP). The resulting mixture was irradiated with a projection lamp (500 W) while oxygen was passed through solution, in which the mixture was stirred for 24 h at room temperature. The ¹H NMR spectrum of the mixture showed that the conversion was 70% and the products **38**, **39**, **40**, and **41** formed were in a ratio of 1.5:1.0:0.3:0.2, respectively (5.60 g). Evaporation of the solvent (30 °C, 20 mmHg) and chromatography of the residue on a silica gel column (200 g) eluting with hexane/ether (3:2) gave as the first fraction hydroperoxide **38**, the second

fraction the endoperoxide **39**, the third fraction **41**, and as the last fraction **40**.

3.4.1. (1R(S),4S(R),5R(S))-1,4-Dimethyl-2,3-dioxabicyclo-[2.2.2]oct-7-en-5-yl hydroperoxide (38). Colorless solid, mp 105–106 °C from ether/hexane (35%). ¹H NMR (400 MHz, CDCl₃) δ 8.1 (br s, 1H, –OOH), 6.49 (d, A-part of AB-system, *J*_{8,3}=8.3 Hz, 1H, H₇ or H₈), 6.26 (d, B-part of AB-system, *J*_{8,3}=8.3 Hz, 1H, H₈ or H₇), 4.42 (dd, *J*_{5,6}=8.1 Hz, *J*_{5,6'}=2.5 Hz, 1H, H₅), 2.40 (dd, A-part of AB-system, *J*_{gem}=14.0 Hz, *J*_{5,6}=8.1 Hz, 1H, H₅), 1.59 (s, 3H, CH₃), 1.58 (dd, B-part of AB-system, *J*_{gem}=14.0 Hz, *J*_{5,6'}=2.5 Hz, 1H), 1.42 (s, 3H, CH₃). ¹³C NMR (100 MHz, CDCl₃) δ 136.8, 132.4, 82.0, 75.5, 74.8, 37.3, 20.3, 18.9. IR (KBr, cm⁻¹) 3429, 2988, 2940, 2916, 1452, 1308, 1124, 1082, 1059, 835, 748. Anal. Calcd for C₈H₁₂O₄: C, 55.81; H, 7.02. Found: C, 55.42; H, 7.08.

3.4.2. (1R(S),4S(R),5R(S))-5,7-Dimethyl-2,3-dioxabicyclo-[2.2.2]oct-7-en-5-yl hydroperoxide (39). Viscous liquid, (20%). ¹H NMR (400 MHz, CDCl₃, acetone-*d*₆) δ 8.71 (s, 1H, –OOH), 6.25 (dq, *J*_{4,8}=6.7 Hz, ⁴*J*_{8,Me}=1.6 Hz, 1H, H₈), 4.72 (dd, *J*_{4,8}=6.7 Hz, *J*_{1,4}=0.8 Hz, 1H, H₄), 4.45 (br dd, *J*_{1,6}=4.0 Hz, *J*_{1,6'}=1.7 Hz, 1H, H₁), 2.10 (dd, A-part of AB-system, *J*_{gem}=14.1 Hz, *J*_{1,6}=4.0 Hz, 1H, H₆), 1.93 (d, *J*_{1,6}=1.6 Hz, 3H, –CH₃), 1.49 (dd, B-part of AB-system, *J*_{gem}=14.1 Hz, *J*_{1,6'}=1.7 Hz, 1H, H_{6'}), 1.27 (s, 3H, –CH₃). ¹³C NMR (100 MHz, acetone-*d*₆) δ 138.3, 119.0, 76.2, 71.2, 71.0, 19.1, 19.0, 14.1. IR (KBr, cm⁻¹) 3384, 2981, 2935, 1323, 1124, 913, 744. Anal. Calcd for C₈H₁₂O₄: C, 55.81; H, 7.02. Found: C, 55.47; H, 6.79.

3.4.3. 4-Hydroperoxy-2,5-dimethylenecyclohexyl hydroperoxide (40). Colorless solid, mp 123–124 °C from ether/hexane (7%). ¹H NMR (400 MHz, CDCl₃, acetone-*d*₆) 9.35 (s, 2H, –OOH), 5.04 (s, 2H, –C=CH₂), 4.99 (s, 2H, –C=CH₂), 4.4 (t, *J*_{1,2}=*J*_{1,2'}=3.1 Hz, 2H, H₁ and H₄), 2.61 (dd, A-part of AB-system, *J*_{gem}=14.6 Hz, *J*_{1,2}=3.1 Hz, 2H, H₂ and H₄ or (H_{2'} and H_{4'})), 2.15 (dd, B-part of AB-system, *J*_{gem}=14.6 Hz, *J*_{1,2'}=3.1 Hz, 2H, H_{2'} and H_{4'} or (H₂ and H₄)). ¹³C NMR (100 MHz, acetone-*d*₆) δ 136.1, 111.7, 80.3, 30.3. IR (KBr, cm⁻¹) 3342, 3028, 2990, 1404, 1061, 847, 787. Anal. Calcd for C₈H₁₂O₄: C, 55.81; H, 7.02. Found: C, 55.50; H, 6.70.

3.4.4. 4-Hydroperoxy-1,4-dimethylcyclohexa-2,5-dien-1-yl hydroperoxide (41). Colorless solid, mp 147–148 °C from ether/hexane (5%). ¹H NMR (400 MHz, acetone-*d*₆) δ 9.9 (s, 2H, –OOH), 5.89 (s, 4H, –CH=CH–), 1.24 (s, 6H, –CH₃). ¹³C NMR (100 MHz, acetone-*d*₆) δ 133.9, 77.9, 23.8. IR (KBr, cm⁻¹) 3331, 2930, 1429, 1057, 995, 931, 744. Anal. Calcd for C₈H₁₂O₄: C, 55.81; H, 7.02. Found: C, 55.17; H, 6.81.

Acknowledgements

The authors are indebted to TUBITAK (104T401), Middle East Technical University and TUBA (Turkish Academy of Sciences) for financial support.

References and notes

1. Wassermann, H. H.; Murray, R. W. *Singlet Oxygen*; Academic: New York, NY, 1979.

2. (a) Clennan, E. L.; Pace, A. *Tetrahedron* **2005**, *61*, 6665–6691; (b) Balci, M. *Chem. Rev.* **1981**, *81*, 91–108.
3. (a) Griesbeck, A. G.; El-Idreesy, T. T.; Adam, W.; Krebs, O. *Ene-reactions with Singlet Oxygen. CRC Handbook of Organic Photochemistry and Photobiology*, 2nd ed.; Horspool, W. M., Song, P.-S., Eds.; CRC: Boca Raton, FL, 2004; (b) Clennan, E. L. *Tetrahedron* **2000**, *56*, 9151–9179; (c) Stratakis, M.; Orfanopoulos, M. *Tetrahedron* **2000**, *56*, 1595–1615; (d) Prein, M.; Adam, W. *Angew. Chem., Int. Ed.* **1996**, *35*, 477–494; (e) Frimer, A. A.; Stephenson, L. M. *Singlet Oxygen. Reactions, Modes and Products*; Frimer, A. A., Ed.; CRC: Boca Raton, FL, 1985; (f) Wasserman, H. H.; Ives, J. L. *Tetrahedron* **1981**, *37*, 1825–1852; (g) Foote, C. S.; Wexler, S. *J. Am. Chem. Soc.* **1964**, *86*, 3979–3981.
4. Schenck, G. O.; Eggert, H.; Denk, W. *Liebigs Ann. Chem.* **1953**, *584*, 177–198.
5. Gorman, A. A. *Chem. Soc. Rev.* **1981**, *10*, 205–231.
6. Harding, L. B.; Goddard, W. A. *J. Am. Chem. Soc.* **1980**, *102*, 439–449.
7. Jefford, C. W. *Tetrahedron Lett.* **1979**, *20*, 985–988.
8. Stephenson, L. M.; Grdina, M. B.; Orfanopoulos, M. *Acc. Chem. Res.* **1980**, *13*, 419–425.
9. (a) Singleton, D. A.; Hang, C.; Szymanski, M. J.; Meyer, M. P.; Leach, A. G.; Kuwata, K. T.; Chen, J. S.; Greer, A.; Foote, C. S.; Houk, K. N. *J. Am. Chem. Soc.* **2003**, *125*, 1319–1328; (b) Maranzana, A.; Canepa, C.; Ghigo, G.; Tonachini, G. *Eur. J. Org. Chem.* **2005**, 3643–3649; (c) Sevin, F.; McKee, M. L. *J. Am. Chem. Soc.* **2001**, *123*, 4591–4600.
10. (a) Orfanopoulos, M.; Grdina, M. B.; Stephenson, L. M. *J. Am. Chem. Soc.* **1979**, *101*, 275–276; (b) Schulte-Elte, K. H.; Rautestrauch, V. *Helv. Chim. Acta* **1978**, *61*, 2777–2783.
11. Schulte-Elte, K. H.; Rautestrauch, V. *J. Am. Chem. Soc.* **1980**, *102*, 1738–1740.
12. (a) Houk, K. N.; Williams, P. A.; Mitchell, P. A.; Yamaguchi, K. *J. Am. Chem. Soc.* **1981**, *103*, 949–950; (b) Foote, C. S. *Acc. Chem. Res.* **1968**, *1*, 104–109; (c) Hurst, J. R.; Wilson, S. L.; Schuster, G. B. *Tetrahedron* **1985**, *41*, 2191–2195.
13. (a) Balci, M.; Sütbeyaz, Y.; Seçen, H. *Tetrahedron* **1990**, *46*, 3715–3742; (b) Balci, M. *Pure Appl. Chem.* **1997**, *69*, 97–104; (c) Gültekin, M. S.; Celik, M.; Balci, M. *Curr. Org. Chem.* **2004**, *8*, 1159–1186.
14. (a) Tang, Y.-Q.; Maul, C.; Höfs, R.; Sattler, I.; Grabley, S.; Feng, X.-Z.; Zeeck, A.; Thriecke, R. *Eur. J. Org. Chem.* **2000**, 149–153; (b) Bach, G.; Breiding-Mack, S.; Grabley, S.; Hammann, P.; Huetter, K.; Thiericke, R.; Uhr, H.; Wink, J.; Zeeck, A. *Liebigs Ann. Chem.* **1993**, 241–250.
15. (a) Secen, H.; Salamci, E.; Sutbeyaz, Y.; Balci, M. *Synlett* **1993**, 609–610; (b) Salamci, E.; Secen, H.; Sutbeyaz, Y.; Balci, M. *J. Org. Chem.* **1997**, *62*, 2453–2457.
16. (a) Gollnick, K. *Adv. Photochem.* **1968**, *6*, 1–122; (b) Kishali-Horasan, N.; Sahin, E.; Kara, Y. *Org. Lett.* **2006**, *8*, 1791–1793.
17. (a) Banwell, M. G.; Halton, B. *Aust. J. Chem.* **1980**, *33*, 2673–2683; (b) Altundas, A.; Menzek, A.; Demirci-Gultekin, D.; Karakaya, M. *Turk. J. Chem.* **2005**, *29*, 513–518.
18. Balci, M. *Basic ¹H- and ¹³C-NMR Spectroscopy*; Elsevier: Amsterdam, 2005.
19. For very similar regioselectivity see: Linker, T.; Fröhlich, L. *J. Am. Chem. Soc.* **1995**, *117*, 2694–2697.
20. (a) Clennan, E. L.; Chen, X.; Koola, J. J. *J. Am. Chem. Soc.* **1990**, *112*, 5193–5199; (b) Orfanopoulos, M.; Stratakis, M.; Elemes, Y. *J. Am. Chem. Soc.* **1990**, *112*, 6417–6418; (c) Adam, W.; Bottke, N.; Krebs, O.; Lykakis, I.; Orfanopoulos, M.; Stratakis, M. *J. Am. Chem. Soc.* **2002**, *124*, 14403–14409; (d) Ensley, H. E. *Reactions of Singlet Oxygen with α,β -Unsaturated Carbonyl Compounds 2*; Baumstark, A. L., Ed.; JAI: Greenwich, Connecticut, CT, 1990; pp 181–202.
21. (a) Chen, Y.-Z.; Wu, L.-Z.; Zhang, L.-P.; Tung, C.-H. *J. Org. Chem.* **2005**, *70*, 4676–4681; (b) Griesbeck, A. G.; Bartoschek, A. *Chem. Commun.* **2002**, 1594–1595.
22. Huckel, W.; Worffel, U. *Chem. Ber.* **1955**, *88*, 338–345.

Auxiliary controlled singlet-oxygen ene reactions of cyclohexenes

Werner Fudickar, Katja Vorndran and Torsten Linker*

Department of Chemistry, University of Potsdam, Karl-Liebknecht-Str. 24-25, 14476 Potsdam/Golm, Germany

Received 18 May 2006; revised 13 July 2006; accepted 14 July 2006

Available online 25 September 2006

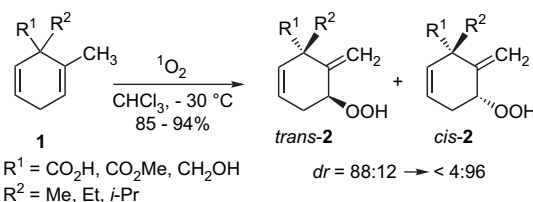
Abstract—The photooxygenation of homochiral cyclohexene ketals, which are easily available from 2-cyclohexenone and L-tartrates, affords hydroperoxides and after reduction the corresponding allylic alcohols in good yields and high regioselectivities. This can be rationalized by electronic repulsions in a perepoxide intermediate and provides evidence for unfavorable 1,3 diaxial interactions with a dioxolane oxygen atom. Only low stereoselectivities were observed, due to the flexibility of the cyclohexene ring. However, the diastereomers could be separated and after cleavage of the auxiliary, 4-hydroxy-2-cyclohexen-1-one was isolated in enantiomerically pure form, which can serve as a building block for natural product synthesis.

© 2006 Elsevier Ltd. All rights reserved.

1. Introduction

Singlet oxygen ($^1\text{O}_2$), which can be conveniently generated by the sensitized photoreaction of molecular oxygen with visible light (photooxygenation), has become an important reagent for the synthesis of oxyfunctionalized products from simple precursors.¹ Especially the ene reaction of $^1\text{O}_2$ with alkenes provides a powerful route to allylic hydroperoxides and after reduction to allylic alcohols. The regioselectivity of this transformation was studied in detail during the last years² and more recently, the selectivities were improved by reactions in zeolites or polymeric containers.³ Singlet-oxygen ene reactions with high diastereoselectivities are based on the pioneering work of Adam.⁴ More recently, auxiliary controlled⁵ and even organocatalytic⁶ enantioselective photooxygenations were realized. Finally, singlet oxygen was applied for reversible light- and air-driven lithography.⁷

Although the singlet-oxygen ene reaction of five- and seven-membered cycloalkenes proceeds with high regioselectivity, the photooxygenation of cyclohexenes affords hydroperoxides with only moderate yield and selectivities.^{2,8} During our work on synthetic applications of singlet oxygen,⁹ we found excellent regio- and high diastereoselectivities in the photooxygenation of cyclohexadienes **1** to afford hydroperoxides **2** (Scheme 1).



Scheme 1. Photooxygenations of the cyclohexadienes **1**.

Furthermore, the reactions are strongly controlled by steric and polar factors and especially carboxylic acids and esters provide high selectivities. This prompted us to investigate chiral auxiliaries with such functional groups in photooxygenations. Commercially available tartaric acid and esters seemed to be the ideal candidates, since they are often used in asymmetric synthesis.¹⁰ Herein we report our results on the singlet-oxygen ene reaction of homochiral cyclohexene ketals, in view of regio- and stereoselectivities as well as synthetic applications.

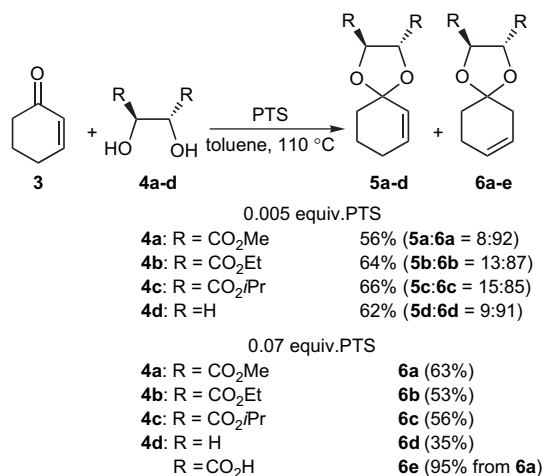
2. Results and discussion

Homochiral ketals can be conveniently prepared by the reaction of a ketone with a chiral diol by azeotropic removal of water.^{10a,11} However, the ketalization of cyclic enones with simple diols might proceed under migration of the double bond, due to the acidic conditions.¹² Indeed, the reaction of 2-cyclohexenone (**3**) with commercially available tartrates **4a–c** or glycol (**4d**) and catalytic amounts of *p*-toluenesulfonic acid (PTS) afforded mixtures of 2-cyclohexene ketals **5a–d** and the rearranged 3-cyclohexene ketals **6a–d** in moderate yields (Scheme 2). Unfortunately, the regioisomers **5** and **6** could not be separated by column

Keywords: Singlet oxygen; Auxiliary control; Regioselectivity; Stereoselectivity.

* Corresponding author. Tel.: +49 331 9775212; fax: +49 331 9775056; e-mail: linker@chem.uni-potsdam.de

chromatography. Therefore, we developed a new procedure for the selective synthesis of the rearranged products by simply increasing the amount of *p*-toluenesulfonic acid (PTS). Under such conditions, the desired 3-cyclohexene ketals **6a–c** were isolated in moderate yields in analytically pure form (Scheme 2). Thus, this one-pot procedure is superior to the literature-known process by a two-step elimination.¹³



Scheme 2. Synthesis of the cyclohexene acetals **6**.

On the other hand, the 2-cyclohexene ketal **5a**, where the double bond is closer to the stereogenic centers, was selectively obtained by a multi-step procedure.¹⁴ To investigate the influence of polar groups, the free dicarboxylic acid **6e** was synthesized by saponification of the methylester **6a** in 95% yield (Scheme 2).

For the ene reactions, singlet oxygen (¹O₂) was conveniently generated at –30 °C from molecular oxygen by irradiation with a sodium lamp in the presence of catalytic amounts of tetraphenylporphin (TPP) as sensitizer (photooxygenations). To establish the influence of the ketal auxiliaries, 2-cyclohexenone (**3**) was employed as substrate for the first photooxygenations. However, even after prolonged irradiation for several days no conversion could be achieved, which can be rationalized by the electron poor double bond. Another explanation for the failure of the singlet-oxygen ene reaction might be the unfavorable conformation of 2-cyclohexenone (**3**). To distinguish between these two effects, the reaction of 2-cyclohexene ketal **5a** was examined next. Furthermore, this substrate should provide higher stereoselectivities than the regioisomer **6a**, since the double bond is located closer to the stereogenic centers. Unfortunately, again no conversion was achieved, which speaks for a preferred conformation of the 2-cyclohexene ketal **5a** with pseudo-equatorial allylic hydrogen atoms, which cannot undergo an ene reaction (Fig. 1).

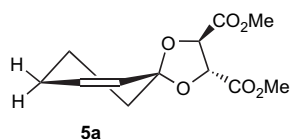


Figure 1. Preferred conformation of the 2-cyclohexene acetal **5a**.

This result is in accordance with our previous studies on the photooxygenation of cyclohexadienes,⁹ which don't react at the bisallylic position (Scheme 1) and points out the importance of pseudo-axial oriented hydrogen atoms in singlet-oxygen ene reactions.

Therefore, the photooxygenations were carried out with the 3-cyclohexene ketals **6a–e**. Indeed, the reactions proceeded smoothly with tetraphenylporphin (TPP) as sensitizer at –30 °C (Table 1). Complete conversion was achieved after 2–4 d and the labile hydroperoxides were directly reduced by dimethylsulfide. To determine the product ratios, ¹H NMR spectra (500 MHz) were directly recorded on the crude reaction mixtures after evaporation of the solvents. Finally, the corresponding allylic alcohols **7** and **8** were isolated in good overall yields by column chromatography (Table 1).

The first photooxygenations were conducted with ketals **6a–c**, derived from chiral tartrates **4a–c** (Table 1, entries 1–3). Interestingly, a high degree of regioselectivity from 81:19 to 89:11 was observed for all substrates. Thus, the allylic alcohols **7a–c** were isolated as main products in good yields. This result is in contrast to the singlet-oxygen ene reaction of substituted cyclohexenes, which afford hydroperoxides with only moderate yield and selectivities.^{2,8} To exclude an influence of the stereogenic centers of the chiral auxiliaries, the achiral ketal **6d** was photooxygenated next (entry 4). Indeed, the same degree of regioselectivity was observed, which can only be rationalized by repulsive interactions of the attacking ¹O₂ with the dioxolane ring. Four different allylic hydrogen atoms are available for the ene reaction and thus four perepoxide intermediates **9** can be discussed (Fig. 2).

The importance of pseudo-axial oriented hydrogen atoms in the singlet-oxygen ene reaction was already pointed out in

Table 1. Photooxygenations of the 3-cyclohexene ketals **6**

Entry	Ketal	R	7:8 ^a	dr 7 ^a	dr 8 ^a	Yield (%) ^b
1	6a	CO ₂ Me	82:18	57:43	62:38	75
2	6b	CO ₂ Et	81:19	53:47	55:45	75
3	6c	CO ₂ <i>i</i> -Pr	89:11	54:46	n.d.	73
4	6d	H	87:13	—	—	77
5	6e	CO ₂ H	n.d.	n.d.	n.d.	<10 ^c
6	6e	CO ₂ H ^d	>95:5	52:48	n.d.	^e
7	6e	CO ₂ ^f	>95:5	56:44	n.d.	^e

^a Ratios determined (dr=diastereomeric ratio) by ¹H NMR analysis of the crude product (500 MHz).

^b Yield of isolated allylic alcohols. Main isomers were separated by column chromatography in analytically pure form.

^c Low yield is due to cleavage of the ketal under the acidic conditions.

^d Addition of tetra-*n*-butylammonium hydroxide as base.

^e Products **7e** were not isolated but are identical to saponified **7a**.

^f Deprotonation with 4 equiv of NaOCD₃, reaction in CD₃OD with rose bengal as sensitizer.

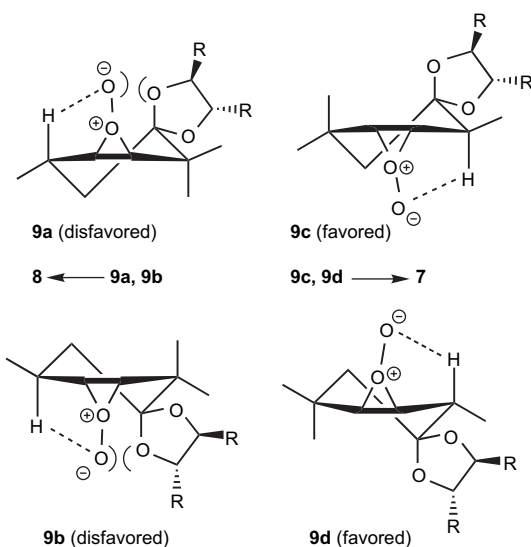


Figure 2. Four possible pereperoxide intermediates **9**.

Figure 1. If the remote allylic position reacts (Fig. 2, pereperoxides **9a** and **9b**), an unfavorable 1,3 diaxial interaction between the negatively charged pereperoxide and one dioxolane oxygen atom results, irrespective of the attack of $^1\text{O}_2$ from the top or bottom of the double bond. Both intermediates afford the regioisomers **8**, which are therefore formed only as side products. On the other hand, if the allylic position adjacent to the ketal reacts (Fig. 2, pereperoxides **9c** and **9d**), no unfavorable 1,3 diaxial interactions are operative and the regioisomers **7** are obtained as the main products.

This result is in accordance with the large group effect,² and very recently steric interactions between $^1\text{O}_2$ and a pseudo-axial methyl group were discussed during the photooxygenation of cyclogeranyl derivatives.¹⁵ However, the herein investigated ketal auxiliaries increase the unfavorable 1,3 diaxial interactions by severe electronic repulsions between the pereperoxide and one dioxolane oxygen atom and thus control the regioselectivity of the singlet-oxygen ene reaction.

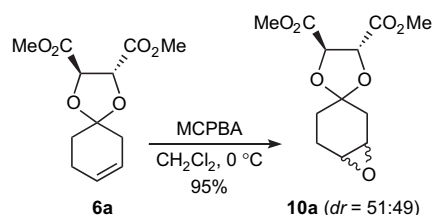
Besides the high regioselectivities, only low stereoselectivities were observed for the chiral esters **6a–c** (Table 1, entries 1–3). The diastereomeric ratios could be determined from the crude products by ^1H NMR spectroscopy (500 MHz) and all isomers showed distinctive chemical shifts. Furthermore, a separation and complete characterization of the main products was possible by column chromatography. Thus, the major diastereomers of the allylic alcohols **7** always have the *S* configuration at the newly formed stereogenic center, which was established by cleavage of the chiral auxiliary (see below). However, because of the low selectivities, an explanation and discussion for the formation of these isomers in excess is not possible.

To increase the stereoselectivities, the free dicarboxylic acid **6e** was photooxygenated next, since strong directing effects of such functional groups were found in the singlet-oxygen ene reaction in our previous studies.⁹ However, the acidic reaction conditions led to the cleavage of the chiral auxiliary (Table 1, entry 5). To overcome this problem, bases were

added to the reaction mixture. Indeed, an increase in the regioselectivity resulted due to the stronger 1,3 diaxial polar repulsions, but no influence on the diastereoselectivity was observed (entries 6 and 7).

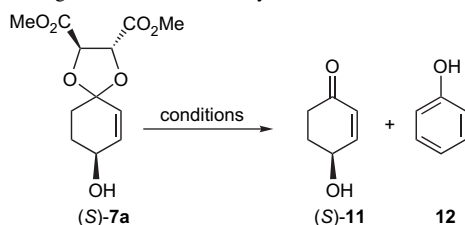
Obviously, the homochiral cyclohexene ketals **6** are too flexible (compare different structures in Fig. 2) to prefer one conformation and induce a high stereoselectivity. Furthermore, the chiral auxiliary is too far away from the newly formed stereogenic center and thus, only a 1,6 induction results. This is in accordance with a somewhat higher stereoselectivity for the minor regioisomer **8a** (Table 1, entry 1), which is formed by a 1,5 induction. The best substrates for a stereoselective photooxygenation would be the 2-cyclohexene ketals **5**, since the double bond is located closer to the chiral auxiliaries. Indeed, alkene **5a** exhibits a higher stereoselectivity in cyclopropanations than the corresponding isomer **6a**.^{13,14} Unfortunately, the 2-cyclohexene ketal **5a** does not undergo a singlet-oxygen ene reaction, due to the pseudo-equatorial allylic hydrogen atoms (Fig. 1).

To compare steric and polar interactions in the oxidation of 3-cyclohexene ketal **6a**, we became interested in the epoxidation with *m*-chloroperbenzoic acid (MCPBA). The reaction proceeded smoothly at 0 °C and the epoxides **10a** were isolated in high yield (Scheme 3). However, both diastereomers were obtained in a ratio of almost 1:1. Thus, the photooxygenation of ketal **6a** proceeds with a higher selectivity, although MCPBA is sterically more demanding than singlet oxygen. This interesting result is a further proof of the importance of polar interactions in the pereperoxide intermediates **9**, leading to stereoselectivities of up to 57:43 for a 1,6 induction.



Scheme 3. Epoxidation of the 3-cyclohexene acetal **6a**.

From the synthetic point of view, it was important that the major allylic alcohols **7** could be conveniently separated by column chromatography and were isolated in diastereomerically and analytically pure form. The absolute configuration of the newly formed stereogenic center could not be established by the coupling constants or NOE effects. Therefore, we examined the cleavage of the chiral auxiliary from the ketal **7a** (Table 2), to afford 4-hydroxy-2-cyclohexen-1-one (**11**), which is literature-known.¹⁶ However, the lability of the desired product under the acidic reaction conditions was problematic. Thus, cleavage with diluted hydrochloric acid led to the elimination of water and formation of phenol (**12**) as the main product (entry 1). After optimization of the reaction conditions, the best results were obtained with buffered clay, which afforded 4-(*S*)-hydroxy-2-cyclohexen-1-one (**11**) in high yield (Table 2, entry 3). The *S* configuration was unequivocally determined by comparison of the optical rotations and thus the major diastereomers **7** have the same absolute configuration. Finally, from 2-cyclohexenone, the

Table 2. Cleavage of the chiral auxiliary from ketal *S*-7a

Entry	Conditions	Conv. (%)	11 (%)	12 (%)
1	MeOH, dil HCl	>98	32	64
2	Montmorillonite	>98	70	18
3	Montmorillonite, NaOAc	76	74 (97) ^a	—

^a Yield based on reisolated starting material.

auxiliary controlled singlet-oxygen ene reaction offers an easy access to the enantiomerically pure ketone **11**, which can serve as a precursor for natural product synthesis.¹⁶

3. Conclusions

Homochiral cyclohexene ketals were conveniently synthesized from 2-cyclohexenone and L-tartrates. Under the acidic reaction conditions an isomerization of the double bond was observed, which afforded 3-cyclohexene ketals regioselectively. The singlet-oxygen ene reactions proceeded smoothly at -30°C and the corresponding allylic alcohols were isolated in good yields after reduction. All reactions exhibited a high degree of regioselectivity, which can be rationalized by electronic repulsions in a perepoxide intermediate and gives evidence for unfavorable 1,3 dipolar interactions with a dioxolane oxygen atom. On the other hand, the photo-oxygenations proceeded with low stereoselectivities, due to the flexibility of the cyclohexene ring. However, compared with the epoxidation of the homochiral cyclohexene ketals, the singlet-oxygen ene reaction provided higher stereoselectivities by a 1,6 induction. The isomeric allylic alcohols could be separated by column chromatography and the major diastereomers were isolated in analytically pure form. Finally, the *S* configuration of the newly formed stereogenic center was unequivocally established by cleavage of the chiral auxiliary with clay in high yield. In summary, starting from 2-cyclohexenone, the auxiliary controlled singlet-oxygen ene reaction offers an easy access to an enantiomerically pure hydroxycyclohexenone, which can serve as a precursor for natural product synthesis.

4. Experimental

4.1. General

Commercially available compounds were used without further purification; solvents were dried according to standard procedures. Flash chromatography was performed using Merck Kieselgel 60 silica. TLC analysis was carried out on Alugram silica gel 60 F₂₅₄ plates (Macherey-Nagel). Molybdatophosphate was used as developing reagent. NMR spectra were measured on a Bruker AC 300 (300 MHz) and AC 500 (500 MHz) spectrometers using deuteriochloroform (CDCl₃), deuterodimethylsulfoxide (DMSO-*d*₆) or

deuteromethanol (CD₃OD) as internal standard. IR spectra were recorded on a Perkin–Elmer 1600 FT-IR and optical rotations on a JASCO P-1020 polarimeter. Elemental analyses were performed on a Vario El 3 instrument (Elementar).

4.2. General procedure for the ketalizations

A solution of 2-cyclohexenone (**3**) (4 g, 42 mmol), the diol (42 mmol), and *p*-toluenesulfonic acid (0.5 g, 2.9 mmol, 0.07 equiv) in dry toluene (200 mL) was refluxed by using a Dean–Stark trap for 8 h. After cooling the reaction mixture was washed with a saturated aqueous solution of NaHCO₃ (100 mL) followed by washing with water (100 mL). After drying (MgSO₄) the solvent was evaporated and the crude product was purified by flash chromatography.

4.2.1. Dimethyl 1,4-dioxaspiro[4,5]dec-7-ene-2(R),3(R)-dicarboxylate (6a). The ketalization was carried out as described above using dimethyl L-tartrate (**4a**) (7.4 g, 42 mmol) to afford after chromatography (hexane/ethyl acetate=3:1, *R_f*=0.43) a colorless oil (6.65 g, 63%).

¹H NMR (300 MHz, CDCl₃) δ 1.84 (t, *J*=6.3 Hz, 1H, 10-H), 2.26–2.50 (m, 4H, 6-H, 9-H), 3.82 (s, 6H, Me), 4.84 (d, *J*=5.0 Hz, 1H, 2-H), 4.88 (d, *J*=5.0 Hz, 1H, 3-H), 5.58–5.62, 5.69–5.74 (2dm, *J*=10 Hz, 2H, 7-H, 8-H); ¹³C NMR (75 MHz, CDCl₃) δ 24.4 (t, C-10), 31.6 (t, C-6), 36.2 (t, C-9), 52.8, 52.8 (2q, Me), 76.9, 77.1 (2d, C-2, C-3), 113.6 (s, C-5), 123.6 (d, C-7), 126.4 (d, C-8), 170.1, 170.4 (2s, COOMe); IR (film) 3034, 2976, 2945, 1765, 1478, 1372, 1237, 1047, 857, 759, 662 cm⁻¹; [α]_D²⁰ -43.2 (c 1.02, CHCl₃). Anal. Calcd for C₁₂H₁₆O₆: C, 56.25; H, 6.29. Found: C, 56.58; H, 6.61.

4.2.2. Diethyl 1,4-dioxaspiro[4,5]dec-7-ene-2(R),3(R)-dicarboxylate (6b). The ketalization was carried out as described above using diethyl L-tartrate (**4b**) (8.6 g, 42 mmol) to afford after chromatography (hexane/ethyl acetate=3:1, *R_f*=0.51) a colorless oil (6.2 g, 53%).

¹H NMR (300 MHz, CDCl₃) δ 1.33 (t, *J*=7.1 Hz, 6H, CH₃), 1.86 (t, *J*=6.2 Hz, 1H, 10-H), 2.26–2.48 (m, 4H, 6-H, 9-H), 4.28 (q, *J*=7.1 Hz, 4H, CH₂CH₃), 4.80 (d, *J*=5.0 Hz, 1H, 2-H), 4.85 (d, *J*=5.0 Hz, 1H, 3-H), 5.61, 5.72 (2dm, *J*=10 Hz, 2H, 7-H, 8-H); ¹³C NMR (75 MHz, CDCl₃) δ 14.1, 14.1 (2q, CH₃), 24.4 (t, C-10), 31.6 (t, C-6), 36.3 (t, C-9), 61.8, 61.9 (2t, CH₂CH₃), 77.0, 77.2 (2d, C-2, C-3), 113.4 (s, C-5), 123.6 (d, C-7), 126.4 (d, C-8), 169.7, 169.9 (2s, COOEt); IR (film) 3030, 2981, 2934, 1759, 1448, 1371, 1218, 1137, 1047, 943, 857, 753, 662 cm⁻¹; [α]_D²⁰ -44.9 (c 1.07, CHCl₃). Anal. Calcd for C₁₄H₂₀O₆: C, 59.14; H, 7.09. Found: C, 59.33; H, 7.27.

4.2.3. Diisopropyl 1,4-dioxaspiro[4,5]dec-7-ene-2(R),3(R)-dicarboxylate (6c). The ketalization was carried out as described above using diisopropyl L-tartrate (**4c**) (9.8 g, 42 mmol) to afford after chromatography (hexane/ethyl acetate=3:1, *R_f*=0.67) a colorless oil (7.3 g, 56%).

¹H NMR (300 MHz, CDCl₃) δ 1.29 (d, *J*=6.2 Hz, 12H, CH₃), 1.83 (m, 1H, 10-H), 2.24–2.53 (m, 4H, 6-H, 9-H), 4.71 (d, *J*=5.2 Hz, 1H, 2-H), 4.78 (d, *J*=5.2 Hz, 1H, 3-H), 5.12 (sept, *J*=6.2 Hz, 2H, CH(CH₃)₂), 5.56, 5.64

(2dm, $J=9.9$ Hz, 2H, 7-H, 8-H); ^{13}C NMR (75 MHz, CDCl_3) δ 21.6, 21.6, 21.7, 21.7 (4q, CH_3), 24.5 (t, C-10), 31.7 (t, C-6), 36.4 (t, C-9), 69.6, 69.7 (2d, $\text{CH}(\text{CH}_3)_2$), 77.2, 78.0 (2d, C-2, C-3), 113.4 (s, C-5), 123.7 (d, C-7), 126.4 (d, C-8), 169.3, 169.5 (2s, $\text{COO}i\text{-Pr}$); IR (film) 3030, 2981, 2935, 1753, 1467, 1376, 1220, 1107, 751, 657 cm^{-1} ; $[\alpha]_{\text{D}}^{20}$ -38.0 (c 0.98, CHCl_3). Anal. Calcd for $\text{C}_{16}\text{H}_{24}\text{O}_6$: C, 61.52; H, 7.74. Found: C, 61.77; H, 7.68.

4.2.4. 1,4-Dioxa-spiro[4,5]dec-7-ene (6d). The ketalization was carried out as described above using ethylene glycol (**4d**) (2.6 g, 42 mmol) to afford after chromatography (hexane/ethyl acetate=3:1, $R_f=0.60$) a colorless oil (2.1 g, 35%).

^1H NMR (300 MHz, CDCl_3) δ 1.51 (t, $J=6.4$ Hz, 2H, 10-H), 1.98–2.06 (m, 4H, 6-H, 9-H), 3.72–3.75 (m, 4H, 2-H, 3-H), 5.36, 5.47 (2dm, $J=9.7$ Hz, 2H, 7-H, 8-H); ^{13}C NMR (75 MHz, CDCl_3) δ 24.7 (t, C-10), 31.2 (t, C-6), 35.9 (t, C-9), 64.4 (2t, C-2, C-3), 107.8 (s, C-5), 124.4 (d, C-7), 126.4 (d, C-8). IR (KBr) 3026, 2925, 1653, 1476, 1432, 1388, 1361, 1335, 1262, 1221, 1172, 1114, 1058, 1027, 948, 850 cm^{-1} . Anal. Calcd for $\text{C}_8\text{H}_{12}\text{O}_2$: C, 68.55; H, 8.63. Found: C, 68.03; H, 9.16.

4.2.5. 1,4-Dioxa-spiro[4,5]dec-7-ene-2(R),3(R)-dicarboxylic acid (6e). To a solution of the methylester **6a** (300 mg, 1.1 mmol) in methanol (10 mL) was added NaOH (360 mg, 9 mmol) dissolved in water (2 mL). After refluxing for 6 h the solvent was evaporated and water (20 mL) and diethyl ether (20 mL) were added. After separation the aqueous phase was acidified with 1 M aqueous HCl and extracted three times with diethyl ether. The combined ether extracts were washed with water, dried (MgSO_4), and the solvent was removed to afford the carboxylic acid **6e** as a yellow solid (240 mg, 95%); mp 114 °C.

^1H NMR (500 MHz, $\text{DMSO}-d_6$) δ 1.79–1.88 (m, 2H, 10-H), 2.16–2.51 (m, 4H, 6-H, 9-H), 4.81, 4.82 (2d, $J=9.2$ Hz, 2H, 2-H, 3-H), 5.45–5.50 (m, $J=11.6$ Hz, 1H, 8-H), 5.65–5.7 (m, $J=11.6$ Hz, 1H, 7-H); ^{13}C NMR (125 MHz, $\text{DMSO}-d_6$) δ 25.1 (t, C-9), 32.3 (t, C-10), 37.1 (t, C-6), 77.4, 77.6 (2d, C-2, C-3), 112.8 (s, C-5), 124.4 (d, C-7), 127.1 (d, C-8), 172.0, 172.4 (2s, COOH); IR (film) 3038, 2934, 1737, 1425, 1361, 1271, 1142, 1042, 944 cm^{-1} ; $[\alpha]_{\text{D}}^{20}$ -2.6 (c 1.0, MeOH). Anal. Calcd for $\text{C}_{10}\text{H}_{12}\text{O}_6$: C, 52.63; H, 5.26. Found: C, 52.54; H, 4.97.

4.2.6. Dimethyl 1,4-dioxa-spiro[4,5]dec-6-ene-2(R),3(R)-dicarboxylate (5a). The ene ketal was prepared via trans-ketalization of 1,1-dimethoxy-2-cyclohexene.¹⁴

^1H NMR (300 MHz, CDCl_3) δ 1.75–1.84 (m, 2H, 9-H), 1.87–1.97 (m, 2H, 10-H), 1.98–2.07 (m, 2H, 8-H), 3.80 (s, 6H, CH_3), 4.83 (s, 2H, 2-H, 3-H), 5.65 (d, $J=10.0$ Hz, 1H, 6-H), 6.02 (dt, $J=3.5, 10.0$ Hz, 1H, 7-H); ^{13}C NMR (75 MHz, CDCl_3) δ 20.7 (t, C-9), 24.9 (t, C-10), 34.4 (t, C-8), 53.2, 53.1 (2s, Me), 77.4, 77.2 (2d, C-2, C-3), 111.4 (s, C-5), 127.1 (d, C-6), 134.8 (d, C-7), 170.4, 170.5 (2s, COOMe); IR (film) 3033, 2978, 2945, 1764, 1478, 1371, 1237, 1045, 857, 759, 662 cm^{-1} ; $[\alpha]_{\text{D}}^{20}$ -7.3 (c 1.0, CHCl_3), lit.:¹⁴ $[\alpha]_{\text{D}}^{24}$ -8.5 (c 3.5, CHCl_3).

4.3. General procedures for the photooxygenations

4.3.1. Procedure A. The ketals **6a–d** (2 mmol) and tetraphenylporphyrin (1 mg) were dissolved in CHCl_3 (4 mL) and CCl_4 (12 mL) in a glass tube. The tube was irradiated at -30 °C with two sodium lamps (250 W) for 2–4 d. During the irradiation a slow stream of oxygen was bubbled through the solution and additional portions of the sensitizer were added, when the color of the solution faded. After completion, dimethylsulfide (1 mL) was added and the reaction solution was kept for 24 h. The solvent was evaporated and the ratio of the isomers was determined from the NMR spectra (500 MHz).

4.3.2. Procedure B. The ketal **6e** (100 mg, 0.4 mmol) was dissolved in 2 mL CD_3OD in a glass tube. After addition of rose bengal (1 mg) and sodium (40 mg, 1.7 mmol) the tube was irradiated under the same conditions as described for the general procedure for a period of 7 d. After completion, dimethylsulfide (1 mL) was added and the reaction solution was kept for 24 h. The solvent was evaporated and the ratio of the isomers was determined from the NMR spectra (500 MHz) in CD_3OD .

4.3.3. Photooxygenation of ketal 6a. Following procedure A, compound **6a** was irradiated for 4 d and the allylic alcohols were isolated as colorless oils. The ratio **7a/8a** (82:18) and the diastereomeric ratios for **7a** (57:43) and **8a** (62:38) were determined from the crude spectra by NMR spectroscopy (500 MHz). Chromatography (hexane/ethyl acetate=1:2, $R_f=0.42$ – 0.50) afforded first the major diastereomer of **8a**, followed by the minor diastereomer of **8a**, the minor diastereomer of isomer **7a**, and finally, the major diastereomer of **7a** (overall yield: 410 mg, 75%).

4.3.3.1. Dimethyl 8(S)-hydroxy-1,4-dioxa-spiro[4,5]-dec-6-ene-2(R),3(R)-dicarboxylate (S-7a) (main product).

^1H NMR (300 MHz, CDCl_3) δ 1.72–1.92 (m, 2H, 9-H), 2.08–2.2 (m, 2H, 10-H), 3.82, 3.83 (2s, 6H, CH_3), 4.21 (m, 1H, 4-H), 4.81, 4.83 (2d, $J=4.5$ Hz, 2H, 2-H, 3-H), 5.69 (d, $J=10.5$ Hz, 1H, 6-H), 5.97–6.04 (dm, $J=10.5$ Hz, 1H, 7-H); ^{13}C NMR (75 MHz, CDCl_3) δ 30.6 (t, C-9), 32.0 (t, C-10), 53.2, 53.3 (2q, Me), 66.4 (d, C-8), 77.8, 77.9 (2d, C-2, C-3), 111.0 (s, C-5), 129.0 (d, C-6), 137.5 (d, C-7), 170.8 (2s, CO_2Me); IR (KBr) 3425, 2975, 2920, 1738, 1402, 1234, 1156, 1042, 931, 745 cm^{-1} ; $[\alpha]_{\text{D}}^{25}$ -54.9 (c 0.25, CHCl_3). Anal. Calcd for $\text{C}_{12}\text{H}_{16}\text{O}_7$: C, 52.94; H, 5.88. Found: C, 52.66; H, 5.88.

4.3.3.2. Dimethyl 8(R)-hydroxy-1,4-dioxa-spiro[4,5]-dec-6-ene-2(R),3(R)-dicarboxylate (R-7a) (minor diastereomer).

^1H NMR (300 MHz, CDCl_3) δ 1.75–1.89 (m, 2H, 9-H), 2.09–2.19 (m, 2H, 10-H), 3.83, 3.84 (2s, 6H, CH_3), 4.27 (m, 1H, 8-H), 4.85, 4.87 (2d, $J=4.5$ Hz, 2H, 2-H, 3-H), 5.73 (d, $J=10.4$ Hz, 1H, 6-H), 5.99–6.03 (dm, $J=10.4$ Hz, 1H, 7-H); ^{13}C NMR (75 MHz, CDCl_3) δ 30.6 (t, C-9), 31.8 (t, C-10), 55.2, 55.3 (2q, Me), 66.0 (d, C-8), 77.2, 77.3 (2d, C-2, C-3), 110.8 (s, C-5), 128.8 (d, C-6), 136.8 (d, C-7), 170.3 (2s, CO_2Me); IR (KBr) 3425, 2975, 2920, 1738, 1402, 1234, 1156, 1042, 931, 745 cm^{-1} ; $[\alpha]_{\text{D}}^{20}$ $+2.3$ (c 1.0, CHCl_3).

4.3.3.3. Dimethyl 7-hydroxy-1,4-dioxo-spiro[4,5]dec-8-ene-2(R),3(R)-dicarboxylate (8a) (major diastereomer). ¹H NMR (300 MHz, CDCl₃) δ 1.95–2.14 (m, 2H, 10-H), 2.25–2.46 (m, 2H, 6-H), 3.76, 3.77 (2s, 6H, CH₃), 4.29 (m, 1H, 7-H), 4.79, 4.84 (2d, *J*=4.7 Hz, 2H, 2-H, 3-H), 5.64–5.71 (dm, *J*=9.7 Hz, 1H, 9-H), 5.8–5.87 (dm, *J*=9.7 Hz, 1H, 8-H); ¹³C NMR (75 MHz, CDCl₃) δ 36.8 (t, C-10), 40.1 (t, C-6), 53.3, 53.4 (2q, Me), 66.4 (d, C-7), 77.0, 77.1 (2d, C-2, C-3), 113.7 (s, C-5), 125.5 (d, C-9), 129.9 (d, C-8), 170.0, 170.5 (2s, CO₂Me); [α]_D²⁰+14.8 (c 0.96, CHCl₃).

4.3.3.4. Dimethyl 7-hydroxy-1,4-dioxo-spiro[4,5]dec-8-ene-2(R),3(R)-dicarboxylate (8a) (minor diastereomer). ¹H NMR (300 MHz, CDCl₃) δ 2.05–2.22 (m, 2H, 10-H), 2.32–2.52 (m, 2H, 6-H), 3.84, 3.85 (2s, 6H, CH₃), 4.37 (m, 1H, 8-H), 4.86, 4.92 (2d, *J*=4.7 Hz, 2H, 2-H, 3-H), 5.72–5.8 (dm, *J*=9.7 Hz, 1H, 9-H), 5.89–5.97 (dm, *J*=9.7 Hz, 1H, 8-H); ¹³C NMR (75 MHz, CDCl₃) δ 36.8 (t, C-10), 39.9 (t, C-6), 53.3, 53.4 (2q, Me), 66.4 (d, C-7), 77.1, 77.6 (2d, C-2, C-3), 113.2 (s, C-5), 125.8 (d, C-9), 129.6 (d, C-8), 170.2, 170.5 (2s, CO₂Me).

4.3.4. Photooxygenation of ketal 6b. Following procedure A, compound **6b** was irradiated for 4 d and the allylic alcohols were isolated as colorless oils. The ratio **7b/8b** (81:19) and the diastereomeric ratios for **7b** (53:47) and **8b** (55:45) were determined from the crude spectra by NMR spectroscopy (500 MHz). Chromatography (hexane/ethyl acetate=1:2, *R_f*=0.50–0.58) afforded first the major diastereomer of **8b**, followed by the minor diastereomer of **8b**, the minor diastereomer of isomer **7b**, and finally, the major diastereomer of **7b** (overall yield: 450 mg, 75%).

4.3.4.1. Diethyl 8(S)-hydroxy-1,4-dioxo-spiro[4,5]dec-6-ene-2(R),3(R)-dicarboxylate (S-7b) (major diastereomer). ¹H NMR (300 MHz, CDCl₃) δ 1.33 (t, *J*=6.6 Hz, 6H, CH₃), 1.73–1.92 (m, 2H, 9-H), 2.0–2.17 (m, 2H, 10-H), 4.21 (m, 1H, 8-H), 4.25 (t, *J*=6.6 Hz, 4H, CH₂), 4.76 (m, 2H, 2-H, 3-H), 5.69 (d, *J*=10.1 Hz, 1H, 6-H), 5.94 (dm, *J*=10.1 Hz, 1H, 7-H); ¹³C NMR (75 MHz, CDCl₃) δ 13.6 (q, CH₃), 29.3 (t, C-9), 30.7 (t, C-10), 61.1 (2t, OCH₂), 64.6 (d, C-8), 76.1 (d, C-2, C-3), 109.1 (s, C-5), 127.4 (d, C-6), 135.3 (d, C-7), 168.6 (2s, CO₂Et); IR (KBr) 3420, 2982, 2940, 1740, 1445, 1395, 1221, 1127, 1022, 939 cm⁻¹. Anal. Calcd for C₁₄H₂₀O₇: C, 55.99; H, 6.71. Found: C, 55.85; H, 6.72.

4.3.4.2. Diethyl 8(R)-hydroxy-1,4-dioxo-spiro[4,5]dec-6-ene-2(R),3(R)-dicarboxylate (R-7b) (minor diastereomer). ¹H NMR (300 MHz, CDCl₃) δ 1.33 (t, *J*=6.6 Hz, 6H, CH₃), 1.73–1.92 (m, 2H, 9-H), 2.0–2.17 (m, 2H, 10-H), 4.21 (m, 1H, 8-H), 4.25 (t, *J*=6.6 Hz, 4H, CH₂), 4.78, 4.82 (2d, *J*=4.7 Hz, 2H, 2-H, 3-H), 5.66 (d, *J*=10.1 Hz, 1H, 6-H), 5.94 (dm, *J*=10.1 Hz, 1H, 7-H); ¹³C NMR (75 MHz, CDCl₃) δ 13.6 (q, CH₃), 29.2 (t, C-9), 30.5 (t, C-10), 61.0 (2t, OCH₂), 64.6 (d, C-8), 76.2 (d, C-2, C-3), 109.3 (s, C-5), 127.5 (d, C-6), 135.4 (d, C-7), 168.4 (2s, CO₂Et).

4.3.4.3. Diethyl 7-hydroxy-1,4-dioxo-spiro[4,5]dec-8-ene-2(R),3(R)-dicarboxylate (8b) (major diastereomer). ¹H NMR (300 MHz, CDCl₃) δ 1.33 (t, *J*=7.1 Hz, 6H, CH₃), 2.05–2.22 (m, 2H, 10-H), 2.32–2.56 (m, 2H, 6-H),

4.30 (q, *J*=7.1 Hz, 4H, OCH₂), 4.35 (m, 1H, 7-H), 4.8–4.91 (m, 2H, 2-H, 3-H), 5.76–5.80 (dm, *J*=9.89 Hz, 2H, 9-H), 5.89–5.97 (dm, *J*=9.89 Hz, 1H, 8-H); ¹³C NMR (75 MHz, CDCl₃) δ 13.6 (2q, CH₃), 35.5 (t, C-10), 39.7 (t, C-6), 62.2, 62.3 (2t, OCH₂), 70.1 (d, C-7), 75.9, 76.1 (2d, C-2, C-3), 112.2 (s, C-1), 124.5 (d, C-9), 128.3 (C-8), 168.6, 168.7 (CO₂Et).

4.3.4.4. Diethyl 7-hydroxy-1,4-dioxo-spiro[4,5]dec-8-ene-2(R),3(R)-dicarboxylate (8b) (minor diastereomer). ¹H NMR (300 MHz, CDCl₃) δ 1.33 (t, *J*=7.1 Hz, 6H, CH₃), 2.05–2.22 (m, 2H, 10-H), 2.32–2.56 (m, 2H, 6-H), 4.30 (q, *J*=7.1 Hz, 4H, OCH₂), 4.29 (m, 1H, 7-H), 4.83–4.96 (m, 2H, 2-H, 3-H), 5.76–5.80 (dm, *J*=9.9 Hz, 2H, 9-H), 5.82–5.91 (dm, *J*=9.9 Hz, 1H, 8-H); ¹³C NMR (75 MHz, CDCl₃) δ 13.6 (2q, CH₃), 35.7 (t, C-10), 39.3 (t, C-6), 65.1, 65.2 (2t, OCH₂), 70.9 (d, C-7), 75.9, 76.1 (2d, C-2, C-3), 112.3 (s, C-1), 124.2 (d, C-9), 128.5 (C-8), 168.6, 168.7 (CO₂Et).

4.3.5. Photooxygenation of ketal 6c. Following procedure A, compound **6c** was irradiated for 4 d and the allylic alcohols were isolated as colorless oils. The ratio **7c/8c** (89:11) and the diastereomeric ratio for **7c** (54:46) were determined from the crude spectra by NMR spectroscopy (500 MHz). Chromatography (hexane/ethyl acetate=1:2, *R_f*=0.65–0.72) afforded first the major diastereomer of **8c**, followed by the minor diastereomer of isomer **7c**, and finally, the major diastereomer of **7c**. The minor diastereomer of **8c** could not be isolated (overall yield: 480 mg, 73%).

4.3.5.1. Diisopropyl 8(S)-hydroxy-1,4-dioxo-spiro[4,5]dec-6-ene-2(R),3(R)-dicarboxylate (S-7c) (major diastereomer). ¹H NMR (300 MHz, CDCl₃) δ 1.23 (d, *J*=6.1 Hz, 12H, CH₃), 1.50–2.14 (m, 4H, 10-H, 12-H), 4.14 (m, 1H, 8-H), 4.59 (m, 2H, 2-H, 3-H), 5.06 (sept, *J*=6.1 Hz, 2H, CH), 5.62–5.72 (d, *J*=10.0 Hz, 1H, 6-H), 5.89–5.96 (d, *J*=10.0 Hz, 1H, 7-H); ¹³C NMR (75 MHz, CDCl₃) δ 21.8 (q, CH₃), 30.3 (t, C-9), 32.0 (t, C-10), 65.7 (d, C-8), 70.1 (2d, CHMe₂), 77.7, 78.1 (2d, C-2, C-3), 110.6 (s, C-5), 128.5 (d, C-6), 137.0 (d, C-7), 169.4, 169.5 (2s, COO*i*-Pr). Anal. Calcd for C₁₆H₂₄O₇: C, 58.53; H, 7.37. Found: C, 58.26; H, 7.29.

4.3.5.2. Diisopropyl 8(R)-hydroxy-1,4-dioxo-spiro[4,5]dec-6-ene-2(R),3(R)-dicarboxylate (R-7c) (minor diastereomer). ¹H NMR (300 MHz, CDCl₃) δ 1.21 (d, *J*=6.1 Hz, 12H, CH₃), 1.62–2.19 (m, 4H, 10-H, 12-H), 4.11 (m, 1H, 8-H), 4.61–5.13 (m, 2H, 2-H, 3-H), 5.06 (sept, *J*=6.1 Hz, 2H, CH), 5.62–5.72 (d, *J*=10.0 Hz, 1H, 6-H), 5.89–5.96 (d, *J*=10.0 Hz, 1H, 7-H); ¹³C NMR (75 MHz, CDCl₃) δ 21.9 (q, CH₃), 30.3 (t, C-9), 31.9 (t, C-10), 65.6 (d, C-8), 70.0 (2d, CHMe₂), 77.2, 77.6 (2d, C-2, C-3), 110.4 (s, C-5), 128.3 (d, C-6), 136.9 (d, C-7), 169.3, 169.4 (2s, COO*i*-Pr).

4.3.5.3. Diisopropyl 7-hydroxy-1,4-dioxo-spiro[4,5]dec-8-ene-2(R),3(R)-dicarboxylate (8c) (major diastereomer). ¹H NMR (300 MHz, CDCl₃) δ 1.29, 1.31 (2d, *J*=6.1 Hz, 12-H, CH₃), 2.05–2.25 (m, 2H, 10-H), 2.25–2.61 (m, 2H, 6-H), 4.41 (m, 1H, 7-H), 4.71, 4.80 (2d, *J*=5.2 Hz, 2H, 2-H, 3-H), 5.12 (sept, *J*=6.2 Hz, 2H, OCH), 5.70–5.79 (m, 1H, 9-H), 5.85–5.92 (m, 1H, 8-H);

^{13}C NMR (75 MHz, CDCl_3) δ 22.0 (q, CH_3), 36.6 (t, C-10), 40.1 (t, C-6), 66.3 (d, C-7), 70.3, 70.7 (2d, CHMe_2), 77.7 (2d, C-2, C-3), 113.4 (s, C-5), 125.5 (d, C-9), 129.9 (d, C-8), 169.6, 169.1 (2s, $\text{COO}i\text{-Pr}$); IR (KBr) 3415, 2980, 2957, 1738, 1365, 1245, 1098, 1024, 754 cm^{-1} ; $[\alpha]_{\text{D}}^{20}$ -4.8 (c 1.02, CHCl_3). Anal. Calcd for $\text{C}_{16}\text{H}_{24}\text{O}_7$: C, 58.53; H, 7.37. Found: C, 58.96; H, 6.89.

4.3.6. Photooxygenation of ketal 6d. Following procedure A, compound **6d** (200 mg, 1.4 mmol) was irradiated for 2 d and the allylic alcohols were isolated as colorless oils. The ratio **7d/8d** (87:13) was determined from the crude spectra by NMR spectroscopy (500 MHz). Chromatography (hexane/ethyl acetate=1:2, R_f =0.35) afforded **8d** in the first fractions, followed by **7d** (overall yield: 170 mg, 77%).

4.3.6.1. 8-Hydroxy-1,4-dioxo-spiro[4,5]dec-6-ene (7d).

^1H NMR (300 MHz, CDCl_3) δ 1.69–1.80 (m, 2H, 10-H), 1.91–2.18 (m, 2H, 9-H), 3.89–4.04 (m, 4H, 2-H, 3-H), 4.22 (br, 1H, 8-H), 5.63 (dt, $J=1.4$, 10.0 Hz, 1H, 6-H), 5.95 (dd, $J=1.1$, 10.0 Hz, 1H, 7-H); ^{13}C NMR (75 MHz, CDCl_3) δ 31.0 (t, C-10), 31.3 (t, C-9), 64.9, 65.0 (2d, C-2, C-3), 66.3 (d, C-8), 105.4 (s, C-1), 129.5 (d, C-6), 135.3 (d, C-7). IR (KBr) 3032, 2948, 2883, 1675, 1396, 1346, 1272, 1066, 1012, 939, 863 cm^{-1} .

4.3.6.2. 7-Hydroxy-1,4-dioxo-spiro[4,5]dec-8-ene (8d).

^1H NMR (300 MHz, CDCl_3) δ 1.96 (d, $J=4.4$ Hz, 2H, 10-H), 2.23 (br, 2H, 6-H), 2.71 (d, $J=10.3$ Hz, 1H, OH), 3.85–3.98 (m, 4H, 2-H, 3-H), 4.24 (m, 1H, 7-H), 5.69 (dt, $J=3.6$, 9.8 Hz, 1H, 8-H), 5.79–5.89 (m, 1H, 9-H); ^{13}C NMR (75 MHz, CDCl_3) δ 36.1 (t, C-10), 39.4 (t, C-6), 64.7 (t, C-2, C-3), 66.7 (d, C-7), 108.4 (s, C-1), 126.5 (d, C-8), 127.7 (d, C-9).

4.3.7. Photooxygenation of ketal 6e. Following procedure B, compound **6e** was irradiated for 7 d. The NMR spectrum (500 MHz) of the crude product showed exclusively regioisomer **7e** in a diastereomeric ratio of 56:44. The configuration of the main diastereomer was established by saponification of the corresponding methylester **8a** (MeOH/ H_2O , catalytic amount of NaOH) and comparison of their NMR spectra.

4.3.7.1. 8(S)-Hydroxy-1,4-dioxo-spiro[4,5]dec-6-ene-2(R),3(R)-dicarboxylic acid (7e) (major diastereomer).

^1H NMR (300 MHz, CD_3OD) δ 1.69–2.0 (m, 2H, 10-H), 2.02–2.30 (m, 2H, 9-H), 4.15 (m, 1H, 8-H), 4.54, 4.56 (2d, $J=6.6$ Hz, 2H, 2-H, 3-H), 5.77 (d, $J=10$ Hz, 1H, 6-H), 5.87 (d, $J=10$ Hz, 1H, 7-H); ^{13}C NMR (75 MHz, CDCl_3) δ 30.3 (t, C-9), 32.0 (t, C-10), 65.7 (d, C-8), 80.4, 80.7 (2d, C-2, C-3), 107.4 (s, C-5), 129.9 (d, C-6), 135.1 (d, C-7), 176.7, 176.8 (2s, COOH).

4.3.7.2. 7(R)-Hydroxy-1,4-dioxo-spiro[4,5]dec-8-ene-2(R),3(R)-dicarboxylic acid (7e) (minor diastereomer).

^1H NMR (300 MHz, CD_3OD) δ 1.69–2.0 (m, 2H, 10-H), 2.02–2.30 (m, 2H, 9-H), 4.15 (m, 1H, 8-H), 4.48, 4.50 (2d, $J=6.2$ Hz, 2H, 2-H, 3-H), 5.77 (d, $J=10$ Hz, 1H, 6-H), 5.87 (d, $J=10$ Hz, 1H, 7-H); ^{13}C NMR (75 MHz, CDCl_3) δ 30.2 (t, C-9), 31.7 (t, C-10), 65.7 (d, C-8), 80.4, 80.7 (2d, C-2, C-3), 107.6 (s, C-5), 130.0 (d, C-6), 134.7 (d, C-7), 177.0, 177.1 (2s, COOH).

4.4. Epoxidation of the ketal 6a

The cyclohexene ketal **6a** (420 mg, 1.6 mmol) was dissolved in dichloromethane (30 mL) and *m*-chloroperbenzoic acid (440 mg, 1.9 mmol) was added at 0 °C in several portions. The course of the reaction was followed by TLC (hexane/ethyl acetate=3:1). After completion (4 h) a saturated solution of NaHCO_3 (100 mL) was added. After separation, the aqueous phase was washed with diethyl ether (100 mL), and the combined organic extracts were washed with water, dried (NaSO_4), and the solvent was evaporated. The diastereomeric ratio (51:49) was determined from the crude spectra by NMR spectroscopy (500 MHz). The product was purified by column chromatography (hexane/ethyl acetate=1:1, R_f =0.19) to afford the epoxides **10** as white solids (415 mg, 95%).

4.4.1. Dimethyl 7,8-epoxy-1,4-dioxo-spiro[4,5]decane-2(R),3(R)-dicarboxylate (10) (major diastereomer).

Mp 56.5 °C; ^1H NMR (300 MHz, CDCl_3) δ 1.47–1.56, 1.65–1.77 (2m, 2H, 10-H), 2.10–2.32 (m, 4H, 6-H, 9-H), 3.12–3.20 (m, 2H, 7-H, 8-H), 3.80, 3.81 (2s, 6H, Me), 4.75, 4.79 (2d, $J=5.1$ Hz, 2H, 2-H, 3-H); ^{13}C NMR (75 MHz, CDCl_3) δ 22.8 (t, C-10), 28.1 (t, C-9), 35.8 (t, C-6), 51.1 (d, C-8), 52.1 (d, C-7), 53.1, 53.2 (2s, Me), 77.1, 77.2 (2d, C-2, C-3), 112.5 (s, C-1), 170.1, 170.3 (2s, COOMe); $[\alpha]_{\text{D}}^{20}$ -29.3 (c 0.98, CHCl_3); IR (KBr) 3015, 2959, 1761, 1436, 1373, 1344, 1254, 1217, 1164, 1125, 1086, 992, 933 cm^{-1} . Anal. Calcd for $\text{C}_{12}\text{H}_{16}\text{O}_7$: C, 52.94; H, 5.88. Found: C, 52.85; H, 6.24.

4.4.2. Dimethyl 7,8-epoxy-1,4-dioxo-spiro[4,5]decane-2(R),3(R)-dicarboxylate (10) (minor diastereomer).

^1H NMR (300 MHz, CDCl_3) δ 1.44–1.56, 1.63–1.78 (2m, 2H, 10-H), 2.0–2.30 (m, 4H, 7-H, 8-H), 3.41 (br, 2H, 7-H, 8-H), 3.77, 3.78 (2s, 6H, Me), 4.74 (m, 2H, 2-H, 3-H); ^{13}C NMR (75 MHz, CDCl_3) δ 23.5 (t, C-10), 29.2 (t, C-9), 36.3 (t, C-6), 52.0 (d, C-8), 52.8 (d, C-7), 53.1, 53.2 (s, Me), 78.0, 78.1 (2d, C-2, C-3), 113.5 (s, C-1), 171.2, 171.3 (2s, COOMe).

4.5. Cleavage of the chiral auxiliary from ketal 7a

4.5.1. Cleavage with HCl. The ketal (*S*)-**7a** (100 mg, 0.36 mmol) was dissolved in methanol (10 mL). Hydrochloric acid (1 N, 0.5 mL) was added dropwise at 0 °C. After 12 h diethyl ether (20 mL) and water (10 mL) were added, the organic phase was separated, dried (MgSO_4), and the solvent was evaporated. NMR analysis of the residue resulted in a 1:2 mixture of the ketone **11** and phenol (**12**).

4.5.2. Cleavage with montmorillonite K-10. The ketal (*S*)-**7a** (100 mg, 0.36 mmol) was dissolved in dichloromethane (10 mL). Montmorillonite K-10 (800 mg) was added at 0 °C and the mixture was stirred at room temperature for 24 h. After filtration and evaporation of the solvent NMR analysis of the residue resulted in a 4:1 mixture of the ketone **11** and phenol (**12**).

4.5.3. Cleavage with buffered montmorillonite K-10. The ketal (*S*)-**7a** (100 mg, 0.36 mmol) was dissolved in dichloromethane (10 mL). Sodium acetate (45 mg, 0.4 mmol) and montmorillonite K-10 (800 mg) were added at 0 °C and

the mixture was stirred at room temperature for 24 h. The conversion was followed by TLC but was not complete even after longer reaction times. However, no phenol could be detected. After filtration and evaporation of the solvent, flash chromatography (hexane/ethyl acetate=1:2, $R_f=0.3$) afforded the ketone **11** as a colorless oil (30 mg, 74%, 97% based on the conversion). In addition, unreacted ketal (*S*)-**7a** was recovered (24 mg, 24%).

4.5.3.1. 4(*S*)-Hydroxy-2-cyclohexen-1-one (11). ^1H NMR (300 MHz, CDCl_3) δ 1.85–2.09 (m, 1H, 5-H), 2.22–2.45 (m, 2H, 6-H), 2.55–2.68 (m, 1H, 5-H), 4.60 (br, 1H, 4-H), 5.99 (d, $J=10.2$ Hz, 1H, 2-H), 6.95 (dt, $J=2.0$, 10.2 Hz, 1H, H-3); ^{13}C NMR (75 MHz, CDCl_3) δ 32.8 (t, C-5), 35.7 (t, C-6), 66.7 (d, C-4), 129.6 (d, C-2), 153.0 (d, C-3), 199.1 (s, CO); $[\alpha]_D^{25} -85.3$ (c 0.16, CHCl_3), lit.:¹⁶ $[\alpha]_D^{20} -90.0$ (c 0.2, CHCl_3).

Acknowledgements

This work was generously supported by the Fonds der Chemischen Industrie and the Deutsche Forschungsgemeinschaft (DFG).

References and notes

- Recent reviews: (a) Clennan, E. L. *Tetrahedron* **2000**, *56*, 9151–9179; (b) Clennan, E. L.; Pace, A. *Tetrahedron* **2005**, *61*, 6665–6691.
- Excellent review: Stratakis, M.; Orfanopoulos, M. *Tetrahedron* **2000**, *56*, 1595–1615.
- (a) Li, X.; Ramamurthy, V. *J. Am. Chem. Soc.* **1996**, *118*, 10666–10667; (b) Clennan, E. L.; Sram, J. P. *Tetrahedron Lett.* **1999**, *40*, 5275–5278; (c) Stratakis, M.; Froudakis, G. *Org. Lett.* **2000**, *2*, 1369–1372; (d) Bartoschek, A.; El-Idreesy, T. T.; Griesbeck, A. G.; Hoinck, L.-O.; Lex, J.; Miara, C.; Neudörfl, J. M. *Synthesis* **2005**, 2433–2444.
- Excellent review: Prein, M.; Adam, W. *Angew. Chem., Int. Ed.* **1996**, *35*, 477–494.
- (a) Dussault, P. H.; Woller, K. R.; Hillier, M. C. *Tetrahedron* **1994**, *50*, 8929–8940; (b) Adam, W.; Güthlein, M.; Peters, E.-M.; Peters, K.; Wirth, T. *J. Am. Chem. Soc.* **1998**, *120*, 4091–4093; (c) Adam, W.; Peters, K.; Peters, E.-M.; Schambony, S. B. *J. Am. Chem. Soc.* **2001**, *123*, 7228–7232; (d) Adam, W.; Bosio, S. G.; Turro, N. J. *J. Am. Chem. Soc.* **2002**, *124*, 8814–8815; (e) Adam, W.; Bosio, S. G.; Turro, N. J.; Wolff, B. T. *J. Org. Chem.* **2004**, *69*, 1704–1715.
- (a) Sundén, H.; Engqvist, M.; Casas, J.; Ibrahim, I.; Córdova, A. *Angew. Chem., Int. Ed.* **2004**, *43*, 6532–6535; (b) Córdova, A.; Sundén, H.; Engqvist, M.; Ibrahim, I.; Casas, J. *J. Am. Chem. Soc.* **2004**, *126*, 8914–8915.
- Fudickar, W.; Fery, A.; Linker, T. *J. Am. Chem. Soc.* **2005**, *127*, 9386–9387.
- (a) Dang, H.-S.; Davies, A. G. *Tetrahedron Lett.* **1991**, *32*, 1745–1748; (b) Maldotti, A.; Andreotti, L.; Molinari, A.; Borisov, S.; Vasil'ev, V. *Chem.—Eur. J.* **2001**, *7*, 3564–3571.
- (a) Linker, T.; Fröhlich, L. *Angew. Chem., Int. Ed. Engl.* **1994**, *33*, 1971–1972; (b) Linker, T.; Fröhlich, L. *J. Am. Chem. Soc.* **1995**, *117*, 2694–2697; (c) Linker, T.; Rebien, F.; Tóth, G. *Chem. Commun.* **1996**, 2585–2586; (d) Nardello, V.; Aubry, J.-M.; Linker, T. *Photochem. Photobiol.* **1999**, *70*, 524–530; (e) Fröhlich, L.; Linker, T. *Synlett* **2004**, 2725–2727.
- (a) Alexakis, A.; Mangney, P. *Tetrahedron: Asymmetry* **1990**, *1*, 477–511; (b) Johnson, R. A.; Sharpless, K. B. *Catalytic Asymmetric Synthesis*; Ojima, I., Ed.; VCH: New York, NY, 1993; pp 101–158; (c) Gawronski, J.; Gawronska, K. *Tartaric and Malic Acids in Synthesis*; Wiley: New York, NY, 1999; (d) Ukaji, Y.; Inomata, K. *Synlett* **2003**, 1075–1087.
- Greene, T. W.; Wuts, P. G. M. *Protecting Groups in Organic Synthesis*, 3rd ed.; Wiley: New York, NY, 1999.
- Fioravanti, S.; Luna, G.; Pellacani, L.; Tardella, P. A. *Tetrahedron* **1997**, *53*, 4779–4786.
- Mash, E. A.; Nelson, K. A. *Tetrahedron* **1987**, *43*, 679–692.
- (a) Mash, E. A.; Nelson, K. A.; Heidt, P. C. *Tetrahedron Lett.* **1987**, *28*, 1865–1868; (b) Mash, E. A.; Hemperly, S. B.; Nelson, K. A.; Heidt, P. C.; Van Deusen, S. J. *Org. Chem.* **1990**, *55*, 2045–2055.
- Tsangarakis, C.; Zaravinos, I.-P.; Stratakis, M. *Synlett* **2005**, 1857–1860.
- (a) Gebauer, O.; Brückner, R. *Liebigs Ann. Chem.* **1996**, 1559–1563; (b) March, P.; Escoda, M.; Figueredo, M.; Font, J.; Garcia-Garcia, E.; Rodriguez, S. *Tetrahedron: Asymmetry* **2000**, *11*, 4473–4483.



ELSEVIER

Available online at www.sciencedirect.com

ScienceDirect

Tetrahedron 62 (2006) 10647–10659

Tetrahedron

A comparative mechanistic analysis of the stereoselectivity trends observed in the oxidation of chiral oxazolidinone-functionalized enecarbamates by singlet oxygen, ozone, and triazolinedione

J. Sivaguru,^a Thomas Poon,^b Catherine Hooper,^b Hideaki Saito,^{a,c,d} Marissa R. Solomon,^a Steffen Jockusch,^a Waldemar Adam,^{e,f} Yoshihisa Inoue^{c,d} and Nicholas J. Turro^{a,g,*}

^aThe Department of Chemistry, Columbia University, New York, NY 10027, USA

^bJoint Science Department, W.M. Keck Science Center, 925 N. Mills Ave., Claremont McKenna, Pitzer, and Scripps Colleges, Claremont, CA 91711, USA

^cThe Department of Applied Chemistry, Osaka University, 2-1 Yamada-oka, Suita 565-0871, Japan

^dThe Entropy Control Project, ICORP, JST, 4-6-3 Kamishinden, Toyonaka 560-0085, Japan

^eInstitute für Organische Chemie, Universität Würzburg, D-97074 Würzburg, Germany

^fThe Department of Chemistry, University of Puerto Rico, Facundo Bueso 110, Rio Piedras, PR 00931, USA

^gThe Department of Chemical Engineering, Columbia University, New York, NY 10027, USA

Received 30 May 2006; revised 26 July 2006; accepted 31 July 2006

Available online 29 September 2006

Abstract—The stereoselectivity in the reactions of the *E/Z* enecarbamates **1**, equipped with the oxazolidinone chiral auxiliary, has been examined for singlet oxygen (¹O₂), ozone (O₃), and 4-phenyl-1,2,4-triazoline-3,5-dione (PTAD) in a variety of solvents as a function of temperature. The oxidative cleavage of the alkenyl functionality by ¹O₂ and O₃ releases the enantiomerically enriched methyldeoxybenzoin (MDB) product. The *extent* (% ee) as well as the *sense* (*R* vs *S*) of the stereoselectivity in the MDB formation depends on the electronic nature of the oxidant. A high stereoselectivity, substantially dependent on solvent and temperature, is displayed for the reactions with ¹O₂, whereas the ground-state reactants O₃ and PTAD are rather unaffected by solvent and temperature variations. The present comparative analysis clearly substantiates our hypothesis of stereoselective vibrational quenching of the attacking ¹O₂, whereas O₃ and PTAD are only subject to steric impositions. The electronically excited ¹O₂ is sensitive to all three stereochemically relevant structural characteristics embodied in the chiral enecarbamates, namely the *R/S* configuration at the C₄ position of the oxazolidinone chiral auxiliary, the *Z/E* geometry of the ‘alkene’ functionality, and *R/S* configuration at the C₃’ position of the enecarbamate side chain.

© 2006 Elsevier Ltd. All rights reserved.

1. Introduction

High enantioselectivity in photochemical reactions^{1–3} depends on effective manipulation of chiral/prochiral faces of the reactant within the short lifetimes of the excited states.⁴ To imprint stereocontrol in the photoproduct, confined media^{5–10} has been employed with considerable success; however, to obtain a high enantioselectivity in solution still constitutes a formidable challenge.^{1–3} In this regard, a novel concept, which we have explored in the stereoselective photooxidative cleavage of chiral enecarbamates, involves selective deactivation (quenching) of one of the diastereomers in a pair of chiral excited states.^{11–13} To demonstrate this concept, we have compared the reaction of enecarbamates **1**

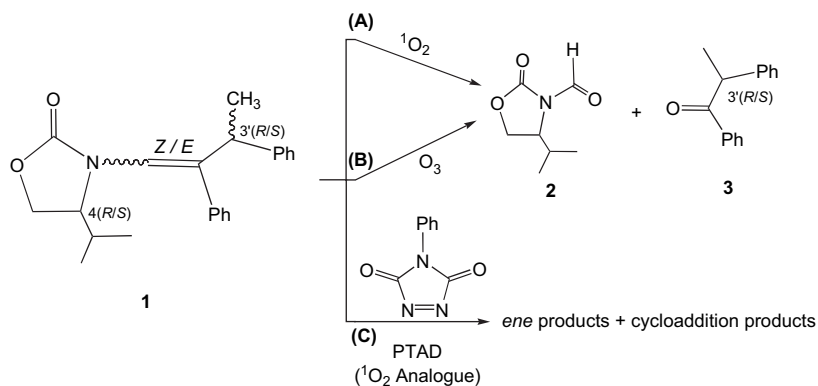
(Scheme 1) with related reactive species viz. singlet oxygen (¹O₂),^{14–17} ozone (O₃),¹⁸ and 4-phenyl-1,2,4-triazoline-3,5-dione (PTAD).^{19–23} Indeed, the high stereoselectivity was observed in the formation of the product MDB **3** (Scheme 1) in the reactions with ¹O₂. The observed high stereoselectivity was hypothesized to result from a combination of steric interactions and selective deactivations of the excited state (Scheme 1).^{11,24}

Previously we have shown^{24–26} that the photooxidation of enecarbamates by ¹O₂ leads to diastereomerically pure dioxetanes (complete conversion), as exemplified for the chiral *Z*-configured enecarbamate 1'*Z*,4*R*(*iPr*),3'(*R/S*)-**1** (Fig. 1).

The salient reactivity feature in the exposed snapshot in Figure 1 is the approach of ¹O₂ on to the double bond, where in addition to the steric hindrance imposed on the ¹O₂, the possible synergistic stereoselective vibrational quenching

Keywords: Kinetic resolution; Ozonolysis; Photooxygenation; Substituent; Solvent and temperature effects; Vibrational quenching.

* Corresponding author. Tel.: +1 212 854 2175; fax: +1 212 932 1289; e-mail: njt3@columbia.edu



Scheme 1. Reactions of oxazolidinone-functionalized *Z/E*-encarbamates **1** with (A) $^1\text{O}_2$, (B) O_3 , and (C) PTAD.

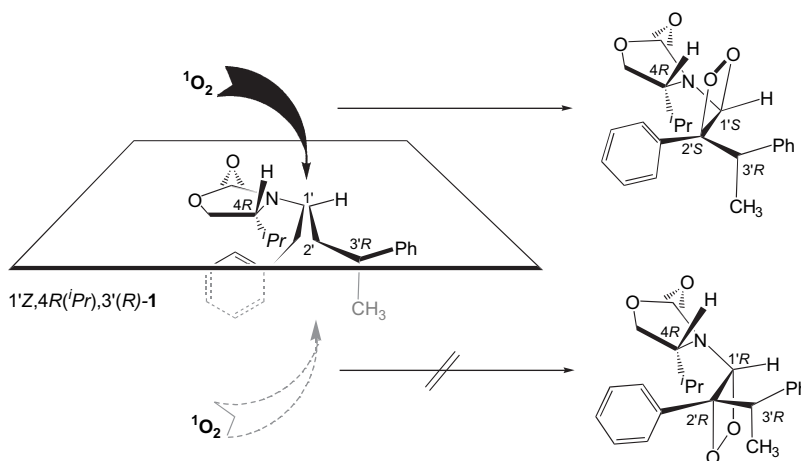


Figure 1. Preferred π -facial attack of $^1\text{O}_2$ from above, controlled by the steric shielding of the 4-isopropyl substituent of the oxazolidinone chiral auxiliary in *Z* encarbamates.

of the $^1\text{O}_2$ from the bottom face could dictate the observed high diastereoselectivity. Moreover, the stereoselection in the dioxetane formation is independent from the configuration of the alkyl side chain at the $\text{C}_{3'}$ position and the size of the alkyl substituent at the C_4 position (*Me*, *iPr*, *Ph*) of the oxazolidinone chiral auxiliary.^{24–26} For example, the diastereomer $1'Z,4R(iPr),3'(R)-1$ (Fig. 1) that possesses the *R* configuration at the C_4 position affords the corresponding $[1'S,2'S]$ dioxetane with complete stereocontrol [diastereomeric ratios (d.r.) of >95:5]. Further, the stereoselection in the MDB product **3** (Scheme 1) upon photooxidative cleavage of these oxazolidinone-functionalized encarbamates by $^1\text{O}_2$ depends not only on the alkene geometry (*Z/E*), the size of the C_4 alkyl substituent (*H*, *Me*, *iPr*) in the oxazolidinone ring, and the configuration (*R/S*) at the $\text{C}_{3'}$ stereogenic center of the phenethyl side chain, but also on the nature of the solvent and the reaction temperature.^{11,27} The stereoselectivity of oxidation of the conformationally more flexible *E* diastereomer responds sensitively to such reaction conditions (ee values of up to 97%), whereas the conformationally more rigid *Z* diastereomer behaves less sensitively to such manipulation (ee values of up to 30%).^{11,27} We proposed that conformational effects (entropy control) are responsible for stereoselective quenching of $^1\text{O}_2$ by vibrational deactivation (a new concept!), in concert with the steric interactions leading to stereoselective oxidative cleavage of the double bond by the attacking $^1\text{O}_2$.^{11,27}

In the present work, we compare the reactivity of singlet oxygen ($^1\text{O}_2$, Scheme 1A) for both *E* and *Z* diastereomers of the encarbamates (Chart 1) with O_3 , an electrophilic oxidant akin to $^1\text{O}_2$ (Scheme 1B) and PTAD, a ground-state analogue of $^1\text{O}_2$ (Scheme 1C). If, indeed, our hypothesis of stereoselective vibrational quenching in the photooxidative cleavage of the encarbamates by $^1\text{O}_2$ proves to be correct, then PTAD would constitute a good test reagent, as it is considered analogous^{19–23} in its chemical reactivity to $^1\text{O}_2$, but as a ground-state molecule PTAD, is not subject to vibrational deactivation.²⁸ Moreover, in view of its much larger size than $^1\text{O}_2$, this bulkier species would be more sensitive to steric effects. Similarly, the highly reactive O_3 oxidant is also a ground-state species and is not subjected to vibrational quenching as in the case of $^1\text{O}_2$. Thus, the electrophilic O_3 , a highly reactive ground-state oxidant would provide an opportunity to probe the importance of the excited-state character in the photooxygenation process. An additional advantage of O_3 over PTAD is the fact that like $^1\text{O}_2$, oxidation of both *Z* and *E* encarbamates **1** by O_3 affords the same MDB product **3**,²⁹ which should facilitate the direct comparison of the stereoselection of these two oxidants.

In the present work, analogous to previous reports,^{11,27} we shall employ both *E* and *Z* oxazolidinone-functionalized encarbamates as 50:50 diastereomeric mixtures of the *R/S* isomers at the $\text{C}_{3'}$ position. Thus, for the purpose of this

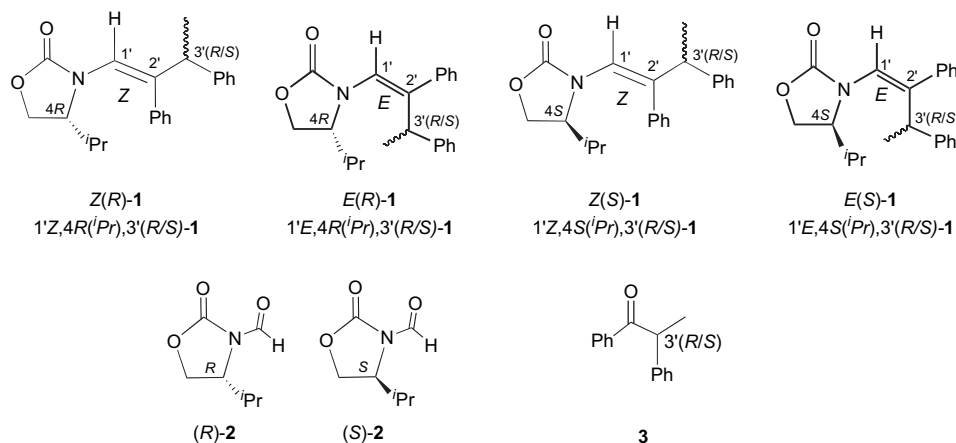


Chart 1. Structure matrix.

study, stereoselectivity will be defined as selective consumption (kinetic resolution) of enecarbamates (upon reaction with $^1\text{O}_2$, O_3 , and PTAD) based upon the C₃' stereochemistry.¹¹ The chemical reactivity of $^1\text{O}_2$, O_3 , and PTAD toward the diastereomeric enecarbamates shall be examined as a function of (i) *E/Z* alkene geometry, (ii) the *R/S* configuration at the C₄ position of the oxazolidinone chiral auxiliary, (iii) the *R/S* configuration of the alkyl substituent at the C₃' position of the oxazolidinone chiral auxiliary, (iv) the solvent, and (v) the reaction temperature. The stereoselectivity for the reactions with PTAD^{19–23} (vs $^1\text{O}_2$) is based on the comparison of diastereomeric composition of the enecarbamates **1** before and after the reaction. On the other hand, for the comparison of $^1\text{O}_2$ with O_3 , the enantiomeric excess in the MDB product **3** was examined (Scheme 1).²⁹

Herein we report the results of an extensive investigation, which for the first time compares the stereochemical behavior of such chemically diverse reactive species ($^1\text{O}_2$, O_3 , and PTAD), whose reactivity are analogous in their reaction with the diastereomeric *E* and *Z* enecarbamates **1**. Evidently, the observed difference in the stereocontrol of these reactive species validates our hypothesis of significant vibrational deactivation (physical quenching) of the electronically excited $^1\text{O}_2$ as a factor for the observed stereoselectivity in the formation of the MDB product. Such selective quenching of diastereomeric excited states constitute a promising *stereochemical tool* to effect enantioselective photoreactions.

2. Experimental

2.1. Materials

All regular solvents were purchased from Aldrich and the deuterated solvents from Cambridge Isotope Labs and used as received. CDCl_3 was stored over sodium bicarbonate prior to use. Flash chromatography was carried out on silica gel, while 2-mm thick silica-gel plates (EMD 60F) were employed for preparative TLC. Commercially available compounds were purified by standard procedures. The *Z* and *E* enecarbamates were synthesized by previously published methods.^{11,12,24–26} The *Z* and *E* enecarbamates **1** were used as 50:50 mixture of *R* and *S* enantiomers at the C₃' position (Chart 1), but the epimeric pair is optically pure at the

C₄ stereogenic center of the oxazolidinone chiral auxiliary. O_3 was generated by means of an OL100 Ozone Generator.

2.2. Instrumentation

GC analyses were carried out on a Varian 3900 gas chromatograph, equipped with an auto-sampler. A Varian Factor-4 VG-1ms column ($l=25$ m, $id=0.25$ mm, $df=0.25$ μm) was employed for the separation on the achiral stationary phase, with a program of 50 °C for 4 min, raised to 225 °C at 10 °C/min, and kept at 225 °C for 10 min. A Varian CP-Chirasil-DEX CB column ($l=25$ m, $id=0.25$ mm, $df=0.25$ μm) was used for the separations on the chiral stationary phase, with a program of 135 °C for 70 min, raised to 200 °C at 15 °C/min, and kept at 200 °C for 30 min. The ^1H NMR and ^{13}C NMR spectra were recorded on BRUKER spectrometers (Model DPX300 or DRX300). For the reaction with PTAD, all ^1H NMR spectra were obtained in CDCl_3 on an AC360 Bruker spectrometer, supplied with NTNMR software version 1.3 and processed with Mestre-C 4.1.1.0.

2.3. Photooxygenation of *Z* and *E* enecarbamates

The appropriate *Z* or *E* enecarbamate epimeric pair **1** (see Chart 1) and the methylene blue sensitizer were dissolved in 0.7 mL of the desired deuterated solvent (the enecarbamate concentration was 3.0×10^{-3} M and that of methylene blue 3.7×10^{-4} M), placed into the NMR tube, sealed with a rubber septum, fitted with a gas delivery needle, and a vent needle. Dry O_2 gas was purged through the sample for 20 min, while irradiating with a 500-W halogen lamp, equipped with a cutoff filter (<500 nm). After irradiation, the samples were submitted to ^1H NMR spectroscopy to determine the conversion (kept below 50%). The mass balance (based on unreacted enecarbamate and formed MDB product) and the conversion (based on unreacted enecarbamate) were determined by GC analysis on an achiral stationary phase, with 4,4'-di-*tert*-butylbiphenyl as calibration standard. The enantioselectivity (% ee) of the MDB product was determined by GC analysis on a chiral stationary phase.

2.4. Reaction of enecarbamates with PTAD

The respective enecarbamate pair (0.013 mmol) in CDCl_3 was placed in the NMR tube followed by the addition of

0.003 mmol of the PTAD dissolved in chloroform-*d*. The amount of PTAD was chosen to give a maximum of 25% conversion. The reaction was allowed to proceed at 24, 7, or -20°C until the disappearance of the characteristic red color of the PTAD indicated that the reaction had terminated. The samples were then subjected to ^1H NMR spectroscopy to record the conversion and diastereomeric excess.

2.5. General procedure for the ozone oxidation of the enecarbamates

An aliquot of the appropriate enecarbamate epimeric pair was taken from a standard solution in dichloromethane and transferred to a NMR tube. Most of the solvent was removed by means of a gentle stream of N_2 , the residual solvent removed by placing the open NMR tube into a vacuum (~ 12 in. Hg) oven at room temperature for at least 2 h. To each NMR tube was added 0.7 mL of the desired deuterated solvent. The NMR tube with the enecarbamate was kept in a cooling bath at the required temperature. A separate test tube with the deuterated solvent of interest was placed into the cooling bath at the required temperature, and saturated with O_3 (generated by OL100 Ozone Generator) by purging with O_3 gas for a minimum of 15–20 min. The required amount of an O_3 -saturated solution was added to the NMR tube and the conversion monitored by ^1H NMR spectroscopy (conversion $<20\%$). The amounts of O_3 -saturated solution used in the case of $\text{CD}_2\text{Cl}_2/\text{CDCl}_3$ were 50 μL at $+20^{\circ}\text{C}$, 40 μL at -15°C , 30 μL at -45°C , and 25 μL at -70°C . For CD_3OD , the amounts of O_3 -saturated solution were 90 μL at $+20^{\circ}\text{C}$, 50 μL at -15°C , 40 μL at -45°C , and 35 μL at -70°C . Because of the lower solubility of ozone in CD_3OD ,³⁰ larger amounts of O_3 -saturated solution were used in the CD_3OD experiments. After addition of the O_3 , the reaction was allowed to proceed at the desired temperature for 15 min, and then analyzed by ^1H NMR spectroscopy, with conversion calculated by integration of the aldehyde (decomposition product) and the unreacted enecarbamates signals. The samples were then subjected to GC analysis on a chiral stationary phase.

2.6. General procedure for the oxidation of the enecarbamates by triphenyl phosphite ozonide

A 0.5 mL aliquot of triphenyl phosphite (1.72×10^{-6} M) in dichloromethane was pipetted into a colorless 1-dram vial, and placed into a cooling bath kept at -70°C . The O_3 gas was bubbled through the chilled solution for a minimum of 10 min until the solution acquired the characteristic purple color of O_3 saturation (O_3 generated by OL100 Ozone Generator), followed by N_2 gas to remove excess O_3 (ca. 5 min). To the colorless triphenyl phosphite ozonide solution was added a pre-cooled solution (kept in the same cooling bath) of *Z(R)*-**1** in dichloromethane, and the mixture was allowed to react for 40 min in the cooling bath at -70°C . After 40 min, the vial was removed from the cooling bath and the contents allowed to warm up to room temperature (ca. 20°C). The reaction mixture was concentrated and submitted to GC analysis on a chiral and an achiral stationary phase, with di-*tert*-butylbiphenyl as calibration standard.

3. Results

The reaction between the chiral enecarbamates **1** and the three different reactive species $^1\text{O}_2$, O_3 , and PTAD was carried out to assess the difference in their reactivity and stereoselectivity. The Evans chiral auxiliary^{31–33} in the enecarbamate diastereomer *Z*-**1** serves as the essential stereochemical director, whereas the 1-phenylethyl substituent at the C_3' position of the double bond minimizes the *ene* reaction during photooxygenation^{24–26} as the required coplanar alignment of the only allylic hydrogen atom is encumbered. The *E*-**1** enecarbamate was prepared from the *Z*-**1** diastereomer by direct or sensitized photochemical isomerization,³⁴ followed by chromatographic separation. Photooxygenation of the enecarbamate **1** gave quantitatively the expected oxazolidinone aldehyde **2** and the chiral methyldeoxybenzoin (MDB) **3** on complete conversion of the substrate. In previous experiments,^{24–26} the thermally labile dioxetane was detected at -35°C and shown to decompose readily at room temperature (ca. 20°C) into aldehyde **2** and MDB **3** (Scheme 1, Chart 1).

The reactivity of chiral *Z* and *E* enecarbamates **1** with $^1\text{O}_2$, O_3 , and PTAD, was compared by examining the selectivity observed with the three different reactants. The product studies for the reactions of *Z* and *E* enecarbamates **1** with PTAD^{19–23} are presented in Table 1. The comparable results for reactions with O_3 ²⁹ and $^1\text{O}_2$,^{11,27} which have been previously published are summarized in Tables 2 and 3, respectively. The reactions with PTAD as with the previous work, employed a 50:50 mixture of C_3' epimers and were conducted to conversions less than 25% to minimize formation of side products.

Examination of Table 1 shows that there is no significant effect of the alkene geometry in the PTAD reaction with the chiral *Z* and *E* enecarbamates **1**. As exemplified in Entry 1 of Table 1, the addition of PTAD to *E(R)*-**1** in CDCl_3 at 24°C accumulated a 14% diastereomeric excess of the

Table 1. Diastereomeric excess in enecarbamate **1** after reaction with PTAD in CDCl_3

Entry	Enecarbamate ^a	Temp ($^{\circ}\text{C}$)	% de enecarbamate ^{b-d}	% Convn ^c
1	<i>E(R)</i> - 1	24	14 [$\text{C}_3'\text{S}$]	17
2		7	8 [$\text{C}_3'\text{S}$]	20
3		-20	11 [$\text{C}_3'\text{S}$]	16
4	<i>E(S)</i> - 1	24	13 [$\text{C}_3'\text{R}$]	13
5		7	10 [$\text{C}_3'\text{R}$]	11
6	<i>Z(R)</i> - 1	24	10 [$\text{C}_3'\text{S}$]	19
7		7	13 [$\text{C}_3'\text{S}$]	13
8		-20	14 [$\text{C}_3'\text{S}$]	19
9	<i>Z(S)</i> - 1	24	0	16
10		7	4 [$\text{C}_3'\text{R}$]	13
11		-20	4 [$\text{C}_3'\text{R}$]	18

^a A ca. 50:50 mixture of diastereomers (total concentration 0.1 M) was used.

^b Average of three runs (error $\pm 4\%$).

^c Conversion was monitored by ^1H NMR spectroscopy; the conversion (error $\pm 3\%$) was kept low to prevent side reactions.^{19–23}

^d It is important to note that the C_3' isomer of the enecarbamate substrate is observed in excess in the product mixture, since it is the less reactive epimer of the starting enecarbamate pair; for example, in entry 1, PTAD is relatively more reactive with the $\text{C}_3'(\text{R})$ epimer and, hence, the $\text{C}_3'(\text{S})$ epimer of *E(R)*-**1** accumulates.

Table 2. Determination of the stereoselectivity factor (*s*) for the formation of (*R/S*)-MDB product in the oxidation^a of **1** by O₃ as a function of solvent and temperature²⁹

Entry	Enecarbamate ^a	Solvent	Temp (°C)	% ee MDB ^b	% Convn ^c	<i>s</i> ^d	$\Delta\Delta H^\ddagger$ (kcal mol ⁻¹) ^d	$\Delta\Delta S^\ddagger$ (cal mol ⁻¹ K ⁻¹) ^d
1	<i>E(R)</i> - 1	CD ₂ Cl ₂	20	22 (<i>S</i>)	6	1.6	0.16	1.49
2			-15	24 (<i>S</i>)	15	1.7		
3			-45	16 (<i>S</i>)	18	1.4		
4			-70	18 (<i>S</i>)	27	1.5		
5	<i>E(R)</i> - 1	CDCl ₃	20	18 (<i>S</i>)	12	1.5	-0.48	-0.97
6			-15	20 (<i>S</i>)	17	1.6		
7			-70	29 (<i>S</i>)	25	2.0		
8	<i>E(R)</i> - 1	CD ₃ OD	20	4 (<i>S</i>)	4	1.1	0.12	0.16
9			-15	2 (<i>S</i>)	6	1.1		
10			-45	0	4	1.0		
11			-70	4 (<i>S</i>)	5	1.1		
12	<i>Z(R)</i> - 1	CD ₂ Cl ₂	20	31 (<i>R</i>)	10	2.0	-0.14	0.79
13			-15	30 (<i>R</i>)	12	1.9		
14			-78	36 (<i>R</i>)	9	2.2		
15	<i>Z(S)</i> - 1	CD ₂ Cl ₂	20	33 (<i>S</i>)	6	2.0	0.6	2.98
16			20	27 (<i>S</i>)	9	1.8		
17			-15	38 (<i>S</i>)	7	2.3		
18			-15	12 (<i>S</i>)	20	1.3		
19			-45	6 (<i>S</i>)	27	1.2		
20			-70	36 (<i>S</i>)	9	2.2		
21			-70	4 (<i>S</i>)	36	1.1		
22	<i>Z(S)</i> - 1	CDCl ₃	20	20 (<i>S</i>)	16	1.6	0.08	1.03
23			-15	16 (<i>S</i>)	17	1.4		
24			-70	18 (<i>S</i>)	14	1.5		
25	<i>Z(S)</i> - 1	CD ₃ OD	20	20 (<i>S</i>)	3	1.5	-0.05	0.62
26			-15	21 (<i>S</i>)	4	1.5		
27			-45	22 (<i>S</i>)	16	1.6		
28			-70	22 (<i>S</i>)	7	1.6		

^a A 50:50 mixture of diastereomers (total concentration 2.3 × 10⁻³ M) was used.^b Average of three runs (error ±6%).^c Conversion monitored by ¹H NMR spectroscopy the conversion was kept low to prevent side reactions.¹⁸^d Calculated from Eqs. 1–3.**Table 3.** Determination of the stereoselectivity factor (*s*) for the formation of (*R/S*)-MDB product in the photooxygenation^a of **1** as a function of solvent and temperature^{11,27}

Entry	Enecarbamate ^a	Solvent	Temp (°C)	MDB ^b (% ee)	Convn ^c (%)	<i>s</i> ^d	$\Delta\Delta H^\ddagger$ (kcal mol ⁻¹) ^d	$\Delta\Delta S^\ddagger$ (cal mol ⁻¹ K ⁻¹) ^d
1	<i>E(R)</i> - 1	CDCl ₃	50	8 (<i>S</i>)	5	1.2	-4.5	-14
2			18	63 (<i>R</i>)	17	5		
3			-15	78 (<i>R</i>)	37	13		
4			-40	88 (<i>R</i>)	43	31		
5	<i>E(R)</i> - 1	CD ₂ Cl ₂	20	34 (<i>S</i>)	25	2.3	-4.0	-15
6			-20	27 (<i>R</i>)	65	2.7		
7			-60	82 (<i>R</i>)	54	40		
8	<i>E(R)</i> - 1	CD ₃ CN	50	64 (<i>S</i>)	23	5.5	-4.5	-17
9			18	30 (<i>S</i>)	34	2.1		
10			-15	0	28	1.0		
11			-40	58 (<i>R</i>)	37	5.2		
12	<i>E(R)</i> - 1	CD ₃ OD	50	70 (<i>R</i>)	30	7.6	-2.5	-4.9
13			18	85 (<i>R</i>)	34	19		
14			-15	90 (<i>R</i>)	17	23		
15			-40	94 (<i>R</i>)	12	37		
16			-70	97 (<i>R</i>)	8	72		
17	<i>E(S)</i> - 1	CD ₂ Cl ₂	20	28 (<i>R</i>)	29	2.0	5.3	19.0
18			-20	36 (<i>S</i>)	59	3.4		
19			-60	88 (<i>S</i>)	56	45		
20	<i>Z(R)</i> - 1	CD ₂ Cl ₂	20	22 (<i>R</i>)	29	1.7	-0.7	1.2
21			-20	22 (<i>R</i>)	59	2.1		
22			-60	30 (<i>R</i>)	56	2.6		

^a The *E* enecarbamate concentration is 3.0 × 10⁻³ M and that for the methylene blue sensitizer is 3.7 × 10⁻⁴ M.^b Determined by GC analysis on a chiral stationary phase.^c Conversion (convn) of enecarbamates determined by GC analysis on an achiral stationary phase with 4,4'-di-*tert*-butylbiphenyl as calibration standard, and by ¹H NMR spectroscopy; averages of three runs, within 5% error of the stated values.^d Calculated from Eqs. 1–3.

C_3 -(*S*)-epimer of *E*(*R*)-**1** after the reaction; thus, the C_3 -(*R*)-epimer of *E*(*R*)-**1** is more reactive. By changing the alkene geometry to the *Z* enecarbamate, the C_3 -(*S*)-epimer of *Z*(*R*)-**1** accumulated in a 10% diastereomeric excess under identical conditions (Entry 6), which indicates that the C_3 -(*R*)-epimer of *Z*(*R*)-**1** is more reactive. Thus, when the *R* configuration at the C_4 position of the oxazolidinone chiral auxiliary was used, the C_3 -(*R*)-epimer was more reactive irrespective of the alkene *Z/E* geometry. For example (Table 1; Entries 1–3), PTAD is more reactive for the C_3 -(*R*)-epimer of *E*(*R*)-**1** and, hence, the C_3 -(*S*)-epimer of *E*(*R*)-**1** was observed in excess after the reaction. Similarly, PTAD is more reactive for the C_3 -(*R*)-epimer of *Z*(*R*)-**1** and, thus, the C_3 -(*S*)-epimer of *Z*(*R*)-**1** results in excess (Table 1; Entries 6–8). The low selectivity observed in the reaction (<15%) indicates that the C_3 stereocenter is not playing a dominant role. Since the sense in the stereoselection was reversed upon changing the configuration at the C_4 position of the oxazolidinone chiral auxiliary from *R* to *S* (Table 1; Entries 4,5 and 9–11), the PTAD reaction is well behaved.

The enantiomeric excesses in the MDB product upon oxidative cleavage of the epimeric pairs of oxazolidinone-derived *E* and *Z* enecarbamates by O_3 are given in Table 2 for three different solvents (CD_2Cl_2 , $CDCl_3$, and CD_3OD) and at various temperatures. The conversion was kept low to avoid side reactions¹⁸ and the enantiomeric excess (ee) was obtained by GC analysis of the methyldeoxybenzoin (MDB) product on a chiral stationary phase. Inspection of Table 2 reveals the following features: (i) The same MDB enantiomer is formed preferentially irrespective of the solvent, that is, employed, but the ee values for both *E* and *Z* enecarbamates change notably, when compared at the same temperature; for example, the ee value for the O_3 oxidation of *E*(*R*)-**1** in CD_2Cl_2 is 18% (Entry 4), in $CDCl_3$ it is 29% (Entry 7), and in CD_3OD it is 4% (Entry 11) at $-70^\circ C$. (ii) The sense of the preferentially generated MDB enantiomer depends on the configuration at the C_4 position of the oxazolidinone ring, as well as the alkene *Z/E* geometry; for example, *E*(*R*)-**1** substrate gave the *S*-MDB product in excess, whereas the corresponding *Z*(*R*)-**1** enecarbamate afforded *R*-MDB in excess. (iii) The same MDB enantiomer is produced irrespective of the temperature. (iv) The change in the configuration at the C_4 position of the oxazolidinone reverses the sense of the MDB enantiomer to the same extent, which indicates that the O_3 oxidation is also well behaved. (v) The observed ee values depend on the extent of conversion; thus, the ee values were moderate at low conversions and small at high conversions.

The stereoselectivity factor (*s*), which represents the ratio of the rates of formation (k_R/k_S) of the enantiomeric products, may be computed from the observed ee values at a given conversion by means of Eqs. 1 and 2.^{35–38} The computed *s* values for the O_3 oxidation are given in Table 2, and are quite low, i.e., at best ~ 2 . Consequently, the stereocontrol in the ozonolysis reaction is relatively poor.

$$s = \frac{k_R}{k_S} = \frac{\ln[1 - C(1 + ee_{MDB})]}{\ln[1 - C(1 - ee_{MDB})]} \quad (1)$$

where *C* is the conversion and ee_{MDB} the ee value of the MDB product

$$\ln(k_R/k_S) = \ln[(100 + \% ee)/(100 - \% ee)] \quad (2)$$

$$\begin{aligned} -\Delta\Delta G^\ddagger_{R-S}/RT &= \ln(k_R/k_S) \\ &= \Delta\Delta S^\ddagger_{R-S}/R - \Delta\Delta H^\ddagger_{R-S}/RT \end{aligned} \quad (3)$$

The effect of the solvent type and polarity was examined by conducting the ozonolysis in the polar, protic solvent CD_3OD , and the low-polarity halogenated solvents CD_2Cl_2 and $CDCl_3$. For the oxidative cleavage of the *E*(*R*)-**1** substrate by O_3 , the solvent dependence of the stereoselectivity follows the order (the ee values are given in parentheses) CD_3OD (4%) < $CDCl_3$ (18%) < CD_2Cl_2 (22%) at the common temperature of about $20^\circ C$ (Table 2; Entries 8, 5, and 1). Similarly, for the O_3 cleavage of the *Z* isomer [*Z*(*S*)-**1**], the solvent dependence of the stereoselectivity follows the order CD_3OD (20%) \approx $CDCl_3$ (20%) < CD_2Cl_2 (33%), also at about $20^\circ C$ (Table 2; Entries 25, 22, and 15). Evidently, the best diastereoselectivity is obtained for CD_2Cl_2 , whereas the lowest stereocontrol is displayed by the hydrogen-bonded solvent methanol at the same temperature. Since the stereoselectivity in $CDCl_3$ and CD_3OD is similar (Table 2; compare Entries 22–24 and 25–28), the solvent polarity alone cannot be the responsible factor for the stereocontrol in the oxidative cleavage of the *Z*(*S*)-**1** enecarbamates by O_3 .

In contrast, the ozonolysis of the *E*(*R*)-**1** diastereomer in $CDCl_3$ and CD_3OD displays significant differences in the observed stereoselectivity (Table 2; compare Entries 5–7 and 8–11). Although not as dramatic as observed for the 1O_2 oxidation, the effect is attributed to the differing alkene geometry (*Z* vs *E* enecarbamate) and the various conformations that these diastereomers may adopt in the two solvents.^{11,27,29} To be noted is the comparatively high ee values for the *Z* versus the *E* enecarbamates. Mechanistically most revealing is the finding that the *R*-MDB enantiomer is the favored product for *Z*(*R*)-**1** (Table 2; Entries 12–14), but the *S*-MDB isomer dominates for *E*(*R*)-**1** (Table 2; Entries 1–11). For example, in CD_2Cl_2 at $20^\circ C$ *E*(*R*)-**1** favors the *S*-MDB product (Table 2; Entry 1), whereas *Z*(*R*)-**1** prefers the *R*-MDB (Table 2; Entry 12) under the identical conditions.

Our previous results on the photooxygenation of *Z* and *E* enecarbamate (Table 3) showed that there is negligible effect of the alkyl substituent (methyl or isopropyl group) at the oxazolidinone C_4 position.^{11–13,24–27} Further, upon employing *R* or *S* antipodes at the C_4 position (Table 3), the sense of the enantioselectivity in the MDB product is reversed, while the extent of the stereocontrol in the photooxidative cleavage of the *E* enecarbamates is the same (within the experimental error). This is clearly displayed by the % ee data for the *E*(*R*)-**1** and *E*(*S*)-**1** diastereomers, as exemplified by their photooxygenation in CD_2Cl_2 at $20^\circ C$ (*s* factor ca. 2 for both; Entries 5 and 17 in Table 3). Thus, *E*(*R*)-**1** (Table 3; Entries 5–7) favors the *S*-MDB enantiomer (34% ee at 25% convn), whereas *E*(*S*)-**1** (Entries 17–19) favors the *R*-MDB (28% ee at 29% convn) enantiomer as the final oxidation products; the reversal in the enantioselectivity sense is expected.

The effect of the solvent type and polarity was examined by conducting the photooxygenation in the polar, aprotic solvent CD_3CN , the polar, protic solvent CD_3OD , and the

low-polarity halogenated solvents CD_2Cl_2 and CDCl_3 . For the photooxidative cleavage of the *E*-**1** substrate, the solvent dependence of the diastereoselectivity follows the order CD_3CN (30%) $\sim\text{CD}_2\text{Cl}_2$ (34%) $<\text{CDCl}_3$ (63%) $<\text{CD}_3\text{OD}$ (85%) at the common temperature of about 18–20 °C (Table 3; Entries 9, 5, 2, and 13); the ee values are given in parentheses. Evidently, the best stereoselectivity is obtained for the hydrogen-bonding solvent methanol (Table 3; Entry 13), whereas the lowest stereoselectivity is displayed by the aprotic acetonitrile (Table 3; Entry 9) at the same temperature of 18 °C. To be noted is the relatively high ee value in chloroform-*d* (Table 3; Entries 1–4). Again, mechanistically most revealing is the finding that the *R*-MDB enantiomer is the favored product in CDCl_3 and CD_3OD (Table 3; Entries 2 and 13), but the *S*-MDB isomer dominates in CD_2Cl_2 and CD_3CN (Table 3; Entries 5 and 9). Thus, also for the photooxidative cleavage of the *E(R)*-**1** enecarbamates, the stereoselectivity cannot be attributed to the solvent polarity alone.

Still more intriguing for mechanistic considerations is the temperature dependence of the ee values upon photooxygenation of the *E(R)*-**1** substrate (Table 3). Only in methanol is the extent of the diastereoselectivity relatively constant (note the high ee value of 97% at –70 °C, i.e., nearly perfect stereocontrol!); moreover, the same enantiomer, namely *R*-MDB, is formed over the entire temperature range from –70 to +50 °C (Table 3; Entries 12–16). In the other solvents, a temperature-dependent change in the sense of stereoselection is observed from the usual *R*-MDB to the *S*-MDB isomer. For example, very good stereocontrol (ee value of 88%) in favor of *R*-MDB is found in chloroform-*d* at –40 °C (Table 3; Entry 4), but the *S*-MDB isomer is favored with only poor diastereoselectivity (ee value of only 8%) at +50 °C (Table 3; Entry 1). This inflection in the enantioselectivity sense (*R* to *S* isomer) occurs in CDCl_3 above +18 °C (Table 3; Entries 1 and 2), whereas in CD_2Cl_2 it takes place between +20 and –20 °C (Table 3; Entries 5 and 6). In the case of CD_3CN , the change in the sense takes place at –15 °C (Table 3; Entry 10), as indicated by the 0% ee value in the MDB product.

The present stereoselectivity data indicate that the solvent and temperature effects are just confined to the reaction of $^1\text{O}_2$ with *E*-**1**. Both the O_3 and PTAD reactions do not show any noticeable dependence of the stereocontrol on either temperature or solvent. These remarkable stereoselectivity trends require careful mechanistic scrutiny, to understand the details of the enecarbamate oxidation. To enable a detailed comparative mechanistic rationalization of these

trends for the three oxidants $^1\text{O}_2$, O_3 , and PTAD, we will rely on the previously published structural details of the chiral *Z*²⁴ and *E*²⁷ enecarbamates.

4. Discussion

Before entering into a mechanistic analysis of the stereochemical control exercised by $^1\text{O}_2$, O_3 , and PTAD with *Z/E* enecarbamates **1**, the established reaction pathways must be recalled. Both $^1\text{O}_2$ and PTAD approach the alkene double bond (on the XY-plane) perpendicularly (*Z*-axis), as shown in Figure 2 for the transition structures **A** ($^1\text{O}_2$) and **C** (PTAD),^{19–23} whereas O_3 ¹⁸ adds to the double bond laterally, as displayed by the transition structure **B** in Figure 2. Additionally, the major differences and similarities between the three reagents are:

- Both O_3 and PTAD are ground-state molecules and will not experience any excited-state vibrational deactivation as observed for the electronically excited $^1\text{O}_2$; their stereoselectivity is expected to be controlled mainly by steric effects, whereas for $^1\text{O}_2$ also physical quenching may play a role.²⁸
- PTAD^{19–23} is a much larger enophile than $^1\text{O}_2$ and if steric control at the $\text{C}_{3'}$ position is the deciding factor, then a higher stereoselectivity should be expected for PTAD compared to $^1\text{O}_2$.^{14–17}
- O_3 ¹⁸ is similar in size to $^1\text{O}_2$ and should be subject to similar steric interactions,²⁹ but differences may arise from its lateral attack on the double bond versus the perpendicular one for $^1\text{O}_2$.

Based on this mechanistic background, we shall now analyze the factors that underlay the stereoselectivity in the oxidation of both *Z* and *E* enecarbamates with O_3 and PTAD, and compare the present results with our previously published ones^{11,24–27} for $^1\text{O}_2$. A brief summary of the salient features of our experimental data is given below:

- A high stereoselectivity is observed in the formation of MDB for the $^1\text{O}_2$ oxidation of *E*-**1**; whereas a low stereoselectivity is observed for both O_3 and PTAD reactions with *E*-**1**.
- $^1\text{O}_2$ is sensitive to all the stereochemical structural features inherent with the chiral enecarbamate substrate (the alkene *Z/E* geometry, the *R/S* configuration at the C_4 position in the oxazolidinone chiral auxiliary, and the *R/S* configuration at the $\text{C}_{3'}$ position of the

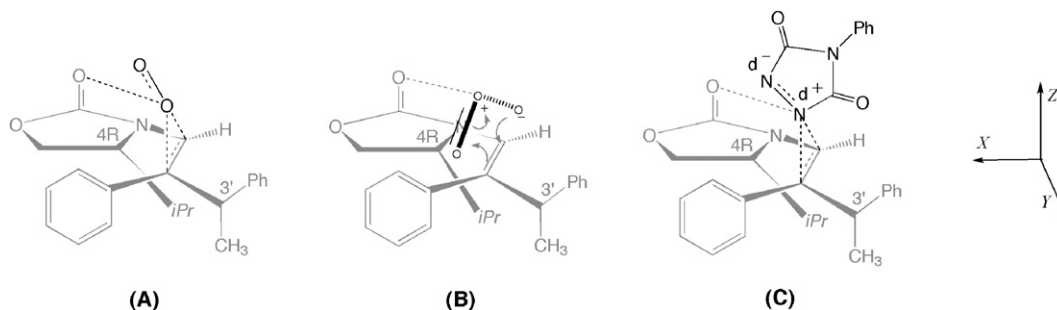


Figure 2. Plausible transition structures for the reactions of $^1\text{O}_2$ (A), O_3 (B), and PTAD (C) with the chiral enecarbamates *Z*-**1**.

phenethyl side chain), as reflected in the vastly different stereoselectivities (Table 3) observed for the *Z* and *E* enecarbamates. This is highlighted by the observation that the photooxidative cleavage of the *E*-1 isomer affords the MDB product in high (up to 97%) enantioselectivity (Table 3), whereas the ee value for the *Z*-1 isomer is low (only 30% at best) under comparable reaction conditions.^{11,24–27} In contrast, both PTAD (Table 1) and O₃ (Table 2), display a very low stereoselectivity for both *Z* and *E* enecarbamates.

- (iii) The sensitivity of the three different reactive species towards C_{3'} stereochemistry follows the order ¹O₂ >> O₃ > PTAD; thus, PTAD reacts preferentially with the C_{3'}(*R*)-epimer irrespective of the alkene *Z/E* geometry, whereas the C_{3'}(*S*)-epimer of the *E* enecarbamate and the C_{3'}(*R*)-epimer of the *Z* enecarbamate are more reactive for O₃.
- (iv) The enantiomeric excess in the MDB product for the ¹O₂ oxidation of the *E*-1 diastereomer depends substantially on the employed solvent and the temperature conditions, but not for the corresponding *Z*-1 enecarbamate (Table 3);^{11,24–27} no significant solvent and temperature effects are evident for the reaction of PTAD (Table 1) and O₃ (Table 2) with both *Z* and *E* enecarbamates.
- (v) Not only does the extent of stereoselection (% ee value) for the *E*-1 diastereomer vary extensively as a function of solvent and temperature (Table 3), but the favored configuration (*R* vs *S* enantiomers of MDB) changes, i.e., there is an inversion in the sense of the stereoselectivity for the ¹O₂ oxidation (Table 3), but not for PTAD (Table 1) or O₃ (Table 2).

This divergent behavior in the stereochemical control displayed by ¹O₂, O₃, and PTAD in their reactivity towards **1** needs to be mechanistically rationalized in terms of the trajectory for the attack on the double bond of the chiral enecarbamate substrate. The configuration at the C_{3'} position is of particular interest in regard to steric blocking (ground-state reactivity) versus vibrational deactivation (excited-state reactivity) by the methyl versus phenyl substituents for attack of the reagent on the double bond.

Since we have employed a 50:50 diastereomeric mixture of enecarbamates *E*-1 (actually, *R/S* epimers at the C_{3'} stereogenic site of the alkyl side chain), the stereoselection in the present case entails *kinetic resolution*.^{11,27} Thus, the enantiomeric excess in the MDB product **3**, which is formed in the double-bond cleavage by ¹O₂ and O₃, reflects the differentiation in the relative reaction rates of the enecarbamate oxidation (Fig. 3). For such *kinetic resolution*, the so-called selectivity factor (*s*),^{35–38} which is a quantitative measure (corrected for the extent of conversion) of the relative reaction rates for the two stereoisomers in question (Eqs. 1 and 2) come to prominence. In the present case, the *s* factor may be computed for the two-epimeric enecarbamates [C_{3'}(*R*) and C_{3'}(*S*) epimers] from the substrate conversion and the MDB enantiomeric excess by using Eqs. 1 and 2. A large *s* value translates to high enantiomeric excess in the MDB product (see Figs. 3 and 4).

For illustration purposes, under identical conditions, the oxidation of *E(R)*-1 by ¹O₂ gave an ee value of 97%

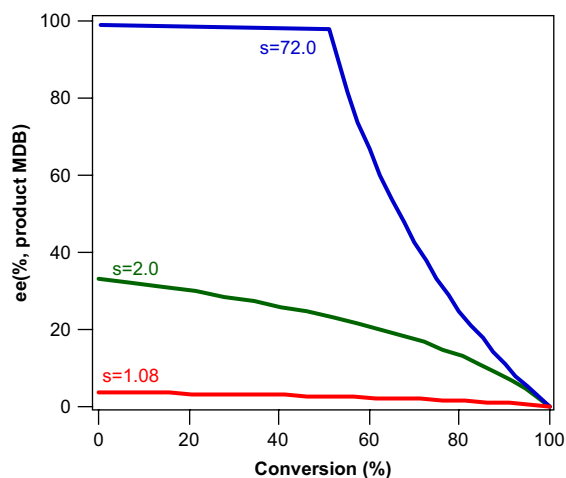


Figure 4. The dependence of the enantiomeric excess of the MDB product on the conversion of the chiral oxazolidinone-functionalized enecarbamates to illustrate the consequences of the difference in the *s* factor.^{35–38}

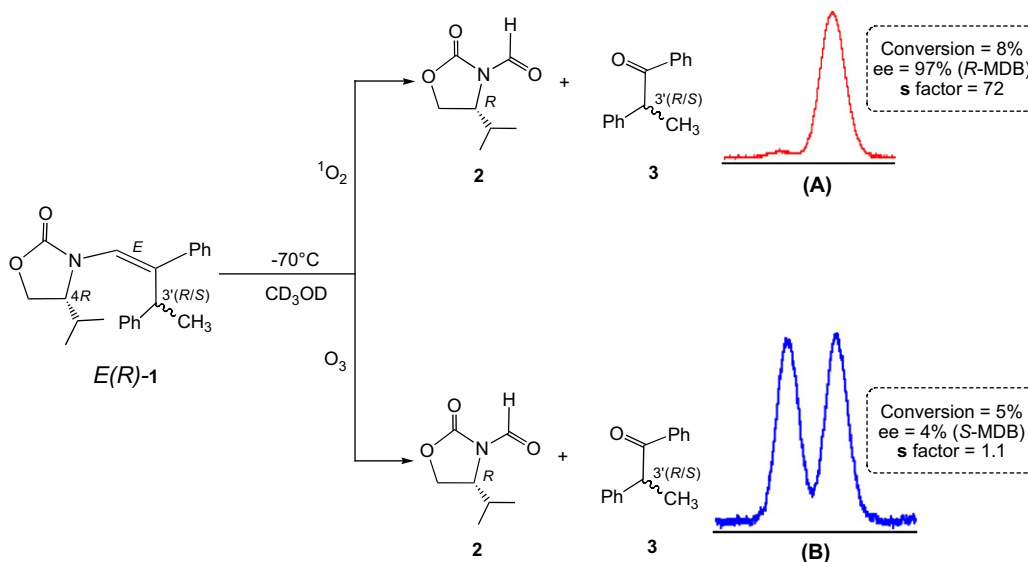


Figure 3. The GC traces of the MDB product for the oxidation of *E(R)*-1 by ¹O₂ (A) and O₃ (B) at –70 °C in CD₃OD.

with a s factor of 72, compared to only 4% for the O₃ oxidation with an s factor of about 1.1 (compare Entry 16 in Table 3 and Entry 11 in Table 2). As a practical utilization of such a high s factor in a kinetic resolution, we previously demonstrated¹¹ that we may photochemically resolve the two epimers with ¹O₂ by running the photooxygenation of *E(R)*-**1** in CD₃OD at -70 °C to nearly 50% conversion. The *R*-MDB product was separated from the reaction mixture by chromatography and an ee value of 97% was obtained. The unreacted 1'*E*,4*R*'(*Pr*),3'*S*'-**1** enecarbamate was then quantitatively photooxidized at room temperature to afford the *S*-MDB product with an ee value of 97%. This remarkable case of stereoselection for ¹O₂ was previously coined as *photochemical Pasteur-type kinetic resolution*.¹¹

The plot of % ee versus conversion in Figure 4 displays that the dependence of the enantioselectivity as a function of conversion for various s factors, as observed for the O₃ oxidation (Table 2), for which the ee values are moderate at low and small at high conversions. For example, 36% ee was observed at 9% conversion and only 4% ee at 36% conversion (Table 2; Entries 20 and 21) for the oxidation of *Z(S)*-**1** by O₃ in CD₂Cl₂ at -70 °C. The consequence of the difference in the s factors is best illustrated in Figure 3, where an ee value of 97% was obtained for ¹O₂ (s factor of 72) compared to an ee value of only 4% for O₃ (s factor of 1.1) in CD₃OD. When stereoselectivity results are rationalized mechanistically in the kinetic-resolution studies, instead of the ee values the s factor should be employed.^{35–38} The reason for this is that the ee value refers to the amount of the enhanced MDB enantiomer uncorrected for the extent of conversion, whereas the s factor reflects the variation in the ee value corrected for the extent of conversion (Eq. 1; Fig. 4).^{35–38} For example, in the case of the O₃ oxidation of *Z(S)*-**1** at -70 °C, in CD₂Cl₂ the ee value is 4% *S*-MDB at 36% conversion and the s factor 1.1 (Table 2; Entry 21), while for CD₃OD the ee value is 22% *S*-MDB at 7% conversion and the s factor 1.6 (Table 2; Entry 28); clearly, there is a large difference in the ee values, but the s factors are almost the same. In the case of the ¹O₂ oxidation of the *E* enecarbamate, there is a significant variation in the s factor upon changing the solvent from CD₂Cl₂ (the s factor varies from 2.3 to 40) to CD₃OD (the s factor varies from 7.6 to 72), but not for the *Z* isomer. Comparison of the stereoselectivity of PTAD, O₃, and ¹O₂ in the various solvents at different temperatures, it is clear that PTAD (Table 1) and O₃ (Table 2), exhibits essentially no temperature effect or solvent effect for both *Z/E* enecarbamates, whereas ¹O₂ (Table 3) displays a substantial temperature effect and solvent effect for the *E* enecarbamates and not for the *Z* enecarbamates. The differential activation parameters ($\Delta\Delta S^\ddagger$ and $\Delta\Delta H^\ddagger$) were determined for the reactivity of O₃ and ¹O₂. Since the temperature profile of the stereoselectivity for PTAD is quite similar to that of O₃, we shall consider only the O₃ and ¹O₂ oxidants, but infer for PTAD from the O₃ results. The $\Delta\Delta S^\ddagger$ and $\Delta\Delta H^\ddagger$ values for the ¹O₂ and O₃ oxidation of *E(R)*-**1** diastereomer in CDCl₃, CD₂Cl₂, and CD₃OD were computed with the help of the Eyring relation (Eq. 3) and the data are given in Table 2 for O₃ and in Table 3 for ¹O₂.^{2,27,39,40} The $\Delta\Delta S^\ddagger$ and $\Delta\Delta H^\ddagger$ values for the O₃ oxidation of the enecarbamate **1** *Z/E* diastereomers reveal a negligible temperature effect in the MDB enantiomeric excess; e.g., the $\Delta\Delta H^\ddagger$ values range

between -0.5 to $+0.6$ kcal mol⁻¹ and the $\Delta\Delta S^\ddagger$ values between -1.0 and $+3.0$ cal mol⁻¹ K⁻¹ over the entire variation of reaction conditions (Table 2). In contrast, a pronounced temperature dependence is displayed for the ¹O₂ oxidation, since the $\Delta\Delta H^\ddagger$ term varies between -5.0 and $+5.0$ kcal mol⁻¹ and the $\Delta\Delta S^\ddagger$ term between -17 and $+19$ cal mol⁻¹ K⁻¹ (Table 3). Clearly, the major contribution derived from the differential activation entropy term ($\Delta\Delta S^\ddagger$), in comparison with the differential activation enthalpy term ($\Delta\Delta H^\ddagger$), cannot be ignored.

The experimental trends in the temperature dependence of the enantioselectivity for the O₃ and ¹O₂ oxidations of the enecarbamates as a function of the solvent nature is given in the Eyring plots for the *E(R)*-**1** diastereomer in Figure 5. The slope of nearly zero in the Eyring plot for the O₃ oxidation in the investigated solvents indicates that this reaction is insensitive to solvent and temperature variations, since the differential activation enthalpy ($\Delta\Delta H^\ddagger$) contributes negligibly.^{41,42} Since the behavior of PTAD parallels that of O₃, we presume that PTAD also exhibits similar Eyring plots. Also note the nearly parallel lines (similar slopes) for the ¹O₂ oxidation, which indicate that the enthalpic contribution ($\Delta\Delta H^\ddagger$) is about the same in the diverse solvents; thus, the stereoselectivity is controlled by the entropic term ($\Delta\Delta S^\ddagger$). Most significant is the crossing of the zero % ee line, which constitutes the inversion point in the sense of the enantioselectivity, i.e., opposite configurations are selected as the favored MDB enantiomer.

The contrasting temperature and solvent dependence of the stereoselectivity observed for the ¹O₂ and O₃ reactants (by inference, PTAD is similar to O₃) in their oxidation of the chiral enecarbamate substrates is convincingly exposed by the $\Delta\Delta S^\ddagger$ and $\Delta\Delta H^\ddagger$ parameters.^{2,39,40} Thus, the stereoselection is a critical balance of the enthalpy and entropy, which are interrelated by Eqs. 1 and 2. Consequently, the large contribution from the differential activation parameters for the ¹O₂ oxidation (Table 3) suggests that the transition state is conformationally flexible and its solvation–desolvation behavior is crucial. Expectedly, the temperature and solvent variations influence the stereo-differentiating step.^{2,39,40} Such entropy effects are indicative of conformational factors,^{2,39,40} which in the present case are dictated, presumably, by the stereogenic center at the C_{3'} position of the phenethyl side chain. In contrast, the low contribution from the differential activation parameters for the O₃ oxidation indicates that the transition state is more rigid and not affected by the variation of the external factors of the system. As expected, there is no significant temperature and solvent dependence in the sense of the stereoselectivity for the O₃ and PTAD oxidations.

These conspicuously complex temperature and solvent effects in the stereoselectivity observed for the oxidation of the *E* and *Z* enecarbamates by ¹O₂, O₃, and PTAD can be mechanistically rationalized in terms of the structural features inherent within the chiral substrate and the electronic nature of the oxidants. We previously proposed^{11,24–27} that the high stereocontrol in the photooxidative cleavage of the enecarbamates by the electronically excited ¹O₂ is the consequence of selective π -facial quenching by the enecarbamate substrate. In this context, it is well known that the lifetime of

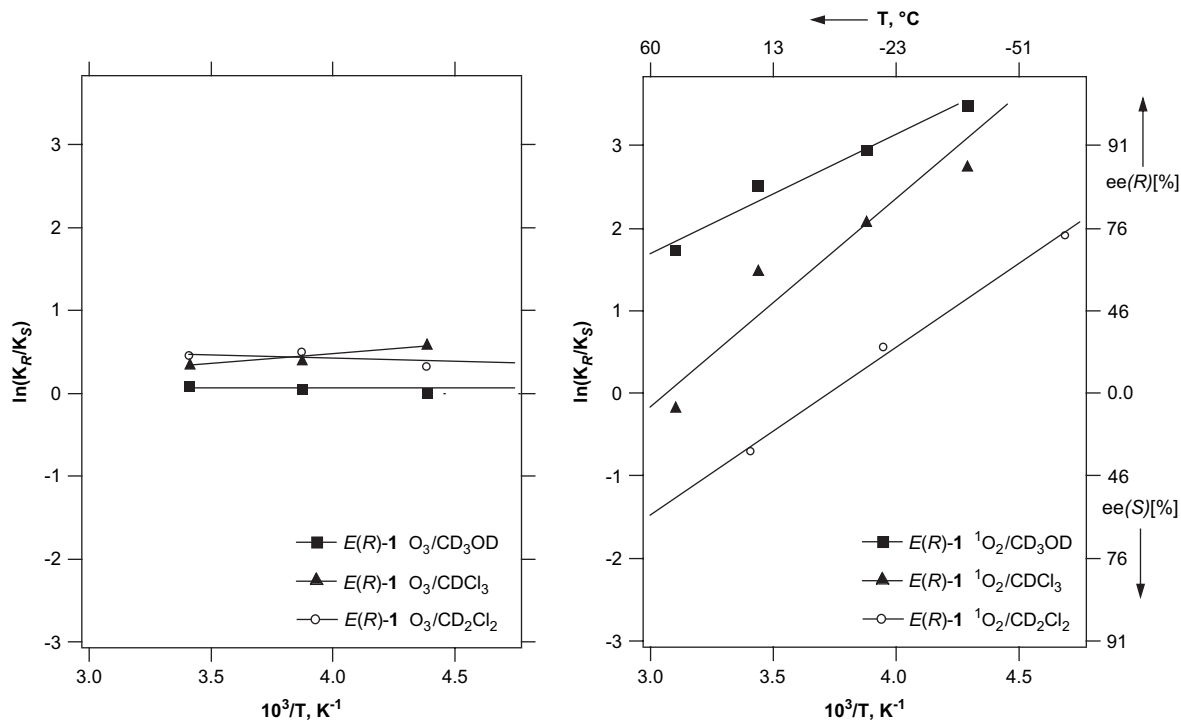


Figure 5. Eyring plots for the stereoselective photooxygenation of *E(R)*-1 by O_3 (left) and 1O_2 (right) in a variety of solvents.

1O_2 in deuterated solvents is much longer than non-deuterated ones,^{14–17} since C–H bond vibrations deactivate 1O_2 to its triplet ground state.²⁸ In view of the higher flexibility of enecarbamates, conformations may be populated, in which one π face of the double bond exposes a larger number of C–H bonds for selective quenching²⁸ of the incoming electronically excited 1O_2 (see Panel A in Fig. 6). Further, deuterium substitution (CD_3 vs CH_3) at the alkene geometry (*cis*- vs *trans*-) in the ene-reaction involving 1O_2 shows a substantial isotope-effect (k_H/k_D for *cis*-: 1.04–1.09 and k_H/k_D for *trans*-: 1.38–1.41).⁴³ If this hypothesis is valid, the ground-state reactive species like PTAD and O_3 will not be vibrationally deactivated like 1O_2 . Thus, for O_3 and PTAD only steric hindrance reflects the observed selectivity. Our analyses of O_3 and PTAD reactivity with the *Z(R)*-1 emphasizes this aspect. As shown in Panel B (O_3) and Panel C (PTAD) of Figure 6, the approach of reactant onto the double bond is hindered from the bottom by the isopropyl group, such that O_3 as well as PTAD are forced to attack from the top. Additionally, kinetic resolution by the stereogenic center at the $C_{3'}$ position of the phenethyl side chain plays a role in enriching one of the MDB enantiomers (Fig. 6).²⁷ For example, in the O_3 oxidation of the 50:50 mixture of the *3'R/S* diastereomers of *Z(R)*-1, the $C_{3'}(R)$ -epimer is more reactive than $C_{3'}(S)$ -epimer, such that the *R*-MDB enantiomer is formed in excess and the $C_{3'}(S)$ -epimer of the *Z* enecarbamate accumulates (see Panel B in Fig. 6). Similar arguments apply also to the reactivity of PTAD with the 50:50 mixture of the *3'R/S* diastereomers of *Z(R)*-1 (see Panel C in Fig. 6), which is corroborated in the observed selectivity (Table 1).

Indeed, if steric effects play a dominant role in the O_3 oxidation, then the observed ee values should be higher when a bulkier ozone-like oxidant is employed in the kinetic resolution of the *R/S* epimers at the $C_{3'}$ position. This expectation was tested with the triphenyl phosphite ozonide

(Scheme 2), which is reported^{44–46} to add at $-70^\circ C$ directly to alkenes through a peroxide-like transition state, i.e., it displays 1O_2 reactivity, but does not involve genuine 1O_2 .

As shown in Scheme 2, an ee value of 83% (*R*-MDB) was observed for the triphenyl phosphite ozonide $[(PhO)_3PO_3]$ oxidation of *Z(R)*-1,^{29,45,46} compared to only 36% (*R*-MDB) for O_3 . Due to the bulkiness of the $(PhO)_3PO_3$ oxidant and its ground-state character, the stereoselectivity displayed in the O_3 (and by inference also PTAD) reactions may be attributed to the steric interference experienced by these reactants with the enecarbamate substrate. Evidently, the much higher stereoselection exhibited by 1O_2 than for O_3 and PTAD suggests that factors other than steric impediments control the stereoselectivity of the 1O_2 oxidations, possibly quenching of the excited state nature of 1O_2 by vibrational interactions.

To understand the intricacies of the complex stereoselectivity trends observed for the 1O_2 , O_3 , and PTAD, the structural characteristics in regard to the stereochemical aspects of the chiral enecarbamates needs to be considered in detail. As shown in Figure 7, the oxazolidinone-functionalized enecarbamate are composed of three distinct stereochemically pertinent structural features, namely the *R/S* configuration at the C_4 position in the oxazolidinone chiral auxiliary, the *Z/E* geometry of the alkenyl double bond (labeled *alkene*), and the *R/S* configuration at the $C_{3'}$ position of the alkyl side chain on the double bond. The following implications on the control of the stereoselectivity imposed by these structural features on the attacking oxidants may be anticipated:

- (i) The reactant may be sterically sensitive to the C_4 position and distinguish between its *R/S* configurations but unable to sense any differences for the *Z/E*

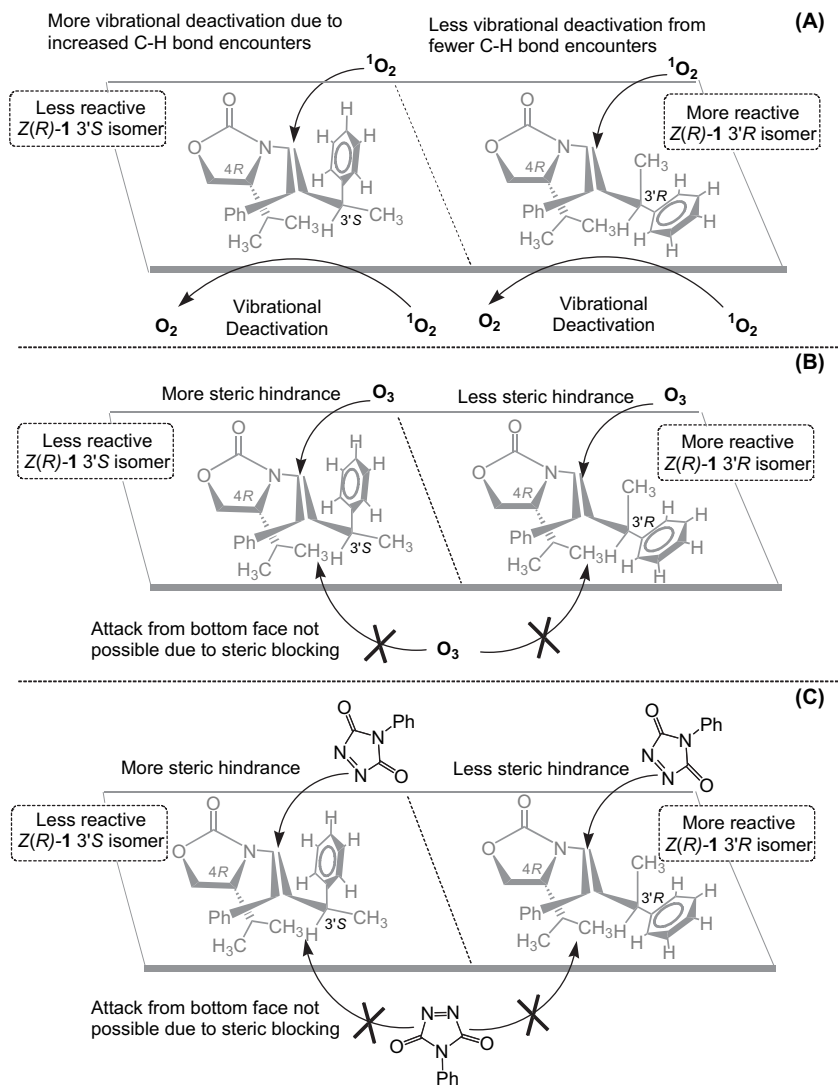
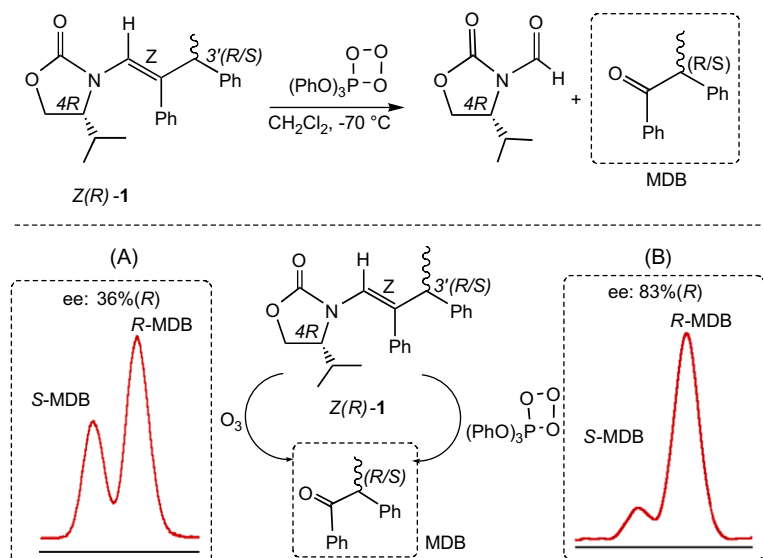


Figure 6. The favored π -facial attack on the alkene double bond of the chiral enencarbamate Z(R)-1 by $^1\text{O}_2$ (A), O_3 (B), and PTAD (C).



Scheme 2. Oxidation of the Z(R)-1 diastereomer by O_3 (A) and by $(\text{PhO})_3\text{PO}_3$ (B); for comparison, the corresponding GC traces (chiral stationary phase) are displayed.

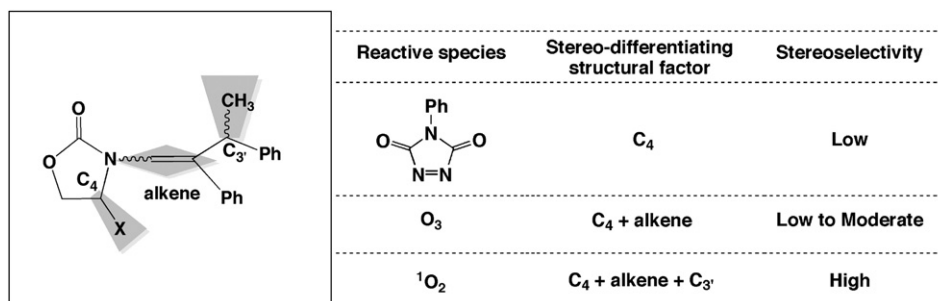


Figure 7. The stereochemically relevant structural composition of the chiral oxazolidinone-functionalized enecarbamates and their implications in regard to stereocontrol.

configurations of the *alkene* geometry nor the *R/S* configurations of the C_{3'} position; a low stereoselectivity should be expected, as displayed by PTAD.

- (ii) The reactant may be sensitive to the C₄ position and the *alkene* geometry, but insensitive to the C_{3'} position; up to a moderate stereoselectivity should be expected, as observed O₃.
- (iii) The reactant may be sensitive to all three stereochemical features, namely the C₄ position, the *alkene* geometry, and the C_{3'} position; a high stereoselectivity should result, as found for ¹O₂.

From the above analysis of the stereochemically relevant structural characteristics of the chiral enecarbamate substrate and the electronic nature of the three reactants, we speculate that the vibrational deactivation (physical quenching) is responsible for the high stereocontrol exhibited by electronically excited ¹O₂ (~97% ee at -70 °C; CD₃OD, Table 2).²⁸ In contrast, the ground-state O₃ and PTAD oxidants are only subject to classical steric effects, which are relatively ineffective for stereoselection. Thus, the product-generating chemical pathway competes with the physical quenching process through vibrational deactivation by C–H bonds.^{28,47} In the vibrational deactivation scenario, the isopropyl group at the C₄ position of the oxazolidinone chiral auxiliary is apparently responsible for the excited-state deactivation of ¹O₂. To compare directly the influence of vibrational deactivation encountered in [2+2] cycloaddition with that of ene reaction should be of pertinent mechanistic interest. In our case, such comparison with the same substrates will not be possible as the phenethyl side chain exclusively gives the [2+2] cycloaddition product. The phenethyl group would need to be replaced with a methyl group, to study the influence of vibrational deactivation for the ene reaction. Previously we have demonstrated that the oxazolidinone chiral auxiliary provides high π -facial selectivity through the C₄ substituent for both the ene and the [2+2] reaction in the case of substrates that have the methyl instead of the phenethyl group.²⁵ It was also shown that the mode selectivity (*ene* vs [2+2]) depends on the *alkene E* versus *Z* geometry, which was explained in terms of an orbital-directing effect of the enamine-type functionality.²⁵ Again, deuterated substrates would be necessary to examine the influence of vibrational deactivation in the ene reaction. A promising mechanistic probe to validate this novel phenomenon of stereoselective quenching of ¹O₂, involves the deuteration of the alkyl substituents at the C₄ and C_{3'} stereogenic centers. Such studies are in progress in our laboratory.

5. Conclusion

The current comparative study involving ¹O₂, O₃, and PTAD with enecarbamates **1** provides detailed insights into the intricate nature of the steric and electronic interactions required to achieve a high selectivity in the photooxygenation of chiral alkenes. The extensive stereochemically relevant structural properties embodied in the chiral oxazolidinone-substituted enecarbamates (i.e., the chiral centers at the C₄ position of the oxazolidinone ring and at the C_{3'} position of the phenethyl side chain, as well as the *E/Z* configurations of the *alkene* functionality) make these substrates informative molecular probes to explore the mechanistic intricacies of the oxidative cleavage of alkenyl double bonds. The stereoselection depends not only on the *alkene* geometry (*Z/E*), the size of the C₄ alkyl substituent (*H*, *Me*, *iPr*) in the oxazolidinone ring, the configuration (*R/S*) at the C_{3'} stereogenic center of the phenethyl side chain, the solvent, and temperature, but also on the electronic nature (excited vs ground state) of the oxidant. The most dramatic effects on the stereocontrol have been seen for the conformationally more flexible *E* diastereomer, which responds to the electronic characteristics of the reactive species, possibly through the selective vibrational quenching by the substituents at the C_{3'} position of the chiral enecarbamates as a function of their configuration. The stereochemical consequence of this novel phenomenon deserves further exploration in photochemical transformations.

Acknowledgements

The authors at Columbia thank the NSF (CHE 01-10655 and CHE-04-15516) for generous support of this research. W.A. is grateful for the financial support from the Deutsche Forschungsgemeinschaft, Alexander-von-Humboldt Stiftung, the Fonds der Chemischen Industrie, and the hospitality of the University of Puerto Rico. T.P. acknowledges the support of the W.M. Keck Foundation. H.S. and Y.I. gratefully acknowledge a JSPS research fellowship for young scientists (08384). The oxidative work with ¹O₂ and O₃ was carried out at the Columbia University, and the PTAD studies were conducted at Claremont McKenna, Pitzer, and Scripps Colleges.

References and notes

- Chiral Photochemistry*; Inoue, Y., Ramamurthy, V., Eds.; Marcel Decker: New York, NY, 2004.
- Inoue, Y. *Chem. Rev.* **1992**, *92*, 741–770.

3. Rau, H. *Chem. Rev.* **1983**, *83*, 535–547.
4. Turro, N. J. *Proc. Natl. Acad. Sci. U.S.A.* **2002**, *99*, 4805–4809.
5. Turro, N. J.; Cheng, C. C.; Abrams, L.; Corbin, D. R. *J. Am. Chem. Soc.* **1987**, *109*, 2449–2456.
6. *Photochemistry in Organized and Constrained Media*; Ramamurthy, V., Ed.; Wiley-VCH: New York, NY, 1991.
7. Garcia-Garibay, M. A. *Acc. Chem. Res.* **2003**, *36*, 491–498.
8. Sivaguru, J.; Natarajan, A.; Kaanumalle, L. S.; Shailaja, J.; Uppili, S.; Joy, A.; Ramamurthy, V. *Acc. Chem. Res.* **2003**, *36*, 509–521.
9. Sivaguru, J.; Shailaja, J.; Uppili, S.; Ponchot, K.; Joy, A.; Arunkumar, N.; Ramamurthy, V. Achieving Enantio and Diastereoselectivities in Photoreactions Through the Use of a Confined Space. In *Organic Solid-State Reactions*; Toda, F., Ed.; Kluwer Academic: Dordrecht, The Netherlands, 2002; pp 159–188.
10. Poon, T.; Turro, N. J.; Chapman, J.; Lakshminarasimhan, P.; Lei, X.; Adam, W.; Bosio, S. G. *Org. Lett.* **2003**, *5*, 2025–2028.
11. Poon, T.; Sivaguru, J.; Franz, R.; Jockusch, S.; Martinez, C.; Washington, I.; Adam, W.; Inoue, Y.; Turro, N. J. *J. Am. Chem. Soc.* **2004**, *126*, 10498–10499.
12. Sivaguru, J.; Poon, T.; Franz, R.; Jockusch, S.; Adam, W.; Turro, N. J. *J. Am. Chem. Soc.* **2004**, *126*, 10816–10817.
13. Singlet Oxygen Feat. *Chem. Eng. News* **2004**, *82*, 7.
14. *Singlet Oxygen*; Wasserman, H. H., Murray, R. W., Eds.; Academic: New York, NY, 1979.
15. Gollnick, K.; Kuhn, H. J. *Singlet Oxygen*; Wasserman, H. H., Murray, R. W., Eds.; Academic: New York, NY, 1979.
16. Foote, C. S. *Acc. Chem. Res.* **1968**, *1*, 104–110.
17. *Singlet Oxygen*; Frimer, A. A., Ed.; CRC: Boca Raton, 1985; Vols. 1–4.
18. Bailey, P. S. *Ozonation in Organic Chemistry*; Academic: New York, NY, 1978; Vols. 1–2.
19. Adam, W.; De Lucchi, O. *Tetrahedron Lett.* **1981**, *22*, 929–932.
20. Adam, W.; Schwarm, M. *J. Org. Chem.* **1988**, *53*, 3129–3130.
21. Adam, W.; Bottke, N.; Krebs, O. *J. Am. Chem. Soc.* **2000**, *122*, 6791–6792.
22. Adam, W.; Bottke, N.; Krebs, O. *Org. Lett.* **2000**, *21*, 3293–3296.
23. Leach, A. G.; Houk, K. N. *Chem. Commun.* **2002**, 1243–1255.
24. Adam, W.; Bosio, S. G.; Turro, N. J.; Wolff, B. T. *J. Org. Chem.* **2004**, *69*, 1704–1715.
25. Adam, W.; Bosio, S. G.; Turro, N. J. *J. Am. Chem. Soc.* **2002**, *124*, 14004–14005.
26. Adam, W.; Bosio, S. G.; Turro, N. J. *J. Am. Chem. Soc.* **2002**, *124*, 8814–8815.
27. Sivaguru, J.; Solomon, M. R.; Saito, H.; Poon, T.; Jockusch, S.; Adam, W.; Inoue, Y.; Turro, N. J. *Tetrahedron* **2006**, *62*, 6707–6717.
28. Turro, N. J. *Tetrahedron* **1985**, *41*, 2089–2098.
29. Sivaguru, J.; Saito, H.; Poon, T.; Omonuwa, T.; Franz, R.; Jockusch, S.; Hooper, C.; Inoue, Y.; Adam, W.; Turro, N. J. *Org. Lett.* **2005**, *7*, 2089–2092.
30. Greenwodd, F. L. *J. Org. Chem.* **1945**, *10*, 414–418.
31. Evans, D. A.; Bartroli, J.; Shih, T. L. *J. Am. Chem. Soc.* **1981**, *103*, 2127–2129.
32. Ager, D. J.; Prakash, I.; Schaad, D. R. *Chem. Rev.* **1996**, *96*, 835–876.
33. Evans, D. A.; Chapman, K. T.; Hung, D. T.; Kawaguchi, A. T. *Angew. Chem., Int. Ed. Engl.* **1987**, *26*, 1184–1186.
34. Saito, H.; Sivaguru, J.; Jockusch, S.; Inoue, Y.; Adam, W.; Turro, N. J. *Chem. Commun.* **2005**, 3424–3426.
35. Kagan, H. B.; Fiaud, J. C. *Top. Stereochem.* **1988**, *18*, 249–330.
36. Keith, J. M.; Larrow, J. F.; Jacobsen, E. N. *Adv. Synth. Catal.* **2001**, *343*, 5–26.
37. Martin, V. S.; Woodward, S. S.; Katsuki, T.; Yamada, Y.; Ikeda, M.; Sharpless, K. B. *J. Am. Chem. Soc.* **1981**, *103*, 6237–6240.
38. Chen, C. S.; Fujimoto, Y.; Girdaukas, G.; Sih, C. J. *J. Am. Chem. Soc.* **1982**, *104*, 7294–7299.
39. Buschmann, H.; Scharf, H.-D.; Hoffmann, N.; Esser, P. *Angew. Chem., Int. Ed. Engl.* **1991**, *30*, 477–515.
40. Otera, J.; Sakamoto, K.; Tsukamoto, T.; Orita, A. *Tetrahedron Lett.* **1998**, *39*, 3201–3204.
41. Leffler, J. E. *J. Org. Chem.* **1966**, *31*, 533–537.
42. Leffler, J. E. *J. Org. Chem.* **1955**, *20*, 1202–1231.
43. Grdina, B. M.; Orfanopoulos, M.; Stephenson, L. M. *J. Am. Chem. Soc.* **1979**, *101*, 3111–3112.
44. Above $-30\text{ }^{\circ}\text{C}$, the ozonide liberates $^1\text{O}_2$ while at lower temperatures, the ozonide itself is an oxidant.
45. Mori, A.; Abe, M.; Nojima, M. *J. Org. Chem.* **2001**, *66*, 3548–3553.
46. Stephenson, L. M.; Zielinski, M. B. *J. Am. Chem. Soc.* **1982**, *104*, 5819–5820.
47. Poon, T.; Turro, N. J.; Chapman, J.; Lakshminarasimhan, P.; Lei, X.; Jockusch, S.; Franz, R.; Washington, I.; Adam, W.; Bosio, S. G. *Org. Lett.* **2003**, *5*, 4951–4953.

Stereoelectronic and solvent effects on the allylic oxyfunctionalization of alkenes with singlet oxygen

Mariza N. Alberti and Michael Orfanopoulos*

Department of Chemistry, University of Crete, Iraklion, Voutes 71003, Crete, Greece

Received 4 June 2006; revised 29 July 2006; accepted 31 July 2006

Available online 25 September 2006

Dedicated to Professor Harry H. Wasserman for his great contribution to this field

Abstract—The factors that control the stereochemistry of sensitized photooxygenation of alkenes via singlet oxygen (ene reaction) are selectively reported. We also introduce our most recent stereoelectronic effects on the singlet oxygen–ene reaction. The origin of site selectivity and solvent-dependent stereoselectivity in this classical ene reaction with simple as well as functionalized alkenes is highlighted. These studies and other similar studies have enhanced substantially the utility of singlet oxygen in the synthesis of natural and non-natural products. © 2006 Published by Elsevier Ltd.

1. Introduction

Molecular oxygen was discovered by Scheele and Priestly more than two centuries ago.¹ Later on, the fall of the powerful theory of phlogiston was followed by a period of exciting discovery of the role of oxygen in life processes. Photosensitized oxidations have been of interest to chemists and biologists since Raab's discovery that microorganisms are killed by light in the presence of oxygen and sensitizers.² These conditions cause pathological effects, referred as 'photodynamic action'.

In the period between 1928 and 1935, Mulliken³ interpreted the paramagnetic nature of molecular oxygen as a result of two outer electrons with parallel spins. Childe and Mecke⁴ spectroscopically identified the $^1\Sigma_g^+$ (37.5 kcal mol⁻¹) higher-energy electronic state and Herzberg⁵ discovered another singlet excited state $^1\Delta_g$ (22.5 kcal mol⁻¹). The $^1\Delta_g$ state is long-lived and survives at least for 10⁸ collisions with methanol in vapor phase, whereas the $^1\Sigma_g^+$ state survives for not more than 10 collisions under the same conditions.⁶

Although singlet oxygen was discovered more than 70 years ago,^{5,7} until the early 1960s it was considered to be of rather limited as a research subject. It was the pioneer work of Foote^{8,9} and Wexler that demonstrated the photosensitized oxidations of organic compounds in solution and brought the singlet oxygen back into the mainstream of chemical

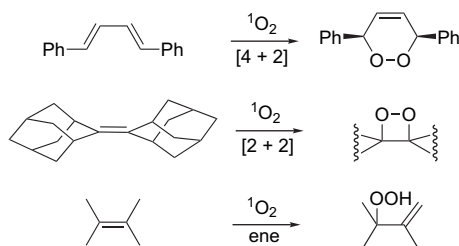
research. The chemical and photochemical generations of singlet oxygen, its ready detection, and its unusual but stereocontrolled¹⁰ chemical reactivity have made this research subject remarkably attractive.^{11–16} Most of the photosensitized oxygenations are now well established to involve $^1\Delta_g$ excited singlet state of molecular oxygen. The most convenient way of generating singlet oxygen is the dye photosensitization, as shown in Eqs. 1–3. These photooxygenations represent one of the most important hydrocarbon functionalization reactions available to the synthetic organic chemists.^{17,18}



Singlet oxygen studies have been reported to such diverse areas, as chemiluminescence,¹⁹ photocarcinogenicity,²⁰ ozonolysis,²¹ photodynamic action,⁹ photosynthesis,¹⁹ polymer degradation,¹⁵ environmental,^{15,22,23} and biological significance.^{24–26} The reaction of singlet oxygen with carbon–carbon double bonds, can be classified into three categories: (1) the [4+2] cycloaddition to conjugated dienes or anthracenes to yield endoperoxides; (2) the reaction with enol ethers, enamines, and electron-rich alkenes, without allylic hydrogens of proper orientation to yield 1,2-dioxetanes; and finally (3) the ene or 'Schenck reaction' with alkenes to form allylic hydroperoxides (Scheme 1). These reactions are very smooth and preparatively useful because of their high yields and specificity.

Keywords: Singlet oxygen; Ene reactions; Stereoselectivity; Electronic effects; Solvent effects.

* Corresponding author. Tel.: +30 2810 545030; fax: +30 2810 545001; e-mail: orfanop@chemistry.uoc.gr



Scheme 1. [4+2], [2+2], and ene addition reactions of singlet molecular oxygen to alkenes.

The ene reaction was originally discovered²⁷ by Schenck in 1943 and it was revived after the pioneering work of Foote in the early 1960s. A great deal of work has focused on whether the ene reaction proceeds through a concerted or a stepwise mechanism. The initially proposed synchronous pathway²⁸ was challenged by a biradical,²⁹ zwitterionic,³⁰ or a peroxide³¹ intermediate. Kinetic isotope effects on the photooxygenation of tetrasubstituted,³² trisubstituted,³³ and *cis*-disubstituted³⁴ alkenes supported the irreversible formation of an intermediate peroxide, while for *trans*-disubstituted alkenes³⁵ a partial equilibration of the intermediate with the reactants was postulated. Consistent with the peroxide intermediate is also the observation that the ene reaction proceeds as a highly suprafacial process, in which the conformational arrangement of the allylic hydrogen controls the stereochemistry of the product allylic hydroperoxides.³⁶

Trapping of the intermediate with sulfoxides,³⁷ phosphites,³⁸ and sulfenates or sulfinate esters³⁹ in the photooxygenation of adamantylidenoadamantane, and theoretical calculations^{40–44} as well, support the peroxide as the most possible intermediate. Many authors consider an intermediate exciplex^{45–47} instead of the polar peroxide. Since the geometry of the intermediate is well defined from the isotope effects and the stereochemical studies, if an intermediate exciplex is formed, its geometrical features must resemble those of a peroxide. Recent theoretical and experimental works by Singleton and co-workers,⁴⁸ however, proposed a two-step no-intermediate mechanism, with a rate-limiting transition state resembling that for the formation of a peroxide in the initially proposed stepwise process. Nevertheless, the mechanistic features of the ¹O₂ ene reaction continue to challenge the scientific community, and it is likely that the mechanism debate will continue in the years to come.

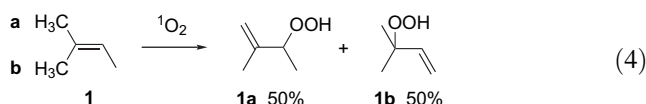
The purpose of this article is to provide a brief overview mainly about our work, both past and current, concentrating

on the factors that control the stereoselectivity of the ¹O₂-alkene ene reaction.

2. Stereoselectivity

2.1. Site selectivity ('cis-effect')

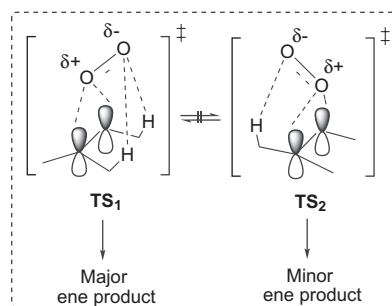
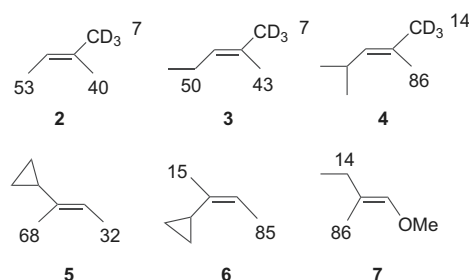
The site selectivity of the singlet oxygen–alkene reactions went unrecognized throughout more than 20 years of mechanistic study. It was generally recognized that methyl and methylene hydrogens are reactive and that the isopropyl C–H and certain conformationally inaccessible hydrogen atoms are not. The equal amounts of photooxidized products **1a** and **1b** obtained from trimethylethylene, as shown in Eq. 4, led to the conclusion that the ene reaction proceeds without any site selectivity. Since product **1a** results from H-abstraction from either methyl group a or b of **1**, Eq. 4, the relative reactivity of these groups was not known.



The stereospecific deuterium labeling and subsequent photooxygenation of olefins **2**, **3**, and **4** revealed the hidden site selectivity of the singlet oxygen–ene reaction (Scheme 2). A strong preference for H-abstraction from the more substituted side of the double bond was found.⁴⁹ This surprising selectivity is referred to as the 'cis-effect'. Selected examples are represented in Scheme 2. Both experimental and theoretical chemists have offered explanations for the 'cis-effect'.⁵⁰ Generally, most of the proposed explanations are consonant with the existence of an interaction between the incoming oxygen and two allylic hydrogens that highly stabilizes the transition state TS₁, versus TS₂, of peroxide formation (inset, Scheme 2).

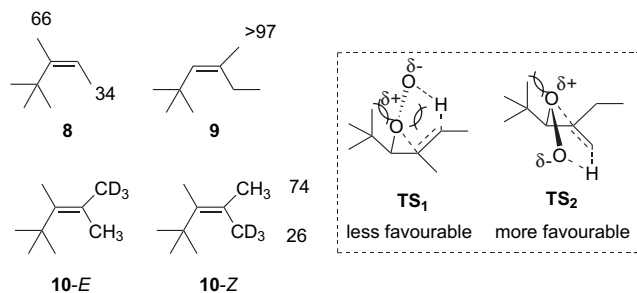
2.2. *anti* 'cis-Effect' selectivity

The proposal that there is a stabilizing effect by the simultaneous interaction of ¹O₂ with two allylic hydrogens on the same side of the olefin during the formation of the peroxide, suffices to explain the rare cases where *anti* 'cis-effect' selectivity has been observed in the photooxygenation of the series of acyclic trisubstituted alkenes shown in Scheme 3.⁵¹ Examination of the possible transition states leading to the major (*anti*) and minor (*syn*) allylic hydroperoxides, provides



Scheme 2. Site selectivity of the photooxygenation of trisubstituted alkenes ('cis-effect'). Numerical values represent percentage of hydrogen abstraction.

reasonable mechanistic rationale into the *anti* selectivity. For example, in TS₁ leading to the minor (*syn*) product (Scheme 3), the non-bonded interactions involving the large *tert*-butyl group and the incoming oxygen are expected to be stronger than those in TS₂, where this steric interaction is less significant (inset, Scheme 3). In general, the *anti* 'cis-effect' selectivity is related: (a) to the degree of crowdedness on the more substituted side of the olefin; (b) to the non-bonded interactions during the formation of the new double bond; and (c) most importantly, to the lack of simultaneous interaction of the incoming oxygen with two allylic hydrogens.



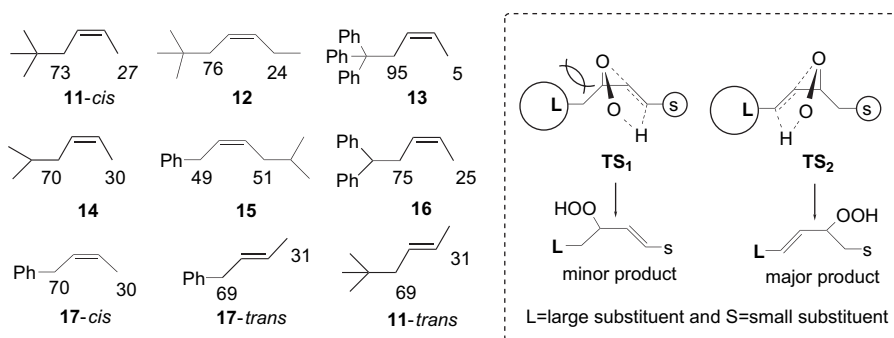
Scheme 3. *anti* 'cis-effect' selectivity of the photooxygenation of certain trisubstituted alkenes.

2.3. The large group non-bonded effect

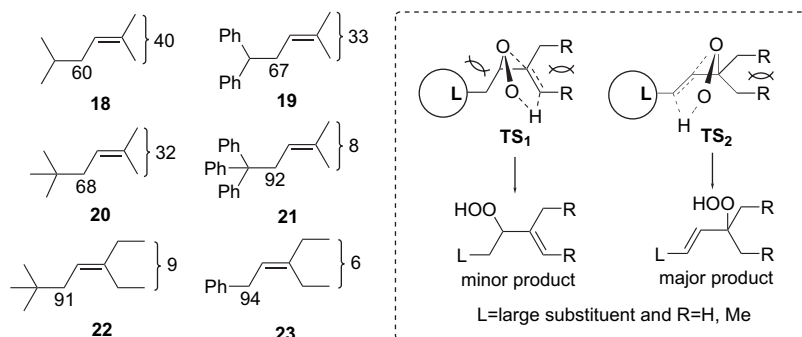
2.3.1. *cis*- and *trans*-Disubstituted alkenes. In the reaction of singlet oxygen with non-symmetrical *cis*- or *trans*-disubstituted alkenes, an unexpected regioselectivity was found.⁵² The allylic hydrogens next to the large alkyl substituent are more reactive than those next to the small group. The

regioselective photooxygenation reaction, some representative disubstituted alkenes, and their regio-limitations are shown in Scheme 4. The site selectivity was explained by examining the possible transition states leading to the allylic hydroperoxides with a general example, where L=large substituent and S=small substituent (inset, Scheme 4). In the transition state TS₂ leading to the major product, the non-bonded interactions involving the large group are smaller than those of the transition state TS₁ leading to the minor product, since TS₂ is expected to have lower energy than TS₁. Considering that the formation of peroxide in the photooxygenation of *trans*-alkenes is reversible,^{35b} the 1,3-non-bonded interactions in the product forming transition states between the oxygen and the alkyl substituents appear to control the site selectivity in a similar fashion to those shown in the inset of Scheme 4.

2.3.2. Dimethyl and diethyl trisubstituted alkenes. The regioselectivity trend in the photooxygenation of geminal dimethyl and diethyl trisubstituted olefins is similar to that observed in *cis*- or *trans*-disubstituted alkenes, with the allylic hydrogens next to the bulky alkyl substituent being more reactive.⁵² The results of some representative alkenes are summarized in Scheme 5. The transition states in the hydrogen abstraction step, as seen earlier in the inset of Scheme 4, help to explain the observed change in site selectivity. In a transition state where there is a strengthening of the C–O bond on the tertiary carbon, a release of the 1,3-non-bonded interactions between the oxygen and the L group (L=large substituent) with respect to the intermediate peroxide occurs. Therefore, transition state TS₂ is expected to be lower in energy than the transition state TS₁ where the non-bonded interactions exist (inset, Scheme 5).



Scheme 4. Site selectivity of the photooxygenation of *cis*- and *trans*-alkenes 11–17.

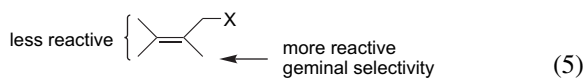


Scheme 5. Regioselectivity of the photooxygenation of alkenes 18–23. Numerical values represent percentage of hydrogen abstraction.

2.4. Geminal selectivity

2.4.1. Geminal selectivity with respect to allylic functionality.

Replacement of an allylic hydrogen in tetramethylethylene (TME-X) with a series of functional groups (sulfides, sulfoxides, sulfones, halides; Eq. 5) undergo selective photooxygenations with a surprising geminal selectivity with respect to the allylic functionality X.⁵³ This selectivity is represented by Eq. 5. Three possible explanations were proposed to account for the observed regioselectivity: (a) anchimeric assistance by the allylic substituent leading to regioselective opening of the possible peroxide intermediate by an S_N2 mechanism; (b) electronic repulsions between the lone pairs of the heteroatoms and the negatively charged oxygen of the peroxide; and (c) different barriers to rotation of methyl groups of the substrate. Similar explanation was earlier reported by Houk and co-workers^{50c} in an effort to rationalize the site selectivity of singlet oxygen–ene reaction with trisubstituted alkenes.



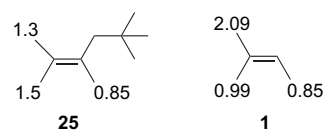
X = SO₂C₆H₄Me-p, SCH₄NO₂-p, Br, SO₂C₆H₄Y-p (Y = NO₂, H, Me, MeO)

2.4.2. Geminal selectivity with respect to a bulky allyl or vinyl substituent.

In order to examine comprehensively the factors affecting geminal selectivity, we synthesized a series of alkyl or phenyl substituted alkenes at the allylic or at the vinylic position.⁵⁴ Photooxygenation of these olefins shows a strong preference for hydrogen abstraction from the methyl group that is geminal to the larger substituent of the alkene. In Scheme 6, selective substrates are represented. Disubstituted olefin **24** impressively illustrates this point; the same trend was also noted in cyclic alkenes **27–29**.^{54b} Examination of the possible transition states leading to the major and the minor products in the reaction of ¹O₂ with L-allylic substituted trimethylethylene, helps to explain the observed regioselectivity (inset, Scheme 6). The transition state TS₁, leading to the major product, is expected to have lower energy than TS₂ and TS₄, because of 1,3-non-bonded interactions. Furthermore, in transition state TS₃, leading to the minor product or absence of product, the non-bonded interactions involving the large alkyl group and the methyl

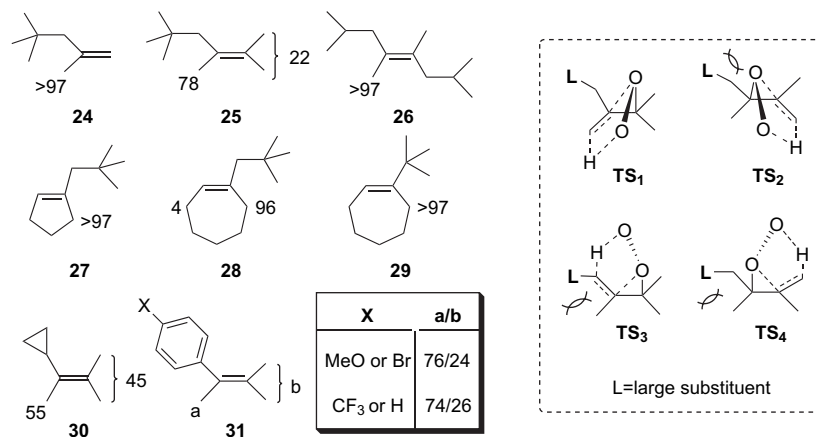
group, which are placed in a cis configuration, are expected to be stronger than those in the transition states TS₁, TS₂, and TS₄, where this steric interaction is absent. Similar examination was provided for the observed regiochemistry in ¹O₂–ene reaction for vinyl substituted tetramethylethylenes.

Previous work,⁵⁵ based on the theoretical model of Houk (MM2 calculations),^{50c} gave an alternative rationalization for the geminal selectivity. This model predicts that the lower the barrier to rotation the higher the hydrogen abstraction from the peroxide. For example, they found, according to this model, that for some alkyl substituted tetramethylethylenes there is a surprising correlation between the rotational barriers and their reactivity toward ¹O₂. Some numerical values in kcal mol⁻¹ are depicted in Scheme 7 for substrates **25** and **1**. In 2,3,5,5-tetramethyl-2-hexene (**25**), for example, the more reactive methyl group (geminal, 78%) has the lowest barrier to rotation (0.85 kcal mol⁻¹) with respect to the other two methyls. Similar trends hold with 2-methyl-2-butene (**1**).



Scheme 7. Calculated rotational barriers in kcal mol⁻¹ by MM2.

However, the barrier to rotation does not always predict the regioselectivity of the ene reaction of ¹O₂ with alkenes. In an earlier work, we calculated the rotational barrier values, with the HF/STO-3G method, for the allylic methyl groups in a series of trisubstituted alkenes, and compared them with the observed experimental ene regioselectivity.⁵⁶ Selective results are represented in Table 1. For alkene **4** there was a correlation between rotational barriers and ene reactivity. However, for alkenes **10-Z** and **10-E**, the *syn* methyl groups have lower rotational barriers than the corresponding *anti* by 0.5 kcal mol⁻¹. The observed ene reactivity of **10-Z** and **10-E** was in the opposite direction to the proposed theoretical model. Furthermore, for alkene **8** the *exo* methyl group has higher rotational barrier than the corresponding *syn* by 2 kcal mol⁻¹. In contrast again to the predictions of the proposed theoretical model, this methyl group was found to be more reactive in ¹O₂–ene reaction than the *syn*. These



Scheme 6. Geminal selectivity in the ene reaction of ¹O₂ with di-, tri-, and tetra-substituted alkenes.

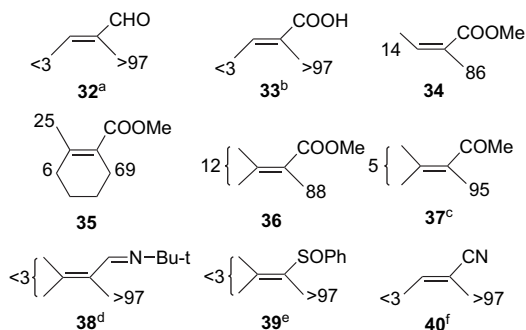
Table 1. Relative yields of ene products and rotational barriers of methyl groups

Substrate	% Ene products with $^1\text{O}_2$	Rotational barriers HF/STO-3G (kcal mol $^{-1}$)
 4	14	1.64
	86	0.40
 8	66	2.91
	34	0.91
 10-Z	74	1.63
	26	1.11
 10-E	76	1.63
	24	1.11

results indicate that there is not always a correlation between the reactivity of the methyl groups and their rotational barriers. More importantly, according to the Curtin–Hammett principle, the rotational barriers are irrelevant to the product distribution since their values are too small (0.5–2.0 kcal mol $^{-1}$) compared to the activation energies of the reactions (6–13 kcal mol $^{-1}$).

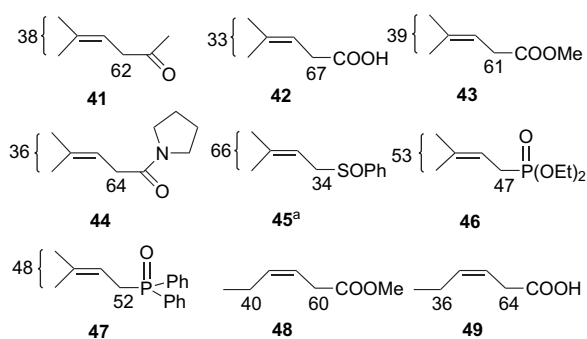
2.5. Electron withdrawing group at the α - and β -position

For alkenes bearing an electron withdrawing group at the α -position, such as aldehyde,⁵⁷ carboxylic acid,⁵⁸ ester,⁵⁹ ketone,⁶⁰ imine,⁶¹ sulfoxide,⁶² and cyano,⁶³ a high degree of geminal selectivity has been demonstrated. In Scheme 8, selective results are represented. Numerical values represent percentage of hydrogen abstraction. The 1,3-non-bonded interactions, which control the site selectivity in the photooxygenation of non-functionalized alkenes (see Sections 2.3–2.4.2), do not contribute significantly to the geminal selectivity of alkenes bearing at the α -position an electron withdrawing group. It was proposed that, in the hydrogen abstraction step, the perepoxide opens preferentially at the C–O bond next to the unsaturated moiety. Due to the forthcoming conjugation in the adduct, the corresponding transition state is favorable.



Scheme 8. Geminal site selectivity in the photooxygenation of alkenes bearing an electron withdrawing group at α -position. (a) See Ref. 57, (b) see Ref. 58, (c) see Ref. 60, (d) see Ref. 61, (e) see Ref. 62, and (f) see Ref. 63.

When the electron withdrawing substituent is at the β -position with respect to the double bond, various trends in site selectivity are observed (Scheme 9).⁶⁴ For substrates 41–44, the observed site selectivity is identical to the site selectivity observed for the alkyl substituted alkene 18, which shows approximately similar substituent stereo demand. In substrates 45–47, where the substituents are sulfide, phosphonate, or phosphine oxide, the double bond formation on the side of the alkene, which is away from the functionality increases significantly. This behavior was attributed to the electronic repulsions between the highly polarized oxygen atoms of the S–O and P–O bonds and the negative oxygen atom of the perepoxide, which directs the intermediate to abstract hydrogen from the methyl group. The results observed in the case of the disubstituted unsaturated ester 48 and acid 49 are similar to that of the trisubstituted substrates 43 and 42, respectively. This reveals that any unfavorable interactions between oxygen and carbonyl in the more substituted side of the double bond probably do not force formation of the intermediate in the less substituted side of the double bond (*anti* ‘cis-effect’ selectivity, see Section 2.2). We conclude that there are three competing factors, which can affect the regiochemistry in the ene reaction of $^1\text{O}_2$ with alkenes bearing an electron withdrawing group at β -position: (1) the driving force to form the new double bond in conjugation with the functionality in the allylic hydroperoxide product; (2) the 1,3-non-bonded interactions between the positively charged oxygen of perepoxide and the allylic functionality, which favor again the conjugated product; and (3) the electronic repulsions between perepoxide and the allylic functionality favoring the unconjugated product. We believe that in the series of substrates examined here, the last factor is the most important and dictates the ene products distribution.



Scheme 9. Geminal selectivity in the photooxygenation of alkenes bearing an electron withdrawing group at β -position. (a) See Ref. 65.

2.6. Solvent and electronic effects on the stereoselectivity of singlet oxygen–ene reaction

2.6.1. α,β -Unsaturated esters and *E/Z*-2,4-dimethylpent-3-en-2-ol-5,5-*d*₃. Previous studies have shown that the rate of the $^1\text{O}_2$ ene reaction with alkenes shows negligible dependence on solvent polarity.⁶⁶ Product distribution depends substantially on solvent polarity and reaction temperature, only in substrates where both ene and dioxetane products are produced.⁶⁷ Furthermore, extensive mechanistic work has shown that there is a negligible solvent effect on the reaction of $^1\text{O}_2$ with α,β -unsaturated ketones,^{60a} olefins, and dienes.⁶⁸

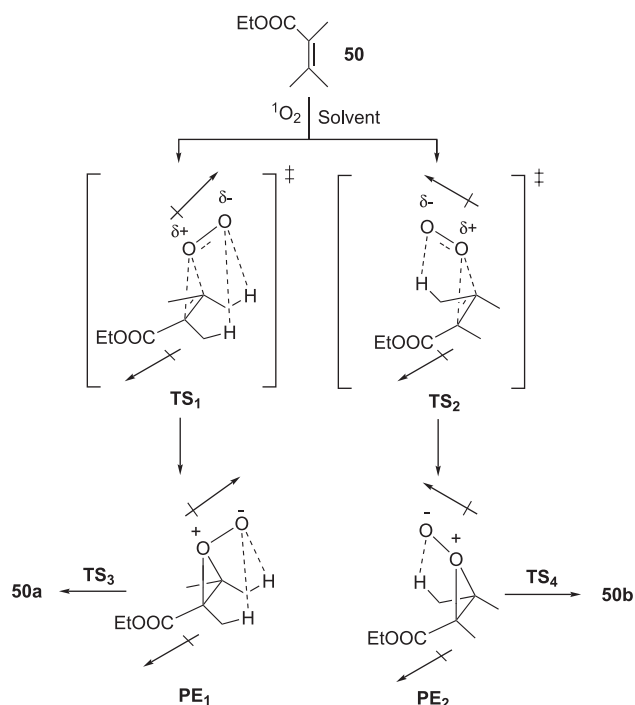
In the reaction of $^1\text{O}_2$ with α,β -unsaturated esters there is a small but significant solvent effect on the variation of the ene products.⁶⁹ As seen from Table 2, the hydrogen abstraction from the methyl group, which is geminal to the ester functionality in compound **50**, producing adduct **50a**, decreases substantially as the solvent polarity increases. For example, the ratio of ene products **50a/50b** decreases by a factor of 5 on going from carbon tetrachloride to the more polar solvent DMSO. It was found that there is a surprising correlation between the dielectric constant (ϵ , Table 2) of the solvent and the distribution of the ene products. By increasing the dielectric constant of the solvent, the percentage of **50b** increases.

Table 2. Solvent effect on the regioselectivity of the photooxygenation of **50**

Solvent	50a/50b	ϵ^a (20 °C)
CCl_4	95/5	2.24
Benzene	94/6	2.283
Acetone	88/12	20.7
CH_3CN	85/15	36.64
DMSO	80/20	47.24

^a See Ref. 70.

Transition state TS_2 , where the oxygen atom is added to the same side of the ester functionality to form the *syn* perepoxide PE_2 , is favored in polar solvents because its dipole moment is higher than that of the transition state TS_1 , where the oxygen adds to the other side of the olefin to form the *anti* perepoxide PE_1 (Scheme 10).

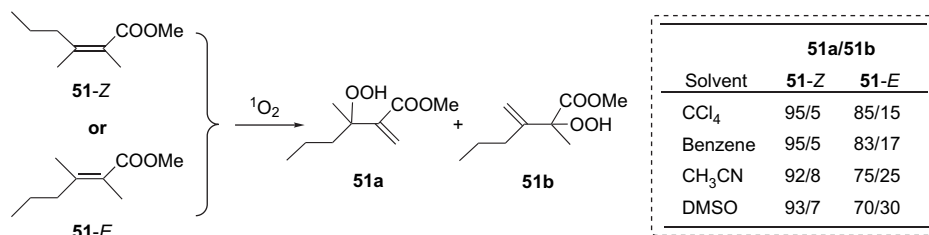


Scheme 10. Proposed mechanism for the solvent-dependent photooxygenation of α,β -unsaturated esters.

To verify this mechanistic possibility, the solvent dependence of the ene products derived from the photooxygenation of the isomeric α,β -unsaturated esters **51-Z** and **51-E** was examined (Scheme 11). For the isomer **51-Z**, both products are formed from the same intermediate (the perepoxide oxygen is placed *anti* to the ester functionality), and no solvent dependence on the ene products was found (inset, Scheme 11). On the other hand, for **51-E** the two ene products are formed from two different perepoxides. When the oxygen atom of the perepoxide intermediate is placed *syn* to the ester group, **51b** is produced, whereas **51a** is formed from the *anti* position. For isomer **51-E**, the expected solvent effect was found: **51a/51b**=85/15 in CCl_4 ; 83/17 in benzene; and 70/30 in DMSO (inset, Scheme 11). These results are consonant with the proposed *syn* (polar) and *anti* (less polar) perepoxide-like transition states similar to TS_1 and TS_2 whose relative stabilities change with solvent polarity. It is constructive to note that the ene product distribution is not affected by solvent polarity when the two sides of the double bond do not compete for the ene product. This is demonstrated with the substrate **51-Z**, where the two methyls are in *cis* position.

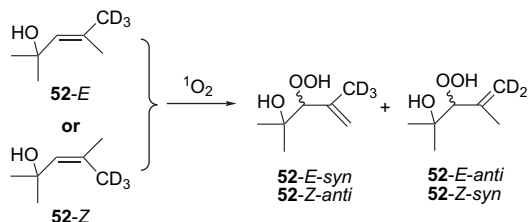
Significant solvent effects on the regioselectivity of the ene reaction have also been observed with allylic alcohols **52-E** and **52-Z**.⁷¹ It is worth mentioning that for **52-E** and **52-Z**, singlet oxygen can interact with only one allylic hydrogen or deuterium on each side of the alkene. No ‘*cis*-effect’ would be expected with these substrates. The results are summarized in Table 3. We define as *syn* the adducts formed by allylic hydrogen abstraction, which is on the same side of the double bond as the hydroxyl. For the case of **52-E**, the *syn* adduct is formed by hydrogen abstraction, while for the case of **52-Z** by deuterium abstraction. In fact, adducts **52-E-syn** and **52-Z-anti** are identical, and **52-E-anti** and **52-Z-syn** are also identical. As seen from Table 3, photooxygenation of **52-E** and **52-Z** in CCl_4 and CH_3CN showed similar *syn* selectivity. This result indicates that the *syn/anti* product selectivity is independent on the specific labeling of the methyl groups. For the case of **52-E**, the ratio of *syn/anti* decreases by a factor of 6 on going from carbon tetrachloride to the polar solvent methanol.

Adam and co-workers, observed high diastereoselectivity (de ~90%) in the photooxygenation of chiral allylic alcohols⁷² and amines.⁷³ This result was rationalized in terms of hydroxyl or amino group coordination with the incoming oxygen. The synergy of oxygen–hydroxyl coordination, as well as the 1,3-allylic strain, provides, in non-polar solvents, high selectivity for the *threo* allylic hydroperoxides. This effect controls the *syn/anti* stereoselectivity in the photooxygenation of allylic alcohols **52-E** and **52-Z**. Examination of the possible transition states in Scheme 12 helps to understand the observed stereoselectivity. In TS_1 (applied to **52-E**), where the electrophile approaches the olefin from the more crowded side to form PE_1 , the oxygen interacts simultaneously with the hydroxyl and one allylic hydrogen. This interaction stabilizes the transition state. Polar solvents interact with the hydroxyl group through hydrogen bonding and reduce its ability to interact with the oxygen. Thus, the activation energy of TS_1 increases significantly and leads to a reversal of selectivity, which is now controlled by steric factors.



Scheme 11. Solvent effect on stereoselectivity of $^1\text{O}_2$ addition to **51-Z** and **51-E**.

Table 3. Solvent effect on the stereoselectivity of the photooxygenation of **52-E** and **52-Z**



Substrate	Solvent	<i>syn/anti</i> selectivity
52-E	CCl ₄	75/25
52-Z	CCl ₄	72/28
52-E	CHCl ₃	66/34
52-Z	CHCl ₃	65/35
52-E	CH ₃ CN	41/59
52-Z	CH ₃ CN	40/60
52-E	MeOH	33/67

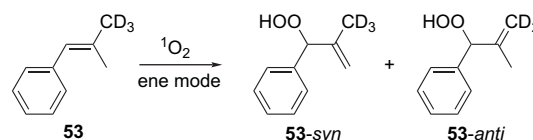
Stensaas and co-workers,^{74a} investigated the photooxygenations of tiglic acid, angelic acid, 2,3-dimethyl-2-butenic acid, and their corresponding methyl esters, using singlet oxygen in methanol and methanol/water solvent mixtures and compared with non-hydrogen-bonding solvents with different dielectric constants. They concluded that principally four factors dictate the site selectivity of singlet oxygen-ene reactions of these substrates in hydrogen-bonding solvents: the 'cis-effect', the polarity of the solvent and substrate, and the most important hydrogen-bonding interactions between the solvent and substrate. Recently, they studied^{74b} the aqueous photooxygenations of some α -substituted alkene salts and the major factor dictating the product distribution of ene products is hydrogen-bonding interactions between the water and the substrate.

2.6.2. *syn* Selectivity of β,β -dimethylstyrene. Surprisingly, in the reaction of $^1\text{O}_2$ with β,β -dimethylstyrene,⁷⁵ the ene products, which are formed, apart from dioxetane and

diendoperoxides,⁷⁶ exhibit an unexpected solvent-dependent *syn* selectivity. Considering that in the more substituted side of the olefin, oxygen is capable of interacting with only one allylic hydrogen, *anti* 'cis-effect' selectivity would be expected. In order to study the *syn/anti* selectivity of the ene products, the stereospecific labeling of the *anti* methyl by deuterium in β,β -dimethylstyrene to produce substrate **53** was required. The photooxygenation of **53** in several solvents revealed that there is a strong selectivity for attack on the methyl *syn* to the phenyl group. The magnitude of this selectivity depends on solvent polarity. By increasing the dielectric constant of the solvent, a substantial increase in the amount of hydrogen abstraction from the *syn* methyl group occurs. For instance, the ratio of *syn/anti* ene products increases by a factor of 3.4 on going from CCl₄ to methanol (Table 4).

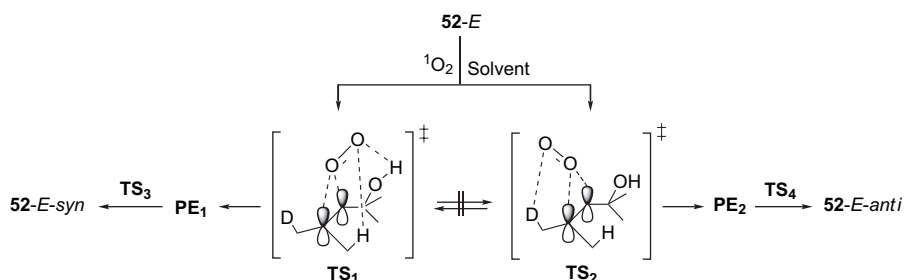
A mechanistic possibility that accounts for the observed *syn* selectivity is shown in Scheme 13. In TS₁, the incoming oxygen is oriented toward the more substituted side of the double bond. There is only one allylic hydrogen interaction with singlet oxygen and TS₁ leading to the major ene product. In TS₂, leading to the minor *anti* product, singlet oxygen

Table 4. Regioselectivity of the photooxygenation of **53** in a variety of solvents

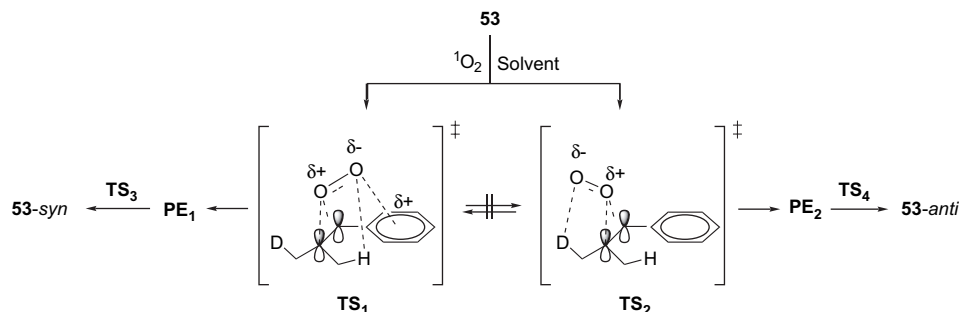


Solvent	<i>syn/anti</i>	ϵ^a (Temp °C)
CCl ₄	56/44	2.24 (20)
Benzene	57/43	2.283 (20)
CHCl ₃	63/37	4.87 (25)
CH ₃ CN	71/29	36.64 (20)
CH ₃ OH	82/18	33.0 (20)

^a See Ref. 70.



Scheme 12. Proposed mechanism for the solvent-dependent photooxygenation of **52-E**.



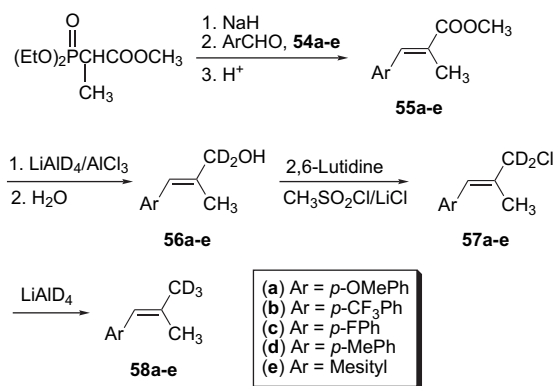
Scheme 13. Proposed mechanism for the photooxygenation of **53**.

again interacts with only one allylic hydrogen. Therefore, the extra stabilization of TS_1 versus TS_2 must arise from ‘positive’ interactions of singlet oxygen with the phenyl ring. In TS_1 , which leads to perezoxide PE_1 , the benzylic carbon is slightly electron-deficient, which is stabilized by electron donation from the phenyl group. Interaction of the negatively charged oxygen of perezoxide with the phenyl ring, which has lost part of its electronic density, results in significant stabilization. Thus, the overall effect stabilizes better the *syn* transition state TS_1 than the *anti* TS_2 where this effect is absent. On increasing the polarity of the solvent, this stabilization becomes more significant because the transition state becomes more polar.

3. Electronic effect

3.1. On site selectivity

In light of the unexpected *syn* selectivity⁷⁵ of the photooxygenation of β,β -dimethylstyrenes **53**, in a variety of solvents (Section 2.6.2), the electronic effect of the reaction of singlet oxygen with *para*-substituted β,β -dimethylstyrenes was studied.⁷⁷ For this purpose, a series of *para*-substituted aryl alkenes **58a–e** were synthesized (Scheme 14). The stereoselective deuterium labeling of the *trans*-methyl group of the *para*-substituted β,β -dimethylstyrenes allows the *syn/anti* hydrogen abstraction determination.



Scheme 14. Synthesis of labeled trisubstituted alkenes **58a–e**.

The preparation of alkenes **58a–e** in 93–98% isomeric purity with the *E* configuration was accomplished through the stereoselective formation of **55a–e**, by a Wittig–Horner reaction⁷⁸ with aldehydes **54a–e**, followed by $LiAlD_4/AlCl_3$ reduction⁷⁹ and subsequent chlorination⁸⁰ of the resulting

allylic alcohols **56a–e**, followed by $LiAlD_4$ reduction⁸¹ of the allylic chlorides **57a–e** (Scheme 14). The conversion of the allylic alcohols **56a–e** to the allylic chlorides **57a–e** proceeds by retention of stereochemistry at least to 95% for *Z*-isomer.

The photooxygenation of alkenes **58a–d** in several solvents, apart from the ene adducts, affords a great amount (~80% relative yield) of oxygenated products arising from [4+2] or [2+2] addition.⁷⁶ The isolation of the ene adducts was accomplished by column chromatography, using methylene chloride as eluent. The ratio of *syn/anti* selectivity was determined by 1H NMR spectroscopy. The photooxygenation results for alkenes **53** and **58a–e** are summarized in Table 5.

For the singlet oxygen–ene reaction of **53** and **58a–d** in chloroform, a distinguishable trend is recognized. Electron withdrawing substituents, such as $-CF_3$ (74% *syn* selectivity) and $-F$ (68% *syn* selectivity), favor in about 40% hydrogen abstraction from the *syn* methyl group of the double bond. In the case of a donating substituent such as $-OMe$, **58a**,

Table 5. Site selectivity of the photooxygenation of **53** and **58a–e**

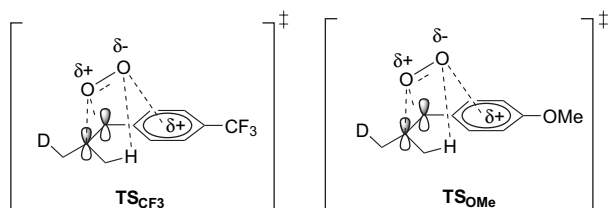
Substrate	Ar	<i>syn/anti</i> selectivity ^a	
		$CHCl_3$	CH_3CN
53		63/37 ^b	71/29 ^b
58a		46/54	54/46
58b		74/26	76/24
58c		68/32	70/30
58d		55/45	57/43
58e		86/14	86/14

^a Determined by 1H NMR integration of the proper hydrogen signals. The error was $\pm 4\%$.

^b Taken from Ref. 75.

the reactivity of the *anti* methyl group is slightly in favor than that of the *syn* methyl. In substrates **53** and **58d**, an intermediate *syn* selectivity was observed, compared to the other substrates. Therefore, the relative stability of transition state TS₁ (Scheme 13), as controlled by the electron density of the aryl ring, affects the *syn/anti* selectivity in the ene products.

The proposed mechanism that accounts for the observed selectivity, which is due to the electronic effects of the aryl rings, is shown in Scheme 15.



Scheme 15. Transition states for the photooxygenation of **58a** and **58b** aryl alkenes.

In transition state TS_{CF₃} the *syn* approach of ¹O₂ to the double bond is better stabilized by the partial positive charge on the phenyl ring, due to the electron withdrawing character of –CF₃, than in TS_{OMe} (Scheme 15), where the positive charge is reduced because of the electron donating ability of the –OMe substituent. Consequently, transition state TS_{CF₃} leads to higher, 74% *syn* selectivity, whereas TS_{OMe} to the lowest 46%.

Taking into account that steric interactions on the reaction center due to the phenyl substituents are negligible, the order of the magnitude of *syn* selectivity depends exclusively on the charge density of each particular substituted phenyl ring. For example, as the positive charge density from –OMe to –CF₃ increases, the hydrogen abstraction from the crowded methyl group increases: $\delta_{\text{CF}_3}^+$ (74%) > δ_{F}^+ (68%) > δ_{H}^+ (63%) > $\delta_{\text{CH}_3}^+$ (55%) > δ_{OMe}^+ (46%).

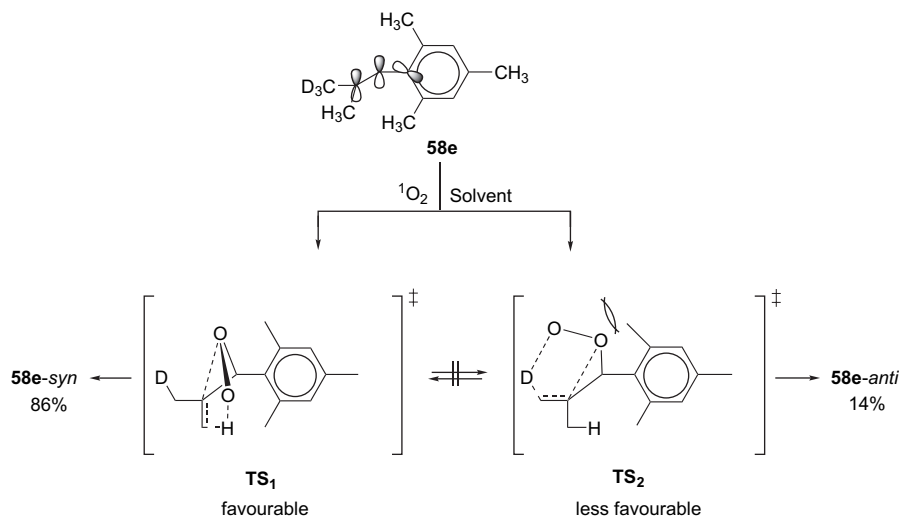
When the above photooxygenations were run in a polar solvent, such as acetonitrile, similar trend for *syn* selectivity was found (Table 5).

In the case of alkene **58e**, bearing a trimethyl substituted phenyl ring (Ar=mesityl) an abnormal high reactivity for the *syn* methyl group (86% relative yield) was found either in non-polar or polar solvent (Table 5, last entry). Unlike the *para*-substituted aryl alkenes, **58a–d** and **53**, where the *syn* selectivity was attributed to electronic effects of the phenyl ring, the high *syn* selectivity of ¹O₂ with alkene **58e**, must be attributed to steric reasons. If the electronic effect would be the case, lower *syn* selectivity would have been expected, due to a lower positive charge density on the phenyl ring, arising from the inductive effect of the three methyl groups. It is expected that the two *ortho* methyl substituents will force the phenyl ring out of the plane of the alkene double bond. We assume that the favorable conformation of the phenyl ring would be the one, which places the ring almost perpendicular to the plane of the double bond. This assumption is in a good agreement with the following experimental results: although in all the cases of *para*-substituted aryl alkenes, **58a–d** and **53**, the reaction with ¹O₂ gave mostly [4+2], [2+2], and diendoperoxides in more than 80% relative yields,⁷⁶ in the case of aryl alkene **58e**, this reaction gave mostly the ene adduct in more than 80% and minor amounts of [4+2] and [2+2] adducts. This result supports the perpendicular phenyl ring conformation, where the alkene double bond and one phenyl double bond are not properly aligned to an *s-cis* conformation, required for a [4+2] cycloaddition.

This remarkable *syn* selectivity can be attributed to the fact that in transition state TS₂, leading to the minor ene adduct, the substantial non-bonded interactions involving the *ortho* methyl substituents and the incoming singlet oxygen are much larger than those in TS₁, where these interactions are diminished, Scheme 16.

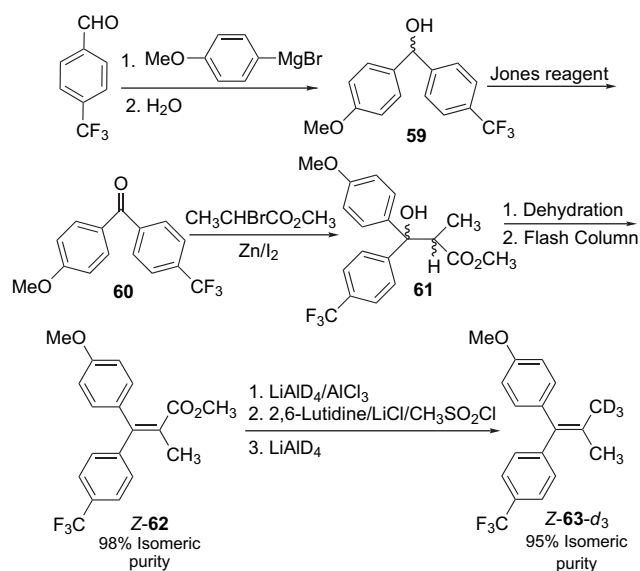
3.2. ‘Push–pull’ electronic effect

To this end, the ‘push–pull’ electronic effect was tested for the site selectivity of this reaction. For this purpose the 1-(*p*-methoxyphenyl)-1-[(*p*-trifluoromethyl)phenyl]-2-methylprop-1-ene-3,3,3-*d*₃ (**Z-63-d₃**, Scheme 17) alkene was designed. This alkene has three distinctive characteristics: (a) two geminal *para*-substituted phenyl rings with an



Scheme 16. Proposed mechanism for the photooxygenation of **58e**.

electron donating (–OMe) and an electron withdrawing (–CF₃) group, respectively (push–pull effect), (b) sterically equivalent sites of the alkene double bond, assuming that variation of *para*-substitution is far enough to sterically influence the double bond reaction center, and (c) stereoselective deuterium labeling such that the two reactive methyl groups are distinguishable on the ene products.

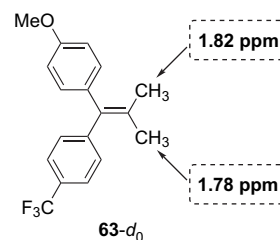


Scheme 17. Synthesis of (*Z*)-1-(*p*-methoxy-phenyl)-1-[(*p*-trifluoromethyl)-phenyl]-2-methyl-prop-1-ene-3,3,3-*d*₃ (*Z*-63-*d*₃).

The stereoselective formation of tetrasubstituted alkenes⁸² is an important and challenging task for the synthesis of many natural products.⁸³ In this case, the successful pathway for the synthesis of *Z*-63-*d*₃ is depicted in Scheme 17. Alcohol **59** was derived from the Grignard coupling of (*p*-trifluoromethyl)benzaldehyde with *p*-methoxy-benzyl magnesium bromide.⁸⁴ Jones oxidation of the secondary alcohol **59** afforded ketone **60**, in good yield.⁸⁵ The key step for the synthesis of *Z*-63-*d*₃ was the Reformatsky reaction between ketone **60** and 2-bromo-propionate in the presence of ‘activated’ zinc and catalytic amount of I₂.⁸⁶ It is worth mentioning that ketones and β-bromo-esters, with increasing steric demands, gave very low yields of the title reaction and in some cases the desired product was hardly detected. Improvements by metals other than zinc and high-intensity ultrasound techniques, promoted successfully Reformatsky reactions with these substrates.⁸⁷ In our case, we managed to isolate **61**, as a mixture of *threoerythro* stereoisomers, in 80% overall yield (see Section 5.4.3). Dehydration of **61** with catalytic amount of *p*-toluenesulfonic acid afforded a mixture of *E/Z*-62 α,β-unsaturated methyl esters. Separation of *E/Z*-62 methyl esters was accomplished by flash column chromatography, using hexane/EtOAc, v/v, 9:1 as eluent. For *E*- and *Z*-α,β-unsaturated methyl esters the isomeric purities were 90 and 98%, respectively. The *Z*-62 isomer was used for the last two steps of the synthesis. The labeled alkene *Z*-63-*d*₃ was prepared according to the previously described procedure for the synthesis of **58a–e** (see Section 5.3). Reduction of *Z*-62 with LiAlD₄ to the corresponding allylic alcohol, subsequent conversion of the latter to the allylic chloride followed by reduction with LiAlD₄, afforded the desired alkene in 95% isomeric purity.

The unlabeled alkene 63-*d*₀ was also prepared by LiAlH₄ reduction of the crude mixture of *E/Z*-62, followed by chlorination and LiAlH₄ reduction of the allylic alcohol-*d*₀.

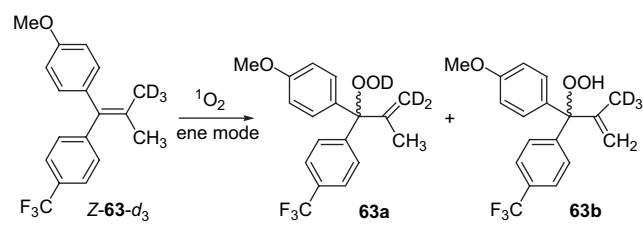
The ¹H NMR spectrum of substrate 63-*d*₀ in the aromatic region revealed two AB systems: one at 7.52 and 7.23 ppm with a coupling constant 8.1 Hz, and the other at 7.02 and 6.83 ppm with a coupling constant 8.6 Hz. The former corresponds to the aromatic protons of the F₃C-substituted phenyl ring and the latter corresponds to the aromatic protons of the MeO-substituted phenyl ring.⁸⁸ Nuclear Overhauser effect (NOE) experiments with deuterium unlabeled 63-*d*₀ alkene confirmed the stereochemistry of *Z*-63-*d*₃. Upon irradiation of protons of F₃C-substituted phenyl ring at 7.23 ppm, two positive NOEs were recorded: (a) hydrogens belonging to this aryl ring at 7.52 ppm and (b) the methyl group at 1.78 ppm. Furthermore, upon irradiation of protons of MeO-substituted phenyl ring at 7.02 ppm, two positive NOEs were recorded: (a) hydrogens belonging to this aryl ring at 6.83 ppm and (b) the methyl group at 1.82 ppm (Scheme 18).



Scheme 18. NOE experiments for 63-*d*₀ revealed the chemical shifts for the methyl groups.

Substrate *Z*-63-*d*₃ reacts smoothly with singlet oxygen generated by a 300-W Xenon lamp irradiation of TPP as sensitizer (10^{−4} M) in CCl₄, at 0 °C, under an oxygen atmosphere. A catalytic amount of galvinoxyl radical was also added to the reaction mixture, as a free radical scavenger. A solution of 0.05 M K₂Cr₂O₇ was used as a light filter during the photooxygenation. The irradiation time was ranged between 2 and 10 min. The ene allylic hydroperoxides were formed as the major adducts along with some unidentified oxygenated products. The ene adducts were stable and purified by flash column chromatography over silica gel, prewashed with triethylamine using a mixture of hexane/EtOAc, v/v, 9/1 as eluent. It is worth mentioning that a recovered small amount of the starting material was not isomerized. Determination of the ratio **63a/63b** was achieved by ¹H NMR spectroscopy before and after the reduction of allylic hydroperoxides. These results are presented in Table 6. The photooxygenation reactions of substrate *Z*-63-*d*₃ were run in various solvents such as carbon tetrachloride, chloroform, acetone, acetonitrile as well as in protic such as MeOH.

As shown from Table 6, a small but persistent preference on the order of 2–10% for hydrogen abstraction from the methyl group, which is *cis* to the CF₃-substituted phenyl ring was observed in non-protic solvents. However, in protic solvents, this preference increases to the range between 15 and 20%. Since the steric effect is identical to both sites of the double bond, the selectivity must be due to the variation of the electron density on the two sites of the double bond. This small but noticeable site selectivity may be rationalized by

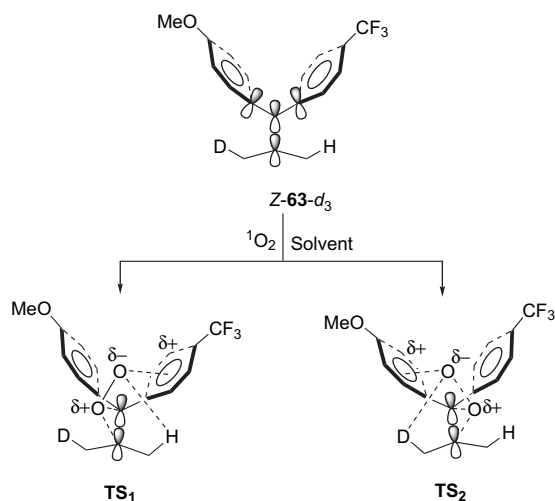
Table 6. Site selectivity of the photooxygenation of *Z*-**63-d**₃ in a variety of solvents


Solvent	ϵ^a (Temp °C)	Sensitizer	63a/63b ^b
CCl ₄	2.24 (20)	TPP	46/54
CHCl ₃	4.87 (25)	TPP	48/52
(CH ₃) ₂ CO	20.7 (20)	RB	49/51
CH ₃ CN	36.64 (20)	RB	49/51
CF ₃ CH ₂ OH	27.68 (20)	MB	40/60
MeOH	33.0 (20)	MB	42/58
MeOH/D ₂ O=4:1	42.44 (20)	MB	42/58

^a See Ref. 70.

^b Determined by ¹H NMR integration of the proper hydrogen signals. The error was $\pm 3\%$.

a similar mechanism proposed above for the case of aryl alkenes (Scheme 13). It is expected that the geminal phenyl groups, for steric reasons, will be out of the plane of the alkene double bond. Therefore, their electronic effects, through resonance, are not fully developed to the benzylic carbon of the double bond during the addition of singlet oxygen. In TS₁ the relative positive interaction of the CF₃-phenyl ring with the incoming oxygen is slightly higher than in TS₂ for similar reasons mentioned previously (Scheme 19). However, the difference in the electronic interactions between singlet oxygen and the two *para*-substituted phenyl rings in *Z*-**63-d**₃ must be relatively smaller than those between singlet oxygen and *para*-substituted alkenes **58a** and **58b** (Scheme 13), where the phenyl rings are more conjugated with the alkene double bond, compared to *Z*-**63-d**₃. This may be the reason for a much smaller site selectivity for hydrogen abstraction for *Z*-**63-d**₃. It is not obvious why in this case (substrate *Z*-**63-d**₃) the site selectivity increases from 2–5% in aprotic solvents to 15–20% in protic solvents. A number of additional factors may contribute to this result, such as (a) hydrogen bonding, (b) better stabilization of the

**Scheme 19.** Proposed mechanism for the photooxygenation of *Z*-**63-d**₃.

more polar transition state, and (c) conformational variations of the phenyl rings in protic solvents.

4. Conclusion

Stereoselective singlet oxygen allylic photooxygenations of alkenes have received remarkable attention over the last few years and will continue to play an important role in the synthesis of natural and non-natural products. In this report, a number of factors, such as solvents, electronic effects, and non-bonded interactions that dictate the ene product selectivity as well as the various mechanisms of this reaction are highlighted. This brief overview constitutes mainly examples taken from previous and recent works from our laboratory.

We have no doubts that the diversity of singlet oxygen will continue to fascinate researchers in chemistry, biology, and medicine, and to make reactions of this species a favored area for the development of new methods and ideas.

5. Experimental

5.1. General

¹H NMR and ¹³C NMR spectra were recorded on 500 and 300 MHz spectrometers, in CDCl₃ solutions. Chemical shifts are reported in parts per million downfield from Me₄Si, by using the residual solvent peak as internal standard. Isomeric purities were determined by ¹H NMR, ¹³C NMR, and by analytical gas chromatography equipped with a 50%–50% phenyl methyl silicone capillary column and a 5971A MS detector. Photooxygenations were achieved with a Xenon Variac Eimac Cermax 300 W lamp. TLC was carried out on SiO₂ (silica gel F₂₅₄). Chromatography refers to flash chromatography and was carried out on SiO₂ (silica gel 60, SDS, 230–400 mesh ASTM). Drying of organic extracts during work-up of reactions was performed over anhydrous MgSO₄. Evaporation of the solvents was accomplished with a rotary evaporator. Preparation of the labeled alkenylarenes **53**⁷⁵ and **58a**⁸⁹ has been described in earlier studies from our lab. UV–vis spectrum for compound **62-d**₀ was performed on a Hitachi U-2001 spectrophotometer, with bandwidth 200–900 nm.

5.2. General procedure for the preparation of labeled isobutenylarenes **58b–e**

5.2.1. Synthesis of esters **55b–e.** In a flame-dried flask were placed 2 g of NaH (60% in paraffin oil, 54.0 mmol) and 60 mL of dry DME. The flask was cooled to 0 °C, and then a solution of methyl diethyl-2-phosphonopropionate (11.2 g, 50.0 mmol) in dry DME (40 mL) was added dropwise under N₂ atmosphere. A vigorous evolution of hydrogen gas was observed. After 1 h of stirring at room temperature, a solution of arylaldehyde (46.0 mmol) in dry DME was injected. Stirring was continued for 2–3 h, and the reaction mixture was quenched with MeOH, poured into H₂O, and extracted with Et₂O. The combined ether layers were dried over MgSO₄ and concentrated, affording exclusively the desired *E*-ester (60% overall yield).

The spectroscopic data for esters **55b–e** are as follows. Compound **55b**: ^1H NMR (CDCl_3 , 500 MHz) δ : 7.69 (s, 1H), 7.64 (d, 2H, $J=8.0$ Hz), 7.47 (d, 2H, $J=8.0$ Hz), 3.84 (s, 3H), 2.11 (s, 3H) ppm; MS $m/z=244$ (100, $m/z=115$). Compound **55c**: ^1H NMR (CDCl_3 , 500 MHz) δ : 7.64 (s, 1H), 7.37 (dd, 2H, $J_{\text{HH}}=8.5$ Hz, $J_{\text{HF}}=5.7$ Hz), 7.08 (dd, 2H, $J_{\text{HH}}=8.5$ Hz, $J_{\text{HF}}=8.5$ Hz), 3.82 (s, 3H), 2.10 (s, 3H) ppm. Compound **55d**: ^1H NMR (CDCl_3 , 500 MHz) δ : 7.69 (s, 1H), 7.34 (d, 2H, $J=7.8$ Hz), 7.16 (d, 2H, $J=7.8$ Hz), 3.81 (s, 3H), 2.37 (s, 3H), 2.08 (s, 3H) ppm; MS $m/z=190$ (100, $m/z=130$). Compound **55e**: ^1H NMR (CDCl_3 , 500 MHz) δ : 7.61 (s, 1H), 6.85 (s, 2H), 3.82 (s, 3H), 2.59 (s, 3H), 2.29 (s, 6H), 2.12 (s, 3H) ppm; MS $m/z=232$ (100, $m/z=187$).

5.2.2. Synthesis of allylic alcohols- d_2 56b–e. A solution of the *E*-ester (32 mmol) in dry Et_2O (20 mL) was added dropwise to a cooled (0 °C) mixture of LiAlD_4 (0.734 g, 17.5 mmol) and AlCl_3 (0.773 g, 5.8 mmol) in dry Et_2O (40 mL), under N_2 atmosphere. The AlCl_3 had been added in portions to the LiAlD_4 at 0 °C over a 15 min period. After 1 h of stirring at room temperature, the reaction mixture was quenched at 0 °C with a 2 N solution of HCl and filtered. The filtrate was washed with brine, dried over MgSO_4 , and concentrated to give the corresponding *E*-alcohol (80% overall yield).

The spectroscopic data for allylic alcohols- d_2 **56b–e** are as follows. Compound **56b**: ^1H NMR (CDCl_3 , 500 MHz) δ : 7.58 (d, 2H, $J=8.2$ Hz), 7.37 (d, 2H, $J=8.2$ Hz), 6.54 (s, 1H), 1.89 (s, 3H) ppm; MS $m/z=199$ (100, $m/z=43$). Compound **56c**: ^1H NMR (CDCl_3 , 500 MHz) δ : 7.23 (dd, 2H, $J_{\text{HH}}=8.5$ Hz, $J_{\text{HF}}=5.7$ Hz), 7.02 (dd, 2H, $J_{\text{HH}}=8.5$ Hz, $J_{\text{HF}}=8.5$ Hz), 6.48 (s, 1H), 1.86 (s, 3H) ppm. Compound **56d**: ^1H NMR (CDCl_3 , 500 MHz) δ : 7.23 (br s, 4H), 6.48 (s, 1H), 2.35 (s, 3H), 1.86 (s, 3H) ppm; MS $m/z=146$ (100, $m/z=106$). Compound **56e**: ^1H NMR (CDCl_3 , 500 MHz) δ : 6.93 (s, 2H), 6.31 (s, 1H), 2.63 (s, 3H), 2.26 (s, 6H), 1.61 (s, 3H) ppm; MS $m/z=192$ (100, $m/z=133$).

5.2.3. Synthesis of allylic chlorides- d_2 57b–e. To a stirred mixture of the *E*-allylic alcohol (25 mmol) and 3.2 mL (27.6 mmol) of 2,6-lutidine, under N_2 atmosphere was added 1.18 g (27.8 mmol) of LiCl dissolved in a minimum amount of anhydrous dimethylformamide (DMF). On cooling to 0 °C, a suspension was formed, which was treated dropwise with MeSO_2Cl (2.14 mL, 27.6 mmol). After 10–12 h of stirring at room temperature, the reaction mixture was poured into a saturated solution of CuSO_4 to remove 2,6-lutidine and extracted with Et_2O . The organic extracts were dried over MgSO_4 and concentrated to afford the allylic chloride in 93–98% geometrical purity (85% overall yield).

The spectroscopic data for allylic chlorides **57b–e** are as follows. Compound **57b**: ^1H NMR (CDCl_3 , 500 MHz) δ : 7.59 (d, 2H, $J=8.0$ Hz), 7.37 (d, 2H, $J=8.0$ Hz), 6.61 (s, 1H), 1.98 (s, 3H) ppm; MS $m/z=236$ (100, $m/z=201$). Compound **57c**: ^1H NMR (CDCl_3 , 500 MHz) δ : 7.25 (dd, 2H, $J_{\text{HH}}=8.5$ Hz, $J_{\text{HF}}=5.7$ Hz), 7.03 (dd, 2H, $J_{\text{HH}}=8.5$ Hz, $J_{\text{HF}}=8.5$ Hz), 6.54 (s, 1H), 1.97 (s, 3H) ppm. Compound **57d**: ^1H NMR (CDCl_3 , 500 MHz) δ : 7.31 (d, 2H, $J=7.7$ Hz), 7.09 (d, 2H, $J=7.7$ Hz), 6.54 (s, 1H), 2.33 (s, 3H), 1.99 (s, 3H) ppm; MS $m/z=182$ (100, $m/z=147$). Compound **57e**: ^1H NMR (CDCl_3 , 500 MHz) δ : 6.98 (s, 2H), 6.45

(s, 1H), 2.67 (s, 3H), 2.21 (s, 6H), 1.75 (s, 3H) ppm; MS $m/z=210$ (100, $m/z=175$).

5.2.4. Synthesis of deuterated alkenes 58b–e. To a cooled (0 °C) mixture of LiAlD_4 (0.44 g, 10.5 mmol) in dry THF (40 mL), under N_2 atmosphere, was added dropwise a solution of allylic chloride (21 mmol) in dry THF (20 mL). After 3–4 h of stirring at room temperature, the reaction mixture was quenched at 0 °C by addition of 1 mL of H_2O , 1 mL of 15% NaOH solution, and 2.5 mL of H_2O , and then filtered. The organic layer was washed with a 5% solution of NaHCO_3 , dried over MgSO_4 , and concentrated. The residue was purified by flash column chromatography (petroleum ether) to afford *trans*-**58-d**₃ in 93–98% geometrical purity.

The spectroscopic data for labeled alkenes **58b–e** are as follows. Compound **58b** (isomeric purity 93%): ^1H NMR (CDCl_3 , 500 MHz) δ : 7.56 (d, 2H, $J=8.2$ Hz), 7.32 (d, 2H, $J=8.2$ Hz), 6.29 (s, 1H), 1.88 (s, 3H) ppm; ^{13}C NMR (CDCl_3 , 125 MHz) δ : 142.30, 137.84, 128.88, 127.76 (q, $J_{\text{CF}}=31.9$ Hz), 124.94 (q, $J_{\text{CF}}=3.5$ Hz), 124.40 (q, $J_{\text{CF}}=270$ Hz), 124.08, 26.03 (septet, $J_{\text{CD}}=19$ Hz), 19.34 ppm; MS $m/z=203$ (100, $m/z=163$). Compound **58c** (isomeric purity 98%): ^1H NMR (CDCl_3 , 500 MHz) δ : 7.20 (dd, 2H, $J_{\text{HH}}=8.5$ Hz, $J_{\text{HF}}=5.9$ Hz), 7.03 (dd, 2H, $J_{\text{HH}}=8.5$ Hz, $J_{\text{HF}}=8.5$ Hz), 6.26 (s, 1H), 1.86 (s, 3H) ppm; ^{13}C NMR (CDCl_3 , 125 MHz) δ : 161.06 (d, $J_{\text{CF}}=243$ Hz), 135.25, 134.67 (d, $J_{\text{CF}}=3.3$ Hz), 130.15 (d, $J_{\text{CF}}=7.6$ Hz), 124.05, 114.80 (d, $J_{\text{CF}}=21$ Hz), 25.81 (septet, $J_{\text{CD}}=19$ Hz), 19.14 ppm; MS $m/z=153$ (100, $m/z=135$). Compound **58d** (isomeric purity 95%): ^1H NMR (CDCl_3 , 500 MHz) δ : 7.18 (br s, 4H), 6.30 (s, 1H), 2.40 (s, 3H), 1.91 (s, 3H) ppm; ^{13}C NMR (CDCl_3 , 125 MHz) δ : 135.79, 135.28, 134.60, 128.71, 128.60, 124.96, 25.97 (septet, $J_{\text{CD}}=19$ Hz), 21.08, 19.29 ppm; MS $m/z=149$ (100, $m/z=134$). Compound **58e** (isomeric purity 98%): ^1H NMR (CDCl_3 , 500 MHz) δ : 6.96 (s, 2H), 6.13 (s, 1H), 2.74 (s, 3H), 2.25 (s, 6H), 1.54 (s, 3H) ppm; ^{13}C NMR (CDCl_3 , 125 MHz) δ : 136.35, 135.46, 134.87, 134.82, 127.73, 123.16, 24.14 (septet, $J_{\text{CD}}=19$ Hz), 20.92, 20.16, 18.95 ppm; MS $m/z=177$ (100, $m/z=162$).

5.3. Photooxygenation of deuterated alkenes 58a–e

A solution of 25–30 mg of isobutenylarene- d_3 , in 8–10 mL of CHCl_3 and TPP as sensitizer (1×10^{-4} M) was bubbled gently with oxygen and irradiated for 30–40 min at 0 °C. Rose bengal was the sensitizer in acetonitrile and methylene blue in methanol. The photooxygenation of those substrates gave complex mixtures of oxygenated adducts. The ene adducts were purified by flash column chromatography over silica gel prewashed with triethylamine, using CH_2Cl_2 as eluent. The ^1H NMR spectroscopic data of the ene allylic hydroperoxides of the isobutenylarenes **58a–e** (d_0) are the following. Ene product from **58a-d**₀: (CDCl_3 , 500 MHz) δ : 7.99 (s, 1H, OOH), 7.29 (d, $J=8.5$ Hz, 2H), 6.90 (d, $J=8.5$ Hz, 2H), 5.33 (s, 1H), 5.14 (br s, 1H), 5.08 (br s, 1H), 3.81 (s, 3H), 1.70 (s, 3H) ppm. Ene product from **58b-d**₀: (CDCl_3 , 500 MHz) δ : 8.09 (s, 1H, OOH), 7.64 (d, $J=8.1$ Hz, 2H), 7.49 (d, $J=8.1$ Hz, 2H), 5.44 (s, 1H), 5.12 (br s, 1H), 5.11 (br s, 1H), 1.70 (s, 3H) ppm. Ene product from **58c-d**₀: (CDCl_3 , 500 MHz) δ : 8.05 (s, 1H, OOH), 7.33 (dd, $J_{\text{HH}}=8.0$ Hz, $J_{\text{HF}}=5.5$ Hz, 2H), 7.06 (dd, $J_{\text{HH}}=8.0$ Hz, $J_{\text{HF}}=8.0$ Hz, 2H), 5.36 (s, 1H), 5.13 (br s, 1H),

5.10 (br s, 1H), 1.69 (s, 3H) ppm. Ene product from **58d-d₀**: (CDCl₃, 500 MHz) δ : 7.98 (s, 1H, OOH), 7.25 (d, 2H, $J=7.9$ Hz), 7.18 (d, 2H, $J=7.9$ Hz), 5.35 (s, 1H), 5.13 (br s, 1H), 5.07 (br s, 1H), 2.36 (s, 3H), 1.70 (s, 3H) ppm. Ene product from **58e-d₀**: (CDCl₃, 500 MHz) δ : 7.81 (s, 1H, OOH), 6.85 (s, 2H), 5.86 (d, 1H), 4.96 (br s, 1H), 4.79 (br s, 1H), 2.32 (s, 6H), 2.27 (s, 3H), 1.54 (s, 3H) ppm.

5.4. Synthesis of (Z)-1-(*p*-methoxyphenyl)-1-[(*p*-trifluoromethyl)phenyl]-2-methylprop-1-ene-3,3,3-*d*₃ (**63-d₃**)

This compound was prepared according to the procedure shown in Scheme 17.

5.4.1. (*p*-Methoxyphenyl)-[(*p*-trifluoromethyl)phenyl]-methanol (59**).** The title compound was prepared by a Grignard reaction between (*p*-trifluoromethyl)benzaldehyde and *p*-methoxybenzylmagnesium bromide. To a solution of Mg (1.46 g, 60 mmol) and catalytic amount of I₂ in 60 mL dry Et₂O was added dropwise 4-bromoanisole (9.35 g, 50 mmol) in 40 mL dry Et₂O. The mixture was refluxed for 2 h. After the solution was cooled to 0 °C (*p*-trifluoromethyl)benzaldehyde (8.36 g, 48 mmol) was added dropwise. After 30 min the mixture was warmed to room temperature and then refluxed for 2–3 h. The solution was worked up with NH₄Cl solution and extracted three times with Et₂O. The organic layers were combined, dried (MgSO₄), filtered, and concentrated to afford **59** as an oil in 75% overall yield. ¹H NMR (CDCl₃, 500 MHz) δ : 7.53 (d, 2H, $J=8.0$ Hz), 7.44 (d, 2H, $J=8.0$ Hz), 7.24 (d, 2H, $J=8.6$ Hz), 6.86 (d, 2H, $J=8.6$ Hz), 5.83 (br s, 1H), 3.81 (s, 3H), 2.23 (br s, 1H, OH) ppm; MS $m/z=282$ (100, $m/z=109$).

5.4.2. 4-Trifluoromethyl-4'-methoxybenzophenone (60**).** Jones reagent was added dropwise to a solution of **59** (10.15 g, 36 mmol) in acetone (40 mL) at 0 °C. The addition was continued until the orange color of the reagent persisted. The solution was stirred at 0 °C for an additional 5 min. The solution was poured into water (200 mL) and extracted with ether. The ether extracts were washed with brine and dried over MgSO₄, and the solvent was removed under reduced pressure. The crude product was chromatographed on silica gel (hexanes/EtOAc=2:1) to give **60** as a yellow solid in 70% overall yield. ¹H NMR (CDCl₃, 500 MHz) δ : 7.83 (m, 4H), 7.75 (d, 2H, $J=8.1$ Hz), 6.98 (d, 2H, $J=8.7$ Hz), 6.86 (d, 2H, $J=8.6$ Hz), 3.90 (s, 3H) ppm; MS $m/z=280$ (100, $m/z=135$).

5.4.3. 3-(*p*-Methoxyphenyl)-3-[(*p*-trifluoromethyl)phenyl]-3-hydroxy-2-methylpropionate (61**).** The title compound was prepared by a Reformatsky reaction between **60** and 2-bromopropionate in the presence of activated Zn and catalytic amount of I₂. The granular Zn was activated in a mixture of H₂SO₄/HNO₃=9/1 for 30 min. Then it was filtered and washed several times with H₂O and finally with acetone. Zn was dried before using. In a flame-dried flask were placed activated Zn (9.9 g, 0.151 mol), 2-bromopropionate (5.62 mL, 50.4 mmol), carbonyl compound **60** (7.06 g, 25.2 mmol), catalytic amount of I₂, and dry benzene/Et₂O=2/1 (80/40 mL). The mixture was refluxed for 2 days. The solution was poured into a solution of 4 N H₂SO₄ (50 mL) and extracted once with H₂O and two times with brine. The organic layers were combined, dried (MgSO₄), filtered, and concentrated. The residue was passed through a

short pad of silica, prewashed with triethylamine (hexane/EtOAc=9:1), to afford **61** (80% overall yield) as a 1:1 mixture of stereoisomers (please note that before column chromatography β -hydroxy-methylester **61** existed as a 3:2 mixture of stereoisomers). ¹H NMR (mixture of two stereoisomers) (CDCl₃, 500 MHz) δ : 7.63 (d, 2H, $J=7.9$ Hz), 7.53 (m, 6H), 7.44 (d, 2H, $J=8.8$ Hz), 7.33 (d, 2H, $J=8.8$ Hz), 6.82 (d, 4H, $J=7.9$ Hz), 4.74 (br s, 1H, OH), 4.71 (br s, 1H, OH), 3.76 (s, 3H), 3.73 (s, 3H), 3.64 (s, 3H), 3.61 (s, 3H), 2.58 (m, 2H), 1.39 (s, 1H), 1.35 (s, 1H), 1.18 (d, 3H, $J=6.9$ Hz), 1.12 (d, 3H, $J=6.9$ Hz) ppm.

5.4.4. Methyl 3-[(*p*-trifluoromethyl)phenyl]-2-methyl-*p*-methoxycinnamate (62**).** A solution of **61** (7.44 g, 20.16 mmol) in benzene (100 mL) containing catalytic amount of *p*-toluenesulfonic acid was heated at 70 °C for 2–3 h. The solution was dried (MgSO₄), filtered, and concentrated to afford substituted α,β -unsaturated methyl-ester (95% overall yield) as a 1:1 mixture of *E/Z*-isomers. The residue passed through a long pad of silica (hexane/EtOAc=9:1) and the two isomers were separated successfully. ¹H NMR (*E*-**62**, isomeric purity 90%) (CDCl₃, 500 MHz) δ : 7.52 (d, 2H, $J=8.1$ Hz), 7.22 (d, 2H, $J=8.1$ Hz), 7.06 (d, 2H, $J=8.8$ Hz), 6.87 (d, 2H, $J=8.8$ Hz), 3.82 (s, 3H), 3.48 (s, 3H), 2.09 (s, 3H) ppm; ¹³C NMR (*E*-**62**, isomeric purity 90%) (CDCl₃, 125 MHz) δ : 170.70, 163.57, 146.43, 145.41, 132.16, 130.80, 130.68, 129.85 (q, $J_{CF}=34.9$ Hz), 128.87, 125.63 (q, $J_{CF}=3.8$ Hz), 124.53 (q, $J_{CF}=271$ Hz), 113.60, 54.88, 51.25, 18.31 ppm; MS $m/z=350$ (100, $m/z=350$). ¹H NMR (*Z*-**62**, isomeric purity 98%) (CDCl₃, 500 MHz) δ : 7.60 (d, 2H, $J=8.1$ Hz), 7.29 (d, 2H, $J=8.1$ Hz), 7.02 (d, 2H, $J=8.7$ Hz), 6.81 (d, 2H, $J=8.7$ Hz), 3.78 (s, 3H), 3.54 (s, 3H), 2.00 (s, 3H) ppm; ¹³C NMR (*Z*-**62**, isomeric purity 98%) (CDCl₃, 125 MHz) δ : 171.50, 159.38, 144.86, 144.64, 133.90, 130.28, 130.04, 129.75 (q, $J_{CF}=34.8$ Hz), 128.36, 125.24 (q, $J_{CF}=3.5$ Hz), 124.14 (q, $J_{CF}=270.5$ Hz), 113.63, 55.20, 51.76, 18.57 ppm; MS $m/z=350$ (100, $m/z=350$).

5.4.5. (Z)-3-(*p*-Methoxyphenyl)-3-[(*p*-trifluoromethyl)phenyl]-2-methylprop-2-en-1-ol-1,1-*d*₂. This compound was prepared according to the previously described procedure for the synthesis of allylic alcohols-*d*₂ **56b–e** (Section 5.2.2). ¹H NMR (*Z*, isomeric purity 98%) (CDCl₃, 500 MHz) δ : 7.55 (d, 2H, $J=8.1$ Hz), 7.25 (d, 2H, $J=8.1$ Hz), 7.03 (d, 2H, $J=8.7$ Hz), 6.83 (d, 2H, $J=8.7$ Hz), 3.78 (s, 3H), 1.88 (s, 3H), 1.57 (br s, 1H, OH) ppm; MS $m/z=306$ (100, $m/z=306$).

5.4.6. (Z)-3-(*p*-Methoxyphenyl)-3-[(*p*-trifluoromethyl)phenyl]-2-methylprop-2-en-1-yl-1,1-*d*₂ chloride. This compound was prepared according to the previously described procedure for the synthesis of allylic chlorides-*d*₂ **57b–e** (Section 5.2.3). ¹H NMR (*Z*, isomeric purity 95%) (CDCl₃, 500 MHz) δ : 7.56 (d, 2H, $J=8.4$ Hz), 7.25 (d, 2H, $J=6.9$ Hz), 7.12 (d, 2H, $J=6.9$ Hz), 6.86 (d, 2H, $J=8.4$ Hz), 3.80 (s, 3H), 1.89 (s, 3H) ppm; MS $m/z=342$ (100, $m/z=307$).

5.4.7. (Z)-1-(*p*-Methoxyphenyl)-1-[(*p*-trifluoromethyl)phenyl]-2-methylprop-1-ene-3,3,3-*d*₃ (Z-63-d₃**).** This compound was prepared according to the previously described procedure for the synthesis of deuterated alkenes **58b–e** (Section 5.2.4). The crude product was chromatographed on

silica gel (hexane) to give Z-**63-d₃** as a yellow oil. ¹H NMR (Z-**63-d₃**, isomeric purity 95%) (CDCl₃, 500 MHz) δ: 7.59 (d, 2H, *J*=7.7 Hz), 7.30 (d, 2H, *J*=7.7 Hz), 7.10 (d, 2H, *J*=8.4 Hz), 6.90 (d, 2H, *J*=8.4 Hz), 3.83 (s, 3H), 1.84 (s, 3H) ppm; ¹³C NMR (CDCl₃, 125 MHz) δ: 158.24, 147.47, 135.68, 135.11, 132.20, 131.09, 130.27, 128.22 (q, *J*_{CF}=32.6 Hz), 124.96 (q, *J*_{CF}=3.75 Hz), 124.51 (q, *J*_{CF}=270.2 Hz), 113.56, 55.32, 22.54, 21.87 (septet, *J*_{CD}=19.05 Hz) ppm; MS *m/z*=309 (100, *m/z*=309).

5.4.8. 1-(*p*-Methoxyphenyl)-1-[(*p*-trifluoromethyl)phenyl]-2-methylprop-1-ene (63-d₀**).** The unlabeled olefin **63-d₀** was prepared by reduction of methyl 3-[(*p*-trifluoromethyl)phenyl]-2-methyl-*p*-methoxycinnamate (crude mixture 1:1 of *E/Z*-isomers) with LiAlH₄ to the respective allylic alcohol, subsequent conversion of the latter to the allylic chloride, and further reduction with LiAlH₄. The residue was chromatographed on silica gel (hexane) to give **63-d₀** as a yellow oil. ¹H NMR (CDCl₃, 500 MHz) δ: 7.52 (d, 2H, *J*=8.1 Hz), 7.23 (d, 2H, *J*=8.1 Hz), 7.02 (d, 2H, *J*=8.6 Hz), 6.83 (d, 2H, *J*=8.6 Hz), 3.79 (s, 3H), 1.82 (s, 3H), 1.78 (s, 3H) ppm; ¹³C NMR (CDCl₃, 125 MHz) δ: 158.24, 147.48, 135.65, 135.11, 132.30, 131.09, 130.27, 128.41 (q, *J*_{CF}=31.8 Hz), 124.96 (q, *J*_{CF}=3.75 Hz), 124.57 (q, *J*_{CF}=270.1 Hz), 113.56, 55.34, 22.71, 22.61 ppm; MS *m/z*=306 (100, *m/z*=306). UV-vis spectra of **63-d₀** in CHCl₃ have characteristic maximum absorption at λ_{max}=245 nm.

5.5. Photooxygenation of Z-**63-d₃**

A solution of 15 mg of Z-**63-d₃** in 8 mL of CCl₄ containing a catalytic amount of galvinoxyl as free radical scavenger (TPP, 1×10⁻⁴ M as sensitizer) was bubbled gently with oxygen and irradiated with a 300-W Xenon lamp, through a 0.05 M K₂Cr₂O₇ filter solution, for 2 min at 0 °C. The same procedure was followed in several solvents. TPP was the sensitizer in CHCl₃. Rose bengal was the sensitizer in acetonitrile and acetone. Methylene blue was the sensitizer in isopropanol, 2,2,2-trifluoroethanol, MeOH, and MeOH/D₂O=4:1. The photooxygenation gave complex mixtures of oxygenated adducts. The ene adducts were purified by flash column chromatography over silica gel prewashed with triethylamine, using a mixture of hexane/EtOAc=9:1 as eluent. The ¹H NMR spectroscopic data of the ene allylic hydroperoxide of **63-d₀** are the following. ¹H NMR (CDCl₃, 500 MHz) δ: 7.61 (s, 4H), 7.32 (d, 2H, *J*=8.8 Hz), 7.24 (s, 1H, OOH), 6.90 (d, 2H, *J*=8.8 Hz), 5.22 (s, 1H), 5.09 (s, 1H), 3.83 (s, 3H), 1.71 (s, 3H) ppm.

Acknowledgements

M.O. thanks Professor R. H. Grubbs for his generous hospitality during his sabbatical stay at Caltech (2006). M.N.A. thanks the financial support of the Greek Secretariat of Research and Technology (PENED, 2001) for a three years graduate fellowship. We also thank Professors I. Smonou and M. Stratakis for useful comments and discussions.

Supplementary data

Supplementary data associated with this article can be found in the online version, at doi:10.1016/j.tet.2006.07.106.

References and notes

- Partington, J. R. *A History of Chemistry*; Macmillan: London, 1970; Vols. 2–4.
- Raab, O. *Z. Biol.* **1900**, 39, 524.
- Mulliken, R. S. *Nature (London)* **1928**, 122, 505.
- Childe, W. H. J.; Mecke, R. *Z. Physik* **1931**, 68, 344.
- Herzberg, G. *Nature (London)* **1934**, 133, 759.
- Gollnick, K.; Schenck, G. O. *1,4-Cycloaddition Reactions*; Hamer, J., Ed.; Academic: New York, NY, 1967.
- Kautsky, H. *Trans. Faraday Soc.* **1939**, 35, 216.
- Foote, C. S.; Wexler, S. *J. Am. Chem. Soc.* **1964**, 86, 3979.
- Foote, C. S. *Science* **1968**, 162, 963.
- Corey, E. J.; Taylor, W. C. *J. Am. Chem. Soc.* **1964**, 86, 3881.
- Wasserman, H. H.; Murray, R. W. *Singlet Oxygen*; Academic: New York, NY, 1979.
- Frimmer, A. A.; Stephenson, L. M. *Reactions, Modes and Products*; Frimer, A. A., Ed.; Singlet Oxygen; CRC: Boca Raton, FL, 1985.
- Wasserman, H. H.; Ives, J. L. *Tetrahedron* **1981**, 37, 1825.
- Foote, C. S.; Clennan, E. L. *Active Oxygen in Chemistry*; Foote, C. S., Valentine, J. S., Greenberg, A., Liebman, J. F., Eds.; Chapman and Hall: London, 1995; pp 105–140.
- Ranby, B.; Rabek, J. F. *Photodegradation, Photooxygenation and Photostabilization of Polymers*; Wiley: London, 1975.
- Kasha, M.; Khan, A. V. *Ann. N.Y. Acad. Sci.* **1970**, 171, 5.
- For recent reviews, see: (a) Margaros, I.; Montagon, T.; Tofi, M.; Pavlakos, E.; Vassilikogiannakis, G. *Tetrahedron* **2006**, 62, 5308; (b) Clennan, E. L.; Pace, A. *Tetrahedron* **2005**, 61, 6665; (c) Casteel, D. A. *Nat. Prod. Rep.* **1999**, 16, 55; (d) Prein, M.; Adam, W. *Angew. Chem., Int. Ed.* **1996**, 35, 477.
- (a) Vassilikogiannakis, G.; Stratakis, M. *Angew. Chem., Int. Ed.* **2003**, 42, 5465; (b) Adam, W.; Saha-Möllner, C. R.; Schmid, K. S. *J. Org. Chem.* **2001**, 66, 7365; (c) Paquette, L. A.; Tae, J.; Arrington, M. P.; Sadoun, A. H. *J. Am. Chem. Soc.* **2000**, 122, 2742; (d) Adam, W.; Braun, M.; Griesbeck, A.; Lucchini, V.; Staab, E.; Will, B. *J. Am. Chem. Soc.* **1989**, 111, 203; (e) Adam, W.; Brünker, H.-G. *Synthesis* **1995**, 1066; (f) Dussault, P. H.; Woller, K. R. *J. Am. Chem. Soc.* **1997**, 119, 3824; (g) Adam, W.; Klung, P. *J. Org. Chem.* **1994**, 59, 2695; (h) Adam, W.; Richter, M. J. *J. Org. Chem.* **1994**, 59, 3341; (i) Adam, W.; Kumar, A. S.; Saha-Möllner, C. R. *Synthesis* **1995**, 1525; (j) Adam, W.; Richter, M. J. *Synthesis* **1994**, 176; (k) Adam, W.; Griesbeck, A.; Staab, E. *Angew. Chem., Int. Ed. Engl.* **1986**, 25, 269.
- Kearns, D. R. *Chem. Rev.* **1971**, 71, 395.
- Khan, A. U.; Kasha, M. *Ann. N.Y. Acad. Sci.* **1970**, 171, 24.
- Murray, R. W.; Lin, J. W. P.; Kaplan, M. L. *Ann. N.Y. Acad. Sci.* **1970**, 171, 121.
- Abdou, M. S. A.; Holdcroft, S. *Macromolecules* **1993**, 26, 2954.
- Scurlock, R. D.; Wang, B.; Ogilby, P. R.; Sheats, J. R.; Clough, R. L. *J. Am. Chem. Soc.* **1995**, 117, 10194.
- Smith, K. C. *The Science of Photobiology*; Plenum Rosetta: New York, NY, 1977.
- Foote, C. S. *Free Radicals in Biology*; Academic: New York, NY, 1976; Vol. 2, pp 85–133.
- Gollnick, K.; Hartmann, H. *Oxygen and Oxy Radicals in Biology*; Academic: New York, NY, 1981; pp 379–395.
- (a) Schenck, G. O. DE-B 933925, 1943 'quoted from Ref. 4'; (b) Schenck, G. O.; Eggert, H.; Denk, W. *Justus Liebigs Ann. Chem.* **1953**, 584, 177.

28. Gorman, A. A. *Chem. Soc. Rev.* **1981**, 10, 205.
29. Harding, L. B.; Goddard, W. A. *J. Am. Chem. Soc.* **1980**, 102, 439.
30. Jefford, C. W. *Tetrahedron Lett.* **1979**, 20, 985.
31. (a) Stratakis, M.; Orfanopoulos, M. *Tetrahedron* **2000**, 56, 1595; (b) Clennan, E. L. *Tetrahedron* **2000**, 56, 9151; (c) Sharp, D. B. *Abstracts of Papers*, 138 National Meeting of the American Chemical Society, Washington, DC, 1960; PSME 79.
32. Grdina, M. B.; Orfanopoulos, M.; Stephenson, L. M. *J. Am. Chem. Soc.* **1979**, 101, 3111.
33. Stratakis, M.; Orfanopoulos, M.; Chen, J.; Foote, C. S. *Tetrahedron Lett.* **1996**, 37, 4105.
34. Orfanopoulos, M.; Foote, C. S. *J. Am. Chem. Soc.* **1998**, 110, 6583.
35. (a) Orfanopoulos, M.; Foote, C. S. *Free Radical Res. Commun.* **1987**, 2, 321; (b) Orfanopoulos, M.; Smonou, I.; Foote, C. S. *J. Am. Chem. Soc.* **1990**, 112, 3607.
36. Orfanopoulos, M.; Stephenson, L. M. *J. Am. Chem. Soc.* **1980**, 102, 1417.
37. Schaap, A. P.; Recher, C. G.; Faler, G. R.; Villasenor, S. R. *J. Am. Chem. Soc.* **1983**, 105, 1691.
38. Stratakis, M.; Orfanopoulos, M.; Foote, C. S. *Tetrahedron Lett.* **1991**, 32, 863.
39. Clennan, E. L.; Chen, M.-F.; Xu, G. *Tetrahedron Lett.* **1996**, 37, 2911.
40. Inagaki, S.; Fukui, K. *J. Am. Chem. Soc.* **1975**, 97, 7480.
41. Dewar, M. J. S.; Thiel, W. *J. Am. Chem. Soc.* **1975**, 97, 3978.
42. Yamaguchi, K.; Yabushita, S.; Fueno, T.; Houk, K. N. *J. Am. Chem. Soc.* **1981**, 103, 5043.
43. Davies, A. G.; Schiesser, C. H. *Tetrahedron* **1991**, 47, 1707.
44. Yoshioka, Y.; Yamada, S.; Kawakami, T.; Nishino, M.; Yamaguchi, K.; Saito, I. *Bull. Chem. Soc. Jpn.* **1996**, 69, 2683.
45. Clennan, E. L.; Nagraba, K. *J. Am. Chem. Soc.* **1983**, 105, 5932.
46. Gorman, A. A.; Hamblett, I.; Lambert, C.; Spencer, B.; Standen, M. C. *J. Am. Chem. Soc.* **1988**, 110, 8053.
47. Aubry, J.-M.; Mandard-Cazin, B.; Rougee, M.; Bensasson, R. V. *J. Am. Chem. Soc.* **1995**, 117, 9159.
48. Singleton, D. A.; Hang, C.; Szymanski, M. J.; Meyer, M. P.; Leach, A. G.; Kuwata, K. T.; Chen, J. S.; Greer, A.; Foote, C. S.; Houk, K. N. *J. Am. Chem. Soc.* **2003**, 125, 1319.
49. (a) Orfanopoulos, M.; Grdina, M. B.; Stephenson, L. M. *J. Am. Chem. Soc.* **1979**, 101, 275; (b) Schulte-Elte, K. H.; Muller, B. L.; Rautenstrauch, V. *Helv. Chim. Acta* **1978**, 61, 2777.
50. (a) Hurst, J. R.; McDonald, J. D.; Schuster, G. B. *J. Am. Chem. Soc.* **1982**, 104, 2065; (b) Gorman, A. A.; Gould, I. R.; Hamblett, I. *J. Am. Chem. Soc.* **1982**, 104, 7098; (c) Houk, K. N.; Williams, P. A.; Mitchell, P. A.; Yamaguchi, K. *J. Am. Chem. Soc.* **1981**, 103, 949.
51. Stratakis, M.; Orfanopoulos, M. *Tetrahedron Lett.* **1995**, 36, 4291.
52. Orfanopoulos, M.; Stratakis, M.; Elemes, Y. *Tetrahedron Lett.* **1989**, 30, 4875.
53. Clennan, E. L.; Chen, X. *J. Org. Chem.* **1988**, 53, 3124.
54. (a) Orfanopoulos, M.; Stratakis, M.; Elemes, Y. *J. Am. Chem. Soc.* **1990**, 112, 6417; (b) Stratakis, M.; Orfanopoulos, M. *Synth. Commun.* **1993**, 23, 425.
55. Clennan, E. L.; Chen, X.; Koola, J. J. *J. Am. Chem. Soc.* **1990**, 112, 5193.
56. Orfanopoulos, M.; Stratakis, M.; Elemes, Y.; Jensen, F. *J. Am. Chem. Soc.* **1991**, 113, 3180.
57. Adam, W.; Catalani, L.; Griesbeck, A. *J. Org. Chem.* **1986**, 51, 5494.
58. Adam, W.; Griesbeck, A. *Angew. Chem., Int. Ed. Engl.* **1985**, 24, 1070.
59. Orfanopoulos, M.; Foote, C. S. *Tetrahedron Lett.* **1985**, 26, 5991.
60. (a) Ensley, H. E.; Carr, R. V. C.; Martin, R. S.; Pierce, T. E. *J. Am. Chem. Soc.* **1980**, 102, 2836; (b) Kwon, B.-M.; Kanner, R. C.; Foote, C. S. *Tetrahedron Lett.* **1989**, 30, 903.
61. (a) Akasaka, T.; Kakeushi, T.; Ando, W. *Tetrahedron Lett.* **1987**, 28, 6633; (b) Akasaka, T.; Misawa, Y.; Goto, M.; Ando, W. *Heterocycles* **1989**, 28, 445.
62. Akasaka, T.; Misawa, Y.; Goto, M.; Ando, W. *Tetrahedron* **1989**, 45, 6657.
63. Adam, W.; Griesbeck, A. *Synthesis* **1986**, 1050.
64. Stratakis, M.; Orfanopoulos, M. *Tetrahedron Lett.* **1997**, 38, 1067.
65. Clennan, E. L.; Cheng, X. *J. Am. Chem. Soc.* **1989**, 111, 8212.
66. (a) Foote, C. S.; Denny, R. W. *J. Am. Chem. Soc.* **1971**, 93, 5168; (b) Gollnick, K.; Griesbeck, A. *Tetrahedron Lett.* **1984**, 25, 725.
67. (a) Asveld, E. W. H.; Kellogg, R. M. *J. Am. Chem. Soc.* **1980**, 102, 3644; (b) Ando, W.; Watanabe, K.; Suzuki, J.; Migita, T. *J. Am. Chem. Soc.* **1974**, 96, 6766; (c) Kwon, B.-M.; Foote, C. S. *J. Org. Chem.* **1989**, 54, 3878; (d) Chan, Y.-Y.; Li, X.; Zhu, C.; Zhang, Y.; Leung, H.-K. *J. Org. Chem.* **1990**, 55, 5497; (e) Gollnick, K.; Knutzen-Mies, K. *J. Org. Chem.* **1991**, 56, 4017; (f) Yoshioka, M.; Sakuma, Y.; Saito, M. *J. Org. Chem.* **1999**, 64, 9247.
68. Gollnick, K.; Kuhn, H. J. *Singlet Oxygen*; Wasserman, H. H., Murray, R. W., Eds.; Academic: New York, NY, 1979; pp 287–427.
69. Orfanopoulos, M.; Stratakis, M. *Tetrahedron Lett.* **1991**, 32, 7321.
70. Dean, J. A. *Lange's Handbook of Chemistry*, 15th ed.; McGraw-Hill: 1999; pp 464–488.
71. (a) Stratakis, M.; Orfanopoulos, M.; Foote, C. S. *Tetrahedron Lett.* **1996**, 37, 7159; (b) Vassilikogiannakis, G.; Stratakis, M.; Orfanopoulos, M.; Foote, C. S. *J. Org. Chem.* **1999**, 64, 4130.
72. (a) Adam, W.; Nestler, B. *J. Am. Chem. Soc.* **1992**, 114, 6549; (b) Adam, W.; Nestler, B. *J. Am. Chem. Soc.* **1993**, 115, 5041.
73. (a) Adam, W.; Brünker, H.-G. *J. Am. Chem. Soc.* **1993**, 115, 3008; (b) Brünker, H.-G.; Adam, W. *J. Am. Chem. Soc.* **1995**, 117, 3976.
74. (a) Stensaas, K. L.; Payne, J. A.; Ivancic, A. N.; Bajaj, A. *Tetrahedron Lett.* **2002**, 43, 25; (b) Stensaas, K. L.; Bajaj, A.; Al-Turk, A. *Tetrahedron Lett.* **2005**, 46, 715.
75. Stratakis, M.; Orfanopoulos, M.; Foote, C. S. *J. Org. Chem.* **1998**, 63, 1315.
76. (a) Matsumoto, M.; Kondo, K. *Tetrahedron Lett.* **1975**, 16, 3935; (b) Matsumoto, M.; Dobashi, S.; Kuroda, K. *Tetrahedron Lett.* **1977**, 18, 3361; (c) Matsumoto, M.; Kuroda, K. *Synth. Commun.* **1981**, 11, 987.
77. A preliminary communication for the electronic effect of singlet oxygen with *para*-substituted aryl alkenes has been already reported, see: Alberti, M. N.; Vougioukalakis, G. C.; Orfanopoulos, M. *Tetrahedron Lett.* **2003**, 44, 903.
78. Brittelli, D. R. *J. Org. Chem.* **1981**, 46, 2514.
79. Jorgenson, M. J. *Tetrahedron Lett.* **1962**, 3, 559.
80. Collington, E. W.; Meyers, A. I. *J. Org. Chem.* **1971**, 36, 3044.
81. Grdina, M. B.; Orfanopoulos, M. *J. Org. Chem.* **1979**, 44, 2936.
82. (a) Takeda, T. *Modern Carbonyl Olefination*; Wiley-VCH: Weinheim, 2004; (b) Grubbs, R. H. *Handbook of Metathesis*; Wiley-VCH: Weinheim, 1993; Vols. 1–3.

83. Wiseman, H. *Tamoxifen: Molecular Basis of Use in Cancer Treatment and Prevention*; Wiley: Chichester, UK, 1994.
84. Vogel, A. I.; Furniss, B. S.; Hannaford, A. J.; Rogers, V.; Smith, P. W. G.; Tatchell, A. R. *Vogel's Textbook of Practical Organic Chemistry*, 4th ed.; Longman: London and New York, NY, 1978; pp 363–366.
85. (a) Babler, J. H.; Coghlan, M. J. *Synth. Commun.* **1976**, *6*, 469; (b) Sundararaman, P.; Herz, W. *J. Org. Chem.* **1977**, *42*, 806; (c) Dauben, W. G.; Michno, D. M. *J. Org. Chem.* **1977**, *42*, 682.
86. (a) Shriner, R. L. *Org. React.* **1942**, *1*, 1; (b) Gaudemar, M. *Organomet. Chem. Rev., A* **1972**, *8*, 183; (c) Rathke, M. W. *Org. React. (N.Y.)* **1975**, *22*, 423; (d) Fürstner, A. *Synthesis* **1989**, 571.
87. (a) Harada, T.; Mukaiyama, T. *Chem. Lett.* **1982**, 161; (b) Ross, N. A.; Bartsch, R. A. *J. Org. Chem.* **2002**, *68*, 360.
88. Günther, H. *NMR Spectroscopy Basic Principles, Concepts and Applications in Chemistry*, 2nd ed.; Wiley: West Sussex PO19 1UD, England, 1996.
89. Vassilikogiannakis, G.; Hatzimarinaki, M.; Orfanopoulos, M. *J. Org. Chem.* **2000**, *65*, 8180.

Unusual endoperoxide isomerizations: a convenient entry into 2-vinyl-2-cyclopentenones from saturated fulvene endoperoxides

Ihsan Erden,^{a,*} Nüket Öcal,^b Jianga Song,^a Cindy Gleason^a and Christian Gärtner^a

^aSan Francisco State University, Department of Chemistry and Biochemistry, 1600 Holloway Avenue, San Francisco, CA 94132, USA

^bYildiz Technical University, Faculty of Arts and Sciences, Department of Chemistry, Davutpasa Campus, 34010 Merter-Istanbul, Turkey

Received 16 June 2006; revised 12 July 2006; accepted 24 July 2006

Available online 14 September 2006

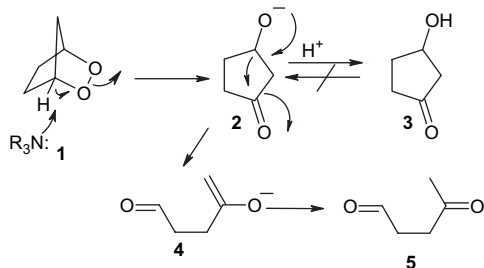
This paper is dedicated to my teacher, friend and associate, Professor Armin de Meijere

Abstract—An unusual peroxide base-promoted isomerization is uncovered. Saturated endoperoxides derived from fulvenes give rise to 2-vinyl-2-cyclopentenones upon treatment with DBU in CH₂Cl₂ in a one-pot reaction. This methodology is applied to a convenient synthesis of dihydrojasmane. Moreover, functional groups placed on the side chain at C-6 participate in the base-catalyzed isomerizations via conjugate attack at the enone moiety to give 2-cyclopentenones carrying oxygen heterocycles at C-2.

© 2006 Elsevier Ltd. All rights reserved.

1. Introduction

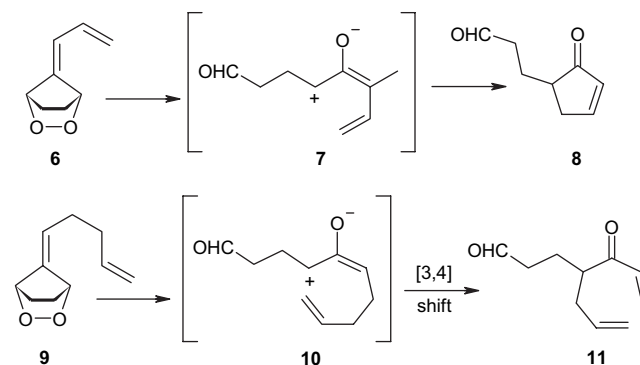
Endoperoxides, readily available in most cases from 1,3-dienes by way of a Diels–Alder reaction with singlet oxygen,¹ are sensitive to thermal, photochemical, and reductive conditions.² In particular, base-catalyzed rearrangements, also known as Kornblum–De la Mare reactions are well-known.³ Treatment of bridged bicyclic endoperoxides typically result in the formation of hydroxyketones. The mechanism of these reactions have been thoroughly studied. In particular, the base-catalyzed disproportionation of 2,3-dioxabicyclo[2.2.1]heptane (**1**) to 3-hydroxycyclopentanone (**3**) and levulinaldehyde (**5**) by amine catalysis has been reported by Salomon and Zagorski in an elegant study.⁴ Isotope labeling studies show that the most likely mechanism for the disproportionation involves initial abstraction of the bridgehead proton in the rate-determining step (Scheme 1).



Scheme 1.

* Corresponding author. Tel.: +1 415 338 1627; fax: +1 415 338 2384; e-mail: ierden@sfsu.edu

Previously, we studied the singlet oxygenations of fulvenes and low-temperature diazene reduction of the unstable endoperoxides⁵ and reported on some novel mechanisms encountered during the thermal isomerizations of saturated fulvene endoperoxide, e.g., **23**, **32**, **42**, and **46**.^{6,7} We have explored the synthetic utility of the allene oxides/cyclopropanones⁸ to prepare functionalized cyclopentenones derived from saturated fulvene endoperoxides, e.g., **6** → **7** → **8**⁹ and also disclosed the first aliphatic examples of [3,4]-sigmatropic shifts on suitably substituted cyclopropanones derived from the corresponding endoperoxides by thermolysis (**9** → **10** → **11**) (Scheme 2).¹⁰

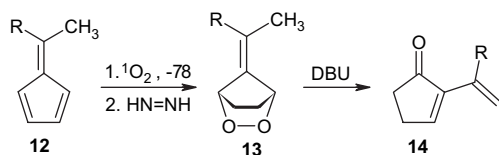


Scheme 2.

2. Results and discussion

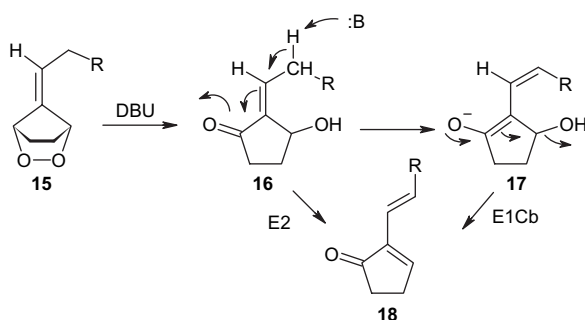
We here report a new and synthetically useful facet of base-catalyzed endoperoxide isomerizations that we observed in

saturated fulvene endoperoxides. The outcome of these reactions has proved particular to the nature of the base. Thus, treatment of fulvene endoperoxides with triethylamine at 0 °C to rt in CH₂Cl₂ results in the formation of the corresponding hydroxyketone as expected.⁵ However, the use of the stronger base, 1,8-diazabicyclo[5.4.0]undec-7-ene (DBU), gave 2-vinyl-2-cyclopentenones, e.g., **14**, in high yields (Scheme 3).



Scheme 3.

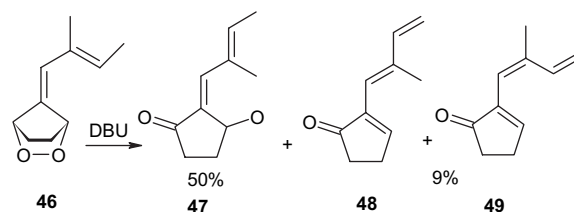
The mechanism presumably commences with initial proton abstraction at the bridgehead. However, the resulting hydroxyketone is prone to further proton abstraction at the allylic position. The timing of the proton elimination is subject to discussion and further studies, and two alternative mechanisms may be advanced for the dehydration step. One possible dehydration pathway would involve deprotonation of the γ -H, enolate formation, followed by hydroxide elimination (presumably via initial protonation by BH⁺), an E1Cb mechanism (Scheme 4). However, the fact that the reaction proceeds in CH₂Cl₂, an aprotic solvent that does not encourage ionic species, points to a concerted 1,4-elimination (E2). Regardless of the mechanism of the dehydration step, the resulting compounds from this tandem isomerization–dehydration process are 2-vinylcyclopentenones, a substance class for which there are very few synthetic methods.^{11–15} The ease with which the 2-vinylcyclopentenones can be constructed from the readily available fulvenes in a one-pot reaction makes this approach particularly attractive. Table 1 depicts some selected systems we have prepared so far.



Scheme 4.

In one case, where the starting fulvene carried a 6-vinyl group, the reaction with DBU led to a mixture of the expected hydroxyketone **47** (50%) and a mixture of the two isomers **48** and **49** (9%). It appears that the protons at the remote methyl group are just acidic enough to permit abstraction, resulting in the formation of a highly conjugated system (Scheme 5).

In another example, we subjected the hydroxyketone **52**, obtained from **51** by treatment with DBU, to the reaction with



Scheme 5.

catalytic trifluoroacetic acid, in hopes of affecting dehydration. The product from this reaction was the alcohol **53**, obviously stemming from a process involving dehydration, double bond shift, and rehydration (Scheme 6).

The presence of functionality on side chain of the exocyclic double bond was tested in the case of **37** (entry 6). The treatment of the endoperoxide **35** with DBU delivered a 3:2 mixture of the dehydration products **36** and **37** (Scheme 7). Obviously the hydroxyl group in the side chain did not suffer elimination. The two products were identified in the mixture by means of their ¹H and ¹³C NMR spectra.

When the hydroxyl group was placed at C-3 on the side chain of the exocyclic double bond in the starting fulvene (entry 7), treatment of the saturated endoperoxides **42** with DBU furnished the tetrahydrofuran derivative **40** exclusively. Compound **40** appears to be a suitable precursor of the hypotensive drug oundenone,¹⁶ and this approach is currently being explored (Scheme 8).

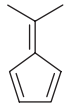
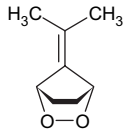
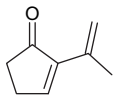
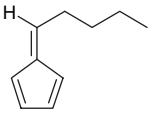
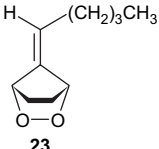
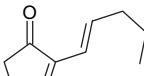
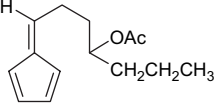
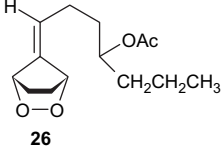
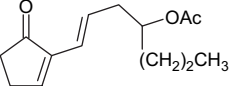
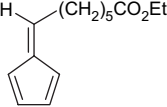
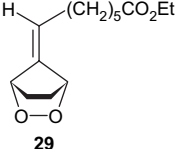
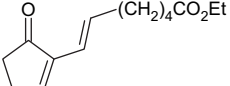
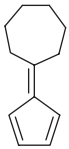
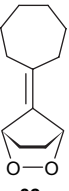
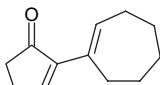
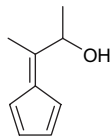
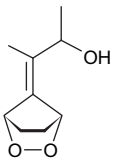
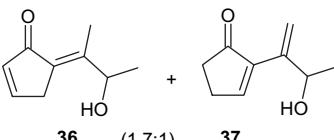
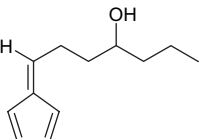
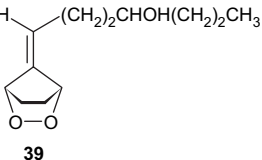
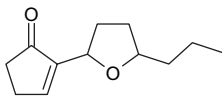
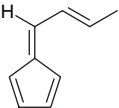
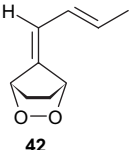
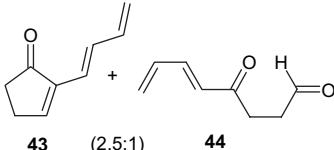
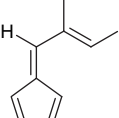
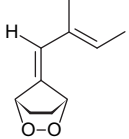
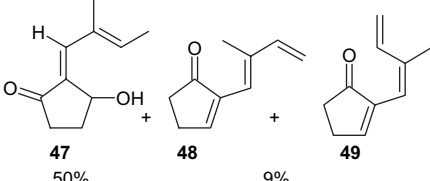
Finally, the fulvene endoperoxide–DBU isomerization–dehydration methodology was implemented in a short synthesis of the naturally occurring fragrant compound dihydrojasnone.¹⁷ Starting with fulvene **22** (entry 2), readily available from valeraldehyde in 77% yield by photooxygenation in CH₂Cl₂ at –78 °C followed by diazene reduction, (generated in situ from azodicarboxylate and acetic acid at low temperatures), endoperoxide **23** was obtained, which without isolation was treated with DBU to give the cyclopentenone **24** in 83% yield. The conversion of **24** to dihydrojasnone was achieved by the well-documented protocol^{18,19} involving methyl lithium addition to the carbonyl group and subsequent treatment with PCC in CH₂Cl₂ to furnish **56** in 50% overall yield from **24** (Scheme 9).

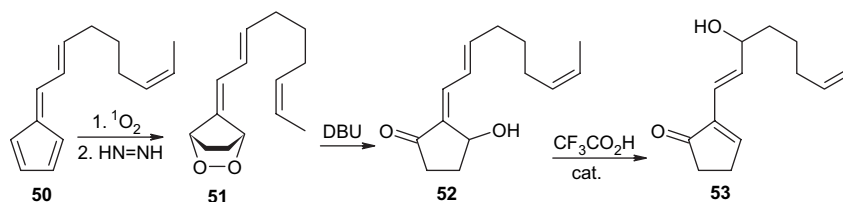
Compound **30** (entry 4) can also be obtained in this manner in a very short sequence from the readily available fulvene. The former represents an important precursor of certain prostaglandins and related compounds. These aspects are currently being explored.

It is noteworthy that the respective unsaturated fulvene endoperoxides do not suffer dehydration after base-catalyzed isomerization with DBU, presumably owing to the unstable nature of the products (cyclopentadienones). Endoperoxide **57**, derived from 6,6-dimethylfulvene for instance, gave a mixture of the hydroxyketones **58** and **59** in a ratio of 5:1 (Scheme 10).²⁰

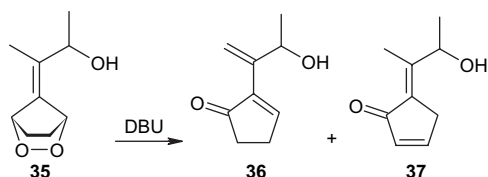
Compound **58** is the expected primary isomerization product, however, **59** is a secondary product that most likely

Table 1. DBU-catalyzed isomerizations–dehydrations of fulvene endoperoxides

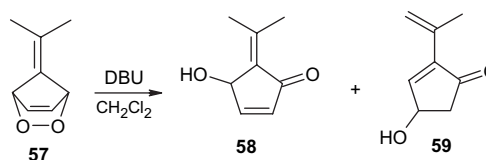
Entry	Fulvene	Endoperoxide	Cyclopentenone	Yield (%)
1	 19	 20	 21	76
2	 22	 23	 24	83
3	 25	 26	 27	81
4	 28	 29	 30	69
5	 31	 32	 33	82
6	 34	 35	 36 (1.7:1) 37	66
7	 38	 39	 40	68
8	 41	 42	 43 (2.5:1) 44	66
9	 45	 46	 47 50% 48 9% 49	59



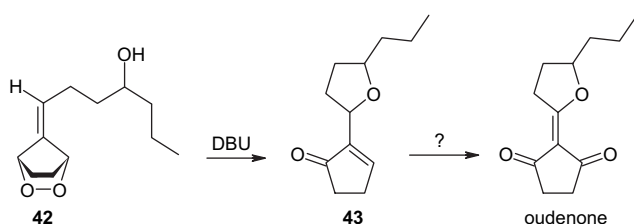
Scheme 6.



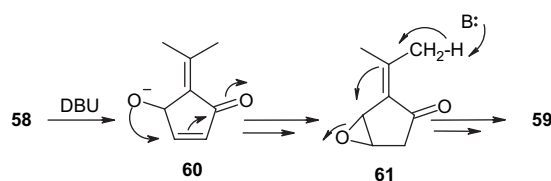
Scheme 7.



Scheme 10.



Scheme 8.



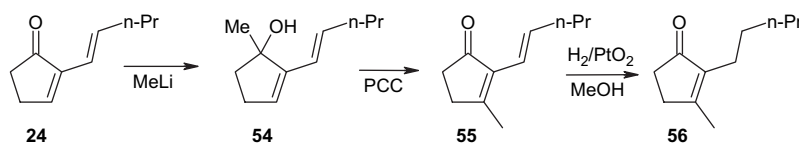
Scheme 11.

forms by further isomerization of **58** by a mechanism outlined in Scheme 11.

It is interesting to note that the base-catalyzed decomposition of unsaturated fulvene endoperoxides appears to be entirely analogous to those of the saturated counterparts, except for the dehydration step in the latter. Intermediates **16** (Scheme 2) and **61** (Scheme 11) differ only in the nature of the leaving groups (alcohol vs epoxide). The epoxide suffers ring opening to the allylic alcohol, whereas the hydroxyl group is eliminated in **16**.

3. Conclusion

In summary, we have uncovered a new useful facet of base-catalyzed endoperoxide rearrangements that result in a Kornblum–De la Mare isomerization followed by dehydration to give 2-vinyl-2-cyclopentenones, which are highly desirable synthetic intermediates. In cases where there are oxygen nucleophiles on the side chain, conjugate attack at the β -carbon of the exocyclic double bond occurs to give 2-cyclopentenones that carry a heterocycle at C-2. Implementation of this methodology in the synthesis of a variety of targets is underway.



Scheme 9.

4. Experimental

4.1. General

^1H and ^{13}C NMR spectra were recorded on a General Electric QE-Plus 300 MHz and Bruker Avance DRX 300 MHz spectrometers, using CDCl_3 as solvent and TMS as internal standard, unless specified otherwise. IR spectra were obtained on a Nicolet Avance 370 DTGS FT-IR spectrometer. Column chromatographic separations were carried out with Davison 6–200 mesh silica gel. For preparative TLC, Merck silica gel (grade 60 PF254) was used. All reactions were conducted under an atmosphere of dry nitrogen or argon. Fulvenes were stored under argon in the freezer at -30°C . Non-deuterated solvents were dried and distilled prior to use. All fulvenes in this study were prepared according to published procedures.^{21,22} Signal multiplicities in the NMR spectra are reported as follows: s-singlet, d-doublet, t-triplet, dd-doublet of doublets, dt-doublet of triplets, q-quartet, quin-quintuplet, sext-sextet, m-multiplet, br-broad.

Spectroscopic data for the synthesis of those fulvenes not found in literature are described below.

4.1.1. Fulvene 25. It was prepared from **38** (vide infra) by stirring with acetic anhydride in the presence of pyridine

for 48 h followed by aqueous work-up in 86% yield. ^1H NMR (CDCl_3 , TMS): δ 6.55 (m, 1H), 6.46 (m, 2H), 6.37 (t, $J=8.0$ Hz, 1H), 6.12 (dt, 1H), 4.95 (m, 1H), 2.55 (m, 2H), 2.02 (s, 3H), 1.8 (m, 2H), 1.55 (m, 2H), 1.33 (m, 2H), 0.9 (t, $J=7.2$ Hz, 3H); ^{13}C NMR (CDCl_3 , TMS): δ 170.8, 146.2, 141.5, 133.4, 131.1, 125.6, 118.9, 73.5, 36.3, 33.9, 27.1, 21.2, 18.7, 14.0 ppm. Anal. Calcd for $\text{C}_{14}\text{H}_{20}\text{O}_2$: C, 76.33; H, 9.15. Found: C, 76.28; H, 9.13.

4.1.2. Fulvene 28. Yield 78%. ^1H NMR (CDCl_3 , TMS): δ 6.6–6.4 (m, 4H), 6.2 (m, 1H), 4.1 (q, $J=7.5$ Hz, 2H), 2.54 (q, $J=7.5$ Hz, 2H), 2.30 (t, $J=7.2$ Hz, 2H), 1.65 (m, 2H), 1.50 (m, 2H), 1.4 (m, 2H), 1.25 (t, $J=7.5$ Hz, 3H); ^{13}C NMR (CDCl_3 , TMS): δ 173.7, 146.1, 142.8, 133.1, 130.8, 125.6, 119.1, 60.2, 34.2, 30.9, 29.1, 28.8, 24.8, 14.3 ppm. Anal. Calcd for $\text{C}_{14}\text{H}_{20}\text{O}_2$: C, 76.33; H, 9.15. Found: C, 76.31; H, 9.15.

4.1.3. Fulvene 38. Yield 49%. ^1H NMR (CDCl_3 , TMS): δ 6.53 (m, 2H), 6.45 (m, 1H), 6.40 (t, $J=7.5$ Hz, 1H), 6.2 (m, 1H), 3.63 (m, 1H), 2.65 (q, $J=7.5$ Hz, 2H), 1.67 (m, 2H), 1.44 (m, 2H), 1.30 (m, 4H), 0.9 (t, $J=7.5$ Hz, 3H); ^{13}C NMR (CDCl_3 , TMS): δ 146.2, 142.6, 133.2, 130.8, 125.6, 119.1, 71.3, 37.6, 36.9, 31.9, 27.5, 25.3, 22.7, 14.1 ppm. Anal. Calcd for $\text{C}_{12}\text{H}_{18}\text{O}$: C, 80.85; H, 10.18. Found: C, 80.82; H, 10.23.

4.1.4. Fulvene 50. Yield 39%. ^1H NMR (CDCl_3 , TMS): δ 6.75 (m, 2H), 6.5–6.2 (m, 5H), 5.4 (m, 2H), 2.3 (m, 2H), 2.2 (m, 2H), 2.05 (m, 2H), 1.0 (t, $J=7.5$ Hz, 3H) ppm. Anal. Calcd for $\text{C}_{14}\text{H}_{18}$: C, 90.26; H, 9.74. Found: C, 90.25; H, 9.73.

4.2. Typical procedure for the preparation of the saturated endoperoxides

A solution of 6,6-dimethylfulvene (1.06 g, 10 mmol) and 5 mg of TPP (*meso*-tetraphenylporphyrin) in 200 mL CH_2Cl_2 was cooled to -78°C in a flat Dewar containing dry ice–acetone. The mixture was stirred while being irradiated with a 250 W high-pressure sodium lamp for 3 h under an oxygen atmosphere (a balloon filled with oxygen served this purpose). Then the lamp was turned off, 8.7 g (45 mmol) of potassium azodicarboxylate was added to the mixture in small portions, a pressure-equalizing dropping funnel fitted with a drying tube containing Drierite was attached to the flask. A solution of 5.1 g (85 mmol) of acetic acid in 20 mL CH_2Cl_2 was added dropwise to the stirred slurry at -78°C , and the mixture was slowly warmed up to -35°C and stirred at this temperature for 1 h. The mixture was then slowly warmed up to 0°C for an additional 30 min. Then the salt was filtered by suction, the filtercake washed with cold CH_2Cl_2 , while keeping the filter flask in an ice bath. The filtrate was washed with saturated aqueous NaHCO_3 , dried over MgSO_4 , filtered into a 250 mL round-bottomed flask. An aliquot was concentrated at reduced pressure (caution: saturated fulvene endoperoxides—when neat—are potentially explosive!), and dissolved in CDCl_3 for NMR spectroscopy. The product was practically pure according to its ^1H NMR spectrum.⁵ For the DBU-catalyzed isomerizations, the endoperoxides need not be isolated.

4.3. Typical procedure for the DBU-catalyzed isomerizations

Three drops of DBU were added to a solution of endoperoxide **57**, obtained as described above, in 250 mL CH_2Cl_2 at 0°C , and the solution was stirred at room temperature for 12–15 h. Then the mixture was concentrated at reduced pressure, and the residue chromatographed on SiO_2 , eluting with hexane/ether (3:1).

4.3.1. 2-Isopropenyl-2-cyclopentenone (21). ^1H NMR (CDCl_3 , TMS): δ 7.5 (t, $J=3.0$ Hz, 1H), 6.07 (s, 1H), 5.16 (s, 1H), 2.60 (m, 2H), 2.47 (m, 2H), 1.94 (s, 3H); ^{13}C NMR (CDCl_3 , TMS): δ 208.5, 158.5, 143.7, 135.1, 117.3, 36.7, 26.3, 22.0 ppm. FTIR (film): 2973, 2927, 2855, 1710, 1453, 1387, 1262, 1177, 1038, 913, 802 cm^{-1} . Anal. Calcd for $\text{C}_8\text{H}_{10}\text{O}$: C, 78.65; H, 8.25. Found: C, 78.61; H, 8.24.

4.3.2. (E)-(2)-Pent-1-enyl-2-cyclopentenone (24). ^1H NMR (CDCl_3 , TMS): δ 7.4 (t, $J=3.0$ Hz, 1H), 6.6 (dt, $J=16.0, 7.0$ Hz, 1H), 6.1 (d, $J=16.0$ Hz, 1H), 2.6 (m, 2H), 2.45 (m, 2H), 2.1 (q, $J=7.0$ Hz, 2H), 1.50 (sext, $J=7.0$ Hz, 2H), 0.94 (t, $J=7.0$ Hz, 3H); ^{13}C NMR (CDCl_3 , TMS): δ 208.3, 156.5, 141.2, 135.7, 119.8, 35.57, 35.52, 26.2, 22.2, 13.7 ppm. Anal. Calcd for $\text{C}_{10}\text{H}_{14}\text{O}$: C, 79.96; H, 9.39. Found: C, 79.95; H, 9.38.

4.3.3. (E)-1-(5-Oxocyclopent-1-enyl)hept-1-en-4-yl acetate (27). ^1H NMR (CDCl_3 , TMS): δ 7.3 (br s, 1H), 6.45 (dt, $J=15.6, 7.2$ Hz, 1H), 6.0 (d, $J=15.6$ Hz, 1H), 4.85 (quin, $J=6.0$ Hz, 1H), 2.5 (m, 2H), 2.35 (m, 2H), 2.26 (m, 2H), 1.94 (s, 3H), 1.45 (m, 2H), 1.24 (m, 2H), 0.82 (t, $J=7.2$ Hz, 3H); ^{13}C NMR (CDCl_3 , TMS): δ 207.8, 170.4, 157.4, 157.2, 140.6, 129.9, 122.3, 72.9, 38.0, 35.3, 26.0, 20.1, 18.3, 13.7, 13.5 ppm. Anal. Calcd for $\text{C}_{14}\text{H}_{23}\text{O}_3$: C, 70.20; H, 9.69. Found: C, 70.17; H, 9.66.

4.3.4. (E)-Ethyl 7-(5-oxocyclopent-1-enyl)hept-6-enoate (30). ^1H NMR (CDCl_3 , TMS): δ 7.3 (t, $J=3$ Hz, 1H), 6.5 (dt, $J=16.0, 7.2$ Hz, 1H), 4.0 (q, $J=7.2$ Hz, 2H), 2.5 (m, 2H), 2.35 (m, 2H), 2.2 (m, 2H), 2.05 (m, 2H), 1.60 (m, 2H), 1.35 (m, 2H), 1.7 (t, $J=7.2$ Hz, 3H); ^{13}C NMR (CDCl_3 , TMS): δ 208.4, 173.6, 157.0, 141.0, 135.1, 120.1, 60.2, 35.6, 34.1, 33.1, 28.4, 26.3, 24.5, 14.2 ppm. Anal. Calcd for $\text{C}_{14}\text{H}_{20}\text{O}_3$: C, 70.20; H, 9.69. Found: C, 70.19; H, 9.66.

4.3.5. 2-Cycloheptenylcyclopent-2-enone (33). ^1H NMR (CDCl_3 , TMS): δ 7.4 (t, $J=3.0$ Hz, 1H), 6.7 (t, $J=6.6$ Hz, 1H), 2.56 (m, 2H), 2.45 (m, 2H), 2.37 (m, 2H), 2.25 (m, 2H), 1.8 (m, 2H), 1.55 (m, 4H); ^{13}C NMR (CDCl_3 , TMS): δ 208.2, 155.5, 145.0, 135.8, 133.0, 36.0, 32.2, 31.1, 28.4, 26.4, 26.3, 25.3 ppm. Anal. Calcd for $\text{C}_{12}\text{H}_{16}\text{O}$: C, 81.77; H, 9.15. Found: C, 81.77; H, 9.14.

4.3.6. (E)-5-(3-Hydroxybutan-2-ylidene)cyclopent-2-enone (36). ^1H NMR (CDCl_3 , TMS): δ 7.54 (m, 1H), 6.30 (m, 1H), 5.2 (br s, 1H, OH), 5.05 (q, $J=7.0$ Hz, 1H), 3.2 (s, 2H), 1.32 (d, $J=7.0$ Hz, 3H) ppm.

4.3.7. 2-(3-Hydroxybut-1-en-2-yl)cyclopent-2-enone (37). ^1H NMR (CDCl_3 , TMS): δ 7.7 (t, $J=3.0$ Hz, 1H), 5.65 (s,

1H), 5.4 (s, 1H), 4.5 (q, $J=6.6$ Hz, 1H), 3.9 (br s, 1H, OH), 2.7 (m, 2H), 2.5 (m, 2H), 1.26 (d, $J=6.6$ Hz, 3H); ^{13}C NMR (CDCl_3 , TMS, **36+37**): δ 209.1, 197.4, 160.7, 156.0, 156.4, 143.5, 142.5, 137.0, 128.5, 114.7, 68.9, 68.2, 35.2, 35.0, 26.3, 22.0, 21.0, 18.2 ppm.

4.3.8. 2-(5-Propyltetrahydrofuran-2-yl)cyclopent-2-enone (40, both epimers). ^1H NMR (CDCl_3 , TMS): δ 7.5 (t, $J=2.7$ Hz, 1H), 4.7 and 4.61 (m, 1H), 4.1 and 3.8 (m, 1H), 2.6 (m, 2H), 2.42 (m, 2H), 2.3–1.9 (m, 2H), 1.2–1.8 (m, 6H), 0.9 (m, 3H); ^{13}C NMR (CDCl_3 , TMS): δ 208.7, 208.5, 157.8, 157.5, 148.4, 148.2, 79.7, 79.4, 74.1, 73.8, 38.25, 38.16, 35.6, 32.0, 31.9, 31.4, 26.63, 26.6, 19.5, 14.3 ppm. Anal. Calcd for $\text{C}_{12}\text{H}_{18}\text{O}_2$: C, 74.19; H, 9.34. Found: C, 74.14; H, 9.33.

4.3.9. (E)-(2-Buta-1,3-dienyl)cyclopent-2-enone (43). ^1H NMR (CDCl_3 , TMS): δ 7.5 (t, $J=3.0$ Hz, 1H), 7.16 (dd, $J=17.0$, 10.5 Hz, 1H), 6.2–6.5 (m, 2H), 5.35 (d, $J=17.0$ Hz, 1H), 5.17 (d, $J=10.5$ Hz, 1H), 2.6 (m, 2H), 2.46 (m, 2H); ^{13}C NMR (CDCl_3 , TMS): δ 208.6, 159.0, 141.6, 138.0, 134.3, 123.0, 120.0, 36.3, 27.2 ppm. HRMS m/z calcd for $\text{C}_9\text{H}_{10}\text{O}$: 134.0732. Found: 134.0733.

4.3.10. (5E,7E)-4-Oxonona-5,7-dienal (44). ^1H NMR (CDCl_3 , TMS): δ 9.8 (s, 1H), 7.35 (m, 1H), 6.4 (t, $J=11.1$ Hz, 1H), 6.1 (m, 1H), 5.9 (d, $J=11.1$ Hz, 1H), 2.75 (m, AA'BB' pattern, 4H), 1.8 (dd, $J=6.6$, 1.0 Hz, 3H); ^{13}C NMR (CDCl_3 , TMS): δ 201.3, 198.7, 144.2, 141.5, 130.9, 127.8, 38.3, 33.2, 19.5 ppm. HRMS m/z calcd for $\text{C}_8\text{H}_{10}\text{O}_2$: 138.0681. Found: 138.0677.

4.3.11. (E)-3-Hydroxy-2-((E)-2-methylbut-2-enylidene)cyclopentanone (47). ^1H NMR (CDCl_3 , TMS): δ 7.0 (s, 1H), 6.2 (q, $J=7.2$ Hz, 1H), 5.2 (d, $J=4.8$ Hz, 1H), 2.6 (m, 2H), 3.3 (br s, 1H, OH), 2.23 (m, 2H), 2.0 (s, 3H), 1.8 (d, $J=7.2$ Hz, 3H) ppm. Anal. Calcd for $\text{C}_{10}\text{H}_{14}\text{O}_2$: C, 72.26; H, 8.49. Found: C, 72.35; H, 8.50.

4.3.12. (E)- and (Z)-2-(2-Methylbuta-1,3-dienyl)cyclopent-2-enone (48 and 49). ^1H NMR (CDCl_3 , TMS): δ 7.6 (t, $J=3.0$ Hz, 1H), 7.5 (t, $J=3.0$ Hz, 1H), 6.8 (dd, $J=17.1$, 10.8 Hz, 1H), 6.5 (dd, $J=17.4$, 10.8 Hz, 1H), 6.2 (s, 1H), 6.13 (s, 1H), 5.4 (dd, $J=17.4$, 10.8 Hz, 1H), 5.2 (dd, $J=17.1$, 10.8 Hz, 1H), 2.7 (m, 2H), 2.4 (m, 2H), 1.97 (s, 3H), 1.95 (s, 3H) ppm.

4.3.13. (E)-3-Hydroxy-2-((2E,6Z)-octa-2,6-dienylidene)cyclopentanone (52). ^1H NMR (CDCl_3 , TMS): δ 7.0 (d, $J=11.4$ Hz, 1H), 6.5 (m, 1H), 6.3 (m, 1H), 5.3 (m, 2H), 5.1 (m, 1H), 2.6 (m, 2H), 1.9–2.4 (m, 8H), 0.9 (t, $J=7.5$ Hz, 3H) ppm; ^{13}C NMR (CDCl_3 , TMS): δ 206.8, 149.4, 137.3, 137.2, 133.5, 128.0, 126.8, 70.2, 36.4, 34.3, 31.0, 26.9, 21.2, 15.0 ppm. Anal. Calcd for $\text{C}_{14}\text{H}_{20}\text{O}_2$: C, 76.33; H, 9.15. Found: C, 76.36; H, 9.12.

4.3.14. 2-((1E,6Z)-3-Hydroxyocta-1,6-dienyl)cyclopent-2-enone (53). ^1H NMR (CDCl_3 , TMS): δ 7.5 (t, $J=3.0$ Hz, 1H), 6.8 (dd, $J=16.0$, 8.0 Hz, 1H), 6.4 (d, $J=16$ Hz, 1H), 5.4 (m, 2H), 5.3 (m, 1H), 2.64 (m, 2H), 2.5 (m, 2H), 1.7–2.2 (m, 6H), 0.9 (t, $J=7.5$ Hz, 3H).

Anal. Calcd for $\text{C}_{14}\text{H}_{20}\text{O}_2$: C, 76.33; H, 9.15. Found: C, 76.29; H, 9.14.

4.4. (E)-1-Methyl-2-(pent-1-enyl)cyclopent-2-enol (54)

To a stirred solution of 1.00 g (6.66 mmol) of **24** in 50 mL of dry ether at -78 °C was added dropwise through a syringe 5.23 mL of an ethereal solution of methyllithium (1.4 M). The reaction mixture was allowed to warm up to room temperature and stirred for 1 h. A saturated aqueous solution of NH_4Cl solution (10 mL) was added dropwise, the layers separated, and the aqueous layers extracted twice with 10 mL portions of ether. The combined organic layers were washed twice with 10 mL of brine each, and the organic layer dried over anhydrous MgSO_4 . The solvent was removed at reduced pressure and the residue chromatographed on SiO_2 (3:1 hexanes/EtOAc), providing 0.8 g (72% yield) of **54**. ^1H NMR (CDCl_3 , TMS): δ 6.15 (dt, $J=16.2$, 6.6 Hz, 1H), 5.95 (d, $J=16.2$ Hz, 1H), 5.6 (narrow m, 1H), 2.4–1.9 (m, 6H), 1.45 (sext, $J=7.2$ Hz, 2H), 1.40 (s, 3H), 0.91 (t, $J=7.2$ Hz, 3H); ^{13}C NMR (CDCl_3 , TMS): δ 146.6, 132.1, 127.5, 123.2, 83.2, 42.5, 35.5, 28.5, 25.8, 22.5, 13.7 ppm.

4.5. (E)-3-Methyl-2-(pent-1-enyl)cyclopent-2-enone (55)

A solution of 1.0 g (6 mmol) of the tertiary alcohol **54** in 5 mL of CH_2Cl_2 was added dropwise to a stirred suspension of 2.58 g (12.0 mmol) of pyridinium chlorochromate (PCC) in 20 mL CH_2Cl_2 at 0 °C. The mixture was stirred at room temperature for 1 h, and was diluted with 25 mL of ether. The ethereal solution was decanted from the solid, which was washed with three 20 mL portions of ether. The combined ethereal phases were washed successively with two 25 mL portions of 5% NaOH, 5% HCl, and two 10 mL portions of saturated aqueous NaHCO_3 , and dried over MgSO_4 . The solvent was removed at reduced pressure and the residue purified by column chromatography on SiO_2 , eluting with 3:1 hexanes/EtOAc, to give 0.74 g (69% yield) of **55** as a pale yellow oil. ^1H NMR (CDCl_3 , TMS): δ 6.7 (dt, $J=16.0$, 7.2 Hz, 1H), 6.06 (d, $J=16$ Hz, 1H), 2.55 (m, 2H), 2.35 (m, 2H), 2.12 (s, 3H), 2.0 (m, 2H), 1.5 (m, 2H), 0.9 (t, $J=7.2$ Hz, 3H). These data are almost identical to those reported for **55**.¹³

4.5.1. 4-Hydroxy-2-(propen-1-en-2-yl)cyclopent-2-enone (59). ^1H NMR (CDCl_3 , TMS): δ 7.3 (d, 1H), 6.1 (s, 1H), 5.2 (s, 1H), 4.9 (m, 1H), 3.4 (br, OH), 2.9 (dd, B part of an ABX system, $^2J=18.6$ Hz, 1H), 2.38 (d, $^2J=18.6$ Hz, 1H), 1.93 (s, 3H); ^{13}C NMR (CDCl_3 , TMS): δ 204.9, 156.2, 144.3, 134.4, 119.9, 68.0, 48.9, 22.5 ppm.

4.6. 3-Methyl-2-pentylcyclopent-2-enone (dihydrojasmane, 56)

Ketone **55** (0.5 g, 3.0 mmol) was dissolved in 10 mL of methanol, 2% PtO_2 was added, and the mixture was hydrogenated at atmospheric pressure at room temperature. Hydrogenation was interrupted after the uptake of 1 equiv of H_2 , and the catalyst filtered off, the residue concentrated at reduced pressure to give **56** in quantitative yield. Its physical and spectroscopic data were identical in all respects with the reported values in literature.

Acknowledgements

This work was supported by funds from the National Science Foundation (CHE-9729001), the National Institutes of Health, MBRS-SCORE Program-NIGMS (Grant No. GM52588), and in part from a grant (P20 MD) from the Research Infrastructure in Minority Institutions Program, NCMHD, NIH.

References and notes

1. *Singlet Oxygen*; Wasserman, H. H., Murray, R. W., Eds.; Academic: New York, NY, 1979.
2. Balci, M. *Chem. Rev.* **1981**, *81*, 91.
3. Kornblum, N.; De La Mare, H. E. *J. Am. Chem. Soc.* **1951**, *73*, 880.
4. Zagorski, M. G.; Salomon, R. G. *J. Am. Chem. Soc.* **1980**, *102*, 2501.
5. Adam, W.; Erden, I. *Angew. Chem.* **1978**, *90*, 223; *Angew. Chem., Int. Ed. Engl.* **1978**, *17*, 210.
6. Erden, I.; Amputch, M. *Tetrahedron Lett.* **1987**, *28*, 3779.
7. Erden, I.; Drummond, J.; Alstad, R.; Xu, F. *Tetrahedron Lett.* **1993**, *34*, 1255.
8. Erden, I.; Drummond, J.; Alstad, R.; Xu, F. *Tetrahedron Lett.* **1993**, *34*, 2291.
9. Erden, I.; Xu, F.; Drummond, J.; Alstad, R. *J. Org. Chem.* **1993**, *58*, 3611.
10. Erden, I.; Xu, F.; Cao, W. *Angew. Chem.* **1997**, *109*, 1557; *Angew. Chem., Int. Ed.* **1997**, *36*, 1516.
11. Ishihara, H.; Inomata, K.; Mukaiyama, T. *Chem. Lett.* **1975**, 531.
12. Funel, J.-A.; Prunet, J. *J. Org. Chem.* **2004**, *69*, 4555.
13. Shimada, J.; Hashimoto, K.; Kim, B. H.; Nakamura, E.; Kuwajima, I. *J. Am. Chem. Soc.* **1984**, *106*, 1759; Nakamura, E.; Shimada, J.; Kuwajima, I. *J. Chem. Soc., Chem. Commun.* **1983**, 498.
14. Stetter, H.; Leinen, H. T. *Chem. Ber.* **1983**, *116*, 254.
15. Johnson, C. R.; Adams, J. P.; Braun, M. P.; Senayake, C. B. W. *Tetrahedron Lett.* **1992**, *33*, 919.
16. For a recent synthesis of oudenone, see: Flynn, B. L.; Silveira, C. C.; de Meijere, A. *Synlett* **1995**, 812.
17. For a review on Jasmonoids, see: Ho, T.-L. *Synth. Commun.* **1974**, *4*, 265.
18. Dauben, W. G.; Michno, D. M. *J. Org. Chem.* **1977**, *42*, 682.
19. Seo, J.; Fain, H.; Blanc, J.-B.; Montgomery, J. *J. Org. Chem.* **1999**, *64*, 6060.
20. Though 2(3*H*)-oxepinones are the sole products from thermal isomerizations of unsaturated fulvene endoperoxides in aprotic, non-nucleophilic solvents, **57** has been reported to give rise to considerable amounts of **58** in methanol; see Refs. **23** and **24**.
21. Stone, K. J.; Little, R. D. *J. Org. Chem.* **1984**, *49*, 1849.
22. Erden, I.; Xu, F.; Sadoun, A.; Smith, W.; Sheff, G.; Ossun, M. *J. Org. Chem.* **1995**, *60*, 813.
23. Harada, N.; Suzuki, S.; Uda, H.; Ueno, H. *J. Am. Chem. Soc.* **1971**, *94*, 1777; Harada, N.; Uda, H.; Ueno, H.; Utsumi, S. *Chem. Lett.* **1973**, 1173.
24. (a) Skorianetz, W.; Schulte-Elte, K. H.; Ohloff, G. *Angew. Chem.* **1972**, *84*, 3111; *Angew. Chem., Int. Ed. Engl.* **1972**, *11*, 330; (b) Skorianetz, W.; Schulte-Elte, K. H.; Ohloff, G. *Helv. Chim. Acta* **1971**, *54*, 1913.

A comparison of hydrogen bonding solvent effects on the singlet oxygen reactions of allyl and vinyl sulfides, sulfoxides, and sulfones

Kristina L. Stensaas,^{*} Brent V. McCarty, Natacha M. Touchette and James B. Brock

Department of Chemistry, Millsaps College, 1701 N. State Street, Jackson, MS 39210-0001, United States

Received 1 June 2006; revised 11 August 2006; accepted 14 August 2006

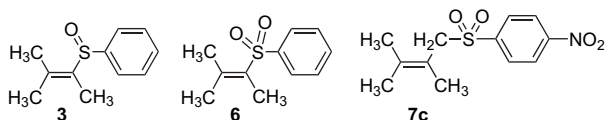
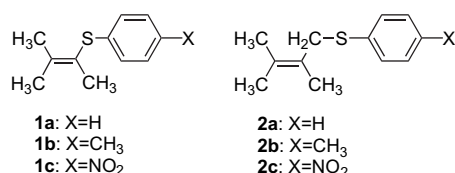
Available online 2 October 2006

Abstract—The singlet oxygen ($^1\Delta_g$) photooxidations of 2-methyl-3-phenylthio-2-butene (**1a**), 1-[(4-nitrophenyl)thio]-2,3-dimethyl-2-butene (**2c**), 2-methyl-3-phenylsulfinyl-2-butene (**3**), 2-methyl-3-phenylsulfonyl-2-butene (**6**), and 1-[(4-nitrophenyl)sulfonyl]-2,3-dimethyl-2-butene (**7c**) were conducted in the following deuterated solvents: acetonitrile, benzene, chloroform, methanol, or methanol/water mixture. In each case the ene allylic hydroperoxide products and/or the [2+2] cycloaddition products were quantified and inspected for possible hydrogen bonding induced differences in product selectivity and regiochemistry. After comparison to literature values for related substrates, the results indicate that only photooxidations of vinyl sulfides are susceptible to hydrogen bonding solvent effects.

© 2006 Elsevier Ltd. All rights reserved.

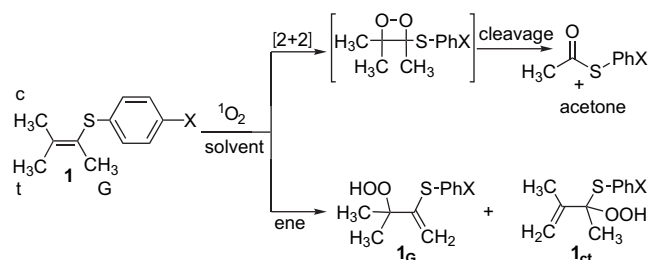
1. Introduction

Hydrogen bonding and specifically aqueous solvent effects have recently been reported^{1,2} for the singlet oxygen ene reactions of α,β -unsaturated esters, acids, and sodium salts. As part of our continued interest in hydrogen bonding solvent effects on the singlet oxygen reactions of substituted alkenes, we have conducted a comparative study of the effects of hydrogen bonding solvents on the photooxidations of 2-methyl-3-phenylthio-2-butene (**1a**), 1-[(4-nitrophenyl)thio]-2,3-dimethyl-2-butene (**2c**), 2-methyl-3-phenylsulfinyl-2-butene (**3**), 2-methyl-3-phenylsulfonyl-2-butene (**6**), and 1-[(4-nitrophenyl)sulfonyl]-2,3-dimethyl-2-butene (**7c**).



The possible reaction modes available to sulfides **1** and **2** certainly make these substituted substrates interesting to study. Vinyl sulfide **1** can conceivably undergo reaction with singlet

oxygen at the alkene double bond via the ene reaction³ to form regioisomeric allylic hydroperoxides **1_G** and **1_{ct}** or a [2+2] cycloaddition to form the dioxetane product (Scheme 1).⁴ Oxidation at sulfur to form a sulfoxide is also a possibility. In conjunction with literature values for previous photooxidations of vinyl sulfides,⁴ allyl sulfides,^{5,6} allyl sulfoxides,^{5,6,14} and allyl sulfones⁶ conducted in a variety of solvents, we will systematically investigate the possibility of hydrogen bonding induced changes in product formation, product distributions, and implications for the mechanisms of these reactions.



2. Results and discussion

2.1. Singlet oxygen photooxidations of vinyl and allyl sulfides

In a typical experiment, 2-methyl-3-phenylthio-2-butene (**1a**, 0.5 M) in benzene-*d*₆ was irradiated at 0 °C with a 500 W tungsten–halogen lamp. Tetraphenylporphine (TPP, 2 × 10^{−4} M) was used as the photosensitizer and dry oxygen

Keywords: Singlet oxygen; Ene reactions; Hydrogen bonding; Sulfides; Sulfoxides; Sulfones.

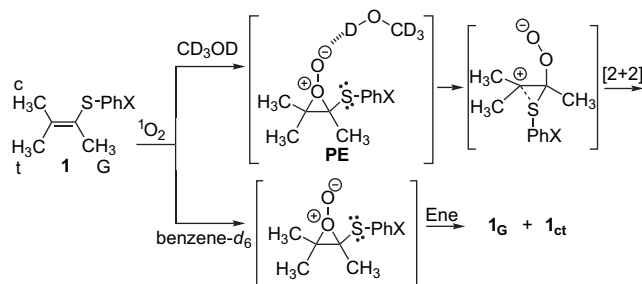
^{*} Corresponding author. Tel.: +1 601 974 1402; fax: +1 601 974 1401; e-mail: stenskl@millsaps.edu

was continuously purged through the system. The photo-oxidation products and their distributions were determined using ^1H NMR. Table 1 lists the quantified products of vinyl sulfides **1a–c** and allyl sulfides **2a–c** in various deuterated solvents.

The results indicate that for **1a** reaction at 0°C occurs at the alkene double bond producing exclusively [2+2] cycloaddition products in CD_3OD and a mixture of ene product and [2+2] product in benzene- d_6 . Clearly a solvent effect is occurring, but initially it was unclear whether hydrogen bonding was involved because Adam⁴ and co-workers previously reported that in CDCl_3 at -25°C only [2+2] products were formed with **1a** and **1b** (Table 1). Furthermore, they reported that the electronic character of the *p*-substituent influences the mode selectivity for vinyl sulfides. Photooxidation of **1c** containing the electron-withdrawing NO_2 group resulted in 70% ene reaction and 30% [2+2] products.

Ando⁷ and co-workers previously suggested that the mode selectivity for vinyl sulfides depends on several factors including solvent and temperature. Protic solvents and low temperatures appear to accelerate the dioxetane mode for vinyl sulfides. Ando indicated that protic solvents would stabilize the proposed perepoxide intermediate (**PE** Scheme 2) by hydrogen bonding with the negatively charged pendant oxygen, thereby allowing the sulfur to attack and form the zwitterion intermediate, which would lead to the [2+2] product. Aprotic solvents would not stabilize **PE** and therefore the ene mode would be expected to predominate.

The different mode selectivity observed in benzene- d_6 and CDCl_3 for **1a** could be attributed to the different temperatures utilized to run these reactions, 0°C in benzene- d_6 and -25°C in CDCl_3 . Again, lower temperatures have been shown⁷ to favor the dioxetane mode. However, as a reviewer indicated, the fact that such a substantial temperature dependence is observed in aprotic solvents indicates that the structure of the transition state leading to products is also important.⁸ Therefore, another contributing factor to the mode selectivity could be the activation entropy leading to a transition state, which resembles the perepoxide. Clearly the structure and subsequent stabilization of the perepoxide is very important in determining the reaction mode with vinyl sulfides.



Scheme 2. Proposed hydrogen bonding stabilization of perepoxide **PE**.

It is interesting to note that when the ene mode does operate with **1** the well-established phenomenon of geminal^{9,10} selectivity, preferential abstraction of the allylic hydrogen geminal to the sulfur group, does not determine the regiochemistry. In benzene- d_6 , 44% cis+trans hydrogen abstraction was observed with **1a** and in CDCl_3 Adam and co-workers reported 60% cis+trans hydrogen abstraction with **1c**. Perhaps this regiochemistry can be explained by a favorable interaction between the incoming electrophilic singlet oxygen and the electron rich sulfur. Frimer et al.¹¹ suggested the importance of an initial interaction between the incoming oxygen and the enol ether in their study of the photooxidations of 2,3-dihydro- γ -pyrans. Sulfur may be inducing the same type of directing 'cis' effect with vinyl sulfides **1**.

Geminal selectivity is slightly favored with allyl sulfides **2**. These substrates appear to be unaffected by polarity or hydrogen bonding solvent effects as the ene product distributions are fairly stable over a wide range of dielectric constants. Under our conditions, neither the [2+2] cycloaddition nor sulfide oxidation was competitive with the ene reaction for **2c**. Methylene hydrogen abstraction was not observed either. Clennan¹² previously reported that only at temperatures below -29°C does the oxidation at sulfur become important for **2b**.

Geminal selectivity has been reported⁵ as preferential for the ene reactions of allylic sulfides, sulfoxides, and sulfones. Several reasons have been suggested for this preference including: (1) electronic repulsions between the lone pairs on the sulfur substituent and the negatively charged pendant

Table 1. Ene product ratios resulting from geminal (G)/cis+trans (ct) hydrogen abstraction or [2+2] cycloaddition products for vinyl sulfides **1a–c** and allylic sulfides **2a–c** where X=H (a), CH_3 (b), and NO_2 (c)

Solvent	Vinyl sulfide 1			Allylic sulfide 2		
	H (1a)	CH_3 (1b)	NO_2 (1c)	H (2a)	CH_3 (2b)	NO_2 (2c)
Benzene- d_6	0/44, 56	—	—	—	—	—
CDCl_3	100 ^a	—	10/60, 30 ^b	—	—	56/44
Acetone- d_6	—	—	—	^d	52/48 ^{b,c}	52/48 ^b
CD_3OD	100	—	—	—	—	54/46
CD_3CN	—	—	—	—	—	54/46

^a Ref. 4.

^b Ref. 5.

^c Ref. 6.

^d Ref. 6. Note only ene products form.

oxygen, which favor the perepoxide intermediate **A** (Fig. 1) that places these groups on opposite sides, and (2) substituted tetramethylethylenes exist in conformations where the geminal hydrogens achieve the perpendicular geometry necessary for abstraction easier than the cis/trans allylic hydrogens.

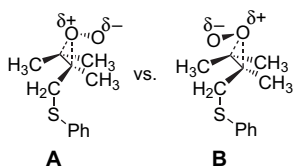


Figure 1. Perepoxide **A** is preferred for allyl sulfides, sulfoxides, and sulfones.

2.2. Singlet oxygen photooxidations of vinyl and allyl sulfoxides

The photooxidation products of vinyl sulfoxide **3**, allyl sulfonides **4a–c**, and the related α,β -unsaturated ester **5d** and acid **5e** are reported in Table 2. Under our conditions only the geminal ene product was formed during photooxidation of **3** in benzene- d_6 ¹³ and CD₃OD. Solvent effects have previously² been reported for **5d** and **5e**; specifically, as the polarity of the solvent increases, geminal selectivity decreases. It has been suggested that the perepoxide leading to **5_G** is somewhat less stabilized in a polar solvent. Therefore, we were surprised to discover that vinyl sulfoxide **3** only forms geminal product, regardless of solvent polarity. Clearly perepoxide **I** leading to **3_G** is more stabilized than the perepoxide intermediate leading to **5_G** (Fig. 2). These results appear to indicate that hydrogen bonding with the solvent is not important in determining the ene product ratio for **3** because only one ene product is formed regardless of solvent choice.

Clennan⁶ and Chen previously reported that the ene product distribution of allyl sulfoxides **4a–c** did not show solvent effects or electronic effects due to the *p*-substituent, and

Table 2. Ene product ratios resulting from geminal (**G**)/cis+trans (**ct**) hydrogen abstraction for vinyl sulfoxide **3**, allylic sulfoxides **4a–c** where X=H (**a**), CH₃ (**b**), and NO₂ (**c**), and **5d,e** where Y=OCH₃ (**d**) and OH (**e**)

Solvent	ϵ^a	Allylic sulfoxides 4			Unsaturated sulfonides 5	
		H (4a)	CH ₃ (4b)	NO ₂ (4c)	OCH ₃ (5d)	OH (5e)
Benzene- d_6	2.3	—	—	—	89/11 ^f	100/0 ^f
CDCl ₃	4.8	—	75/25 ^d	—	—	—
Acetone- d_6	20.7	74/26 ^c	75/25 ^c	75/25 ^c	—	—
CD ₃ OD	33	100/0	75/25 ^d	—	85/15 ^f	91/9 ^f
CD ₃ CN	36.6	—	—	—	83/17 ^f	86/14 ^f
CD ₃ OD/D ₂ O ^b	51.8	—	—	—	82/18 ^f	90/10 ^f

^a Dielectric constants (ϵ) were taken from Ref. 16.

^b A mixture of 90% CD₃OD and 10% D₂O.

^c Ref. 5.

^d Ref. 6.

^e Ref. 14.

^f Ref. 1.

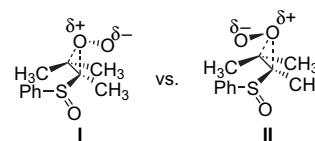


Figure 2. Perepoxide **I** is preferred for vinyl sulfoxides.

only minimal temperature effects were noted with **4b**; at -77 °C a 75/25 ratio of **G/ct** was reported but at 20 °C a 67/33 ratio of **G/ct** resulted. It is clear that geminal selectivity is overwhelming with all of these substrates.

2.3. Singlet oxygen photooxidations of vinyl and allyl sulfones

Table 3 lists the photooxidation products for vinyl sulfone **6** and allyl sulfones **7a–c**. Under our conditions only ene products were formed from photooxidation of **6** and **7c**. Again, overwhelming geminal selectivity was observed. Neither the *p*-substituent nor choice of solvent affected the product ratios for **7a–c**. Clennan⁵ suggested that the conformational arrangement of the geminal hydrogens in the allylic substrates favors the abstraction of the geminal hydrogens.

Table 3. Ene product ratios resulting from geminal (**G**)/cis+trans (**ct**) hydrogen abstraction for vinyl sulfone **6** and allylic sulfones **7a–c** where X=H (**a**), CH₃ (**b**), and NO₂ (**c**)

Solvent	Allylic sulfones 7		
	H (7a)	CH ₃ (7b)	NO ₂ (7c)
CDCl ₃	—	—	81/19
Acetone- d_6	83/17 ^b	83/17 ^b	—
CD ₃ OD	100/0	—	73/27
CD ₃ OD/D ₂ O ^a	100/0	—	—

^a Solvent mixtures of CD₃OD/D₂O (95/5 and 90/10) were used.

^b Ref. 6.

3. Conclusions

Several interesting conclusions can be drawn from this work:

- (1) The singlet oxygen mode selectivity for vinyl sulfides are susceptible to a combination of factors including the solvent, reaction temperature, and the electronic character of the *p*-substituent. In particular, hydrogen bonding stabilization of the peroxide by a protic solvent favors formation of the dioxetane.
- (2) The overall trend for geminal selectivity in allyl sulfides, sulfoxides, and sulfones increases with increasing size of the allyl substituent; allyl sulfide **2b** produced 52%, allyl sulfoxide **4b** produced 75%, and allyl sulfone **7b** produced 83% of the ene hydroperoxide resulting from geminal hydrogen abstraction.
- (3) Vinyl sulfoxides and sulfones show no solvent effects, which is unexpected when compared to their solvent dependent α,β -unsaturated ester and acid counterparts.

4. Experimental

4.1. General

¹H NMR spectra were recorded on a 60 MHz Varian EM 360-L spectrometer and referenced internally to tetramethylsilane. Melting points were taken in open capillaries on a Mel-Temp II apparatus and are uncorrected. Thin layer chromatography was carried out on 250 μ m layer silica gel flexible plates and column chromatography was carried out with SilicAR CC-4 silica gel obtained from Mallinckrodt. Methyl isopropyl ketone and thiophenol were obtained from Eastman and used as received. Anhydrous HCl, *m*-chloroperoxybenzoic acid, 2,3-dimethyl-2-butene, *N*-bromosuccinimide, benzoyl peroxide, and *p*-nitrothiophenol were purchased from Aldrich and used without further purification. Hydrogen peroxide (30%) and dichloromethane were obtained from Fisher and used as received. Sodium methoxide from Mallinckrodt and formic acid from JT Baker were also used without further purification. Deuterated solvents (benzene, methanol, chloroform, acetonitrile, and deuterium oxide) and photosensitizers (rose bengal, methylene blue, and tetraphenylporphine) were used as received.

4.1.1. 2-Methyl-3-phenylthio-2-butene (1a). It was synthesized according to literature procedures¹⁵ from the reaction of methyl isopropyl ketone (6.55 g, 0.076 mol) and thiophenol (6.06 g, 0.055 mol). After the reaction was cooled to 0 °C, anhydrous HCl was bubbled through the system as thiophenol (10.69 g, 0.097 mol) was added from an addition funnel dropwise for 40 min. After the solution warmed to room temperature, the excess ketone was distilled off at atmospheric pressure (bp 94–95 °C). The crude product then underwent reduced pressure distillation to yield 6 mL of distillate; this was then dissolved in ether, extracted with 2 M NaOH to remove excess thiophenol, and dried with NaSO₄. Lit. bp: 49.5–50 °C (0.03 mm Hg), ¹H NMR (C₆D₆): δ 1.6 (s, 3H), 1.95 (s, 3H), 2.01 (s, 3H), 7.05–7.35 (m, 5H).

4.1.2. 2-Methyl-3-phenylsulfinyl-2-butene (3). Compound **1a** (1.77 g, 0.0099 mol) was oxidized with 30% hydrogen

peroxide (1.127 g, 0.0374 mol) by literature procedures¹⁵ in methanol (39.76 mL) with a formic acid catalyst (0.994 mL). The reaction mixture was extracted with 50 mL of distilled water and 35 mL fractions of ethyl ether, and the organic layer was dried with MgSO₄. Compound **3** was recrystallized with petroleum ether. Lit. mp: 75–76.5 °C, ¹H NMR (CDCl₃) δ 1.6 (s, 3H), 1.8 (s, 3H), 2.2 (s, 3H), 7.2–7.5 (m, 5H).

4.1.3. 2-Methyl-3-phenylsulfonyl-2-butene (6). It was synthesized by the oxidation of **1a** (1 g, 0.0056 mol) with 2.5 molar equiv of *meta*-chloroperoxybenzoic acid (2.42 g, 0.014 mol). Compound **1a** was dissolved in dichloromethane with 1 equiv of sodium bicarbonate. *m*-CPBA was dissolved in dichloromethane in an addition funnel and added dropwise to the sulfide solution for 15 min. The solution was then stirred and cooled over ice for an additional 45 min. The product was washed with 2 \times 20 mL portions of distilled water, 3 \times 20 mL portions of 2 M NaOH, and 20 mL portions of distilled water. The organic layer was dried over MgSO₄ and purified on a silica gel column using 7:3 hexane/ethyl acetate ¹H NMR (CDCl₃) δ 1.93 (s, 3H), 2.08 (s, 3H), 2.28 (s, 3H), 7.4–8.0 (m, 5H).

4.1.4. 1-Bromo-2,3-dimethyl-2-butene. It was prepared using literature procedures¹⁴ by the reaction of 2,3-dimethyl-2-butene (40.4 mmol) and *N*-bromosuccinimide (41.1 mmol) in a solution of carbon tetrachloride (25 mL) with benzoyl peroxide (0.129 mol). The product mixture was distilled under reduced pressure at 65 °C (24 mm Hg). ¹H NMR (CDCl₃) δ 1.7 (s, 3H), 1.77 (s, 6H), 4.08 (s, 2H).

4.1.5. 1-[(4-Nitrophenyl)thio]-2,3-dimethyl-2-butene (2c). It was synthesized from the reaction⁶ of 1-bromo-2,3-dimethyl-2-butene (1.0 g, 6.13 mmol) with *p*-nitrothiophenol (1.18 g, 6.20 mmol) in a solution of absolute ethanol (45 mL) and sodium methoxide (0.335 g, 6.22 mmol). The product was extracted using diethyl ether and water, dried with MgSO₄, and purified through recrystallization from hexanes. Mp: 67–69 °C (lit. mp: 67–68 °C), ¹H NMR (CD₃OD) δ 1.65–2.0 (m, 9H), 3.85 (s, 2H), 7.6 (d, 2H, *J*=9 Hz), 8.3 (d, 2H, *J*=9 Hz).

4.1.6. 1-[(4-Nitrophenyl)sulfonyl]-2,3-dimethyl-2-butene (7c). Compound **2c** (0.217 mmol) was oxidized with 2 equiv of *m*-chloroperoxybenzoic acid (0.434 mmol) in a solution of dichloromethane (5 mL) as per literature procedure.¹⁴ The *m*-CPBA was extracted using saturated NaHCO₃, the products were washed with ether and a saturated NaCl solution, and dried with MgSO₄ before undergoing reduced pressure distillation to remove the solvent. ¹H NMR (CD₃OD) δ 1.2–1.65 (m, 9H), 3.9 (s, 2H), 8.05 (d, 2H, *J*=6 Hz), 8.35 (d, 2H, *J*=6 Hz).

4.2. Singlet oxygen photooxidation procedure for 1a

Samples of **1a** (0.5 M) immersed in an ice bath were photooxidized in benzene-*d*₆ using 2 \times 10⁻⁴ M tetraphenylporphine (TPP) as the photosensitizer and a sodium nitrite filter solution (75 g NaNO₂/100 mL H₂O). After 4 h of photooxidation, all the starting material reacted to form either **1a_{ct}** [¹H NMR (C₆D₆) δ 1.63 (s, 3H), 1.77 (s, 3H), 5.35 (s, 1H, *J*=8 Hz), 5.47 (s, 1H, *J*=8 Hz), 6.92–7.57 (m, 5H)] or

the cleavage products (Scheme 1) of the dioxetane, the thioester [$^1\text{H NMR}$ (C_6D_6) δ 1.12 (s, 3H)] and acetone [$^1\text{H NMR}$ (C_6D_6) δ 1.93 (s, 6H)].

Compound **1a** was completely converted in 12 h by the photooxidation in CD_3OD using 2×10^{-4} M methylene blue as the photosensitizer and a sodium dichromate filter solution (50.25 g $\text{Na}_2\text{Cr}_2\text{O}_7/50$ mL H_2O). The only products observed were the cleavage products of the dioxetane (Scheme 1) the thioester [$^1\text{H NMR}$ (CD_3OD) δ 1.32 (s, 3H)] and acetone [$^1\text{H NMR}$ (CD_3OD) δ 2.5 (s, 6H)].

4.3. Singlet oxygen photooxidation procedure for **3**

Samples of **3** (0.5 M) immersed in an ice bath were photooxidized in both benzene- d_6 using 2×10^{-4} M tetraphenylporphine (TPP) photosensitizer and a sodium nitrite filter solution (75 g $\text{NaNO}_2/100$ mL H_2O). After 2 h of reaction time, **3_G** was the only product. $^1\text{H NMR}$ (C_6D_6) δ 1.0 (s, 3H), 1.32 (s, 3H), 5.39 (s, 1H), 5.77 (s, 1H), 7.0–7.7 (m, 5H), 9.67 (s, 1H).

For the photooxidation of **3** in CD_3OD , a 2×10^{-4} M solution of methylene blue photosensitizer and a sodium dichromate filter solution (50.25 g $\text{Na}_2\text{Cr}_2\text{O}_7/50$ mL H_2O) were used. After 6 h of photooxidation, the only product was **3_G**. $^1\text{H NMR}$ (CD_3OD) δ 1.02 (s, 3H), 1.42 (s, 3H), 6.04 (s, 1H), 6.25 (s, 1H), 7.23–7.8 (m, 5H).

4.4. Singlet oxygen photooxidation procedure for **6**

Samples of **6** (0.25 M) immersed in an ice bath were photooxidized in deuterated methanol and 95/5 and 90/10 mixtures of CD_3OD and D_2O using a 5×10^{-4} M solution of rose bengal photosensitizer and a potassium dichromate filter solution (1.0001 g $\text{K}_2\text{Cr}_2\text{O}_7/200$ mL H_2O). After 18 h of photooxidation, **6_G** formed as the only product. $^1\text{H NMR}$ (CD_3OD) δ 1.42 (s, 6H), 6.4 (s, 1H), 6.62 (s, 1H).

4.5. Singlet oxygen photooxidation procedures for **2c** and **7c**

Compound **2c** was photooxidized in deuterated chloroform, acetonitrile, and methanol, while **7c** was reacted in both deuterated chloroform and methanol. A 2×10^{-4} M solution of methylene blue photosensitizer and a 0.2% w/v filter solution of rhodamine B were used in these photooxidations and all were conducted in an ice bath. Ratios of **2c_G**/**2c_{ct}** and **7c_G**/**7c_{ct}** were produced for each reaction.

2c_G: $^1\text{H NMR}$ (CD_3CN) δ 1.40 (s, 6H), 3.9 (s, 2H), 5.3 (s, 1H), 5.4 (s, 1H), 7.5 (d, 2H), 8.2 (d, 2H), 9.3 (s, 1H).

2c_{ct}: $^1\text{H NMR}$ (CD_3CN) δ 1.42 (s, 3H), 1.80 (s, 3H), 3.5 (s, 2H), 5.1 (s, 2H), 7.5 (d, 2H), 8.2 (d, 2H), 9.3 (s, 1H).

7c_G: $^1\text{H NMR}$ (CD_3OD) δ 1.26 (s, 6H), 4.18 (s, 2H), 5.5 (s, 2H), 8.1 (d, 2H), 8.4 (d, 2H).

7c_{ct}: $^1\text{H NMR}$ (CD_3OD) δ 1.57 (s, 3H), 1.72 (s, 3H), 3.84 (s, 2H), 4.80 (s, 2H), 8.1 (d, 2H), 8.4 (d, 2H).

Acknowledgements

We thank the Donors of The Petroleum Research Fund, administered by the American Chemical Society, for their generous support of this research. We also thank Millsaps College and the Wiener Fellowship program for their support.

References and notes

- Stensaas, K.; Bajaj, A.; Al-Turk, A. *Tetrahedron Lett.* **2005**, *46*, 715–718.
- Stensaas, K.; Payne, J.; Ivancic, A.; Bajaj, A.; Al-Turk, A. *Tetrahedron Lett.* **2002**, *43*, 25–27.
- Stratakis, M.; Orfanopoulos, M. *Tetrahedron* **2000**, *56*, 1595–1615.
- Adam, W.; Kumar, A.; Saha-Moller, C. *Tetrahedron Lett.* **1995**, *36*, 7853–7854.
- Clennan, E.; Chen, X. *J. Org. Chem.* **1988**, *53*, 3124–3125.
- Clennan, E.; Chen, X. *J. Am. Chem. Soc.* **1989**, *111*, 8212–8218.
- Ando, W.; Watanabe, K.; Suzuki, J.; Migita, T. *J. Am. Chem. Soc.* **1974**, *96*, 6766–6768.
- Recent computational studies conducted by Singleton and Houk suggest that the ene reaction may proceed through a two-step no intermediate process involving a transition state with the symmetry of a peroxide rather than a discrete peroxide intermediate. Singleton, D. A.; Hang, C.; Szymanski, M. J.; Meyer, M. P.; Leach, A. G.; Kuwata, K. T.; Chen, J. S.; Greer, A.; Foote, C. S.; Houk, K. N. *J. Am. Chem. Soc.* **2003**, *125*, 1319–1328.
- Orfanopoulos, M.; Foote, C. *Tetrahedron Lett.* **1985**, 5991–5994.
- Adam, W.; Richter, M. *Tetrahedron Lett.* **1993**, *34*, 8423–8426.
- Frimer, A.; Bartlett, P.; Boschung, A.; Jewett, J. *J. Am. Chem. Soc.* **1977**, *99*, 7977–7986.
- Clennan reported that at <10% conversion, only 68% ene reaction occurs and 32% sulfur oxidation occurs. Sulfur oxidation becomes unimportant at temperatures above -29°C . See Ref. 6.
- Akasaka, T.; Misawa, Y.; Goto, M.; Ando, W. *Tetrahedron* **1989**, *45*, 6657–6666. This reference reported the same result as ours at 15°C .
- Clennan, E.; Chen, X. *J. Am. Chem. Soc.* **1989**, *111*, 5787–5792.
- Parham, W.; Edwards, L. *J. Org. Chem.* **1968**, *33*, 4150–4154.
- CRC Handbook of Chemistry and Physics*, 81st ed.; Lide, D. R., Ed.; Chemical Rubber: Boca Raton, FL, 2000.

Synthesis of α,β -unsaturated γ -lactones via photooxygenation of 2,3-dihydrofurans followed by ferrous ion-catalyzed *gem*-dehydration

Yu-Zhe Chen, Li-Zhu Wu,* Ming-Li Peng, Dong Zhang, Li-Ping Zhang and Chen-Ho Tung*

Technical Institute of Physics and Chemistry, Chinese Academy of Sciences, Beijing 100080, China

Received 24 June 2006; revised 14 August 2006; accepted 15 August 2006

Available online 25 September 2006

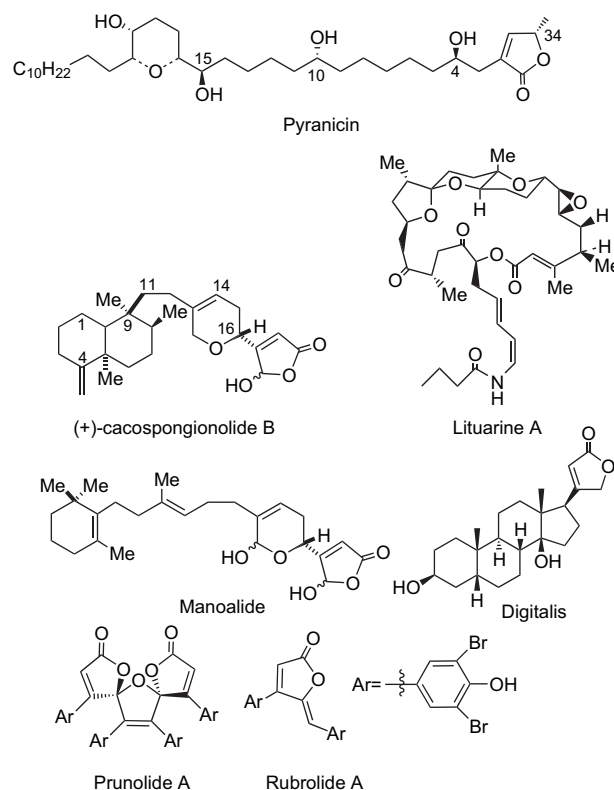
This paper is dedicated to Professor Xihui Jiang on the occasion of his 80th birthday

Abstract—Several alkyl and aryl substituted 2,3-dihydrofurans **1a–1e** were synthesized and their reactions with singlet oxygen were investigated. Photooxygenation of **1a–1e** in carbon tetrachloride at ambient temperature exclusively yields allylic hydroperoxides **4a–4e**. Treatment of these hydroperoxides with aqueous ferrous sulfate solution affords the corresponding α,β -unsaturated γ -lactones **6a–6e** with high yields. This work provides an efficient route to the preparation of butenolide moiety, an important functionality in the structures of many natural products that exhibit biological properties.

© 2006 Elsevier Ltd. All rights reserved.

1. Introduction

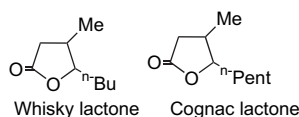
α,β -Unsaturated γ -lactone moiety is an important functionality in the structures of many natural products that exhibit interesting biological properties.^{1–3} For example, pyranicin,⁴ cacospongionolide,⁵ lituarine,⁶ manolide, rubrolide, prunolide,⁷ and digitalis⁸ all are known to include this butenolide subunit (Scheme 1). Furthermore, five-membered lactones have a specific odoriferous impression, and α,β -unsaturated γ -lactones are advanced intermediates on the way to naturally occurring flavoring materials such as whisky lactone and cognac lactone (Scheme 2).⁹ In this regard, the development of efficient strategies for the synthesis of α,β -unsaturated γ -lactones is greatly demanded, and a number of methods have been developed.¹⁰ Among these methods, selective oxidation of furans by singlet oxygen holds special promise. For example, Schenck and co-workers¹¹ irradiated furan, 2-hydroxymethylfuran, furfural, and 2-methylfuran in alcohol in the presence of a singlet oxygen photosensitizer, and obtained 5-alkoxybutenolide. The formation of butenolide was assumed to occur via the 1,4-cycloaddition of singlet oxygen to the 1,3-diene in furans to yield ozonides, which then underwent solvolysis to give the product. 5-Hydroxybutenolides were also synthesized by singlet oxygen oxidation of furans.¹² For 3-alkylfuran the singlet oxygen oxidation generally produces the mixture



Scheme 1. Structure of pyranicin, cacospongionolide, lituarine, manolide, rubrolide, prunolide, and digitalis.

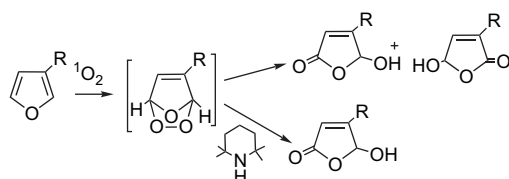
Keywords: α,β -Unsaturated γ -lactones; Photooxygenation of 2,3-dihydrofurans; Ferrous ion-catalyzed *gem*-dehydration of hydroperoxides.

* Corresponding authors. Tel./fax: +86 10 82543580 (L.-Z.W.); tel./fax: +86 10 82543578 (C.-H.T.); e-mail addresses: lzwu@mail.ipc.ac.cn; chtung@mail.ipc.ac.cn

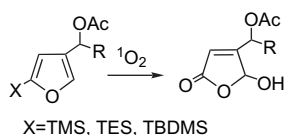


Scheme 2. Whisky lactone and cognac lactone.

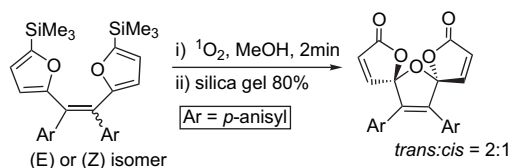
of the C-3 and C-4 isomers of 5-hydroxybutenolides. To increase the regioselectivity of this reaction, Kernan and Faulkner¹³ carried out the oxidation in the presence of a hindered base such as 2,2,6,6-tetramethylpiperidine and selectively obtained the C-4 isomer (**Scheme 3**). Lee et al.¹⁴ introduced a trimethylsilyl group into the 5-position of 3-alkylfurans, then performed the singlet oxygen oxidation. They also obtained the regioisomer, 4-alkyl-5-hydroxybutenolides (**Scheme 4**). Recently, Snapper and co-workers⁵ synthesized the 5-hydroxybutenolide functionality in cacospongionolides B and E via photooxygenation of furan moiety in the presence of a hindered base. Vassiliko-*giannakis* et al.⁷ synthesized the spirocyclic core of the prunolides by using a double photooxygenation of a 1,2-di-[2-(5-trimethylsilyl) furyl]-alkene (**Scheme 5**).



Scheme 3. Oxidation of 3-substituted furan.



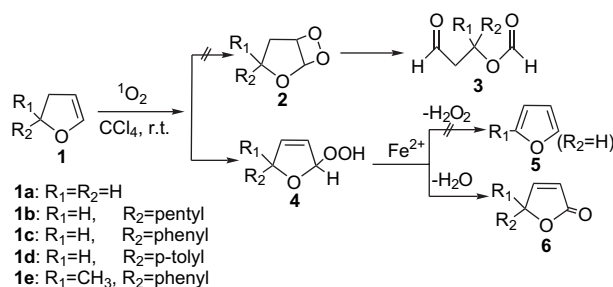
Scheme 4. Oxidation of 3,5-disubstituted furan.



Scheme 5. The spirocyclic core of prunolides.

The photosensitized oxidation of 2,3-dihydrofurans also has been extensively investigated.¹⁵ These substrates can undergo [2+2] cycloadditions and ene reaction with singlet oxygen to give 1,2-dioxetane **2** and allylic hydroperoxides **4**, respectively¹⁶ (**Scheme 6**). It has been established¹⁵ that in addition to the structure details of the substrates, the nature of the solvent (aprotic/protic solvents; polarity) and the reaction temperature may affect the extent to which the two reaction modes compete with each other for singlet oxygen. Generally, polar solvents and low temperature favor [2+2] cycloaddition products over ene products. On heating, the

dioxetanes **2** decompose to yield the dicarbonyl compounds **3**, while the allylic hydroperoxides **4** can eliminate H₂O₂ to give the corresponding furans **5** if the 2-position of the 2,3-dihydrofuran is unsubstituted or monosubstituted. Although the photooxygenation of 2,3-dihydrofurans has been extensively investigated,^{15,16} utilization of this photooxidation as a route to synthesize α,β -unsaturated γ -lactones has not been reported. In the present work we describe a versatile route to butenolides. Our approach involves the singlet oxygen oxidation of 2,3-dihydrofurans **1** in non-polar solvents at room temperature to give exclusively the allylic hydroperoxides **4** followed by ferrous ion-catalyzed *gem*-dehydration of these hydroperoxides. α,β -Unsaturated γ -lactones **6** are generally produced with excellent yields.



Scheme 6. Photooxygenation of 2,3-dihydrofurans.

2. Results and discussion

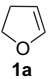
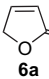
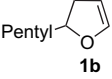
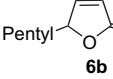
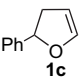
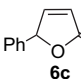
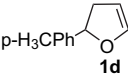
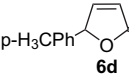
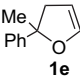
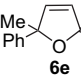
2.1. Photooxygenation of 2,3-dihydrofuran (1a)

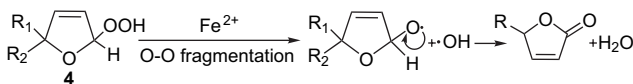
As mentioned above, 2,3-dihydrofuran can undergo ene reaction and [2+2] cycloaddition with singlet oxygen to yield allylic hydroperoxide **4** and 1,2-dioxetane **2**, respectively, and polar solvents and low temperature favor the formation of **2** over **4**. Thus, we performed the photooxygenation of 2,3-dihydrofuran in a non-polar solvent, carbon tetrachloride, at ambient temperature in order to generate the allylic hydroperoxide in high yield. Tetraphenylporphyrin (TPP) was used as the sensitizer, and a 450 W Hanovia high-pressure lamp was used as the light source. A glass filter was employed to cut off the light with $\lambda < 400$ nm, thus only the sensitizer in the irradiation sample absorbed the light. Irradiation of oxygen-bubbling solution of **1a** in carbon tetrachloride in the presence of 10^{-5} M TPP exclusively resulted in the formation of 5-hydroperoxy-2,5-dihydrofuran **4a** (**Scheme 6**). Generally, after 30 min irradiation the conversion of **1a** was close to 100%. The assignment of the structure of **4a** mainly relies on its ¹H and ¹³C NMR spectra, which were extracted from those of the crude reaction mixture. The ¹³C NMR spectrum showed four signals at δ 74.6 (t), 112.0 (d), 122.8 (d), and 134.2 (d) ppm. These chemical shifts are attributed to carbon atoms C-2, C-5, C-3, and C-4 of **4a**, respectively. The ¹H NMR spectrum exhibited four multiplets at δ 4.72 (H-2), 5.58 (H-3), 6.13 (H-4), and 6.37 (H-5) and a broad singlet at 8.39 (OOH) ppm in a ratio of 2:1:1:1 attributed to protons H-2 through H-5 and OOH of **4a** as indicated in brackets. These ¹³C and ¹H NMR data are consistent with those reported in the literature.¹⁵

With the allylic hydroperoxide **4a** in hand, then we conducted the transformation of **4a** into butenolide **6a**. It has

been established¹⁷ that α -alkoxybenzyl hydroperoxides can be converted into corresponding arylcarboxylate esters via ferrous ion-catalyzed *gem*-dehydration. This prompted us to investigate the possibility of the ferrous ion-catalyzed dehydration of **4**. To the solution of **4a** in carbon tetrachloride immediately obtained by photooxygenation described above was added a solution of ferrous sulfate (1 equiv) in water, and the mixture was stirred at room temperature overnight. α,β -Unsaturated γ -lactone **6a** was isolated by dichloromethane extraction in an overall yield of 95% based on the consumed **1a** (Table 1). This product was characterized by ¹H NMR spectrum that is consistent with the literature.¹⁵ It is suggested that this ferrous ion-catalyzed *gem*-dehydration proceeds via the oxy radical generated by homolytic fragmentation of the O–O bond of the allylic hydroperoxide in the presence of ferrous ion (Scheme 7).^{17,18}

Table 1. The yield of α,β -unsaturated γ -lactones produced by photooxygenation of 2,3-dihydrofurans followed by ferrous ion-catalyzed or triethylamine-catalyzed *gem*-dehydration

Substrate	Treatment of the oxidation product	Product	Yield (%)
	FeSO ₄ Et ₃ N		>95 90
	FeSO ₄ Et ₃ N		84 81
	FeSO ₄		60
	FeSO ₄		67
	FeSO ₄		76



Scheme 7. Ferrous ion-catalyzed *gem*-dehydration.

In the efforts to transform allylic hydroperoxide **4** into butenolide **6**, we also tested another method that involves the treatment of **4** with a triethylamine.¹⁷ Addition of equivalent amount of triethylamine to the solution of **4a** in carbon tetrachloride immediately obtain by photooxygenation and stirring the solution overnight led to complete conversion of **4a** into **6a**, as evidenced by ¹H NMR spectrum changes. Compound **6a** was isolated by chromatograph on silica in the yield greater than 90% (Table 1).

Gollnick and co-workers¹⁵ performed the photooxygenation of **1a** under similar reaction condition described above, but at low temperatures (–78 to 13 °C). In contrast to our result, a large amount of [2+2] cycloaddition product **2a** (24% of the products) was obtained. Compound **2a** transformed

into 3-(formyloxy) propanal **3a** at elevated temperature (Scheme 6). In our study since we isolated **6a** in 95% yield after the ferrous ion-catalyzed dehydration, the formation of **2a**, if any, must not be significant. Evidently, temperature is an important factor determining the pathway in the reaction of olefins with singlet oxygen. Furthermore, Gollnick¹⁵ reported that allylic hydroperoxide **4a** undergoes elimination of hydrogen peroxide to give furan **5a** rather than dehydration to give the lactone **6a**. Indeed, we kept the solution of **4a** in carbon tetrachloride at 50 °C for 4 h, and found that quantitative furan **5a** was produced.

2.2. Photooxygenation of 2-pentyl-2,3-dihydrofuran (**1b**), 2-phenyl-2,3-dihydrofuran (**1c**), and 2-*p*-tolyl-2,3-dihydrofuran (**1d**)

α,β -Unsaturated γ -lactone moiety is often connected to natural products at its 5-position. To exploit the possibility of utilization of the above mentioned photooxygenation of 2,3-dihydrofurans as a tool for the synthesis of natural products, we have investigated the ene reaction and the subsequent ferrous ion-catalyzed dehydration of several 2,3-dihydrofurans with alkyl or aryl at its 2-position. Photoirradiation of oxygen-bubbling 0.1 M solution of **1b** in carbon tetrachloride at room temperature in the presence of 10^{–5} M TPP led to the formation of 2-pentyl-5-hydroperoxy-2,5-dihydrofuran **4b** as evidenced by ¹H NMR spectrum of the reaction mixture. No corresponding 1,2-dioxetane **2b** was detected. After 30 min irradiation the conversion of **1b** is completed. Addition of aqueous solution of ferrous sulfate to the reaction mixture and stirring the mixture overnight resulted in the formation of 5-pentyl-substituted butenolide **6b**. The isolated yield of this product was ca. 84% based on the consumed **1b** (Table 1). As in the case of **1a**, when the photooxygenation mixture was treated with triethylamine, the allylic hydroperoxide **4b** transformed into the 5-pentyl-substituted butenolide **6b** with the yield of 81% (Table 1).

The 2-aryl-substituted 2,3-dihydrofurans **1c** and **1d** also can be used as starting materials to produce the corresponding 5-aryl-substituted butenolides via photooxygenation in non-polar solvents at ambient temperature, followed by ferrous ion-catalyzed *gem*-dehydration. Under the conditions mentioned above, the 5-aryl-butenolides **6c** and **6d** were isolated in 60 and 67% yields, respectively (Table 1). Interestingly, the efficiency of the photooxygenation of substrates **1c** and **1d** is remarkably larger than those for **1a** and **1b**. Generally, irradiation of the solutions of the former substrates under above conditions for several minutes led to complete conversion to the corresponding allylic hydroperoxides.

2.3. Photooxygenation of 2-methyl-2-phenyl-2,3-dihydrofuran (**1e**)

In order to elucidate the feasibility of the synthesis of 5,5-disubstituted butenolide by the above methods, we investigated the photooxygenation of 2-methyl-2-phenyl-2,3-dihydrofuran **1e**. As expected, TPP-sensitized photooxygenation of **1e** in carbon tetrachloride at room temperature yielded the allylic hydroperoxide **4e** exclusively. No [2+2] cycloaddition product was detected from the ¹H NMR spectrum of the reaction mixture. Treatment of the reaction mixture with aqueous ferrous sulfate solution resulted in the conversion

of **4e** to 5-methyl-5-phenyl butenolide **6e**. The isolated yield of **6e** was ca. 76% (Table 1).

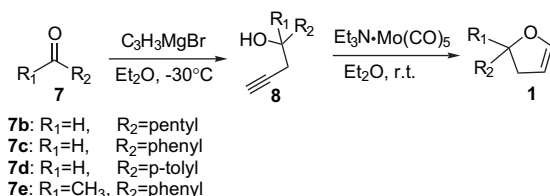
3. Conclusion

Photosensitized oxidation of 2,3-dihydrofuran and its derivatives with alkyl and/or aryl substituent(s) at its 2-position in a non-polar solvent at ambient temperature exclusively yield the corresponding allylic hydroperoxides. 1,2-Dioxetanes were not detected. Treatment of the photooxygenation solutions with ferrous sulfate aqueous solution or triethylamine quantitatively resulted in the conversion of the allylic hydroperoxides into α,β -unsaturated γ -lactones. The overall yields of the α,β -unsaturated γ -lactones were in the region of 60–95% based on the consumed 2,3-dihydrofurans. The high product yield, mild conditions under which the reactions occur, and the low cost of the reagents used make this reaction sequence to be an efficient strategy for the synthesis of α,β -unsaturated γ -lactones.

4. Experimental

4.1. Materials

Solvents of reagent grade from Beijing Chemical Works and 2,3-dihydrofuran of analytical grade from Acros Co. were used without further purification. 2-Pentyl-2,3-dihydrofuran **1b**, 2-phenyl-2,3-dihydrofuran **1c**, 2-*p*-tolyl-2,3-dihydrofuran **1d**, and 2-methyl-2-phenyl-2,3-dihydrofuran **1e** were synthesized according to the literatures¹⁹ as shown in Scheme 8.



Scheme 8. Preparation of 2,3-dihydrofurans.

4.1.1. Preparation of alkynols (8). In a typical experiment a solution of Grignard reagent, C₃H₅MgBr in Et₂O was prepared by a literature procedure.²⁰ This solution was cooled to –30 °C and a solution of the corresponding aldehyde or ketone **7** in Et₂O was added dropwise. The mixture was slowly warmed to room temperature and stirred for 1 h. It was then poured into ice water. Saturated aqueous NH₄Cl solution was added to dissolve the precipitate and the organic layer was separated. The aqueous layer was extracted with ether and the extracts were combined with the above organic layer. The combined solution was dried over MgSO₄. After evaporation of the solvent the residue was purified by distillation at reduced pressure.

Compound **8b**: ¹H NMR (400 MHz, CDCl₃): δ=3.75 (1H, m, CHOH), 2.43 (1H, ddd, *J*=16.5, 4.9, 2.6 Hz, CH₂-C_{sp}), 2.31 (1H, ddd, *J*=16.5, 6.6, 2.6 Hz, CH₂-C_{sp}), 2.05 (1H, t, *J*=2.6 Hz, C_{sp}-H), 2.05 (1H, br, OH), 1.60–1.20 (8H, m, (CH₂)₄), 0.89 (3H, t, *J*=6.6 Hz, CH₃).

Compound **8c**: ¹H NMR (400 MHz, CDCl₃): δ=7.40–7.10 (5H, m, Ph), 4.75 (1H, m, CHOH), 2.61 (1H, d, *J*=3.3 Hz, OH), 2.51 (2H, dd, *J*=6.6, 2.6 Hz, CH₂), 1.96 (1H, t, *J*=2.6 Hz, C_{sp}H).

Compound **8d**: ¹H NMR (400 MHz, CDCl₃): δ=7.29 (2H, d, *J*=7.9 Hz, Ph), 7.18 (2H, d, *J*=7.9 Hz, Ph), 4.84 (1H, t, *J*=6.3 Hz, CHOH), 2.63 (2H, dd, *J*=6.2, 2.6 Hz, CH₂), 2.46 (1H, br, OH), 2.37 (3H, s, -CH₃), 2.07 (1H, t, *J*=2.1 Hz, C_{sp}H).

Compound **8e**: ¹H NMR (400 MHz, CDCl₃): δ=7.50–7.20 (5H, m, Ph), 2.78 (2H, dd, *J*=15.4, 2.6 Hz, CH₂), 2.62 (1H, s, OH), 2.06 (1H, t, *J*=2.6 Hz, C_{sp}H), 1.66 (3H, s, -CH₃).

4.1.2. Preparation of 2,3-dihydrofurans (1). In a typical experiment, to 0.21 g (0.78 mmol) of molybdenum hexacarbonyl was added 14 mL of dry triethylamine under nitrogen atmosphere, then 12 mL of dry ether was added. The mixture was stirred for 10–15 min until the molybdenum hexacarbonyl had dissolved. The solution was irradiated with 350 nm light for 1 h. To the yielded yellow solution of Et₃N·Mo(CO)₅ was added the solution of alkynol (**8**, 6 mmol) in ether, and the mixture was stirred for 72 h at room temperature under nitrogen. The solvent was then removed by rotary evaporation. The remaining liquid was chromatographed on silica with *n*-hexane and ether mixture (10:1, v:v) as eluent and 2,3-dihydrofurans were obtained.

Compound **1b**: ¹H NMR (400 MHz, CDCl₃): δ=6.28 (1H, dd, *J*=4.9, 2.3 Hz, OCH=), 4.85 (1H, dd, *J*=4.9, 2.2 Hz, OCH=CH), 4.52 (1H, m, -OCH-), 2.68 (1H, m, =CH-CH₂), 2.21 (1H, ddt, *J*=15.1, 7.7, 2.2 Hz, =CH-CH₂), 1.8–1.2 (8H, m, (CH₂)₄), 0.9 (3H, t, *J*=6.6 Hz, CH₃).

Compound **1c**: ¹H NMR (400 MHz, CDCl₃): δ=7.40–7.20 (5H, m, Ph), 6.43 (1H, dd, *J*=4.9, 2.3 Hz, OCH=), 5.49 (1H, dd, *J*=10.7, 8.5 Hz, CHPh), 4.92 (1H, dd, *J*=4.9, 2.4 Hz, -OCH=CH), 3.05 (1H, ddt, *J*=15.4, 10.7, 2.4 Hz, CH₂, *H-trans*), 2.58 (1H, ddt, *J*=15.4, 8.4, 2.4 Hz, CH₂, *H-cis*).

Compound **1d**: ¹H NMR (400 MHz, CDCl₃): δ=7.40–7.10 (4H, m, Ph), 6.45 (1H, dd, *J*=4.9, 2.3 Hz, OCH=), 5.50 (1H, dd, *J*=10.6, 8.6 Hz, CH₃Ph-CH), 4.96 (1H, m, OCH=CH), 3.06 (1H, m, CH₂, *H-trans*), 2.62 (1H, m, CH₂, *H-cis*), 2.36 (3H, s, -CH₃).

Compound **1e**: ¹H NMR (400 MHz, CDCl₃): δ=7.50–7.20 (5H, m, Ph), 6.40 (1H, dd, *J*=4.9, 2.4 Hz, OCH=), 4.86 (1H, m, -OCH=CH), 2.87 (1H, dt, *J*=15.0, 2.3 Hz, =CH-CH₂), 2.80 (1H, dt, *J*=15.0, 2.3 Hz, =CH-CH₂), 1.67 (3H, s, -CH₃).

4.1.3. Photooxygenation and ferrous ion-catalyzed gem-dehydration. The photooxidation of 2,3-dihydrofurans **1** was carried out in carbon tetrachloride in a Pyrex reactor with tetraphenylporphyrin (TPP) as the sensitizer. The light source was a 450 W Hanovia high-pressure mercury lamp with a glass filter to cut off the light with wavelength below 400 nm, thus to ensure the absence of direct excitation of the substrates. During irradiation, oxygen was bubbled

through the solution. The photooxygenation process was followed by ^1H NMR of the reaction mixture. After the oxidation was completed, to the reaction mixture was added equivalent amount of ferrous sulfate aqueous solution (or triethylamine). The mixture was stirred overnight, and then the organic layer was separated and dried over MgSO_4 . Evaporation of the solvent afforded α,β -unsaturated γ -lactones.

Compound **6a**: ^1H NMR (400 MHz, CDCl_3): $\delta=7.60$ (1H, m, $\text{CH}_2\text{-CH=}$), 6.21 (1H, m, $\text{CH}_2\text{CH=CH}$), 4.93 (2H, m, CH_2).

Compound **6b**: ^1H NMR (400 MHz, CDCl_3): $\delta=7.47$ (1H, dd, $J=5.7, 1.2$ Hz, CHCH=CH), 6.13 (1H, dd, $J=5.7, 1.9$ Hz, CHCH=CH), 5.06 (1H, m, CHCH=CH), 1.2–1.8 (8H, m, $(\text{CH}_2)_4$), 0.92 (3H, t, $J=6.7$ Hz, CH_3).

Compound **6c**: ^1H NMR (400 MHz, CDCl_3): $\delta=7.2\text{--}7.5$ (5H, m, Ph), 7.52 (1H, dd, $J=5.6, 1.7$ Hz, CHCH=CH), 6.23 (1H, dd, $J=5.6, 2.1$ Hz, CHCH=CH), 6.03 (1H, dd, $J=2.0, 1.7$ Hz, PhCH).

Compound **6d**: ^1H NMR (400 MHz, CDCl_3): $\delta=7.1\text{--}7.4$ (4H, m, Ph), 7.51 (1H, dd, $J=5.5, 1.5$ Hz, CHCH=CH), 6.22 (1H, dd, $J=5.7, 2.0$ Hz, CHCH=CH), 5.99 (1H, dd, $J=2.0, 1.5$ Hz, CHCH=CH), 2.37 (3H, s, $-\text{CH}_3$).

Compound **6e**: ^1H NMR (400 MHz, CDCl_3): $\delta=7.63$ (1H, d, $J=5.6$ Hz, PhCCH=CH), 7.5–7.2 (5H, m, Ph-), 6.06 (1H, d, $J=5.6$ Hz, PhC-CH=CH), 1.83 (3H, s, $-\text{CH}_3$).

Acknowledgements

Financial support from the Ministry of Science and Technology of China (Grant no. 2004CB719903 and 2007CB808004), the National Science Foundation of China (nos. 20333080, 20332040, 20472091, 50473048, 20472092, 20403025), and the Chinese Academy of Sciences (no. KJCX2-SW-H15) is gratefully acknowledged.

References and notes

- For recent examples, see: (a) Chia, Y.; Chang, F.; Wu, Y. *Tetrahedron Lett.* **1999**, *40*, 7513–7514; (b) Takahashi, S.; Maeda, K.; Hirota, S.; Nakata, T. *Org. Lett.* **1999**, *1*, 2025–2028; (c) Siddiqui, B. S.; Afshan, F.; Ghiasuddin; Faizi, S.; Naqvi, S. N.-H.; Tariq, R. M. *J. Chem. Soc., Perkin Trans. 1* **1999**, 2367–2370; (d) Cortez, D. A. G.; Fernandes, J. B.; Vieria, P. C.; Silva, M. F. G. F.; Ferreira, A. G.; Cass, Q. B.; Pirani, J. R. *Phytochemistry* **1998**, *49*, 2493–2496.
- (a) Otsuka, H.; Kotani, K.; Bando, M.; Kido, M.; Takeda, Y. *Chem. Pharm. Bull.* **1998**, *46*, 1180–1181; (b) Guo, S.; Wang, L.; Chen, D. *Indian J. Chem., Sect. B* **1997**, *36B*, 339–342; (c) Evidente, A.; Sparapano, L. *J. Nat. Prod.* **1994**, *57*, 1720–1725; (d) Damtoft, S.; Jensen, S. R. *Phytochemistry* **1995**, *40*, 157–159; (e) Estevez-Reyes, R.; Estevez-Braun, A.; Gonzalez, A. G. *J. Nat. Prod.* **1993**, *56*, 1177–1181; (f) Claydon, N.; Hanson, J. R.; Truneh, A.; Avent, A. G. *Phytochemistry* **1991**, *30*, 3802–3803.
- (a) Seki, T.; Satake, M.; Mackenzie, L.; Kaspar, H. F.; Yasumoto, T. *Tetrahedron Lett.* **1995**, *36*, 7093–7096; (b) Cambie, R. C.; Bergquist, P. R.; Karuso, P. *J. Nat. Prod.* **1988**, *51*, 1014–1016; (c) Ahmed, M.; Ahmed, A. A. *Phytochemistry* **1990**, *29*, 2715–2716; (d) De Guzman, F. S.; Schmitz, F. J. *J. Nat. Prod.* **1990**, *53*, 926–931; (e) Marshall, J. A.; Piettre, A.; Paige, M. A.; Valeriote, F. *J. Org. Chem.* **2003**, *68*, 1780–1785.
- Strand, D.; Rein, T. *Org. Lett.* **2005**, *7*, 199–202.
- Cheung, A. K.; Murelli, R.; Snapper, M. L. *J. Org. Chem.* **2004**, *69*, 5712–5719.
- Robertson, J.; Meo, P.; Dallimore, J. W. P.; Doyle, B. M.; Hoarau, C. *Org. Lett.* **2004**, *6*, 3861–3863.
- Sofikiti, N.; Tofi, M.; Montagnon, T.; Vassilikogiannakis, G.; Stratakis, M. *Org. Lett.* **2005**, *7*, 2357–2359.
- Stork, G.; Weat, F.; Lee, Y.; Isaacs, R. C. A.; Manabe, S. *J. Am. Chem. Soc.* **1996**, *118*, 10660–10661.
- (a) Fráter, G.; Bajgrowicz, J. A.; Kraft, P. *Tetrahedron* **1998**, *54*, 7633–7703; (b) Otzuka, K.; Zenibayashi, Y.; Itoh, M.; Totsuka, A. *Agric. Biol. Chem.* **1974**, *38*, 485–490.
- For recent reviews on the synthesis of butenolides, see: (a) Negishi, E.; Kitora, M. *Tetrahedron* **1997**, *53*, 6707–6738; (b) Deshong, P.; Sidler, D. R.; Slough, G. A. *Tetrahedron Lett.* **1987**, *28*, 2233–2236; (c) Marshall, J. A.; Wolf, M. A. *J. Org. Chem.* **1996**, *61*, 3238–3239; (d) Yu, W.; Alper, H. *J. Org. Chem.* **1997**, *62*, 5684–5687; (e) Xiao, W.; Alper, H. *J. Org. Chem.* **1997**, *62*, 3422–3423; (f) Arcadi, A.; Bernocchi, E.; Burini, A.; Cacchi, S.; Marinelli, F.; Pietroni, B. *Tetrahedron* **1988**, *44*, 481–490; (g) Marshall, J. A.; Bartley, G. S.; Wallace, E. M. *J. Org. Chem.* **1996**, *61*, 5729–5735; (h) Clough, J. M.; Pattenden, G.; Wight, P. G. *Tetrahedron Lett.* **1989**, *30*, 7469–7472; (i) Chen, J.; Sanner, M. A.; Carlson, R. M. *Synth. Commun.* **1990**, *20*, 901–906; (j) Marshall, J. A.; Wallace, E. M.; Coan, P. S. *J. Org. Chem.* **1995**, *60*, 796–797; (k) Yoneda, E.; Kaneko, T.; Zhang, S.; Onitsuka, K.; Takahashi, S. *Org. Lett.* **2000**, *2*, 441–443; (l) Renurd, M.; Ghosez, L. A. *Tetrahedron* **2001**, *57*, 2597–2608; (m) Langer, P.; Friefold, I. *Synlett* **2001**, 523–525; (n) Linclau, B.; Boydell, A. J.; Clarke, P. J.; Horan, R.; Jaequet, C. *J. Org. Chem.* **2003**, *68*, 1821–1826.
- (a) Koch, E.; Schenck, G. O. *Chem. Ber.* **1966**, *99*, 1984–1990; (b) Schenck, G. O.; Appel, R. *Naturwissenschaften* **1946**, *33*, 122–123; (c) Schroeter, S. H.; Brammer, R.; Schenck, G. O. *Justus Liebigs Ann. Chem.* **1966**, *697*, 42–61; (d) Gollnick, K.; Schenck, G. O. *1,4-Cycloaddition Reactions: The Diels–Alder Reaction in Heterocyclic Synthesis*; Hammer, J., Ed.; Academic: New York, NY, 1967; Chapter 10, p 255.
- For recent reviews, see: (a) Feringa, B. L. *Recl. Trav. Chim. Pays-Bas* **1987**, *106*, 469–488; (b) Wasserman, H. H.; Ives, J. L. *Tetrahedron* **1981**, *37*, 1825–1852; (c) Mataumoto, M. *Singlet Oxygen*; Frimer, A. A., Ed.; CRC: Boca Raton, FL, 1985; Vol. II.
- Kernan, M. R.; Faulkner, D. J. *J. Org. Chem.* **1988**, *53*, 2773–2776.
- Lee, G. C. M.; Syage, E. T.; Harcourt, D. A.; Holmes, J. M.; Garst, M. E. *J. Org. Chem.* **1991**, *56*, 7007–7014.
- (a) Gollnick, K.; Mies, K. K. *J. Org. Chem.* **1991**, *56*, 4017–4027; (b) Adam, W.; Griesbeck, A. G. *J. Org. Chem.* **1988**, *53*, 1492–1495.
- For Tetrahedron Symposia-in-Print Number 20, see: Jefford, C. W.; Boukouvalas, J.; Kohmoto, S. *Tetrahedron* **1985**, *41*, 2037–2235 (Guest editors: Saito, I., Matsuura, T.).

17. Sharp, D. B.; Patrick, T. M. *J. Org. Chem.* **1961**, *26*, 1389–1394.
18. Nonami, Y.; Baran, J.; Sosnicki, J.; Mayr, H.; Masuyama, A.; Nojima, M. *J. Org. Chem.* **1999**, *64*, 4060–4063 and the reference therein.
19. (a) McDonald, F. E.; White, B. H. *Org. Synth.* **2002**, *79*, 27–34; (b) Schmidt, B.; Kocienski, P.; Reid, G. *Tetrahedron* **1996**, *52*, 1617–1630.
20. Viola, A.; MacMillan, J. H. *J. Am. Chem. Soc.* **1968**, *90*, 6141–6145.

Dye-sensitized photooxygenation of sugar-furans as synthetic strategy for novel C-nucleosides and functionalized *exo*-glycals

Flavio Cermola* and M. Rosaria Iesce

Dipartimento di Chimica Organica e Biochimica, Università di Napoli Federico II, Complesso Universitario di Monte Sant'Angelo, Via Cinthia 4, 80126 Napoli, Italy

Received 5 June 2006; revised 26 July 2006; accepted 27 July 2006

Available online 18 September 2006

Abstract—The methylene blue-sensitized photooxygenation of β -ribofuranosyl furan **1e** followed by in situ Et_2S treatment afforded the conformationally stable β -ribofuranoside **4e** almost quantitatively. The latter was converted to pyridazine C-nucleoside **6e** by cyclization with NH_2NH_2 and to pyrazoline **7e** through a 1,3-dipolar cycloaddition with diazomethane. Attempts to epoxidize the double bond failed both by dimethyldioxirane (DMDO), which left **4e** unchanged, and by $\text{NEt}_3/t\text{-BuOOH}$ or $\text{NaOO-}t\text{-Bu}$ which respectively afforded the new and unexpected *exo*-glycals *E,Z*-**8e** and the novel furan derivative **9**.
© 2006 Published by Elsevier Ltd.

1. Introduction and background

C-Glycoside synthesis represents a field of great interest due to the potential biological relationships, which often characterize these molecules.¹ Many synthetic approaches have been developed and others are being investigated for the purpose of furnishing more efficient procedures.² Two main synthetic pathways provide C-nucleosides as well as glycosides in general.³ The most common approach is based on promoted coupling between a donor sugar and an acceptor, the latter being the desired aglycone.^{2,3} The other approach involves transforming a suitable pre-existent aglycone by means of regio- and stereoselective reactions.³ Although the first approach has wider applicability, it has definite limitations including isomerization or decomposition of the acceptor during the reaction due to the harsh conditions required. When this approach fails, the second strategy could represent the only possibility to achieve the target molecule.³

Furans are versatile and useful starting materials in the field of organic synthesis. For example, they are good diene-type compounds in [4+2] cycloaddition with singlet oxygen ($^1\text{O}_2$).⁴ This excited state of oxygen can be easily produced starting from atmospheric oxygen, solar light and a sensitizer, which together constitute a reaction system of very low environmental impact. On the other hand, pericyclic reactions are known to proceed with very high regio- and stereoselectivity, the first of which fails when singlet oxygen

is the dienophile,⁵ as well as with good yields.⁶ [4+2] Cycloaddition of singlet oxygen to furans has been applied with success in approaching highly functionalized molecules, which in turn can serve as building blocks in constructions of more complicated organic structures.⁴ The reaction quantitatively affords 2,3,7-trioxabicyclo[2.2.1]hept-5-enes, usually named endoperoxides (Fig. 1),^{4,5} which are thermally unstable. The rearrangement pathways strictly depend on the electronic nature of the substituents on the furan ring, providing useful approaches to a wide range of functionalized cyclic or acyclic compounds.^{4,5,7}

Previous studies aimed at controlling dye-sensitized photooxygenation of furans bearing a sugar and investigated the reaction of glucosyl furans α -**1a,b** (Scheme 1).⁸ The results showed that the sugar ring at the α -position of a furan strongly influences the chemical behaviour of the corresponding endoperoxides **2a,b**; they thermally rearranged into the corresponding α -O-glycosides **3a,b** through a Baeyer—Villiger-type mechanism (Scheme 1). This uncommon C- to O-glycoside transposition is promoted by the electrophilicity of the anomeric carbon and does not depend on the ring-sugar size. Indeed, similar results were obtained starting from the arabinosyl furans **1c,d**, which led quantitatively to the O-furanosides **3c,d** (Scheme 1).⁹ Moreover, the use of the β -anomer of **1c** confirmed that the observed

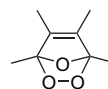
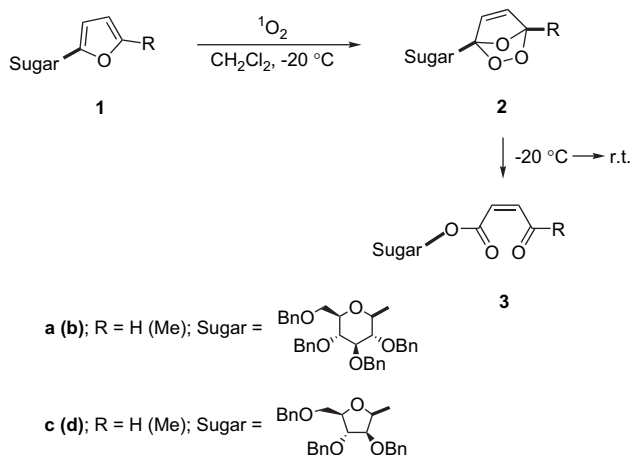


Figure 1. 2,3,7-Trioxabicyclo[2.2.1]hept-5-ene.

Keywords: Photooxygenation; [4+2] Cycloadditions; C-Nucleosides; 1,3-Dipolar cycloadditions.

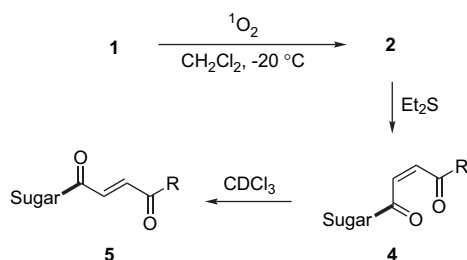
* Corresponding author. E-mail: cermola@unina.it

stereoselectivity is due to retention of the configuration in the sugar moiety from C- to O-migration (Scheme 1).⁹



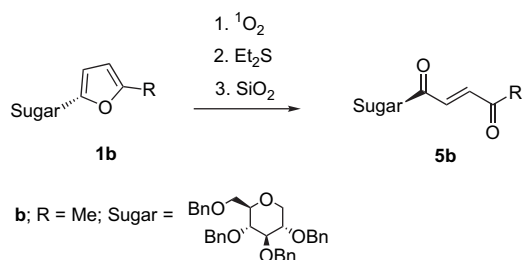
Scheme 1.

Although thermally unstable, the endoperoxides **2** could be used in approaching novel and functionalized C-glycosides. Indeed, when the photooxygenation mixtures of **2** were treated with a precooled ($-20\text{ }^{\circ}\text{C}$) solution of Et_2S , the C-glycosides **4** were formed almost quantitatively (Scheme 2).^{8,9} They were obtained with complete *cis*-stereoselectivity, owing to the bicyclic structure of the parent endoperoxides, but the use of chloroform or other slightly acid conditions promoted a complete isomerization into *trans*-derivatives **5** (Scheme 2).



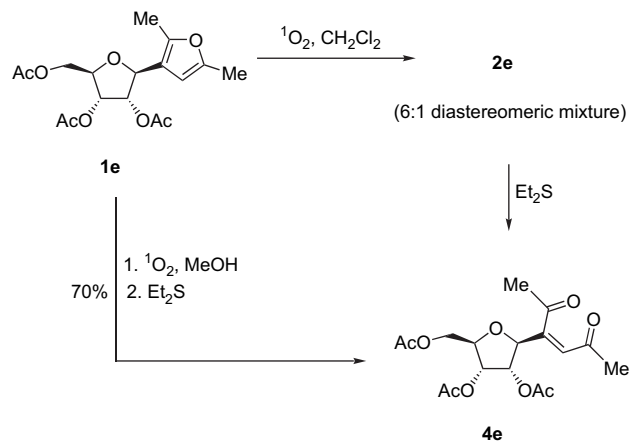
Scheme 2.

The development of the one-pot procedure shown in Scheme 3 is of considerable interest. It offers an easy synthetic approach for β -C-glycosides such as the derivative β -**5b**, starting from the corresponding α -glucosyl furans, for example, α -**1b**, which can be more easily prepared than the β -analogues.⁸



Scheme 3.

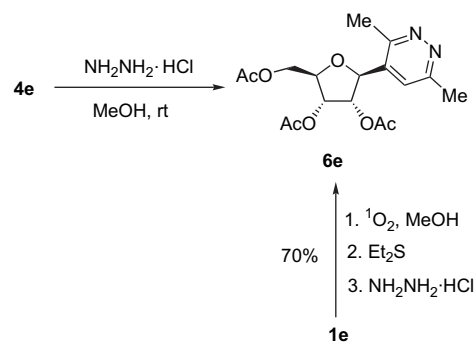
Subsequently, we decided to apply the photooxygenation procedure to β -ribofuranosides in the hope of producing novel C-nucleosides of pharmacological interest. Thus we synthesized the β -ribofuranosyl furan **1e**,⁹ previously unknown, to obtain functionalized furanosides with configurationally stable unsaturated aglycones as well as to avoid the C- to O-rearrangement. The photooxygenation of β -**1e** in dichloromethane at $-20\text{ }^{\circ}\text{C}$ was complete after 30 min (TLC) and afforded the 6:1 diastereomeric mixture of the endoperoxide **2e**, which by Et_2S reduction quantitatively gave the *cis*-diketone **4e** (Scheme 4). As expected, compound **4e** showed a configurational stability, and did not isomerize at all into the corresponding *trans*-alkene.⁹ Here we report some synthetic applications based on the use of the β -ribofuranoside **4e** as starting material for interesting new C-nucleosides and *exo*-glycals. Compound **4e** is easily prepared by a one-pot procedure based on the dye photooxygenation of the furanosyl furan **1e** followed by in situ Et_2S reduction (Scheme 4). Due to the high yield as well as the stereoselectivity, compound **4e** can be used without chromatographic purification.



Scheme 4.

2. Results and discussion

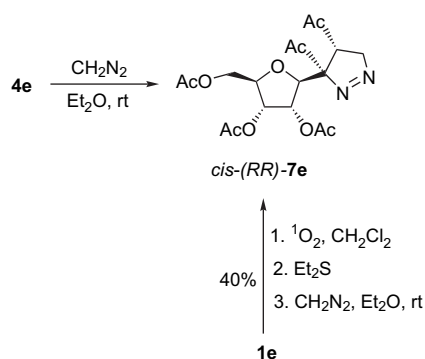
The *cis*-relationship of the two carbonyl groups of β -ribofuranoside **4e** and its configurational stability led us to carry out a cyclization into a pyrimidine-base system by the addition of hydrazine hydrochloride. The reaction was performed using dry methanol as the solvent and led to the new pyridazine C-nucleoside β -**6e** (Scheme 5). A one-pot process starting



Scheme 5.

from furan **1e** was then developed and afforded compound **6e** in 70% yield (based on furan **1e**).⁹

The presence of the peracetylated sugar ring as well as of two acetyl groups at the unsaturated carbons suggested the use of **4e** as a dipolarophile in [4+2] cycloadditions with electron-rich diene compounds as well as in [3+2] reaction with suitable 1,3-dipoles, providing six- and five-membered cyclic compounds, respectively. As 1,3-dipoles, diazoalkanes are usually able to give cycloadditions, which are HOMO-controlled by the dipole, the reactions proceeding faster with electron-poor alkenes.¹⁰ Thus we chose diazomethane as the dipole and the reaction was carried out by adding an excess of a freshly prepared ether solution of CH₂N₂ to the ribofuranoside **4e** (0.5 mmol), while stirring at room temperature. After 30 min the reaction was complete (TLC), and the ¹H NMR spectrum showed the presence of an unknown derivative as the main product. On the basis of 2D-NMR experiments, we assigned the C-pyrazoline structure **7e** to the new product (Scheme 6).



Scheme 6.

The correctness of the assigned regiochemistry was easily established by the presence of the CH–CH₂ system in the ¹H NMR spectrum, which has to be absent in the regioisomer. The *cis*-facial relationship of the two acetyl groups was given on the basis of the concerted mechanism, which represents the usual pathway working in 1,3-dipolar cycloaddition reactions.¹⁰ At present the configurations of the two new chiral centres have still to be assigned.

Nevertheless, considering the cycloadducts similar to the transition states, we tentatively assigned the 4'*R*,5'*R* configurations to **7e**, on the basis of comparison of calculated thermodynamical stabilities of the two isomers. Indeed, a MM⁺ conformational analysis assigned a lower energy to the *cis*-(*RR*)-**7e** of ca. 5 kcal/mol compared to the *cis*-(*SS*)-pyrazoline isomer **7e'** (Fig. 2). All the spectroscopic data were collected on the crude reaction mixture, and this shows that the cycloaddition proceeds with very high yields and with almost complete regio- and stereoselectivity.

We next tested the possibility of oxidizing the double bond of **4e** using diverse epoxidizing reagents in order to achieve a new C-nucleoside characterized by an epoxidic aglycone. Treatment at –20 °C of a crude glycoside **4e** with freshly prepared dimethyldioxirane (DMDO) did not work, even after a week. This was only to be expected considering the electron-poor character of the double bond together with the electrophilicity of the oxidant.¹¹ We then attempted to epoxidize the alkene moiety by using a *t*-BuOOH/NET₃ mixture, a nucleophilic oxidizing system usually used in the epoxidation of alkenes substituted with two or three electron-withdrawing groups.¹² Unlike DMDO, the hydroperoxide/triethylamine solution generally leads to a mixture of *cis*- and *trans*-epoxides, the mechanism involved not being concerted.¹² The reaction was carried out by adding 6 equiv of the epoxidizing system to a stirred dichloromethane solution of **4e** at room temperature. Surprisingly, the work-up of the reaction after 12 h did not afford trace of any stereoisomeric epoxide; instead it produced the diastereomeric *exo*-glycals *E,Z*-**8e** in very high yields (Scheme 7). The molar ratio of *E*- and *Z*-**8e** changed from an initial 9:1 to 3:2 in the course of time.

The structure of *exo*-glycals for the two observed products was assigned on the basis of spectral data. The stereochemistry was firstly assigned by correlating the large differences in chemical shifts of the AB system protons of CH₂CO group to the different spacial closeness to the sugar chiral centres (ca. 0.5 ppm in *E*-**8e** vs 1 ppm in *Z*-**8e**). The assigned stereochemistry was then confirmed by 2D-NOESY experiments run on the diastereomeric mixture. In particular, the 2D-spectrum showed a strong NOE correlation between the methylene protons with the larger AB system and the

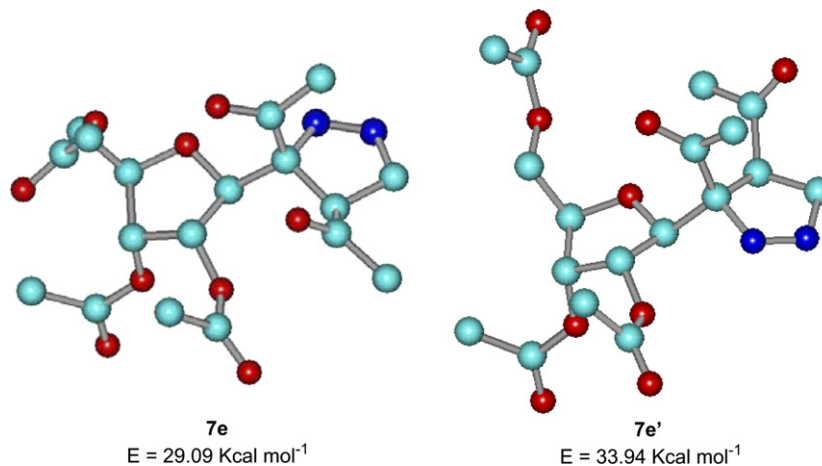
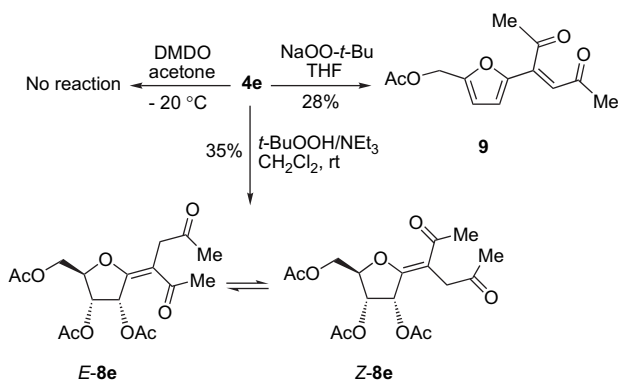


Figure 2. Conformational analysis (MM⁺) for the *cis*-(*RR*)-**7e** and (*SS*)-**7e'** pyrazolines.

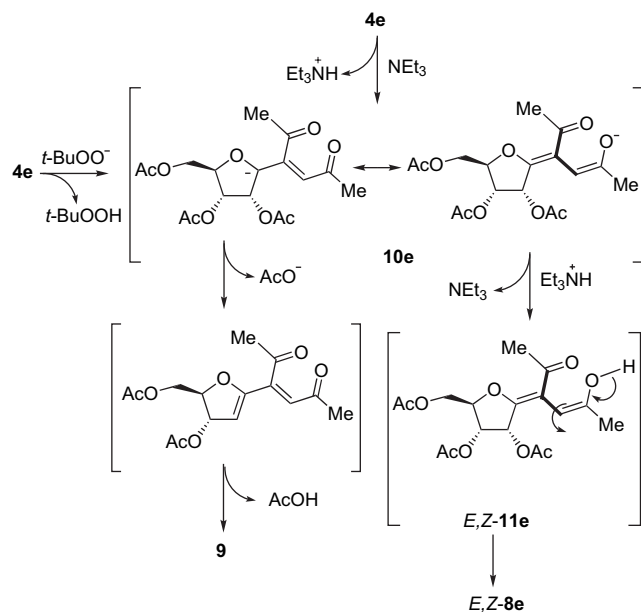


DMSO = dimethyldioxirane

Scheme 7.

doublet at δ 5.99 in agreement with the CH_2CO group at the same side of H-2, as occurs in the *Z*-configuration. Obviously, the same correlation was absent in the isomer *E*-**8e**.

This uncommon result shows that the acidity of the anomeric proton in **4e** is higher than that of the hydroperoxidic proton. This explains how triethylamine promotes the anion **10e** shown in **Scheme 8**. Due to the high conjugation of the system, subsequent re-protonation of the carbonyl oxygen should afford the undetected enol *E,Z*-**11e**, which tautomerizes into *Z*-**8e** and *E*-**8e**, the latter being initially the major isomer. The hypothesis was confirmed by control experiments. Indeed, when only NEt_3 was added to a solution of **4e**, compounds *Z*-**8e** and *E*-**8e** were the only products in the crude reaction mixture (^1H NMR).



Scheme 8.

The higher acidity of H-1 compared to *t*-BuOOH was demonstrated by the use of $\text{NaOO-}t\text{-Bu}$, freshly prepared by adding 1 equiv of NaH to the hydroperoxide at $0\text{ }^\circ\text{C}$ in anhydrous THF.¹³ With this reagent, the epoxidation reaction was still overcome by the acid–base reaction but surprisingly the furan **9** was formed (**Scheme 7**). The explanation

may be that, due to the absence of an acid–base equilibrium, the fate of the anion **10e** is different from that previously observed in the presence of mild base NEt_3 . It undergoes deacetylation of the sugar ring, the second elimination being very fast owing to the aromatization of the intermediate dihydrofuran system (**Scheme 8**).

It is noteworthy that deacetylation did not occur whether starting from furan **1e** or from 1,2,3,5-tetra-*O*-acetyl- β -D-ribofuranose. Thus the electron-poor aglycone in **4e** should be responsible for the two observed reactions in that it increases the H-1 acidity, which represents the drawing force.

Although it was not possible to synthesize the planned epoxide, the above results illustrate the synthetic potential of the photooxygenation procedure applied to the sugar-furans **1**. They also highlight the high reactivity of unsaturated ribofuranoside systems such as **4e**, leading to a wide range of differently functionalized compounds, which in turn can be used as starting material for more complex glycosyl derivatives.

The synthesis of the new functionalized *exo*-glycals **8e** is of interest both for the potential biological activity¹⁴ and for their synthetic application in producing pharmacologically active derivatives.¹⁵

Moreover, the work demonstrated the use of glycosides with α,β -unsaturated systems, such as compound **4e**, in [3+2] dipolar cycloadditions towards suitable 1,3-dipoles. This provides an easy access to C-nucleosides of pharmacological interest. Indeed, the reaction of **4e** with diazomethane leads regio- and stereoselectively to the novel pyrazoline C-nucleoside **7e**, which is structurally related to pyrazole C-nucleosides, compounds widely used for their pharmacological properties.¹⁶

3. Experimental

3.1. General

Nuclear magnetic resonance (NMR) spectra were recorded at 500 MHz for [^1H] and 125 MHz for [^{13}C] on a Fourier Transform NMR Varian 500 Unity Inova spectrometer. The carbon multiplicity was evidenced by DEPT experiments. The proton couplings were evidenced by ^1H – ^1H COSY experiments. The heteronuclear chemical shift correlations were determined by HMQC and HMBC pulse sequences. ^1H – ^1H proximities through space within a molecule were determined by NOESY. Analytical TLC was performed on pre-coated silica gel plates (Macherey-Nagel) with 0.2 mm film thickness. Column chromatography was performed on silica gel (Macherey-Nagel). Reagent-grade commercially available reagents and solvents were used.

3.1.1. Synthesis of 2',5'-dimethyl-3'-(2,3,5-tri-*O*-acetyl- β -D-ribofuranosyl)furan **1e.** To a stirred solution of 2,3,5-tri-*O*-acetyl-1-*O*-(acetyl)- β -D-ribofuranose (320 mg, 1 mmol) in dry CH_2Cl_2 (10 mL) under argon and in the presence of molecular sieves 2,5-dimethylfuran (96 mg, 1 mmol) and, successively, a dichloromethane solution of SnCl_4 (1 M,

16 mL) were added. The resulting mixture was stirred at room temperature for 3 h. The reaction was then quenched by saturated solution of NaHCO_3 (5 mL). The organic layer was separated and the aqueous layer was extracted with CHCl_3 (3×10 mL). The combined organic extracts were washed with brine and dried over anhydrous MgSO_4 . After filtration the solvent was removed under reduced pressure. ^1H NMR spectrum showed that glycosyl furan **1e** was present as a mixture of α and β -anomers in ca. 1:8 molar ratio.¹⁷ Silica gel chromatography using *n*-hexane/EtOAc (85:15, v/v) as eluent afforded glycosyl furan β -**1c** in 35% yield: ^1H NMR (CDCl_3) δ 2.04 (s, 3H, CH_3CO_2), 2.10 (s, 6H, $2\text{CH}_3\text{CO}_2$), 2.20 (s, 3H, CH_3 -2'), 2.24 (s, 3H, CH_3 -5'), 4.21 (m, 2H, H-4 and H-5_A), 4.31 (dd, $J=13.4$, 4.6 Hz, 1H, H-5_B), 4.81 (d, $J=7.0$ Hz, 1H, H-1), 5.08 (dd, $J=7.0$, 5.7 Hz, 1H, H-2), 5.27 (dd, $J=5.7$, 4.1 Hz, 1H, H-3), 5.86 (s, 1H, H-4'); ^{13}C NMR (CDCl_3) δ 15.9 (q, CH_3 -2'), 16.8 (q, CH_3 -5'), 20.6 (q, CH_3CO_2), 20.7 (q, CH_3CO_2), 20.8 (q, CH_3CO_2), 63.8 (t, C-5), 71.7 (d, C-3), 74.8 (d, C-2), 75.2 (d, C-1), 79.6 (d, C-4), 104.2 (d, C-4'), 116.5 (s, C-3'), 148.4 (s, C-2'), 150.5 (s, C-5'), 169.6, 169.7 and 170.5 (3s, 3CO_2).

3.1.2. One-pot synthesis of β -furanoside **4e** by MB-sensitized photooxygenation of β -**1e** and Et_2S reduction.

A 0.02 M solution of β -**1e** (0.25 mmol) in dry CH_2Cl_2 was irradiated at -20°C with a halogen lamp (General Electric, 650 W) in the presence of methylene blue (MB, 1×10^{-3} mmol) while dry oxygen was bubbled through the solution. The progress of the reaction was checked by periodically monitoring the disappearance of **1e** (TLC or ^1H NMR). When the reaction was complete (90 min), a pre-cooled dichloromethane solution of Et_2S (2 equiv) was added to the photooxygenation mixture. The latter was kept at -20°C for 1 h and then transferred at room temperature. When the reduction was complete (2 h, ^1H NMR), the solvent and unreacted Et_2S were removed under reduced pressure. The residue was taken up in Et_2O , the suspension filtered to remove the insoluble sensitizer (MB) and the filtrate evaporated to give crude *cis*- β -**4e** (yield >90%). Silica gel chromatography on a short column gave pure compound **4e** in 70% yield.^{9,18}

Compound **4e**: ^1H NMR (CDCl_3) δ 2.07 (s, 3H, CH_3CO_2), 2.08 (s, 3H, CH_3CO_2), 2.13 (s, 3H, CH_3CO_2), 2.26 (s, 3H, CH_3CO), 2.29 (s, 3H, CH_3CO), 4.14 (dd, $J=12.1$, 3.7 Hz, 1H, H-5_A), 4.20 (m, 1H, H-4), 4.35 (dd, $J=12.1$, 3.0 Hz, 1H, H-5_B), 4.60 (dd, $J=6.0$, 1.2 Hz, 1H, H-1), 5.22 (m, 2H, H-2 and H-3), 6.31 (d, $J=1.2$ Hz, 1H, H-3'); ^{13}C NMR (CDCl_3) δ 20.4 (q, CH_3CO_2), 20.5 (q, CH_3CO_2), 20.8 (q, CH_3CO_2), 30.5 (2q, $2\text{CH}_3\text{CO}$), 62.8 (t, C-5), 71.4 (d, C-3), 73.7 (d, C-2), 80.5 (d, C-4), 80.9 (d, C-1), 124.4 (d, C-3'), 153.9 (s, C-2'), 169.3 (s, CO_2), 169.6 (s, CO_2), 170.6 (s, CO_2), 196.5 (s, C-4'), 200.4 (s, C-1').

In the subsequent reactions, crude *cis*- β -**4e** was used without further purification since control experiments showed that the presence of non-volatile Et_2SO was irrelevant.

3.1.3. Treatment of **4e with diazomethane.** To the crude ribofuranoside **4e** (0.25 mmol) in dry Et_2O was added a diethyl ether solution of freshly prepared CH_2N_2 (ca. 1 mmol) and the resulting mixture was kept at room temperature under

stirring. After 1 h the reaction was complete and the ^1H NMR showed the presence of pyrazoline **7e** as the only identifiable product (ca. 80%). After evaporation of the solvent, TLC chromatography of the residue (*n*-hexane/ Et_2O , 1:4, v/v) afforded pure **7e** (50%; 40% based on starting furan **1e**).

cis-(*R,R*)-**7e**: ^1H NMR (CDCl_3) δ 2.06, 2.08, 2.14 (3s, 9H, $3\text{CH}_3\text{CO}_2$), 2.25 and 2.41 (2s, 6H, $2\text{CH}_3\text{CO}$), 3.26 (dd, $J=8.8$, 3.8 Hz, 1H, H-5'), 4.15 (m, 1H, H-4), 4.23 and 4.30 (2dd, $J=12.6$, 4.4, 3.3 Hz, 2H, H-2-5), 4.55 (dd, $J=18.1$, 8.8 Hz, 1H, H-4'_A), 4.67 (d, $J=6.1$ Hz, 1H, H-1), 4.76 (dd, $J=18.1$, 3.8 Hz, 1H, H-4'_B), 4.87 (t, $J=6.1$ Hz, 1H, H-2), 5.05 (dd, $J=6.1$, 5.5 Hz, 1H, H-3); ^{13}C NMR (CDCl_3) δ 20.5 (q, $2\text{CH}_3\text{CO}_2$), 20.8 (q, CH_3CO_2), 31.1 (q, CH_3CO), 32.4 (q, CH_3CO), 46.2 (d, C-5'), 62.5 (t, C-5), 70.5 (d, C-2), 71.2 (d, C-3), 79.8 (d, C-4), 81.6 (t, C-4'), 82.5 (d, C-1), 110.9 (s, C-1'), 169.1 (s, CO_2), 169.3 (s, CO_2), 173.4 (s, CO_2), 203.9 (s, CO), 208.0 (s, CO).

No other isomer was detected either by careful NMR analysis of the crude reaction mixture or by chromatography, and only polymeric material was found in addition to *cis*-(*R,R*)-**7e**.

3.1.4. Treatment of **4e** with $\text{NET}_3/t\text{-BuOOH}$.

12 Triethylamine (6 equiv) and *tert*-butyl hydroperoxide (6 equiv)¹⁹ were added to a 0.1 M solution of crude ribofuranoside **4e** (1 mmol) in dry dichloromethane, and the resulting solution was kept at room temperature under stirring. When the reaction was complete (12 h, TLC), the mixture was partitioned between water and dichloromethane and the aqueous layer was extracted with further dichloromethane. The combined organic layers were then dried over Na_2SO_4 . After evaporation of the solvents and unchanged reactants, the residue was chromatographed on silica gel eluting with *n*-hexane/ AcOEt (2:3, v/v) and AcOEt , which afforded a mixture of *E*- and *Z*-**8e** in ca. 9:1 molar ratio, respectively (35%; 23% based on the starting furan). The ^1H NMR recorded on the same mixture kept at room temperature for 24 h showed that the molar ratio was changed to 3(*E*):2(*Z*).

E-**8e**: ^1H NMR (CDCl_3) δ 2.05, 2.08, 2.13, 2.16 and 2.20 (5s, 15H, $5\text{CH}_3\text{CO}$), 3.48 and 3.55 (2d, $J=17.5$ Hz, CH_2CO), 4.09 (m, 1H, H-5_A), 4.54 (m, 2H, H-4 and H-5_B), 5.37 (dd, $J=8.2$, 6.0 Hz, 1H, H-3), 6.31 (d, $J=6.0$ Hz, 1H, H-2); ^{13}C NMR (CDCl_3) δ 20.4 (q, CH_3CO_2), 20.5 (q, CH_3CO_2), 20.8 (q, CH_3CO_2), 28.7 (q, CH_3CO), 29.5 (q, CH_3CO), 41.5 (t, CH_2CO), 61.8 (t, C-5), 69.3 (d, C-2), 69.4 (d, C-3), 79.4 (d, C-4), 111.9 (s, C=), 162.3 (s, O-C=), 169.1 (s, CO_2), 169.3 (s, CO_2), 170.4 (s, CO_2), 196.7 (s, CO), 205.0 (s, CO).

Z-**8e** (in 2:3 mixture with *E*-**8e**): ^1H NMR (CDCl_3) δ 2.41 (s, 3H, CH_3CO), 3.22 and 3.33 (2d, $J=17.5$ Hz, CH_2CO), 4.25 (dd, $J=12.4$, 4.4 Hz, 1H, H-5_A), 4.54 (partially overlapped to the signal of *E*-**8e**, H-5_B), 4.75 (m, 1H, H-4), 5.26 (dd, $J=8.1$, 5.9 Hz, 1H, H-3), 5.99 (d, $J=6.0$ Hz, 1H, H-2); ^{13}C NMR (CDCl_3) δ 29.6 (q, CH_3CO), 31.9 (q, CH_3CO), 41.4 (t, CH_2CO), 61.1 (t, C-5), 69.0 (d, C-2), 70.3 (d, C-3), 81.7 (d, C-4), 111.7 (s, C=), 161.0 (s, O-C=), 169.2 (s, CO_2), 169.4 (s, CO_2), 170.3 (s, CO_2), 197.2 (s, CO), 205.7 (s, CO). The signals not reported are overlapped to those of *E*-**8e**.

3.1.5. Treatment of 4e with NEt₃. NEt₃ (1 equiv) in CDCl₃ (0.5 mL) was added to a solution of crude ribofuranoside **4e** in the same solvent (0.5 mL), and the resulting mixture was monitored by ¹H NMR. After 10 min, the spectrum showed the presence of the *E*- and *Z*-**8e** mixture in ca. 9(*E*):1(*Z*) molar ratio.

3.1.6. Treatment of 4e with NaOO-*t*-Bu.¹³ A suspension of oil-free NaH (washed with hexane and dried) (50 mg, 2 mmol) in dry THF (20 mL) under the atmosphere of argon was cooled to 0 °C and 1.2 mL (6 equiv) of *t*-BuOOH (solution 5.0 M in decane) was added. The resulting mixture was warmed under stirring to 25 °C for 30 min, then cooled to 0 °C and a solution of the crude ribofuranoside **4e**, previously dried on P₂O₅ (95 mg, 0.25 mmol) in dry THF (10 mL), was added dropwise. The reaction mixture was stirred at 0 °C until the disappearance of compound **4e** (16 h, by TLC). Then, the solvents were removed under reduced pressure and the crude mixture was chromatographed on silica gel, using *n*-hexane/EtOAc (4:1) as eluent, to give furan **9** (28%; 22% based on the starting furan): ¹H NMR (CDCl₃) δ 2.11 (3H, s, CH₃CO₂), 2.32 and 2.47 (6H, 2s, 2COCH₃), 5.07 (2H, s, CH₂), 6.48 (2H, br s, H-3 and H-4), 6.61 (1H, s, CH); ¹³C NMR (CDCl₃) δ 20.5 (q, CH₃CO₂), 30.1 (q, CH₃CO), 30.9 (q, CH₃CO), 67.2 (t, CH₂), 114.2 (d, C-3), 116.2 (d, C-4), 118.9 (d, CH), 148.5 and 148.5 (2s, C-5 and C=), 152.1 (s, C-2), 169.3 (s, CO₂), 197.4 (s, CO), 202.6 (s, CO).

Acknowledgements

Financial support from MIUR (FIRB 2003–2005 and PRIN 2006–2008) is gratefully acknowledged. NMR experiments were run at the Centro di Metodologie Chimico-Fisiche, Università di Napoli Federico II.

References and notes

1. Simons, C. *Nucleoside Mimetics Their Chemistry and Biological Properties*; Gordon and Breach Science: Australia, Canada, 2001; (b) Peasley, K. *Med. Hypotheses* **2000**, *55*, 408.
2. See for example: Wu, Q.; Simons, C. *Synthesis* **2004**, 1533.
3. Postema, H. D. M. *C-Glycoside Synthesis*; CRC: London, 1995; (b) Du, Y.; Linhardt, R. J. *Tetrahedron* **1998**, *54*, 9913.
4. (a) Iesce, M. R.; Cermola, F.; Temussi, F. *Curr. Chem. Org.* **2005**, *9*, 109; (b) Matsumoto, M. *Singlet Oxygen*; Frimer, A. A., Ed.; CRC: Boca Raton, 1985; Vol. II, pp 205–272; (c) Bloodworth, A. J.; Eggelte, H. J. *Singlet Oxygen*; Frimer, A. A., Ed.; CRC: Boca Raton, 1985; Vol. II, pp 93–203.
5. Iesce, M. R. *Synthetic Organic Photochemistry*; Griesbeck, A. G., Mattay, J., Eds.; Marcel Dekker: New York, NY, 2005; Vol. 12, pp 299–363.
6. See for example: (a) Morgan, K. M. *Ann. Rep. Prog. Chem., Sect B: Org. Chem.* **2005**, *101*, 284; (b) Nicolaou, K. C.; Snyder, S. A.; Montagnon, T.; Vassilikogiannakis, G. *Angew. Chem., Int. Ed.* **2002**, *41*, 1668; (c) Wiest, O.; Houk, K. N. *Top. Curr. Chem.* **1996**, *183*, 1.
7. Scarpati, R.; Iesce, M. R.; Cermola, F.; Guitto, A. *Synlett* **1998**, 17; Gollnick, K.; Griesbeck, A. *Tetrahedron* **1985**, *41*, 2057.
8. Cermola, F.; Iesce, M. R.; Montella, S. *Lett. Org. Chem.* **2004**, *1*, 271.
9. Cermola, F.; Iesce, M. R.; Buonerba, G. *J. Org. Chem.* **2005**, *70*, 6503.
10. Regitz, M.; Heydt, H. *1,3-Dipolar Cycloaddition Chemistry*; Padwa, A., Ed.; Wiley: New York, NY, 1984; pp 393–558.
11. Singh, M.; Murray, R. W. *J. Org. Chem.* **1992**, *57*, 4263.
12. Graziano, M. L.; Iesce, M. R.; Scarpati, R. *Synthesis* **1984**, 66.
13. Fernandez de la Pradilla, R.; Castro, S.; Manzano, P.; Martin-Ortega, M.; Priego, J.; Viso, A.; Rodriguez, A.; Fonseca, I. *J. Org. Chem.* **1998**, *63*, 4954.
14. For some recent examples, see: Lin, C.-H.; Lin, H.-C.; Yang, W.-B. *Curr. Top. Med. Chem.* **2005**, *5*, 1431; Stolz, F.; Reiner, M.; Blume, A.; Reutter, W.; Schmidt, R. R. *J. Org. Chem.* **2004**, *69*, 665; Tatibouet, A.; Rollin, P.; Martin, O. R. *J. Carbohydr. Chem.* **2000**, *19*, 641.
15. Tailliefumier, C.; Chapleur, Y. *Chem. Rev.* **2004**, *104*, 263; Yang, W.-B.; Yang, Y.-Y.; Gu, Y.-F.; Wang, S.-H.; Chang, C.-C.; Lin, C.-H. *J. Org. Chem.* **2002**, *67*, 3773; Lay, L.; Nicotra, F.; Panza, L.; Russo, G.; Sello, G. *J. Carbohydr. Chem.* **1998**, *17*, 1269; Link, J. T.; Gallant, M.; Danishefsky, S. J.; Huber, S. *J. Am. Chem. Soc.* **1993**, *115*, 3782.
16. See for example Elgemeie, G. H.; Zaghary, W. A.; Amin, K. M.; Nasr, T. M. *Nucleosides Nucleotides Nucleic acids* **2005**, *24*, 1227; Nishiyama, Y.; Nishimura, N.; Kuroyanagi, N.; Maeba, I. *Carbohydr. Res.* **1997**, *300*, 183.
17. The β-anomer **1e** was the main product (β:α=8:1) owing to the neighbouring group of the acetyl at C-2 of the glycosyl donor.
18. Diacetylenes may undergo polymerization, mainly on contact with chromatographic adsorbents (Graziano, M. L.; Iesce, M. R.; Scarpati, R. *Synthesis* **1983**, 125).
19. High equivalents of the reactants were used to balance those oxidating diethyl sulfoxide present in the crude reaction mixture.

Reactions of urocanic acid (UCA) methyl esters with singlet oxygen and 4-methyl-1,2,4-triazoline-3,5-dione (MTAD)

Roberto Roa and Kevin E. O'Shea*

Department of Chemistry and Biochemistry, Florida International University, Miami, FL 33199, United States

Received 12 June 2006; revised 30 July 2006; accepted 30 July 2006

Dedicated in memory of Professor Christopher S. Foote

Abstract—Singlet oxygen adds to the imidazole ring of *cis*- and *trans*-methyl urocanate (MUC) to yield the corresponding 2,5-endoperoxides, which are modestly stable at low temperature but decompose upon warming to form complex reaction mixtures. MTAD, a singlet oxygen mimic, reacts with *cis*- and *trans*-MUC to yield stereospecific [4+2] reaction products involving the olefinic side chain and the C₄–C₅ double bond of the imidazole ring. *trans*-MUC forms a 1:2 MTAD adduct while the *cis* isomer yields only the 1:1 adduct at 25 °C. The stereospecificity and absence of MeOH trapping adducts indicate that these reactions may not involve open or trappable dipolar intermediates. © 2006 Elsevier Ltd. All rights reserved.

1. Introduction

3-(1*H*-Imidazol-4(5)-yl)-2-propenoic acid commonly referred to as urocanic acid (UCA) is a metabolite of histidine and is present in the stratum corneum of the human skin. UCA, produced naturally as the *trans* isomer, accumulates in the upper layers of the epidermis and isomerizes to *c*-UCA upon absorption of UV light^{1,2} (Fig. 1). *t*-UCA was found to absorb ultraviolet B light and thus considered to be a natural sunscreen against harmful UV rays. This led to the addition of UCA to sunscreens and skin lotions to help prevent skin cancer and skin related diseases. However, subsequent studies indicated that *t*-UCA can act as an initiator of immunosuppression, which may be critical to UV-induced pathogenesis of skin cancer and other cutaneous diseases.^{3,4}

It was recently reported that photoexcited *t*-UCA can lead to the formation of reactive oxygen species, which are linked to a number of diseases and disorders, i.e., enzyme inactivation,

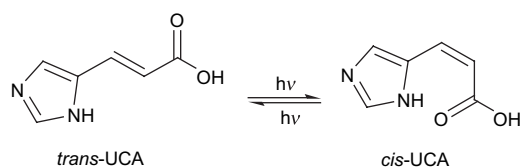


Figure 1. Photoisomerization of UCA.

Keywords: Photooxygenation; Singlet oxygen; Endoperoxides; Urocanic acid.

* Corresponding author. Tel.: +1 305 348 3968; fax: +1 305 348 3772; e-mail: osheak@fiu.edu

mutations, premature aging, DNA damage, and respiratory problems.⁵ The oxidative products of UCA are proposed to be responsible for UV-induced immune suppression. In 2002, Elton and Morrison confirmed that the irradiation of UCA with monochromatic light at 351 nm produces singlet oxygen.⁶ They concluded that UCA is a better scavenger than generator of singlet oxygen and may play an important role as an antioxidant. Colorimetric tests (EM Quant peroxide strip) on the reaction products of singlet oxygen with UCA showed the presence of peroxides,⁶ but detailed product studies have not been reported. UCA-singlet oxygen products catalyze further photo-destruction of UCA and UCA peroxides can be major contributors to photo-initiated nicking of plasmid DNA.⁶

The reactions of singlet oxygen with imidazole ring containing systems, especially histidine and guanine analogs, have received considerable attention. Early studies on the photo-oxygenation of histidine demonstrated that complex reaction mixtures are produced, i.e., the reaction of singlet oxygen with *N*-benzoyl histidine leads to the formation of 17 products.⁷ Wasserman and Lipshutz conducted extensive studies on the reactions of singlet oxygen with substituted imidazoles, proposed the involvement of 2,5-endoperoxides, and reported two main pathways of oxidation depending on the substitution pattern of the imidazole ring.⁸ When the imidazole ring bears a hydrogen atom at the 2- and/or 5-position, a carbonyl group is produced at that specific site. In the absence of a proton at the 2- or 5-position the formation of the dioxetane by [2+2] addition of singlet oxygen to the C₄–C₅ bond in the imidazole appears to be operative. Ryang and Foote later reported the direct observation of imidazole 2,5-endoperoxides as products of singlet oxygen.⁹

Singlet oxygenation of guanine and its nucleosides (guanosine) have received considerable attention because of the implications on the function of DNA and its importance during photodynamic therapy (PDT) used for the treatment of malignant tumors.^{10,11} Because of the limited solubility of guanine substrates, the instability of intermediates and complexity of the product mixtures, the mechanism of photosensitized oxidation of guanine and its nucleosides was unclear until recently.¹¹ Foote and co-workers used a variety of substituted guanosine adducts, isotopic labeling, and low temperature NMR to suggest that singlet oxygenation of guanosine involves a series of reactive intermediates, including endoperoxides, hydroperoxides, and dioxiranes.^{11b,c} The reaction pathways are highly sensitive to solvent effects and the substitution pattern, i.e., only the C-8 methylated substrate reacts to form an observable endoperoxide, which collapses to yield singlet oxygen and the starting substrate (Fig. 2). Kang and Foote conducted detailed product studies on isotopically labeled imidazole ring systems and demonstrated that the reaction pathways are dramatically influenced by N-alkylation of the parent compound¹² (Fig. 2).

The photooxidation of UCA may be a main pathway for premature aging, UV-induced immune suppression, and skin cancer,^{13,14} yet the mechanisms and products of photooxidation have not been clearly established. While previous studies on the singlet oxygenation of imidazole ring systems provide tremendous insight about the possible reaction pathways of singlet oxygen with UCA, the presence of the conjugated enone side chain in UCA may lead to different singlet oxygen reactivities.

Because of the insoluble nature of UCA in organic solvents, the methyl ester, MUC, was used as a model for UCA. MUC is modestly soluble in the organic solvents required for low temperature NMR studies. MUC is expected to exhibit the same reactivity as UCA toward singlet oxygen. We report herein singlet oxygenation of *cis*- and *trans*-MUC yields 2,5-endoperoxides, which are modestly stable at low temperature but decompose at room temperature to afford complex

product mixtures. Given the unstable nature of the endoperoxides and the complexity of the reaction product mixtures we also studied the reactions of MUC with MTAD, a singlet oxygen mimic. Surprisingly, MTAD and singlet oxygen exhibit dramatically different reactivities toward MUC.

2. Results and discussion

2.1. Reactions of singlet oxygen with MUC

Since the solubility of UCA in organic solvents is too low to conduct detailed NMR studies, *trans*-UCA was converted to the corresponding methyl, *n*-butyl, and *tert*-butyl esters, using acid promoted esterification. *t*-MUC showed the best solubility among the esters in the organic solvents commonly used for low temperature NMR. *t*-MUC is easily isomerized to *c*-MUC by irradiation with 254 nm light under argon-saturated conditions.¹⁵ The *cis* isomer was purified using standard flash column chromatography.

For the typical experiment, MUC was dissolved in 0.5–1 mL of the appropriate NMR solvent (CD_2Cl_2 , acetone- d_6 , CD_3CN , or CDCl_3) along with Rose bengal, the singlet oxygen sensitizer. The solution was transferred to a 5 mm NMR tube and placed in ice water in a windowed Dewar. The sample was gently purged with oxygen and irradiated using 200 W Hg–Xe lamp. Pyrex glass was employed to filter light ≤ 320 nm. Control experiments showed no conversion of the *cis*- or *trans*-MUC in the absence of oxygen (argon saturated) or by direct photolysis (in the absence of Rose bengal). The photosensitized oxidation of *t*-MUC, monitored by ^1H NMR, was complete within 5 min and continued irradiation did not change the product distribution.

Likely pathways for the reaction of the MUC with singlet oxygen are illustrated below (Fig. 3). They include [4+2] cycloaddition to the imidazole ring to form a 2,5-endoperoxide **1**, [4+2] across the double bond of the side chain

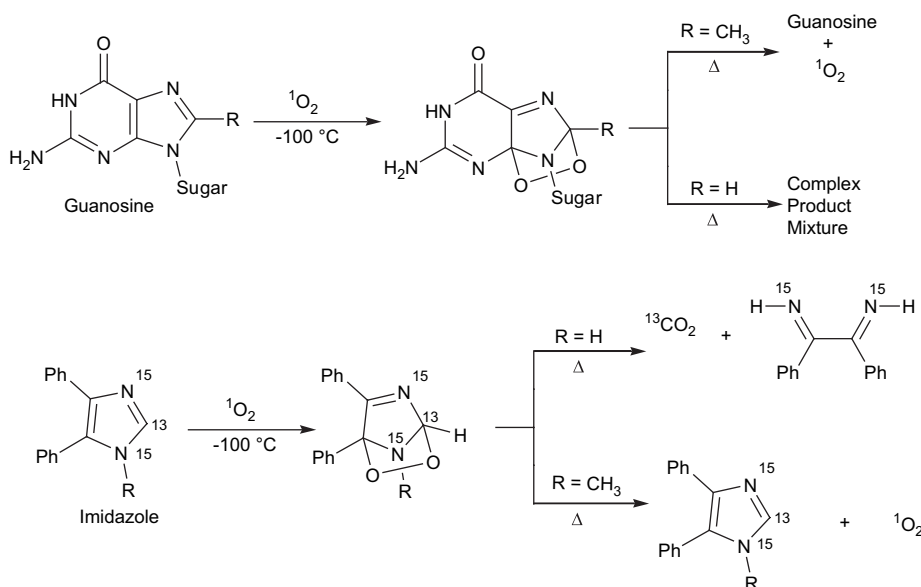


Figure 2. Singlet oxygenation products of guanosine¹¹ and labeled imidazole.¹²

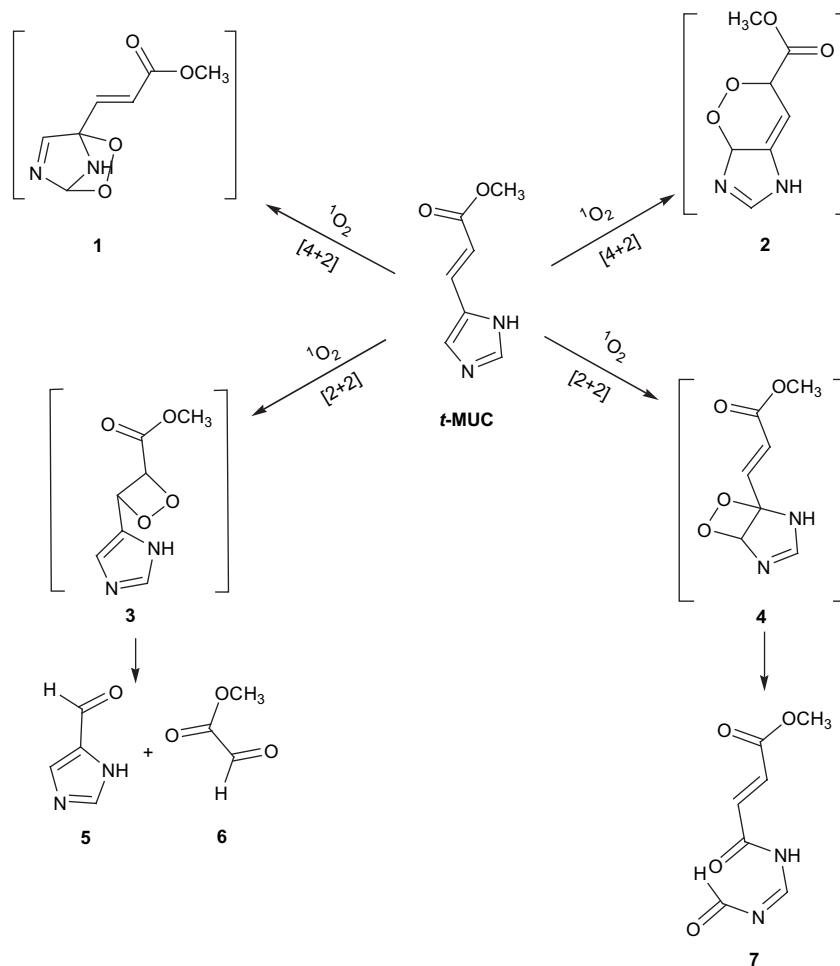


Figure 3. Likely pathways for the reaction of singlet oxygen with *t*-MUC.

and the C_4 – C_5 double bond of the imidazole ring to yield endoperoxide **2**, and [2+2] cycloadditions to the side chain to form dioxetane **3** or across the C_4 – C_5 double bond of the ring to form **6**. Dioxetanes generally collapse to the corresponding carbonyl compounds at room temperature.

The reaction products of singlet oxygen and *t*-MUC at room temperature exhibit a nearly continuous series of overlapping ^1H NMR peaks between 6 and 8 ppm. The complex nature of the ^1H NMR spectrum indicates a considerable number of products formed at room temperature. The [2+2] addition to the side chain would result in the formation of the dioxetane **3**, which will collapse to **5** and **6**. ^1H NMR and GC–MS analyses of the reaction solution show no evidence of **5** or **6**, thus indicating the [2+2] reaction does not occur at the side chain of *t*-MUC under our experimental conditions. The room temperature ^1H NMR spectrum also does not correspond to endoperoxide **1** in accordance with chemical shifts reported for analogous compounds.¹² To test for the formation of endoperoxide **2** we subjected the reaction mixture at low temperature to treatment with cobalt(II) tetraphenylporphyrin, which is known to convert endoperoxides to furans via loss of water.¹⁶ Subsequent ^1H NMR and GC–MS analyses showed no evidence that the corresponding furan was formed. These results indicate that singlet oxygen does not react at the side chain of *t*-MUC.

Given the complex nature of the product mixtures observed at room temperature and the fact that endoperoxides and dioxetanes often decompose at room temperature the photooxygenation and ^1H NMR characterization were conducted at low temperature. The NMR tube containing the reaction solution was kept at -78°C throughout the photooxygenation (dry ice/acetone bath in a windowed Dewar). The NMR tube was transferred to a pre-cooled NMR magnet and the proton spectrum collected at -78°C . The solution was gradually warmed within the NMR magnet and proton spectra collected at -40 , -20 , 0 , and 25°C . Dramatic differences were observed in the spectra obtained at 0 and 25°C . The predominant peaks in the low temperature ^1H NMR spectrum are singlets at 8.02 and 4.90 ppm (1H/ea); a pair of doublets at 6.80 (1H) and 6.51 ppm (1H) with $J=16.1$ Hz indicating the trans double bond is not oxidized; and a methoxy resonance at 3.63 ppm. While solubility limitations at low temperatures did not allow for acquisition of a carbon NMR spectrum, the proton spectrum for the reaction mixture at low temperature is consistent with **1** *trans* based on the literature values for the endoperoxide of 1-methylimidazole (Fig. 4). There are no peaks indicating the presence of dioxetane products down to -78°C .

Singlet oxygenation of *c*-MUC was also conducted at low temperature. The ^1H NMR of the product is shown below (Fig. 5). The characteristic ^1H NMR peaks are as

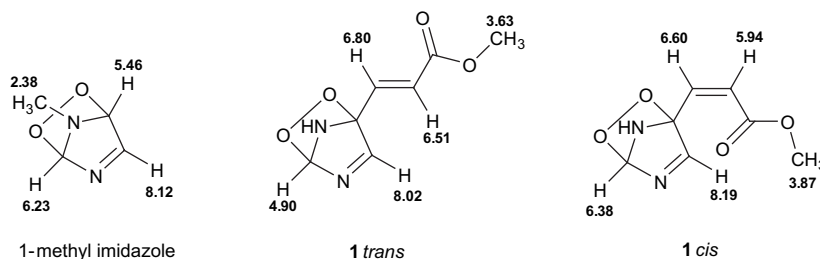


Figure 4. Comparison of the ^1H NMR chemical shifts for the 2,5-endoperoxides of 1-methyl imidazole⁹ with **1 trans** and **1 cis**.

follows: 8.19 (1H) and 6.38 (1H) ppm, a pair of doublets at 6.57 (1H) and 5.94 (1H) ppm with $J=11.6$ Hz indicating the *cis* double bond is not oxidized, and a singlet at 3.87 (3H) corresponding to the methoxy resonance. The results are consistent with the formation of the endoperoxide formed by [4+2] addition of singlet oxygen to the imidazole ring.

A number of 2,5-endoperoxides decompose via retro Diels–Alder reaction to yield starting material and singlet oxygen. Tetramethylethylene singlet oxygen trapping experiments indicate the endoperoxides of MUC do not decompose to singlet oxygen upon warming from -78 °C to room temperature. The formation of the endoperoxides can occur by concerted or non-concerted processes.¹⁷ To test for the possible involvement of dipolar intermediates, 3 equiv of methanol was added to the solvent prior to running the reaction. Under these conditions the formation of methanol adducts indicates the involvement of dipolar intermediates.^{18,19} The ^1H NMR spectra of the reaction run in the presence of MeOH did not indicate the formation of MeOH adducts or any change in the product distribution at -78 and 0 °C. While the presence of MeOH adducts would clearly indicate the involvement of dipolar intermediates, under our experimental conditions, where MeOH (3 equiv) was added to a relatively non-polar solvent a dipolar intermediate may be too short lived to be trapped. There was also no significant change in the product distribution using CD_2Cl_2 , acetone- d_6 , CDCl_3 , or CD_3CN as solvents, suggesting that the polar intermediates may not involve in the product forming reaction pathways.

2.2. Reactions of MTAD

Due to the instability of the endoperoxides and limited solubility of MUC we were unable to further characterize the complex reaction mixtures produced from singlet oxygenation. With this in mind we chose to study the reactions of MUC with MTAD, a singlet oxygen mimic. MTAD, a powerful electrophile, undergoes the same type of reactions as singlet oxygen, namely [4+2], [2+2], and the ene reactions.²⁰ We expected analogous products for the reactions of MTAD and singlet oxygen with MUC, but unlike the peroxide products formed from singlet oxygen, the expected [2+2] and [4+2] products from MTAD (Fig. 6) should be stable at room temperature and readily characterized using NMR.

t-MUC was dissolved in 0.5–1 mL of CDCl_3 in an NMR tube and 1 equiv of MTAD was added. Upon addition of MTAD to the *t*-MUC solution, the color immediately turns from red to deep purple, but quickly fades to a very light pink. Positive mode APCI-MS established the molecular ion, $\text{MH}^+=266$, indicating the addition of 1 equiv of MTAD. The proton NMR spectrum of the product shows a clean set of three triplets at 5.75, 5.49, and 5.24 ppm (1H each), with coupling constants ~ 3.4 Hz, as well as singlets at 7.45 (1H), 3.05 (3H), and 3.75 ppm (3H). The spectrum does not contain peaks in the olefinic region with a characteristic *trans* coupling constant. The absence of *trans* olefinic peaks rules out the presence of **8** and **9**. The diazetidine product, **11** would exhibit a pair of doublets ~ 5.0 – 6.0 ppm with characteristic

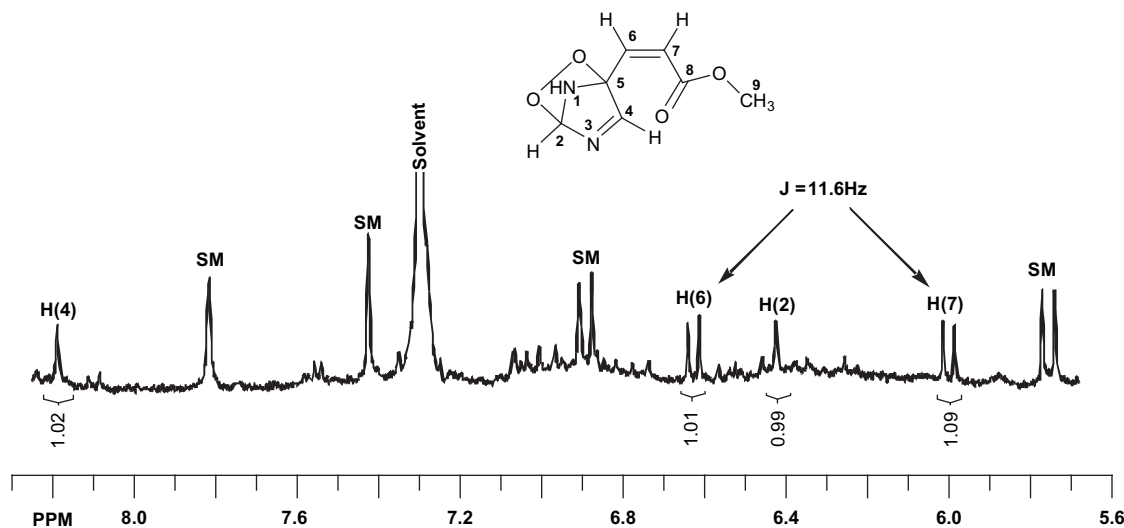


Figure 5. ^1H NMR spectrum of the products from reaction of singlet oxygen of *c*-MUC at 0 °C in CDCl_3 .

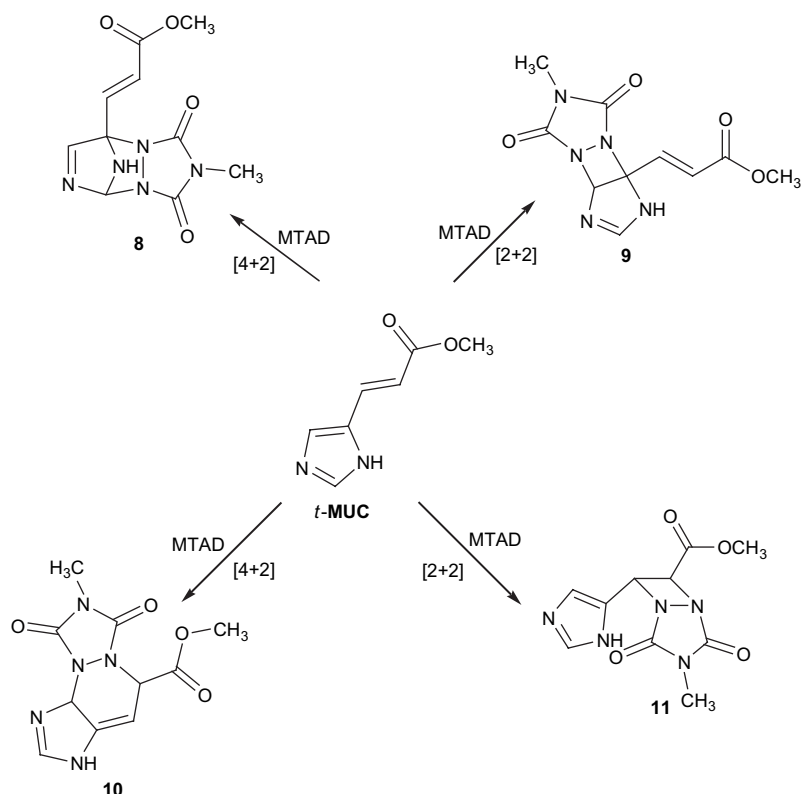


Figure 6. Likely products from the reactions of MTAD with *t*-MUC.

trans coupling constants^{20c} as well as singlets corresponding to the imidazole ring hydrogens. The ¹H NMR spectrum does not possess peaks consistent with diazetidines. The [4+2] addition of MTAD across the olefinic side chain and the C₄-C₅ double bond of the imidazole ring yields **10**. While analogous [4+2] reactions of MTAD with styrenes have been reported,^{21,22} the reaction product of MUC is not expected to lead to the observed set of triplets in the ¹H NMR spectrum. The H-shift product presented below (Fig. 7) would lead to the re-aromatization of the imidazole ring system possessing –CHH'–CH''– set protons and may exhibit three triplets in the ¹H NMR spectrum.

To test the presence of such a product, low temperature experiments were monitored by ¹H NMR at –30 °C. No rearrangement of the product was observed upon warming to 25 °C. The initial product, however, does slowly degrade at room temperature. Carbon, DEPT, and ¹H–¹³C HETCOR NMR spectra were obtained at –30 °C. The DEPT spectra indicate that the reaction product does not contain any methylene groups ruling out the presence of the H-shifted product. Based on the NMR data summarized below (Figs. 8 and 9), we propose that the observed reaction product is **10**.

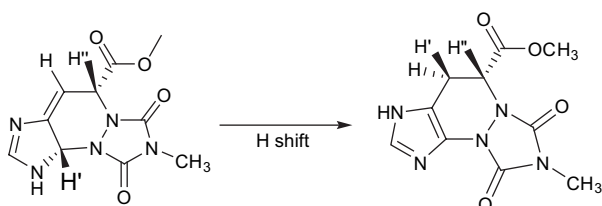


Figure 7. Potential H-shifted product of **10 cis**.

The reaction of *c*-MUC with MTAD was run at –30 °C and exhibits the same color changes as the reaction of *t*-MUC. The proton NMR spectrum of the product contains three doublets of doublets at 5.93, 5.88, and 5.29 ppm (1H each) as shown in Figure 8. The spectrum indicates a single product and is consistent with, **10 trans**, the [4+2] cycloaddition of MTAD across the double bond of the side chain and the C₄-C₅ double bond of the imidazole ring.

The ¹H NMR spectra of the MTAD products from the *cis*- and *trans*-MUC indicate each isomer leads to a single diastereomer (likely enantiotopic pairs). The observation of three clean triplets in the proton NMR spectrum of the *t*-MUC product and three doublets of doublets from *c*-MUC product is rationalized in terms of long range and different coupling constants due to geometrical differences. The results are in accordance with the Woodward–Hoffmann rules, with MTAD reacting in a disrotatory fashion to yield the *cis* or *trans* product depending on the stereochemistry of the starting material. One might expect **10** would be susceptible to a retro Diels–Alder transformation. However, upon heating to 50 °C they decompose yielding complex mixtures, which do not include MUC.

Addition of MTAD to a solution containing **10 cis** results in its disappearance with the clean formation of a secondary product. The ¹H NMR spectrum of the secondary product has the following characteristics: a singlet at 7.93 ppm (1H), a pair of doublets at 6.01 and 5.37 ppm (1H each, *J* = 1.6 Hz), singlets at 3.80, 3.10, and 3.03 ppm (3H each). The ¹H and ¹³C NMR spectra indicate a second equivalent of MTAD reacts via an ene reaction to form a stable 2:1 adduct. The reaction of MTAD with β,β-dimethyl-*p*-methoxy

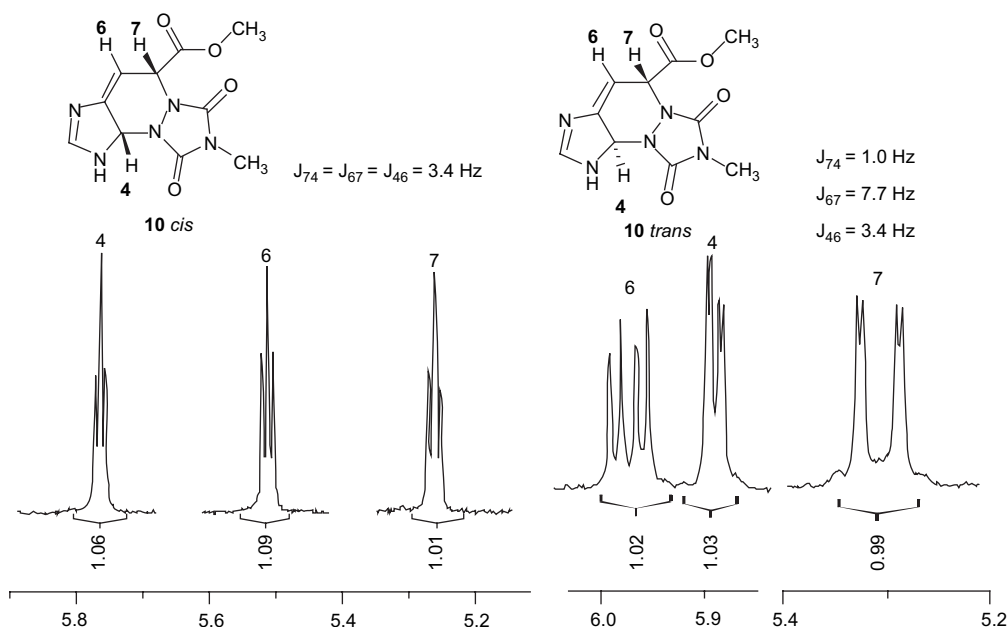


Figure 8. Expansion of ^1H NMR spectral regions for **10** *cis* and *trans*.

styrene yields an analogous 2:1 [4+2]/ene adduct, but via trappable dipolar intermediates.²¹ Addition of MTAD to the **10** *trans* did not result in the formation of a 2:1 adduct at room temperature. While warming the solution to 50 °C promotes the formation of the 2:1 adduct as a minor product, the mixture readily decomposes.

Based on these results we propose the following mechanism (Fig. 10) for the reactions of MTAD with MUC. The addition of the first equivalent of MTAD to *trans*- and *cis*-MUC occurs via a suprafacial disrotatory [4+2] cycloaddition such that the relative stereochemistries of the homo-allylic protons are *cis* and *trans*, respectively. The *cis* homo-allylic protons in **10** *cis* are susceptible to the ene reaction with MTAD to form a 2:1 [4+2]/ene adduct, where as the ene reaction of MTAD with **10** *trans* is inhibited by steric factors

induced by the *trans* geometry. It is also possible that the geometry of the allylic proton in **10** *trans* is not properly aligned (co-planar with the π system) for the ene reaction to occur.

To probe the involvement of dipolar intermediates in the reaction of MTAD with MUC,^{23,24} 3 equiv of MeOH was added to the solvent prior to adding MTAD to MUC. Detailed analysis of the ^1H NMR spectrum from the MeOH trapping studies did not indicate the formation of any methanol adducts under our experimental conditions from either the *cis* or the *trans* isomers at -30 and 0 °C. While the formation of MeOH adducts is strong evidence for the involvement of dipolar intermediates the absence of such adducts suggest that dipolar intermediates are not involved or too short lived to be trapped.

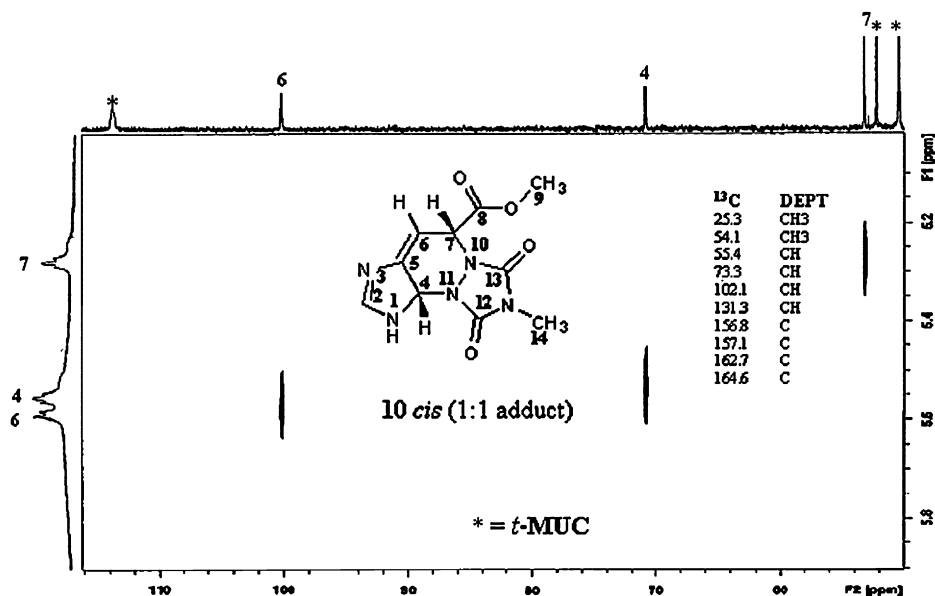


Figure 9. Summary of the ^{13}C , DEPT, and ^1H - ^{13}C HETCOR NMR spectra for **10** *cis*.

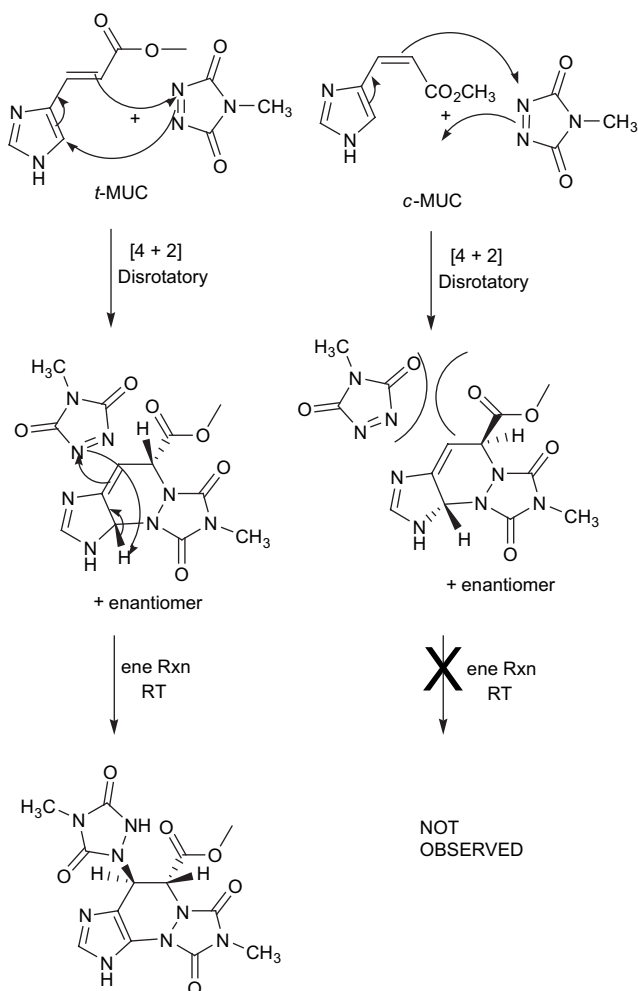


Figure 10. Proposed mechanism for the reaction of MTAD with *cis*- and *trans*-MUC.

Singlet oxygen and MTAD exhibit different reactivities toward MUC. One might expect that the imidazole ring system is more electron rich than the diene, which includes the enone side chain and C₄–C₅ double bond of the imidazole ring. If the reaction was controlled primarily by electronic factors, addition to the imidazole ring may be predominant as was observed with singlet oxygen. On the other hand, the observed [4+2] addition of MTAD involves the enone side chain. The observed different reactivities may be due to steric factors induced during secondary orbital interactions of MTAD with MUC (Fig. 11). The *endo* transition

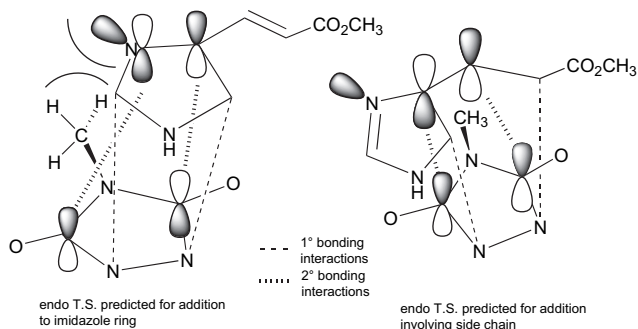


Figure 11. Possible transition states for [4+2] additions of MTAD to *t*-MUC.

state leading to addition of MTAD to the imidazole ring will exhibit significant steric interactions between the *N*-methyl group on MTAD and the lone pair of the pyridine nitrogen atom of the imidazole ring. The [4+2] addition of MTAD involving the enone side chain, the observed reaction pathway, does not possess such steric interactions. Since singlet oxygen is not subject to such secondary orbital interactions or steric constraints a different reaction pathway is observed compared to MTAD.

3. Conclusions

Singlet oxygen and MTAD exhibit dramatically different reactivities toward *cis*- and *trans*-MUC. Singlet oxygen undergoes [4+2] cycloaddition to the imidazole ring in MUC, while MTAD undergoes [4+2] stereospecific cycloaddition involving the olefinic side chain and C₄–C₅ double bond of the imidazole ring. The observed different reactivities may be due to secondary orbital interactions of MTAD during the cycloaddition and/or steric factors not presented by singlet oxygen. *t*-MUC forms a 1:2 MTAD [4+2]/ene adduct while the *cis* isomer only yields the [4+2] adduct at room temperature. While stereospecificity and absence of MeOH trapping adducts indicate the reactions of MTAD with MUC do not involve open or trappable dipolar intermediates, the vivid short lived color changes during the primary stages of the reactions indicate a charge transfer complex may be involved in the reaction process. The endoperoxides formed from the reaction of singlet oxygen with MUC are modestly stable at low temperature and decompose upon warming to form complex reaction mixtures. Studies are underway to characterize the products formed from the collapse of the MUC endoperoxides in an attempt to better understand the antioxidant role of UCA.

4. Experimental

4.1. General

Acetone-*d*₆, CDCl₃, CD₂Cl₂, CD₃CN, *t*-UCA, Rose bengal, cobalt(II) tetraphenylporphyrin, and MTAD were purchased from Aldrich and used as received. TLC analyses were performed on 0.2 mm thick plates pre-coated with fluorescent silica (Whatman), using short wavelength UV light to visualize the spots. ¹H and ¹³C NMR spectra were recorded on a Bruker ARX-400 spectrometer equipped with a variable temperature probe. Chemical shifts values are in parts per million based on the chemical shift of the solvent. ¹³C NMR peak multiplicity was determined by DEPT experiments. MS measurements were made using a direct probe on a Thermoquest Navigator Mass Spectrometer.

4.2. Reactions

4.2.1. Synthesis of *trans*-methyl, *n*-butyl, and *tert*-butyl urocanate. *trans*-UCA (1.0 g, 7.2 mmol) and 11 mL of 10% v/v solution of concentrated sulfuric acid in the appropriate alcohol were placed into a 50 mL round bottom flask. The solution was then heated to reflux for ~20 h. The resultant solution was allowed to cool to room temperature and 18 mL of the corresponding alcohol was added. The pH of

the solution was adjusted to 8–8.5 by adding solid anhydrous sodium carbonate. The basic solution was then gravity filtered and the solvent was removed under vacuum. The crude product was extracted with hot ethyl acetate. Evaporation of the solvent gave the desired ester in 90–95% yield. TLC analysis and column chromatography were performed using a 4:1 mixture of CHCl₃/EtOH. *trans*-Methyl urocanate: 400 MHz ¹H NMR (CD₃CN): δ (ppm) 7.63 (s, 1H), 7.57 (d, *J*=15.7 Hz, 1H), 7.33 (s, 1H), 6.41 (d, *J*=15.7 Hz, 1H), 3.69 (s, 3H); 100 MHz ¹³C NMR: 167.3, 138.0, 136.4, 134.6, 123.8, 113.4, 51.3; *trans* *n*-butyl urocanate: 400 MHz ¹H NMR (acetone-*d*₆): δ (ppm) 7.65 (s, 1H), 7.53 (d, *J*=15.6 Hz, 1H), 7.30 (s, 1H), 6.39 (d, *J*=15.6 Hz, 1H), 4.12 (t, 2H), 1.55 (m, 2H), 1.30 (m, 2H), 0.92 (t, 3H); *trans* *tert*-butyl urocanate: 400 MHz ¹H NMR (acetone-*d*₆): δ (ppm) 7.64 (s, 1H), 7.55 (d, *J*=15.7 Hz, 1H), 7.32 (s, 1H), 6.40 (d, *J*=15.7 Hz, 1H), 1.38 (s, 9H).

4.2.2. Synthesis of *cis*-MUC. *trans*-MUC (0.760 g, 5 mmol) was mixed with 250 mL of dichloromethane and purged with argon for 2 min. The solution was prepared in a sealed quartz reaction vessel and irradiated in a Rayonet photochemical reactor equipped with sixteen 254 nm emitting bulbs for ~4 h at 34 °C. Analysis by ¹H NMR indicates a *trans*–*cis* ratio of 20:80. TLC analysis and column were performed using CHCl₃/EtOH in a ratio 9:1. ¹H NMR indicates the purified sample was of high purity with no traces of the *trans* isomer. 400 MHz ¹H NMR (CD₂Cl₂): δ (ppm) 7.70 (s, 1H), 7.34 (s, 1H), 6.88 (d, *J*=12.5 Hz, 1H), 5.70 (d, *J*=12.5 Hz, 1H), 3.78 (s, 3H); 100 MHz ¹³C NMR: δ (ppm) 168.7, 137.4, 136.7, 131.2, 127.4, 110.7, 51.7.

4.2.3. Reactions of *cis*- and *trans*-MUC with singlet oxygen. MUC (2 mg, 13 μmol) was mixed with 1 mL of deuterated solvent (CD₂Cl₂, acetone-*d*₆, CD₃CN, or CDCl₃) in an NMR tube. Rose bengal (10 μM) was used as the sensitizer. A 200 W Hg–Xe lamp was used to irradiate the sample. A water filter was placed in front of the lamp as a heat filter and Pyrex glass was employed to filter light ≤320 nm. The NMR tube containing the sample was placed inside a windowed Dewar flask and oxygen was gently bubbled through the solution during irradiation. ¹H NMR spectra were taken at 5-min intervals at the same temperature of irradiation. The peaks in the ¹H NMR spectrum at low temperature assigned to endoperoxide, **1** *trans* are as follows: 400 MHz (CDCl₃): δ (ppm) 8.02 (s, 1H), 6.80 (d, *J*=16.1 Hz, 1H), 6.51 (d, *J*=16.1 Hz, 1H), 4.90 (s, 1H), 3.63 (s, 3H). The ¹H NMR signals for endoperoxide **1** *cis* are as follows: 400 MHz (CDCl₃): δ (ppm) 8.19 (s, 1H), 6.57 (d, *J*=11.6 Hz, 1H), 6.38 (s, 1H), 5.94 (d, *J*=11.6 Hz, 1H), 3.87 (s, 3H).

4.2.4. Reactions of *cis*- and *trans*-MUC with MTAD. MUC (2 mg, 13.1 μmol) was dissolved in 1 mL of deuterated chloroform. The solution was then reacted with 1 equiv of MTAD (1.5 mg, 13.1 μmol). The reactions of MTAD were carried out at temperatures down to –30 °C in a 5 mm NMR tube. NMR characterizations were run at the same temperature as the reaction. A summary of the chemical shift information for the major reaction products is provided below 400 MHz (CDCl₃): δ (ppm) 1:1 adduct, **10** *cis*: 7.45 (s, 1H), 5.75 (t, *J*=3.4 Hz, 1H), 5.49 (t, *J*=3.4 Hz, 1H), 5.24 (t, *J*=3.4 Hz, 1H), 3.75 (s, 3H), 3.05 (s, 3H); 1:1 adduct, **10** *trans*: 7.51 (s, 1H), 5.93 (d of d, *J*=7.7 and 3.4 Hz, 1H),

5.88 (d of d, *J*=3.4 and 1.1 Hz, 1H), 5.29 (d of d, *J*=7.7 and 1.1 Hz, 1H), 3.80 (s, 3H), 3.13 (s, 3H). 100 MHz (CD₃CN): δ (ppm) 25.3, 54.1, 55.4, 73.3, 102.1, 131.3, 156.8, 157.1, 162.7, 164.6. Positive mode APCI-MS of the **10** *cis* and *trans* yielded a molecular ion (MH⁺: 266) indicating 1:1 adducts.

1:2 *t*-MUC/MTAD adduct 7.93 (s, 1H), 6.01 (d, *J*=1.6 Hz, 1H), 5.37 (d, *J*=1.6 Hz, 1H), 3.80 (s, 3H), 3.10 (s, 3H), 3.03 (s, 3H). 100 MHz (CD₃CN): δ (ppm) 24.8, 25.1, 50.1, 53.2, 60.0, 123.1, 132.4, 139.9, 153.5, 155.1, 155.4, 157.3, 168.4.

Acknowledgements

R.R. was supported by NIH/NIGMS R25GM061347. We thank Yali Hsu for his assistant with the NMR experiments.

References and notes

- Morrison, H.; Avnir, D.; Bernasconi, C.; Fagan, G. *Photochem. Photobiol.* **1980**, *32*, 711–714.
- Baden, H. P.; Pathak, M. A. *J. Invest. Dermatol.* **1967**, *48*, 11–17.
- Morrison, H. *Photodermatology* **1985**, *2*, 158–165.
- Norval, M.; Simpson, T. J. *Photochem. Photobiol.* **1989**, *50*, 267.
- Haralampus-Grynaviski, N.; Ransom, C.; Ye, T.; Rozanowska, M.; Wrona, M.; Sarna, T.; Simon, J. D. *J. Am. Chem. Soc.* **2002**, *124*, 3461–3468.
- Elton, L. M.; Morrison, H. *Photochem. Photobiol.* **2002**, *75*, 565–569.
- Tomita, M.; Irie, M.; Ukita, T. *Tetrahedron Lett.* **1968**, 4933–4949.
- Wasserman, H. H.; Lipshutz, B. H. Reactions of Singlet Oxygen with Heterocyclic Systems. In *Organic Chemistry. A Series of Monographs*; Academic: New York, NY, 1979; pp 430–506.
- Ryang, H. S.; Foote, C. S. *J. Am. Chem. Soc.* **1979**, *101*, 6683–6687.
- Ravanat, J.-L.; Berger, M.; Bernad, F.; Langlois, R.; Ouellet, R.; van Lier, J. E.; Cadet, J. *Photochem. Photobiol.* **1992**, *55*, 809–814 and references within.
- (a) Ye, Y.; Muller, J. G.; Luo, W.; Mayne, C. L.; Shallop, A. J.; Jones, R. A.; Burrows, C. J. *J. Am. Chem. Soc.* **2003**, *125*, 13926–13927; (b) Kang, P.; Foote, C. S. *J. Am. Chem. Soc.* **2002**, *124*, 4865–4873; (c) Sheu, C.; Kang, P.; Khan, S.; Foote, C. S. *J. Am. Chem. Soc.* **2002**, *124*, 3905–3913.
- (a) Kang, P.; Foote, C. S. *Tetrahedron Lett.* **2000**, 9623–9626; (b) Kang, P.; Foote, C. S. *J. Am. Chem. Soc.* **2002**, *124*, 9629–9638.
- (a) Kammeyer, A.; Eggelte, T. A.; Overmars, H.; Bootsma, A.; Bos, J. D.; Teunissen, M. B. M. *Biochim. Biophys. Acta, Gen. Subj.* **2001**, *1526*, 277–285; (b) Ramu, A.; Mehta, M. M.; Leaseburg, T.; Aleksic, A. *Cancer Chemother. Pharmacol.* **2001**, *47*, 338–346; (c) Morrison, H.; Deibel, R. M. *Photochem. Photobiol.* **1988**, *48*, 153–156.
- (a) Cadet, J.; Douki, T.; Gasparutto, D.; Ravanat, J. L. *Mutat. Res.* **2003**, *531*, 5–35; (b) Ravanat, J. L.; Douki, T.; Cadet, J. *J. Photochem. Photobiol. B: Biol.* **2001**, *63*, 88–102.
- Mohammad, T.; Morrison, H. *Org. Prep. Proced. Int.* **2000**, *32*, 581–584.
- O'Shea, K. E.; Foote, C. S. *J. Org. Chem.* **1988**, *54*, 3475–3477 and references within.
- O'Shea, K. E.; Foote, C. S. *J. Am. Chem. Soc.* **1988**, *110*, 7167.

18. Early examples include (a) Jefford, C. W.; Rimaubt, C. G. *J. Am. Chem. Soc.* **1978**, *100*, 6437–6438; (b) Asveld, E. W. H.; Kellogg, R. M. *J. Am. Chem. Soc.* **1980**, *102*, 3644–3648.
19. The involvement of dipolar intermediates in singlet oxygen reactions has recently been questioned. See: (a) Singleton, D. A.; Hang, C.; Szymansky, M. J.; Meyer, M. P.; Leach, A. G.; Kuwata, K. T.; Chen, J. S.; Greer, A.; Foote, C. S.; Houk, K. N. *J. Am. Chem. Soc.* **2003**, *125*, 1319; (b) Singleton, D. A.; Hang, C.; Szymansky, M. J.; Greenwald, E. E. *J. Am. Chem. Soc.* **2003**, *125*, 1176.
20. (a) Smonou, I.; Orfanopoulos, M.; Foote, C. S. *Tetrahedron Lett.* **1988**, *29*, 2769–2772; (b) Orfanopoulos, M.; Foote, C. S.; Smonou, I. *Tetrahedron Lett.* **1987**, *28*, 15–18; (c) Jensen, F.; Foote, C. S. *J. Am. Chem. Soc.* **1987**, *109*, 6376–6385; (d) Clennan, E. L.; Earlywine, A. D. *J. Am. Chem. Soc.* **1987**, *109*, 7104–7110.
21. Stratakis, M.; Hatzimarinaki, M.; Froudakis, G. E.; Orfanopoulos, M. *J. Org. Chem.* **2001**, *66*, 3682–3687.
22. Lai, Y.-C.; Mallakpour, S. E.; Butler, G. B.; Palenik, G. L. *J. Org. Chem.* **1985**, *50*, 4378–4381.
23. The role and involvement of dipolar intermediates during the reactions of triazolinedione have received considerable attention recently, see: (a) Singleton, D. A.; Hang, C. *J. Am. Chem. Soc.* **1999**, *121*, 11885–11893; (b) Roubelakis, M. M.; Vougioukalakis, G. C.; Angelis, Y. S.; Orfanopoulos, M. *Org. Lett.* **2006**, *8*, 39–42; (c) Kim, D. K.; O'Shea, K. E. *J. Am. Chem. Soc.* **2003**, *126*, 7000–7001; (d) Vassilikogiannakis, G.; Stratakis, M.; Orfanopoulos, M. *Org. Lett.* **2000**, *2*, 2245–2248.
24. For an excellent review of the mechanisms of triazolinedione ene reactions, see: Vougioukalakis, G. C.; Orfanopoulos, M. *Synlett* **2005**, 713–731.



ELSEVIER

Singlet oxygen oxidation of 2'-deoxyguanosine. Formation and mechanistic insights

Jean-Luc Ravanat,^a Glaucia R. Martinez,^{b,c} Marisa H. G. Medeiros,^c
Paolo Di Mascio^c and Jean Cadet^{a,*}

^aLaboratoire 'Lésions des Acides Nucléiques', DRFMC/LCIB UMR-E n°3 CEA/UJF, CEA/Grenoble,
F-38054 Grenoble cedex 9, France

^bDepartamento de Bioquímica e Biologia Molecular, Setor de Ciências Biológicas, Universidade Federal do Paraná,
Curitiba-PR, Brazil

^cDepartamento de Bioquímica, Instituto de Química, Universidade de São Paulo, CP 26077,
CEP 05513-970 São Paulo, SP, Brazil

Received 7 July 2006; revised 9 August 2006; accepted 16 August 2006

Available online 25 September 2006

Abstract—Emphasis was placed in this work on the delineation of mechanistic aspects of the singlet oxygen-mediated oxidation reactions of 2'-deoxyguanosine **1** used as a DNA model compound in aerated aqueous solution. For this purpose a thermolabile naphthalene endoperoxide derivative was used allowing the generation of [¹⁸O]-labeled singlet oxygen for dedicated mechanistic studies. The analysis and characterization of the oxidized nucleosides of the ¹O₂ reactions were achieved on the basis of accurate HPLC–tandem mass spectrometry measurements. Thus it was found that primary oxidation products include, in addition to the previously identified 8-oxo-7,8-dihydro-2'-deoxyguanosine **5** and the two diastereomers of spiroiminodihydantoin **8**, two relatively minor nucleosides, namely the two diastereomers of 4-hydroxy-8-oxo-4,8-dihydro-2'-deoxyguanosine **9**.

© 2006 Elsevier Ltd. All rights reserved.

1. Introduction

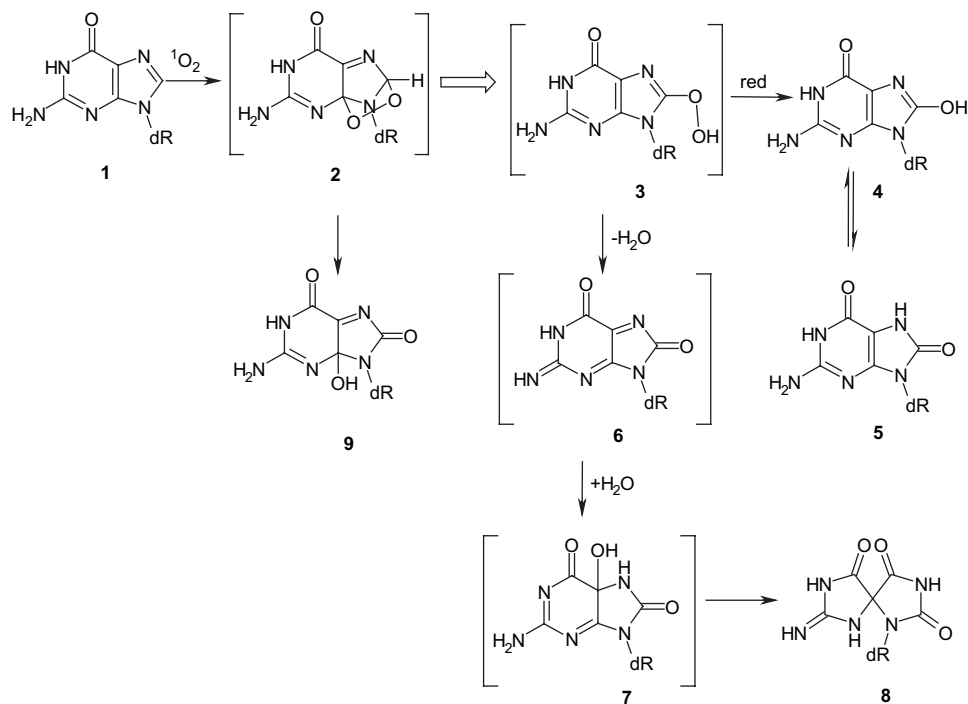
Guanine is the only normal nucleic acid base that significantly reacts with singlet oxygen (¹O₂) in the ¹Δ_g state ($E=22.4$ kcal) at neutral pH.¹ This is illustrated by the comparison of the values of the total rate constant (k_T) of ¹O₂ with nucleic acid components that is the sum of chemical quenching (k_r) and physical quenching (k_q). The reactivity of the main DNA and RNA nucleosides toward ¹O₂ in organic solvents was found to decrease in the following order: guanine >> cytosine > adenine > uracil > thymine.^{2,3} Similar observations were made in water in which the measured value of k_T for guanosine⁴ was established to be $5.3 \times 10^6 \text{ M}^{-1} \text{ s}^{-1}$, which is close to the value determined for 2',3',5'-*O*-*tert*-butyldimethylsilylguanosine in 1,1,2-trichlorotrifluoroethane ($k_T=3.0 \times 10^6 \text{ M}^{-1} \text{ s}^{-1}$).² It may be

pointed out that the contribution of the chemical quenching to the overall k_T value is rather low, in fact less than 2% as inferred from the measurement of the k_r rate constant of guanosine with ¹O₂ in acetone-*d*₆ that was found to be $1.36 \times 10^5 \text{ M}^{-1} \text{ s}^{-1}$.⁵ Earliest experiments have shown that guanine components including nucleosides and nucleotides were highly susceptible to ¹O₂ generated by type II photosensitizers, hydrogen peroxide–sodium hypochlorite reaction, peroxochromate or microwave electric discharge.^{6–14} Several degradation products including 2-deoxy-D-erythro-pentose and the 2'-deoxyribonucleosides of urea, cyanuric acid, and oxamide whose formation is not very informative from a mechanistic point of view were isolated and characterized.^{13,14} Almost 15 years were necessary to gain relevant insights into the mechanism of ¹O₂ oxidation of guanine components. The isolation and identification of the main degradation products of guanine nucleosides have been facilitated by the availability of highly resolutive HPLC analytical tools. This has involved the use of suitable LC columns such as those packed with an amino substituted silica gel stationary phase that have been shown to be appropriate to achieve the separation of the rather polar spiroiminodihydantoin 2'-deoxyribonucleoside diastereomers **8** (dSp).^{15–17} Major progress has been made in the measurement of analytes at the output of the HPLC columns with the advent of

Keywords: Singlet oxygen; Cycloaddition; Endoperoxide; Dioxetane; 8-Oxo-7,8-dihydroguanine; Spiroiminodihydantoin.

Abbreviations: dGuo, 2'-deoxyguanosine; 8-oxodGuo, 8-oxo-7,8-dihydro-2'-deoxyguanosine; dSp, spiroiminodihydantoin 2'-deoxyribonucleoside; 4-OH-8-oxodGuo, 4-hydroxy-8-oxo-4,8-dihydro-2'-deoxyguanosine; DHPNO₂, *N,N'*-di(2,3-dihydroxypropyl)-1,4-naphthalenediopropanamide endoperoxide.

* Corresponding author. Tel.: +33 4 38 78 49 87; fax: +33 4 38 78 50 90; e-mail: jean.cadet@cea.fr



Scheme 1. Degradation pathway of 2'-deoxyguanosine (**1**) mediated by singlet oxygen.

the tandem mass spectrometry detection technique involving an electrospray ionization source (EIS). This allows accurate and sensitive quantitation of the stable primary oxidation products of 2'-deoxyguanosine (**1**) (dGuo) under conditions where the formation of secondary decomposition compounds of 8-oxo-7,8-dihydro-2'-deoxyguanosine (**5**) (8-oxodGuo), which is a much better target for $^1\text{O}_2$ than the precursor **1**, is minimized.¹⁷ As discussed below in more detail it was found that in addition to relatively minor 8-oxodGuo **5**, the two main $^1\text{O}_2$ oxidation products of dGuo **1** were the two diastereomers of dSp **8**¹⁸ (Scheme 1) and not the two diastereomeric forms of 4-hydroxy-8-oxo-4,8-dihydro-2'-deoxyguanosine (**9**) as proposed initially.^{15–19}

In the present work, evidence is provided from tandem mass spectrometry measurement that the pair of diastereomers **9** is in fact generated as primary $^1\text{O}_2$ oxidation products of dGuo **1**. Efforts were also made, using the chemical precursor of labeled singlet oxygen, to gain further insights into the mechanism of formation of the two diastereomers of dSp **8** that involves either a direct oxidation of dGuo **1** or a secondary efficient reaction of $^1\text{O}_2$ with 8-oxodGuo **5** initially generated.

2. Results and discussion

2.1. Formation of the 4R* and 4S* diastereomers of 4-hydroxy-8-oxo-4,8-dihydro-2'-deoxyguanosine (**9**)

Numerous investigations have been aimed at elucidating the mechanism of $^1\text{O}_2$ oxidation reactions of the guanine moiety of nucleosides and other nucleic acid components in aqueous solutions during the last twenty years in relation with the known genotoxic effects of this reactive oxygen species. It

was found in earlier studies that UVA excited photosensitizers including phthalocyanine and methylene blue, two predominant type II ($^1\text{O}_2$) photosensitizers, are able to efficiently degrade 2'-deoxyguanosine (**1**) giving rise to two main oxidized nucleosides.^{15–17} The structures of the two compounds that were tentatively assigned as a pair of (4R*)- and (4S*)-diastereomers of 4-hydroxy-8-oxo-4,8-dihydro-2'-deoxyguanosine (**9**)^{15–17} have been subsequently revisited. Thus, it was reported that the base moiety of the main $^1\text{O}_2$ oxidation products of guanosine in aerated aqueous solution has the same spiroiminodihydroantoin structure¹⁸ that the overwhelming modified nucleosides that arise from one-electron oxidation of 8-oxo-7,8-dihydroguanosine^{19–21} (structure **8**, Scheme 1). Further support for the spirocyclic connectivity of related dSp 2'-deoxyribonucleosides **8** was provided from SELINQUATE ^{13}C NMR measurements, a method allowing assessment of carbon connectivity through the consideration of ^{13}C scalar couplings.²² It may be also pointed out that relevant chemical and conformational features on dSp diastereomers **8** either as free nucleosides or when inserted into DNA duplexes as inferred from theoretical calculations are now available.^{23–25}

Further investigation on the singlet oxygen oxidation reactions of dGuo **1** was recently performed using *N,N'*-di(2,3-dihydroxypropyl)-1,4-naphthalenedipropionamide endoperoxide (DHPNO₂) as a clean source of $^1\text{O}_2$ ²⁶ and HPLC–MS/MS as the analytical tool for the accurate detection of the degradation products. Thus, the presence of two major peaks in the elution profile provided by HPLC analysis on a graphite column was observed using the neutral loss scan mode detection. This is based on the search of fragments corresponding to a constant loss of 116 amu that is characteristic of the fragmentation of most 2'-deoxyribonucleosides.²⁷ It may be noted that the MS spectrum of the targeted nucleosides exhibits a signal corresponding to the

molecular ion $[M+H]^+$ at $m/z=300$ in agreement with the dSp structure **8**. As relevant fragments that were acquired with the cone potential at 30 V we may note those of the protonated base $[BH+H]^+$ at $m/z=184$ and the 2-deoxyribose residue $[dR]^+$ at $m/z=117$. Interestingly, two new oxidized nucleosides that exhibit similar ESI-MS/MS fragmentation than the predominant dSp diastereomers **8** were found to be present in the reaction mixture (Fig. 1).

The detection of the two latter nucleosides was achieved by using the specific transition $300 \rightarrow 184$ that was previously applied to detect **8** by HPLC-MS/MS in the multiple reaction monitoring (MRM) mode.²⁸ The two new oxidized nucleosides **9**, which are produced in a relatively low yield compared to dSp **8** were found to be less rapidly eluted on the highly hydrophobic graphite HPLC column than the two diastereomers of dSp (**8**) (Fig. 1). It may be noted that these two compounds were not previously detected when the amino substituted silica gel column was used for the separations of the 1O_2 oxidation products of dGuo **1**. This may be explained by the fact that under these analytical conditions the minor oxidation products co-elute with the overwhelming 2'-deoxyguanosine (**1**). It may be added that the two latter products **9**, together with dSp diastereomers **8** are not retained on the usual octadecylsilyl silica gel columns even when water was used as the mobile phase. This most likely explains why the two oxidized dGuo decomposition compounds **9** were not detected so far despite extensive investigations. Several pieces of information that were inferred from complementary studies were considered for the assignment of the nucleosides. First, it was found in contrast to what was observed for diastereomers **8** (vide infra) that the two products are not formed upon incubation of 8-oxodGuo **5** in the presence of the chemical generator of

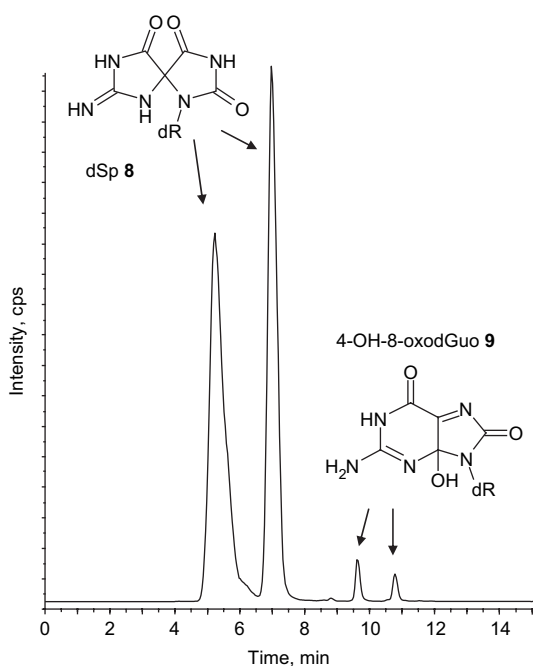


Figure 1. HPLC-MS/MS chromatogram obtained by analysis of oxidation products of 2'-deoxyguanosine (**1**) upon incubation with DHPN $_2$. The MS/MS detection was achieved using the specific transition $300 \rightarrow 184$ for dSp (**8**). Separation was performed using the Hypercarb column (see Section 4).

1O_2 . This is strongly indicative that they are primary oxidation products of singlet oxygen oxidation of dGuo **1**. Another relevant piece of information was gained from the experiments that have involved the reaction of dGuo **1** with isotopically labeled 1O_2 generated from thermolabile DHPN $^{18}O_2$. HPLC-MS/MS analysis indicates that both nucleosides have incorporated two labeled oxygen atoms ($m/z=304 \rightarrow 188$). On the basis of these observations and taking into consideration the fact that only two diastereomers of **8** are possible, the two newly isolated dGuo oxidation products were assigned as the (4R*)- and (4S*)-diastereomers of 4-hydroxy-8-oxo-4,8-dihydro-2'-deoxyguanosine (**9**). It may also be added that the third possible structure that could exhibit similar MS features, namely 5-hydroxy-8-oxo-7,8-dihydro-2'-deoxyguanosine regioisomer **7**, the precursor of dSp **8**, was ruled out due to its high instability at room temperature.²¹ The ESI-MS patterns of **8** and **9** that are reported in Figure 2 show similar fragmentation patterns that are dominated by the cleavage of the N-glycosidic bond and further splitting of the 2-deoxyribose moiety as is usually observed for 2'-deoxyribonucleosides. However, we note the presence of a specific fragment at $m/z=210.2$ in the mass spectrum of dSp **8**, which has not yet been characterized.

The formation of **9** as already pointed out is a relatively minor process of the 1O_2 -mediated oxidation of dGuo **1**. Interestingly, this provides further support for the occurrence of a second mode of degradation pathway of 1,4-endoperoxides **2** that was initially proposed and then discarded. It would be of interest to check in forthcoming studies whether nucleosides **9** are produced in DNA and oligonucleotides.

2.2. Mechanistic aspects on the formation of spiroiminodihydantoin nucleosides as the result of primary and secondary oxidation reactions

The use of a clean source of 1O_2 that can be isotopically labeled with ^{18}O atoms has been shown to be particularly suitable for mechanistic studies dedicated to oxidation of **1** and **5** in aqueous solution.²⁹ As already discussed it is well documented that 1O_2 oxidation of dGuo **1** in water at neutral pH gives rise to the predominant formation of a diastereomeric pair of **8**.^{29–31} The HPLC-MS/MS analysis of the two dSp nucleosides generated upon the incubation of dGuo **1** with DHPN $^{18}O_2$, as a generator of $^{18}[^1O_2]$, showed the presence of two sets of molecules (Fig. 3).

One is labeled with two [^{18}O]-labeled atoms whereas only one ^{18}O has been incorporated in the second molecule during the $^{18}[^1O_2]$ oxidation of dGuo **1**. The formation of the latter nucleosides **8** whose ESI-MS spectra exhibit a molecular ion at $m/z=302$ may be rationalized in terms of initial 1O_2 cycloaddition across the 4,8-bond leading to the transient formation of an oxidized quinonoid **6** that upon reaction with a water molecule gives rise to **8** as shown in Scheme 1. There is another route leading to dSp **8** through the intermediacy of **5**, which has been found to be a primary 1O_2 oxidation product of dGuo **1**. The observation of a doubly [^{18}O]-labeled dSp molecule **8** as inferred from the presence of a pseudo-molecular ion at $m/z=304$ in the HPLC-mass spectrum is fully supportive of the significant involvement of a secondary oxidation process in the formation of **8**. This is in agreement with the fact that 8-oxodGuo **5**, which is more susceptible

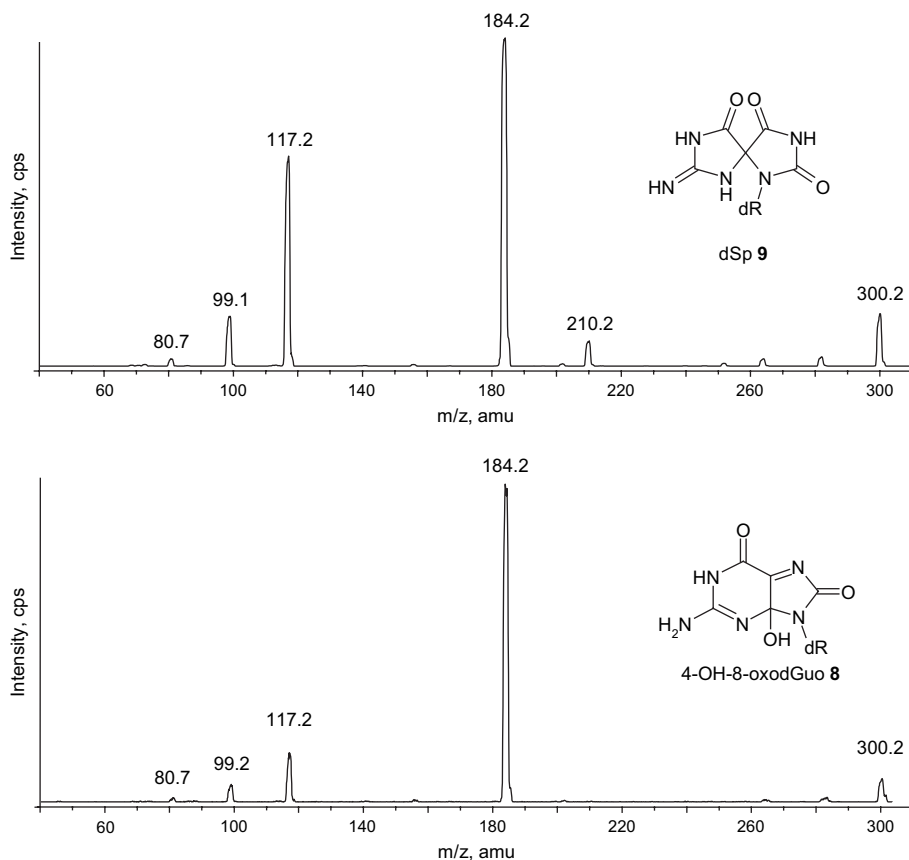


Figure 2. Collision-induced dissociation mass spectra of ion $m/z=300$ (positive mode) of either dSp **8** (upper panel) or 4-OH-8-oxodGuo **9** (lower panel).

than dGuo **1** to ^{18}O oxidation almost by two orders of magnitude,⁴ is gradually consumed as soon it is produced in a reaction with $^1\text{O}_2$.¹⁵ The secondary formation of a diastereomeric mixture of dioxetane **10** as the result of a [2+2] cycloaddition of $^1\text{O}_2$ across the 4,5-ethylenic bond of **5**. In a subsequent step, **10** is likely to rearrange giving rise to the 5-hydroperoxide **11**, which upon reduction leads to the formation of

5-hydroxy-8-oxo-7,8-dihydro-2'-deoxyguanosine (**7**), the unstable regioisomer of **9**. Subsequent acyl shift rearrangement, which is favored at neutral and alkaline pHs, is likely to explain the formation of **8**. Strong support for this pathway was provided by the observation of key intermediates including related ribonucleoside derivatives of dioxetane **10** and 5-hydroperoxide **11** in the photosensitized organic solution of the 2',3',5'-tri-*O-tert*-butyl dimethylsilyl

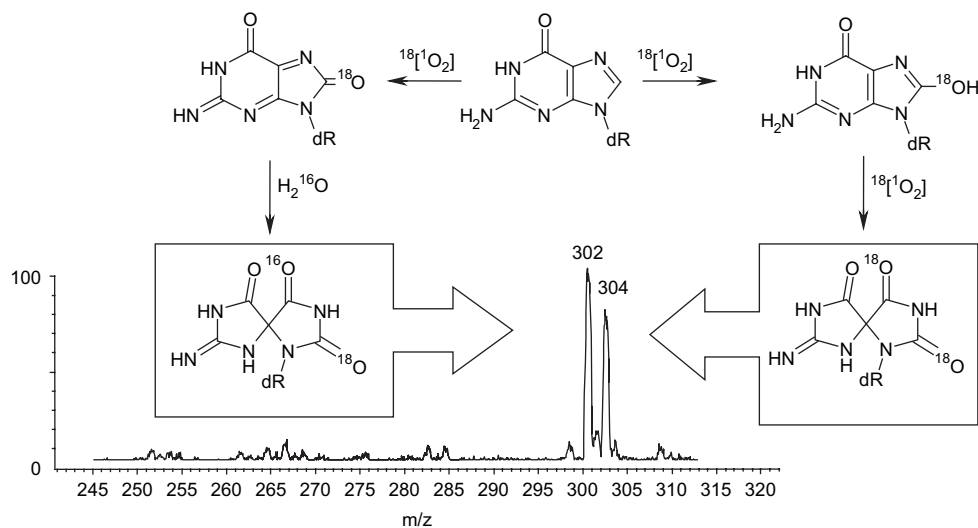


Figure 3. Mass spectra of dSp **8** generated upon incubation of dGuo **1** with DHPN $^{18}\text{O}_2$, a chemical generator of [^{18}O]-labeled singlet oxygen.

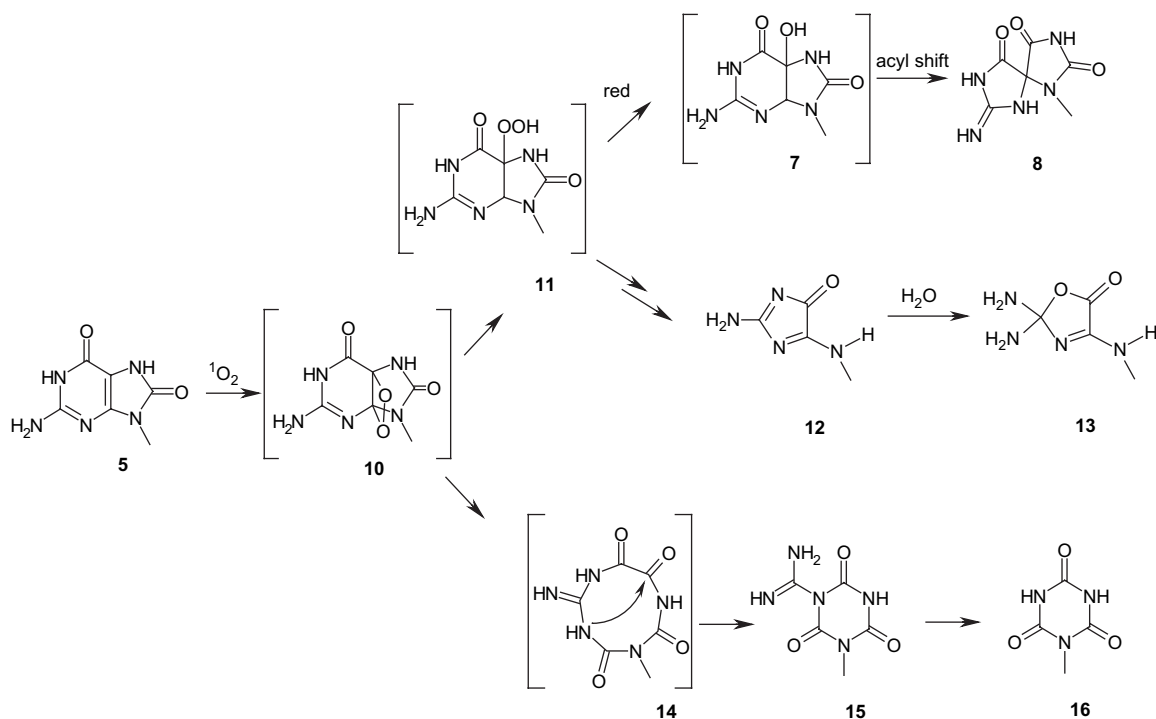
derivative of 8-oxo-7,8-dihydroguanosine.^{31,32} This was achieved by both ¹³C NMR and 2-D HMBC measurements performed at -60°C . It may be added that support for the assignment of the ¹³C chemical shifts was provided by hybrid Hartree–Fock density functional theory calculations.³¹ Evidence for the dimethylsulfide-mediated reduction of 5-hydroperoxy-8-oxo-7,8-dihydro-2'-deoxyguanosine (**11**) into the alcohol precursor **7** of spiroiminodihydantoin nucleosides **8** was also gained from NMR measurements carried out at -40°C .³¹

The delineation of mechanistic aspects concerning the formation of other ¹O₂ oxidation products of 8-oxodGuo **5** has been the subject of recent studies that have involved the use of either unlabeled DHPNO₂ or DHPN¹⁸O₂.²⁹ It appears that the oxidized nucleosides so far identified arise from the initial formation of dioxetane precursors **10**. In addition to the conversion of **10** into the linear 5-hydroperoxide **11**, a second major degradation pathway was found to occur. Thus the cleavage of the 1,2-bond of **10** was proposed to generate the nine-membered ring intermediate **14**, which is converted into 1,3,5-triazine-1(2*H*)-carboximidamide, 3-(2-deoxy-β-D-erythro-pentofuranosyl)-tetrahydro-2,4,6-trioxo- (**15**) upon intramolecular cyclization.³³ Subsequent slow hydrolysis of the six-membered ring nucleoside **15** leads to the formation of 1-(2-deoxy-β-D-erythro-pentofuranosyl)-cyanuric (**16**) that is accompanied by the release of urea (Scheme 2).

Another degradation pathway whose mechanism remains to be established gives rise to the imidazolone nucleoside **12**, the precursor of oxazolone nucleoside **13** that has been shown previously to be the main one-electron oxidation product of dGuo **1** in aqueous aerated solutions.³⁴

2.3. Mechanism of ¹O₂ oxidation of 2'-deoxyguanosine

The formation of the main primary ¹O₂ oxidation products of dGuo **1** including the two diastereomers of dSp **8**, 8-oxodGuo **5**, and the recently characterized (4*R**)- and (4*S**)-4-OH-8-oxodGuo **9** may be rationalized in terms of a Diels–Alder [4+2] cycloaddition of ¹O₂ across the 4,8-bond of the imidazole ring of the guanine moiety of **1**. This gives rise to unstable 4,8-endoperoxides **2** whose characterization has not been so far achieved even at temperature lower than -80°C . However, related endoperoxides that were generated by type II photosensitization of the 2',3',5'-*O*-*tert*-butyldimethylsilyl derivative of 8-methylguanosine in organic solvents were found to be produced and their structures assigned on the basis of NMR measurements at low temperature.^{34,35} The endoperoxides **2** are likely to undergo in aqueous solution a predominant rearrangement that leads to putative 8-hydroperoxy-2'-deoxyguanosine **3** for which direct structural proofs are also lacking. In a subsequent step, **3** may be reduced into 8-hydroxy-2'-deoxyguanosine (**4**), which is known to be in a dynamic equilibrium with its 6,8-diketo tautomer namely 8-oxo-7,8-dihydro-2'-deoxyguanosine (**5**) (Scheme 1). It may be mentioned that 2,6-diamino-4-hydroxy-5-formamidopyrimidine (FapyGua), a degradation product that may be formed by hydration of guanine radical cation followed by the opening of the imidazole ring according to a reductive pathway,^{36,37} is not generated at least in detectable amount within isolated DNA.³⁸ This was achieved using a thermolabile naphthalene endoperoxide derivative as a clean chemical source of ¹O₂.²⁶ This has led to rule out the possibility for ¹O₂ to act as a one-electron oxidant in contrast to a previous proposal.³⁹ The main degradation pathway of **3** involves dehydration, which leads to the formation of oxidized quinonoid **6**. In a subsequent



Scheme 2. Singlet oxygen oxidation of 8-oxo-7,8-dihydro-2'-deoxyguanosine (**5**).

step hydration would give rise to 5-hydroxy-8-oxo-7,8-dihydro-2'-deoxyguanosine (**7**) that through an acyl shift, which is favored at neutral pH, leads to the formation of the two diastereomers of **8**. It should be added that support for a common precursor to both 8-oxodGuo **5** and dSp **8** is provided by the fact that the presence of reducing agent such as thiols or Fe²⁺ ions leads to a significant increase in the yield of 8-oxodGuo **5** at the expense of **8**.^{18,40} The second degradation pathway is likely to involve the cleavage of the peroxidic bond of **2** with subsequent formation of 4-hydroxy-8-oxo-4,8-dihydro-2'-deoxyguanosine (**9**).

3. Conclusion

The use of a pure source of singlet oxygen, together with the possibility of producing [¹⁸O]-labeled singlet oxygen, in association with HPLC–MS/MS analysis allowed us to propose a coherent mechanism for the singlet oxygen-mediated decomposition of dGuo **1** as a free nucleoside. Interestingly, the formation of the two diastereomers of 4-hydroxy-8-oxo-4,8-dihydro-2'-deoxyguanosine (**9**) may be rationalized in terms of cleavage of the peroxidic bond of **2**, which constitutes a minor reaction with respect to the predominant rearrangement into the hydroperoxide **3**. It may be noted that the chemical reactions of ¹O₂ with the guanine moiety of both isolated and cellular DNAs are partly different since so far only 8-oxodGuo **5** has been shown to be produced in detectable amount.⁴¹ Further efforts should be made to check for the putative ¹O₂-mediated formation in DNA of other oxidized nucleosides including **8** and **9** by taking advantage of the recent availability of more sensitive HPLC–MS/MS apparatus and optimized conditions of enzymatic release of the targeted lesions.

4. Experimental

4.1. Chemicals

DHPNO₂ and DHPN¹⁸O₂ were prepared as previously described.²⁶ Nucleosides including dGuo **1** and 8-oxodGuo **5** were obtained from Sigma (St Quentin-Fallavier, France) and used without further purification.

4.2. Incubation of 2'-deoxyguanosine with the chemical source of singlet oxygen

Incubation of dGuo **1** was performed using a 5 mM solution of the nucleoside in a deuterated aqueous solution of either DHPNO₂ or DHPN¹⁸O₂ at a 20 mM concentration. The resulting solution was heated for 2.5 h at 37 °C to allow the total decomposition of the endoperoxide.

4.3. HPLC–MS/MS analysis

The diastereomeric mixture of spiroiminodihydantoin 2'-deoxyribonucleosides **8** (dSp) was analyzed using an HPLC system that consisted of two Shimadzu LC-10AD/VP pumps (Shimadzu, Tokyo, Japan) connected to a 7125 Rheodyne injector valve (Rheodyne, Cotati, CA, USA). The separation was performed either on a Supelcosil™ (Supelco, Bellefonte, PA, USA) LC-NH₂ column (5 μm, 250×4.6 mm),

using a mobile phase composed of 80% of acetonitrile and 20% of ammonium formate (25 mM) at a flow rate of 0.8 ml/min or using a 150×2.1 mm Hypercarb column (Thermo Electron corporation, Cheshire, UK) using a linear gradient (0–50% in 30 min) of acetonitrile in 2 mM ammonium formate. Detection of the products was achieved using a Shimadzu SPD-10Avp UV–visible detector (Shimadzu, Tokyo, Japan) set at 230 nm. ESI-MS experiments were carried out on a Quattro II instrument (Micromass, Manchester, UK) or using an API3000 (Applied Biosystems, Toronto, Canada) as described in detail elsewhere.²⁸ The spectra were obtained in the positive ion mode. The source temperature was maintained at 100 °C. The optimal flow-rates of the drying and nebulizing gas (nitrogen) were found to be 300 and 30 L/h, respectively. The capillary and HV electrode potentials were set at 3.50 and 0.5 kV, respectively. The cone voltage was set at 15 and 30 V to the ESI-MS-scan mode and 60 V for the ESI-MS/MS analysis; besides, a pressure of 5.5×10⁻⁴ mbar was used in the gas cell and the collision energy was set at 26 eV. The data were processed and transformed into values in a mass/charge scale by means of the Mass Lynx NT™ data system 3.20 version (Micromass, Manchester, UK).

Acknowledgements

The following Brazilian research funding institutions including FAPESP (Fundação de Amparo à Pesquisa do Estado de São Paulo), CNPq (Conselho Nacional para o Desenvolvimento Científico e Tecnológico), CNPq-Instituto do Milênio Redoxoma, and John Simon Guggenheim Memorial Foundation (P.D.M. Fellowship) are acknowledged for financial support. G.R.M. was a post-doctorate recipient of an FAPESP fellowship. Partial support was also provided to J.C. from the European EU Marie Curie Training and Mobility program (project n° MRTN-CT2003 'CLUS-TOXDNA').

References and notes

- Cadet, J.; Sage, E.; Douki, T. *Mutat. Res.* **2005**, *571*, 3.
- Prat, F.; Houk, N.; Foote, C. S. *J. Am. Chem. Soc.* **1997**, *119*, 3951.
- Lee, P. C. C.; Rodgers, M. A. J. *Photochem. Photobiol.* **1987**, *45*, 79.
- Sheu, C.; Foote, C. S. *J. Am. Chem. Soc.* **1995**, *117*, 6439.
- Sheu, C.; Kang, P.; Khan, S.; Foote, C. S. *J. Am. Chem. Soc.* **2002**, *124*, 3905.
- Simon, M. I.; Van Vunakis, H. *J. Mol. Biol.* **1962**, *4*, 488.
- Simon, M. I.; Van Vunakis, H. *Arch. Biochem. Biophys.* **1964**, *105*, 197.
- Waskell, L. A.; Sastry, K. S.; Gordon, M. P. *Biochim. Biophys. Acta* **1966**, *129*, 42.
- Simon, M. I.; Van Vunakis, H. *Biochim. Biophys. Acta* **1966**, *129*, 49.
- Hallett, P. R.; Hallett, B. P.; Snipes, W. *Biophys. J.* **1970**, *10*, 305.
- Rosenthal, I.; Pitts, J. N., Jr. *Biophys. J.* **1971**, *11*, 963.
- Saito, I.; Inoue, K.; Matsuura, T. *Photochem. Photobiol.* **1975**, *21*, 27.
- Cadet, J.; Téoule, R. *Photochem. Photobiol.* **1978**, *28*, 661.
- Cadet, J.; Balland, A.; Voituriez, L.; Hahn, B.-S.; Wang, S. Y. *Oxygen and Oxy-Radicals in Chemistry and Biology*;

- Rodgers, M. A. J., Powers, E. L., Eds.; Academic: New York, NY, 1981; p 610.
15. Ravanat, J.-L.; Berger, M.; Benard, F.; Langlois, R.; Ouellet, R.; van Lier, J. E.; Cadet, J. *Photochem. Photobiol.* **1992**, *55*, 809.
 16. Buchko, G. W.; Cadet, J.; Berger, M.; Ravanat, J.-L. *Nucleic Acids Res.* **1992**, *20*, 4847.
 17. Ravanat, J.-L.; Cadet, J. *Chem. Res. Toxicol.* **1995**, *8*, 379.
 18. Niles, J. C.; Wishnok, J. S.; Tannenbaum, S. R. *Org. Lett.* **2001**, *3*, 963.
 19. Luo, W.; Muller, J. G.; Rachlin, E. M.; Burrows, C. J. *Org. Lett.* **2000**, *2*, 613.
 20. Luo, W.; Muller, J. G.; Burrows, C. J. *Org. Lett.* **2001**, *3*, 2801.
 21. Luo, W.; Muller, J. G.; Rachlin, E. M.; Burrows, C. J. *Chem. Res. Toxicol.* **2001**, *14*, 927.
 22. Adam, W.; Arnold, M. A.; Grune, M.; Nau, W. M.; Pischel, U.; Saha-Möller, C. R. *Org. Lett.* **2002**, *4*, 537.
 23. Jia, L.; Shafirovich, V.; Shapiro, R.; Geacintov, N. E.; Broyde, S. *Biochemistry* **2005**, *44*, 6043.
 24. Jia, L.; Shafirovich, V.; Shapiro, R.; Geacintov, N. E.; Broyde, S. *Biochemistry* **2005**, *44*, 13342.
 25. Karwowski, B.; Dupeyrat, F.; Bardet, M.; Ravanat, J.-L.; Krajewski, P.; Cadet, J. *Chem. Res. Toxicol.*, in press.
 26. Martinez, G. R.; Ravanat, J.-L.; Medeiros, M. H. G.; Cadet, J.; Di Mascio, P. *J. Am. Chem. Soc.* **2000**, *122*, 10212.
 27. Regulus, P.; Spessotto, S.; Gateau, M.; Cadet, J.; Favier, A.; Ravanat, J.-L. *Rapid Commun. Mass Spectrom.* **2004**, *16*, 2223.
 28. Ravanat, J.-L.; Remaud, G.; Cadet, J. *Arch. Biochem. Biophys.* **2000**, *374*, 118.
 29. Martinez, G. R.; Medeiros, M. H. G.; Ravanat, J.-L.; Cadet, J.; Di Mascio, P. *Biol. Chem.* **2002**, *383*, 607.
 30. Ye, Y.; Muller, J. G.; Luo, W.; Mayne, C. L.; Shalopp, A. J.; Jones, R. A.; Burrows, C. J. *J. Am. Chem. Soc.* **2003**, *125*, 13926.
 31. McCallum, J. E. B.; Kuniyoshi, C. Y.; Foote, C. S. *J. Am. Chem. Soc.* **2004**, *126*, 16777.
 32. Sheu, C.; Foote, C. S. *J. Am. Chem. Soc.* **1995**, *117*, 474.
 33. Raoul, S.; Cadet, J. *J. Am. Chem. Soc.* **1996**, *118*, 1892.
 34. Cadet, J.; Berger, M.; Buchko, G. W.; Joshi, P. C.; Raoul, S.; Ravanat, J.-L. *J. Am. Chem. Soc.* **1994**, *116*, 7403.
 35. Kang, P.; Foote, C. S. *J. Am. Chem. Soc.* **2002**, *124*, 4865.
 36. Cadet, J.; Douki, T.; Gasparutto, D.; Ravanat, J.-L. *Mutat. Res.* **2003**, *531*, 5.
 37. Douki, T.; Ravanat, J.-L.; Angelov, D.; Wagner, J. R.; Cadet, J. *Top. Curr. Chem.* **2004**, *236*, 1.
 38. Ravanat, J.-L.; Saint-Pierre, C.; Di Mascio, P.; Martinez, G. R.; Medeiros, M. H. G.; Cadet, J. *Helv. Chim. Acta* **2001**, *84*, 3702.
 39. Boiteux, S.; Gajewski, E.; Laval, J.; Dizdaroglu, M. *Biochemistry* **1992**, *31*, 106.
 40. Buchko, G. W.; Wagner, J. R.; Cadet, J.; Raoul, S.; Weinfeld, M. *Biochim. Biophys. Acta* **1995**, *1263*, 17.
 41. Ravanat, J.-L.; Di Mascio, P.; Martinez, G. R.; Medeiros, M. H. G.; Cadet, J. *J. Biol. Chem.* **2000**, *275*, 40601.

Reaction of singlet oxygen with some benzylic sulfides

Sergio M. Bonesi,^{a,b} Maurizio Fagnoni,^b Sandra Monti^c and Angelo Albini^{b,*}

^aCHIDECAR-CONICET, Dep. Quim. Org., Fac. Cien. Ex. Nat., Universidad de Buenos Aires, Ciudad Universitaria, 1428 Buenos Aires, Argentina

^bDepartment of Organic Chemistry, University of Pavia, v. Taramelli 10, 27100 Pavia, Italy
^cISOF-CNR Institute, v. Gobetti 123, 40129 Bologna, Italy

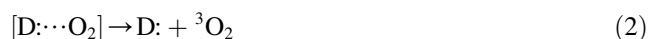
Received 8 June 2006; revised 25 July 2006; accepted 28 July 2006
Available online 27 September 2006

Abstract—Product distribution, total quenching rate (k_T), and rate of chemical reaction (k_r) with singlet oxygen have been determined for some alkyl, benzyl, α -methylbenzyl, and cumyl sulfides. Their contributions depend on the steric hindering around the sulfur atom. In protic solvents, the sulfoxide is the main product via a hydrogen-bonded persulfoxide. In apolar solvents, intramolecular α -H abstraction leads to oxidative C–S bond cleavage, with varying efficiency. The behavior of sulfides is compared to that of alkenes and amines.

© 2006 Elsevier Ltd. All rights reserved.

1. Introduction

The fascinating chemistry of singlet oxygen remains an appealing field of research and continues to reveal new mechanistic facets and synthetic applications.^{1,2} This strong electrophile attacks either a π nucleophile (alkenes, polyenes, electron-rich aromatics, and heterocycles) or a nucleophile (organic sulfur or phosphorous derivatives). The interaction with most nucleophiles (D:) leads to a weakly bonded complex that evolves either toward the formation of a stable product or toward the starting compound and triplet oxygen (Eqs. 1–3).³



Thus, a single intermediate leads both to chemical reaction and to physical quenching. Both the extent to which the initial complex is formed (in competition with singlet oxygen decay) and the ratio between the ensuing processes vary greatly depend on the structure of the nucleophile as well as on the experimental conditions (solvent, temperature, pressure, catalysis by various additives). As an example,

chemical reaction is all important with alkenes, while both aromatic and aliphatic amines mainly act as physical quenchers and sulfides lie in between, with the portion of chemical reaction varying from a few percent to almost quantitative. The important role that oxygen and its excited states have in chemical and biological reactions of sulfur-containing compounds has stimulated a host of experimental and computational studies aimed at the rationalization of the mechanism(s) involved.^{4–10} Several years ago we initiated a program to study the photooxygenation of sulfides, in particular benzyl sulfides.^{11–14} Presently, we report some new results on related substrates and attempt to frame the findings in the general picture of singlet oxygen reactions.

2. Results

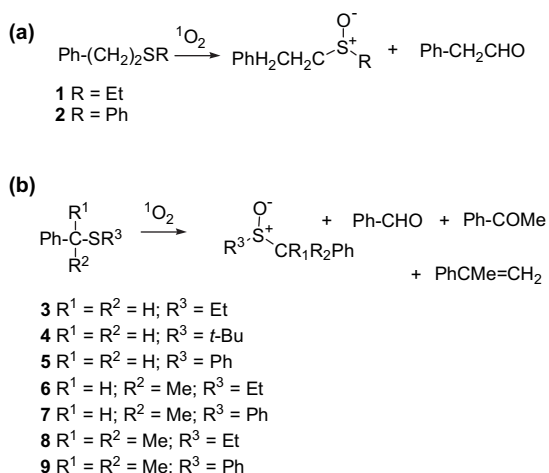
The oxygenation of a series of benzyl sulfides was carried out by visible light irradiation of a sensitizer (Rose Bengal in alcohols and in acetonitrile, tetraphenylporphine in benzene) in an oxygen saturated solution. The conversion was limited to ca. 30%, in order to limit secondary photoreactions, and the mass balance was good, except when noted. The solvents used were apolar benzene, polar acetonitrile, and protic methanol. The results are reported in Table 1. It is well known that aliphatic sulfides yield the sulfoxides with a small amount of the sulfones. We examined phenethyl ethyl sulfide (**1**) and found that, while the sulfoxide is virtually the only product in methanol, in acetonitrile, and in benzene a significant amount of phenylacetaldehyde (43% in the last solvent) was formed (see Scheme 1, Table 1). Essentially the same pattern was followed when using phenethyl phenyl sulfide (**2**).

* Corresponding author. Tel.: +39 0382 987316; fax: +39 0382 987323; e-mail: angelo.albini@unipv.it

Table 1. Products from the photosensitized oxidation of some sulfides^a

Sulfide	Solvent	Products, %	
		S-Oxidation	Cleavage
1, PhCH ₂ CH ₂ SEt	MeOH	PhCH ₂ CH ₂ SOEt, 74	—
	MeCN	PhCH ₂ CH ₂ SOEt, 61	PhCH ₂ CHO, 15
	C ₆ H ₆	PhCH ₂ CH ₂ SOEt, 57	PhCH ₂ CHO, 43
2, PhCH ₂ CH ₂ SPh	MeOH	PhCH ₂ CH ₂ SOPh, 100	—
	MeCN	PhCH ₂ CH ₂ SOPh, 80	PhCH ₂ CHO, 20
	C ₆ H ₆	PhCH ₂ CH ₂ SOPh, 58	PhCH ₂ CHO, 42
3, PhCH ₂ SEt	MeOH	PhCH ₂ SOEt, 63	PhCHO, 25
	MeCN	PhCH ₂ SOEt, 6	PhCHO, 90
	C ₆ H ₆	PhCH ₂ SOEt, 2	PhCHO, 89
4, PhCH ₂ S- <i>t</i> -Bu	MeOH	PhCH ₂ SO- <i>t</i> -Bu, 95	PhCHO, 5
	MeCN	PhCH ₂ SO- <i>t</i> -Bu, 18	PhCHO, 45
	C ₆ H ₆	PhCH ₂ SO- <i>t</i> -Bu, 27	PhCHO, 43
5, PhCH ₂ SPh	MeOH	PhCH ₂ SOPh, 65; PhCH ₂ SO ₂ Ph, 4	PhCHO, 27; (PhS) ₂ , 4
	MeCN	PhCH ₂ SOPh, 11	PhCHO, 77; (PhS) ₂ , 17
	C ₆ H ₆	PhCH ₂ SOPh, 13	PhCHO, 51; (PhS) ₂ , 11
6, PhCHMeSEt	MeOH	PhCHMeSOEt, 51; PhCHMeSO ₂ Et, 2	PhCOMe, 2
	MeCN	PhCHMeSOEt, 66; PhCHMeSO ₂ Et, 1	PhCOMe, 6
	C ₆ H ₆	PhCHMeSOEt, 37; PhCHMeSO ₂ Et, 15	PhCOMe, 7
7, PhCHMeSPh	MeOH	PhCHMeSOPh, 53; PhCHMeSO ₂ Ph, 5	PhCOMe, 1
	MeCN	PhCHMeSOPh, 21	PhCOMe, 73; (PhS) ₂ , 11
	C ₆ H ₆	PhCHMeSOPh, 36	PhCOMe, 37; (PhS) ₂ , 13
8, PhCMe ₂ SEt	MeOH	—	PhCOMe, 16; (PhCMe ₂ S) ₂ , 1
	MeCN	—	PhCOMe, 5; PhCMe=CH ₂ , 1; (PhCMe ₂ S) ₂ , 8
	C ₆ H ₆	—	PhCOMe, 15; PhCMe=CH ₂ , 3; (PhCMe ₂ S) ₂ , 23
9, PhCMe ₂ SPh	All	—	—

^a The dye-sensitized photooxidation of sulfides **3** and **6** has been previously reported (Ref. 14). The small differences in the product distribution depend on the different irradiation time.



Scheme 1.

With benzyl ethyl sulfide (**3**), as already known,^{13–15} cleavage to benzaldehyde is an important path, which predominates in nonprotic solvents. Similar results were obtained with other benzyl derivatives, viz. the *tert*-butyl (**4**) and the phenyl sulfides (**5**, see Scheme 1 and Table 1); some phenyl disulfide was also obtained in the last case.

α -Methylbenzyl sulfides were next examined. With the ethyl derivative (**6**) the sulfoxide was the main product in all of the solvents tested, with acetophenone remaining below 7%. On the other hand, the corresponding phenyl derivative (**7**) exhibited again a medium-depending oxygenation, with a large predominance of the sulfoxide in methanol, but

acetophenone (accompanied by some phenyl disulfide) was the main product in the other cases.

Finally, cumyl ethyl sulfide (**8**) was consumed under photo-oxygenation conditions, but gave no sulfoxide. The products formed were acetophenone and α -methylstyrene along with some cumyl disulfide. The yields were low in this case, possibly because the oxygenation was quite sluggish and secondary photodecomposition was important. The corresponding phenyl derivative (**9**) was virtually stable under photooxygenation conditions.

The kinetics of these photooxygenations was then studied by measuring the total rate constant for the quenching of singlet oxygen (k_T) through the change in the luminescence lifetime. As it appears in Table 2, the values varied considerably, dropping by 3 orders of magnitude from ethyl sulfide to cumyl phenyl sulfide. These values were measured in deuteriochloroform in order to obtain meaningful data also for the entire range of sulfides including the least reactive derivatives, which would not be possible in solvents where the singlet oxygen lifetime is shorter. On the other hand, previous studies showed that k_T changes very little with the solvent characteristics, including polarity, for example, by <10% with benzyl ethyl sulfide¹³ and by <20% for diethyl sulfide¹⁶ in solvents of different polarity, for example, when passing from benzene to acetonitrile. Therefore, the reported values should be reasonably valid also for the other solvents.

The rate for chemical reaction (k_c), as opposed to physical quenching, was then measured in competition experiments, as previously done in the literature, by using the oxidation of

Table 2. Rate of total quenching (k_T) and rate of chemical reaction (k_r) for the singlet oxygen reaction with some sulfides

Sulfide	Solvent	$k_r \times 10^7, \text{M}^{-1} \text{s}^{-1}$	S-Oxidation versus cleavage	k_r/k_T	$k_T \times 10^7, \text{M}^{-1} \text{s}^{-1}$ in CDCl_3
Et ₂ S	MeOH	6.6×10^{7a}		1.8	3.0 ^b
	C ₆ H ₆	0.39 ^a		0.11	
1, PhCH ₂ CH ₂ SEt	MeOH	0.9	95:5	0.6	1.5
	MeCN	0.24	80:20	0.16	
	C ₆ H ₆	0.2	57:43	0.13	
2, PhCH ₂ CH ₂ SPh	MeOH	0.027	100:0	0.51	0.53
	MeCN	0.004	80:20	0.08	
	C ₆ H ₆	0.008	58:42	0.15	
3, PhCH ₂ SEt	MeOH	1.2	72:28	1	1.2
	MeCN	0.61	4:96	0.51	
	C ₆ H ₆	0.55	2:98	0.46	
4, PhCH ₂ S- <i>t</i> -Bu	MeOH	0.027	72:28	0.08	0.35
	MeCN	0.085	29:71	0.24	
	C ₆ H ₆	0.062	39:61	0.18	
5, PhCH ₂ SPh	MeOH	0.026	72:28	0.45	0.058
	MeCN	0.017	13:87	0.29	
	C ₆ H ₆	0.016	20:80	0.28	
6, PhCHMeSEt	MeOH	0.11	96:4		
	MeCN	0.07	92:8		
	C ₆ H ₆	0.03	84:16		
7, PhCHMeSPh	MeOH	0.018	98:2		
	MeCN	0.009	22:78		
	C ₆ H ₆	0.001	50:50		
8, PhCMe ₂ SEt	MeOH	0.026	≈0:100	0.16	0.165
	MeCN	0.12	≈0:100	0.73	
	C ₆ H ₆	0.17	≈0:100	1.03	
9, PhCMe ₂ SPh	All	<0.001		<0.3	0.0034

^a From Ref. 16.

^b In benzene, from Ref. 16.

an alkene (octaline) under the same conditions as the standard.^{16,17} The values obtained are reported in Table 2.

3. Discussion

3.1. Physical and chemical quenching by sulfides: dependence on the structure

All of the present reactions likely occur via a persulfoxide,¹⁸ generally accepted as the first intermediate in the reaction of singlet oxygen with sulfides, and the extent of chemical versus physical quenching is determined by the relative importance of the different paths from this species. As for the formation of this intermediate, the k_T data in Table 2 support earlier observations¹⁹ and show that the total quenching rate is decreased when the sulfur atom is bonded to a phenyl group (by a factor 20–50, see the pairs 1/2, 3/5, 8/9) or to a tertiary carbon (by a factor 4–15, see the pairs 3/4, 3/8, 5/9). This correlates with steric hindrance, and thus with nucleophilicity, rather than with oxidizability (see below).

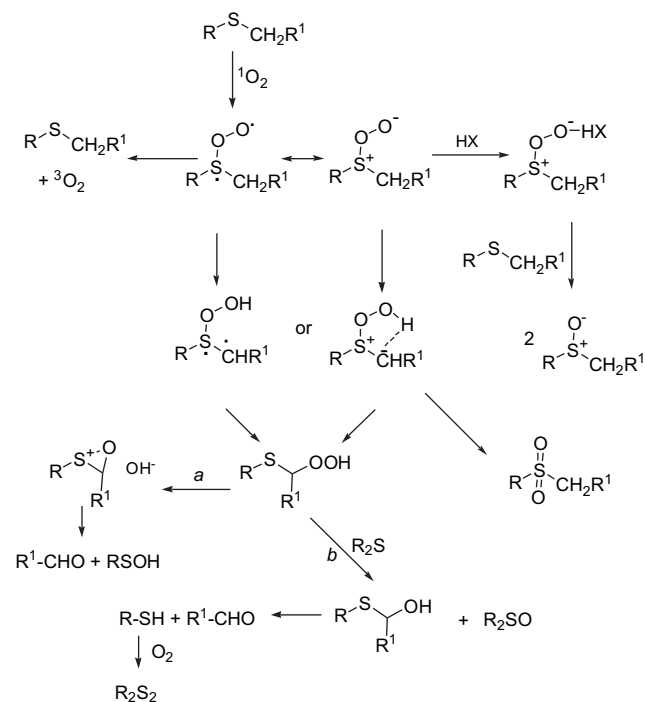
As for the ensuing chemistry, two different reactions occur, viz. sulfoxidation and C–S bond cleavage to yield carbonyl derivatives. Table 2 shows that chemical reaction is the main path ($k_r > 0.5k_T$) for nonhindered sulfides (Et₂S, 1–3, 5) in methanol and in this case the product is the sulfoxide. This is attributed to hydrogen bonding of the persulfoxide that makes it a stronger electrophile and thus facilitates oxygen transfer to a second sulfide molecule (the ‘single intermediate’ mechanism initially proposed by Foote,⁵ and known to

be promoted by acids).^{13,16} Accordingly, the limiting value of k_r is $2k_T$, as indeed observed with dialkyl sulfides (see diethyl sulfide in Table 2). The presence of substituents in α -position in the chain makes the reaction less effective, reasonably because of the steric hindrance encountered by the approaching sulfides makes oxygen transfer less competitive with decay of the persulfoxide. The effect of inserting two methyl groups in α is apparent: with both 4 and 8 k_r is $< 0.15k_T$ and the reaction in methanol becomes slower than that in aprotic solvents. A phenyl group likewise limits k_r , but in this case some effect is exerted also when the substituent is in the β -position.

In aprotic solvent, however, chemical reaction is generally less competitive with physical decay and may be dominated by C–S bond cleavage. This process involves hydrogen transfer to form an intermediate ylide (see below).^{20–23} Contrary to sulfoxide formation, this is scarcely affected by bulky groups around the sulfur atoms (the efficiency moderately changes in *S*-ethyl, phenyl, and *tert*-butyl derivatives, see the series 3–5), while its role depends on the presence of a weak α C–H bond. Thus, with diethyl and dibutyl sulfide C–S cleavage has been detected as an inefficient process ($k_r/k_T \leq 0.05$), though this is more important for phenethyl sulfides ($k_r/k_T \approx 0.1$). With benzyl sulfides, however, the value of k_r increases up to $0.5k_T$. Furthermore, with the first two sulfides cleavage is always accompanied by an equally efficient sulfoxidation, while with benzyl derivatives sulfoxidation is all but negligible in aprotic solvents (the sluggish C–S cleavage in sulfide 8, lacking a α -H apparently involves a different path).

The dependence on the C–H bond strength suggests that, as proposed earlier,^{13,24} this is a radical process and the ylide is to be regarded as a diradical rather than as a zwitterion (with anion stabilizing substituent the situation is different).^{24,25} However, stereoelectronic factors also operate. In low-energy conformations the S⁺–O–O[−] moiety bisects the angle between the S-bonded groups R–S–R' and the outer oxygen may be close to an α -CH.^{20,21} This determining factor depends on the nature of both R and R'. Thus, the inefficient C–S bond cleavage from the α -methylbenzyl ethyl sulfide **5**, as opposed to the high reactivity of the non-methylated analogue **5** has been rationalized through PM3 calculations as due to a long O[−]⋯H distance in two out of four of the low-energy conformations of the corresponding persulfoxide.²⁶ However, Table 1 shows that with the S-phenyl analogue **7** C–S bond cleavage is restored as the main process in aprotic solvents, reasonably because the bulky phenyl group pushes the oxygen toward the benzylic hydrogen.

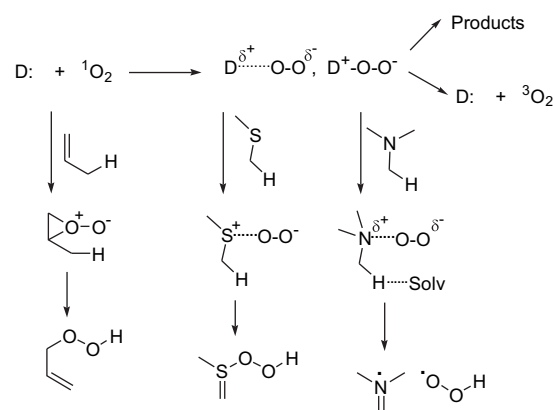
In turn, the ylide rearranges to a α -hydroperoxy sulfide and this intermediate gives the end product via either intramolecular or intermolecular oxygen transfer, as suggested by Clennan (Scheme 2).²⁴ The first path (a in Scheme 2) gives the carbonyl derivatives along with sulfinates or other oxidized sulfurated products, the latter one (path b) equimolecular amounts of sulfoxide, carbonyl, and mercaptan (the latter oxidized under these conditions to the disulfide). Table 1 shows that path b is followed by the alkyl sulfides **1** and **2** in benzene. As for the benzyl sulfides, the reaction in the same solvent shifts from path a exclusively for **3** to increasing component of path b in **4** and **5** and path b exclusively with **7**. Apparently, sterical hindering at the sulfur atom discourages formation of the thioxiranium ring more than accepting an oxygen from a hydroperoxide.



Scheme 2.

3.2. The oxidation of sulfides versus that of alkenes and amines: the first intermediate

It may be useful to consider the mechanism in Scheme 2 in the general frame of singlet oxygen reactions. A first-sight comparison of the oxidation of sulfides via persulfoxide and the ylide with the ene reaction of alkenes via a peroxide as well as with the oxidation of amines via a complex and α -deprotonation (Scheme 3) seems to imply an analogous reaction course, involving transfer of an α -hydrogen after electrophilic attack. One may wonder, how far can the analogy be carried; as an example, is there a similar structure dependence? This is not the case: introducing a phenyl ring onto the reacting moiety increases k_T with amines (PhNR₂>R₃N), but decreases it with sulfides and moderately affects the k_f/k_T ratio in both cases; with alkenes, phenyl substitution induces only a partial regioselectivity.^{27a} A phenyl group in α greatly increases k_f/k_T in sulfides by making intramolecular hydrogen abstraction possible, but has little effect with alkenes (attack at the benzylic hydrogen is not or moderately preferred in benzyltrimethylethylene);^{27b,c} k_T does not change in both cases. Below we consider in some detail the three photooxygenations.



Scheme 3.

Both with π (alkenes) and with n (sulfides or amines) donors, the first intermediate is a more or less labile adduct where one of the oxygen atom is engaged. Clearly the CT character of such complexes is much stronger with good donors such as amines with respect to the other cases, as evidenced, for example, by the dramatic dependence of k_T on the solvent polarity with these donors^{3,28–30} in contrast to the near independence with alkenes and sulfides. However, singlet oxygen is a relatively poor oxidant [$E^0(\text{O}_2^{\cdot-}/^1\text{O}_2)=0.11$ V vs SCE]³¹ and even with amines [e.g. E^0 (DABCO) 1.02 V, PhNMe₂ 0.71 V] 'full' electron transfer remains endothermic (Table 3). There is a dependence of k_T on ΔG_{ET} and for various families of donors the total quenching rate constants roughly follow such dependence (notice however that with amines k_T changes over 2–4 orders of magnitude with solvent polarity; therefore care is required in the evaluation of the results with these substrates).^{3,32,33} This is illustrated in Figure 1, where a plot of $\log(k_T)$ versus E^0 for sulfides, amines, alkenes, and aromatics is presented (see Table 3 for details on the data used). It is apparent that aromatic sulfides (like alkenes and amines) show some dependence, while aliphatic sulfides do not (points lie on an almost vertical line).

Table 3. Total quenching rate of singlet oxygen and oxidation potential for various donors used in Figure 1

	k , $M^{-1} s^{-1}$	$\log k$	E^0 , V versus SCE
<i>Aliphatic amines^a</i>			
Et ₃ N	6.5×10^7	7.80	1.53
<i>n</i> -Bu ₃ N	5.8×10^7	7.76	1.34
<i>N</i> -Methylpiperidine	5.3×10^7	7.72	1.73
DABCO	5.2×10^7	7.71	1.02
(<i>n</i> -Pr) ₂ NH	1.8×10^7	7.25	1.96
Et ₂ NH	1.5×10^7	7.18	2.04
Piperidine	5.8×10^6	6.76	2.07
(<i>i</i> -Pr) ₂ NH	1.8×10^6	6.25	1.83
<i>i</i> -BuNH ₂	4.1×10^5	5.61	2.66
<i>n</i> -PrNH ₂	2.3×10^5	5.36	2.75
<i>Aromatic amines (in MeCN)^b</i>			
TMPD	5.2×10^9	9.71	0.16
<i>p</i> -Phenylenediamine	2.8×10^{10}	10.45	0.18
<i>p</i> -Aminodiphenylamine	1.1×10^9	9.04	0.27
<i>N,N</i> -Diphenyl- <i>p</i> -phenylenediamine	4.5×10^8	8.65	0.34
<i>N,N,N',N'</i> -Tetramethylbenzidine	1.0×10^9	9.25	0.43
<i>o</i> -Phenylenediamine	8.0×10^8	8.90	0.40
2-Aminoanthracene	2.3×10^8	8.36	0.44
1-Naphthylamine	2.7×10^8	8.43	0.54
<i>N,N</i> -Dimethyl- <i>p</i> -toluidine	1.0×10^9	9.00	0.65
<i>N,N</i> -Dimethylaniline	2.85×10^8	8.45	0.71
Diphenylamine	1.8×10^7	7.25	0.83
<i>N</i> -Methyl- <i>N,N</i> -diphenylamine	4.1×10^6	6.61	0.84
Aniline	1.06×10^7	7.02	0.87
<i>p</i> -Iodoaniline	5.1×10^6	6.70	0.88
<i>p</i> -Bromoaniline	7.1×10^6	6.85	0.89
<i>p</i> -Chloroaniline	7.6×10^6	6.88	0.90
Triphenylamine	4.1×10^7	7.61	0.92
<i>N,N</i> -Dimethyl- <i>p</i> -nitroaniline	1.1×10^6	6.04	1.19
<i>Alkenes (in MeOH)^c</i>			
Tetramethylethylene	4.35×10^7	7.64	1.78
1,2-Dimethylcyclohexene	7.35×10^6	6.87	1.64
2-Methyl-2-butene	2.45×10^6	6.39	2.21
1-Butene	1.2×10^4	4.08	2.50
1-Methylcyclopentene	7.3×10^5	5.86	2.06
1-Methylcyclohexene	1.2×10^5	5.08	2.00
Cyclopentene	8.7×10^4	4.94	2.49
Cyclohexene	5.4×10^3	3.73	2.33
<i>Aromatics (in MeCN)^b</i>			
1,2,4-Trimethoxybenzene	4.4×10^7	7.64	1.12
1,4-Dimethoxybenzene	6.4×10^6	6.81	1.34
1,2,3-Trimethoxybenzene	1.7×10^5	5.23	1.42
1,2-Dimethoxybenzene	7.4×10^5	5.87	1.45
Hexamethylbenzene	6.4×10^6	6.81	1.46
1,3-Dimethoxybenzene	2.2×10^5	5.34	1.49
1,3,5-Trimethoxybenzene	2.6×10^5	5.41	1.49
Pentamethylbenzene	1.2×10^6	6.08	1.58
1,2,4,5-Tetramethylbenzene	3.2×10^5	5.50	1.59
1,2,4-Trimethylbenzene	4.1×10^4	4.61	1.71
<i>Aliphatic sulfides</i>			
EtSEt ^d	3.0×10^7	7.50	1.57 ⁱ
<i>t</i> -BuS- <i>t</i> -Bu ^e	4.7×10^4	4.67	1.59 ^j
PhCH ₂ CH ₂ SEt ^f	1.5×10^7	7.18	1.65 ^j
PhC(CH ₃) ₂ SEt ^f	1.6×10^6	6.20	1.60 ^k
PhCH ₂ SEt ^g	1.0×10^7	7.00	1.60 ^k
<i>Aromatic sulfides</i>			
PhS- <i>t</i> -Bu ^e	1.2×10^4	4.08	1.70 ^l
PhSPh ^c	3.9×10^4	4.59	1.43 ⁱ
PhSMe ^h	2.3×10^6	6.36	1.34 ^h
<i>p</i> -MePhSMe ^h	4.6×10^6	6.66	1.24 ^h
<i>p</i> -MeOPhSMe ^h	7.6×10^6	6.88	1.13 ^h
<i>p</i> -BrPhSMe ^h	1.1×10^6	6.04	1.41 ^h
<i>p</i> -CNPhSMe ^h	7.3×10^4	4.86	1.61 ^h
<i>p</i> -NO ₂ PhSMe ^h	8.7×10^4	4.94	1.70 ^h
PhCH ₂ CH ₂ SPh ^f	5.3×10^5	5.72	1.21 ^m

(continued)

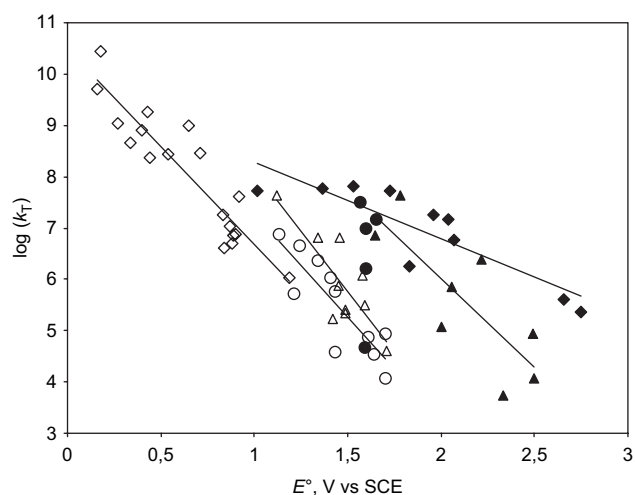
Table 3. (continued)

	k , $M^{-1} s^{-1}$	$\log k$	E^0 , V versus SCE
PhCH ₂ SPh ^f	5.8×10^5	5.76	1.43 ⁿ
PhC(CH ₃) ₂ SPh ^f	3.4×10^4	4.53	1.64 ^k

^a Ref. 36.^b Ref. 33.^c Ref. 57.^d Ref. 16.^e Ref. 12.^f This work.^g Ref. 13.^h Ref. 11.ⁱ Ref. 58.^j Assumed equal to that of diethyl sulfide.^k Ref. 59.^l Ref. 60.^m Ref. 61.ⁿ Ref. 62.

When donors of the same family and similar bulk at the reacting site are compared, a good correlation with calculated ΔG_{ET} is observed as is the case for 4-substituted thioanisoles. As shown in Figure 1, a good correlation of k_T with E^0 of the donor has been found (or with the substituent σ values, themselves proportional to E^0).¹¹ The correlation with σ is consistent with the strong electrophilic character of singlet oxygen (when compared with the ρ value obtained with other oxygen transfer reagents, ρ (¹O₂) is larger than with negatively charged species, though smaller than with the positive ones (see Table 4).

However, when donors with different steric hindrance are considered the correlation with calculated ΔG_{ET} breaks

**Figure 1.** Rate constants for total quenching of singlet oxygen by sulfides (circles) and amines (diamonds) (filled symbols, aliphatic; empty symbols, aromatic derivatives) as well as alkenes (▲) and electron-rich aromatics (△) versus the nucleophile E^0 . See Table 3 for details.**Table 4.** ρ Values from the oxidation of some thioanisoles

Reagent	ρ	Ref.
Me ₂ B(OH) ₂ (OOH) ²⁻	-0.65	53
Me ₂ B(OH) ₃ (OOH) ⁻	-1.5	53
¹ O ₂	-1.97	11
<i>tert</i> -Butylperoxyiodanes	-3.32	54

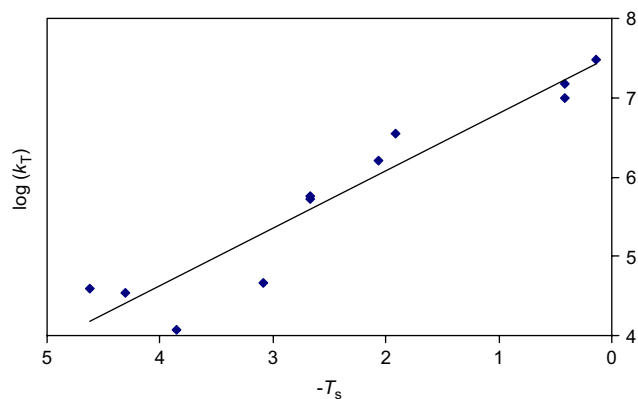


Figure 2. Rate constants for total quenching of singlet oxygen by aliphatic and aromatic sulfides versus the Taft steric parameters T_s .^{55,56} See Table 5 for details.

down.³⁴ The order of reactivity of aliphatic sulfides depends here on nucleophilicity, and thus on bulky substituents ($R_2S \approx PhCH_2SR > PhSR > Ph_2S$, the same order observed in sulfoxidation by metal oxo complexes).³⁵ The slowing effect of substituents close to the moiety involved in the interaction with singlet oxygen has been observed with amines^{36,37} and sulfides.³⁸ Indeed, Clennan showed that $\log(k_T)$ linearly correlated with the Taft steric parameter T_s with hydrazines (slope 0.9)³⁹ and sulfenamides (1.47),⁴⁰ although this was not the case for disulfides.⁴⁰

In the present case, we observed that the various families of sulfides we considered (RSEt, RS-*tert*-Bu, RSPH) all had a similar dependence on the T_s value of substituent R. Indeed, when a single correlation with the parameters of both substituents for sulfides RSR^1 according to Eq. 2 was attempted, a trend, if not a linear dependence was observed, with a slope somewhat lower than those quoted above (slope -0.72 , r^2 0.91, see Fig. 2, both the presently studied substrates and other bulky aliphatic and aromatic sulfides are included, see Table 5).

$$\log(k_T) = \text{constant} + K [T_s(R) + T_s(R^1)] \quad (4)$$

Table 5. Total quenching rate of singlet oxygen and Taft parameters for various sulfides used in Figure 2

Sulfide RSR^1	$\log(k_T)^a$	T_s^b	Summed up T_s for the two substituents
EtSEt	7.48	Et, 0.07	0.14
<i>t</i> -BuSt-Bu	4.67	<i>t</i> -Bu, 1.54	3.08
PhSt-Bu	4.08	Ph, 2.31	3.85
PhSPH	4.59		4.62
PhCH ₂ CH ₂ SEt	7.18	PhCH ₂ CH ₂ , 0.38	0.42
PhCH ₂ St-Bu	6.54	PhCH ₂ , 0.38	1.92
PhC(CH ₃) ₂ SEt	6.2	PhC(CH ₃) ₂ , 2	2.07
PhCH ₂ CH ₂ SPh	5.72		2.67
PhCH ₂ SPh	5.76		2.67
PhC(CH ₃) ₂ SPh	4.53		4.31
PhCH ₂ SEt	7.0		0.42

^a For the k_T values see previous¹² and present work.

^b The T_s parameters are taken from the compilations by Taft⁵⁵ and Dubois.⁵⁶ The value for the PhCMe₂ group is not available in these references. It has been taken as 2.0 by correcting the value for the benzyl group proportionally to the change observed in passing from Et to *iso*-Pr and *tert*-Bu.

We feel that this result is informative. Recent calculations show that singlet oxygen, besides being a strong electrophile, has also some nucleophilic character due to the presence of a high energy HOMO geometrically orthogonal to the LUMO.^{41,42} This has been recognized as the source of the asynchronicity of the ene reaction, due to the tendency for both the HOMO and the LUMO of the alkene to be involved in an interaction with a single oxygen atom. Thus, tendency toward 1,1 bond formation distinguishes the ene reaction, 'as opposed to the simultaneous 1,2-bond formation distinctive of synchronous, concerted transition states of the Diels–Alder reaction'.⁴²

On the other hand, with *n* donors such as sulfides and amines the nucleophilic contribution scarcely operates (and if it does, more with the former donors). The initial adduct appears to be slightly less stable than the reagents (by 6.6 kcal/mol, or at most isoenergetic depending on the method used) with the sulfides^{20,21,43,44} and markedly less stable with amines (8 to >20 kcal/mol).⁴⁵ Notice that also in the latter case a close proximity between nitrogen and one of the oxygen atoms is required in the complex. Summing up, steric factors are important and k_T depends on the nucleophilicity of the quencher.

3.3. The chemical reaction

The comparison can be extended to the ensuing evolution of the first intermediate, which determines the chemical or physical nature of the quenching. The ene reaction with alkenes is concerted and bonding of the *second* oxygen atom occurs as the first intermediate evolves to the products via a valley ridge with no barrier. As for sulfides, a path involving bonding of the second oxygen atom would be the formation of a thiadioxirane, which has been located as a reasonably stable intermediate, but is separated from the initial persulfoxide by an insurmountable barrier of 10–20 kcal/mol.²⁰

The other intramolecular possibility is the above discussed hydrogen (or proton) transfer from the position α to the heteroatom, a path that is indeed analogous to the perepoxide–alkylhydroperoxide conversion with alkenes, but differs from that case in that it is not barrierless. In the case of dimethylpersulfoxide, a 6–7 kcal/mol activation energy has been calculated for this path, which is only 1/20th of physical quenching in apolar, nonhydrogen bonding solvents, but is made more effective by α -phenyl substitution (k_r can be as large as 50% of k_T for some benzyl sulfides, provided that conformational factors do not prevent it).

This path is even less efficient with amines ($k_r < 0.1k_T$ with tertiary aliphatic amines, negligible with aromatic tertiary amines).⁴⁶ The role of this path increases both in a nucleophilic solvent, which is able to accept the α -proton, and when a better electrofugal group is present, as with α -trimethylsilyl derivatives.⁴⁶

Finally, intermolecular activation of the first intermediate is possible, provided that this is sufficiently long-lived. With sulfides indeed activation by acids (or by nucleophiles) is effective, so that a more active species is formed and transfers oxygen to a second molecule of sulfide (see Scheme 1;

this step, as mentioned above, is again subjected to steric hindrance). This mechanism is followed in methanol and, when intramolecular activation is slow, also in a polar aprotic solvent such as MeCN. However, this path is less important with amines (the barely bonded CT complex is too short-lived for activation) as well as, for the opposite reason, with alkenes (the strength of the bonds formed leaves little room for improvement).

In conclusion, the reaction of singlet oxygen with a series of benzyl sulfides was examined. The total quenching rate (k_T) depends on the nucleophilicity of the sulfide, since the persulfoxide is formed over an essentially flat surface and bulky substituents tilt the balance against bonding with singlet oxygen, drastically lowering k_T . The strength of the S–O bond formed with sulfides is intermediate between the strong C–O bond formed with alkenes and the weak N–O bond with amines, resulting in largely variable proportion of chemical quenching (k_r/k_T). Two types of chemical reactions contribute. The path leading to sulfoxide via the protonated persulfoxide observed in a protic medium depends again on the sulfide nucleophilicity (making the overall dependence quadratic). The photocleavage reaction observed in aprotic solvent depends on the strength of the α -CH bond.

4. Experimental

4.1. Materials

Sulfides **1**, **2**,⁴⁷ **3–5**,⁴⁸ **6**, **7**,⁴⁹ **8**, and **9**⁵⁰ were prepared according to the published procedures. 5,10,15,20-Tetraphenyl-21H-porphine (Aldrich) and CDCl_3 (Carlo Erba) were used without further purification. Samples of sulfioxides and sulfones⁵¹ as well as of diphenyl disulfide⁵² for the quantitative analysis of the photoproducts were prepared according to the published procedures. The other photooxidation products were commercially available.

4.2. Photoreactions

The photooxidations were carried out by using 0.01–0.1 M solutions of the sulfides in the presence of Rose Bengal (in methanol or acetonitrile) or of tetraphenylporphine in benzene. The solutions were contained in rubber-stoppered Pyrex tubes. These were exposed to four phosphor-coated 15 W lamps (Applied Photophysics) emitting from 350 to 700 nm while a stream of dry oxygen saturated with the appropriate solvent was passed in the solution through a needle.

The products formed were determined by capillary GC (HP1) on the basis of calibration curves in the presence of cyclododecene as the internal standard or by reverse phase HPLC with MeCN– H_2O mixture as the eluant, λ 230 and 260 nm, respectively, with biphenyl as the internal standard.

4.3. Rate of photoreactions

Rate constants for the quenching of singlet oxygen were obtained from the shortening of the $(\text{O}_2)^1\Delta_g$ emission lifetime

at 1.27 μm in the presence of known amounts of sulfides in aerated CDCl_3 . Singlet oxygen was generated by energy transfer to O_2 from the triplet state of TPP, populated by laser excitation (Nd:YAG laser, 532 nm). The near-IR luminescence of molecular oxygen was observed at 90° geometry through a 5 mm thick AR coated silicon metal filter with wavelength pass $>1.1 \mu\text{m}$ and an interference filter at 1.27 μm by means of a preamplified (low-impedance) Ge-photodiode cooled at 77 K (Applied Detector Corporation, Model 403 HS, time resolution 300 ns). Single exponential analysis of the emission decay was performed with the exclusion of the initial part of the signal, affected by scattered light, sensitizer fluorescence, and formation profile of the emission signal itself. The rate of chemical reaction was determined by comparing the oxidation of octaline ($k_r=1.83 \times 10^6 \text{ M}^{-1} \text{ s}^{-1}$) under the same conditions.

Acknowledgements

Partial support of this work by MURST, Rome, is gratefully acknowledged.

References and notes

- Clennan, E. L.; Pace, A. *Tetrahedron* **2005**, *61*, 6665.
- Clennan, E. L. *Tetrahedron* **2000**, *56*, 9151.
- Schweitzer, C.; Schmidt, R. *Chem. Rev.* **2003**, *103*, 1685.
- First reported by Schenck: Schenck, G. O.; Krauch, C. H. *Angew. Chem.* **1962**, *74*, 510.
- Liang, J. J.; Gu, C. L.; Kacher, M. L.; Foote, C. S. *J. Am. Chem. Soc.* **1983**, *105*, 4717.
- Clennan, E. L. *Sulfur Rep.* **1996**, *19*, 171.
- Ando, W. *Sulfur Rep.* **1981**, *1*, 147.
- Ishiguro, K.; Sawaki, Y. *Bull. Chem. Soc. Jpn.* **2000**, *73*, 535.
- Clennan, E. L. Sulfide Photooxygenation. A Question of Mechanism. In *Advances in Oxygenated Processes*; Baustark, A. L., Ed.; Jay: Greenwich, CT, 1995; Vol. 4, p 49.
- Jensen, F. Theoretical Aspects of the Reaction of Organic Sulfur and Phosphorus Compounds with Singlet Oxygen. In *Advances in Oxygenated Processes*; Baustark, A. L., Ed.; Jay: Greenwich, CT, 1995; Vol. 4, p 1.
- Bonesi, S. M.; Fagnoni, M.; Albini, A. *J. Org. Chem.* **2004**, *69*, 928.
- Bonesi, S. M.; Fagnoni, M.; Monti, S.; Albini, A. *Photochem. Photobiol. Sci.* **2004**, *3*, 489.
- Bonesi, S. M.; Mella, M.; d'Alessandro, N.; Aloisi, G. G.; Vanossi, M.; Albini, A. *J. Org. Chem.* **1998**, *63*, 9946.
- Bonesi, S. M.; Torriani, R.; Mella, M.; Albini, A. *Eur. J. Org. Chem.* **1999**, 1723.
- Corey, E. J.; Ouannès, C. *Tetrahedron Lett.* **1976**, *27*, 4263.
- Clennan, E. L.; Greer, A. *J. Org. Chem.* **1996**, *61*, 4793.
- Higgins, R.; Foote, C. S.; Cheng, H. *Advances in Chemistry Series*; Gould, R. F., Ed.; American Chemical Society: Washington, DC, 1968; Vol. 77, p 102.
- Clennan, E. L. *Acc. Chem. Res.* **2001**, *34*, 875.
- Monroe, B. M. *Photochem. Photobiol.* **1979**, *29*, 761.
- Jensen, F.; Greer, A.; Clennan, E. L. *J. Am. Chem. Soc.* **1998**, *120*, 4439.
- McKee, M. L. *J. Am. Chem. Soc.* **1998**, *120*, 3963.
- Ishiguro, K.; Hayashi, M.; Sawaki, Y. *J. Am. Chem. Soc.* **1996**, *118*, 7265.

23. Greer, A.; Chen, M. F.; Jensen, F.; Clennan, E. L. *J. Am. Chem. Soc.* **1997**, *119*, 4380.
24. Touchkine, A.; Aebischer, D.; Clennan, E. L. *J. Am. Chem. Soc.* **2001**, *123*, 4966.
25. See also, Takada, T.; Ando, W. *Tetrahedron Lett.* **1986**, *27*, 1591.
26. Bonesi, S. M.; Freccero, M.; Albini, A. *J. Phys. Org. Chem.* **1999**, *12*, 703.
27. (a) Adam, W.; Arnold, M. A.; Grüne, M.; Nau, W. M.; Pisdchel, U.; Saha-Möller, C. R. *Org. Lett.* **2002**, *4*, 537; (b) Joy, A.; Robbins, R. J.; Oitichumani, K.; Ramamurthy, V. *Tetrahedron Lett.* **1997**, *45*, 4875; (c) Orfanopoulos, M.; Stephenson, L. M. *J. Am. Chem. Soc.* **1980**, *102*, 1417.
28. Gollnick, K.; Lindner, J. H. E. *Tetrahedron Lett.* **1973**, *21*, 1903.
29. Clennan, E. L.; Noe, L. J.; Wen, T.; Szneler, E. *J. Org. Chem.* **1989**, *54*, 3581.
30. For a detailed discussion of the medium effect on the quenching by amines, see: Lemp, E.; Günther, G.; Castro, R.; Curitol, M.; Zanocco, A. L. *J. Photochem. Photobiol. A: Chem.* **2005**, *175*, 146.
31. Fukuzumi, S.; Fujita, S.; Suenobu, T.; Yamada, H.; Imamura, H.; Araki, Y.; Ito, O. *J. Phys. Chem. A* **2002**, *106*, 1241.
32. Lemp, E.; Zanocco, A. L.; Lissi, E. A. *Curr. Org. Chem.* **2003**, *7*, 799.
33. Darmanyan, A. P.; Jenks, W. S.; Jardon, P. *J. Phys. Chem. A* **1998**, *102*, 7420.
34. It should also be considered that E^0 values for the—generally irreversible—oxidation of organic compounds are subject to a considerable error and not easily compared when the structure is different.
35. Caroling, G.; Rajaram, J.; Kuriacose, J. C. *J. Mol. Catal.* **1989**, *49*, 153.
36. Monroe, B. M. *J. Phys. Chem.* **1977**, *81*, 1861.
37. Li, H. R.; Wu, L. Z.; Tung, C. H. *J. Am. Chem. Soc.* **2000**, *122*, 2446.
38. Kacher, M. L.; Foote, C. S. *Photochem. Photobiol.* **1979**, *29*, 765.
39. Clennan, E. L.; Wang, D.; Clifton, C.; Chem, M. F. *J. Am. Chem. Soc.* **1997**, *119*, 4717.
40. Clennan, E. L.; Greer, A. *Tetrahedron Lett.* **1996**, *37*, 7093.
41. Leach, A. G.; Houk, K. N. *Chem. Commun.* **2002**, 1243.
42. Singleton, D.; Hang, C.; Szymanski, M. J.; Meyer, M. P.; Leach, A. G.; Kuwata, K. T.; Chen, J. S.; Greer, A.; Foote, C. S.; Houk, K. N. *J. Am. Chem. Soc.* **2003**, *125*, 1319.
43. Baciocchi, E.; Del Giacco, T.; Elisei, F.; Gerini, M. F.; Guerra, M.; Lapi, A.; Liberali, P. *J. Am. Chem. Soc.* **2003**, *125*, 16444.
44. Bonesi, S. M.; Manet, I.; Freccero, M.; Fagnoni, M.; Albini, A. *Chem.—Eur. J.* **2006**, *12*, 4844.
45. Martin, N. H.; Allen, N. W., III; Cottle, C. A.; Marscke, C. K., Jr. *J. Photochem. Photobiol. A: Chem.* **1997**, *103*, 33.
46. Baciocchi, E.; Del Giacco, T.; Lapi, A. *Org. Lett.* **2006**, *8*, 1783.
47. Bacon, W. E.; LeSuer, W. M. *J. Am. Chem. Soc.* **1954**, *76*, 670.
48. Fehnel, E. A.; Carmack, M. *J. Am. Chem. Soc.* **1949**, *71*, 84.
49. Nishihato, K.; Nishio, M. *J. Chem. Soc., Perkin Trans. 2* **1973**, 758.
50. Screttas, C. S.; Micha-Screttas, M. *J. Org. Chem.* **1979**, *40*, 713.
51. Bordwell, F. G.; Boutan, P. *J. Am. Chem. Soc.* **1957**, *79*, 717.
52. McAllan, D. T.; Cullum, T. V.; Dean, R. A.; Fidler, F. A. *J. Am. Chem. Soc.* **1951**, *73*, 3627.
53. Davies, D. M.; Deary, M. E.; Quill, K.; Smith, R. A. *Chem.—Eur. J.* **2005**, *11*, 3552.
54. Ochiai, M.; Nakanishi, A.; Ito, K. *J. Org. Chem.* **1997**, *62*, 4253.
55. Taft, R. W., Jr. *Steric Effects in Organic Chemistry*; Newman, M. S., Ed.; Wiley: New York, NY, 1956; p 556.
56. MacPhee, J. A.; Panaye, A.; Dubois, J. E. *Tetrahedron* **1978**, *34*, 3553.
57. Gollnick, K.; Kuhn, H. J. *Singlet Oxygen*; Wasserman, H. H., Murray, R. W., Eds.; Academic: New York, NY, 1979; p 287.
58. Fukuzumi, S.; Shimoosako, K.; Suenobu, T.; Watanabe, Y. *J. Am. Chem. Soc.* **2003**, *125*, 9074.
59. Koizumi, T.; Fuchigami, T.; Nonaka, T. *Bull. Chem. Soc. Jpn.* **1989**, *62*, 219.
60. Matsumura, Y.; Yamada, M. *Tetrahedron* **1995**, *51*, 6411.
61. Watanabe, M.; Suga, S.; Yoshida, J. *Bull. Chem. Soc. Jpn.* **2000**, *73*, 243.
62. Shaaban, M. R.; Fuchigami, T. *Tetrahedron Lett.* **2002**, *43*, 273.

The hydroperoxysulfonium ylide. An aberration or a ubiquitous intermediate?

Edward L. Clennan* and Chen Liao

Department of Chemistry, University of Wyoming, 1000 East University Avenue, Laramie, WY 82071, United States

Received 26 June 2006; revised 19 July 2006; accepted 19 July 2006

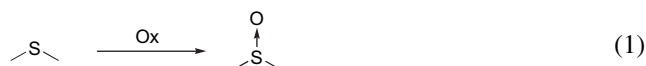
Available online 29 September 2006

Abstract—An intramolecular isotope effect has been measured for the reaction of singlet oxygen with 2,2,8,8-tetradeuterio-1,5-dithia-cyclooctane, **4d₄**. The magnitude of the isotope effect, 1.21 ± 0.09 , provides verification of removal of an α -hydrogen during the product determining step to form a hydroperoxysulfonium ylide and ultimately the sulfoxide product. The absence of any *special* structural features in **4d₄** to enhance the propensity of hydrogen removal is used to suggest that the hydroperoxysulfonium ylide is a ubiquitous intermediate in the reactions of sulfides with singlet oxygen.

© 2006 Elsevier Ltd. All rights reserved.

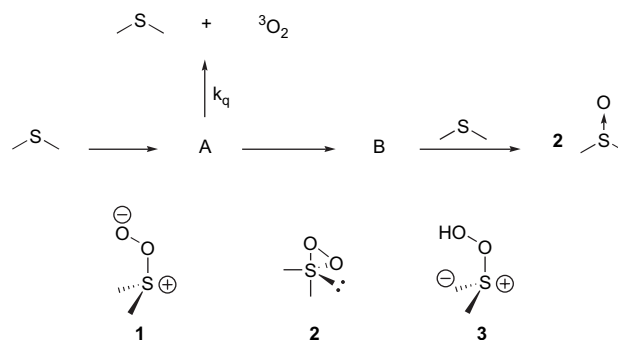
1. Introduction

The oxidation of a sulfide to a sulfoxide despite its apparent simplicity is an extremely important process. A large number of different natural products contain the sulfoxide functional group.¹ It has been reported that oxidation of a single methionine residue in amyloid β -peptide plays a key role in the neurotoxicity responsible for Alzheimer's disease.² Although many reagents are available for sulfide oxidation, the oxygenation process with singlet oxygen is perhaps one of the most convenient.



The ability of singlet oxygen ($^1\Delta_g$) at the time believed to be a sensitizer oxygen complex to perform the transformation shown in Eq. 1 was first demonstrated by Schenck and Krauch in 1962.³ However, the mechanism of this singlet oxygen reaction has proven to be surprisingly complex. The gross features of the potential energy surface were delineated in, what is now, a classic paper published by Foote and co-workers in 1983.⁴ In this manuscript a kinetic study using the 'inert' trapping agents, diphenylsulfide and diphenylsulfoxide, was used to convincingly demonstrate the presence of two intermediates (Scheme 1). Subsequently, the general applicability of this 'two-intermediate' mechanism has been established⁵ for a wide range of sulfonyl

derivatives including disulfides,^{6,7} sulfenamides,^{8–10} and sulfonate esters.¹¹



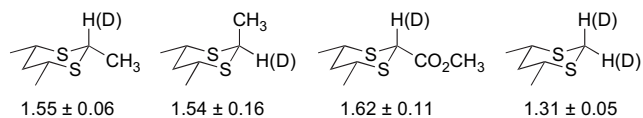
Scheme 1.

The first intermediate was characterized as a nucleophilic oxidant capable of transferring an oxygen atom to an exogenous electrophilic acceptor. The structure of this intermediate was reasonably assigned the persulfide structure, **1**. A wide variety of selective chemical transformations of this intermediate has served to solidify this assignment.¹² The second intermediate was characterized as an electrophilic oxidant capable of donating a single oxygen atom to nucleophilic acceptors. A thiadioxirane, **2**, structure was assigned to this intermediate. Unfortunately, the meta-stability of these intermediates prevented direct spectroscopic characterization.

In 1998, as a result of a detailed computational study, we suggested that a more viable alternative for the second intermediate was a hydroperoxysulfonium ylide, **3**.¹³ This

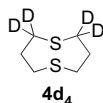
* Corresponding author. Tel.: +1 307 766 6667; fax: +1 307 766 2807; e-mail: clennane@uwyo.edu

suggestion was based on the computational evidence that revealed that the collapse of the persulfoxide to **3** occurs with a barrier of approximately 6 kcal/mol in comparison to an insurmountable barrier of 20 kcal/mol for its rearrangement to **2**. Experimental data to support this suggestion rapidly following in 1999¹⁴ with the report of substantial kinetic isotope effects for the reactions of singlet oxygen with the series of 1,3-dithianes shown in Scheme 2.¹⁵



Scheme 2.

Deprotonations of 1,3-dithianes and their derivatives are well-established procedures for the generation of synthetically useful acyl anion equivalents.¹⁶ In order to alleviate any concern that these 1,3-dithianes are ‘unique’ singlet oxygen substrates as a result of the acidity of their 2-protons (Scheme 2), we report here a kinetic isotope effect study of the specifically deuterated 1,5-dithiacyclooctane, **4d₄**.

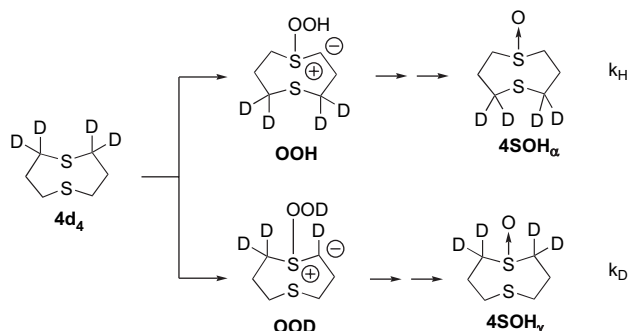


2. Results and discussion

The deuterated 1,5-dithiacyclooctane, **4d₄**, was synthesized as shown in Scheme 3. A high dilution technique was first used to produce a modest yield of 1,5-dithiacyclooctane, **4**, which was converted to **4SO** with sodium periodate in methanol. Deuterium was washed into this sulfoxide by stirring it at 100 °C in a solution of sodium deuterium oxide in D₂O. Finally, **4SOH_γ** was reduced with sodium iodide in perchloric acid followed by treatment with Na₂S₂O₃ to give a 74% yield of **4d₄** with greater than 96% deuterium incorporation.

The isotope effect studies with **4d₄** were conducted under the high concentration conditions (0.05–0.1 M) known to convert **4** cleanly to the sulfoxide, **4SO**. High conversions (i.e., long irradiation times), which are known to convert **4SO** to a 86:14 mixture of the *cis*- and *trans*-(bis)sulfoxides,¹⁷ and low concentrations,¹⁸ which are known to

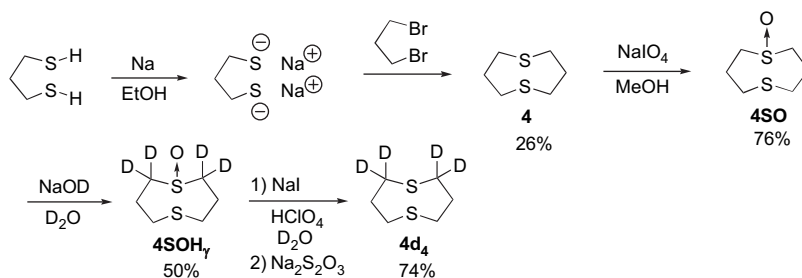
promote formation of cleavage products, were avoided. Under these carefully controlled conditions, two products, **4SOH_α** and **4SOH_γ**, are exclusively formed in the singlet oxygen reaction. The NMR spectra for the 6-spin system, **4SO**, and the 4-spin system **4SOH_γ** (Scheme 4), which was available in pure form from the synthesis depicted in Scheme 3, were fit using WINDNMR¹⁹ simulation software. The derived spectral data for **4SO** are given in Table 1. These assignments were subsequently used to assist in the analysis of the isotope effect experiment (vide infra).



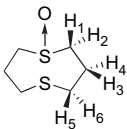
Scheme 4.

The isotope effect, *k_H*/*k_D*, measured in this study is a product isotope effect as depicted in Scheme 4. The isotope effect (i.e., product ratio [**4SOH_α**]/[**4SOH_γ**]) is also equal to [**OOH**]/[**OOD**] since **4SOH_α** and **4SOH_γ** can only form via hydroperoxysulfonium ylides **OOH** and **OOD**, respectively. The most stable conformation of the hydroperoxysulfonium ylide has the hydrogen of the OOH group directly above the negatively charged α-carbon¹³ poised for re-delivery back to this carbon upon reaction of the peroxy linkage with a molecule of sulfide substrate to give two sulfoxide products.

The isotope effect *k_H*/*k_D* = [**4SOH_α**]/[**4SOH_γ**] = [**OOH**]/[**OOD**] = 1.21 ± 0.09 was measured by integration of the α-hydrogen multiplet (H₁ and H₂) between 3.0 and 3.2 ppm and the γ-hydrogen multiplet (H₅ and H₆) between 2.5 and 2.7 ppm from five independent reactions. Figure 1 depicts an example of a typical reaction mixture showing both the multiplet between 2.5 and 2.7 ppm for the γ-hydrogens in **4SOH_γ** and the multiplet between 3.0 and 3.2 ppm for the α-hydrogens in **4SOH_α**. This figure also illustrates the baseline separation between these two multiplets and the large residual peak for **4d₄** in these low conversion reaction mixtures.



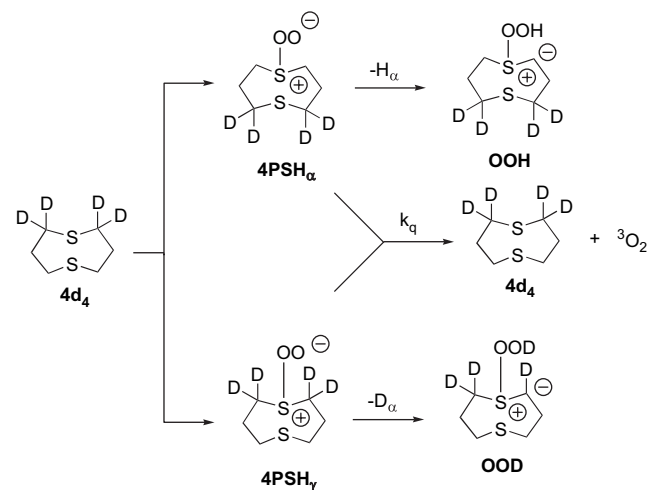
Scheme 3.

Table 1. Spectral Data for **4SO**^{a,b}


Spin	δ (Hz)	J (Hz)
H ₁	1269.17	ddd; $J_{12}=-13.08$; $J_{13}=3.59$; $J_{14}=7.89$
H ₂	1246.56	ddd; $J_{12}=-13.08$; $J_{23}=3.85$; $J_{24}=7.04$
H ₃	876.18	dddd; $J_{13}=3.59$; $J_{23}=3.85$; $J_{34}=-15.77$; $J_{35}=4.72$; $J_{36}=7.59$
H ₄	924.31	dddd; $J_{14}=7.89$; $J_{24}=7.04$; $J_{34}=-15.77$; $J_{45}=8.10$; $J_{46}=4.13$
H ₅	1067.41	ddd; $J_{35}=4.72$; $J_{45}=8.10$; $J_{56}=-14.7$
H ₆	1031.39	ddd; $J_{36}=7.59$; $J_{46}=4.13$; $J_{56}=-14.7$

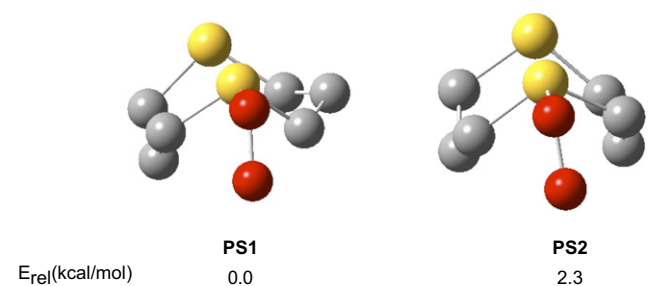
^a The simulation assisted/derived spectral parameters for **4SOH** _{γ} were used as a guide to fit the spectral data for **4SO**.

^b Data collected at 400 MHz.

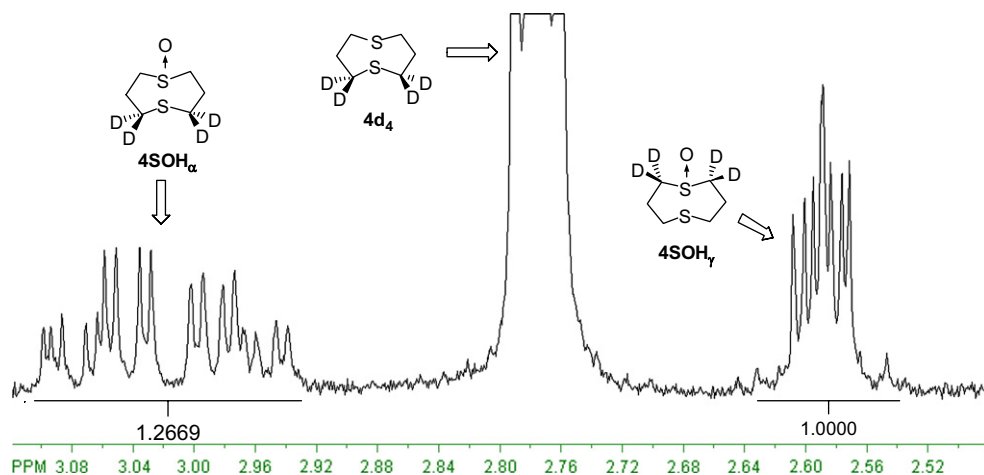
**Scheme 5.**

The observation of a significant isotope effect (1.21 ± 0.09) is consistent with formations of hydroperoxysulfonium ylides from persulfoxides **4PSH** _{α} and **4PSH** _{γ} as shown in **Scheme 5**. Previous studies with **4** have demonstrated that its diminished efficiency ($\sim 70\%$) in its reactions with singlet oxygen is a result of decomposition of the persulfoxide intermediate to starting material and triplet oxygen (path k_q in **Scheme 5**).¹⁷ It is the competition between this physical deactivation pathway and formation of the hydroperoxysulfonium ylide, which is responsible for the observed isotope effect. Hydrogen abstraction in **4PSH** _{α} to form hydroperoxysulfonium ylide **OOH** competes more effectively with physical quenching, k_q , than deuterium abstraction in **4PSH** _{γ} to form **OOD**.

The hydrogen isotopes abstracted in **4PSH** _{α} and **4PSH** _{γ} to form their corresponding hydroperoxysulfonium ylides, **OOH** and **OOD**, respectively, do not enjoy the electronic environment found in 1,3-dithianes (**Scheme 2**) that lead to enhanced acidity. An extensive search of persulfoxide, **4PS** conformational space with MP2/6-31G(d) computational method located only two low energy conformations. (i.e., the global minimum and only one conformation within 3 kcal/mol of the global minimum; **Scheme 6**).²⁰ The lowest energy persulfoxide, **PS1**, adopts a boat–chair, and the

**Scheme 6.**

persulfoxide at 2.3 kcal/mol above the global minimum, **PS2**, adopts a boat–boat conformation. Both conformations have α -hydrogens accessible for abstraction (removed for clarity from the structures in **Scheme 6**) by the persulfoxide terminal oxygen atom. In addition, in both conformations, the remote sulfur, the persulfoxide sulfur, and the oxygen attached to the persulfoxide sulfur are collinear. This suggests that the remote sulfur dissipates the positive charge on the persulfoxide sulfur by donation of lone electron pair density. This was confirmed in a natural bond orbital analysis of

**Figure 1.** ¹H NMR from 2.48 to 3.12 ppm of reaction mixture during photooxygenation of **4d**₄.

persulfoxide conformations **PS1** and **PS2** that detected a depletion of the electron density on the remote sulfur consistent with delocalization of the positive charge in the persulfoxide over both sulfur atoms.²¹ We argue that this diminished charge on the persulfoxide sulfur should further decrease the acidity of the α -hydrogens in comparison to those found in simple dialkylpersulfoxides.

3. Conclusion

We have demonstrated that 2,2,8,8-tetradeuterio-1,5-dithiacyclooctane, **4d₄**, exhibits a significant (20%) isotope effect for the site of product formation in its reaction with singlet oxygen. Consequently, enhanced acidity of the α -hydrogens is not a prerequisite for the observation of an isotope effect and suggests that the hydroperoxysulfonium ylide is a ubiquitous intermediate formed in a wide range of sulfide photooxygenations.

4. Experimental

4.1. General

4.1.1. 1,5-Dithiacyclooctane (4). In a 1000 mL three-necked flask equipped with an overhead stirrer, a condenser, and an adaptor for a syringe pump, 6 g of freshly cut sodium (0.261 mol) was added under nitrogen to 500 mL of rapidly stirred absolute ethanol. After the Na reacted, the solution was heated to 50 °C and 5.3 mL of 1,3-dibromopropane ($d=1.989$ g/mL, 10.54 g, 52.2 mmol) in 20 mL of absolute ethanol and 5.25 mL of 1,3-propanedithiol ($d=1.078$ g/mL, 5.66 g, 52.29 mmol) in 20 mL of absolute ethanol were simultaneously added by a syringe pump at a rate of 0.17 mL/min over a 2 h period. After addition of the reagents the cloudy white solution was refluxed at 50 °C and then allowed to cool to room temperature. It was then filtered to remove the white precipitate. Excess ethanol was removed at reduced pressure by roto-evaporation that induces the formation of more precipitate. Water (200 mL) was added and the solution was then extracted with 3 \times 150 mL dichloromethane. The dichloromethane extract was dried with anhydrous MgSO₄, filtered, and removed slowly under reduced pressure. The crude product was purified by vacuum distillation with freshly cut Na to give a colorless liquid product with a distinctive smell. Yield: 2 g (13.5 mmol, 26%). ¹H NMR (CDCl₃) δ 2.1 (m, 4H), 2.8 (m, 8H).

4.1.2. 1,5-Dithiacyclooctane-1-oxide (4SO). A solution of 0.35 g (1.77 mmol) of sodium periodate in 7.5 mL of water was added to a solution of 0.26 g (1.76 mmol) of **4** in 20 mL of methanol at room temperature over a 10-min period. This mixture was stirred for 20 h then filtered, and the volatile solvent removed. Water was added to the residue and then extracted three times with chloroform. The combined chloroform extracts were washed with sodium thiosulfate and then dried over anhydrous MgSO₄. Purification by column chromatography was accomplished by increasing the eluting solvent polarity from 20% methanol in ethyl acetate (EA) to 45% methanol in EA to give colorless crystals with a low melting point. Yield: 220 mg (1.34 mmol, 76%). ¹H NMR (CDCl₃) δ 2.1–2.3 (m, 4H), 2.5–2.7 (m, 4H), 3.0–3.2 (m, 4H).

4.1.3. 2,2,8,8-Tetradeuterio-1,5-dithiacyclooctane 1-oxide (4SOH_γ). A solution of **4SO** (0.41 g, 2.50 mmol) in 2 mL deuterium oxide was added to a ca. 30% solution of sodium deuterium oxide in 8 mL of deuterium oxide (D content 99.8%). After stirring under an N₂ atmosphere at 100 °C for 24 h, the solvent was concentrated under reduced pressure and the mixture was then extracted with chloroform. The combined organic phase was dried over anhydrous MgSO₄. After removal of the solvent, the mixture was separated by column chromatography, using a mixture of ethyl acetate and methanol (1:4). Yield: 209.6 mg (1.25 mmol, 49.9%). The content of deuterium was 96% as determined by ¹H NMR spectroscopy. ¹H NMR (CDCl₃) δ 3.12–3.16 (m, residual α -hydrogens), 2.55–2.70 (m, 4H), 2.16–2.35 (m, 4H).

4.1.4. 2,2,8,8-Tetradeuterio-1,5-dithiacyclooctane (4d₄). A solution of sodium iodide (0.536 g, 3.57 mmol) and 70% perchloric acid (0.239 g, 2.38 mmol) in 10 mL D₂O was added to a solution of **4SOH_γ** (0.2 g, 1.19 mmol) in 2 mL D₂O. The reaction immediately turned to a cloudy orange color. The reaction was kept at room temperature for 4 h followed by addition of 30% Na₂S₂O₃ to reduce the I₃⁻. The mixture was extracted three times with chloroform and the combined extracts were washed with NaHCO₃. The mixture was dried with anhydrous MgSO₄ and then the solvent was removed. The product was purified by column chromatography, ethyl acetate/hexane=1:4. Yield: 134 mg (0.88 mmol, 74%). ¹H NMR (CDCl₃) δ 2.63–3.00 (m, 4H), 1.87–2.22 (m, 4H). ¹³C NMR (CDCl₃) δ 30.23, 30.78, 29.47 (quintet, $J=21$ Hz).

4.2. Photooxygenation reactions

The photooxygenation reactions were carried out by irradiation of a CD₃CN solution containing 6.25 \times 10⁻⁴ M methylene blue and 0.0125 M **4d₄**, under continuous oxygen agitation with a 150 W tungsten/halogen lamp through 1 cm of a saturated NaNO₂ filter solution for 10 min. The reaction mixtures were analyzed immediately by proton NMR and the isotope effects determined by integration of the appropriate regions.

Acknowledgements

We thank the National Science Foundation for the generous support of this research.

References and notes

- Oae, S.; Doi, J. T. *Organic Sulfur Chemistry: Structure and Mechanism*; CRC: Boca Raton, FL, 1991; p 433.
- Huang, M. L.; Rauk, A. *J. Phys. Chem. A* **2004**, *108*, 6222–6230.
- As quoted in: Ando, W.; Takata, T. *Singlet O₂ Reaction Modes and Products. Part 2*; Frimer, A. A., Ed.; CRC: Boca Raton, FL, 1985; pp 1–117.
- Liang, J.-J.; Gu, C.-L.; Kacher, M. L.; Foote, C. S. *J. Am. Chem. Soc.* **1983**, *105*, 4717–4721.
- Clennan, E. L. *Sulfur Rep.* **1996**, *19*, 171–214.
- Clennan, E. L.; Wang, D.; Clifton, C.; Chen, M.-F. *J. Am. Chem. Soc.* **1997**, *119*, 9081–9082.

7. Clennan, E. L.; Wang, D.; Zhang, H.; Clifton, C. H. *Tetrahedron Lett.* **1994**, *35*, 4723–4726.
8. Clennan, E. L.; Chen, M.-F.; Greer, A.; Jensen, F. *J. Org. Chem.* **1998**, *63*, 3397–3402.
9. Clennan, E. L.; Zhang, H. *J. Am. Chem. Soc.* **1994**, *116*, 809–810.
10. Greer, A.; Chen, M.-F.; Jensen, F.; Clennan, E. L. *J. Am. Chem. Soc.* **1997**, *119*, 4380–4387.
11. Clennan, E. L.; Chen, M.-F. *J. Org. Chem.* **1995**, *60*, 6444–6447.
12. Clennan, E. L. *Acc. Chem. Res.* **2001**, *34*, 875–884.
13. Jensen, F.; Greer, A.; Clennan, E. L. *J. Am. Chem. Soc.* **1998**, *120*, 4439–4449.
14. Touthkine, A.; Clennan, E. L. *J. Org. Chem.* **1999**, *64*, 5620–5625.
15. The formation of an oxidative elimination product in the reactions of β -chlorosulfides also serves as experimental verification of hydroperoxysulfonium ylide intermediates. Touthkine, A.; Clennan, E. L. *Tetrahedron Lett.* **1999**, *40*, 6519–6522.
16. Aggarwal, V. K.; Schade, S.; Adams, H. *J. Org. Chem.* **1997**, *62*, 1139–1145.
17. Clennan, E. L.; Wang, D.-X.; Yang, K.; Hodgson, D. J.; Oki, A. R. *J. Am. Chem. Soc.* **1992**, *114*, 3021–3027.
18. Sheu, C.; Foote, C. S.; Gu, C.-L. *J. Am. Chem. Soc.* **1992**, *114*, 3015–3021.
19. WINDNMR is an NMR simulation program written by Professor Hans Reich, University of Wisconsin, Madison. It is available at <http://www.chem.wisc.edu/areas/reich/plt/windnrmr.htm>.
20. Clennan, E. L.; Hightower, S. E.; Greer, A. *J. Am. Chem. Soc.* **2005**, *127*, 11819–11826.
21. Clennan, E. L.; Hightower, S. E. *J. Org. Chem.* **2006**, *71*, 1247–1250.



ELSEVIER

Chemistry of singlet oxygen with arylphosphines

Dong Zhang,^a Bin Ye,^a David G. Ho,^a Ruomei Gao^b and Matthias Selke^{a,*}^aDepartment of Chemistry and Biochemistry, California State University, Los Angeles, CA 90032, USA^bDepartment of Chemistry, Jackson State University, 1325 J. R. Lynch St., P.O. Box 17910, Jackson, MS 39217, USA

Received 1 June 2006; revised 21 July 2006; accepted 27 July 2006

Available online 26 September 2006

Abstract—The chemistry of singlet oxygen with a variety of arylphosphines has been studied. Rates of singlet oxygen removal by *para*-substituted arylphosphines show good correlation with the Hammett σ parameter ($\rho = -1.53$ in CDCl_3), and with the Tolman electronic parameter. The only products for the reactions of these phosphines with singlet oxygen are the corresponding phosphine oxides. Conversely, for *ortho*-substituted phosphines with electron-donating substituents, there are two products, namely a phosphinate formed by intramolecular insertion and phosphine oxide. Kinetic analyses demonstrate that both products are formed from the same intermediate, and this allows determination of the rate ratios for the competing pathways. Increasing the steric bulk of the phosphine leads to an increase in the amount of insertion product. VT NMR experiments show that peroxidic intermediates can only be detected for very hindered and very electron-rich arylphosphines.

© 2006 Published by Elsevier Ltd.

1. Introduction

The chemistry of singlet dioxygen with heteroatoms, i.e., organic sulfides^{1–5} and, more recently, phosphines^{5–9} has been the subject of numerous papers, as these reactions possess rather complicated mechanisms. Elucidation of the nature of reactive intermediates, and, ideally, their direct observation, have been a major goal of these studies. Such intermediates are of fundamental interest, as they should be even better oxidants than singlet dioxygen itself. In particular, many kinetic and trapping studies have been carried out to determine the nature of the peroxidic intermediates formed during the photooxidation of organic sulfides. The oxidation of phosphines has attracted somewhat less attention. An early paper by Bolduc and Goe¹¹ suggested an open zwitterionic species formed as a primary intermediate, but trapping studies by Sawaki and co-workers⁷ indicated that the primary intermediate in the photooxidation of triphenyl phosphines and tributyl phosphite is electrophilic. This is in contrast with the nucleophilic behavior of the persulfoxide intermediate in the photooxidation of organic sulfides.¹ Ab initio calculations by Foote and co-workers⁸ suggested a cyclic phosphadioxirane intermediate, which would indeed be expected to behave as an electrophile. Arylphosphines have also been investigated as fuel-stabilizers for jet fuels, and very recently Beaver and co-workers have provided strong evidence that phosphadioxiranes may play a key role during this antioxidant activity.^{12,13} Arylphosphines

represent an interesting target for studying reactive intermediates and reaction channels, since their electronic and steric parameters are well defined and can be varied in a systematic manner. Electronic parameters that can be used to assess the donor abilities of arylphosphines include Hammett constants as well as the Tolman electronic parameter.¹⁴ The latter parameter is given by the CO stretching frequency of the carbonyl group trans to the phosphine in a Ni complex of the type $\text{Ni}(\text{CO})_3(\text{PR}_3)$. The stronger the electron-donating ability of the phosphine, the stronger the backbonding to the trans CO ligand, and hence the lower the CO stretching frequency. Chemical properties of arylphosphines are also influenced by the steric bulk of the aryl groups, and the cone angle of a phosphine ligand has long been used as a measure of its bulk.¹⁴ The cone angle is obtained by taking a space-filling model of the $\text{MP}(\text{R}_3)$ group. The metal is the apex of the cone, and the entire ligand forms the actual cone.^{4,5} We have reported the special case of tris(*ortho*-methoxyphenyl)phosphine: the exceptionally large steric bulk of this phosphine (cone angle of 205°)¹⁵ slows down the reactions of peroxidic intermediate so that it can be directly observed at very low temperatures by VT NMR. ³¹P and ¹⁷O NMR measurements at -80° strongly suggest that the peroxidic intermediate is a three-membered ring containing a phosphorus and two oxygen atoms, that is, a phosphadioxirane.¹⁰ We report herein, the products for the reaction of a variety of arylphosphines with singlet oxygen, kinetic data, as well as attempts to observe and characterize products and peroxidic intermediates of these reactions. Electronic parameters for the different arylphosphines were simply varied by using different substituents in the *para* position; the cone angle is the same for all of these *para*-substituted phosphines, namely 145° .

Keywords: Singlet oxygen; Cone angle; Arylphosphine; Phosphadioxirane.

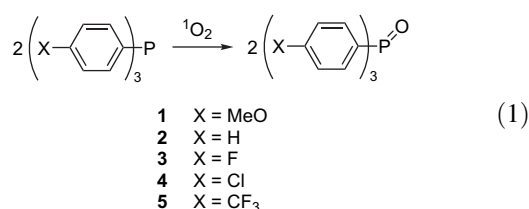
* Corresponding author. Tel.: +1 323 343 2347; fax: +1 323 343 6490; e-mail: mselecte@calstatela.edu

Conversely, steric parameters were changed by employing different substituents in the *ortho* position. All of these arylphosphines are unreactive with triplet oxygen, thus allowing kinetic investigations of their reactions with singlet oxygen.

2. Results and discussion

2.1. Photooxidation of *para*-substituted arylphosphines

Reaction of singlet oxygen at room temperature with *para*-substituted arylphosphines **1–5** leads to the corresponding phosphine oxides in quantitative yield (Eq. 1).



Total rate constants of singlet oxygen removal (k_T) by phosphines **1–5** have been measured by luminescence quenching experiments in a deuterated benzene and chloroform. The k_T values and the corresponding σ values as well as the Tolman electronic parameters for various phosphines are summarized in Table 1.

The logs of the k_T values ($k_{\text{Subst}}/k_{\text{H}}$) yield a good correlation with the Hammett σ parameters; the Hammett plot gives a negative slope of -1.53 in CDCl₃ (Fig. 1), and -1.93 in C₆D₆ ($r^2=0.987$). Since there are three aryl rings per phosphine, the actual ρ values for the electronic effect of one aryl ring are -0.51 and -0.64 , respectively. The reason for the larger value in benzene is unclear at the moment, although it may simply be caused by the smaller dielectric constant of benzene, similar to what has recently been predicted by ab initio calculations for solvent effects on ρ values in benzhydryl cations.¹⁶ The negative ρ value is in agreement with the electrophilic character of the initial singlet oxygen attack on the arylphosphine. The magnitude of ρ for one arylphosphine is smaller than that for the corresponding attack of singlet oxygen on aryl sulfides in thioanisoles.¹⁷

A plot of the k_T values versus the Tolman electronic parameter also gives a good linear correlation ($r^2=0.971$) for

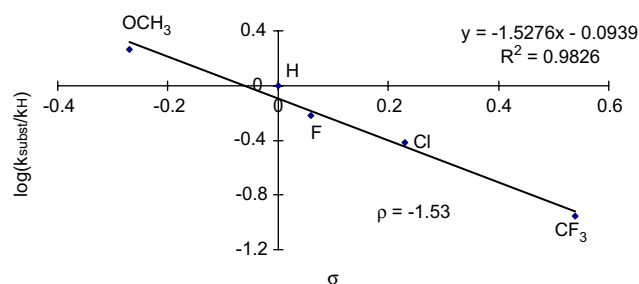


Figure 1. Hammett plot for the reaction of *para*-substituted arylphosphines with singlet oxygen.

phosphines **1–4** (the Tolman electronic parameter for phosphine **5** has not been determined). Since the Tolman electronic parameter is a measure of the σ -donating ability of the phosphine, it is apparent that in the absence of steric variation, the σ -donation of the arylphosphine to the empty degenerate π^* MO of the singlet oxygen molecule determines the reaction rate of singlet oxygen with the *para*-substituted arylphosphines.

In the absence of physical quenching, the value of k_T is the rate of formation of the peroxidic intermediate (i.e., the phosphadioxirane). For all *para*-substituted arylphosphines, the corresponding phosphine oxide was the only major product observed by ³¹P NMR (other products such as the corresponding phosphinates⁷ were 1% or less). In order to determine whether or not all of the peroxidic intermediates lead to the formation of the reaction products or whether loss of dioxygen from the intermediate (indirect physical quenching) is a major process, competition experiments have been carried out. These competition experiments are done under continuous irradiation of a solution containing a singlet oxygen acceptor with a known chemical reaction rate constant and the arylphosphine that is being studied. Thus the two substrates compete for one reactive intermediate (i.e., singlet oxygen) that is produced under steady-state conditions. 9,10-Dimethylanthracene (DMA) was used as a singlet oxygen acceptor in these experiments. DMA is known to interact with singlet oxygen by chemical reaction only. As reference values, we have used k_T values for the reaction of DMA with singlet oxygen from the recent literature,⁹ namely $2.5 \pm 0.1 \times 10^7 \text{ M}^{-1} \text{ s}^{-1}$ in CDCl₃ and $2.9 \pm 0.2 \times 10^7 \text{ M}^{-1} \text{ s}^{-1}$ in deuterated benzene. Loss of DMA and compounds **1–5** was monitored by ¹H and ³¹P NMR. The relative reaction rate ratio for the k_T values of

Table 1. Summary of kinetic data, electronic, and steric parameters for phosphines

Phosphine	k_T in CDCl ₃ (M ⁻¹ s ⁻¹) × 10 ⁶	k_r in CDCl ₃ (M ⁻¹ s ⁻¹) × 10 ⁶	k_T in C ₆ D ₆ (M ⁻¹ s ⁻¹) × 10 ⁶	k_r in C ₆ D ₆ (M ⁻¹ s ⁻¹) × 10 ⁶	k_o/k_i in CDCl ₃	σ_p	Cone angle (deg) ^d	Tolman electronic parameter (cm ⁻¹) ^d
(<i>p</i> -CH ₃ OC ₆ H ₄) ₃ P ^a	14.9 ± 1.6	32.4 ± 1.2	33.1 ± 4.3	59.4 ± 0.9		-0.27	145	2066.1
(C ₆ H ₅) ₃ P ^b	8.1 ± 0.3	16.2 ± 1.6	10.5 ± 0.6	21.5 ± 1.1		0	145	2068.9
(<i>p</i> -FC ₆ H ₄) ₃ P ^b	4.9 ± 0.2	11.0 ± 1.0	5.5 ± 0.2	11.0 ± 0.8		0.06	145	2071.3
(<i>p</i> -ClC ₆ H ₄) ₃ P ^b	3.1 ± 0.2	7.1 ± 0.7	3.3 ± 0.3	8.0 ± 0.8		0.23	145	2072.8
(<i>p</i> -CF ₃ C ₆ H ₄) ₃ P ^c	0.9 ± 0.05	2.2 ± 0.3	0.9 ± 0.06	2.6 ± 0.6		0.54	145	
(<i>o</i> -CH ₃ C ₆ H ₄) ₃ P ^b	5.4 ± 0.5		8.0 ± 0.2		80 ± 7		194	2066.6
(<i>o</i> -CF ₃ C ₆ H ₄) ₃ P ^c	0.1 ± 0.01	Not measurable		Not measurable			205	
(<i>o</i> -CH ₃ OC ₆ H ₄) ₃ ^a	2.8 ± 0.4		5.0 ± 0.2		25 ± 3		205	2058.3

^a Ref. 9.

^b This work.

^c Ref. 10.

^d Ref. 14.

the phosphine and the singlet oxygen acceptor (i.e., DMA) was obtained from the equation of Higgins and co-workers.¹⁸

$$\frac{\log\left\{\frac{[\text{Arylphosphine}]^f/[\text{Arylphosphine}]^0}{[\text{DMA}]^f/[\text{DMA}]^0}\right\}}{\log\left\{\frac{[\text{DMA}]^f/[\text{DMA}]^0}{[\text{DMA}]^f/[\text{DMA}]^0}\right\}} = \frac{k_r(\text{Arylphosphine})}{k_r(\text{DMA})} \quad (2)$$

For all of the *para*-substituted arylphosphines (compounds 1–5), the rate of formation of the corresponding phosphine oxides (k_r) is twice the rate of singlet oxygen removal k_T , both in benzene and chloroform. Thus indirect physical quenching (loss of dioxygen from the periodic intermediate) is not detectable, and all of the phosphadioxirane intermediates are converted to product. We also conducted competition experiments in benzene (Table 1), and found that the reaction rates (i.e., k_r values) follows the same trend, but are somewhat larger than in chloroform. The reason for this increase is unclear at this time.

2.2. *ortho*-Substituted arylphosphines

Generally, k_T values are lower for these phosphines compared to their *para*-substituted counterparts. It is particularly instructive to compare the k_T values for tris(*ortho*-methoxyphenyl)phosphine (6), tris(*ortho*-tolyl)phosphine (9), and triphenylphosphine (2). Despite the fact that the electron density at the phosphorus atom is decreasing from 6 to 9 to 2 (cf. the Tolman electronic parameters), the corresponding k_T values are increasing. This illustrates the strong sensitivity of reactions of singlet oxygen with arylphosphines to steric effects, similar to what has been observed for organic sulfides.

We have recently reported an unusual intramolecular oxidation pathway during the photooxidation of tris(*ortho*-methoxyphenyl)phosphine (6). In addition to tris(*ortho*-methoxyphenyl)phosphine oxide (7), significant amounts of *ortho* methoxyphenyl di(*ortho*-methoxyphenyl)phosphinate (8) are obtained. In fact, at low concentration, this intramolecular oxidation product becomes the major reaction product. We have demonstrated that there exists a phosphine cone angle dependence for this reactive channel of the putative peroxidic intermediate by comparison with the

corresponding *meta* and *para* isomers, which do not form the insertion product.⁹ We now report that the behavior of the tris(*ortho*-tolyl)phosphine (9) is quite similar: reaction of singlet oxygen with 9 leads to the formation of tris(*ortho*-tolyl)phosphine oxide (10) and *ortho* tolyl di(*ortho*-tolyl)-phosphinate (11).

If the phosphine oxides and phosphinates are formed from the same intermediate (i.e., a phosphadioxirane), we can use a simple steady-state treatment to obtain the rate ratio for the intramolecular (k_i) and intermolecular (k_o) reaction rates: according to Scheme 1, the rate of formation of the phosphinates (compounds 7 and 10) is given by Eq. 3:

$$d[\text{Phosphinate}]/dt = k_i[\text{Phosphadioxirane}] \quad (3)$$

Likewise, the rate of formation of the phosphine oxides (compounds 8 and 11) can be expressed by Eq. 4:

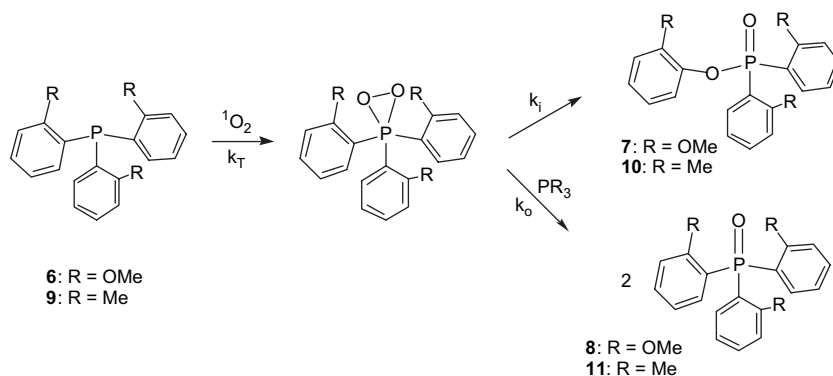
$$d[\text{Phosphine oxide}]/dt = 2k_o[\text{Phosphadioxirane}][\text{Phosphine}] \quad (4)$$

Assuming a steady-state concentration of the phosphadioxirane, and working at low conversion of the starting phosphine, we can combine Eqs. 3 and 4 to obtain an integrated expression for the rate ratio of intramolecular versus intermolecular oxidation:

$$[\text{Phosphine oxide}]/[\text{Phosphinate}] = (2k_o[\text{Phosphine}])/k_i \quad (5)$$

According to Eq. 5, a plot of the product ratio versus starting material concentration should be linear with a slope of twice the rate ratio k_o/k_i . A plot of the photooxidation product ratio (11/10) for tris(*ortho*-tolyl)phosphine versus starting concentration of tris(*ortho*-tolyl)phosphine (in CDCl₃) indeed gives a good linear correlation with a slope of 161±14 (Fig. 2).

The rate ratio of intermolecular versus intramolecular oxidation for tris(*ortho*-tolyl)phosphine is thus 80±7. This ratio is considerably larger than that of the reaction of phosphine 6 with singlet oxygen where k_o/k_i is 25±3 in CDCl₃. Intramolecular oxidation is thus less favorable for



Scheme 1. Reaction of electron-rich *ortho*-substituted arylphosphines with singlet oxygen.

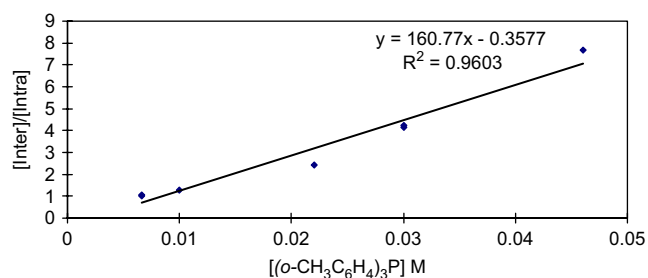


Figure 2. Product ratio of phosphine oxide (intermolecular product)/phosphinate (intramolecular product) versus starting phosphine concentration for the reaction of tris(*ortho*-tolyl)phosphine with singlet oxygen.

tris(*ortho*-tolyl)phosphine as compared to tris(*ortho*-methoxyphenyl)phosphine (**6**). This could be due to the smaller cone angle of this phosphine (194° compared to 205° for phosphine **6**, see Table 1) or due to a combination of the smaller cone angle and an electronic effect, i.e., decreased electron density at the phosphorus atom. The latter effect can be quite drastic, as illustrated by the behavior of tris(*ortho*-trifluoromethyl)phenyl phosphine (**12**). The cone angle of phosphine **12** is similar to that of **6**, but tris(*ortho*-trifluoromethyl)phenyl phosphine obviously is highly electron deficient. Phosphine **12** does quench singlet oxygen with a rather slow rate constant $k_T = 1 \times 10^5 \text{ M}^{-1} \text{ s}^{-1}$, as determined by a singlet oxygen luminescence quenching experiment. However, we were unable to detect any products either at room temperature or temperatures as low as -80°C . Phosphine **12**, therefore, represents the first known example of *physical* quenching of singlet oxygen by a phosphine. It is quite possible that the quenching mechanism involves a transient dioxygen–phosphine complex, i.e., indirect physical quenching.¹⁹ The lack of reactivity of **12** is not merely an electronic effect, since the corresponding *para* isomer tris(*para*-trifluoromethyl)phenyl phosphine (**5**) reacts with singlet oxygen to form phosphine oxide, albeit at a low rate ($k_T = 9 \times 10^5 \text{ M}^{-1} \text{ s}^{-1}$, see Table 1), and without any concomitant physical quenching. It, therefore, appears that electron-rich substituents in the *ortho* position are needed for the intramolecular oxygen atom insertion reaction to become a major pathway.

2.3. Low temperature photooxidation of arylphosphines

We were unsuccessful in detecting any peroxidic intermediates at temperatures as low as -80°C for the *para*-substituted phosphines **1–5**. It appears that the cone angle of these phosphines (145°) is simply too small to prevent the reaction with starting material even at such low temperatures from being too fast to allow spectroscopic detection of any peroxidic intermediate.

In contrast to the *para*-substituted arylphosphines **1–5**, the reaction of tris(*ortho*-methoxyphenyl)phosphine (**6**) and singlet dioxygen at -80°C in methylene chloride or methylene chloride/toluene mixtures leads to the rapid formation of a new phosphine species, namely tris(*ortho*-methoxyphenyl)phosphadioxirane.¹⁰ This phosphadioxirane can be identified by its ^{31}P NMR signal at -45 ppm. The only other peak observed in the ^{31}P NMR spectrum during the low temperature photooxidation of **6** is the signal for the corresponding tris(*ortho*-methoxyphenyl)phosphine oxide (**8**)

(26 ppm at -80°C).⁹ Compound **8** is formed due to the reaction of phosphadioxirane with unreacted starting material. Formation of **8** relative to phosphadioxirane is diminished in CH_2Cl_2 /toluene mixtures compared to neat CH_2Cl_2 solution. In the present work, we noted that tris(*ortho*-tolyl)phosphine (**9**) shows similar behavior compared to **6** at room temperature. We, therefore, reasoned that phosphine **9** might also form a phosphadioxirane that can be directly detected at low temperature. However, despite numerous attempts, we were unable to observe any peroxidic intermediate for phosphine **9** at -80°C , and only the corresponding phosphine oxide **11** was obtained, regardless of solvent. It appears that the relatively small decrease in the cone angle of **9** compared to **6** and possibly the decrease in the electron density at the phosphorus atom are sufficient to make the phosphadioxirane intermediate too short-lived for direct observation. Interestingly, formation of the phosphinates **7** and **10** is greatly diminished if the photooxidation is carried out at low temperature and completely suppressed below -60°C . This appears to be in agreement with the very recent observation by Beaver and co-workers¹³ who noted that the phosphinate–phosphine oxide ratio is actually increased at elevated temperatures.

3. Experimental

3.1. Materials

All solvents and materials were the purest commercially available products and used as received, except for tris(*ortho*-trifluoromethylphenyl)phosphine, which was synthesized according to a literature method.²⁰

3.2. Instrumentation

^1H and ^{31}P NMR spectra were obtained on a Bruker AC300 and DRX400 instrument. Low temperature spectra were obtained by standard VT NMR techniques. Absorption spectra were recorded on a Carey 300 UV–vis spectrophotometer.

3.3. Time-resolved singlet oxygen measurements

A nanosecond Nd:YAG laser (model MiniLaseII/10 Hz; New Wave Research Inc., USA) doubled (532 nm) or tripled (355 nm) in frequency is used as an excitation source. Singlet oxygen luminescence is monitored at right angle. The detector is a cryogenic germanium photodiode detector (model 403HS; Applied Detector Corp., USA) cooled by liquid nitrogen and specialized for detection of near-infrared radiation. Three different filters are used to remove undesired radiation. A Schott color glass filter (model RG850; cut-on 850 nm; Newport, USA) is taped to the sapphire entrance of the detector to block any additional ultraviolet and visible light from entering. The port opening to the detector contains the remaining filters. The long wave pass filter (silicon filter model 10LWF~1000; Newport, USA) transmits in the range of 1100–2220 nm and blocks in the range of 800–954 nm. A band pass filter (model BP-1270-080-B*; CWL 1270 nm; Spectrogen, USA) blocks in the UV, visible, and IR regions and only transmits in the range of 1200–1310 nm with maximum transmission of 60% at 1270 nm. Signals were digitized on a LeCroy 9350CM 500 MHz

oscilloscope and analyzed using Origin software. Generally, four to six runs were conducted per phosphine, and errors are reported as one standard deviation.

3.4. General procedures for arylphosphines photo-oxidation by singlet oxygen

Photooxidation reaction mixtures of 0.01–0.10 M in tris-(*ortho*-methoxyphenyl)phosphine and singlet oxygen sensitizers (tetraphenylporphyrin or C_{70} , max absorption was generally kept between 0.5 and 0.6) were prepared in test tubes or NMR tubes. For NMR analyses, deuterated solvents were employed during the photooxidation. The samples were presaturated with oxygen for 1–2 min and then irradiated under a constant stream of oxygen with a 250 W tungsten–halogen lamp. A 492 nm cutoff filter was used so that the arylphosphines themselves were not irradiated.

3.5. Competition experiments between phosphines and 9,10-dimethylanthracene

The phosphine compounds were irradiated in the presence of a singlet oxygen acceptor namely 9,10-dimethylanthracene (DMA), which removes singlet oxygen by chemical reaction only so that $k_T=k_r=2.5 \times 10^7 \text{ M}^{-1} \text{ s}^{-1}$ in CDCl_3 .⁹ We used tetraphenylporphyrin (TPP) or C_{70} as sensitizers. Phosphine concentration ranged from 0.0005 to 0.003 M, and DMA concentration ranged from 0.0005 to 0.004 M. Irradiation times ranged from 5 to 30 min (for compound **5**). Conversion of each compound was generally kept between 20 and 80%. DMA concentrations were monitored by ^1H NMR while phosphine concentrations were monitored by ^{31}P NMR. All of the NMR peaks used to determine concentrations are summarized below.

Phosphine	^{31}P NMR in CDCl_3 , ppm	^1H NMR in CDCl_3 (methyl) ppm
(<i>p</i> - $\text{CH}_3\text{OC}_6\text{H}_4$) $_3\text{P}$ (1)	–17.8	3.81
(<i>p</i> - $\text{CH}_3\text{OC}_6\text{H}_4$) $_3\text{PO}$	21.4	3.84
(C_6H_5) $_3\text{P}$ (2)	–13.0	
(C_6H_5) $_3\text{PO}$	21.2	
(<i>p</i> - FC_6H_4) $_3\text{P}$ (3)	–16.6	
(<i>p</i> - FC_6H_4) $_3\text{PO}$	18.9	
(<i>p</i> - ClC_6H_4) $_3\text{P}$ (4)	–16.0	
(<i>p</i> - ClC_6H_4) $_3\text{PO}$	19.0	
(<i>p</i> - $\text{CF}_3\text{C}_6\text{H}_4$) $_3\text{P}$ (5)	–13.7	
(<i>p</i> - $\text{CF}_3\text{C}_6\text{H}_4$) $_3\text{PO}$	17.7	
DMA		3.11
DMAO $_2$		2.16
(<i>o</i> - $\text{CH}_3\text{C}_6\text{H}_4$) $_3\text{P}$ (9)	–37.2	
(<i>o</i> - $\text{CH}_3\text{C}_6\text{H}_4$) $_3\text{PO}$ (10)	29.1	
(<i>o</i> - $\text{CH}_3\text{C}_6\text{H}_4$) $_3\text{PO}_2$ (11)	22.2	
(<i>o</i> - $\text{CH}_3\text{OC}_6\text{H}_4$) $_3\text{P}$ (6)	–39.2	3.76
(<i>o</i> - $\text{CH}_3\text{OC}_6\text{H}_4$) $_3\text{PO}$ (7)	26.0	3.58
(<i>o</i> - $\text{CH}_3\text{OC}_6\text{H}_4$) $_3\text{PO}_2$ (8)	27.0	3.60, 3.73

Generally, four to six runs were conducted per phosphine, and errors are reported as one standard deviation. A control experiment demonstrated that the DMA endoperoxide does not oxidize the arylphosphines during the timeframe of the competition experiments (i.e., 1 h or less).

3.6. Low temperature NMR studies

Samples were directly irradiated in NMR tubes placed in a transparent Dewar flask. Acetone/liquid N_2 and 80%

acetone–20% methylene chloride/liquid N_2 were used for controlling the irradiation temperatures at -80 and -90 °C, respectively. After the photooxidation, the NMR tubes were frozen in liquid N_2 and subsequently placed into the precooled NMR spectrometer.

Acknowledgements

This research was supported by a Henry Dreyfus Teacher–Scholar Award. Support by the NIH-NIGMS MBRS program (Award number GM08101) is also gratefully acknowledged.

References and notes

- Clennan, E. L. *Acc. Chem. Res.* **2001**, *34*, 875 and references therein.
- Jensen, F.; Greer, A.; Clennan, E. L. *J. Am. Chem. Soc.* **1998**, *120*, 4439.
- Liang, J.-J.; Gu, C.-L.; Kacher, M. L.; Foote, C. S. *J. Am. Chem. Soc.* **1983**, *105*, 4717.
- Gu, C.-L.; Foote, C. S.; Kacher, M. L. *J. Am. Chem. Soc.* **1981**, *103*, 5949.
- Clennan, E. L.; Pace, A. *Tetrahedron* **2005**, *61*, 6665.
- Nahm, K.; Foote, C. S. *J. Am. Chem. Soc.* **1989**, *111*, 909.
- Tsuji, S.; Kondo, M.; Ishiguro, K.; Sawaki, Y. *J. Org. Chem.* **1993**, *58*, 5055.
- Nahm, K.; Li, Y.; Evanseck, J. D.; Houk, K.; Foote, C. S. *J. Am. Chem. Soc.* **1993**, *115*, 4879.
- Gao, R.; Ho, D. G.; Dong, T.; Khuu, D.; Franco, N.; Sezer, O.; Selke, M. *Org. Lett.* **2001**, *3*, 3719.
- Ho, D. G.; Gao, R.; Chung, H.-Y.; Celaje, J.; Selke, M. *Science* **2003**, *302*, 259.
- Bolduc, P. R.; Goe, G. L. *J. Org. Chem.* **1974**, *39*, 3178.
- Beaver, B. D.; Gao, L.; Fedak, M.; Coleman, M. M.; Sobkowiak, M. *Energy Fuels* **2002**, *16*, 1134.
- Beaver, B. D.; Burgess-Clifford, C.; Fedak, M. G.; Gao, L.; Iyer, P. S.; Sobkowiak, M. *Energy Fuels* **2006**, *20*, 1639.
- Tolman, C. A. *Chem. Rev.* **1977**, *77*, 313.
- Hirsivaara, L.; Guerricabeitia, L.; Haukka, M.; Suomalainen, P.; Laitinen, R. H.; Pakkanen, T. A.; Pursiainen, J. *Inorg. Chim. Acta* **2000**, *307*, 47. Ab initio calculations by these authors indicate that smaller cone angles, which would make the phosphorous atom more exposed to intermolecular attack, correspond to higher energy conformers.
- Kim, K. C.; Lee, K. A.; Sohn, C. K.; Sung, D. D.; Oh, H. K. J.; Lee, I. J. *J. Phys. Chem. A* **2005**, *109*, 2978.
- Bonesi, S. M.; Fagnoni, M.; Albini, A. *J. Org. Chem.* **2004**, *69*, 928.
- Higgins, R.; Foote, C. S.; Cheng, H. *Adv. Chem. Ser.* **1968**, *77*, 102.
- We use the term indirect physical quenching to describe deactivation of singlet oxygen via the formation of an unstable intermediate, which then loses a dioxygen molecule. Direct physical quenching refers to physical deactivation without the formation of any unstable adduct (i.e., energy transfer). This terminology has been used for the reaction of singlet oxygen with organic sulfides. Foote, C. S.; Peters, J. W. *IUPAC Congr., 23rd, Spec. Lec.* **1971**, *4*, 129.
- Eapen, K. C.; Tamborski, C. *J. Fluorine Chem.* **1980**, *15*, 239.

Solvent effect on the sensitized photooxygenation of cyclic and acyclic α -diimines

Else Lemp,^{*} Antonio L. Zanocco, German Günther and Nancy Pizarro

Universidad de Chile, Facultad de Ciencias Químicas y Farmacéuticas, Departamento de Química Orgánica y Fisicoquímica, Casilla 233, Santiago-1, Santiago, Chile

Received 1 June 2006; revised 14 August 2006; accepted 18 August 2006

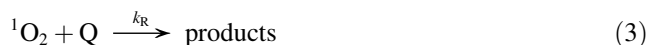
Available online 2 October 2006

Abstract—The reaction of singlet molecular oxygen with a series of cyclic and acyclic α -diimines was studied. Time-resolved methods were used to measure total reaction rate constants and steady-state methods were used to determine chemical reaction rate constants. GC–MS was used to tentatively assign the reaction products. 5,6-Disubstituted cyclic α -diimines are singlet oxygen quenchers, but become more effective in polar solvents. A reaction mechanism involving a peroxide intermediate or transition state leading to a hydroperoxide seems to be a key reaction path for product formation. A replacement of the phenyl substituent for a methyl substituent opens up an additional reaction involving a peroxide-like exciplex, which increases singlet oxygen quenching of the cyclic α -diimines. The reactivity of 5,6-disubstituted cyclic α -diimines towards singlet oxygen is highly dependent on steric interactions arising from vicinal phenyl rings and from electronic effects. 1,4-Disubstituted acyclic α -diimines are, by comparison, moderate or poor singlet oxygen quenchers. Total rate constants are scarcely dependent on solvent properties, but instead correlate with the Hildebrand parameter. These results are explained in terms of a mechanism involving a dioxetane-like exciplex that gives rise to a charged intermediate leading to products.

© 2006 Elsevier Ltd. All rights reserved.

1. Introduction

The interaction of singlet oxygen ($O_2(^1\Delta_g)$) with a target molecule (Q) involves physical (deactivation) and/or chemical (reactive) processes. This process can be represented in Eqs. 1–3



where k_d is the solvent dependent decay rate of singlet oxygen that determines its unperturbed lifetime ($\tau_o=1/k_d$), k_Q corresponds to a second-order rate constant of physical deactivation and k_R is the second-order rate constant of the reactive pathway. Measurement of the lifetime of singlet oxygen at different concentrations of Q permits one to obtain a k_T value, where $k_T=k_Q+k_R$. Evaluation of k_R requires the measurement of quantum yields of oxygen consumption and/or product formation, where these values can be difficult to

obtain. Values of k_Q and k_R can be solvent dependent, where solvent may modify each to a similar extent, thus keeping k_R/k_T constant. Such a similar behaviour can then be ascribed to an analogous mechanism and/or a common transition state. However, differences in the solvent effect between k_Q and k_R would suggest dissimilar transition states for each process. For example, a reaction containing different intermediates or different pathways may still follow from a common intermediate. Thus, the analysis of solvent effect on k_T and/or k_R provides valuable information regarding the nature of the reaction process. Many singlet oxygen reaction rate constants measured before 1999 have been compiled by Wilkinson et al.¹ Solvent effects on singlet oxygen reactions have been reviewed,^{2–6} where rate constant differences have been correlated with solvent dielectric constants,^{7–9} solvent hydrogen bonding (with the target molecule),¹⁰ and/or hydrophobic interactions.¹¹ In the last decade, linear solvation energy relationships (LSER) and theoretical linear solvation energy relationships (TLSER) have been employed to interpret singlet oxygen reaction mechanisms with amine,^{5,12–16} polycyclic aromatic compounds,¹¹ furan,¹⁷ alkaloids,^{5,18,19} and biologically active (polyfunctional) compounds.^{14,17,18,20,21} Such LSER treatments allow a quantitative evaluation of solvent effect in terms of different descriptors. The relative contribution of each descriptor included in the correlation equation depends on the substrate. Common features are observed for compounds belonging to the same family reacting through the same mechanism.

^{*} Corresponding author. Tel.: +56 2 9782877; fax: +56 2 9782868; e-mail: elemp@ciq.uchile.cl

The determination of a model compound correlation equation permits to calibrate and validate the linear free energy relationship in a given solvent set, giving a basis for predictions to the behaviour in other solvents. The formalism may be used to determine the main reaction site in polyfunctional compounds, to detect changes in the reaction mechanism with solvent properties, and to evaluate the relative contribution of tautomers in equilibrium to the total reaction rate. Also, the analysis could be extended to singlet oxygen reactivity in microheterogeneous systems to predict relative rate constants in such systems. However, when using this formalism, several limitations should be considered. First, this type of multilinear correlation is based on the assumption that the various descriptors are orthogonal, i.e., for a given parameter there is no cross-correlation with the other. Second, the barely reproducible rate constant values reported by different laboratories must be carefully stated to improve data reproducibility, which depends on various experimental critical points—e.g., sensitizer stability and reactivity, solvent purity, time of reaction and substrate consumption fraction in steady-state experiments, laser power and number of accumulated shots in time-resolved techniques.

A large number of studies have focused on reactions of singlet oxygen with molecules containing C=C double bonds. On the contrary, little data is available on reactions of singlet oxygen with molecules containing C=N double bonds.^{22–26} A product distribution may depend on temperature and substituents in reactions of $O_2(^1\Delta_g)$ with imino compounds and may involve several intermediates (Scheme 1), i.e., dioxazetidines (**1**) from [2+2] concerted cycloaddition to the carbon–nitrogen double bond;^{23,24} peroxide ions (**2**) from electrophilic attack on iminic carbon²³ and hydroperoxides (**4**) from rearrangement of pernitrones (**3**) in reactions with substituted 2,3-dihydropyrazines.²⁷ The involvement of a pernitron intermediate (**3**) may arise by the interaction of 1O_2 with the imine nitrogen lone pair.

Previous studies do not permit one to conclude whether the reaction of singlet oxygen and the imino group is similar to homologous alkenes or whether it departs significantly from this chemistry due to the presence of the nitrogen atom. In previous works,²⁸ we reported the total rate constant values, k_T , and the chemical reaction rate constant values, k_R , for the reactions between two 5,6-disubstituted-2,3-dihydropyrazines and singlet oxygen in various solvents. Chemical

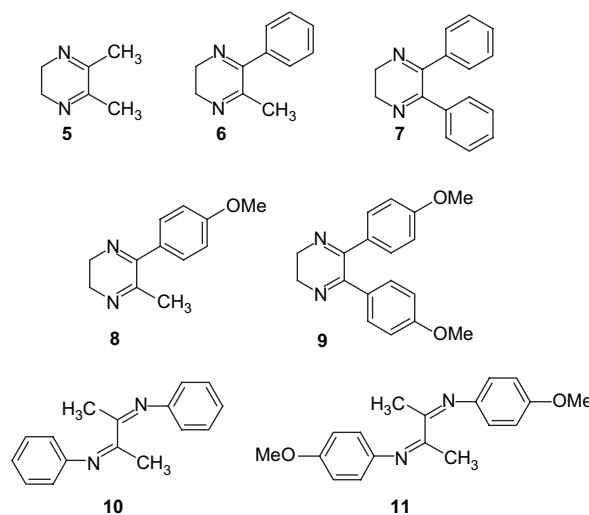
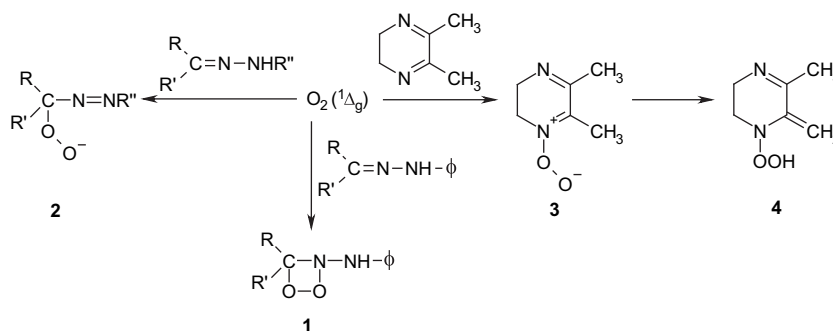


Figure 1. Structures of cyclic α -diimines: 5,6-dimethyl-2,3-dihydropyrazine (**5**), 5-methyl-6-phenyl-2,3-dihydropyrazine (**6**), 5,6-diphenyl-2,3-dihydropyrazine (**7**), 5-methyl-6-(*p*-methoxyphenyl)-2,3-dihydropyrazine (**8**), 5,6-bis(*p*-methoxyphenyl)-2,3-dihydropyrazine (**9**), and acyclic α -diimines: 1,4-diaza-1,4-diphenyl-2,3-dimethyl-1,3-butadiene (**10**), 1,4-diaza-1,4-bis(*p*-methoxyphenyl)-2,3-dimethyl-1,3-butadiene (**11**).

reaction rate constants, k_R , for 5,6-dimethyl-2,3-dihydropyrazine (**5**) were very close to k_T in polar solvents such as propylencarbonate, whereas the contribution of the chemical channel to the total reaction is very low for methyl and phenyl derivatives. Analysis of solvent effect on k_T for the dimethyl derivatives using the semiempirical solvatochromic equation (LSER) of Taft, Kamlet et al.,^{29,30} reveals a dependence on the solvent microscopic parameters α and π^* . When the phenyl group is replaced with a methyl group, the dihydropyrazine ring reactivity increases towards singlet oxygen and modifies the dependence of k_T on solvent parameters. The importance with the Hildebrand parameter is apparent.

In the present work, we study reactions of singlet oxygen with cyclic and acyclic α -diimines that possess different substituents on the iminic carbon (Fig. 1). Our aim is to understand the reaction mechanism based on product distributions and kinetics, which includes measurements of rate constants for chemical and physical reaction channels in several solvents. Solvent effects are analyzed in terms of linear solvation energy relationships (LSER).^{29–31} LSER relations are



Scheme 1.

of great value in interpreting mechanisms of singlet oxygen reactions since they may permit a quantitative explanation of solvent effects.⁵

2. Results

2.1. Total reaction of singlet oxygen with cyclic α -diimines

The total quenching rate constant (physical and chemical), k_T , for reaction of $O_2(^1\Delta_g)$ with the 5,6-disubstituted-2,3-dihydropyrazines (Fig. 1) in several solvents was obtained from the first-order decay of $O_2(^1\Delta_g)$ in the absence (τ_o^{-1}) and the presence of dihydropyrazine (τ^{-1}) according to Eq. 4.

$$\tau^{-1} = \tau_o^{-1} + k_T [\text{dihydropyrazine}] \quad (4)$$

Linear plots of τ^{-1} vs [dihydropyrazine] were obtained for all solvents employed (Fig. 2). Intercepts of these plots match closely with those reported²⁰ and measured (in a large number of experiments from our laboratory) for singlet oxygen lifetimes in the identical solvents. Values of k_T calculated from slopes of these plots are given in Table 1. The k_T values were independent of the laser pulse energy (between 2 and 5 mJ) allowing us to disregard secondary processes involving $O_2(^1\Delta_g)$. Singlet oxygen decays after dye laser excitation at 532 nm, with Rose Bengal as sensitizer in acetone, in the absence and the presence of 5,6-dimethyl-2,3-dihydropyrazine (**5**) are shown in the inset of Figure 2. As can be observed, both traces have nearly the same amplitude, indicating that the excited states of the sensitizer were not deactivated by the addition of **5** at the concentrations employed to quench $O_2(^1\Delta_g)$. The same behaviour was observed with TPP—the sensitizer employed in most solvents—in the presence of the different dihydropyrazines studied. The same k_T values were obtained for some solvents (data not shown) either by using competitive steady-state methods, such as the inhibition of the autoxidation rate of rubrene ($\lambda_{\max}=520$ nm)³² or by following the

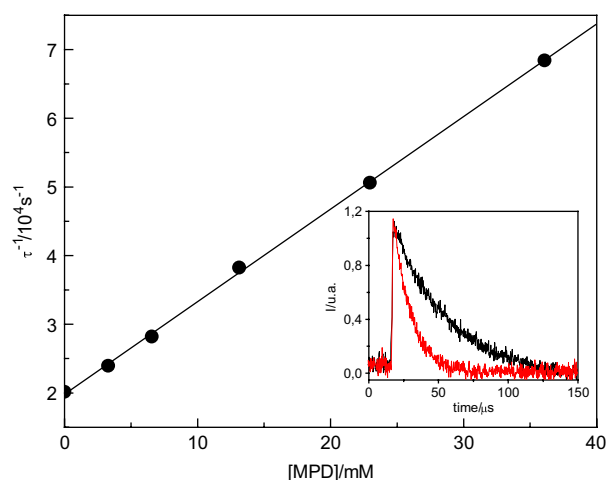


Figure 2. Stern–Volmer plot for deactivation of singlet oxygen by DMD in acetone. Inset (a) Singlet oxygen phosphorescence decay at 1270 nm, following dye laser excitation at 532 nm, with Rose Bengal as sensitizer in acetone. (b) as (a), but with 13.6 mM DMD.

consumption rate of 9,10-dimethylantracene in the absence and the presence of dihydropyrazine derivatives.¹⁸ Thus, possible rapid chemical changes of samples during illumination or interference on $O_2(^1\Delta_g)$ luminescence with the scattered laser light and the tail end of the sensitizer fluorescence³³ can be dismissed.

A solvent dependence is observed in the total quenching rate constants for all reactions of 5,6-disubstituted-2,3-dihydropyrazines with singlet oxygen (Table 1). The largest effect was found for **5**, for which k_T increases by more than 2 orders of magnitude when the solvent was changed from hexafluoro-2-propanol to *N,N*-dimethylacetamide. Similar trends were observed for **6**, **7**, **8** and **9**. The total rate constant value increases by more than 1 order of magnitude when the solvent is changed from protic to non-protic solvents, such as trifluoroethanol vs *N,N*-dimethylformamide. In addition, in all solvents the total rate constant for **6** was considerably larger than those for the other cyclic α -diimines. Dihydropyrazines exhibit similar results to those reported for dienes.¹ Thus, the reactivity of the compounds towards singlet oxygen depends both on dihydropyrazine structure as well as solvent properties.

However, solvent effects observed here are larger than those for dienes² and cannot be associated merely with changes in macroscopic solvent properties due to the existence of specific solute–solvent interactions.^{2,5,28} Thus, a deeper rationalization of solvent effects and interactions of singlet oxygen with dihydropyrazines can be obtained from the analysis of the quenching rate constant dependence on microscopic solvent parameters. The semiempirical solvatochromic equation (LSER) of Taft, Kamlet et al.^{29–31} (Eq. 5) was employed.

$$\log k = \log k_o + s\pi^* + d\delta + a\alpha + b\beta + h\rho_H^2 \quad (5)$$

In Eq. 5, π^* accounts for polarizability and dipolarity of solvent,^{31,34} δ is a correction term for polarizability, α corresponds to the hydrogen bond donor solvent ability, β indicates solvent capability as a hydrogen bond acceptor, and ρ_H is the Hildebrand parameter, a measure of disruption of solvent–solvent interactions in creating a cavity.³⁵ The constant term $\log k_o$ in Eq. 5 arises from the method of multiple linear regression and does not have a clear-cut physical meaning. For correlation equations independent of the cavity term, the constant term $\log k_o$ is equal to $\log k$ in solvents such as alkanes, in which all the other parameters are near to zero.

The coefficients in the LSER equation (Eq. 5), s , d , a , b and h , are obtained by a multilinear correlation analysis on k_T dependence with solvent parameters (Table 2). This analysis is supported on purely statistical criteria. Sample size N , product correlation coefficient R , standard deviation SD, and the Fisher index of equation reliability F , indicate the quality of the overall correlation equation. The reliability of each term is indicated by t -statistic t -stat, and the variance inflation factor VIF. Suitable quality is indicated by large N , F , and t -stat values; small SD values; and R and VIF close to one.³⁶

Results in Table 2 show that not all descriptors are statistically reliable. Descriptor coefficients accepted in the correlation equation were those having a significance level ≥ 0.95 .

Table 1. Values of k_T for reactions of cyclic α -diimines with $O_2(^1\Delta_g)$ in different solvents

Solvent	$k_T/10^5 \text{ M}^{-1} \text{ s}^{-1}$				
	5	6	7	8	9
Hexafluoro-2-propanol	0.26±0.01	—	0.28±0.01	—	0.44±0.02
Trifluoroethanol	1.52±0.16	5.74±0.25	1.75±0.08	3.54±0.18	0.87±0.04
Methanol	5.23±0.22	26.4±1.15	10.6±0.50	20.1±0.99	1.67±0.07
Ethanol	3.69±0.19	22.1±0.99	8.98±0.46	13.0±0.66	2.34±0.11
<i>n</i> -Propanol	8.60±0.38	25.5±1.09	7.20±0.32	12.7±0.64	2.83±0.12
<i>n</i> -Butanol	4.94±0.22	—	—	19.1±0.96	3.36±0.18
<i>n</i> -Pentanol	5.44±0.19	—	—	—	3.06±0.17
Benzyl alcohol	4.48±0.21	23.3±0.09	7.56±0.35	12.7±0.67	3.11±0.17
<i>n</i> -Hexane	3.60±0.17	—	—	10.7±0.56	—
<i>n</i> -Heptane	4.31±0.18	28.9±1.15	—	12.1±0.55	—
Chloroform	3.16±0.13	12.0±0.06	3.56±0.21	—	1.67±0.08
Benzene	5.34±0.21	49.5±1.98	5.66±0.29	18.5±0.89	2.78±0.15
Anisole	6.01±0.33	63.0±2.29	11.4±0.33	24.5±1.29	3.36±0.17
Diethyl ether	6.08±0.31	37.7±1.69	9.32±0.41	16.8±0.70	4.81±0.27
Benzonitrile	6.25±0.41	41.9±1.65	8.35±0.31	24.8±1.17	2.97±0.18
Methylene chloride	7.36±0.31	37.1±1.29	4.56±0.24	12.8±0.59	2.50±0.15
Acetonitrile	9.87±0.41	67.3±3.02	7.99±0.32	23.1±1.11	2.83±0.14
Tetrahydrofuran	12.9±0.48	50.6±2.85	11.7±0.51	25.5±1.15	4.63±0.28
Ethyl acetate	13.6±0.58	51.6±2.12	11.1±0.48	32.1±1.70	3.53±0.20
Acetone	13.7±0.43	60.4±2.63	11.2±0.31	31.1±1.59	3.95±0.19
Dioxane	14.6±0.55	60.8±3.00	11.7±0.37	42.7±2.01	2.99±0.17
<i>N,N</i> -Dimethylformamide	19.3±0.72	101.0±4.19	23.6±1.08	46.5±2.22	5.93±0.31
Propylencarbonate	20.3±0.89	68.1±3.27	18.4±0.90	45.9±2.30	4.70±0.24
Tributyl phosphate	56.8±2.34	159.0±4.38	12.6±0.65	—	3.03±0.17
<i>N,N</i> -dimethylacetamide	58.3±2.61	—	—	—	—

Table 2. LSER correlation equations for the reaction of singlet oxygen with cyclic α -diimines

$\log k = \log k_o + s\pi^* + d\delta + a\alpha + b\beta + h\rho_H^2$							
5	$\log k_o$	s	D	a	b	h	
Coeff.	5.577	0.629	−0.406	−0.602	0.439	—	
±	0.081	0.140	0.102	0.054	0.125	—	
<i>t</i> -Stat.	68.802	4.500	−3.964	−11.053	3.507	—	
<i>P</i> (2-tail)	<0.0001	0.0002	0.0008	<0.0001	0.0024	—	
VIF	—	1.536	1.808	1.006	1.572	—	
<i>N</i> =24, <i>R</i> =0.956, <i>SD</i> =0.144, <i>F</i> =50.029							
6	$\log k_o$	s	D	a	b	h	
Coeff.	6.395	—	—	−0.692	0.203	0.003	
±	0.056	—	—	0.050	0.084	0.001	
<i>t</i> -Stat.	114.69	—	—	−13.855	2.430	4.561	
<i>P</i> (2-tail)	<0.0001	—	—	<0.0001	0.00291	0.0004	
VIF	—	—	—	1.613	1.379	2.088	
<i>N</i> =18, <i>R</i> =0.970, <i>SD</i> =0.075, <i>F</i> =74.475							
7	$\log k_o$	s	D	a	b	h	
Coeff.	5.426	—	—	−0.596	0.595	0.004	
±	0.072	—	—	0.046	0.112	0.001	
<i>t</i> -Stat.	75.320	—	—	−12.853	5.299	4.855	
<i>P</i> (2-tail)	<0.0001	—	—	<0.0001	<0.0001	0.0002	
VIF	—	—	—	1.300	1.449	1.587	
<i>N</i> =19, <i>R</i> =0.976, <i>SD</i> =0.101, <i>F</i> =99.432							
8	$\log k_o$	s	D	a	b	h	
Coeff.	5.959	—	—	−0.589	0.376	0.003	
±	0.065	—	—	0.060	0.093	0.001	
<i>t</i> -Stat.	92.242	—	—	−9.873	4.048	4.198	
<i>P</i> (2-tail)	<0.0001	—	—	<0.0001	0.0011	0.0008	
VIF	—	—	—	1.585	1.402	2.036	
<i>N</i> =19, <i>R</i> =0.943, <i>SD</i> =0.094, <i>F</i> =40.038							
9	$\log k_o$	s	D	a	b	h	
Coeff.	5.381	—	—	−0.363	0.469	—	
±	0.034	—	—	0.029	0.060	—	
<i>t</i> -Stat.	159.483	—	—	−12.458	7.803	—	
<i>P</i> (2-tail)	<0.0001	—	—	<0.0001	<0.0001	—	
VIF	—	—	—	1.000	1.000	—	
<i>N</i> =21, <i>R</i> =0.961, <i>SD</i> =0.074, <i>F</i> =109.904							

For this reason ρ_H was not included in LSER correlation for **5**. Similarly, equations for **6**, **7**, **8** and **9** were independent of π^* parameter. According to the LSER coefficients in Table 2, k_T values for **5** increase in solvents with larger capacity to stabilize charges and dipoles and decrease in strong HBD solvents.

Furthermore, for other compounds under study, the rate constants increase in HBA solvents with high cohesive energy and decrease in strong HBD solvents, although rate constant for **9** does not depend on the Hildebrand parameter.

2.2. Chemical reaction of $O_2(^1\Delta_g)$ with dihydropyrazines

Irradiation of aerated solutions of **5**, **6** and **8** in the presence of TPP or RB, at the wavelength where only the sensitizer absorbs, decreases the concentration of these dihydropyrazine compounds. Plots of \ln [dihydropyrazine] versus t indicate that the photooxidation reaction follows a first-order kinetics, Eq. 6.

$$r = k_R[{}^1O_2][\text{dihydropyrazine}] = k_{\text{obs}}[\text{dihydropyrazine}] \quad (6)$$

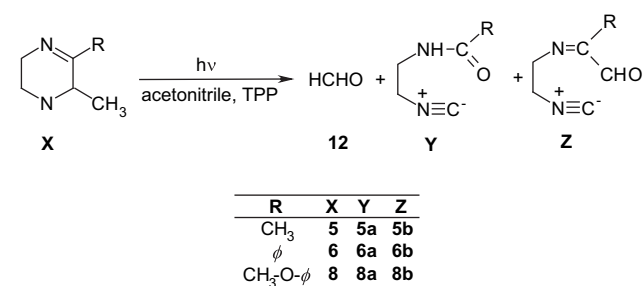
A compound of known reactivity towards singlet oxygen, such as dimethylantracene (DMA) has been employed as actinometer to evaluate the steady-state concentration of $O_2(^1\Delta_g)$. The reactive rate constants for dihydropyrazines can be evaluated from Eq. 7:

$$k_R^{\text{dihydropyrazine}} = k_R^{\text{actinometer}} \frac{k_{\text{obs}}^{\text{dihydropyrazine}}}{k_{\text{obs}}^{\text{actinometer}}} \quad (7)$$

We previously reported the rate constant values, k_R , for chemical quenching of $O_2(^1\Delta_g)$ by **5** and **6**, in various solvents (for compound **5**, k_R (*n*-hexane) = $0.06 \times 10^5 \text{ M}^{-1} \text{ s}^{-1}$; k_R (propylencarbonate) = $21.0 \times 10^5 \text{ M}^{-1} \text{ s}^{-1}$; for compound **6**, k_R (benzene) = $2.18 \times 10^5 \text{ M}^{-1} \text{ s}^{-1}$; k_R (propylencarbonate) = $1.53 \times 10^5 \text{ M}^{-1} \text{ s}^{-1}$).²⁸ For compound **8**, we found values of k_R very close to those obtained for MPD (k_R (benzene) = $1.96 \times 10^5 \text{ M}^{-1} \text{ s}^{-1}$). For **7** and **9**, we found neither substrate consumption nor product formation when monitoring the photosensitized oxidation of these compounds up to 60 h of irradiation—in ethanol or propylencarbonate as solvent—according to gas chromatography with NPD detection. For **9** in acetonitrile as solvent and TPP as sensitizer, we determined a consumption of 4% after 60 h irradiation. With a careful control of experimental conditions (photon flux, temperature and cell geometry) we measured a singlet oxygen steady-state concentration to be equal to $(1.2 \pm 0.3) \times 10^{-10} \text{ M}$ with DMA as actinometer. This result implies that k_R values for **7** and **9** would be $\leq 10^3 \text{ M}^{-1} \text{ s}^{-1}$, and the chemical quenching of singlet oxygen is negligible.

Because of the low substrate concentrations employed and the low conversion yields, no attempts were made to isolate reaction products for spectroscopic characterization. Tentative evidence for product distribution was obtained by GC–MS analysis. GC–MS analyses were carried out after irradiation for 6 h, where 0.001 M substrate (~30 to 40% conversion) was used in acetonitrile solution with TPP as sensitizer. Chromatograms were obtained operating the

spectrometer in both the positive chemical ionization (CI+) as well as the electron impact (EI+) modes. A chromatogram of **6** shows only three major peaks. Unreacted **6** is the main one. The CI+ and EI+ mass spectra corresponding to peaks with largest retention times indicate that 1-isocyano-2-(benzoylamino)ethane (**6a**) and 1-isocyano-4-phenyl-4-carboxaldehyde-3-aza-3-butene (**6b**) are the probable main products of photooxidation of **6** (Scheme 2). Additionally, in separate experiments in benzene, we confirmed the formation of formaldehyde (**12**) as one of the photooxidation products by comparison with a chromatogram obtained for formaldehyde in benzene. For **5** we found formaldehyde (**12**), 1-isocyano-2-(acylamino)ethane (**5a**) and 1-isocyano-4-carboxaldehyde-3-aza-3-pentene (**5b**) and for **8** we detected formaldehyde (**12**), 1-isocyano-2-(4-methoxybenzoylamino)ethane (**8a**) and 1-isocyano-4-(4-methoxyphenyl)-4-carboxaldehyde-3-aza-3-butene (**8b**) as the probable main reaction products (Scheme 2). These results show that the photooxidation of **5**, **6** and **8** follows the same reaction path.



Scheme 2.

2.3. Total reaction of singlet oxygen with acyclic α -diimines

The total quenching rate constant (physical and chemical), k_T , for reaction of $O_2(^1\Delta_g)$ with acyclic α -diimines (Fig. 1) in several solvents was obtained from the first-order decay of singlet oxygen luminescence as described for cyclic compounds (Eq. 6). The values of k_T obtained from these experiments are summarized in Table 3.

The reactivity of acyclic α -diimines (**10** and **11**) towards singlet oxygen is diminished compared to the cyclic homologous. The total quenching rate constants are 1–2 orders of magnitude smaller compared to those for 5,6-disubstituted-2,3-dihydropyrazines (Table 3).

1,4-Diaza-1,4-bis(*p*-methoxyphenyl)-2,3-dimethyl-1,3-butadiene (**11**) is the more reactive compared to 1,4-diaza-1,4-diphenyl-2,3-dimethyl-1,3-butadiene (**10**) and is strongly solvent dependent with respect to the total rate constant. For **11**, k_T increases by more than 1 order of magnitude when the solvent is changed from trifluoroethanol ($k_T = 1.37 \pm 0.07 \times 10^5 \text{ M}^{-1} \text{ s}^{-1}$) to *N,N*-dimethylformamide ($k_T = 15.2 \pm 0.80 \times 10^5 \text{ M}^{-1} \text{ s}^{-1}$). The acyclic α -diimine **10** shows a smaller reactivity with total rate constant values in the order of $10^4 \text{ M}^{-1} \text{ s}^{-1}$ and sparingly solvent dependent. In Table 4 the equation coefficients obtained from the LSER analysis for **11** are included. Our results show that k_T increases in solvents with a larger capacity to stabilize charges and dipoles, high cohesive energy and decrease in strong HBD solvents.

Table 3. Values of k_T for reactions of acyclic α -diimines with $O_2(^1\Delta_g)$ in different solvents

Solvent	$k_T/10^5 \text{ M}^{-1} \text{ s}^{-1}$	
	10	11
Hexafluoro-2-propanol	0.14±0.01	—
Trifluoroethanol	0.26±0.01	1.37±0.07
Ethanol	0.49±0.02	3.39±0.15
<i>n</i> -Propanol	0.41±0.02	1.69±0.07
<i>n</i> -Butanol	0.48±0.02	2.40±0.13
<i>n</i> -Pentanol	0.35±0.02	2.15±0.12
Acetonitrile	0.16±0.01	10.1±0.49
Acetone	0.12±0.01	8.05±0.38
Ethyl acetate	0.12±0.01	4.71±0.25
<i>N,N</i> -Dimethylformamide	0.35±0.02	15.2±0.80
<i>N,N</i> -Dimethylacetamide	0.34±0.02	12.5±0.65
Benzene	0.37±0.02	6.48±0.35
<i>n</i> -Hexane	0.17±0.01	1.81±0.10
<i>n</i> -Heptane	0.14±0.01	2.19±0.11
Chloroform	0.42±0.02	3.70±0.17
Dioxane	0.24±0.01	6.25±0.32
Propylencarbonate	0.29±0.01	14.6±0.70
Benzonitrile	0.16±0.01	8.55±0.44
Tetrahydrofuran	0.15±0.01	4.51±0.20
Anisole	0.28±0.01	6.05±0.31
Diethyl ether	0.21±0.01	2.73±0.11

Table 4. LSER correlation equations for the reaction of singlet oxygen with 1,4-diaza-1,4-bis(*p*-methoxyphenyl)-2,3-dimethyl-1,3-butadiene (**11**)

	$\log k = \log k_0 + s\pi^* + d\delta + a\alpha + b\beta + h\rho_H^2$					
	$\log k_0$	s	D	a	b	h
Coeff.	5.114	0.592	—	-0.597	—	0.003
±	0.058	0.085	—	0.050	—	0.001
<i>t</i> -Stat.	87.440	6.945	—	-11.867	—	4.746
<i>P</i> (2-tail)	<0.0001	<0.0001	—	<0.0001	—	0.0002
VIF	—	1.647	—	1.553	—	2.208

$N=20, R=0.975, SD=0.079, F=103.392$

In all statistical tests performed for compound **10** including simple linear regression, forward and backward ANOVA test and multiple regression, only we found dependence with the Hildebrand parameter. The correlation shows a coefficient h equal to 0.003, with a regression coefficient between 0.6 and 0.75 (highly dependent on the number of data points considered) and a Fisher index near to 10. Although non-acceptable statistical parameters are found, we believe that the total rate constant for this compound depends primarily on the solvent cohesive energy and the poor correlation is due to the narrow range of k_T values.

2.4. Chemical reaction of singlet oxygen with acyclic α -diimines

Chemical rate constants for reactions of acyclic α -diimines with singlet oxygen were determined in steady-state experiments by irradiating 0.001 M substrate in benzene or propylencarbonate solutions with TPP as the sensitizer. GC-NPD was used to monitor the substrate consumption (up to 30%). In these experiments, 9,10-dimethylanthracene (DMA, k_R (benzene)³⁷ = $2.1 \times 10^7 \text{ M}^{-1} \text{ s}^{-1}$) was used as the actinometer. The values for k_R calculated with Eq. 7 are summarized in Table 5.

The data in Table 5 show that chemical rate constant increases when solvent is changed from benzene to propylencarbonate. Comparison of k_R values with k_T values shows

Table 5. Chemical reaction rate constants, k_R , for reactions of 1,4-diaza-1,4-diphenyl-2,3-dimethyl-1,3-butadiene (**10**) and 1,4-diaza-1,4-bis(*p*-methoxyphenyl)-2,3-dimethyl-1,3-butadiene (**11**) with $O_2(^1\Delta_g)$ in different solvents

Solvent	$k_R/10^5 \text{ M}^{-1} \text{ s}^{-1}$	
	10	11
Benzene	0.035±0.002	0.216±0.012
Propylencarbonate	0.0686±0.038	2.120±0.090

that there is a small contribution (in the order of 20%) of the chemical reaction to the total singlet oxygen quenching. The physical quenching is the major deactivation process.

Similar to the dihydropyrazines (low substrate concentration, low conversion yields), we did not attempt to isolate reaction products for spectroscopic characterization, although evidence of product distribution was obtained by GC-MS. For the acyclic α -diimines studied, **10** and **11**, the product distribution was independent of the solvent, but not the relative concentrations. When 0.001 M **11** in benzene was irradiated for 49 h in the presence of TPP, the chromatogram shown in Figure 3a was obtained with the mass spectrometer in the electron impact (EI+) operation mode. Two major peaks are observed, along with two secondary reaction products. Unreacted **11** corresponds to the main peak with a retention time of 22.79 min (Fig. 3b shows the EI+ mass spectrum of **11**).³⁸ Analyses of the positive chemical ionization (CI+) (not included) and the EI+ mass spectra (Fig. 3e) corresponding to peak with retention time of 25.03 min, indicate that the main photooxidation product in benzene was *N*-(4-methoxyphenyl)-2-[(4-methoxyphenyl)imino]propanamide (**11c**). The peaks at 8.54 and 15.22 min suggest that 1-isocyano-4-methoxybenzene (**11a**) and *N*-(4-methoxyphenyl)acetamide (**11b**) are secondary products of the photooxidation of **11** in benzene (Scheme 3).

Figure 3c and d shows mass spectra ionization patterns and the corresponding proposed structures. In the same way that we previously described, we determined the formation of formaldehyde (**12**) as one of the photooxidation products. The same experiment carried out in propylencarbonate yields 1-isocyano-4-methoxybenzene (**11a**) and *N*-(4-methoxyphenyl)acetamide (**11b**) as main products whereas the product with retention time equal to 25.03 is the minor product. A similar behaviour was observed for **10**. Photooxidation in benzene yields *N*-phenyl-2-(phenylimino)propanamide (**10c**) as the main product. In propylencarbonate, the main reaction products were the 1-isocyano (**10a**) and acetamide derivatives (**10b**).

3. Discussion

3.1. Cyclic α -diimines

The quenching of singlet oxygen by **5** has been discussed earlier by Gollnick et al.²⁷ Product distribution was explained in terms of a hydroperoxide intermediate resulting from the rearrangement of a primary reaction intermediate, 'pernitron' or 'nitron oxide' (**13**) (Scheme 4). Other possible reaction pathways, involving interaction of singlet oxygen with C-5 of the dihydropyrazine to give hydroperoxides

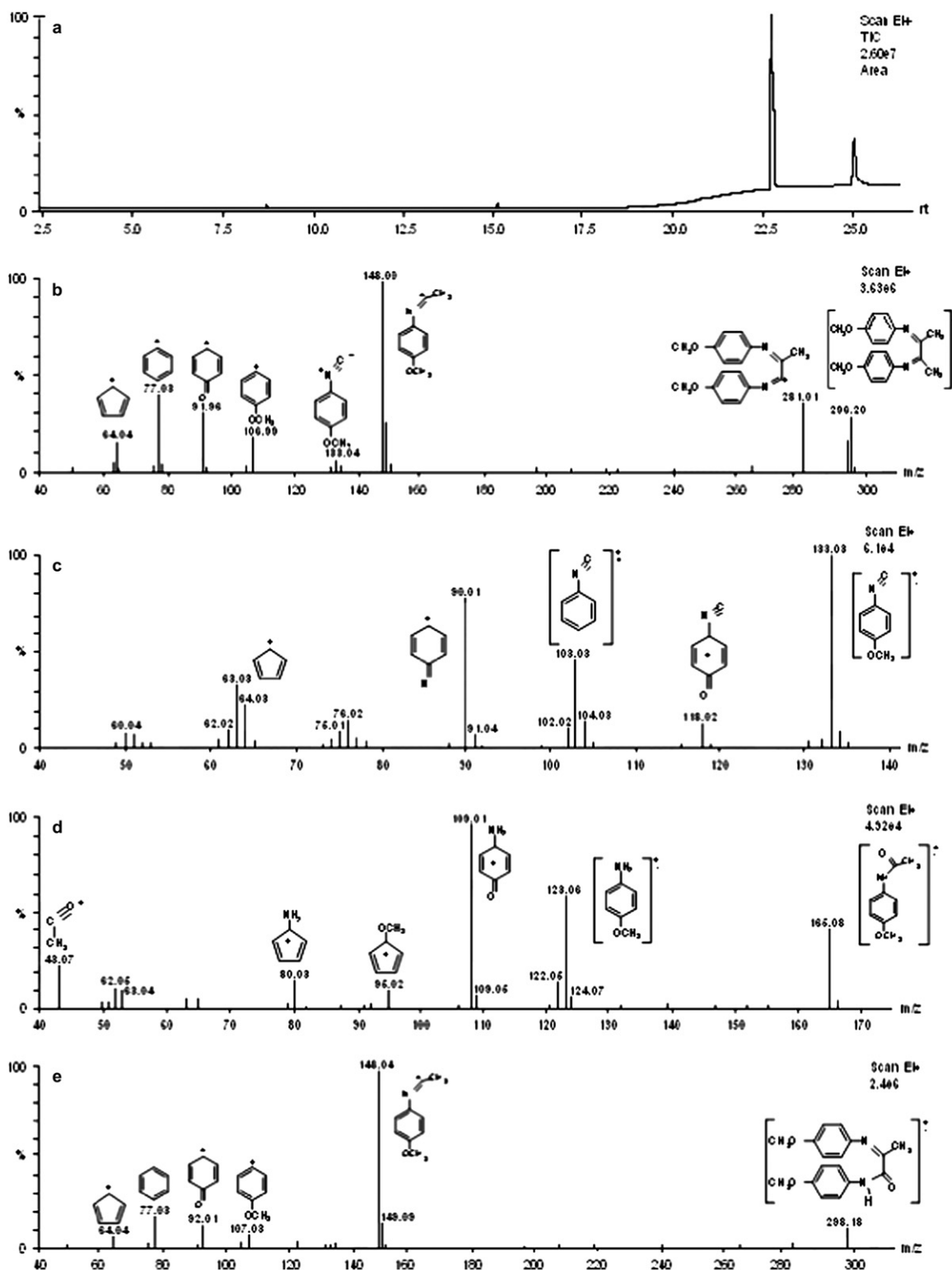
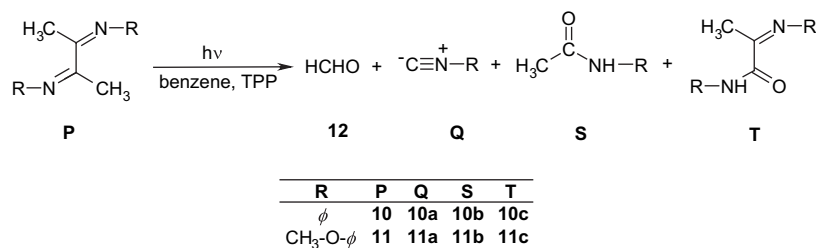


Figure 3. (a) GC–MS chromatogram of 1 mM 1,4-diaza-1,4-bis(*p*-methoxyphenyl)-2,3-dimethyl-1,3-butadiene (**11**) in benzene after 49 h of irradiation in the presence of TPP; (b) EI+ mass spectrum of **11**; (c) EI+ mass spectrum of compound with retention time 8.54 min; (d) EI+ mass spectrum of compound with retention time 15.22 min; (e) EI+ mass spectrum of compound with retention time 25.03 min.

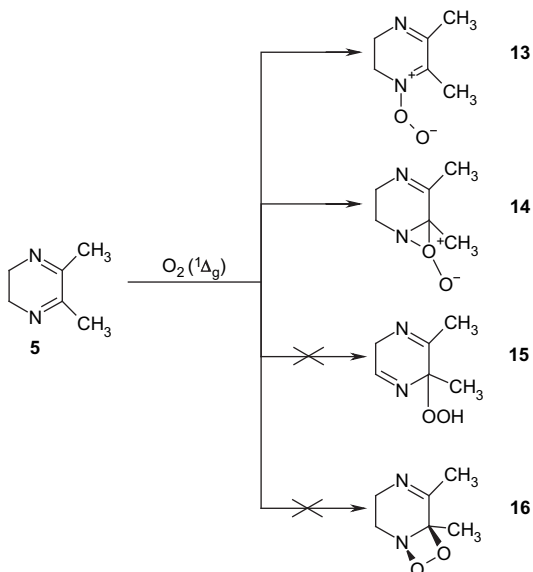
(**15**) or addition of $O_2(^1\Delta_g)$ to the C=N double bond giving peroxaziridines (**16**) were disregarded on the basis of observed products.

Kinetic results obtained in this work indicate that k_T values for singlet oxygen quenching by dihydropyrazines are

highly dependent on solvent properties (Table 1). A meaningful interpretation of k_T solvent dependence was obtained by using LSER solvatochromic equation. LSER correlations listed in Table 2 indicate that the singlet oxygen reaction with **5** has a different solvent dependence compared to that found for with other compounds. For **5**, the reaction rate



Scheme 3.



Scheme 4.

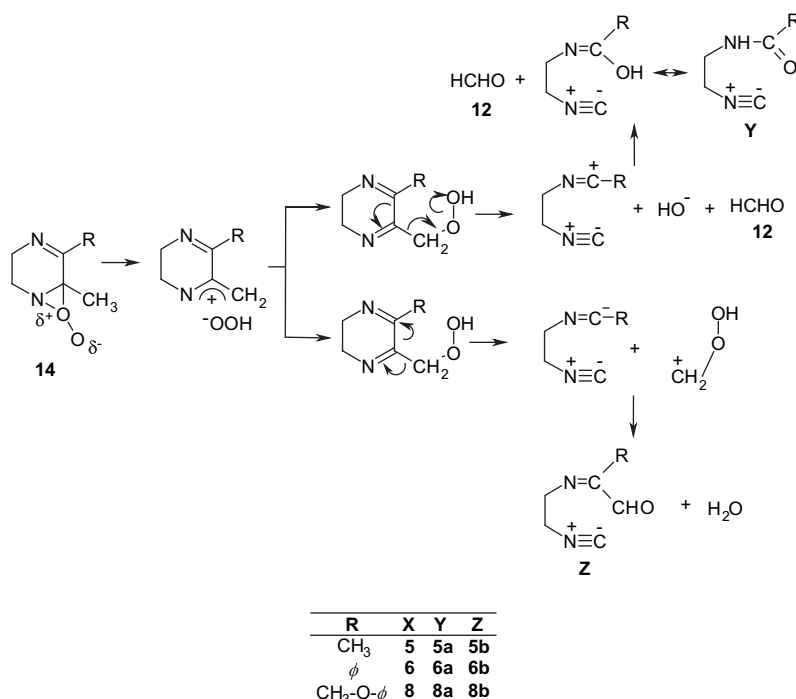
increases in solvents with higher capabilities to stabilize charges and dipoles, and decreases in strong hydrogen bond donor solvents. Data are compatible with an exciplex formation with considerable charge separation. This result could be in agreement with the formation of both peroxide (**14**) and zwitterionic (**13**) intermediates as proposed by Gollnick et al.²⁷ Formation of these species as intermediates, in the ene reaction of singlet oxygen with alkenes, prior to the product determining step has been extensively discussed,^{39–49} although recent theoretical studies predict two adjacent transition states without an intervening intermediate.⁵⁰

Our results support the formation of a peroxide as the primary intermediate arising from the interaction between singlet oxygen and **5**. The LSER equation for this compound shows that the relative statistical weight of the coefficient associated with the α parameter is smaller than the generally observed for electrophilic attack of singlet oxygen on a nitrogen lone pair in amino compounds. This result implies steric hindrance as a factor, likely due to hydrogen bonding between solvent and the nitrogen atom, inhibiting the reaction but not in the extent observed with tertiary amines.^{2,17} This result could be understood if nitrogen is not the reactive centre but is close to it. In the same way, we also found that the coefficient associated with the π^* parameter is larger than that of reactions of $\text{O}_2(^1\Delta_g)$ with amines. Solvent dependence on k_R for reaction of **5** with $\text{O}_2(^1\Delta_g)$ is more significant than that observed for k_T . The chemical rate constant

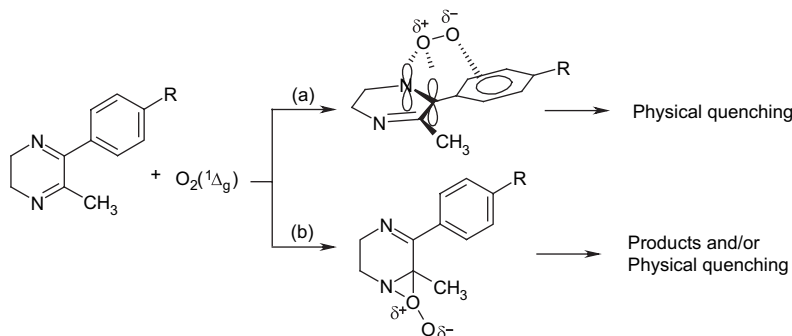
increases by more than 2 orders of magnitude when the solvent is changed from non-polar (e.g., hexane) to polar (e.g., propylencarbonate).²⁸ The contribution of the chemical reaction in non-polar solvents is negligible, whereas in highly polar solvents it represents the main deactivation channel. Solvent dependence of k_R can be explained if intermediates along the reaction coordinate have more localized charge than the initial complex. This result is compatible with involvement of ion pairs in controlling the final product distribution as depicted in Scheme 5.

The k_T value for reactions of **6** and **8** with singlet oxygen is substantially larger compared to **5**, in most solvents. The k_T value for **7** is comparable or slightly larger than that of **5**. Solvent effects for **6**, **7** and **8** analyzed in terms of LSER are characterized by Hildebrand parameter dependence of k_T . Dependence of rate constant on Hildebrand parameter has been ascribed to $\text{O}_2(^1\Delta_g)$ reactions, which involve a concerted or partially concerted cycloaddition of singlet oxygen to an activated diene.¹¹ The dependence on the Hildebrand parameter is explained in terms of formation of an encounter complex of smaller molecular volume compared to the parent compounds. Furthermore, these reactions are also affected by solvent dipolarity–polarizability. Moreover, examination of LSER equations for **6**, **7** and **8** shows that the reaction is also assisted by HBA and inhibited by HBD solvents. These results can be explained if phenyl substitution opens a further reactive channel in which the peroxide is stabilized by interaction with the π system of a phenyl group.^{28,51} A reaction mechanism compatible with our results is depicted in Scheme 6.

Reaction path (a), leads only to physical quenching through intersystem crossing to produce oxygen and the parent α -diimine. The geometry of the exciplex hinders intramolecular hydrogen abstraction processes more that it stabilizes it. Invoking the peroxide structure (Scheme 6a) provides an explanation for the observed solvent dependence. Decrease of total reaction rate constants in HBD solvents can be understood in terms of interactions with the reactive centre (the phenyl substituted $\text{C}=\text{N}$ double bond). Furthermore, the increase in sensitivity to HBA solvents may be due to electrostatic stabilizing interactions with a positive charge on the complex. In addition, dependence of k_T on the Hildebrand parameter can be understood in terms of a phenyl group–peroxide interaction. This interaction would be favourable in solvents with high cohesive energy because interaction of negatively charged oxygen with the neighbouring phenyl disrupts solvent–phenyl group interactions in the substrate. In addition, this hypothesis permits us to explain the low values of the chemical reaction constant measured



Scheme 5.



Scheme 6.

for **6** and **8** even in polar solvents and the absence of photooxidation products for **7** and **9**. As mentioned above, the only reaction products detected for **6** and **8** arise from singlet oxygen attack on a methyl substituted N–C double bond. The total reaction rate constant for **6** and **8** is larger than for the dimethyl substituted analogs. These data are consistent with the mechanism of sensitized photooxidation of **6** proposed in Scheme 6. The increased reactivity of **6** and **8** towards singlet oxygen, relative to the dimethyl substituted α -diimine (**5**), implies that the main path of reaction involves the interaction of $O_2(^1\Delta_g)$ with the phenyl substituted N–C double bond, to give a peroxide-like exciplex that exclusively evolves by intersystem crossing since there is no any accessible α -hydrogen. Even though this mechanism would be the only path for reaction of singlet oxygen with **8**, this molecule is not much more reactive than **5**. This behaviour can be easily understood by considering results of restricted DFT_B3LYP/6-311G* molecular modelling. These calculations predict phenyl rings appreciably deviated

from the coplanarity regarding the imino double bond. For **5** we found a dihedral angle of 39.7° between the phenyl and imino groups, while in the diphenyl substituted compound, **7**, the dihedral angle increases to 56.6° , due to the larger steric hindrance between the phenyl rings. If exciplex leading to physical quenching in Scheme 6 is considered, it can be noticed that a larger dihedral angle between the imino bond and the phenyl substituent would diminish the stabilizing interaction between the partially negative oxygen and the π system of the phenyl substituent, and consequently lower total rate constants would be expected. Compound **9** was the cyclic α -diimine that exhibits the smallest solvent effect. The LSER analysis for this compound shows that the reaction is assisted by HBA and inhibited by HBD solvents. This dependence on the microscopic solvent parameters was similar to that observed for **6**, **7** and **8** but k_T for **9** was found independent on the Hildebrand parameter. This behaviour can be explained by the effect of *p*-methoxyphenyl substituent. Important resonant electron donor effects cannot

be expected due to the lack of coplanarity among the imino and phenyl groups, on the contrary, the inductive electron acceptor effect would be predominant. This effect, more important for the methoxyphenyl group than the phenyl group,³⁹ diminishes the electron density on the imino bond and increases the negative charge on the phenyl ring π system, restricting both, the easiness of singlet oxygen electrophilic attack and the stabilizing interaction between the π system and the negative oxygen once the exciplex is formed. The effect permits us to explain the larger reactivity of **6** and **7** in comparison to the reactivity of **8** and **9**, respectively.

3.2. Acyclic α -diimines

Theoretical calculations predict a *trans* configuration of the two coplanar imino bonds as the most probable structure, with the phenyl substituents on the nitrogen slightly out of the plane due to steric interactions with methyl groups in positions 2 and 3. This configuration does not permit an eventual [2+4] cycloaddition of singlet oxygen to the conjugated double bonds. As mentioned above, the reactivity of acyclic α -diimines towards singlet oxygen is lower than that for the cyclic homologous by a factor 10–100, probably because of the most flexible linear structure. In addition, the data show k_T values strongly dependent on phenyl ring substituent, being more reactive than the *p*-methoxy substituted compound. The k_T values for **11** increase in solvents both with larger capacity to stabilize charges and dipoles, and with high cohesive energy. Also, they decrease in strong HBD solvents (Table 4). The dependence on the π^* parameter implies the formation of an exciplex with appreciable charge separation. Furthermore, the dependence on ρ_H^2 means a more compact exciplex than the parent compounds. This dependence is similar to that found for reaction of $O_2(^1\Delta_g)$ with 1,4-dimethylnaphthalene.¹¹ In this case, a partially concerted cycloaddition mechanism has been suggested to account for the dependence of the rate constant with solvent microscopic parameters. For **11** reaction with $O_2(^1\Delta_g)$, a partially concerted [2+2] cycloaddition, as shown in Scheme 7 is proposed to account for k_T dependence on the solvent. Decrease of k_T in HBD solvents can be explained in terms of interaction of acidic solvents with the nitrogen lone pair, which sterically hinders the access of excited oxygen to the reactive centre.

The lower reactivity of **10**, the reduced solvent effect on k_T and the dependence of k_T on the Hildebrand parameter in spite of the poor correlation can be interpreted based on two factors. First, the exciplex for this compound is formed through a concerted [2+2] cycloaddition with no charge

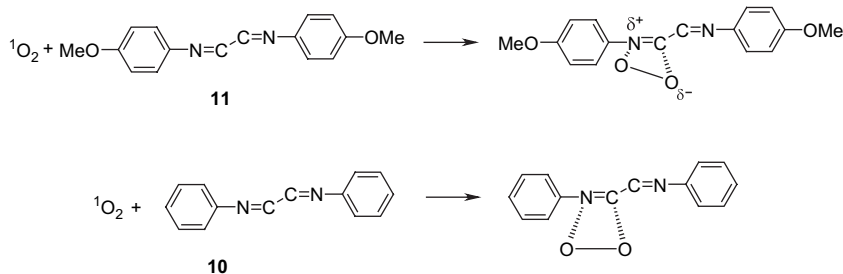
separation, as shown in Scheme 7. Second, reactivity of acyclic α -diimines is dependent on resonant effects of *p*-substituent in the phenyl group. The large resonant electron donor capacity of *p*-methoxy substituent in **11** increases the reactivity of this compound relative to the non-substituted **10**.

A concerted or partially concerted cycloaddition reaction mode would allow us to rationalize product distribution over extended periods of time in photooxidation experiments and similarly explain the dependence on solvent polarity. Identical product distributions are found in polar and non-polar solvents, but their relative concentrations change according to the media. This implies that at least two different intermediates lead to the detected products. The first intermediate may be highly favoured in polar solvents because of larger k_R values in these solvents. The intermediate could then rearrange to a non-polar intermediate in non-polar solvents. Scheme 8 shows a mechanism explaining these results.

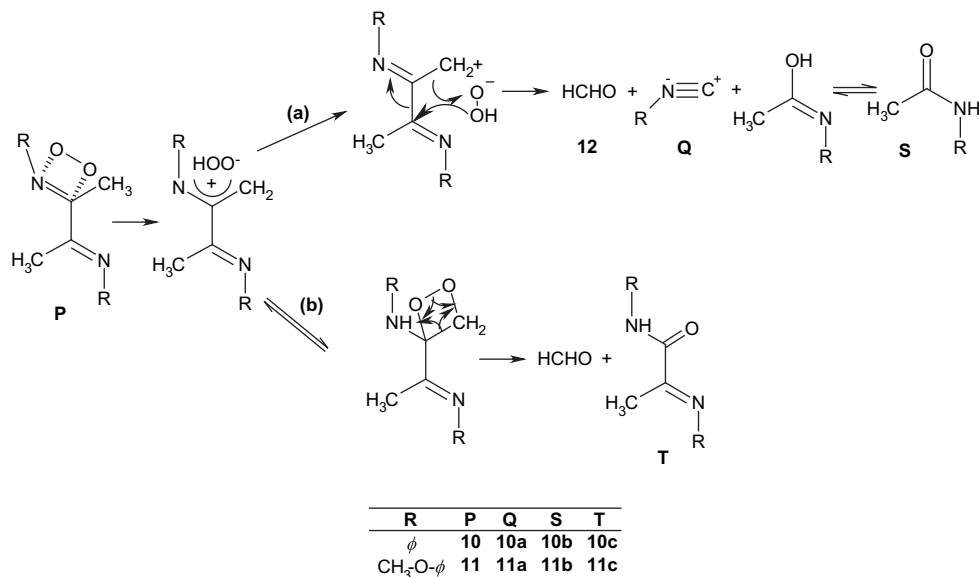
In Scheme 8, path (a) accounts for 1-isocyano-4-methoxybenzene (**11a**) and *N*-(4-methoxyphenyl)acetamide (**11b**), the main products observed in the photooxygenation of **11** in propylencarbonate. Path (b) explains the smaller reactivity in benzene as solvent and the increase in *N*-phenyl-2-(phenylimino)propanamide (**11c**) relative concentration. A similar mechanism has been proposed by Ito et al.²³ to explain product distribution in sensitized oxidation of hydrazones.

3.3. Conclusions

The 5,6-disubstituted cyclic α -diimines are moderate to efficient singlet oxygen quenchers, and are most effective in polar solvents. A reaction mechanism involving a peroxide intermediate that forms a hydroperoxide appears to be the main reaction path from which the products arise. The replacement of a phenyl substituent with a methyl substituent opens an additional reaction path involving a peroxide-like exciplex in which a stabilizing interaction of the negative charge on the free oxygen of a peroxide with aromatic π system contributes to an increased singlet oxygen quenching ability of cyclic α -diimines. 1,4-Disubstituted acyclic α -diimines are moderate to poor singlet oxygen quenchers. The total rate constants are scarcely dependent on the solvent properties. A reaction mechanism involving a dioxetane-like exciplex that evolves to a charged intermediate from which products are formed is most likely the main reaction path in polar solvents.



Scheme 7.



Scheme 8.

4. Experimental

4.1. General

Melting points (not corrected) were determined employing both a modified Koffler and a Electrothermal 9200 apparatus. NMR spectra were obtained from a Bruker DRX-300 spectrometer. Chemical shifts are referred to internal tetramethylsilane, TMS. Elemental analyses were performed on a Fisons EA 1108 instrument. IR spectra were obtained on a Fourier transform Bruker IFS-56 spectrometer. UV–vis measurements were made in a Unicam UV-4 spectrophotometer. A Fisons MD-800 GC–MS system with a Hewlett Packard Ultra-2 capillary column (25 m) was used to obtain electron impact mass spectra. All spectroscopic measurements were performed at room temperature.

4.2. Materials

All solvents used in the synthesis were of reagent grade. In spectroscopic and kinetic measurements, spectroscopic or HPLC quality solvents were used. 5,10,15,20-Tetraphenyl-21*H*,23*H*-porphine (TPP), 99%, and 9,10-dimethyl-anthracene, (DMA), 99%, from Aldrich were used without further purification. Rose Bengal (RB), 96%, from Fluka, was recrystallized twice from ethanol prior to use.

4.3. Methods

Chemical reaction rate constants were determined in several selected solvents using a 10 ml double wall cell, light-protected by black paint. A centred window allowed irradiation with light of a given wavelength using *Schott* cut-off filters. Circulating water maintained the cell temperature at 22 ± 0.5 °C. Sensitizer irradiation, RB or TPP was performed with a visible, 200 W, Par lamp. A *Hewlett Packard 5890* gas chromatograph equipped with a NPD detector and a *Hewlett Packard Ultra-2* capillary column was used to monitor substrate consumption. In a typical run, 0.001 M substrate

solution was irradiated in the presence of the sensitizer up to ~30 to 40% conversion. At least six duplicate 50 μL samples at different time intervals were taken for GC analysis. DMA was used as actinometer.

Time-resolved luminescence measurements were carried out in 1 cm path fluorescence cells. TPP or RB were excited by the second harmonic (532 nm, ca. 9 mJ per pulse) of 6-ns light pulse of a *Quantel Brilliant Q-Switched Nd:YAG* laser. A liquid-nitrogen cooled *North Coast model EO-817P* germanium photodiode detector with a built-in preamplifier was used to detect infrared radiation from the cell. Detector was coupled to the cell at right angle. An interference filter (1270 nm, *Spectrogon US, Inc.*) and a cut-off filter (995 nm, *Andover Corp.*) were the only elements between cell face and the diode cover plate. Preamplifier output was fed into the 1 M Ω input of a digitizing oscilloscope *Hewlett Packard model 54540 A*. Computerized experiment control, data acquisition and analysis were performed with a LabView based software developed in our laboratory.

Restricted density functional theory calculations were made using Gaussian 03W software. All structures were geometry optimized at the B3LYP/6-311G* level.

Equation coefficients and statistical parameters of LSER and TLSER correlations were obtained by multilinear correlation analysis with STAT VIEW 5.0 (SAS Institute Inc.). Results agreed with the *t*-statistic of descriptors.

4.4. Chemical synthesis

4.4.1. Synthesis of cyclic α -diimines. 5,6-Disubstituted-2,3-dihydropyrazines were synthesized as previously described.⁵² Typically, a solution of the corresponding diketone (5 g) in ethyl ether (10 ml) was added to ethylenediamine (2 g) in 10 ml of ethyl ether maintained at 0 °C. The mixture was refluxed for 30 min and the ethereal solution

was dried over sodium sulfate and solvent removed in vacuum. The remaining oil was cooled in a freezer during several hours producing a solid from which pure 5,6-disubstituted-2,3-dihydropyrazine was obtained as yellow needles by recrystallization from ethyl ether–hexane.

4.4.1.1. 5-Methyl-6-phenyl-2,3-dihydropyrazine (6).

This compound was prepared in 50% yield from 1-phenyl-1,2-propanedione according to the already described procedure; mp 34–37 °C (lit.^{27,53} mp 38–39 °C). ¹H NMR (CDCl₃): δ 2.1 ppm (s, 3H), 3.35–3.55 ppm (m, 4H), 7.3–7.4 (m, 5H). IR (KBr, ν, cm⁻¹): 2944, 2833, 1636, 1569, 1440. MS *m/e*=172 (M⁺), 157, 131, 103, 77.

4.4.1.2. 5,6-Dimethyl-2,3-dihydropyrazine (5). Following the procedure for the preparation of MPD, the condensation reaction between ethylenediamine and 2,3-butanedione afforded a liquid reaction crude. Careful distillation under nitrogen was required to obtain pure DMD, yield 40%, bp 58 °C (15 mmHg) (lit.^{52,53} bp 53–54 °C (12 Torr), 60–62 °C (18 Torr)). ¹H NMR (CDCl₃): δ 1.87 ppm (s, 6H), 3.07 ppm (s, 4H). IR (KBr, ν, cm⁻¹): 2949, 2845, 1655, 1598, 1439. MS *m/e*=110 (M⁺), 95, 69, 54, 42.

4.4.1.3. 5,6-Diphenyl-2,3-dihydropyrazine (7). In a reaction similar to that of DMD, 4.2 g (20 mmol) of benzyl and 1.2 g (20 mmol) of ethylenediamine yields 85% of DPD; mp 163–165 °C (lit.^{27,53} mp 162.5–163.5 °C). ¹H NMR (CDCl₃): δ 3.72 ppm (s, 4H), 7.26–7.43 ppm (m, 10H). IR (KBr, ν, cm⁻¹): 2942, 2831, 1553, 1490. MS *m/e*=234 (M⁺), 176, 131, 103, 77.

4.4.1.4. 5,6-Bis(*p*-methoxyphenyl)-2,3-dihydropyrazine (9). Following the same procedure to synthesize DMD 2.2 g (8.3 mmol) of 4,4'-dimethoxybenzyl and 0.5 g (8.3 mmol) of ethylenediamine afforded a pale yellow solid, after purification by employing a chromatographic column packed with silica and chloroform as the eluent. Subsequent recrystallization from ethanol yield 75% of pure BMPD; mp 127–129 °C with dec. ¹H NMR (CDCl₃): δ 3.56 ppm (s, 4H), 3.71 ppm (s, 6H), 6.76–7.38 ppm (m, 8H). IR (KBr, ν, cm⁻¹): 2938, 2835, 1633, 1441. MS *m/e*=294 (M⁺), 263, 133, 103, 77. Elem. anal. calcd %C: 73.47, %H: 6.12, %N: 9.52; exp. %C: 73.26, %H: 6.17, %N: 9.78.

4.4.1.5. 5-Methyl-6-(*p*-methoxyphenyl)-2,3-dihydropyrazine (8). This compound was prepared in 75% yield from 0.5 g (2.7 mmol) of 1-(*p*-methoxyphenyl)-1,2-propanedione according to the already described procedure. ¹H NMR (CDCl₃): δ 2.05 ppm (s, 3H), 3.38–3.48 ppm (m, 4H), 3.77 ppm (s, 3H), 6.86 ppm (d, 2H), 7.37 ppm (d, 2H). IR (KBr, ν, cm⁻¹): 2940, 2837, 1581, 1512, 1439 cm⁻¹. MS *m/e*=202 (M⁺), 171, 133, 103, 77. Elem. anal. calcd %C: 71.26, %H: 6.98, %N: 13.85; exp. %C: 71.06, %H: 7.04, %N: 14.23.

4.4.2. Synthesis of acyclic α-diimines. Acyclic α-diimines were synthesized through the condensation reaction of aromatic amines with 2,3-butanedione.⁵⁴ Typically, a solution of the corresponding aromatic amine (5 g) in 10 ml of ethanol was added to butanedione (2 g) in 5 ml of ethanol. The mixture was gently warmed for 30 min and stirred at room temperature for 24 h to obtain a crystalline yellow

solid. The solid was filtered, washed with cold ethanol and recrystallized from ethanol to obtain the pure product.

4.4.2.1. 1,4-Diaza-1,4-diphenyl-2,3-dimethyl-1,3-butadiene (10). This compound was prepared in 49% yield from aniline according to the already described procedure; mp 137–139 °C (lit.⁵⁴ mp 136–137 °C). ¹H NMR (CDCl₃): δ 2.15 ppm (s, 6H), 6.77–6.81 ppm (m, 2H), 7.08–7.14 ppm (m, 1H), 7.33–7.40 ppm (m, 2H). IR (KBr, ν, cm⁻¹): 3058, 1634, 1590, 1480, 1445. MS *m/e*=236 (M⁺), 118, 103, 77, 51. Elem. anal. calcd %C: 81.35, %H: 6.78, %N: 11.86; exp. %C: 81.14, %H: 7.02, %N: 12.22.

4.4.2.2. 1,4-Diaza-1,4-bis(*p*-methoxyphenyl)-2,3-dimethyl-1,3-butadiene (11). In a reaction similar to that of DPDM, 3.8 g (31 mmol) of *p*-anisidine and 1.2 g (14 mmol) of 2,3-butanedione yields 52% of DMPDM; mp 185–186 °C. ¹H NMR (CDCl₃): δ 2.18 ppm (s, 6H), 3.82 ppm (s, 6H), 6.78 ppm (d, 2H), 6.91 ppm (d, 2H). IR (KBr, ν, cm⁻¹): 2960, 1633, 1501, 1469. MS *m/e*=296 (M⁺), 281, 148, 92, 77. Elem. anal. calcd %C: 72.97, %H: 6.76, %N: 9.46; exp. %C: 72.67, %H: 7.01, %N: 9.48.

Acknowledgements

Financial support from FONDECYT (grant 2990096) and Departamento de Postgrado de la Universidad de Chile (grants PG/037/98 and PG/51/99) are gratefully acknowledged.

References and notes

- Wilkinson, F.; Brummer, J. G. *J. Phys. Chem. Ref. Data* **1981**, *10*, 809–899; Wilkinson, F.; Helman, W. P.; Ross, A. B. <http://allen.rad.nd.edu/compilations/SingOx>.
- Lissi, E. A.; Encinas, M. V.; Lemp, E.; Rubio, M. A. *Chem. Rev.* **1993**, *93*, 699–723.
- Lissi, E. A.; Rubio, M. A. *Pure Appl. Chem.* **1990**, *62*, 1503–1510.
- Lissi, E. A.; Lemp, E.; Zanicco, A. L. *Understanding and Manipulating Excited-state Processes*; Ramamurthy, V., Schanze, K. S., Eds.; Marcel Dekker: New York, NY, 2001; Vol. 4, pp 287–316.
- Lemp, E.; Zanicco, A. L.; Lissi, E. A. *Curr. Org. Chem.* **2003**, *7*, 799–819.
- Schweitzer, C.; Schmidt, R. *Chem. Rev.* **2003**, *103*, 1685–1757.
- Palumbo, M. C.; García, N. A.; Arguello, G. A. *J. Photochem. Photobiol. B, Biol.* **1990**, *7*, 33–42.
- Mandard-Cazin, B.; Aubry, J.-M.; Rigaudy, J. *J. Chem. Soc., Chem. Commun.* **1986**, 952–953.
- Gollnick, K.; Griesbeck, A. *Tetrahedron Lett.* **1984**, *25*, 725–728.
- Mártire, D. O.; Braslavsky, S. E.; García, N. A. *J. Photochem. Photobiol. A, Chem.* **1991**, *61*, 113–124.
- Aubry, J.-M.; Mandard-Cazin, B.; Rougee, M.; Bensasson, R. V. *J. Am. Chem. Soc.* **1995**, *117*, 9159–9164.
- Encinas, M. V.; Lemp, E.; Lissi, E. A. *J. Chem. Soc., Perkin Trans. 2* **1987**, 1125–1127.
- Clennan, E. L.; Noe, L. J.; Wen, T.; Szneler, E. *J. Org. Chem.* **1989**, *54*, 3581–3584.
- Zanicco, A. L.; Günther, G.; Lemp, E.; De la Fuente, J. R.; Pizarro, N. *J. Photochem. Photobiol. A, Chem.* **2001**, *140*, 109–115.

15. Darmanyan, A. P.; Jenksh, W. S. *J. Phys. Chem. A* **1998**, *102*, 7420–7426.
16. Catalan, J.; Diaz, C.; Barrio, L. *Chem. Phys.* **2004**, *300*, 33–39.
17. Zanooco, A. L.; Günther, G.; Lemp, E.; de la Fuente, J. R.; Pizarro, N. *Photochem. Photobiol.* **1998**, *68*, 487–493.
18. Zanooco, A. L.; Lemp, E.; Günther, G. *J. Chem. Soc., Perkin Trans. 2* **1997**, 1299–1302.
19. Lemp, E.; Gunther, G.; Castro, R.; Curitol, M.; Zanooco, A. L. *J. Photochem. Photobiol. A, Chem.* **2005**, *175*, 146–153.
20. Lemp, E.; Pizarro, N.; Encinas, M. V.; Zanooco, A. L. *Phys. Chem. Chem. Phys.* **2001**, *3*, 5222–5225.
21. Lemp, E.; Valencia, C.; Zanooco, A. L. *J. Photochem. Photobiol. A, Chem.* **2004**, *168*, 91–96.
22. George, M. V.; Bhat, V. *Chem. Rev.* **1979**, *79*, 447–478.
23. Ito, Y.; Kyono, K.; Matsuura, T. *Tetrahedron Lett.* **1979**, 2253–2256.
24. Vaidya, V. K. *J. Photochem. Photobiol. A, Chem.* **1994**, *81*, 135–137.
25. Castro, C.; Dixon, M.; Erden, I.; Ergonec, P.; Keeffe, J.; Sukhovistsky, A. *J. Org. Chem.* **1989**, *54*, 3732–3738.
26. Erden, I.; Griffin, A.; Keeffe, J.; Brinck-Kohn, V. *Tetrahedron Lett.* **1993**, *34*, 793–796.
27. Gollnick, K.; Koegler, S.; Maurer, D. *J. Org. Chem.* **1992**, *57*, 229–234.
28. Lemp, E.; Zanooco, A. L.; Günther, G.; Pizarro, N. *J. Org. Chem.* **2003**, *68*, 3009–3016.
29. Reichardt, C. *Solvents and Solvent Effects in Organic Chemistry*, 2nd ed.; VCH: Weinheim, 1990.
30. Kamlet, M. J.; Abboud, J. L. M.; Abraham, M. H.; Taft, R. W. *J. Org. Chem.* **1983**, *48*, 2877–2887.
31. Abraham, M. H.; Doherty, R. M.; Kamlet, M. J.; Harris, J. M.; Taft, R. W. *J. Chem. Soc., Perkin Trans. 2* **1987**, 913–920.
32. Carlson, D. J.; Mendenhall, E. D.; Suprunchuk, T.; Wiles, D. M. *J. Am. Chem. Soc.* **1972**, *94*, 8960–8963.
33. Michaeli, A.; Feitelson, J. *Photochem. Photobiol.* **1994**, *59*, 284–288.
34. Kamlet, M. J.; Carr, P. W.; Taft, R. W.; Abraham, M. H. *J. Am. Chem. Soc.* **1981**, *103*, 6062–6066.
35. Barton, A. F. M. *Chem. Rev.* **1975**, *75*, 731–752.
36. Belsley, D. A.; Kuh, E.; Welsch, R. E. *Regression Diagnostics. Identifying Influential Data and Sources of Collinearity*; Wiley: New York, NY, 1980.
37. Gunther, G.; Lemp, E.; Zanooco, A. L. *Bol. Soc. Chil. Quim.* **2000**, *45*, 637–644.
38. Pretsch, E.; Bühlmann, P.; Affolter, C.; Herrera, A.; Martínez, R. *Determinación Estructural de Compuestos Orgánicos*; Springer: Barcelona, 2001.
39. Stratakis, M.; Orfanopoulos, M.; Foote, C. S. *J. Org. Chem.* **1998**, *63*, 1315–1318.
40. Jefford, C. W.; Rimbault, C. G. *J. Am. Chem. Soc.* **1978**, *100*, 295–296.
41. Jefford, C. W.; Rimbault, C. G. *J. Am. Chem. Soc.* **1978**, *100*, 6437–6445.
42. Manring, L. E.; Foote, C. S. *J. Am. Chem. Soc.* **1983**, *105*, 4710–4717.
43. Wilson, S. L.; Schuster, G. B. *J. Org. Chem.* **1986**, *51*, 2056–2060.
44. Fenical, W.; Kearns, D. R.; Radlick, P. *J. Am. Chem. Soc.* **1969**, *91*, 3396–3398.
45. Frimer, A. A.; Bartlett, P. D.; Boschung, A. F.; Jewett, J. G. *J. Am. Chem. Soc.* **1977**, *99*, 7977–7986.
46. Poon, T. H. W.; Pringle, K.; Foote, C. S. *J. Am. Chem. Soc.* **1995**, *117*, 7611–7618.
47. Stratakis, M.; Orfanopoulos, M.; Foote, C. S. *J. Am. Chem. Soc.* **1991**, *32*, 863–866.
48. Orfanopoulos, M.; Stephenson, L. M. *J. Am. Chem. Soc.* **1980**, *102*, 1417–1418.
49. Grdina, B.; Orfanopoulos, M.; Stephenson, L. M. *J. Am. Chem. Soc.* **1979**, *101*, 3111–3112.
50. Singleton, D. A.; Hang, Ch.; Szymanski, M. J.; Meyer, M. P.; Leach, A. G.; Kuwata, K. T.; Chen, J. S.; Greer, A.; Foote, C. S.; Houk, K. N. *J. Am. Chem. Soc.* **2003**, *125*, 1319–1328.
51. Stratakis, M.; Orfanopoulos, M. *Tetrahedron* **2000**, *56*, 1595–1615.
52. Flamet, I. F.; Stoll, M. *Helv. Chim. Acta* **1967**, *50*, 1754–1758.
53. Beak, P.; Miesel, J. L. *J. Am. Chem. Soc.* **1967**, *80*, 2375–2384.
54. Ferguson, L.; Goodwin, T. *J. Am. Chem. Soc.* **1949**, *71*, 633–637.

‘Reductive ozonolysis’ via a new fragmentation of carbonyl oxides

Chris Schwartz, Joseph Raible, Kyle Mott and Patrick H. Dussault*

Department of Chemistry, University of Nebraska-Lincoln, Lincoln, NE 68588-0304, United States

Received 12 June 2006; revised 13 August 2006; accepted 13 August 2006

Available online 28 September 2006

Abstract—This account describes the development of methodologies for ‘reductive’ ozonolysis, the direct ozonolytic conversion of alkenes into carbonyl groups without the intermediacy of 1,2,4-trioxolanes (ozonides). Ozonolysis of alkenes in the presence of DMSO produces a mixture of aldehyde and ozonide. The combination of DMSO and Et₃N results in improved yields of carbonyls but still leaves unacceptable levels of residual ozonides; similar results are obtained using secondary or tertiary amines in the absence of DMSO. The influence of amines is believed to result from conversion to the corresponding *N*-oxides; ozonolysis in the presence of amine *N*-oxides efficiently suppresses ozonide formation, generating high yields of aldehydes. The reactions with amine oxides are hypothesized to involve an unprecedented trapping of carbonyl oxides to generate a zwitterionic adduct, which fragments to produce the desired carbonyl group, an amine, and ¹O₂. © 2006 Elsevier Ltd. All rights reserved.

1. Introduction

The ozonolysis of alkenes, first reported in 1840, remains one of the most important methods for oxidative cleavage of alkenes.¹ For example, a *SciFinder* search for ozone-related conversion of terminal alkenes to aldehydes returns thousands of examples. A powerful oxidant directly available from oxygen, ozone is also an attractive reagent for sustainable oxidations. However, whereas alkene cleavage with high-valent metal oxides typically results in the direct formation of aldehydes and ketones, ozonolysis initially generates ozonides and other peroxides, species often capable of spontaneous and dangerously exothermic decomposition reactions.² The formation of energetic intermediates is particularly problematic for large-scale processes, but even laboratory-scale reactions must typically be accompanied by a subsequent work-up reaction, most often a reduction.^{3,4} The most effective reducing agents can lead to problems with functional group compatibility (Pt/H₂, BH₃, Zn/HOAc, LiAlH₄) or product separation (PPh₃).⁵ The use of more selective and easily separated reagents (Me₂S) can leave high concentrations of residual 1,2,4-trioxolane (ozonide), leading to explosions upon reaction concentration.⁶ We hoped to exploit the mechanism of alkene ozonolysis to achieve the direct production of carbonyl products, avoiding generation or isolation of peroxidic intermediates. In this account, we describe the development of a practical methodology for ‘reductive ozonolysis’ in which trapping and fragmentation of carbonyl oxides by amine oxides results in the direct formation of aldehydes and ketones.⁷

In approaching this problem, it is instructive to overview the mechanism of alkene ozonolysis (Fig. 1).⁸ A highly exothermic cycloaddition of ozone with an alkene generates a *primary ozonide* (1,2,3-trioxolane).⁹ The primary ozonide has limited stability, and, under typical reaction conditions (>−80 °C) undergoes immediate cycloreversion to a *carbonyl oxide* and a carbonyl. The fate of the carbonyl oxide, which is so short lived as to be undetectable in solution-phase chemistry, determines the distribution of reaction products.¹⁰ A nearly activationless cycloaddition of the carbonyl oxide with a reactive dipolarophile, often the co-generated aldehyde or ketone, produces *ozonides* or 1,2,4-trioxolanes.¹¹ Alternatively, trapping of carbonyl oxides by unhindered alcohols¹² and related nucleophiles generates hydroperoxyacetals and similar addition products.^{8,10} When neither addition nor cycloaddition pathways are available, carbonyl oxides can undergo dimerization or oligomerization to furnish 1,2,4,5-tetraoxanes or polymeric peroxides.¹³ For simplicity, only ozonide formation is illustrated.

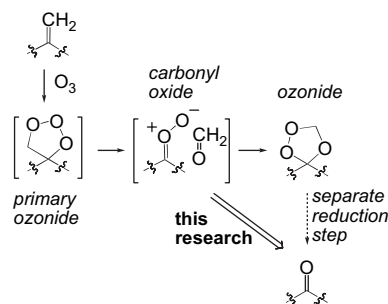


Figure 1. Overview of alkene ozonolysis.

* Corresponding author. Tel.: +1 402 472 3634; fax: +1 402 472 9402; e-mail: pdussault1@unl.edu

Ozonides possess a dangerous combination of kinetic stability and thermochemical instability; they are typically isolable yet often capable of spontaneous and dangerously exothermic decomposition reactions.² Our goal was to develop methodology that would avoid generation of ozonides or other peroxides, and instead directly deliver the desired carbonyl products. Our approach required a reagent capable of intercepting the primary ozonide, the carbonyl oxide, or the ozonide (1,2,4-trioxolane), yet compatible with ozone, one of the strongest oxidants in organic chemistry. Ozonides appeared too stable to be the targets of such an approach. Primary ozonides (1,2,3-trioxolanes) have been generated at very low temperature and separately reacted with strong nucleophiles, but this process has not been accomplished in the presence of ozone.¹⁴ This leaves carbonyl oxides, the most reactive intermediates in an ozonolysis, as the most logical targets for in situ capture.

2. Results and discussion

Our initial approach focused on cycloaddition of carbonyl oxides with X=O reagents (Fig. 2). An optimal trapping reagent would be a readily available and reactive dipolarophile containing a central atom (X) in an incompletely oxidized state. The derived heteroozonides would be expected to undergo internal fragmentation with liberation of O=X=O and a carbonyl group, achieving net oxidation of the X=O reagent and net reduction of the carbonyl oxide. Literature reports suggested that sulfinyl dipolarophiles reduce carbonyl oxides, presumably via intermediate 3-thia-1,2,4-trioxolanes.¹⁵ Moreover, electron rich carbonyl oxides preferentially oxidize sulfoxides (to sulfones), even in the presence of a sulfide.¹⁶ A similar strategy has recently been applied to the reduction of persulfoxides with aryl selenoxides.¹⁷

Our investigations began with dimethyl sulfoxide (DMSO). Whereas ozonolysis of decene provides a nearly quantitative yield of isolated ozonide (3-octyl-1,2,4-trioxolane),¹⁸ the same reaction in the presence of 2.0 equiv of DMSO generated a mixture of aldehyde and ozonide in which the former was predominant (Table 1). While these results were intriguing, we were unable to find conditions able to effectively suppress ozonide formation. For example, the use of 5 equiv of DMSO offered little improvement in yield of aldehyde,¹⁹ while attempts to employ even larger amounts of reagent resulted in phase separation or freezing.

The addition of protic nucleophiles provided an opportunity to test the role of the carbonyl oxide in the DMSO-promoted reductions (Table 2). The presence of methanol resulted in the formation of hydroperoxyacetal at the expense of aldehyde. The same effect was observed to a lesser extent for isopropanol, as would be expected based upon the reported rates of trapping by primary and secondary alcohols.^{10,12}

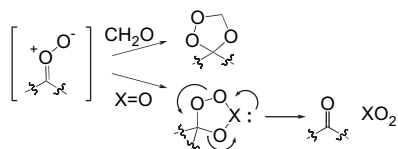
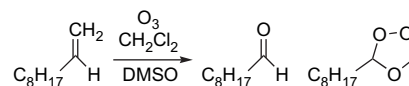


Figure 2. Capture by reductive dipolarophile.

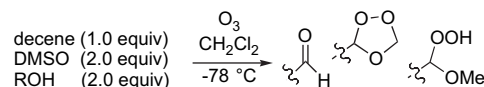
Table 1. Reduction with DMSO



DMSO (equiv)	T (°C)	Aldehyde (%) ^a	Ozonide (%) ^a
0	-78 or 0	Trace	>95%
2	-78	52	35
2	0	61	22

^a Isolated yield.

Table 2. Competition for carbonyl oxide



ROH	Aldehyde (%) ^a	Ozonide (%) ^a	Hydroperoxide (%) ^a
MeOH	11	16	31
<i>i</i> -PrOH	34	19	23

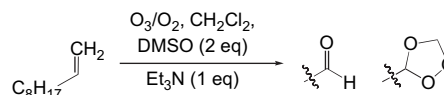
^a Isolated yield.

The DMSO-mediated reduction was unaffected by the addition of a proton donor (HOAc), but was actively suppressed by Sc(OTf)₃. Although we had hoped that the Lewis acid might serve to bring together the reactants, the results suggest that the Sc⁺³ is simply sequestering the sulfoxide. In contrast, ozonolysis at -78 °C in the presence of both DMSO and Et₃N achieved a noticeable improvement in the yield of aldehyde (Table 3); an even better yield was obtained upon reaction at 0 °C. The formation of aldehyde appeared to be enhanced by trace moisture; performing the reaction with deliberate exclusion of water (including drying the incoming stream of O₃/O₂ through a -78 °C U-tube), resulted in a reduced yield. For reasons that would later become clear, the use of excess Et₃N slowed the reaction and resulted in the isolation of recovered decene (not shown).

The combination of DMSO and Et₃N provides a useful protocol for syntheses of aldehydes and ketones (Table 4).

To our surprise, a control reaction investigating ozonolysis in the presence of Et₃N furnished better yields of nonanal than had been obtained with DMSO (Table 5). The amine-promoted reduction appeared general for secondary and tertiary amines; primary amines, which react with carbonyl oxides to form oxaziridines, were not investigated.²⁰ The use of anhydrous conditions again resulted in a decreased yield of aldehyde.

Table 3. Reaction with DMSO and Et₃N



T (°C)	Wet/dry	Aldehyde (%) ^a	Ozonide (%) ^a
-78	Dry	43	17
-78	Wet ^b	65	29
0	Wet	84	12

^a Isolated yield.

^b H₂O (0.05%) in CH₂Cl₂.

Table 4. Application to other substrates

Alkene	$\xrightarrow{\text{O}_3^a}$	carbonyl ^b	ozonide ^b
	\longrightarrow	 93%	 trace
	\longrightarrow	 65%	 28%
	\longrightarrow	 64%	 7%

^a O_3 , DMSO (2 equiv), Et_3N (1 equiv), wet CH_2Cl_2 , 0 °C.

^b Isolated yield.

The sole precedent for this process was a report describing isolation of adipaldehyde upon ozonolysis of cyclohexene in the presence of Et_3N .²¹ The reduction of carbonyl oxides by pyridine has been reported and later refuted.²² However, several observations led us to question the role of the amines. First, as had been previously observed during the experiments with DMSO/ Et_3N , the use of excess amine slowed consumption of alkene. Second, directing the gaseous stream of O_3/O_2 onto or into a CH_2Cl_2 solution of alkene and amine resulted in intense fuming, which persisted for a period proportional to the amount of amine. Similar fuming was observed for ozonolysis of solutions of Et_3N or *N*-methylmorpholine (NMM); in contrast, no fuming was observed when a stream of ozone was directed onto or into a solution of decene. Moreover, monitoring (TLC or NMR of quenched aliquots) of the ozonolysis of mixtures of amine and alkene detected very little formation of aldehyde or ozonide until after fuming had ceased. Third, ozonolysis of a solution of amine, followed by addition of decene and continued ozonolysis, produced a mixture of aldehyde and ozonide. These results suggested the intermediacy of *N*-oxides. The ozonolysis of tertiary amines is known to

Table 5. Ozonolysis in presence of amines

Amine	T (°C)	Wet/dry	Aldehyde (%)	Ozonide (%)
Et_3N	-78	Wet ^a	79	13
Et_3N	-78	Dry	50	30
Et_3N	0	Wet	75	14
Et_3N (2 equiv)	0	Wet	64 ^b	14
NMM	0	Wet	68	12
NMM	0	Dry	57	10
Morpholine	0	Wet	62	10
Morpholine	0	Dry	56	18
$\text{Et}_3\text{Ni-Pr}_2$	0	Dry	58	9
$(\text{C}_{12}\text{H}_{25})_2\text{NMe}$	0	Wet	55	15
DABCO	0	Dry	48	10
Pyridine		Dry	16	11

^a H_2O (0.05%) in CH_2Cl_2 .

^b Unreacted alkene also recovered.

furnish both *N*-oxides and products of side chain cleavage, the latter process accounting for our observation of acetaldehyde in the crude products from reactions employing Et_3N .²³ Furthermore, the ratio of *N*-oxide formation to side chain cleavage is enhanced in the presence of a proton donor, accounting for the influence of moisture on the reactions involving amines.

The role of *N*-oxides was explicitly tested by ozonolysis of 1-decene in the presence of commercial *N*-methylmorpholine-*N*-oxide (NMMO). Reaction proceeded without fuming to furnish *exclusively* nonanal (Table 6).²⁴ Predominant formation of aldehyde was also observed for reactions in the presence of DABCO-*N*-oxide and pyridine *N*-oxide. The latter reduction, while complicated by the formation of intensely colored byproducts, is noteworthy given the very limited amount of reduction observed in the presence of pyridine.

The intermediacy of carbonyl oxides in these reactions was supported by a simple set of competition reactions. The products obtained from ozonolysis of a CH_2Cl_2 solution of decene were compared under three sets of conditions: (1) no additives; (2) addition of stoichiometric MeOH; and (3) addition of stoichiometric amounts of both MeOH and NMMO (Table 7). The results demonstrate competition between the amine oxide and the alcohol for capture of the intermediate nonanal-*O*-oxide.²⁵ Furthermore, 1-methoxydecene, which generates the same carbonyl oxide but cannot easily form an ozonide, also produces nonanal as the major product in the presence of NMMO.¹⁰

Table 6. Reduction by amine oxides

Amine oxide (equiv)	T (°C)	RCHO (%) ^a	Ozonide (%) ^a
NMMO (1.0)	-78 or 0	88	0
NMMO (3.0)	0	94	0
Et_3NO^b (1.0)	0	80	Trace
Me_3NO^c (1.0)	0	68	12
DABCO- <i>N</i> -oxide (1.0)	0	62	10
Pyridine <i>N</i> -oxide (1.0)	0	58	9

^a Isolated yields.

^b Generated in situ.

^c Poor solubility.

Table 7. Competition for the carbonyl oxide^a

X	Additive	A	B	C
H	None	—	—	Major
H	MeOH	Trace	Major	Minor
H	MeOH+NMMO	Major	Minor	Trace
OMe	MeOH+NMMO	Major	Trace	Trace

^a Ratios assessed by ^1H NMR of reaction mixtures.

2.1. Role of base-promoted fragmentation

Amines and pyridines are known to cleave terminal ozonides to a 1:1 mixture of aldehyde and formate through a Kornblum-type E₁CB fragmentation (Fig. 3).^{26–28} Although amine oxides are less basic than amines,²⁹ we were curious as to whether the putative reductions might also result from base-promoted fragmentation. In fact, treatment of a CH₂Cl₂ solution of purified decene ozonide with NMMO did generate a 1:1 mixture of nonanal and formate. However, the reaction was slower than the in situ reductions described above. More convincingly, analysis of the crude reaction mixtures from ozonolysis of decene in the presence of NMMO consistently found ratios of aldehyde/formate greater than 4:1, indicating that the base-promoted fragmentation is a minor contributor to the direct formation of aldehyde in the ozonolysis medium.

However, the base-promoted fragmentation may serve a useful role as a scavenging reaction. For example, if the solution resulting from ozonolysis of a mixture of decene and NMMO (1.0 equiv) is quenched into pH 6 buffer prior to concentration, a small amount of ozonide (up to 7%) is isolated; in the absence of an acidic quench, no ozonide is present after concentration. If the reaction is conducted with three or more equivalents of NMMO, no ozonide is observed regardless of work-up, suggesting that capture of the carbonyl oxide is complete at the higher reagent concentration. For more substituted systems such as the ozonides of methyl oleate (vida infra), the base-promoted fragmentation is much slower, and even less likely to play a significant role in the formation of aldehydes during ozonolysis.

2.2. Other substrates

In situ reduction was successfully applied to the ozonolysis of a 1,2-disubstituted alkene, methyl oleate; the disparity in the isolated yields of the two products appears to result from the volatility of nonanal (Fig. 4). Application of the same protocol to 2-methylundecene provided a moderate yield of 2-undecanone as well as a number of unidentified minor byproducts; similar results were obtained for other 1,1-disubstituted alkenes (not shown). The lower yield observed for a ketone compared with aldehydes could result from a lower efficiency of nucleophilic addition to the ketone



Figure 3. Base-promoted fragmentation.

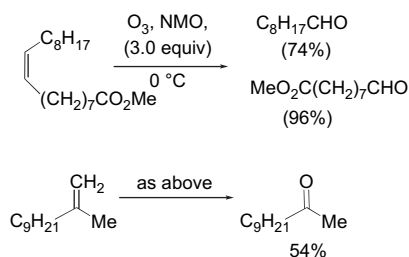


Figure 4. Other substrates.

O-oxide, allowing more time for side reactions such as tautomerization or polymerization.¹⁰ We continue to investigate this process in the hope of identifying optimal conditions for ketone synthesis.

2.3. Mechanism

There is no mechanistic precedent for ‘reductive’ ozonolysis in the presence of amine oxides. Our hypothesis is that the process is not actually a reduction, but instead a fragmentation driven by the reactivity of carbonyl oxides (Fig. 5). Nucleophilic addition of the amine oxides generates an unstable zwitterionic peroxyacetal, which undergoes decomposition to generate aldehyde or ketone, amine, and dioxygen. The proposed mechanism bears a topological resemblance to the Grob fragmentations of diol monosulfonates³⁰ and to the conversion of ketones to dioxiranes.³¹

Verification of the mechanism may prove challenging. Quantification of the liberated amine will be complicated by rapid oxidation by ozone. Decomposition of a ground state zwitterion would be expected to liberate dioxygen in the singlet state; however, detection of ¹O₂ will be constrained by the compatibility of probe molecules with ozone. Although an alternative route to carbonyl oxides is available through photosensitized oxidation of diazoalkanes,³² the amine produced by the predicted mechanism would quench ¹O₂ and suppress the photooxidation. The extent of transfer of ¹⁸O from a labeled amine oxide to the carbonyl products would provide unambiguous evidence for the proposed mechanism. However, no preparation of a labeled amine oxide has been reported and we were unable to find a method for oxidation of tertiary amines that would be practical for use of ¹⁸O-labeled reagents.

The success of the reductive ozonolysis reflects attributes of both carbonyl oxides and amine oxides. Carbonyl oxides are highly reactive species typically represented as either zwitterions or diradicals.¹⁰ Although calculations suggest that the diradical is more representative of gas phase structure, our previous work demonstrated the ability to exploit the zwitterionic character to enhance additions of nucleophiles.³³ Amine oxides are not only nucleophilic but also contain an easily fragmented N–O bond, characteristics that form the basis of a conversion of activated halides to aldehydes.³⁴ In addition, the coordinative saturation of the

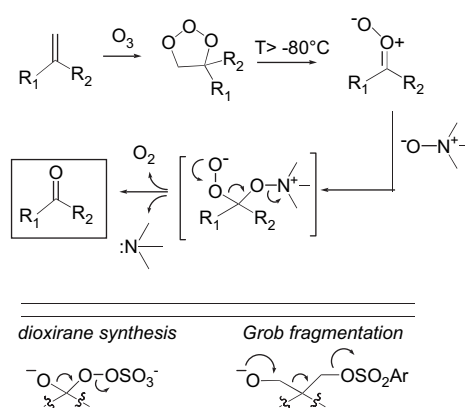


Figure 5. Proposed mechanism.

ammonium leaving group blocks hetero-ozonide formation, leaving fragmentation as the most favorable option. The successful reductions in the presence of morpholine (Table 5) suggests that either hydroxylamines or nitrones may also promote a similar fragmentation.³⁵

While the oxidative regeneration of the amine oxide would seem to offer the possibility of catalytic reactions, the need to competitively capture the carbonyl oxide sets a realistic lower threshold on the concentration of reagent. Moreover, the lower yields of aldehyde obtained for ozonolyses in the presence of stoichiometric NMM (Table 5) versus NMMO (Table 6) may reflect not only the competing formation of ozonide during early stages of the reaction (when amine oxide concentration is necessarily low) but also the fact that the ozonolysis of amines furnishes amine oxides in less than quantitative yields.³⁶ However, regeneration of amine oxides may hold promise in batch reactions and for regeneration of supported reagents.

Finally, the observed fragmentation of carbonyl oxides could be the first example of a new class of reactions. The key structural feature in the amine oxides, a nucleophilic center weakly bonded to a leaving group, is found in other α -nucleophiles, suggesting that a similar fragmentation may be possible with reagents such as hypohalites and peroxysulfates (Fig. 6). Along these lines, it is interesting to note that reaction of amine oxides with dioxiranes generates amines and $^1\text{O}_2$, presumably via an intermediate peroxyammonium zwitterion.³⁷

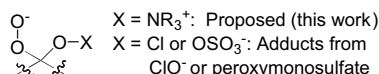


Figure 6. Alternative fragmentation precursors.

3. Conclusion

The ozonolysis of alkenes in the presence of amine oxides directly generates aldehydes and ketones through an unprecedented mechanism involving nucleophilic trapping of carbonyl oxides and fragmentation of the derived zwitterionic peroxides. The methodology, which avoids formation of ozonides or related energetic intermediates, offers a safer alternative to traditional ozonolyses and may expand the synthetic applications of an already versatile oxidative cleavage.

Acknowledgements

We are grateful for support from the Petroleum Research Fund, and for technical assistance from Paul Unverzagt and Fred Zinnel. We thank Dennis Schilling for pointing out Ref. 22 (Slomp et al.) NMR spectra were acquired, in part, on spectrometers purchased with support from NSF (MRI 0079750 and CHE 0091975). A portion of this research was conducted in facilities remodeled with support from NIH (RR016544-01).

References and notes

- Bailey, P. S. *Ozonation in Organic Chemistry*; Academic: New York, NY, 1978; Vol. 1.
- Kula, J. *Chem. Health Saf.* **1999**, *6*, 21; Gordon, P. M. *Chem. Eng. News* **1990**, *68*, 2.
- For an overview of ozonide reduction, see: Kropf, H. *Houben-Weyl Methoden Der Organische Chemie*; Kropf, H., Ed.; Georg Thieme: Stuttgart, 1988; Vol. E13/2, p 1111.
- Ozonolysis of electron-poor alkenes in methanolic base results in the direct formation of methyl esters: Marshall, J. A.; Garofalo, A. W.; Sedrani, R. C. *Synlett* **1992**, 643.
- The use of more effective reducing agents such as PPh₃ (Griesbaum, K.; Kiesel, G. *Chem. Ber.* **1989**, *122*, 145; Clive, D. L. J.; Postema, M. H. D. *J. Chem. Soc., Chem. Commun.* **1994**, 235); BH₃ (Flippin, L. A.; Gallagher, D. W.; Jalali-Araghi, K. *J. Org. Chem.* **1989**, *54*, 1430); LiAlH₄ (Greenwood, F. L. *J. Org. Chem.* **1955**, *20*, 803); NaBH₄ (Witkop, B.; Patrick, J. B. *J. Am. Chem. Soc.* **1952**, *74*, 3855); and Mg/MeOH or Zn/HOAc (Dai, P.; Dussault, P. H.; Trullinger, T. K. *J. Org. Chem.* **2004**, *69*, 2851) can lead to problems with separation of byproducts or functional group compatibility.
- Chen, L.; Wiemer, D. F. *J. Org. Chem.* **2002**, *67*, 7561; Lavallée, P.; Bouthillier, G. *J. Org. Chem.* **1986**, *51*, 1362, footnote 27.
- Schwartz, C.; Raible, J.; Mott, K.; Dussault, P. H. *Org. Lett.* **2006**, *8*, 3199.
- Criegee, R. *Angew. Chem.* **1975**, *87*, 767.
- Anglada, J. M.; Creheut, R.; Maria Bofill, J. *Chem.—Eur. J.* **1999**, *5*, 1809.
- Bunnelle, W. H. *Chem. Rev.* **1991**, *91*, 335.
- Kuczkowski, R. L. *Chem. Soc. Rev.* **1992**, *21*, 79.
- Yamamoto, Y.; Niki, E.; Kamiya, Y. *Bull. Chem. Soc. Jpn.* **1982**, *55*, 2677.
- Barton, M.; Ebdon, J. R.; Foster, A. B.; Rimmer, S. *J. Org. Chem.* **2004**, *69*, 6967; Barton, M.; Ebdon, J. R.; Foster, A. B.; Rimmer, S. *Org. Biomol. Chem.* **2005**, *3*, 1323.
- Murray, R. W. *Acc. Chem. Res.* **1968**, *1*, 313.
- Ando, W.; Miyazaki, H.; Kohmoto, S. *Tetrahedron Lett.* **1979**, 1317.
- Sawaki, Y.; Kato, H.; Ogata, Y. *J. Am. Chem. Soc.* **1981**, *103*, 3832; Adam, W.; Durr, H.; Haas, W.; Lohray, B. *Angew. Chem.* **1986**, *98*, 85; Miura, M.; Nojima, M.; Kusabayashi, S. *J. Chem. Soc., Perkin Trans. 1* **1980**, 1950.
- Sofikiti, N.; Rabalakos, C.; Statakis, M. *Tetrahedron Lett.* **2004**, *45*, 1335.
- Any work involving peroxides should follow standard precautions: Medard, L. A. *Accidental Explosions: Types of Explosive Substances*; Ellis Horwood: Chichester, UK, 1989; Vol. 2; Patnaik, P. *A Comprehensive Guide to the Hazardous Properties of Chemical Substances*; Van Nostrand Reinhold: New York, NY, 1992; Shanley, E. S. *Organic Peroxides*; Swern, D., Ed.; Wiley-Interscience: New York, NY, 1970; Vol. 3, p 341.
- Based upon ¹H NMR of crude reaction mixtures.
- Schulz, M.; Rieche, A.; Becker, D. *Chem. Ber.* **1966**, *99*, 3233.
- Pokrovskaya, I. E.; Ryzhankova, A. K.; Menyailo, A. T.; Mishina, L. S. *Neftekhimiya* **1971**, *11*, 873.
- See: Slomp, G., Jr.; Johnson, J. L. *J. Am. Chem. Soc.* **1958**, *80*, 915; and; Griesbaum, K. *J. Chem. Soc., Chem. Commun.* **1966**, 920.
- Bailey, P. S. *Ozonation in Organic Chemistry*; Academic: New York, NY, 1978; Vol. 2; pp 155–201; Maggiolo, A.; Niegowski, S. J. *Ozone Chemistry and Technology*; American Chemical Society: Washington, DC, 1959; pp 202–204.

24. Typical procedure: to a dry 100-mL round bottom flask was added 3.0 mmol of decene, 20 mL of methylene chloride, and 9.0 mmol of *N*-methylmorpholine-*N*-oxide (NMMO). The stirred solution was cooled to 0 °C and a solution of 2% O₃/O₂ (nominal output of 1 mmol O₃/min) was introduced directly above the solution via a glass pipette for 6.6 min (nominally 2.2 equiv ozone relative to alkene). This mode of ozone addition furnished the most consistent results. The solution was then sparged with O₂ for 2 min and warmed to room temperature. Following confirmation of the absence of ozonide (TLC), the solution was concentrated and the residue was purified by flash chromatography using 5% diethyl ether/pentane. Alternatively, the crude reaction was quenched into pH 6 phosphate buffer and extracted with ether prior to concentration and chromatography.
25. Control experiments demonstrated that the hydroperoxyacetal is relatively stable to the presence of NMMO.
26. Baldwin, F. P.; Burton, G. W.; Griesbaum, K.; Hanington, G. *Adv. Chem. Ser.* **1969**, 91, 448.
27. Isobe, M.; Iio, H.; Kawai, T.; Goto, T. *Tetrahedron Lett.* **1977**, 703.
28. Hon, Y. S.; Lin, S.-W.; Lu, L.; Chen, Y.-J. *Tetrahedron* **1995**, 51, 5019.
29. Kakehashi, R.; Shizuma, M.; Yamamura, S.; Maeda, H. *J. Colloid Interface Sci.* **2005**, 289, 498.
30. Grob, C. A. *Angew. Chem., Int. Ed. Engl.* **1969**, 8, 535.
31. Murray, R. W. *Chem. Rev.* **1989**, 89, 1187.
32. Higley, D. P.; Murray, R. W. *J. Am. Chem. Soc.* **1974**, 96, 3330.
33. Dussault, P. H.; Raible, J. R. *Org. Lett.* **2000**, 2, 3377.
34. Mukaiyama, S.; Inanaga, J.; Yamaguchi, M. *Bull. Chem. Soc. Jpn.* **1981**, 54, 2221; Godfrey, A. G.; Ganem, B. *Tetrahedron Lett.* **1990**, 31, 4825.
35. Bailey, P. S.; Southwick, L. M.; Carter, T. P., Jr. *J. Org. Chem.* **1978**, 43, 2657.
36. Bailey, P. S.; Lerdal, D. A.; Carter, T. P., Jr. *J. Org. Chem.* **1978**, 43, 2662.
37. Ferrer, M.; Sanchez-Baeza, F.; Messeguer, A.; Adam, W.; Golsch, D.; Goerth, F.; Kiefer, W.; Nagel, V. *Eur. J. Org. Chem.* **1998**, 2527.



ELSEVIER

Available online at www.sciencedirect.com

ScienceDirect

Tetrahedron 62 (2006) 10753–10761

Tetrahedron

Dark singlet oxygenation of organic substrates in single-phase and multiphase microemulsion systems

Jean-Marie Aubry,^{a,*} Waldemar Adam,^{b,c} Paul L. Alsters,^d Cédric Borde,^a
Sébastien Queste,^a Jean Marko^a and Véronique Nardello^a

^a*LCOM, Equipe 'Oxydation & Formulation', UMR CNRS 8009, École Nationale Supérieure de Chimie de Lille, BP 90108, F-59652 Villeneuve d'Ascq Cedex, France*

^b*Department of Chemistry, University of Puerto Rico, Facundo Bueso, 110, Rio Piedras, PR 00931, USA*

^c*University of Wuerzburg, Institute of Organic Chemistry, Am Hubland, D-97074 Wuerzburg, Germany*

^d*DSM Pharma Chemicals, Advanced Synthesis, Catalysis and Development, PO Box 18, 6160 MD Geleen, The Netherlands*

Received 13 June 2006; revised 11 August 2006; accepted 16 August 2006

Available online 29 September 2006

This paper is dedicated to the memory of Professor Jean Rigaudy from the Laboratoire de Chimie Organique of the Ecole Supérieure de Physique et Chimie Industrielle de Paris

Abstract—The disproportionation of hydrogen peroxide catalyzed by molybdate anions provides an effective non-photochemical source of singlet oxygen $^1\text{O}_2$ ($^1\Delta_g$). Microemulsions are the preferred media to carry out 'dark' singlet oxygenation of labile and hydrophobic substrates. Single-phase and multiphase microemulsion systems have been developed and improved for the last decade and their respective advantages and limitations are shortly reviewed and discussed.

© 2006 Elsevier Ltd. All rights reserved.

1. Introduction

'Ordinary' oxygen, $^3\text{O}_2$, is somewhat 'extraordinary' since its HOMO is degenerated and contains two electrons with parallel spins, one in each orbital. Therefore, it behaves chemically as a diradical, which reacts slowly with most organic molecules that are in the ground singlet state and very quickly with free radicals and molecules in the triplet excited states. On the contrary, its first excited state is a singlet state with both electrons into the same orbital. The so-called singlet oxygen, $^1\text{O}_2$ ($^1\Delta_g$), is therefore a highly reactive, yet selective, bielecronic oxidizer that received many applications in organic synthesis, mainly at the laboratory scale.¹ Most commonly, it is generated by photosensitization of triplet molecular oxygen, but may also be generated in high yields in a number of chemical reactions.² These have been employed mainly in mechanistic studies, but scarcely used in organic synthesis. The reasons are that they involve either highly oxidizing inorganic reagents (ClO^-),³ which may cause side reactions, or polycyclic aromatic endoperoxides (anthracene and naphthalene derivatives)⁴ that require previous preparation. A more serious

disadvantage of endoperoxides is the fact that they are used in stoichiometric amounts and large quantities of aromatic polycyclic co-products are simultaneously generated, which encumber the isolation of the wanted oxidation product.

In 1980s, a catalytic chemical source has been discovered, in which $^1\text{O}_2$ is quantitatively generated in a mild and convenient method by the disproportionation of hydrogen peroxide induced catalytically by sodium molybdate.^{2,5} The reaction proceeds efficiently in alkaline aqueous solutions⁶ or in highly polar organic solvents such as methanol⁷ in which hydrosoluble⁸ or low-molecular-weight organic substrates⁹ can be effectively oxidized on the preparative scale.

However, the intermediate peroxomolybdates generated by the $\text{H}_2\text{O}_2/\text{MoO}_4^{2-}$ system exhibit a double reactivity, either they can release $^1\text{O}_2$ by cleavage of the Mo–O bonds or they can epoxidize labile substrates under acidic¹⁰ or neutral conditions.¹¹ Two strategies have been developed to avoid the epoxidation side reaction. One uses heterogeneous molybdate-based catalysts that prevent close contact between organic substrates and peroxomolybdates.¹² The other one uses microemulsions (pems), which are stable microdispersions of water and an immiscible organic solvent. The hydrophilic reactants (H_2O_2 , Na_2MoO_4) and the organic substrate are separately solubilized in the aqueous and in the organic compartments of the microemulsion, respectively.

Keywords: Microemulsion; Singlet oxygen; Multiphase media; Hydrogen peroxide.

* Corresponding author. Tel./fax: +33 3 20 33 63 64; e-mail: jean-marie.aubry@univ-lille1.fr

Singlet oxygen is chemically generated into the aqueous microdroplets and then it diffuses out, before deactivation, to the organic solvent phase where it reacts with the substrate.¹³

This article describes the successive developments and the respective advantages/drawbacks of various microemulsion systems starting from a complex and chlorinated single-phase microemulsion to simple and thermo-sensitive multi-phase systems containing an environmentally friendly microemulsion in equilibrium with an excess organic phase or/and an excess aqueous phase.

2. Available strategies for dark singlet oxygenation in microemulsion systems

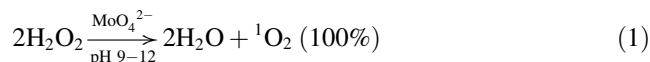
Singlet oxygen, $^1\text{O}_2$, exhibits enhanced reactivity and selectivity compared to those of ground state oxygen, $^3\text{O}_2$. Singlet oxygen has found considerable synthetic utility since it can undergo selective reactions with a wide range of electron-rich molecules (olefin,^{1,14} conjugated dienes,^{15,16} polycyclic aromatic hydrocarbons,⁴ phenols,¹⁷ sulfides¹⁸ and heterocycles¹⁹). Singlet oxygenation is usually carried out by dye-sensitized photooxidation based on molecular oxygen and visible light.²⁰ This method can be conducted in a large variety of nonpolar and polar solvents and a wide range of temperature (-100 to $+100$ °C); the low temperatures are particularly advantageous when labile oxidation products such as dioxetanes have to be prepared. However, it requires specially designed gas/liquid photo-reactors, which are seldom available in research laboratories or industrial plants. Moreover, large-scale photooxidation entails hazardous processing conditions because of the combination of light, organic solvents and dioxygen. As a result of the foregoing disadvantages, photooxidation has found little industrial applications except for the preparation of low tonnages of valuable flavours and fragrances.²¹ By contrast, 'dark' singlet oxygenation, via catalytic disproportionation of hydrogen peroxide, provides a safe and inexpensive alternative to photooxidation that can be carried out in ordinary multi-purpose plant stirred tank reactors.²²

2.1. Chemical generation of singlet oxygen

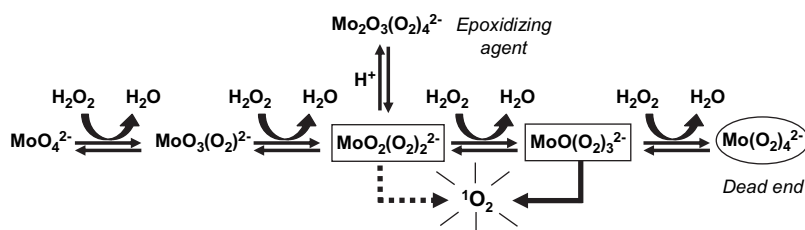
Chemical sources of $^1\text{O}_2$ belongs to a special type of reaction able to produce molecules in an electronically excited state through a chemiexcitation pathway. Such reactions are uncommon and, most often, the excited species is generated in poor yield except in the particular case of $^1\text{O}_2$. Several chemical processes are known to release $^1\text{O}_2$ in high yields.^{2,23} This remarkable behaviour results from two specific features of $^1\text{O}_2$: (i) the low excitation energy of $^1\text{O}_2$

(94 kJ) is easily attainable by many chemical reactions; (ii) the chemical formation of a molecule in the triplet state such as $^3\text{O}_2$ from singlet state reactants is unfavourable with regard to Wigner's rule. Reagents are typically in a singlet state and when the release of O_2 occurs through a *heterolytic* or a *concerted mechanism*, Wigner's rule foresees the conservation of the total spin and thus the formation of oxygen in the singlet state. A historical example of this type of reaction is the oxidation of H_2O_2 by ClO^- that provides Cl^- , H_2O and $^1\text{O}_2$ in 100% yield.²⁴ Since the discovery, in 1963, of the formation of $^1\text{O}_2$ by the system $\text{H}_2\text{O}_2/\text{ClO}^-$, there has been a surge of interest in quest of other chemical sources of $^1\text{O}_2$. In particular, a systematic screening of the whole periodic classification has been conducted in 1985 searching for $^1\text{O}_2$ in the decomposition of aqueous basic H_2O_2 induced by mineral oxides, hydroxides or oxoanions. Singlet oxygen was detected by specific trapping with a water-soluble rubrene derivative. About 30 new chemical sources of $^1\text{O}_2$ were thus identified such as alkaline earths hydroxides, lanthanides and actinide oxides, oxoanions of transition metals in d^0 configuration and the strong oxidizers Au^{3+} , IO_3^- and IO_4^- . Most of the active mineral compounds were not acting as ClO^- through oxidation of H_2O_2 but rather as catalysts for the disproportionation of H_2O_2 .²

Among them, the $\text{MoO}_4^{2-}/\text{H}_2\text{O}_2$ system has been investigated in detail because the reaction efficiently generates $^1\text{O}_2$ in homogeneous phase. It was shown that decomposition proceeds only in basic solutions and is catalytic with respect to molybdate. It was found that all the oxygen released by the disproportionation of H_2O_2 is in the singlet state (Eq. 1).



The reaction is first order with respect to molybdate but a much more complex rate law was observed for H_2O_2 . The reaction is second order at low concentration of H_2O_2 (<0.1 M), zero order at higher concentration (0.1–0.2 M) and then the rate decreases with further increase of H_2O_2 concentration.⁵ These results were rationalized by identifying and quantifying the intermediate peroxometallates by ^{95}Mo NMR and UV-vis spectroscopy.⁶ At natural pH, four peroxomolybdates $\text{MoO}_{4-n}(\text{O}_2)_n^{2-}$, namely the mono-, di-, tri- and tetra- peroxomolybdates, are successively formed by increasing the H_2O_2 concentration. Comparison of these results with kinetic studies, performed under similar conditions, leads to the conclusion that the triperoxomolybdate, $\text{MoO}(\text{O}_2)_3^{2-}$, is the main precursor of $^1\text{O}_2$. ^{95}Mo NMR also reveals that in neutral and slightly acidic media, a dimeric form of the protonated diperoxoanion $\text{HMoO}_2(\text{O}_2)_2^{2-}$ is the main peroxo compound present in the solution. Since all these peroxo species are in slow equilibrium (Scheme 1), it is



Scheme 1. Different peroxomolybdates formed by mixing molybdate anion with hydrogen peroxide in basic or slightly acidic aqueous solutions.

of utmost importance to maintain the pH value between 9 and 12 and the concentration of uncomplexed H_2O_2 ($0.1\text{--}0.5\text{ mol L}^{-1}$) within the optimal conditions to maximize the rate of $^1\text{O}_2$ generation and to limit the epoxidizing action of peroxomolybdates.

From the ^{95}Mo NMR experiments, equilibrium constants between all the peroxo compounds have been calculated. They allowed us to build a predominance diagram showing the prevalent peroxo complexes as a function of pH and H_2O_2 concentration on a logarithmic scale (Fig. 1).¹⁰ The best conditions for $^1\text{O}_2$ generation coincide with the shaded area corresponding to the prevalence of triperoxomolybdate $\text{MoO}(\text{O}_2)_3^{2-}$.

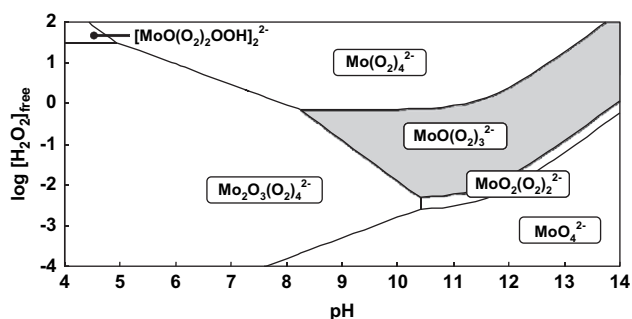


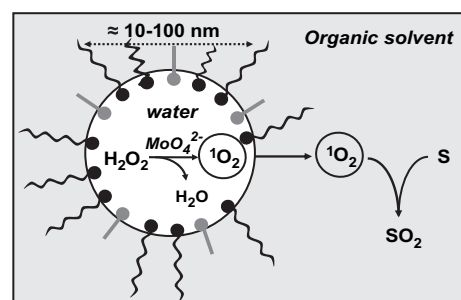
Figure 1. Predominance diagram of the $\text{MoO}_4^{2-}/\text{H}_2\text{O}_2$ system as a function of pH and H_2O_2 concentration. The shaded area corresponds to the optimum conditions for $^1\text{O}_2$ generation.

2.2. Reaction media compatible with the source of $^1\text{O}_2$ based on the $\text{MoO}_4^{2-}/\text{H}_2\text{O}_2$ system

The $\text{MoO}_4^{2-}/\text{H}_2\text{O}_2$ system is able to quantitatively convert an inexpensive, environmentally friendly and storable source of oxygen, i.e., H_2O_2 , into a valuable short-live oxidizing species, i.e., $^1\text{O}_2$, according to reaction 1. High flux of $^1\text{O}_2$ can be efficiently produced at room temperature in water and may be used to perform singlet oxygenation of water-soluble substrates at the preparative level. For moderately hydrophobic substrates, polar solvents such as methanol or DMF may be used instead of water since they can dissolve all the reactants and may sustain the formation of $^1\text{O}_2$, with lower yield and slower rate than in water. Those media are not suitable for highly hydrophobic substrates nor for organic substrates such as allylic alcohols, which suffer competitive side reactions with peroxomolybdates.¹¹

In order to overcome those problems, two-phase systems, water/organic solvent, have been tested. Hydrophilic reactants (H_2O_2 , Na_2MoO_4) lie in the aqueous phase whereas the hydrophobic substrate is localized in the immiscible organic solvent phase. The chemical generation of $^1\text{O}_2$ takes place in the aqueous layer but this short-live species is not able to reach the organic phase before deactivation since the mean travel distance of $^1\text{O}_2$ in water ($\approx 200\text{ nm}$) is much smaller than the diameter of the droplets ($\approx 10^6\text{ nm}$) formed under vigorous stirring of the biphasic system. Therefore most of the available $^1\text{O}_2$ is wasted through deactivation by water molecules and a large excess of H_2O_2 is thus required to bring about appreciable conversion of the substrate.

By contrast, microemulsions are suitable for the chemical formation of $^1\text{O}_2$ and the oxidation of highly hydrophobic or fragile substrates on the preparative scale with a minimum loss of $^1\text{O}_2$. These macroscopically homogeneous mixtures consist of a microscopically heterogeneous dispersion of an oil and water submicrodomains stabilized by an interfacial monolayer of surface-active molecules (Scheme 2). Although more complex in composition than traditional reaction media, microemulsions present definite advantages: (i) they dissolve large amounts of hydrophilic compounds, which are confined in the aqueous microdroplets, as well as nonpolar organic molecules, which are localized in the organic microdomains; (ii) they protect substrates and products sensitive to H_2O_2 or to peroxomolybdates or to alkaline conditions. In addition, the typical size of the microdroplets ($\approx 10\text{--}100\text{ nm}$) is much smaller than the mean travel distance of $^1\text{O}_2$ in water. Hence, in spite of its short lifetime in H_2O ($\tau_\Delta \approx 4\text{ }\mu\text{s}$), $^1\text{O}_2$ can diffuse freely, before deactivation, from the aqueous droplets to the organic phase, where it can react with the substrate.



Scheme 2. Schematic representation of a W/O microemulsion used to oxidize hydrophobic or fragile organic substrates S with $^1\text{O}_2$ chemically generated by the system $\text{H}_2\text{O}_2/\text{MoO}_4^{2-}$.

2.3. Designing single-phase and multiphase microemulsion systems

How can microemulsions be thermodynamically stable? A rough picture for describing microemulsion formation is to consider a subdivision of the dispersed phase into very small droplets with a radius r . Then the entropy change, ΔS , can be approximately expressed as a function of the number of droplets of dispersed phase n , the Boltzmann constant k and the dispersed phase volume fraction Φ (Eq. 2).

$$\Delta S = -nk[\ln \Phi + \{(1 - \Phi)/\Phi\}\ln(1 - \Phi)] \quad (2)$$

So, the entropy of mixing is of the order of nk . The associated free energy change is the sum of the enthalpy for increasing the O/W interface ($\Delta A\gamma_{O/W}$) and of the entropy change (Eq. 3).

$$\Delta G = \Delta A\gamma_{O/W} - T\Delta S \quad (3)$$

where ΔA is the change in interfacial area A ($=n4\pi r^2$) and $\gamma_{O/W}$ is the interfacial tension between oil (O) and water (W). Therefore, the spontaneous microemulsification is thermodynamically favoured ($\Delta G=0$) if the surfactant can reduce the interfacial tension to a sufficiently low value (Eq. 4).²⁵

$$\gamma_{O/W} \approx kT/4\pi r^2 \quad (4)$$

At room temperature, $kT \approx 4 \times 10^{-18}$ mJ and if $r \approx 10$ nm is assumed in a rough calculation, it follows from Eq. 4 that very low interfacial tensions ($\gamma_{O/W} \approx 0.01$ mN m⁻¹) between oil and water would be required to attain a stable droplet radius. A few surfactants (some double chain ionics and some non-ionics) can produce extremely low interfacial tensions, typically 10^{-2} to 10^{-4} mN m⁻¹, but in most cases, such low values cannot be achieved by a single surfactant.

The addition of a co-surfactant (medium-chain alcohol) is an effective way to further decrease $\gamma_{O/W}$. It also confers to the interfacial film the flexibility required to avoid the formation of liquid crystalline phases. Moreover, addition of salts is often necessary to reduce the electrostatic repulsion between head groups of ionic surfactants.

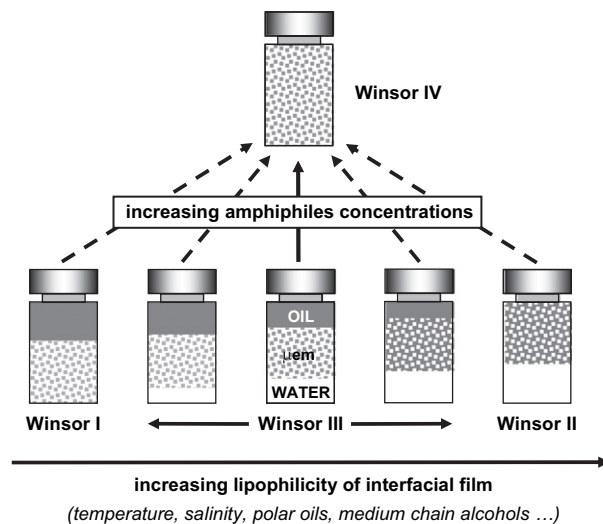
To get the required low interfacial tension, the affinity of the interfacial monolayer of surface-active molecules (surfactant plus co-surfactant) must be high for both the aqueous phase and the organic phase. Depending on the surfactant concentration and on the relative affinities for W and O, different types of microemulsions can be obtained according to Winsor's classification:²⁶

- W I systems: the surfactant is preferentially soluble in water and O/W microemulsions form in equilibrium with an excess oil phase;
- W II systems: the surfactant lies mainly in the oil phase and W/O microemulsions form with an excess aqueous phase;
- W III systems: a three-phase system where a bicontinuous microemulsion coexists with both excess aqueous and oil surfactant-poor phases;
- W IV systems: a single phase that forms upon addition of a sufficient quantity of amphiphiles (surfactant plus co-surfactant).

According to the aimed application it may be desirable to tune the formulation in order to get the wanted type of Winsor system. Many physicochemical formulation parameters are able to modify the relative affinity of the amphiphiles for O and W. All the variables that increase the lipophilicity of the interfacial monolayer will shift the system from W I to W III and finally to W II and vice versa (Scheme 3 and Table 1). In this formulation scan, the W III systems play a central role since they correspond to well-balanced interfacial films.²⁷

2.4. Single-phase W/O microemulsions for singlet oxygenation

2.4.1. Single-phase W/O microemulsions based on chlorinated hydrocarbon as the oil phase. The first microemulsion designed to sustain singlet oxygenation with a chemical source of ¹O₂ was based on sodium dodecyl sulfate (SDS) as the surfactant.¹³ This highly hydrophilic surfactant does not provide microemulsion alone and it spontaneously gives direct micelles in water instead of the reverse micelles that are required to obtain the wanted W/O microemulsion. So, all the parameters that decrease $\gamma_{O/W}$ and that increase both the flexibility and the lipophilicity of the interfacial film (see Table 1) have to be favoured in order to compensate for the excessive hydrophilicity of SDS. A satisfactory W/O



Scheme 3. Modification of the Winsor type of microemulsion systems by scanning one of the formulation variables or by increasing surfactant concentration. The system shown is based on a non-ionic surfactant and has equal volumes of water and oil, μem corresponds to microemulsion phase.

Table 1. Qualitative effect of formulation variables on the lipophilicity of amphiphilic interfacial film between O and W

Formulation variables	Lipophilicity of interfacial film
<i>Surfactant molecular structure</i>	
Lipophilic chain length	↗ ↗
Lipophilic chain branching	↘
Ethylene oxide polyether chain length	↘ ↘ ↘
Surfactant concentration	No influence
<i>Temperature increase</i>	
Non-ionic surfactant	↗ ↗ ↗
Ionic surfactant	↘
<i>Aqueous phase salinity</i>	
Non-ionic surfactant	↗
Ionic surfactant	↗ ↗ ↗
<i>Oil phase molecular structure</i>	
Hydrocarbon chain length	↘
Hydrocarbon chain branching or cyclisation	↗
Polarity of the oil	↗ ↗
<i>Alcohol (co-surfactant)</i>	
Short-chain alcohol concentration (C ₂ or C ₃)	Slight influence
Medium-chain alcohol concentration (C ₄ to C ₆)	↗ ↗

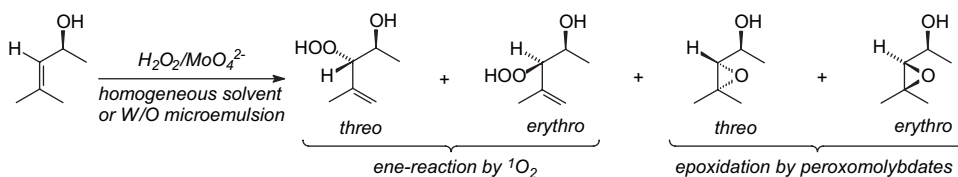
microemulsion was prepared by mixing SDS with *n*-butanol as the hydrophobic co-surfactant, methylene chloride as a rather polar solvent and sodium molybdate as electrolyte and catalyst. This optically isotropic, fluid and transparent liquid meets all the requirements in order to be a preparatively useful medium: (i) no phase separation during storage and during the oxidation process; (ii) high solubility of the reactants; (iii) chemical inertness of the microemulsion components towards H₂O₂, Na₂MoO₄ or the intermediates derived thereof (¹O₂ and peroxomolybdates); (iv) relatively high lifetime of ¹O₂ ($\tau_{\Delta} \approx 40$ μs). Various typical organic substrates (polycyclic aromatic hydrocarbons, heterocycles, conjugated dienes, olefins, sulfides) were successfully oxidized on the preparative scale by the MoO₄²⁻/H₂O₂ system in order to illustrate four standard types of ¹O₂ reactions, namely, the ene reaction, the [2+2] cycloaddition, the [4+2] cycloaddition and the sulfide oxidation. More recently, this

method was applied to the selective oxidation of labile chiral allylic alcohols into allylic hydroperoxides. High chemoselectivity (up to 97%) and diastereoselectivity (up to 92% *threo* preference) can be achieved in proper W/O microemulsion whereas the unwanted epoxides were the major products (93% in water and 61% in MeOH) when the reaction was conducted in homogeneous solvents (Scheme 4).¹¹

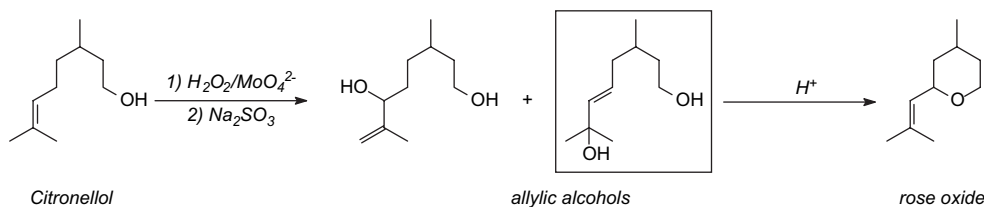
2.4.2. Single-phase environmentally friendly W/O microemulsions. Despite its demonstrated synthetic usefulness, industrial use of this SDS/*n*-BuOH/CH₂Cl₂-based microemulsion is hampered for several reasons: (i) environmental legislation aims at reducing the use of chlorinated solvents; (ii) a large amount of SDS relative to the substrate is required in order to obtain a stable microemulsion; (iii) notably for substrates that are only moderately reactive towards ¹O₂, space time yields are low because a large excess of aqueous H₂O₂ has to be added in order to compensate for the loss of ¹O₂, most of which being deactivated before reaction.

The development of microemulsion media that meet all the demands from a preparative and industrial point of view is not straightforward. In particular, a major challenge is finding a substitute for CH₂Cl₂, in which ¹O₂ has a relatively long lifetime, thus reducing the required amount of aqueous H₂O₂ and the risk of phase separation. The formulation of microemulsions based on polar solvents is critical because polar molecules are likely to interact with the interfacial film impeding a straightforward formation of the microdispersed medium. The composition of the microemulsion was optimized by resorting to the experimental design methodology (simplex). Therefore, suitable compositions for stable microemulsions based on ethyl acetate as organic solvent in the highly complex seven components system (organic solvent, H₂O, SDS, BuOH, substrate, Na₂MoO₄ and H₂O₂) have been found that allow 'dark' singlet oxygenation of lipophilic substrates.²⁸

In a further step, solvent-free microemulsion conditions were developed by replacing the organic solvent by the liquid substrates themselves, i.e., α -terpinene and β -citronellol. This latter substrate is particularly relevant as a model since this substrate is industrially photooxidized with ¹O₂ during the first step of the preparation of rose oxide, an important perfumery ingredient (Scheme 5).²⁸



Scheme 4. Chemical oxidation of mesityllole by the MoO₄²⁻/H₂O₂ system in homogeneous solvents (water or methanol) or in W/O microemulsions.



Scheme 5. Chemical oxidation of citronellol by singlet oxygen and conversion of one of the hydroperoxide into rose oxide.

2.4.3. One phase W/O microemulsions combined with a dewatering process. Monophasic microemulsions are particularly suitable for the peroxidation of labile or highly hydrophobic compounds. However, they present two major drawbacks:

Firstly, the addition of hydrogen peroxide during the reaction results in an increase of the water proportion, which modifies the composition of the microemulsion. In particular, high substrate concentrations or poorly reactive organics require large amounts of H₂O₂ that generate high amounts of water and thus destabilize the system. Ultimately, demixing occurs leading to the formation of an emulsion that is inappropriate for efficient singlet oxygenation. Such a drawback limits the use of one-phase microemulsions either to highly reactive substrates or to relatively low concentrations of substrate.

Secondly, the use of reaction mixtures containing high concentration of amphiphiles hampers facile recovery of the desired products. Moreover, at the end of the oxidation process, the reaction medium is relatively complex, since it is made up of more than six constituents, namely water, oil, surfactant, co-surfactant, catalyst and oxidation product(s). Hence, isolation of the products requires a tedious treatment of the microemulsion.

To avoid composition alterations after the addition of H₂O₂ during the peroxidation, a pervaporation membrane process was combined with the oxidizing microemulsion. A semi-batch oxidation process in which water is continuously and selectively removed from the system to maintain the initial composition of the microemulsion was developed. The efficiency of such a process was illustrated with the peroxidation of a poorly reactive substrate, namely, β -pinene.²⁹

2.5. Multiphase microemulsions for singlet oxygenation

Obtaining single-phase microemulsions requires considerable amounts of surfactant and often some co-surfactant as well, typically 15–25%. This makes recovery of the reaction products from these complex media somewhat problematic. To overcome work-up problems, two- or three-phase systems can be prepared by decreasing the amount of surfactant required to obtain single-phase microemulsions (Scheme 3).

In these multiphase systems, namely W I, W II and W III systems, the microemulsion phase coexists, respectively, with oil, water or both, depending on the relative affinity of the interfacial film for oil and water, respectively.

W III system is a yardstick in the formulation of micro- and macro-emulsions since it corresponds to a 'balanced state' for the interfacial film separating the aqueous and the organic microdomains. It is obtained under well-defined physicochemical conditions of salinity, temperature or hydrophilic-lipophilic balance of the surfactant. In this case, both interfacial tensions between the microemulsion phase on one side and the oil phase or the aqueous phase on the other side are ultralow (10^{-4} – 10^{-2} mN m⁻¹). A yet more important aspect is that the phase separation of a well-balanced W III system is also extremely rapid (a few minutes) after stirring making these systems ideal for easy recovery of the products.³⁰ Most of the surfactant lies in the microemulsion phase whereas organic product partitions between the microemulsion and the oil phases. Hence, the product can be recovered easily from the microemulsion by several extractions with fresh solvent while the surfactant and the catalyst, which are in the microemulsion phase, can be reused. Two multiphase systems have already been investigated, the first one is formulated with an anionic surfactant³¹ whereas the second one, based on a non-ionic one, has never been reported before and will be discussed in Section 3.

2.5.1. Multiphase microemulsions based on an anionic surfactant plus a medium-chain alcohol as co-surfactant.

Five components were mixed, namely, water, sodium molybdate, sodium dodecyl sulfate (SDS), *n*-propanol and toluene to prepare multiphase microemulsion systems. Representing the whole phase diagram for this system would require a prohibitive number of experiments. Binary diagrams showing the percentage of amphiphiles as a function of a scan variable, known as 'optimization diagrams', are usually preferred to investigate the influence of one parameter on the phase behaviour. Formulation scans can be achieved at fixed SDS/PrOH (=1/1) and W/O (=1/1) ratios by changing one of the formulation variables (Table 2) namely, salinity.³² Addition of sodium molybdate actually induces W I → W III → W II transitions (Fig. 2) since this electrolyte decreases the repulsion between the surfactant polar heads, leading to a curvature inversion of the interfacial film.

In order to decrease the amount of amphiphilic molecules, which are responsible for work-up problems, two- or

Table 2. Dependence of the substrate conversion on the microemulsion type and composition

Entry	Winsor type	Composition		α -Terpinene conversion (%)	
		Na ₂ MoO ₄ ·2H ₂ O (mol kg ⁻¹)	SDS+ <i>n</i> -PrOH (% w/w)	Without modification	Excess water phase removed
A	IV	0.15	25	78	—
B	I	0.45	6	65	—
C	III	0.54	—	36	75 (C*)
D	II	0.64	—	20	74 (D*)

Toluene/(water+catalyst)=1:1 (w/w); SDS/*n*-PrOH=1:1 (w/w); α -terpinene=0.1 mol kg⁻¹; H₂O₂=0.15 mol kg⁻¹.

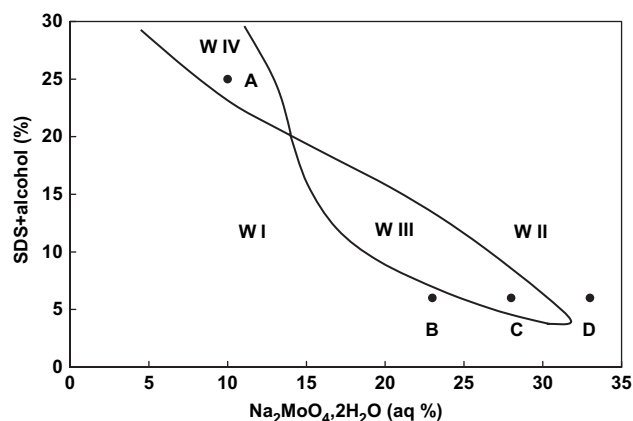
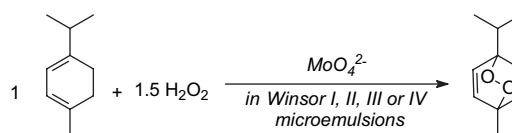


Figure 2. Optimization diagrams for toluene/water/SDS/aPrOH/Na₂MoO₄ system at 25 °C. (SDS/PrOH=1:1 (w/w); toluene/(water+catalyst)=1:1 (w/w); abscissa=% catalyst/(water+catalyst) (w/w)). For dots A–D, see Table 2.

three-phase systems B, C and D were prepared with very low amounts of surfactant and co-surfactant (6%), as indicated in Figure 2. In addition, the presence of an excess oil phase as in the case of W I or W III systems allows an easier recovery of the oxidation product as it partitions between the organic and the microemulsion phases. The single-phase microemulsion A has also been prepared for comparison. To investigate the influence of the microemulsion type on the peroxidation yield, i.e., to determine if globular (W/O or O/W) or bicontinuous microstructures are preferable for the reaction of ¹O₂ with organic compounds, α -terpinene was chosen as a model substrate (Table 2). Hydrogen peroxide was added to the media A–D in a lower amount than required by stoichiometry (Eq. 1) in order to obtain a partial peroxidation of the substrate (Scheme 6).



Scheme 6. Dark singlet oxygenation of α -terpinene in single-phase and multiphase microemulsion systems.

The four types of microemulsion systems (entries A–D) are rather different with regard to substrate conversion. Performances decrease in the order W IV > W I >> W III > W II (Table 2). The dramatic decrease of substrate conversion observed for W III and W II systems can be ascribed to the presence of an excess aqueous phase. Indeed, under stirring, the catalyst and hydrogen peroxide equally partition between the aqueous microdomains (10–100 nm) of the microemulsion and the macrodroplets (10–100 μ m) of the excess aqueous phase. Unfortunately, all the molecules of ¹O₂ generated in the macrodroplets are wasted through physical deactivation by water before reaching the organic phase since the droplets radius is much larger than the mean travel distance of ¹O₂ in water (\approx 200 nm). The elimination of the water excess phase in W III and W II systems (entries C* and D* in Table 2) induces an increase in the substrate conversion, in agreement with our previous explanation.

These results show that multiphase systems can be used for the chemical oxidation of hydrophobic substrates provided

that $^1\text{O}_2$ is exclusively generated in aqueous microdomains ($\varnothing < 200$ nm), which implies that no water excess phase exists or is formed as hydrogen peroxide is added. Winsor I systems consisting in an O/W microemulsion with an excess oil phase are thus suitable to oxidize fairly reactive substrates. They are, however, inappropriate to oxidize poorly reactive compounds since the large amount of H_2O_2 needed over-dilutes the O/W microemulsion and the mean distance between the aqueous microdroplets becomes much larger than 200 nm.

3. Results and discussion

3.1. Multiphase microemulsions based on a non-ionic surfactant without co-surfactant

Single- and multi-phase microemulsion systems may also be obtained by using non-ionic surfactants instead of ionic ones. In particular, the well-known surfactants *n*-alkyl-polyglycol ether (C_iE_j) exhibit three useful features with regard to the aimed application: (i) they do not require any co-surfactant to microemulsify oil and water; (ii) they are much less sensitive to electrolyte than ionic surfactants; (iii) their hydrophilicity/lipophilicity balances can be reversibly tuned by changing temperature; (iv) they are stable over a wide range of pH unlike SDS that suffers hydrolysis under acidic conditions. Moreover, by choosing properly the chemical structure of the surfactant and of the oil, the temperature at which W III systems are observed can be fixed at any given value. In this work, C_{10}E_4 and *n*-octane were chosen as the surfactant and the oil, respectively, because the so-called ‘fish tail’ point of the optimization diagrams (Fig. 3) is localized at a convenient temperature (24.3 °C).³³

When sodium molybdate and α -terpinene are dissolved in water and octane, respectively (Table 3), the gamma shape curve shown in Figure 3 is shifted by approximately 3 °C to lower temperatures. Such a mixture forms a single-phase microemulsion (W IV) by adding 20% of C_{10}E_4 whereas two-phase (W I) and three-phase (W III) systems were prepared with lower surfactant concentrations (7.5% and 5%). Those three reaction media were used to carry out the peroxidation of 0.1 mol kg⁻¹ α -terpinene at 22 °C for the W III and W IV and at 15 °C for the W I in the presence of

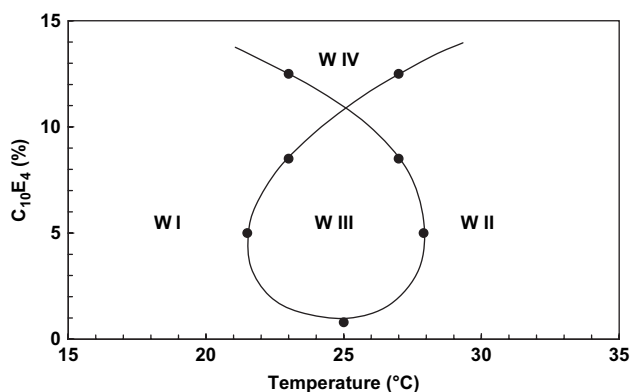


Figure 3. ‘Optimization diagram’ of the ternary system *n*-octane/water/ C_{10}E_4 system as a function of temperature and surfactant concentration and at a fixed ratio octane/water=1:1 (w/w).

Table 3. Amounts of C_{10}E_4 and corresponding temperatures required for obtaining W I, W III and W IV microemulsion systems with the ternary system C_{10}E_4 /water/*n*-octane

C_{10}E_4 (mg)	Temperature (°C) ^a		Winsor system
	Initial	Final	
400 (20%)	22	19	IV
150 (7.5%)	22	18	I
100 (5%)	15	<15	III

^a During the reaction, the temperature must be adjusted and lowered in order to keep the same Winsor system.

a slight excess of H_2O_2 (0.25 mol kg⁻¹). The reaction was completed in about 5 h in the W IV system whereas, at the same temperature, the W III exhibits a loss of efficiency after about 50% conversion due to a loss of $^1\text{O}_2$ in the excess aqueous phase. In that latter case, complete peroxidation of terpinene was obtained by the addition of a second batch of H_2O_2 . The W I exhibits a similar efficiency for the singlet oxygenation as the Winsor IV, as already shown with anionic surfactants, the slower kinetics of the reaction being due to the lower temperature (Fig. 4). Actually, it is known that the rate determining step, i.e., the generation of $^1\text{O}_2$ from peroxomolybdates, depends strongly on the temperature⁵ whereas the fast step, i.e., the competitive interaction of $^1\text{O}_2$ with the substrate and the solvent, does not.

Finally, in spite of apparently different kinetics behaviours, the microstructure of the microemulsion systems does not seem to have a major influence on the peroxidation reaction.

It is noteworthy that the formation of a polar oxidation product, ascaridole, during the reaction modifies the polarity of the oil resulting in a shift of the gamma shape curve to lower temperatures. Hence, the temperature must be adjusted during the reaction in order to maintain the Winsor type in which the reaction has to be conducted and also, to avoid the formation of W II systems. However, at the end of the reaction, the temperature can be decreased of approximately 5 °C for the W III and W IV, in order to obtain a W I that allows the ready recovery of ascaridole from the octane phase.

Contrary to ionic surfactants, the use of thermo-sensitive non-ionic C_iE_j surfactants is particularly interesting since

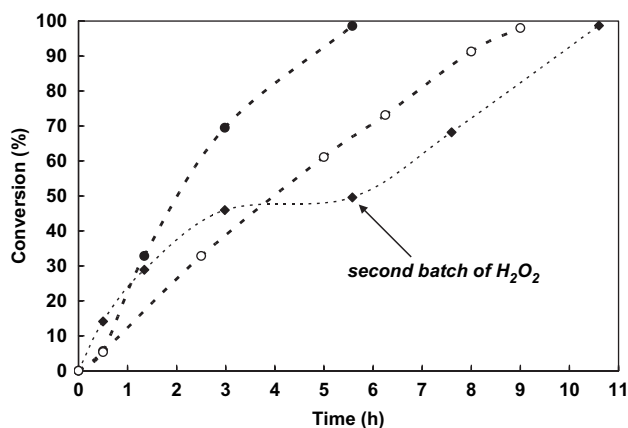


Figure 4. Conversion of α -terpinene 0.1 M in various microemulsion systems based on C_{10}E_4 /water/octane. ● Winsor IV ($T_{\text{initial}}=22$ °C), ○ Winsor I ($T_{\text{initial}}=15$ °C), ◆ Winsor III ($T_{\text{initial}}=22$ °C).

the temperature can be used to adjust reversibly the stability region of the microemulsion and the phase separation can be induced, also reversibly, just by temperature change after the reaction process.

4. Conclusions

Single-phase or multiphase microemulsion systems are ideal media to carry out 'dark' singlet oxygenation of hydrophobic and labile substrates since they offer several benefits: (i) cosolubilization of great amounts of hydrophilic and hydrophobic compounds; (ii) compartmentalization of hydrophilic and hydrophobic species avoiding side reactions; (iii) nanometric size (10–100 nm) of the droplets. This latter feature is of utmost importance for an uncharged short-live species such as $^1\text{O}_2$ since, once generated in aqueous microdroplets, it diffuses freely through the interfacial film to the organic compartment where it reacts with the organic substrate.

Single-phase microemulsions are easy to formulate and to handle but they require large amounts of surfactants that impede recovery of oxidized products. Multiphase microemulsion systems must be prepared under well-defined physicochemical conditions of salinity, temperature or hydrophilic–lipophilic balance of the surfactant. They require much lower amounts of surfactants and they allow simple recovery of the products localized in the oil excess phase. They can sustain effective dark singlet oxygenation provided that the possible excess water phase is removed beforehand.

5. Experimental

5.1. Chemicals

Sodium molybdate dihydrate (99%), *n*-propanol (99%), sodium hydroxide (98%) and 1-isopropyl-4-methyl-1,3-cyclohexadiene (α -terpinene, 85%) were purchased from Aldrich and used without further purification. Sodium dodecyl sulfate (SDS) (98%), toluene (99%), ethyl acetate (99%), dichloromethane (99%), *n*-butanol (98.5%) and hydrogen peroxide (50%) were obtained from Prolabo. Milli-Q water (18.2 M Ω cm) was used.

5.2. Procedures

Salinity scans: samples (5 ml) were prepared in SVL tubes by mixing appropriate amounts of oil, co-surfactant, water, catalyst and surfactant. Mixtures were gently stirred and maintained at a constant temperature (25 ± 0.1 °C) for a sufficient time in order to get thermodynamically stable systems. To further identify each phase according to Winsor label, water was coloured in blue and oil in yellow so that the microemulsion phase was green. Comparative oxidations: 40 g of μem were prepared by predissolving SDS and sodium molybdate in water+*n*-PrOH and by adding toluene to the mixture. After shaking, the systems were allowed to stabilize overnight at 25 ± 0.1 °C. For modified W II and W III systems, greater volumes were prepared. After sufficient time to reach thermodynamic stability, the

phases were separated and mixed again in the desired proportions. Finally, α -terpinene was added to the mixtures (0.1 mol kg^{-1}). Oxidations were performed at 25 °C under vigorous stirring, by adding hydrogen peroxide in two batches (1 and 0.5 mol kg^{-1} after 30 min). The substrate conversion was followed by gas chromatography and the peroxidation products were characterized by ^1H NMR.

A certain amount of C_{10}E_4 (see Table 3) is dissolved into 1 g of octane and 1 g of water containing $10^{-2} \text{ mol L}^{-1}$ of sodium molybdate. To this microemulsion system, placed in a thermostated bath at a given temperature, was added α -terpinene (40 μL , 0.1 mol L^{-1}) followed by a batch of 30 μL H_2O_2 (50%) at zero time leading to an orange-red mixture. The reaction was monitored by HPLC. The values of x and of the temperature which define the Winsor-type system are given in Table 3.

5.3. Instrumentation

Gas chromatography (GC) analyses were performed on a Agilent 6890 N chromatograph equipped with an apolar HP-1 (60 $\text{m} \times 0.32 \text{ mm} - 0.25 \mu\text{m}$) column. ^1H NMR of the peroxidation products was carried out on a AC 200 Bruker spectrometer. Molybdate concentrations were determined by UV spectrometry on a Varian spectrometer at $\lambda = 204 \text{ nm}$.

High-performance liquid chromatography analyses were carried out with a reversed-phase column (Nova-pack C18, 4 μm , $4.6 \times 250 \text{ mm}$) using a 600 controller pump from Waters, a mixture of $\text{CH}_3\text{CN}/\text{H}_2\text{O}$ (90:10) as the eluent, and UV detection with a Waters 490E programmable multi-wavelength detector.

Acknowledgements

We gratefully appreciate financial support by the DSM company and by the EU Growth Program (G1RD-CT-2000-00347); Sustox Project (<http://www.sustox.com>). W.A. thanks the Alexander von Humboldt-Stiftung and the Fonds der Chemischen Industrie for generous support.

References and notes

1. Prein, M.; Adam, W. *Angew. Chem., Int. Ed.* **1996**, *35*, 477–494; Clennan, E. L. *Tetrahedron* **2000**, *56*, 9151–9179; Wahlen, J.; De Vos, D. E.; Jacobs, P. A.; Alsters, P. L. *Adv. Synth. Catal.* **2004**, *346*, 152–164.
2. Aubry, J.-M. *J. Am. Chem. Soc.* **1985**, *107*, 5844–5849; Aubry, J. M. New Chemical Sources of Singlet Oxygen. In *Membrane Lipid Oxidation*; Vigo-Pelfrey, Ed.; CRC: Boca Raton, 1991; Vol. II, pp 65–102.
3. Foote, C. S.; Wexler, S. *J. Am. Chem. Soc.* **1964**, *86*, 3879–3880.
4. Aubry, J. M.; Pierlot, C.; Rigaudy, J.; Schmidt, R. *Acc. Chem. Res.* **2003**, *36*, 668–675.
5. Aubry, J. M.; Cazin, B. *Inorg. Chem.* **1988**, *27*, 2013–2014.
6. Nardello, V.; Marko, J.; Vermeersch, G.; Aubry, J. M. *Inorg. Chem.* **1995**, *34*, 4950–4957.
7. Nardello, V.; Bogaert, S.; Alsters, P. L.; Aubry, J. M. *Tetrahedron Lett.* **2002**, *43*, 8731–8734.

8. Aubry, J. M.; Cazin, B.; Duprat, F. *J. Org. Chem.* **1989**, *54*, 726–728.
9. Jin, H. X.; Liu, H. H.; Wu, Y. K. *Chin. J. Chem.* **2004**, *22*, 999–1002; Emsenhuber, M.; Kwant, G.; Van Straaten, K.; Janssen, M.; Alsters, P.; Hoving, H. Eur. Pat. Appl., EP 1403234, 2004.
10. Nardello, V.; Bouttemy, S.; Aubry, J. M. *J. Mol. Catal. A: Chem.* **1997**, *117*, 439–447.
11. Nardello, V.; Caron, L.; Aubry, J. M.; Bouttemy, S.; Wirth, T.; Chantou, R. S. M.; Adam, W. *J. Am. Chem. Soc.* **2004**, *126*, 10692–10700.
12. McGoran, E. C.; Wyborne, M. *Tetrahedron Lett.* **1989**, *30*, 783–786; Wahlen, J.; De Vos, D. E.; Sels, B. F.; Nardello, V.; Aubry, J. M.; Alsters, P. L.; Jacobs, P. A. *Appl. Catal. A: Gen.* **2005**, *293*, 120–128; Wahlen, J.; De Hertogh, S.; De Vos, D. E.; Nardello, V.; Bogaert, S.; Aubry, J. M.; Alsters, P. L.; Jacobs, P. A. *J. Catal.* **2005**, *233*, 422–433.
13. Aubry, J. M.; Bouttemy, S. *J. Am. Chem. Soc.* **1997**, *119*, 5286–5294.
14. Stratakis, M.; Orfanopoulos, M. *Tetrahedron* **2000**, *56*, 1595–1615.
15. Iesce, M. R. *Mol. Supramol. Photochem.* **2005**, *12*, 299–363.
16. Griesbeck, A. G.; Bartoschek, A.; Adam, W.; Bosio, S. G. *Photooxygenation of 1,3-Dienes in Handbook of Organic Photochemistry and Photobiology*, 2nd ed.; Hosspool, W. M., Lenci, F., Eds.; CRC: London, 2003; Chapter 25, pp 1–19.
17. Carreno, M. C.; Gonzalez-Lopez, M.; Urbano, A. *Angew. Chem., Int. Ed.* **2006**, *45*, 2737–2741.
18. Clennan, E. L. *Acc. Chem. Res.* **2001**, *34*, 875–884; Iesce, M. R.; Cermola, F.; Temussi, F. *Curr. Org. Chem.* **2005**, *9*, 109–139.
19. Clennan, E. L.; Pace, A. *Tetrahedron* **2005**, *61*, 6665–6691.
20. Braun, A. M.; Maurette, M. T.; Oliveros, E. *Technologie Photochimique, Presses Polytechniques Romandes* **1986**, 429–481.
21. Gollnick, K. *Chim. Ind.* **1982**, *64*, 156–166.
22. Aubry, J. M. French Patent 2,612,512, 1987; *Chem. Abstr.* *111*, 133,340; Alsters, P. L.; Nardello, V.; Aubry, J. M. WO 00/61524 (PCT/EP00/02552); *Chem. Abstr.* *133*, 281,926; Alsters, P. L.; Nardello, V.; Aubry, J. M. WO 00/64842 (PCT/EP00/02553); *Chem. Abstr.* *133*, 334,856.
23. Adam, W.; Kazakov, D. M.; Kazakov, V. P. *Chem. Rev.* **2005**, *105*, 3371–3387.
24. Held, A. M.; Halko, D. J.; Hurst, J. K. *J. Am. Chem. Soc.* **1978**, *5732–5740*.
25. Overbeek, J. Th. G. *Faraday Discuss. Chem. Soc.* **1978**, *65*, 7–19.
26. Winsor, P. A. *Trans. Faraday Soc.* **1948**, *44*, 376–398.
27. Salager, J. L.; Anton, R.; Anderez, J. M.; Aubry, J. M. *Techn. Ing.* **2001**, *J2157*, 1–20.
28. Nardello, V.; Herve, M.; Alsters, P. L.; Aubry, J. M. *Adv. Catal.* **2002**, *344*, 184–191.
29. Caron, L.; Nardello, V.; Mugge, J.; Hoving, E.; Alsters, P. L.; Aubry, J. M. *Colloid Interface Sci.* **2005**, *282*, 478–485.
30. Kabalnov, A.; Weers, J. *Langmuir* **1996**, *12*, 1931–1935.
31. Caron, L.; Nardello, V.; Alsters, P. L.; Aubry, J. M. *J. Mol. Catal. A: Chem.* **2006**, *251*, 194–199.
32. Bourrel, M.; Schechter, R. S. *Microemulsions and Related Systems*; Marcel Dekker: New York, NY, 1988.
33. Burauer, S.; Sachert, T.; Sottmann, T.; Strey, R. *Phys. Chem. Chem. Phys.* **1999**, *1*, 4299–4306.

Synthesis of a hydrophilic and non-ionic anthracene derivative, the *N,N'*-di-(2,3-dihydroxypropyl)-9,10-anthracenedipropanamide as a chemical trap for singlet molecular oxygen detection in biological systems

Glaucia R. Martinez,^{a,d} Flávia Garcia,^b Luiz H. Catalani,^b Jean Cadet,^c Mauricio C. B. Oliveira,^d Graziella E. Ronsein,^d Sayuri Miyamoto,^{d,†} Marisa H. G. Medeiros^d and Paolo Di Mascio^{d,*}

^aDepartamento de Bioquímica e Biologia Molecular, Setor de Ciências Biológicas, Universidade Federal do Paraná, Curitiba-PR, Brazil

^bDepartamento de Química Fundamental, Instituto de Química, Universidade de São Paulo, São Paulo, SP, Brazil

^cLaboratoire 'Lésions des Acides Nucléiques', DRFMC/LCIB-UMR-E n°3 (CEA/UJF), CEA/Grenoble, F-38054 Grenoble cedex 9, France

^dDepartamento de Bioquímica, Instituto de Química, Universidade de São Paulo, CP 26.077, 05513-970 São Paulo, SP, Brazil

Received 8 June 2006; revised 5 August 2006; accepted 18 August 2006

Available online 25 September 2006

Abstract—We report herein the synthesis of a new hydrophilic and non-ionic anthracene derivative, the *N,N'*-di-(2,3-dihydroxypropyl)-9,10-anthracenedipropanamide. The evaluation of this compound as chemical trap of singlet molecular oxygen by using labeling experiments and HPLC–MS analysis showed that it could be efficiently used in biological investigations.

© 2006 Elsevier Ltd. All rights reserved.

1. Introduction

Considerable evidence supports the involvement of singlet molecular oxygen ($^1\text{O}_2$) in biological processes. Enzymatic reactions, lipid peroxidation, photooxidation, and phagocytosis are among the most studied ones.^{1,2} Other studies have found tentative evidence that antibodies are able to use $^1\text{O}_2$ as substrate to generate hydrogen peroxide and ozone in phagocytosis.^{3,4}

The investigation of $^1\text{O}_2$ generation in biological systems requires sensitivity and specificity. Some studies have employed deuterated solvents and the addition of quenchers of $^1\text{O}_2$. It is well known that deuterated solvents increase the lifetime of $^1\text{O}_2$,⁵ and quenchers reduce it. Thus, if $^1\text{O}_2$ is involved in a reaction, its lifetime and chemistry will be influenced by the media and additives. Chemical probes to detect $^1\text{O}_2$ may provide the needed data. This approach is particularly interesting considering the reactivity of $^1\text{O}_2$

toward different substances. The products formed can be detected at very low concentrations. However, the efficiency of the overall process depends on the reactivity and the solubility of the trap.⁶

For some time, traps used were derived from furans.⁷ Furans are oxidized to dicarbonylic products as the result of the formation of ozonide intermediates (Fig. 1). Although furans are highly reactive toward $^1\text{O}_2$, these traps can also react with other oxidants, such as hydrogen peroxide, generating the same products observed with $^1\text{O}_2$.⁶

Cholesterol is a known chemical trap of $^1\text{O}_2$ because the product of the reaction is the 5- α -hydroperoxide, which is considered as a fingerprint of $^1\text{O}_2$ oxidation in biological systems; however, there are limitations that include the low reactivity and stability of the product formed. Moreover, 5- α -hydroperoxide can undergo rearrangement to 7- α -hydroperoxides.⁸

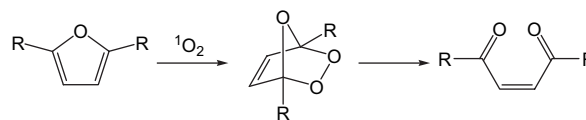


Figure 1. Reaction of furan derivative with $^1\text{O}_2$. R is any substituent.

Keywords: Anthracene; Endoperoxide; HPLC–MS; Singlet oxygen; Trap; Probe.

* Corresponding author. Tel.: +55 11 3091 3815x224; fax: +55 11 3815 5579; e-mail: pdmascio@iq.usp.br

† Present address: Centro de Ciências Naturais e Humanas, Universidade Federal do ABC, Santo André, SP, Brazil.

The typical reaction of $^1\text{O}_2$ by the [2+2] mechanism generating dioxetane was exploited in the design of a trap-and-trigger chemiluminescent probe, namely 2-[1-(3-*tert*-butyldimethylsilyloxy)-phenyl-3,6,9,12-tetraoxa-1-tridecyl-13-hydroxy-methylene]tricyclo[3.3.1.1]decane.⁹ This compound forms an intermediate dioxetane that decomposes under treatment with tetra-*n*-butylammonium fluoride for generating a chemiluminescent signal (Fig. 2).

The reversible binding of $^1\text{O}_2$ to aromatic compounds by the [4+2] mechanism has been exploited to produce chemical traps since the endoperoxide formed represents a specific product for the reaction with $^1\text{O}_2$. Furthermore, the endoperoxides formed with anthracene derivatives are stable at room temperature and their decomposition occurs only at elevated temperatures (around 100 °C).

The first polycyclic aromatic hydrocarbon endoperoxide studied was that derived from rubrene in 1926, when Dufraisse et al. observed that a benzene solution of rubrene became colorless upon exposure to solar light (Fig. 3). They also observed that the peroxide formed was able to regenerate the parent hydrocarbon and oxygen after heating at 150 °C.¹⁰

In the next two decades, many other endoperoxides were prepared and studies were performed to better understand their behavior. In 1942, Dufraisse and Velluz demonstrated that 1,4-dimethoxy-9,10-diphenylanthracene endoperoxide was able to release oxygen at room temperature. They also reported that liberated oxygen was in an 'activated' state.¹¹ The precise nature of the reactive oxygen species was established in 1967 by Wasserman and Scheffer who made a crucial observation.¹² It was found that the products of the reaction of 2,5-diphenyl-4-methyloxazole or 1,3-diphenylisobenzofuran with 9,10-diphenylanthracene endoperoxide were the same to those generated by photooxidation.

Non-substituted aromatic compounds are not able to react significantly with $^1\text{O}_2$. Suitable modification in the polycyclic aromatic structure has to be made in order to increase the reactivity of $^1\text{O}_2$. Thus, at least one, and preferably two, electron-donating groups must be present at certain positions to allow the [4+2] cycloaddition of $^1\text{O}_2$ and to stabilize the endoperoxide. The substituted compounds exhibit large differences in their reactivity toward $^1\text{O}_2$. This is related to the electron density of the aromatic core and the steric hindrance induced by either the substituents themselves or by additional groups located on the other positions.¹³ All these features have to be taken into consideration prior to design a new $^1\text{O}_2$ trap.

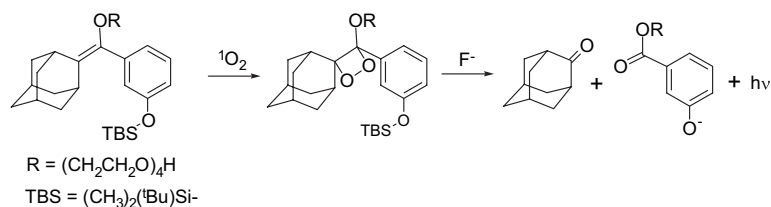


Figure 2. Scheme for the chemiluminescence detection of the stable dioxetane formed by the reaction with $^1\text{O}_2$.

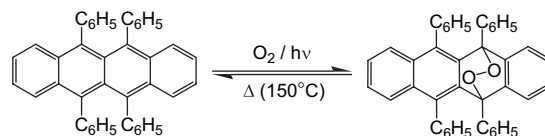


Figure 3. Reaction of rubrene with $^1\text{O}_2$ and the thermal decomposition of its endoperoxide.

Anthracene traps have indeed demonstrated that $^1\text{O}_2$ is generated from lipid hydroperoxides treated with metals, peroxyxynitrite or hypochlorite using the hydrophobic molecule 9,10-diphenylanthracene (DPA) and ^{18}O -labeled lipid hydroperoxides (Fig. 4). The detection of the endoperoxides formed in the reaction was provided by HPLC–MS analysis. The formation of the ^{18}O -labeled endoperoxide of DPA indicated the occurrence of reaction between two lipid peroxy radicals according to the Russell mechanism.^{14–16}

However, as the biological environment is not restricted to the hydrophobic moiety of the membranes and lipoproteins, these traps show some limitations for the investigation of biological systems because of their low water solubility. This problem may be overcome by modifying their structures in order to make them more hydrophilic.¹⁷

Anthracene derivatives with hydrophilic substituents can serve as chemical traps in aqueous solution. Furthermore, the substituent type and position on the aromatic ring can be modified, thus resulting in different reactivity.

The addition of carboxylic groups is an interesting option. A hydrophilic anthracene derivative, a 9,10-anthracenedipropionic acid¹⁸ or the potassium salt of a rubrene-2,3,8,9-tetracarboxylic acid¹⁷ has been reported (Fig. 5). The former was used for time-resolved laser photolysis experiments to determine the lifetime of $^1\text{O}_2$ in D_2O . The latter compound showed solubility at around 1 mM in neutral aqueous solution; however, it was largely insoluble in acid media. Moreover, the rubrene-containing endoperoxide was stable for just a few hours in water.

The anthracene-9,10-diyl-diethyl disulfate (EAS) has many adequate properties: it reacts with $^1\text{O}_2$ generating the corresponding endoperoxide (Fig. 6), its solubility is not pH dependent, it is stable up to 120 °C, and it is detectable in small amounts by HPLC.¹⁹

A compound similar to EAS has also been reported, the anthracene-9,10-bisethanesulfonic acid (AES), which is soluble in water and buffer solutions, is stable over a wide range of pH, and has a reactivity constant (k_r) of

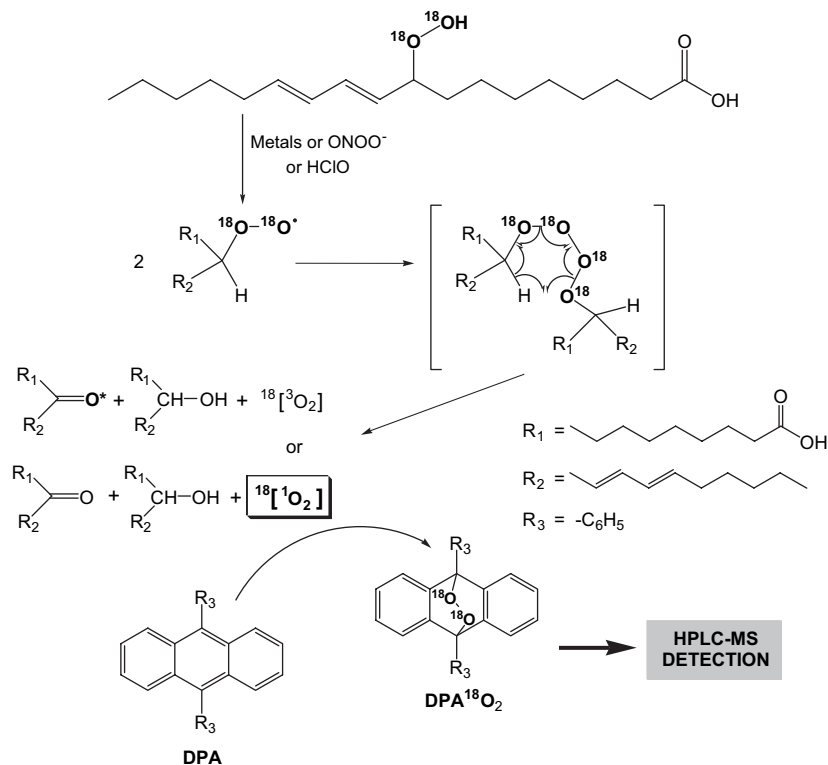


Figure 4. ^{18}O -labeled lipid hydroperoxides treated with metals, peroxyntirite or hypochlorite generates $^{18}\text{O}^1\text{O}_2$ that was detected by using the hydrophobic chemical trap 9,10-diphenylanthracene (DPA) and HPLC–MS analysis.

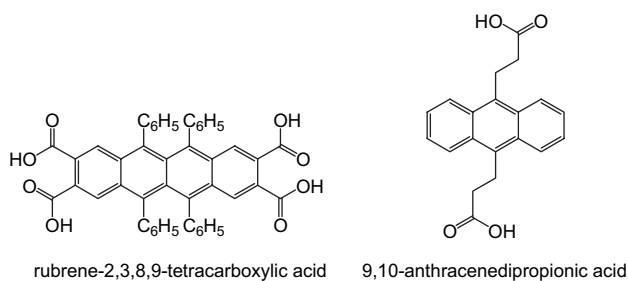


Figure 5. Hydrophilic aromatic compounds with carboxylic groups.

$1.15 \times 10^8 \text{ M}^{-1} \text{ s}^{-1}$ (Fig. 6).²⁰ AES was prepared from 9,10-dibromoanthracene (DBA) by a three-step synthesis. An alternative method for the synthesis of AES has also been demonstrated.²¹ This was achieved by the conversion of

DBA into anthracene-9,10-divinylsulfonate (AVS) through a Pd-catalyzed Heck reaction based on the use of aqueous sodium vinylsulfonate followed by hydrogenation catalyzed by Pd/C catalyst. Interestingly, it was shown that the intermediate AVS could be a suitable $^1\text{O}_2$ chemical trap.

The characteristic $^1\text{O}_2$ reaction with the anthracene moiety was the basis for the development of fluorescein-based fluorescence probe, the 9-[2-(3-carboxy-9,10-dimethyl)-anthryl]-6-hydroxy-3H-xanthen-3-one (DMAX) described by Nagano et al. (Fig. 6).²² It exhibits a weak fluorescence in the native state, but becomes highly fluorescent upon reaction with $^1\text{O}_2$.

A possible disadvantage of these anionic traps is the interaction with cationic photosensitizers, such as methylene blue, or the interaction with some cations that are important to

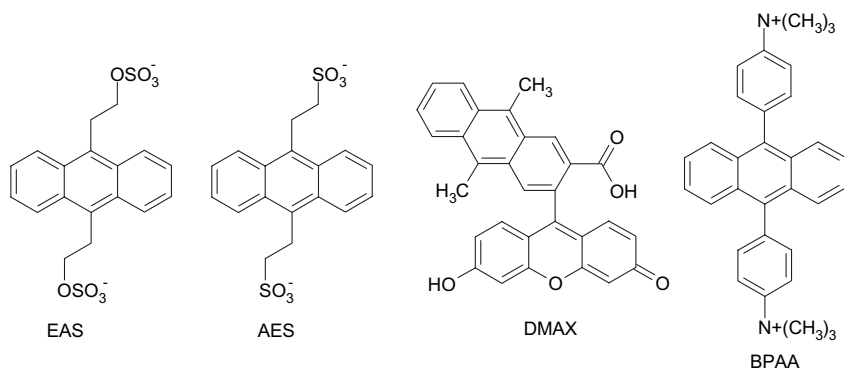


Figure 6. Hydrophilic aromatic compounds.

some chemical reactions that generates $^1\text{O}_2$. In order to avoid these problems, it has been reported the synthesis of an anthracene derivative with a cationic substituent, the bis-9,10-anthracene-(4-trimethylphenylammonium)dichloride (BPAA) (Fig. 6), this compound is hydrophilic and has an overall quenching constant of $2.0 \times 10^7 \text{ M}^{-1} \text{ s}^{-1}$.²³

It should be added that the main limitation of anthracenic compounds is light absorption particularly in photochemical studies. In this way, it was reported that disodium 1,3-cyclohexadiene-1,4-diethanoate is more appropriate in such situations.²⁴ It was shown that the measurement of the amount of $^1\text{O}_2$ generated in aqueous solution by irradiation above 310 nm is well suited when CHDDE was used as the chemical trap and the quantum yield for photosensitizers in D_2O may be easily determined.²⁵

Naphthalene endoperoxides are generally employed as $^1\text{O}_2$ generators. Their stability and solubility follow the same rules of anthracene ones, however, their decomposition to the respective naphthalene derivative and $^1\text{O}_2$ occurs at room temperature. A fact of great importance in this field was the preparation of *N,N'*-di(2,3-dihydroxypropyl)-1,4-naphthalenedipropionamide (DHPN) by Aubry et al.²⁶ The compound has a diol group attached to a propionic arm by an amide linkage. Its hydrophilic and non-ionic character is of fundamental importance for suitable utilization in biological systems. The corresponding endoperoxide (DHPN O_2) named *N*-(2,3-dihydroxy-propyl)-3-{8-[2-(2,3-dihydroxypropylcarbamoyl)-ethyl]-9,10-dioxo-tricyclo[6.2.2.0*2,7*]-dodeca-2,4,6,11-tetraen-1-yl]-propionamide) may be prepared at low temperature by photosensitization with methylene blue and, after removal of the sensitizer from the solution, it is ready to be used. Its decomposition at 37 °C follows first order kinetics and 60% of the oxygen is released as $^1\text{O}_2$.²⁶ We had chosen the naphthalene derivative DHPN to prepare a ^{18}O -labeled endoperoxide (DHPN $^{18}\text{O}_2$).²⁷ This water-soluble naphthalene endoperoxide acts as a chemical source for [^{18}O] isotopically labeled singlet oxygen ($^{18}[^1\text{O}_2]$) and it is particularly interesting to assess the reactivity of $^1\text{O}_2$ toward biological targets (Fig. 7).

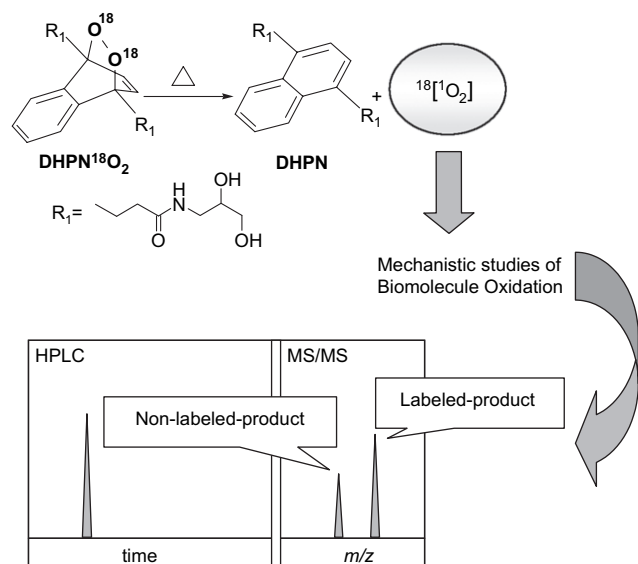


Figure 7. DHPN $^{18}\text{O}_2$ as a chemical source of $^{18}[^1\text{O}_2]$.

Oxidation products thus formed will be labeled with, at least, the incorporation of one ^{18}O -oxygen atom. Therefore, the oxidation products that contain the labeled oxygen can be detected and quantified using appropriate methods, as HPLC coupled to mass spectrometry. It was known that $^1\text{O}_2$ is able to oxidize the guanine bases of DNA. However, it was not possible to distinguish between two possible processes: the direct reaction of $^1\text{O}_2$ within cellular DNA or the oxidative stress induced by the intracellular production of $^1\text{O}_2$. In order to clarify this issue, the labeled endoperoxide was incubated with cells; then nuclear DNA was extracted and HPLC–MS/MS analysis of the labeled product allowed to demonstrate the formation of 8-oxo-7,8-dihydro-2'-deoxyguanosine (8-oxodGua) in DNA by the direct reaction with $^1\text{O}_2$.²⁸

In addition, the labeled endoperoxide DHPN $^{18}\text{O}_2$ was successfully used to study the reaction of $^1\text{O}_2$ with 8-oxodGua inserted into oligodeoxynucleotides²⁹ or as the free nucleoside in aqueous solution.³⁰ Interestingly, when analyzing the products in those studies some amount of non-labeled products were also detected. Using the chemical trap EAS, we were able to show that an energy transfer from labeled $^1\text{O}_2$ to ground state molecular oxygen occurs in aqueous solution. The products of the reaction were analyzed by ESI-MS measurement at the output of a HPLC column.³¹

We report in the present work, the synthesis of a new hydrophilic and non-ionic anthracene derivative containing the same group found in DHPN, the *N,N'*-di-(2,3-dihydroxypropyl)-9,10-anthracenedipropionamide (DHPA, Fig. 8). The evaluation of this compound as a chemical trap of $^1\text{O}_2$ showed that it could be efficiently used in biological investigations, since it is soluble in water, has no charge on its structure, its solubility does not depend on pH, and the product is stable at temperatures above 37 °C, and it may be quantified by appropriate means.

2. Results and discussion

2.1. Synthesis of *N,N'*-di(2,3-dihydroxypropyl)-9,10-anthracenedipropionamide (DHPA)

The first step of the DHPA synthesis was the bromination of DMA resulting in the DBMA (yield of 71%). DBMA structure was assigned by ^1H NMR analysis. In the next step, malonic synthesis resulted in the derivative tetracid, which was characterized by its typical fragmentation in the ESI $^-$ mass spectrum. In the same way, the structure of the expected decarboxylated product (ADPA) was confirmed by ESI $^-$ mass spectrometry. After esterification, HPLC–MS analysis of DEADP showed the presence of a molecular ion $[\text{M}+\text{H}]^+$ at $m/z=379$ and the sodium adduct $[\text{M}+\text{Na}]^+$ at $m/z=396$. In the final step, DEADP amidation resulted in DHPA with a yield of 41%. DHPA was characterized by its ^1H and ^{13}C NMR features and HPLC–MS analysis in the ESI $^+$ mode.

2.2. Formation of DHPA endoperoxide

After 3 h of photosensitization about 75% of DHPA (retention time=15 min, Fig. 9A) was consumed and a new product was detected (retention time=13 min, Fig. 9B). The

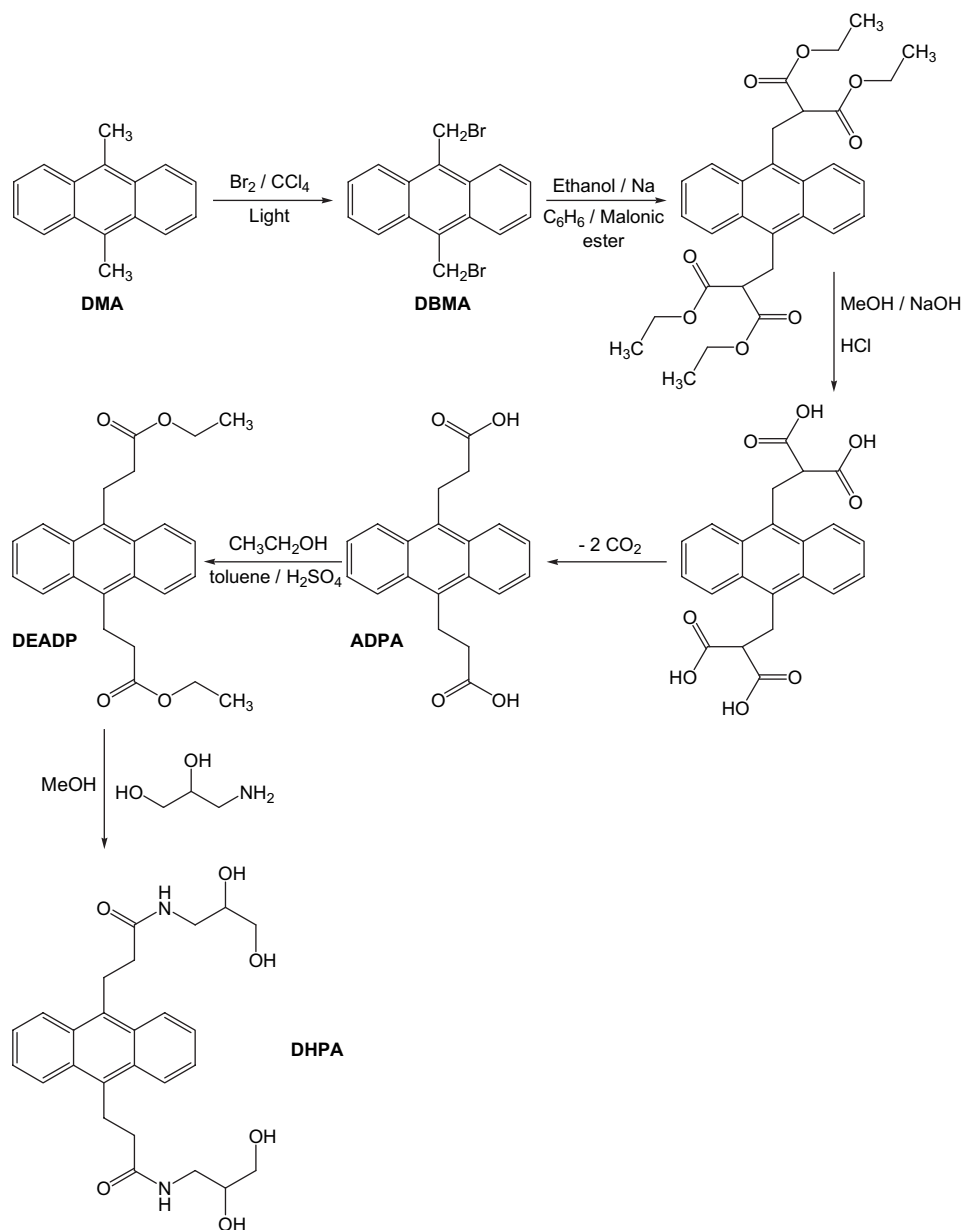


Figure 8. DHPA synthesis.

UV–vis spectra of these compounds are shown in Fig. 9C and D. Contrasting with DHPA (Fig. 9C), the UV–vis spectrum of 13-min product peak did not show the characteristic band of anthracene (Fig. 9D).

In order to further evaluate the ability of DHPA to react with $^1\text{O}_2$, DHPNO₂ was used as a chemical source of $^1\text{O}_2$. For comparison, the reaction with DHPNO₂ was also carried out with EAS, a frequently used $^1\text{O}_2$ -trap. Spectra in

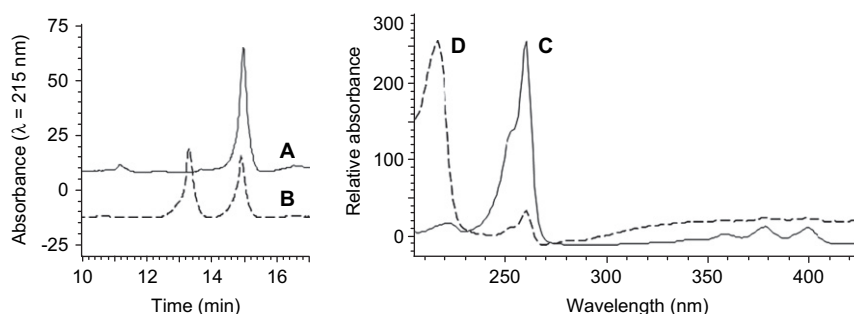


Figure 9. HPLC analysis of DHPA irradiation. (A) Chromatogram of DHPA in methanol, (B) chromatogram of DHPA in methanol after 1 h of irradiation, (C) UV–vis spectrum of the 15-min eluting product peak in chromatogram A, and (D) UV–vis spectrum of the 13-min eluting product peak in chromatogram B.

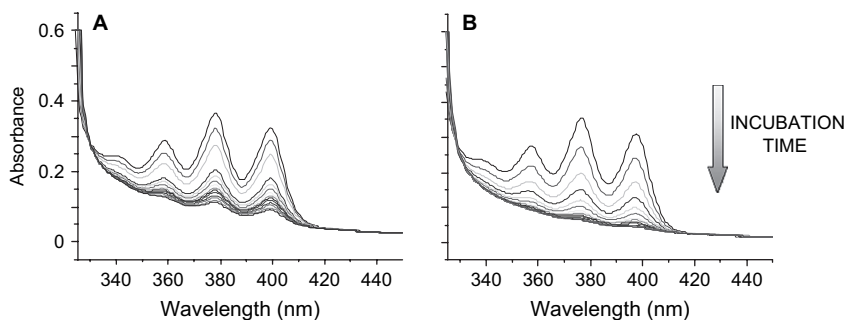


Figure 10. UV-vis spectra during incubation with DHPNO₂. (A) DHPA spectra and (B) EAS spectra.

the visible region show that the products lose the characteristic anthracene moiety absorption, suggesting the formation of respective endoperoxides with a similar reactivity (Fig. 10).

After the incubation of DHPA with DHPNO₂ for 2 h at 37 °C, three product peaks were formed with retention times of 10, 12 and 13 min in an HPLC elution profile ($\lambda=215$ nm, Fig. 11A). The mass spectra of the compounds reveal that the observed peaks correspond to DHPN ($m/z=419$ [M+H]⁺, Fig. 11B), DHPAO₂ ($m/z=501$ [M+H]⁺, Fig. 11C) and DHPA ($m/z=469$ [M+H]⁺, Fig. 11D), respectively. These results suggest that DHPA effectively traps the ¹O₂ produced by thermolysis of DHPNO₂, since the product with

$m/z=501$ (DHPAO₂) corresponds to an increment of one O₂ molecule in DHPA structure ($m/z=469+32$).

Further insights into DHPA-trapping ability of ¹O₂ were gained upon incubation with ¹⁸O-labeled DHPNO₂. We observed the formation of a product with the same retention time as that of DHPA¹⁶O₂ (data not shown), that exhibits a molecular weight and molecular ion at $m/z=505$ (Fig. 12). This new product corresponds to DHPA¹⁸O₂, since it shows an increment of 4 units in the m/z of DHPA¹⁶O₂. A small amount of non-labeled product was also observed resulting from energy transfer to residual O₂ in solution as previously demonstrated.³¹ The results obtained are summarized in Figure 13.

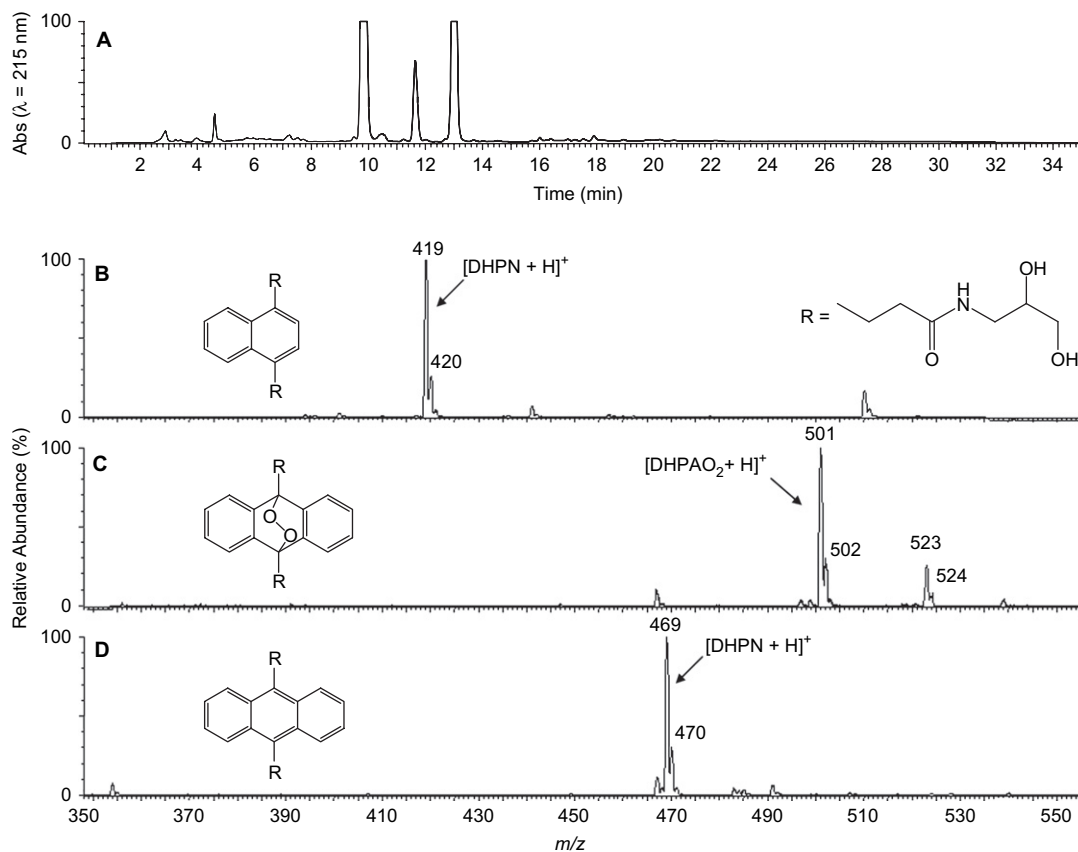


Figure 11. HPLC-MS (ESI⁺) analysis of DHPA reaction with DHPNO₂. (A) UV detection at $\lambda=215$ nm, (B) ESI⁺ mass spectrum of the 10-min eluting product (DHPN), (C) ESI⁺ mass spectrum of the 12-min eluting product peak (DHPAO₂), and (D) ESI⁺ mass spectrum of 13-min eluting product peak (DHPA).

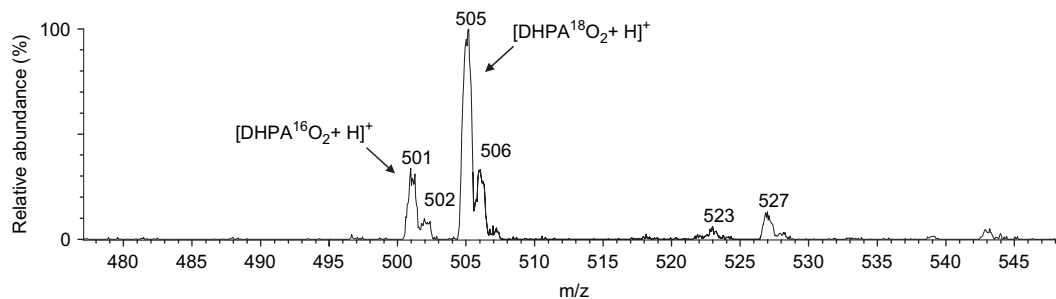


Figure 12. ESI⁺ mass spectrum of DHPA¹⁸O₂.

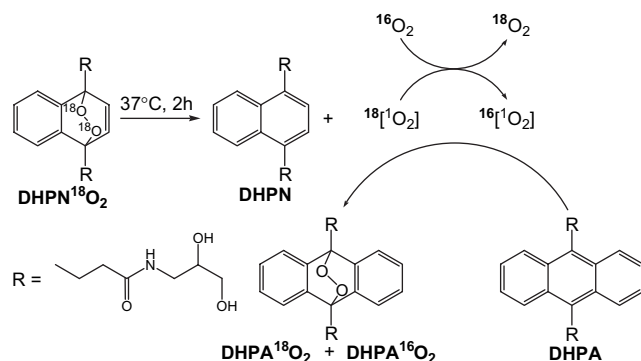


Figure 13. ¹O₂-trapping ability of DHPA.

3. Conclusion

Recent findings suggest the involvement of ¹O₂ in biological processes. However, adequate strategies must be employed to detect this transient species. The development of traps, with controllable properties in their structure, e.g., solubility, reactivity, and specificity, represents important strategies to detect ¹O₂. Thus, the reported synthesis of a new hydrophilic and non-ionic chemical trap may contribute to a better evaluation of ¹O₂ participation in biological processes. We showed that DHPA reacts with ¹O₂ generated by photosensitization or by thermolysis of DHPNO₂ or DHPN¹⁸O₂. The DHPA endoperoxide product was detected by the loss of the absorbance from the anthracene moiety and by mass spectrometry confirming the incorporation of two oxygen atoms on the DHPA structure. The main advantage of this compound is the absence of charge and its hydrophilicity that may allow an easier traffic inside the cell.

4. Experimental

4.1. General

Malonic ester, 3-amino-1,2-propanediol, 9,10-dimethylanthracene, sodium bicarbonate, sodium hydroxide, bromine, and sodium were obtained from Sigma (St. Louis, MO). Benzene, methanol, isopropanol, carbon tetrachloride, toluene, ethanol, acetone, *n*-hexane, hydrochloric acid, sulfuric acid, chloroform and acetonitrile (HPLC grade) were acquired from Merck (Rio de Janeiro, Brazil). The water used in the experiments was treated with the Nanopure Water System (Barnstead, Dubuque, IA). ¹H NMR spectra were recorded on Bruker DRX 500 series Advance

(Bruker–Biospin, Germany). Mass spectra were determined on a Quattro II instrument (Micromass, UK) in the positive or negative ESI mode (cone voltage was set to 25 V). HPLC analyses were recorded on a Shimadzu LC-10AD/VP system (Shimadzu, Japan) with a SupelcosilTM (Supelco, PA) LC-18 column (5 μm, 150×4.6 mm) and UV detection (λ=260 nm). A gradient of water–acetonitrile was used, starting from 15% acetonitrile, reaching 30% acetonitrile in 10 min, and 80% in the next 5 min, followed by an isocratic elution for 5 min, ending with a decreasing gradient back to 15% within 5 min, at a flow rate of 0.6 mL/min. At the output of the UV detector, the eluent was split and a small fraction was directed into the MS spectrometer at a flow rate of 150 μL/min.

4.2. Synthesis of 9,10-dibromomethylanthracene (DBMA)

The route employed was adapted from previous works that describe the synthesis of hydrophilic naphthalene derivatives.^{19,32–34} In the first step, 300 μL of Br₂ (5.8 mmol) was added to 0.5 g (2.43 mmol) of 9,10-dimethylanthracene (DMA) dissolved in 50 mL of CCl₄. The solution was refluxed and irradiated with an Hg lamp (500 W) for 4 h prior to stand overnight at room temperature. The reaction was followed by measuring the pH from the fume released and DBMA formation was checked by thin-layer chromatography (80% CHCl₃ and 20% *n*-hexane). The solvent was removed by rotatory-evaporation under reduced pressure and the solid was purified by recrystallization in chloroform (yield: 0.63 g, 71%). ¹H NMR (CDCl₃) δ 5.52 (4H, s), 7.68 (4H, dd, *J*=6.9, 3.3 Hz), 8.36 (4H, dd, *J*=6.9, 3.3 Hz).

4.3. Synthesis of 9,10-anthracenedipropionic acid (ADPA)

To synthesize ADPA, 1.5 g of sodium (0.0625 mol) was added to 250 mL of ethanol in a dry 1 L flask and then 20 mL of malonic ester (0.132 mol) was introduced. During the course of the reaction, the system was kept warm (~50 °C) to prevent precipitation. After that, 350 mL of dry benzene and 0.55 g (1.51 mmol) of DBMA were added to the reaction mixture. The system was maintained under reflux for 4 h. The mixture was neutralized with 200 mL of 10% HCl aqueous solution. The organic phase was separated and the solvents were removed by rotatory-evaporation under reduced pressure. The saponification was performed with the residue obtained, by adding 100 mL of 6 M NaOH, 100 mL of methanol, and 5 mL of CHCl₃. The system was kept under reflux for 3 h. Then, HCl was added

until pH \sim 1 and the solid was separated by filtration. MS (ESI⁻): $m/z=409$ [M-H]⁻, 365 [M-CO₂-H]⁻, 321 [M-2CO₂-H]⁻, and 277 [M-3CO₂-H]⁻. The decarboxylation was done by keeping the solid at 120 °C for 5 days to get ADPA. MS (ESI⁻): $m/z=321$ [M-H]⁻ and 277 [M-CO₂-H]⁻.

4.4. Synthesis of diethyl 9,10-anthracenedipropionate (DEADP)

The ADPA was subsequently used for the synthesis of DEADP by acid-catalyzed esterification.³⁵ In this way, 150 mg of ADPA (0.47 mmol) was refluxed in 23 mL of ethanol and 0.1 mL of H₂SO₄ (95%) during 2 h. Dean–Stark trap was settled in the presence of 6 mL of toluene and the reflux was left for 4 h. The organic phase was washed with 5% aqueous NaHCO₃, dried, and evaporated to yield DEADP as a oil. MS (ESI⁺): $m/z=379$ [M+H]⁺ and 396 [M+Na]⁺.

4.5. Synthesis of *N,N'*-di(2,3-dihydroxypropyl)-9,10-anthracenedipropanamide (DHPA)

The amidation of the diester DEADP with 3-amino-1,2-propanediol was made by stirring, under reflux, a solution of DEADP (80 mg, 0.21 mmol) and 3-amino-1,2-propanediol (0.2 g, 2.2 mmol) in 7 mL methanol and 4 mL of isopropanol for 24 h. After evaporation of the solvent, the residue was triturated with 20 mL of acetone. The colorless precipitate was filtered by suction, rinsed with acetone, and recrystallized in methanol (yield: 40.5 mg, 41%). MS (ESI⁺): $m/z=491$ [M+Na]⁺. ¹H NMR (CD₃OD): δ 2.66 (4H, t, $J=8.3$ Hz), 3.17 (2H, dd, $J=13.8, 6.8$ Hz), 3.31 (2H, dd), 3.38 (2H, dd, $J=11.5, 4.9$ Hz), 3.59 (2H, m), 3.95 (4H, t, $J=8.3$ Hz), 7.54 (4H, dd, $J=6.9, 3.3$ Hz), 8.41 (4H, dd, $J=6.9, 3.2$ Hz). ¹³C NMR (CD₃OD): δ 24.8 (CH₂), 38.0 (CH₂), 43.2 (CH₂), 64.5 (CH₂), 71.5 (CH), 125.8 (CH), 126.2 (CH), 130.4 (C), 133.2 (C), 175.4 (C=O). The solubility in water is around 0.8 mM.

4.6. Endoperoxide of *N,N'*-di(2,3-dihydroxypropyl)-9,10-anthracenedipropanamide

The chemical trap capacity of DHPA was evaluated by the reaction with ¹O₂, generated by photooxidation or by naphthalene endoperoxide thermolysis. The photooxidation was performed in methanol without sensitizer and it was followed by the loss of UV–vis absorption in 372 nm and by HPLC analysis. In order to further confirm the identity of the product formed, the reaction was performed with DHPA (0.8 mM) and DHPNO₂ (0.5 mM) or ¹⁸O-labeled naphthalene endoperoxide (DHPN¹⁸O₂, 0.5 mM) under argon atmosphere at 37 °C for 2 h. The products were submitted to HPLC separation and ESI⁺-MS analysis. The DHPA UV–vis spectrum was followed along the time of incubation. For comparison, a known chemical trap (EAS, 0.8 mM) was also submitted to the same conditions of reaction and its spectrum was also recorded.

Acknowledgements

This work was supported by the Brazilian research funding institutions: CNPq (Conselho Nacional para o

Desenvolvimento Científico e Tecnológico)—Instituto do Milênio Redoxoma, FAPESP (Fundação de Amparo à Pesquisa do Estado de São Paulo) and the John Simon Memorial Guggenheim Foundation (P.D.M. Fellowship). G.R.M. was post-doctorate recipients of FAPESP fellowship. G.E.R. and M.C.B.O. are Ph.D. and post-doctorate recipients of FAPESP fellowship, respectively.

References and notes

1. Kanofsky, J. R. *Chem. Biol. Interact.* **1989**, *70*, 1.
2. Steinbeck, M.; Khan, A.; Karnovsky, M. *J. Biol. Chem.* **1992**, *267*, 13425.
3. Babior, B. M.; Takeuchi, C.; Ruedi, J.; Gutierrez, A.; Wentworth, P. *Proc. Natl. Acad. Sci. U.S.A.* **2003**, *100*, 3031.
4. Wentworth, P.; Jones, L. H.; Wentworth, A. D.; Zhu, X. Y.; Larsen, N. A.; Wilson, I. A.; Xu, X.; Goddard, W. A.; Janda, K. D.; Eschenmoser, A.; Lerner, R. A. *Science* **2001**, *293*, 1806.
5. Foote, C. S.; Peterson, E. R.; Lee, K. W. *J. Am. Chem. Soc.* **1972**, *94*, 1032.
6. McCall, D. B. Ph.D. Thesis, Wayne State University, 1984.
7. Kreitner, M.; Ebermann, R.; Alth, G. *J. Photochem. Photobiol., B* **1996**, *36*, 109.
8. Foote, C. S.; Clennan, E. L. *Active oxygen in chemistry*; Foote, C. S., Valentine, J. S., Greenberg, A., Liebman, J. F., Eds.; Chapman and Hall: London, 1995; Vol. 2, p 105.
9. MacManus-Spencer, L. A.; Latch, D. E.; Kroncke, K. M.; McNeill, K. *Anal. Chem.* **2005**, *77*, 1200.
10. Moureu, C.; Dufraisse, C.; Dean, P. M. *C.R. Acad. Sci.* **1926**, *182*, 1584.
11. Dufraisse, C.; Velluz, L. *Bull. Soc. Chim. Fr.* **1942**, *9*, 171.
12. Wasserman, H.; Scheffer, J. R. *J. Am. Chem. Soc.* **1967**, *89*, 3073.
13. Aubry, J. M.; Pierlot, C.; Rigaudy, J.; Schmidt, R. *Acc. Chem. Res.* **2003**, *36*, 668.
14. Miyamoto, S.; Martinez, G. R.; Rettori, D.; Augusto, O.; Medeiros, M. H. G.; Di Mascio, P. *Proc. Natl. Acad. Sci. U.S.A.* **2006**, *103*, 293.
15. Miyamoto, S.; Martinez, G.; Medeiros, M. H. G.; Di Mascio, P. *J. Am. Chem. Soc.* **2003**, *125*, 6172.
16. Miyamoto, S.; Martinez, G.; Martins, A. P. B.; Medeiros, M. H. G.; Di Mascio, P. *J. Am. Chem. Soc.* **2003**, *125*, 4510.
17. Aubry, J. M.; Rigaudy, J.; Cuong, N. K. *Photochem. Photobiol.* **1981**, *33*, 149.
18. Lindig, B. A.; Rodgers, M. A. J.; Schaap, A. P. *J. Am. Chem. Soc.* **1980**, *102*, 5590.
19. Di Mascio, P.; Sies, H. *J. Am. Chem. Soc.* **1989**, *111*, 2909.
20. Botsivali, M.; Evans, D. F. *J. Chem. Soc., Chem. Commun.* **1979**, 1114.
21. Nardello, V.; Aubry, J.-M.; Johnston, P.; Bulduk, I.; Vries, A. H. M.; Alsters, P. L. *Synlett* **2005**, 2667.
22. Tanaka, K.; Miura, T.; Umezawa, N.; Urano, Y.; Kikuchi, K.; Higuchi, T.; Nagano, T. *J. Am. Chem. Soc.* **2001**, *123*, 2530.
23. Nardello, V.; Aubry, J. M. *Tetrahedron Lett.* **1997**, *38*, 7361.
24. Nardello, V.; Azaroual, N.; Cerveise, I.; Vermeersch, G.; Aubry, J. M. *Tetrahedron* **1996**, *52*, 2031.
25. Nardello, V.; Brault, D.; Chavalle, P.; Aubry, J. M. *J. Photochem. Photobiol., B* **1997**, *39*, 146.
26. Dewilde, A.; Pellieux, C.; Pierlot, C.; Wattré, P.; Aubry, J. M. *Biol. Chem.* **1998**, *379*, 1377.

27. Martinez, G. R.; Ravanat, J.-L.; Medeiros, M. H. G.; Cadet, J.; Di Mascio, P. *J. Am. Chem. Soc.* **2000**, *122*, 10212.
28. Ravanat, J.-L.; Di Mascio, P.; Martinez, G. R.; Medeiros, M. H. G.; Cadet, J. *J. Biol. Chem.* **2000**, *275*, 40601.
29. Duarte, V.; Gasparutto, D.; Yamaguchi, L. F.; Ravanat, J. L.; Martinez, G. R.; Medeiros, M. H. G.; Di Mascio, P.; Cadet, J. *J. Am. Chem. Soc.* **2000**, *122*, 12622.
30. Martinez, G. R.; Medeiros, M. H. G.; Ravanat, J. L.; Cadet, J.; Di Mascio, P. *Biol. Chem.* **2002**, *383*, 607.
31. Martinez, G. R.; Ravanat, J. L.; Cadet, J.; Miyamoto, S.; Medeiros, M. H. G.; Di Mascio, P. *J. Am. Chem. Soc.* **2004**, *126*, 3056.
32. Lock, G.; Walter, E. *Chem. Ber.* **1942**, *75B*, 1158.
33. Marvel, C. S.; Wilson, B. D. *J. Org. Chem.* **1958**, *23*, 1483.
34. Pierlot, C.; Aubry, J.; Briviba, K.; Sies, H.; Di Mascio, P. *Methods Enzymol.* **2000**, *319*, 3.
35. Vogel, A. I. *Vogel's Textbook of Practical Organic Chemistry*; Wiley: New York, NY, 1989; p 695.

Possible singlet oxygen generation from the photolysis of indigo dyes in methanol, DMSO, water, and ionic liquid, 1-butyl-3-methylimidazolium tetrafluoroborate

Naveen Gandra,^a Aaron T. Frank,^b Onica Le Gendre,^b Nahed Sawwan,^b David Aebisher,^b Joel F. Liebman,^c K. N. Houk,^d Alexander Greer^{b,*} and Ruomei Gao^{a,*}

^aDepartment of Chemistry, Jackson State University, Jackson, MS 39217, USA

^bDepartment of Chemistry, Graduate Center and The City University of New York (CUNY), Brooklyn College, Brooklyn, NY 11210, USA

^cDepartment of Chemistry and Biochemistry, University of Maryland, Baltimore County, Baltimore, MD 21250, USA

^dDepartment of Chemistry and Biochemistry, University of California, Los Angeles, CA 90095, USA

Received 7 July 2006; revised 25 July 2006; accepted 8 August 2006

Available online 25 September 2006

Abstract—We suggest that singlet molecular oxygen [¹O₂ (¹Δ_g)] is formed upon irradiation of indigo **1** [in air or O₂-saturated DMSO and DMSO (0.5% H₂SO₄)] and indigo carmine **2** [in air or O₂-saturated CH₃OH, D₂O, and 1-butyl-3-methylimidazolium tetrafluoroborate (BmIm-BF₄)]. The quantum yield for production of ¹O₂ is estimated to be 0.6 for **1** and 0.3–0.5 for **2**. The rates of reaction of ¹O₂ with **1** and **2** were determined by monitoring the emission of ¹O₂ at 1270 nm over time. Low molar absorptivities (at 532 nm) and rapid physical quenching caused by **1** and **2** limit their utility as ¹O₂ photosensitizers in solution. Compounds **1** and **2** degrade slowly during the photolysis due to a self-sensitized (type I or II) photooxidation reaction. Oxidative cleavage of **1** by singlet oxygen and superoxide, and **2** by superoxide has been noted before (Kuramoto, N.; Kitao, T. *J. Soc. Dyers Color.* **1979**, *95*, 257–261; Kettle, A. J.; Clark, B. M.; Winterbourn, C. C. *J. Biol. Chem.* **2004**, *279*, 18521–18525).

© 2006 Elsevier Ltd. All rights reserved.

1. Introduction

Indigo (**1**) possesses a blue color, and has been of scientific interest given its historic provenance and esthetic hue. Indigo is a naturally derived dye that comes from a variety of plant species.^{1,2} Biosynthetic and laboratory preparations of **1** have been reported.^{3–6} Indigo **1** and indigo carmine **2** represent stable dyes and colorants, and are composed of a central carbon double bond with two imine nitrogens and two carbonyl groups affixed (Chart 1).⁷

Both **1** and **2** are quite photostable⁸ and this led us to raise the following question: *How efficiently might they generate*

¹O₂ by photosensitization? The yield of ¹O₂ formed by irradiation of triplet O₂ plus sensitizer varies depending on the structure of the photosensitizer, the nature of the photosensitizer's excited state, and on the solvents used. Studies of indigo dye spectroscopy,^{8–12} excited state chemistry,^{13–24} and photofading^{25,26} date back to the 1950s. The mechanism of quenching of electronically excited states of thioindigo dyes (S replacing NH) by triplet molecular oxygen has been studied.^{27–35} Wyman and co-workers observed that dissolved oxygen quenched the photoisomerization of **3** without diminishing the intensity of the fluorescence.³⁶ This suggested that the trans–cis isomerization of **3** may involve the excited triplet state. The triplet energy of **3** was determined to be 27–32 kcal/mol,^{16,17} which is greater than the 22.5 kcal/mol required to excite O₂ from its ground state to its first excited singlet state. The triplet state energies of **1** and **2** have not yet been reported.

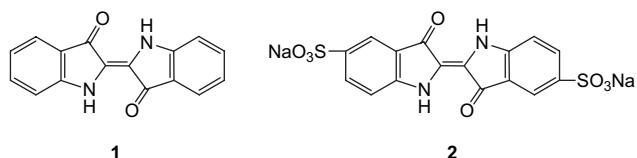
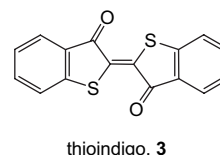


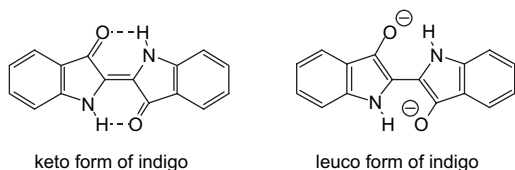
Chart 1. Structures of indigo and indigo carmine in their keto forms.



* Corresponding authors. E-mail addresses: agreer@brooklyn.cuny.edu; ruomei.gao@ccaix.jsu.edu

The photostability of indigo **1** has been attributed by Kobayashi and Rentzepis to the high internal conversion from excited singlet state S_1 to ground singlet state S_0 rather than trans to cis isomerization.¹⁴ The internal conversion process may be enhanced by excited state intramolecular proton transfer. However, Elsaesser et al. have concluded that the internal conversion is related to the vibrations of the N–H bonds, which are part of the intramolecular hydrogen bonds.¹³

Despite the importance of indigo dyes, little information is available about whether they may serve as 1O_2 sensitizers.³⁶ Recent work by Seixas de Melo and co-workers showed that the fluorescence efficiency Φ_F is favored by the leuco, but not keto forms, e.g., Φ_F of indigo is 0.0023 for the keto form, but 0.348 for the leuco form in DMF.³⁷ The structures of the keto and leuco forms of indigo are shown below. The low fluorescence of indigo dyes in their keto form was explained by the small energy gap between S_0 and S_1 . According to the golden rule for radiationless transitions, a small value in the S_1 – S_0 energy gap favors a nonradiative decay pathway by increasing the vibrational overlap (Franck–Condon integrals) of the wave functions for the nonradiative modes of these two states.^{22,23}



The formation of 1O_2 is predominantly a triplet quenching process. The 1O_2 quantum yields (Φ_Δ) were determined using Eq. 1.³⁸ Eq. 1 represents a theoretical understanding of quantum yields of 1O_2 generation.

$$\Phi_\Delta = \Phi_T P_{T,^3O_2} f_{T,\Delta} \quad (1)$$

Here Φ_T is the quantum yield of triplet formation for the photosensitizer, $P_{T,^3O_2}$ the proportion of triplet quenched by ground state oxygen and $f_{T,\Delta}$ the fraction of triplet state quenched by ground state oxygen that leads to the formation of 1O_2 .

There is limited solubility of **1** in DMSO (~ 0.7 mM) and in $CHCl_3$, CH_2Cl_2 , CH_3CN , and CH_3OH (< 0.1 mM). However, because of its pair of sulfonate groups, indigo carmine **2** dissolves in water (~ 0.02 M) and $MeOH$ (~ 0.8 M) to a higher extent. A number of reports discussing photochemistry in ionic liquids have appeared in the past several years.^{39–43} The ability of ionic liquids to retain other ionic compounds suggested the idea of using a photosensitizer bearing a charge, thereby making it preferentially soluble in the ionic liquid. Imidazole-tagged aryl ketones have been developed that can efficiently sensitize photochemical reactions in ionic liquids and are isolated simply by extraction of the ionic liquid solution with an appropriate organic solvent after use.⁴⁴ The [2+4] reaction between 1O_2 and 1,4-dimethylnaphthalene has been investigated in several 1-methyl-3-butylimidazolium cation ($BmIm^+$) ionic liquids along with the following counter anions: PF_6^- , SbF_6^- , and BF_4^- .⁴⁵

Information regarding the quantum efficiency of 1O_2 generation in ionic liquids is unavailable.

We report that absorption of visible light by **1** and **2** in the presence of O_2 leads to the production of 1O_2 . Singlet oxygen generation was measured for **1** in DMSO, and **2** in CH_3OH , D_2O , and $BmIm-BF_4$ using a time-resolved method. Oxidizing intermediates produced during the reaction led to the decomposition of **1** and **2**.

2. Experimental

2.1. General aspects

Indigo **1**, indigo carmine **2**, isatin **4**, rose bengal, methylene blue, and di-*n*-butyl sulfide were purchased commercially and used without further purification. The solvents used (DMSO, D_2O , CH_3OH , and $BmIm-BF_4$) were of spectroscopic or equivalent grade and were used as received. Light at 532 nm was obtained from a time-resolved Nd:YAG laser set-up with pulse width 3–4 ns and maxima energy 50 mJ at 532 nm (Polaris II-20, New Wave Research Merchantek Products). A liquid N_2 cooled germanium photodetector (Applied Detector Corporation) was used for the determination of quantum yields and luminescence quenching rates of 1O_2 . A Rayonet 250 W tungsten lamp equipped with a 1 cm 1.5 M $NaNO_3$ solution cutoff filter was used for steady-state generation of 1O_2 . UV–visible spectra were recorded on a Varian 300 Bio (Cary) spectrophotometer. Mass spectrometry data was collected on an Agilent 1100 LC/MSD instrument using either electrospray ionization or atmospheric pressure photoionization methods. All experiments were carried out at room temperature and with air or O_2 -saturated solutions. Shaking, stirring, and/or sonication were conducted to dissolve **2** and methylene blue in $BmIm-BF_4$.

2.2. 1O_2 Quantum yield measurements

Absorbances of **1** and **2** ranged from 0.03 to 0.6 at the excitation wavelength 532 nm. The absorbance of **1** and **2**, and rose bengal (known to possess a quantum yield of 1O_2 generation 0.76 in DMSO, methanol, and heavy water)^{46,47} all matched to within 80%. The quantum yield values may change according to the reference used. The initial 1O_2 intensity is extrapolated to $t=0$. The data points of the initial 3–4 ns are not used due to electronic interference signals from the detector. The intensity of the pulses at 532 nm were controlled between 40 and 50 mJ. The quantum yield for production of 1O_2 is calculated according to Eq. 2. Unlike Eq. 1, Eq. 2 is practical to use along with the time-resolved method.

$$\frac{\Phi_{\Delta\text{sample}}}{\Phi_{\Delta\text{reference}}} = \frac{S_{\text{sample}}}{S_{\text{reference}}} \quad (2)$$

Here $\Phi_{\Delta\text{sample}}$ and $\Phi_{\Delta\text{reference}}$ are the quantum yields for samples and the reference. Rose bengal was used as a reference sensitizer. S_{sample} and $S_{\text{reference}}$ represent the slopes obtained from the plot of initial intensity of 1O_2 via the absorbance at excitation wavelength 532 nm for the sample and the reference, respectively.

2.3. Quenching rate constants of $^1\text{O}_2$

The phosphorescence of $^1\text{O}_2$ at 1270 nm was measured as previously described.⁴⁸ The $^1\text{O}_2$ quenching rates were measured by monitoring the deactivation of $^1\text{O}_2$ by **1** and **2**. Stern–Volmer analyses were conducted with rose bengal as the sensitizer in DMSO, methanol, and D_2O .

3. Results and discussion

3.1. Spectral properties of **1** and **2**

Normalized UV–visible spectra for **1** and **2** are shown in Figure 1. The λ_{max} and absorptivity at maxima of **1** and **2** and their 532 nm excitation wavelengths are collected in Table 1. The absorption of **1** and **2** consists of a band in the visible region between 500 and 700 nm with a small inflection or shoulder at shorter wavelengths (Fig. 1). The high absorptivity indicates that **1** and **2** can be excited upon the absorption of light in this range.

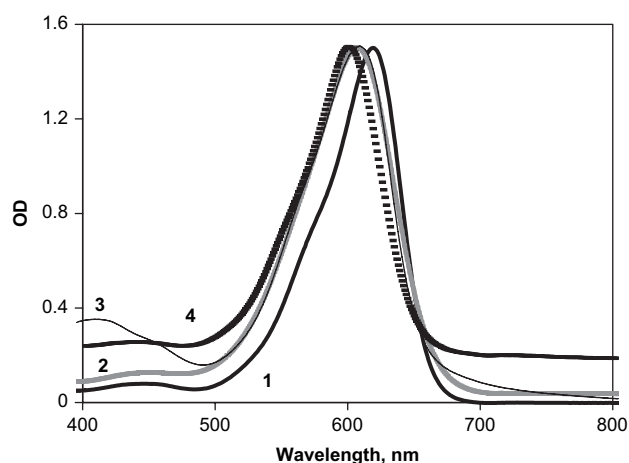


Figure 1. Normalized absorption spectra of **1** and **2**. (1) DMSO solution of **1**. (2) D_2O solution of **2**. (3) BmIm– BF_4 solution of **2**. (4) CH_3OH solution of **2**.

Table 1. Absorption maxima and extinction coefficients of solutions containing **1**, **2**, and methylene blue

Sensitizer	Solvent	λ_{max} , nm	ϵ_{max} , $\text{M}^{-1}\text{cm}^{-1}$	$\epsilon_{532\text{nm}}$, $\text{M}^{-1}\text{cm}^{-1}$
1	DMSO	620	2.26×10^3	3.26×10^2
2	CH_3OH	598	4.76×10^3	1.59×10^3
2	D_2O	607	7.92×10^3	2.02×10^3
2	BmIm– BF_4	609	—	—
Methylene blue	BmIm– BF_4	661	—	—

3.2. Possible $^1\text{O}_2$ quantum yields and quenching rates

The quantum yields for $^1\text{O}_2$ generation were determined by time-resolved laser measurements of its near-infrared luminescence (1270 nm) upon excitation at 532 nm with rose bengal $\Phi_{\Delta}=0.76$ as the reference in DMSO,⁴⁶ CH_3OH , and D_2O (Fig. 2).⁴⁷ Ideally, the straight lines should go

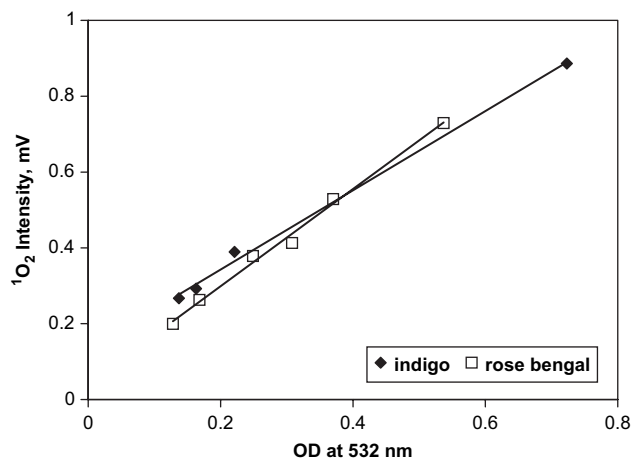


Figure 2. $^1\text{O}_2$ Emission intensity as a function of absorbance in DMSO with the excitation wavelength of 532 nm.

through zero in Figure 2, and we attribute the deviation to systematic errors. Thus, the quantum yields were determined from the slopes of the plots. Triplet–triplet annihilation appears to be negligible at absorbances ranging from 0.03 to 0.60 from excitation at 532 nm, as indicated by the $^1\text{O}_2$ intensity showing a linear correlation with the absorption of the complexes. We estimate that the Φ_{Δ} for **1** is 0.6, and for **2** is 0.3–0.6, where these Φ_{Δ} 's were obtained in the common solvents noted above. No reference photosensitizer is available for ionic liquids. Thus, the relative Φ_{Δ} for **2** in BmIm– BF_4 was calculated assuming $\Phi_{\Delta}=1.0$ for methylene blue. Our results show that Φ_{Δ} for **2** is about half that of methylene blue (Table 2).

The total $^1\text{O}_2$ quenching rate constants (k_T) of **2** with $^1\text{O}_2$ were determined in D_2O and CH_3OH by Stern–Volmer analyses, since a large quenching rate would severely limit their potential as photosensitizers. The quenching rate constants range from 5×10^7 to $3 \times 10^8 \text{ M}^{-1} \text{ s}^{-1}$ for **2** in CH_3OH and D_2O . This is similar to other photosensitizers, e.g., rose bengal ($2 \times 10^7 \text{ M}^{-1} \text{ s}^{-1}$ in CH_3OH ⁴⁹) and methylene blue ($2.3 \times 10^8 \text{ M}^{-1} \text{ s}^{-1}$ in CH_3OH ⁵⁰ and $4 \times 10^8 \text{ M}^{-1} \text{ s}^{-1}$ in D_2O ⁵¹). The quenching rates of $^1\text{O}_2$ by **1** in DMSO and **2** in BmIm– BF_4 cannot be observed because of their limited solubility. The self-decay rate constants (k_d , s^{-1}) measured in the present work are comparable to published values of $7.1 \times 10^4 \text{ s}^{-1}$ in DMSO,⁵² $8.9 \times 10^4 \text{ s}^{-1}$ in CH_3OH ,⁵³ $1.8 \times 10^4 \text{ s}^{-1}$ in D_2O ,⁵⁴ and $6.3 \times 10^4 \text{ s}^{-1}$ in BmIm– BF_4 .⁴⁵

Indigo **1** and indigo carmine **2** exhibit absorption bands in the range of 500–700 nm, and can be activated to higher energy levels by absorbing excitation light in this region. Photosensitization processes have been reviewed in detail by Wilkinson and Brummer.²⁷ A brief summary is given below (Eqs. 3–10). A Type II mechanism involves the generation of $^1\text{O}_2$ via energy transfer between T_1 of a photosensitizer and ground state $^3\text{O}_2$ (Eq. 7). A Type I mechanism involves hydrogen-atom abstraction or electron-transfer between the excited photosensitizer and a substrate, and the subsequent generation of oxygen radicals. One example of the Type I reaction is an electron-transfer from an excited sensitizer to $^3\text{O}_2$, to form superoxide (Eq. 8).

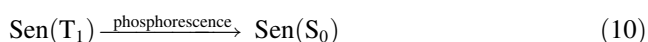
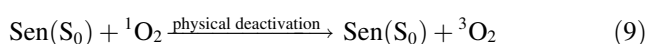
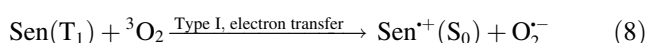
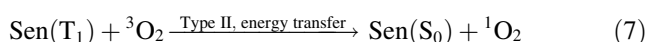
Table 2. Summary of $^1\text{O}_2$ quantum yields (Φ_Δ), total quenching rate constants (k_T , $\text{M}^{-1} \text{s}^{-1}$) and self-decay rate constants in various solvents (k_d , s^{-1})^a

Photosensitizer	Solvent	$\Phi_\Delta \pm \text{S.D.}$	Reference	k_T , $\text{M}^{-1} \text{s}^{-1}$	k_d , s^{-1}
1	DMSO	0.61±0.09	Rose bengal 0.76	—	$(9.1 \pm 2.0) \times 10^4$
1	DMSO/0.5% H_2SO_4	0.62±0.05	Rose bengal 0.76	—	$(6.0 \pm 1.0) \times 10^4$
2	CH_3OH	0.53±0.07	Rose bengal 0.76	$(5.6 \pm 0.1) \times 10^7$	$(8.1 \pm 0.5) \times 10^4$
2	D_2O	0.31±0.03	Rose bengal 0.76	$(3.2 \pm 0.7) \times 10^8$	$(1.9 \pm 0.3) \times 10^4$
2	BmIm-BF ₄ ^b	0.53±0.11	Methylene blue ^c	—	$(6.1 \pm 0.9) \times 10^4$

^a All experiments were measured at room temperature in air-saturated solutions with an excitation wavelength of 532 nm.

^b There is no reference $^1\text{O}_2$ photosensitizer available for BmIm-BF₄.

^c The $^1\text{O}_2$ quantum yield for indigo carmine **2** in BmIm-BF₄ was calculated assuming $\Phi_\Delta=1.0$ for methylene blue.



The apparent production of $^1\text{O}_2$ by the photolysis of **1** and **2** suggests that a triplet energy transfer process takes place. The proposal of energy transfer from excited **1** or **2** to $^3\text{O}_2$ is consistent with measured E_T 27–32 kcal/mol for thioindigo compounds since the triplet ground and first excited singlet state of O_2 is 22.5 kcal/mol.^{16,17} Indigo dyes in their excited triplet states may react with $^3\text{O}_2$ and generate $^1\text{O}_2$ via Eq. 7. Alternatively, the redox potential of $\text{O}_2/\text{O}_2^{\cdot-}$ and $\text{O}_2/\text{HO}_2^{\cdot}$ are -0.60 V and 0.12 V versus NHE in DMF,⁵⁵ respectively, also suggests that electron-transfer is thermodynamically favored, in particular by increasing the acidity of the solution. The excited state redox potentials E ($\text{Sen}^{+\cdot/\cdot}$) for **1** and **2** are unknown. Our results do not appear to support the Type I mechanism (Eq. 8) due to the fact that constant and unvarying high quantum yields (Φ_Δ) for $^1\text{O}_2$ generation are observed in both of DMSO and DMSO/0.5% H_2SO_4 for **1**. The quantum yields for $^1\text{O}_2$ generation suggest intersystem crossing and the formation of triplet states of **1** and **2** under these conditions. However, the quantum efficiency of singlet oxygen can potentially vary with the excitation wavelength, light intensity, solvent, solute, etc. Our results support the notion of low fluorescence efficiency and the formation of excited triplet state of **1** and **2** in their keto form.^{16,17,37,56}

The Φ_Δ for $^1\text{O}_2$ generation from indigo carmine **2** in D_2O (0.31) is lower compared to that in CH_3OH (0.53). This may be explained by a larger acidic dissociation of indigo carmine in water than methanol. We conclude that the k_T

values measured for **1** and **2** are mainly the result of physical quenching since photooxidation products are only observed after extended irradiation periods (several hours) under visible light and oxygen. Physical quenching of $^1\text{O}_2$ may be related to trans–cis isomerization or the presence of the imide nitrogens. The k_T value for **2** is $5.6 \times 10^7 \text{ M}^{-1} \text{ s}^{-1}$ in CH_3OH , and $3.2 \times 10^8 \text{ M}^{-1} \text{ s}^{-1}$ in D_2O .

Due to the lack of reference photosensitizers in ionic liquids, the relative Φ_Δ values were determined by assuming $\Phi_{\Delta(\text{methylene blue})}=1.0$ in BmIm-BF₄, yielding $\Phi_{\Delta(\text{methylene blue})}/\Phi_{\Delta(\text{indigo carmine } 2)}=2:1$. In contrast, the Φ_Δ ratio of methylene blue to indigo carmine **2** is 1:1 in CH_3OH . Furthermore, the Φ_Δ is 0.5 for methylene blue in CH_3OH has been reported previously.⁴⁷ The change in relative $^1\text{O}_2$ quantum yields may result from a competition reaction for the triplet state. The enhancement of the lifetimes of triplet state and radical ions is observed for xanthone in 1-butyl-3-methylimidazolium hexafluorophosphate (BmIm-PF₄).⁴³ This statement is speculative since influence of ionic liquids on the deactivation of triplet states is not established. Thus, it is difficult to assess whether the quantum yields for $^1\text{O}_2$ generation from rose bengal and indigo carmine **2** are significantly increased or decreased in different solvents.

3.3. Possible $^1\text{O}_2$ sensitization

Singlet oxygen may be formed under the conditions we have used in our experiments. Figure 3 contains the data of a representative 1270 nm signal decay produced by irradiation of **2** in CH_3OH . We attribute the 1270 nm signal to $^1\text{O}_2$, which is quenched by addition of NaN_3 (0.20 mM) to the solution. The self-decay rate constants k_d measured in various solvents are consistent with the literature values,^{45,52–54} where the k_d ranges from 10^4 to 10^5 s^{-1} , which correspond to $^1\text{O}_2$ lifetimes between 10 and 100 μs (vide supra, Section 3.2). The 1270 nm signal also decreases with a decreasing concentration of oxygen in the solution. The generation of $^1\text{O}_2$ can be very sensitive to reaction conditions. The amount of $^1\text{O}_2$ produced by **1** and **2** is likely influenced by the concentrations of the sensitizer and oxygen, temperature, and irradiation time. Although the quenching rate constant of $^1\text{O}_2$ by **2** measured in this paper ($5.6 \times 10^7 \text{ M}^{-1} \text{ s}^{-1}$ in methanol) is similar to that of rose bengal ($2.0 \times 10^7 \text{ M}^{-1} \text{ s}^{-1}$ in methanol), higher concentrations of **2** will be required to obtain the same absorbance at the excitation wavelength because of a lower absorptivity [compare ϵ (**2** at 532 nm) = $1600 \text{ M}^{-1} \text{ cm}^{-1}$ with ϵ (rose bengal at 532 nm) = $30,000 \text{ M}^{-1} \text{ cm}^{-1}$]. Therefore, low concentration, high excitation intensity, and long irradiation times should be employed when using **1** or **2** as $^1\text{O}_2$ photosensitizers.

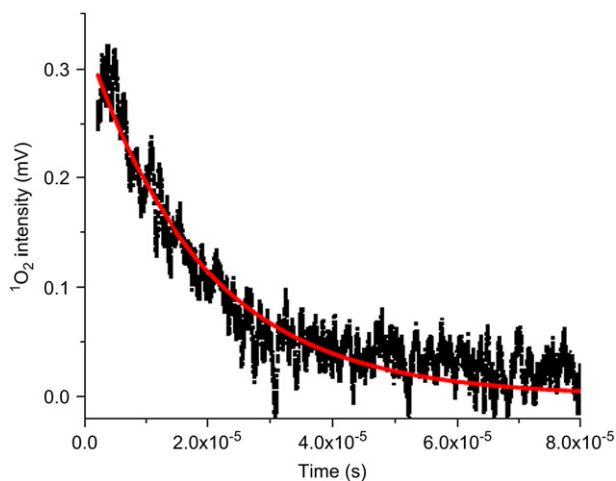
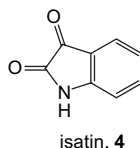


Figure 3. Decay kinetics of $^1\text{O}_2$ for **2** (OD=0.4 at 532 nm; 40 mJ) in CH_3OH . The phosphorescence emission of $^1\text{O}_2$ was monitored at 1270 nm. The dots are experimental data, and the solid line is calculated from a 1st order kinetic fitting.

3.4. Indigo and indigo carmine sensitized photooxidations

In 1979, Kuramoto and Kitao attributed the photofading of indigo **1** in solution to a self-sensitized photooxidation involving singlet oxygen.²⁵ We observed a cleavage of **1** into isatin (**4**) after 8 h of visible light irradiation in an O_2 -saturated solution of $\text{DMSO}-d_6$, or in an O_2 -saturated solution of CDCl_3 in the presence of methylene blue. The LC–MS data is indicative of isatin **4** since we find a molecular ion peak m/z 148 ($\text{M}+\text{H}^+$), and under various ionization conditions find m/z 146 ($\text{M}-\text{H}^-$), m/z 165 ($\text{M}+\text{NH}_4^+$), m/z 180 ($\text{M}+\text{CH}_3\text{OH}_2^+$), m/z 183 ($\text{M}+\text{Cl}^-$) representing the addition of solvent molecules or ions. Isatin **4** was also identified by ^1H NMR spectroscopy and the comparison to a commercial sample of isatin **4**. Singlet oxygen may contribute to the oxidative degradation of **1** by a reaction with the central $\text{C}=\text{C}$ double bond of **1**. Alternatively, oxidation of **1** may take place via a Type I photooxidation pathway, similar to the reaction of **2** with superoxide reported recently.⁵⁷ The mechanism by which active oxygen species initiates a process leading to the oxidative cleavage of the double bond of **1** and **2** will require further investigation. Greater yields of **4** are observed when a co-sensitizer, such as methylene blue is present.²⁵



A sulfide trapping experiment was conducted to study the indigo carmine **2**–sensitized photochemical reaction. We detect dibutyl sulfoxide (51%) by GC–MS in a reaction of **2** (6×10^{-4} M) with dibutyl sulfide (0.15 M) in O_2 -saturated CD_3OD after 48 h of visible light irradiation with a Rayonet lamp. An experiment with rose bengal (6×10^{-4} M) and butyl sulfide (0.15 M) in O_2 -saturated CD_3OD led to 88% conversion to dibutyl sulfoxide after 1 h of visible light

irradiation. These preliminary results may point to the intermediacy of $^1\text{O}_2$, which then oxidizes dibutyl sulfide. However, we have not explored this reaction in sufficient detail to confirm whether $^1\text{O}_2$ is trapped and responsible for the oxidation of dibutyl sulfide.

4. Conclusion

Quantum yields for the possible generation of $^1\text{O}_2$ by indigo **1** and indigo carmine **2** have been measured, which suggest that ISC competes with fluorescence and internal conversion for S_1 . We believe that **1** and **2** may serve as $^1\text{O}_2$ photosensitizers in conventional polar solvents and an ionic liquid. However, low molar absorptivities and physical quenching of **1** and **2** limits their utility as $^1\text{O}_2$ photosensitizers. High intensity of excitation light, longer irradiation times, and low concentrations of **1** or **2** would be needed when attempting to use them as $^1\text{O}_2$ photosensitizers. A better understanding of the photooxidation mechanism of **1** and **2** under the conditions will require further study.

Acknowledgements

This work was supported by research grants to R.G. from the NSF-PREM program (DMR-0611539), A.T.F. from the NIH-MARC program (2T34 GM008078), and to A.G. from the National Institutes of Health (S06 GM076168-01) and PSC-CUNY. We thank Mark Kobrak (Brooklyn College) for useful comments on the manuscript, Cliff Soll (Hunter College Mass Spectrometry Facility) for conducting several mass measurements, and Bin Ye and Matthias Selke (California State University, Los Angeles) for carrying out several laser experiments. We thank a reviewer for comments on the manuscript.

References and notes

- Watson, W. N.; Penning, C. H. *Ind. Eng. Chem.* **1926**, *18*, 1309–1312.
- McGovern, P. E.; Michel, R. H. *Acc. Chem. Res.* **1990**, *23*, 152–158.
- Padden, A. N.; Dillon, V. M.; John, P.; Edmonds, J.; Collins, M. D.; Alvarez, N. *Nature* **1998**, *396*, 225.
- Furuya, T.; Takahashi, S.; Ishii, Y.; Kino, K.; Kirimura, K. *Biochem. Biophys. Res. Commun.* **2004**, *313*, 570–575.
- Compton, R. G.; Perkin, S. J.; Gamblin, D. P.; Davis, J.; Marken, F.; Padden, A. N.; John, P. *New J. Chem.* **2000**, *24*, 179–181.
- Ensley, B. D.; Ratzkin, B. J.; Osslund, T. D.; Simon, M. J.; Wackett, L. P.; Gibson, D. *Science* **1983**, *222*, 167–169.
- Wille, E.; Lüttke, W. *Angew. Chem., Int. Ed. Engl.* **1971**, *83*, 853–854.
- Weinstein, J.; Wyman, G. M. *J. Am. Chem. Soc.* **1956**, *78*, 2387–2390.
- Wyman, G. M. *J. Am. Chem. Soc.* **1956**, *78*, 4599–4604.
- Rogers, D. A.; Margerum, J. D.; Wyman, G. M. *J. Am. Chem. Soc.* **1957**, *79*, 2464–2468.
- Wyman, G. M.; Zenhausern, A. F. *J. Org. Chem.* **1965**, *30*, 2348–2352.
- Wyman, G. M.; Zenhausern, A. *Ber. Bunsen-Ges. Phys. Chem.* **1968**, *72*, 326–328.

13. Elsaesser, T.; Kaiser, W.; Luttko, W. *J. Phys. Chem. A* **1986**, *90*, 2901–2905.
14. Kobayashi, T.; Rentzepis, P. M. *J. Chem. Phys.* **1979**, *70*, 886–892.
15. Suehnel, J.; Gustav, K. *Mol. Photochem.* **1977**, *8*, 437–458.
16. Andree, D. K.; Wyman, G. M. *J. Phys. Chem.* **1977**, *81*, 413–420.
17. Andree, D. K.; Wyman, G. M. *J. Phys. Chem.* **1975**, *79*, 543–544.
18. Wyman, G. M.; Zarnegar, B. M. *J. Phys. Chem.* **1973**, *77*, 1204–1207.
19. Wyman, G. M.; Zarnegar, B. M. *J. Phys. Chem.* **1973**, *77*, 831–837.
20. Wyman, G. M.; Zarnegar, B. M.; Whitten, D. G. *J. Phys. Chem.* **1973**, *77*, 2584–2586.
21. Wyman, G. M. *J. Chem. Soc., Chem. Commun.* **1971**, 1332–1334.
22. Becker, R. S. *Theory and Interpretation of Fluorescence and Phosphorescence*; Wiley-Interscience: New York, NY, 1969; 283 p.
23. Siebrand, W. *J. Chem. Phys.* **1967**, *47*, 2411–2422.
24. Giuliano, C. R.; Hess, L. D.; Margerum, J. D. *J. Am. Chem. Soc.* **1968**, *90*, 587–594.
25. (a) Kuramoto, N.; Kitao, T. *J. Soc. Dyers Colour.* **1979**, *95*, 257–261; (b) Kuramoto, N.; Kitao, T. *J. Soc. Dyers Colour.* **1982**, *98*, 334–340.
26. Kuramoto, N.; Kitao, T. *J. Soc. Dyers Colour.* **1982**, *98*, 159–162.
27. Wilkinson, F.; Brummer, J. G. *J. Phys. Chem. Ref. Data* **1981**, *10*, 809–999.
28. Wilkinson, F.; Helman, W. P.; Ross, A. B. *J. Phys. Chem. Ref. Data* **1993**, *22*, 113–262.
29. Ogilby, P. R. *Acc. Chem. Res.* **1999**, *32*, 512–519.
30. Wilkinson, F.; Abdel-Shafi, A. A. *J. Phys. Chem. A* **1999**, *103*, 5425–5435.
31. Poulsen, T. D.; Ogilby, P. R.; Mikkelsen, K. V. *J. Phys. Chem. A* **1998**, *102*, 9829–9832.
32. Weldon, D.; Wang, B.; Poulsen, T. D.; Mikkelsen, K. V.; Ogilby, P. R. *J. Phys. Chem. A* **1998**, *102*, 1498–1500.
33. Scurlock, R. D.; Nonell, S.; Braslavsky, S. E.; Ogilby, P. R. *J. Phys. Chem.* **1995**, *99*, 3521–3526.
34. Grewer, C.; Brauer, H. D. *J. Phys. Chem.* **1994**, *98*, 4230–4235.
35. Montejano, H. A.; Avila, V.; Garrera, H. A.; Previtali, C. M. *J. Photochem. Photobiol., A* **1993**, *72*, 117–122.
36. Wyman, G. M. *EPA Newslett.* **1994**, *50*, 9–13.
37. Seixas de Melo, J.; Moura, A. P.; Melo, M. J. *J. Phys. Chem. A* **2004**, *108*, 6975–6981.
38. Wang, S.; Gao, R.; Zhou, F.; Selke, M. *J. Mater. Chem.* **2004**, *14*, 487–493.
39. Paul, A.; Mandal, P. K.; Samanta, A. *Chem. Phys. Lett.* **2005**, *402*, 375–379.
40. Ding, J.; Desikan, V.; Han, X.; Xiao, T. L.; Ding, R.; Jenks, W. S.; Armstrong, D. W. *Org. Lett.* **2005**, *7*, 335–337.
41. Lee, C.; Winston, T.; Unni, A.; Pagni, R. M.; Mamantov, G. *J. Am. Chem. Soc.* **1996**, *118*, 4919–4924.
42. Muldoon, M. J.; McLean, A. J.; Gordon, C. M.; Dunkin, I. R. *Chem. Commun.* **2001**, 2364–2365.
43. Alvaro, M.; Ferrer, B.; Garcia, H.; Narayana, M. *Chem. Phys. Lett.* **2002**, *362*, 435–440.
44. Hubbard, S. C.; Jones, P. B. *Tetrahedron* **2005**, *61*, 7425–7430.
45. Swiderski, K.; McLean, A.; Gordon, C. M.; Vaughan, D. H. *Chem. Commun.* **2004**, 2178–2179.
46. Alegria, A. E.; Krishna, C. M.; Elespuru, P. K.; Riesz, P. *Photochem. Photobiol.* **1989**, *49*, 257–265.
47. DeRosa, M. C.; Crutchley, R. J. *Coord. Chem. Rev.* **2002**, *233–234*, 351–371.
48. Gao, R.; Ho, D. G.; Dong, T.; Khoo, D.; Franco, N.; Sezer, O.; Selke, M. *Org. Lett.* **2001**, *3*, 3719–3722.
49. Tanielian, C.; Golder, L.; Wolff, C. *J. Photochem.* **1984**, *25*, 117–125.
50. Acs, A.; Schmidt, R.; Brauer, D. *Ber. Bunsen-Ges. Phys. Chem.* **1987**, *91*, 1331–1337.
51. Schmidt, H.; Al-Ibrahim, A.; Dietzel, U.; Bieker, L. *Photochem. Photobiol.* **1981**, *33*, 127–130.
52. Yu, C.; Canteenwala, T.; El-Khouly, M. E.; Araki, Y.; Pritzker, K.; Ito, O.; Wilson, B. C.; Chiang, L. Y. *J. Mater. Chem.* **2005**, *15*, 1857–1864.
53. Harriman, A.; Luengo, G.; Guliya, K. S. *Photochem. Photobiol.* **1990**, *52*, 735–740.
54. Zahir, K. O.; Haim, A. *J. Photochem. Photobiol., A* **1992**, *63*, 167–172.
55. Sawyer, D. T.; Valentine, J. S. *Acc. Chem. Res.* **1981**, *14*, 393–400.
56. Selvi, S.; Pu, S. C.; Cheng, Y. M.; Fang, J. M.; Chou, P. T. *J. Org. Chem.* **2004**, *69*, 6674–6678.
57. Kettle, A. J.; Clark, B. M.; Winterbourn, C. C. *J. Biol. Chem.* **2004**, *279*, 18521–18525.